COMPARATIVE SEDIMENTOLOGY AND PALEOECOLOGY OF FOSSIL GIANT OYSTER BEDS IN SOME TERTIARY STRATA OF NEW ZEALAND AND ARGENTINA

A thesis

submitted in partial fulfilment

of the requirements for the degree

of

Master of Science in Earth Sciences

at

The University of Waikato

by

LARISSA CLAIRE MACMILLAN

THE UNIVERSITY OF
WAIKATO
Te Whare Wānanga o Waikato

The University of Waikato
2010

"Make them like me adorers of the good science of rock-breaking."
-Charles Darwin giving advice to Charles Lyell

Impressive outcrop of haphazard and densely packed giant-fossil oysters contained in preferentially weathered Orahiri Limestone at Waitomo.

ABSTRACT

Shell concentrations are useful indicators of relative sea-level changes, systems tracts, and depositional sequence and boundary surfaces. Shellbeds can equally act as archives of paleoenvironmental information and aid in the reconstruction of past environmental and ecological conditions. These considerations are applied in this study to occurrences of giant oyster reefs and shellbeds in Tertiary sequences in North Island, New Zealand, and in Patagonia, southern Argentina.

Large recliner morphotype Flemingostreini Stenzel oysters are common in the Oligocene Orahiri Limestone in the vicinity of Waitomo, New Zealand. The oysters occur in tabular beds typically 0.5-2 m, but up to 9 m thick within highly indurated biomicritic limestone. Individual valves reach 15 cm in length, 10 cm in width and 2.5 to 5 cm in thickness. The occurences at Waitomo are characteristic of multi-event shellbeds and can be interpreted as onlap (transgressive lag) and backlap shellbeds within a transgressive systems tract. Shell $\delta^{18}O$ (-2.1 to 1.4‰) and $\delta^{13}C$ (0.4 and 2.5‰) values, and minimal seasonal isotopic ranges with little variability, confirm that these oysters lived in a fully marine environment. The environment of Oligocene Flemingstreini Stenzel was probably similar to modern *Ostrea chilensis* from Foveaux Strait off southern New Zealand, living on coarse shelly and gravelly tide swept substrates in 18-40 m water depth, under normal marine salinity conditions and temperatures around 13^{o}C, forming *in situ* biostromes of haphazardly packed oyster shells.

Specimens of "*Ostrea" patagonica* in the Late Miocene Puerto Madryn Formation, Península Valdés, Patagonia, are held in a weakly calcareous fine sand host. They reach 20 cm in length, 5 cm thick and weigh as much as 3 kg. The 'reef' has a lens (or bioherm) geometry and is composed of articulated, well preserved oysters set in a fine sand matrix. The reef is interpreted as a downlap shellbed within a highstand systems tract. Oyster shell $\delta^{18}O$ (-4.4 to -3.2‰) and $\delta^{13}C$ (-2.0 to -3.2‰) values are low and show large seasonal isotopic ranges, with a large amount of variability, collectively supporting a marginal marine setting receiving extensive freshwater input and mixing. The environment of these

oysters is comparable with modern *Crassostrea gigas* reefs at San Blas, Patagonia. *"Ostrea" patagonica* occupied a low energy intertidal zone in water depths of only 1-2 m. Temperatures ranged from 20°C (summer maximum) to 8°C (winter minimum). The oysters were not cemented firmly to the substrate, but reclined on the muddy sediment and formed an *in situ* bioherm of loosely packed oysters, with the living animals concentrated over time to the outside of the accumulation.

The Pliocene Wilkies Shellbed in the Wanganui Basin, New Zealand, comprises oyster accumulations up to 15 m thick involving the extinct oyster *Crassostrea ingens.* Individuals are up to 30 cm long, 7 cm thick and weigh as much as 2 kg. The shellbed consists of a lower onlap shellbed (transgressive lag) and an overlying backlap shellbed (biostrome). The widespread shell $\delta^{18}O$ (-3.0 to 3.0‰) and $\delta^{13}C$ (-2.6 to 1.8‰) isotopic values support a range of marginal marine to marine environmental conditions. The lower onlap shellbed had estuarine influence, while the upper part had affinities with a nearshore (<40 m) marine setting of more normal salinity. As the thick backlap shellbed migrated shoreward a depth was maintained in which *Crassostrea* could live *in situ* within a weakly calcareous very fine muddy sand in favourable conditions of low turbidity and sedimentation.

All species of fossil oysters in this study are easily distinguished by the large size and thickness of their valves. The 'reefs' formed by these oysters provided hard substrata for a diverse community of encrusting and boring organisms which includes the likes of *Gastrochaenolites* (bivalve), *Maeandropolydora* (polychaete), *Clionolithes* (boring algae), *Entobia* (sponge), *Leptichnus* (bryozoan) and *Radulichnus* (gastropod). These communities are comparable to those seen on extant oyster reefs. They can thus be termed autogenic ecosystem engineers. Non-random distribution of euendoliths and epiliths on oyster valves may be accounted for by different survival adaptations of larvae. Shell morphotypes and exterior architectures are inferred to have prompted active rugophilic (groove-seeking), geophobic (anti-gravity) and rheophilic (current-seeking) behaviour of larvae, which enhanced their survival rate. Preference for the external surface of shells suggests that traces were created during the life time of the oysters, while most internal traces are post-mortem features.

ACKNOWLEDGEMENTS

My first thanks go to my supervisors Cam Nelson, Silvio Casadío and Steve Hood. Cam, my chief supervisor for providing me with an interesting and challenging research topic and giving me the amazing opportunity to do field work abroad. Your constant drive and encouragement for me to "work hard and play hard" got me to where I am today. Silvio, for making me feel welcome in your home in Argentina and for inspiring me with your intense passion for oysters! Thanks to Steve for keeping "in the loop", always being approachable and helping out wherever needed, especially with petrographic work.

The Griffin family and Leo for collecting me from the airport in Argentina and welcoming me into your home. Thank you to all the staff at the University of La Pampa in Santa Rosa for being so friendly and helpful, despite the obvious language barrier. Thanks to Sole and Virginia for all the good times during my stay in Santa Rosa. I acknowledge all the landowners in the Waitomo and Wanganui study areas who gave me permission to access their land throughout the course of my research, and also Dave Smith from DoC, Te Kuiti with assistance with cleaning Piripiri Cave.

I am so grateful for all the generous scholarships I received, including the AusIMM New Zealand Branch Minerals Industry Scholarship, the Geological Society of New Zealand S.J Hastie Award for 2009, a University of Waikato Masters Research Scholarship and the Broad Memorial Fund. Field travel funds were provided by Cam and the Department of Earth and Ocean Sciences is thanked for financial assistance towards geochemical analyses.

Thank you to the Department of Earth and Ocean Sciences technical staff for all their assistance; Steve Cooke, Annette Rodgers, Jacinta Parenzee, Renat Radosinsky, Xu Ganqing and Chris McKinnon. Dr Rochelle Hansen for assistance with sequence stratigraphy. Thank to Steve Cameron and Megan Grainger from the Department of Chemistry for assistance with use of the LA-ICP-MS. Thank you to Keith Michael from NIWA for provision of some modern oyster samples samples and assistance on my topic.

Special thanks to Glen Treweek and Michael Tayler who helped with the initial reconnaissance study and New Zealand field work for my project. My fellow MSc students, you are my colleagues and, most importantly, my very best friends. Thanks to all of you who helped me in the field: Ben, Dirk, Robin, Melissa, Rebecca. Thank you for putting up with the long drop, mud, thistles, hayfever attacks, small bedrooms and bad neighbourhoods!

Last but not least a huge thankyou to my friends and family, in particular Dad, Mum, Gareth, Grandma, Grandad and my girls, for all the loving support they have given me when times have been stressful and difficult for me financially. Mum and Dad, I am really grateful for all the food donations I received on my visits home and the care I received when I got sick. I would not have been able to do this without you.

TABLE OF CONTENTS

LIST OF FIGURES

CHAPTER SIX: Oyster geochemistry

CHAPTER SEVEN: Petrography of oysters and their host sediments

CHAPTER EIGHT: Oysters and associated communities

LIST OF TABLES

CHAPTER ONE
Introduction

The usefulness of shell concentrations as indicators of relative sea-level changes, systems tracts and depositional sequences and boundary surfaces has been recognised for more than a decade (Abbot 1997; Kondo et al. 1998). Shell beds can equally act as useful environmental indicators such as the orientation and packing of the shells to infer transport conditions, or the degree of fragmentation, dissolution, bioerosion, encrustation and disarticulation as indicators of burial rates. Sclerochronological and laser ablation inductively coupled plasma mass spectrometry (LA-ICP-MS) analysis of periodic skeletal increments can also be used to unravel aspects of a shell's life history and growth environment (Kirby et al. 1998).

Oysters are commonly preserved as fossils and are a well known component of the fossil record (Powell 2006; Klünder et al. 2008). The sessile nature of oysters and the fact that oyster larvae (or spat) prefer to settle where there are other oysters, results in large assemblages of oysters on suitable substrates. Oysters are unlike other bivalves as they have a highly irregular shell form (Powell 2006). The shape of the shell is typically dictated by environmental conditions; however oysters are capable of growing over or around adjacent objects, including other oysters. The extant oyster *Crassostrea virginica* is particularly well known for large three-dimensional reefs that build as successive generations of oysters settle on one another (Fig. 1.1). The larger structures formed by the accumulation of oysters have been variously named reefs, beds, bars, banks or the likes (Powell 2006). In the mid and late Cenozoic era in New Zealand and Argentina those corresponding to giant oysters are among the most spectacular.

As seen in extant species, oyster reefs play an important role in establishment of very diverse community assemblages, providing hard substrata for a variety of encrusting and boring organisms. The large irregular surface that is provided by oyster reefs is important in ecosystems that are largely devoid of other hard substrates (Parras & Casadío 2006). The formation of oyster reefs provides a

Figure 1.1 The extant eastern oyster (*Crassostrea virginica*) is widespread in the Northern Hemisphere and forms impressive reef structures, like the above reef in Florida (FRWI, 2005).

restricted resource not only for the attachment of young oysters but also for associated boring and encrusting organisms. Physical modification, maintenance or creation of habitats by organisms such as the extant *Crassostrea* species are positive interactions that have been termed physical ecosystem engineering by Jones et al. (1994b, 1997). A physical ecosystem engineer controls the availability of resources such as energy, space, food or a combination of these factors for other species (Parras & Casadío 2006).

Analysis of the abundance and distribution of encrusting and boring organisms associated with fossil shell specimens can shed light on the role of the specimen as a physical ecosystem engineer. The placement position of organisms on the oyster shell is analysed and the preferential settling of encrusters and borers assessed to provide a better understanding of factors such as life position of the shell and rates of burial (Mauna et al. 2005).

A vast amount of information about past and present day environments is contained within the skeleton of fossil and living organisms (Rhoads & Lutz 1980). External growth lines, microstructural patterns and biogeochemical profiles provide basic tools for studying environmental parameters recorded within the skeletal growth of a bivalve shell, with possible paleoecological applications (Schein et al. 1991). Oysters, like many other bivalves, deposit shell material incrementally (Fig. 1.2) and are therefore able to preserve a biogeochemical time.

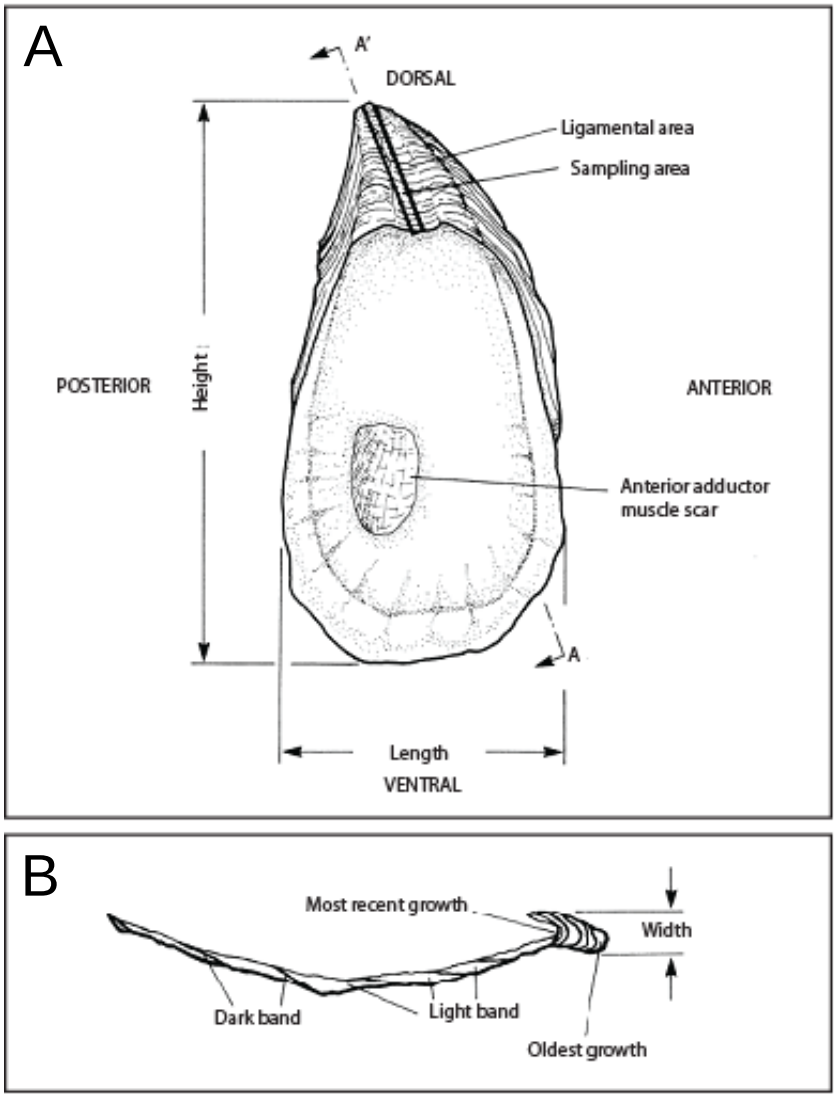

Figure 1.2 (A) Schematic of left valve of *Crassostrea virginica,* showing shell structures and ligament area where growth lines are sampled to provide a biogeochemical time series. (B) Cross section A – A' of the left valve. Adapted from Andrus & Crowe (2000).

Sequence stratigraphy provides an integrated framework within which historical patterns of paleontological phenomena can be analysed. Depositional sequences are the stratigraphic record of fluctuations of sea level and sedimentation, while

environmental parameters also strongly influence the distribution of shallow marine organisms, and the preservation and build up of their skeletal remains (Brett 1995). Sequence stratigraphy can be used to gain a fuller picture of environmental change documented in the sedimentary record through time (Coe & Church 2003). Several studies on the formation of giant oyster shellbeds or 'reefs' have concluded that they are associated with transgressive marine conditions and so can be placed within a sequence stratigraphic framework (Scasso & del Río 1987; del Río et al. 2001; McIntyre 2002; Casadío et al. 2005).

Giant oyster reefs and shellbeds occur in Paleogene and Neogene sequences in the North Island, with similar occurrences also in Patagonia, southern Argentina (Fig. 1.3B). Study sites in the North Island include the large oysters common in the Oligocene Orahiri Limestone (Fig 1.4) of the Te Kuiti Group found in the vicinity of Waitomo (Fig. 1.3C) and the oyster beds in the Pliocene Wilkies Shellbed (Fig. 1.5) in the Wanganui Basin (Fig. 1.3C). In the Waitomo region the oyster Flemingostreini Stenzel can be found in bands up to 9 m thick within highly indurated temperate limestones (Nelson et al. 1983). Individual specimens reach 15 cm in length, 10 cm in width and 2.5 to 5 cm in thickness. The Wilkies Shellbed, up to 15 m thick, comprises the oyster *Crassostrea ingens* (Zittel 1864) within weakly calcareous silty very fine sandstone. Individuals are up to 30 cm long, 7 cm thick and weigh as much as 2 kg (McIntyre 2002). Specimens of "*Ostrea" patagonica* (Fig. 1.6) (d'Orbigny 1842) in the Late Miocene Puerto Madryn Formation, Península Valdés, Patagonia, are held in a weakly calcareous medium sandstone host. They reach 20 cm in length, 5 cm thick and weigh up to > 3 kg (Mauna et al. 2005).

1.1 BACKGROUND TO STUDY LOCATIONS

1.1.1 Waitomo (Late Oligocene)

Early geological studies in the Waitomo-King Country region (Fig. 1.3), such as those by Henderson & Ongley (1923) and Marwick (1946), focused on a general overview of the geology in a large region with the purpose of constructing a geological map. On a still wider regional scale useful data in the form of stratigraphic columns and lithological descriptions were provided by Glennie (1956), Kear & Schofield (1958) and Stainton (1964). From this information a general idea of the sedimentary paleoenvironments represented in the oyster-

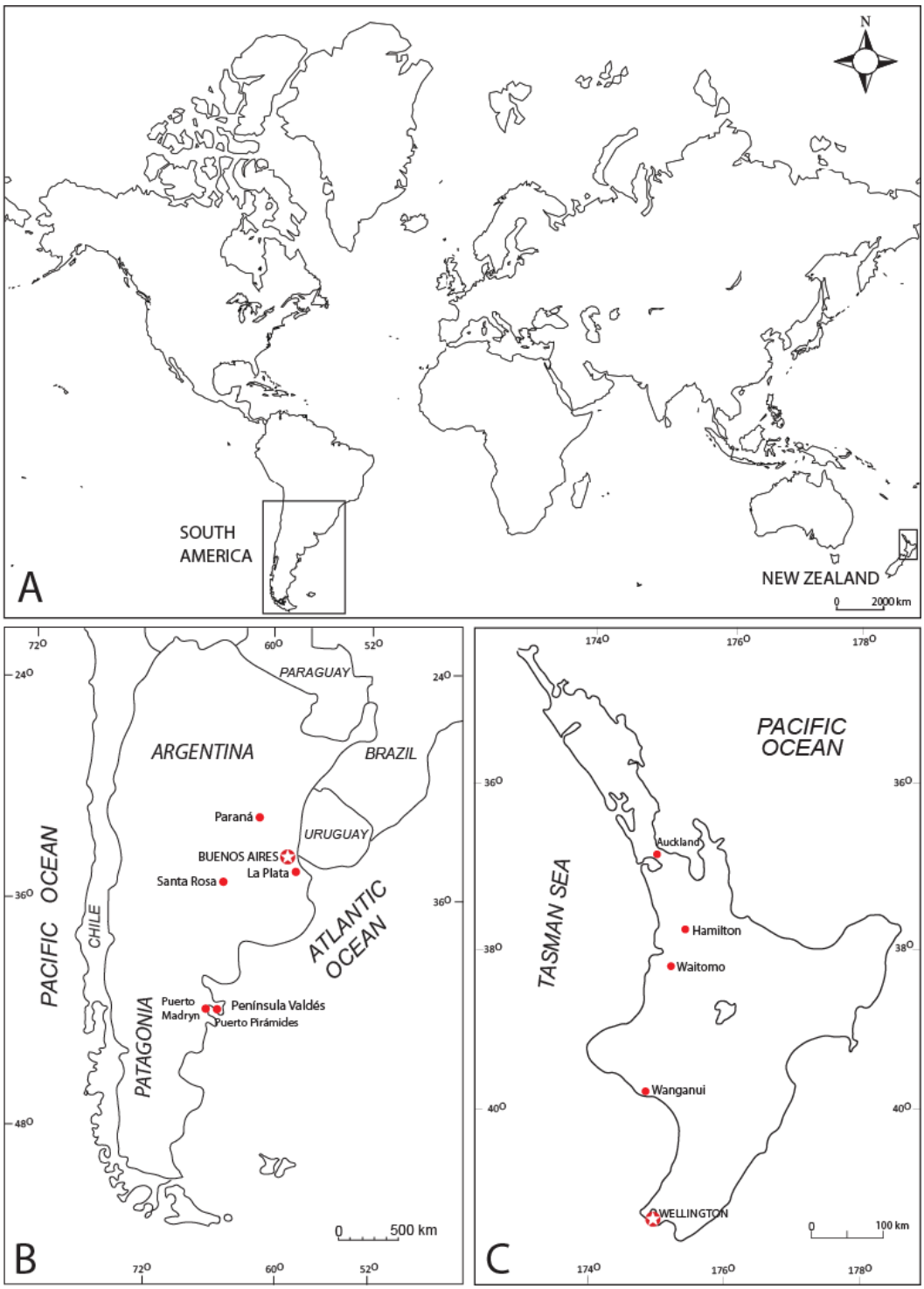

Figure 1.3 (A) Location of field sites on a global scale. (B) Field site located at Puerto Pirámide, Península Valdés, Argentina (see Chapter Four for more detail). (C) North Island field site locations situated at Waitomo and Wanganui (see Chapters Three and Five respectively for more detail).

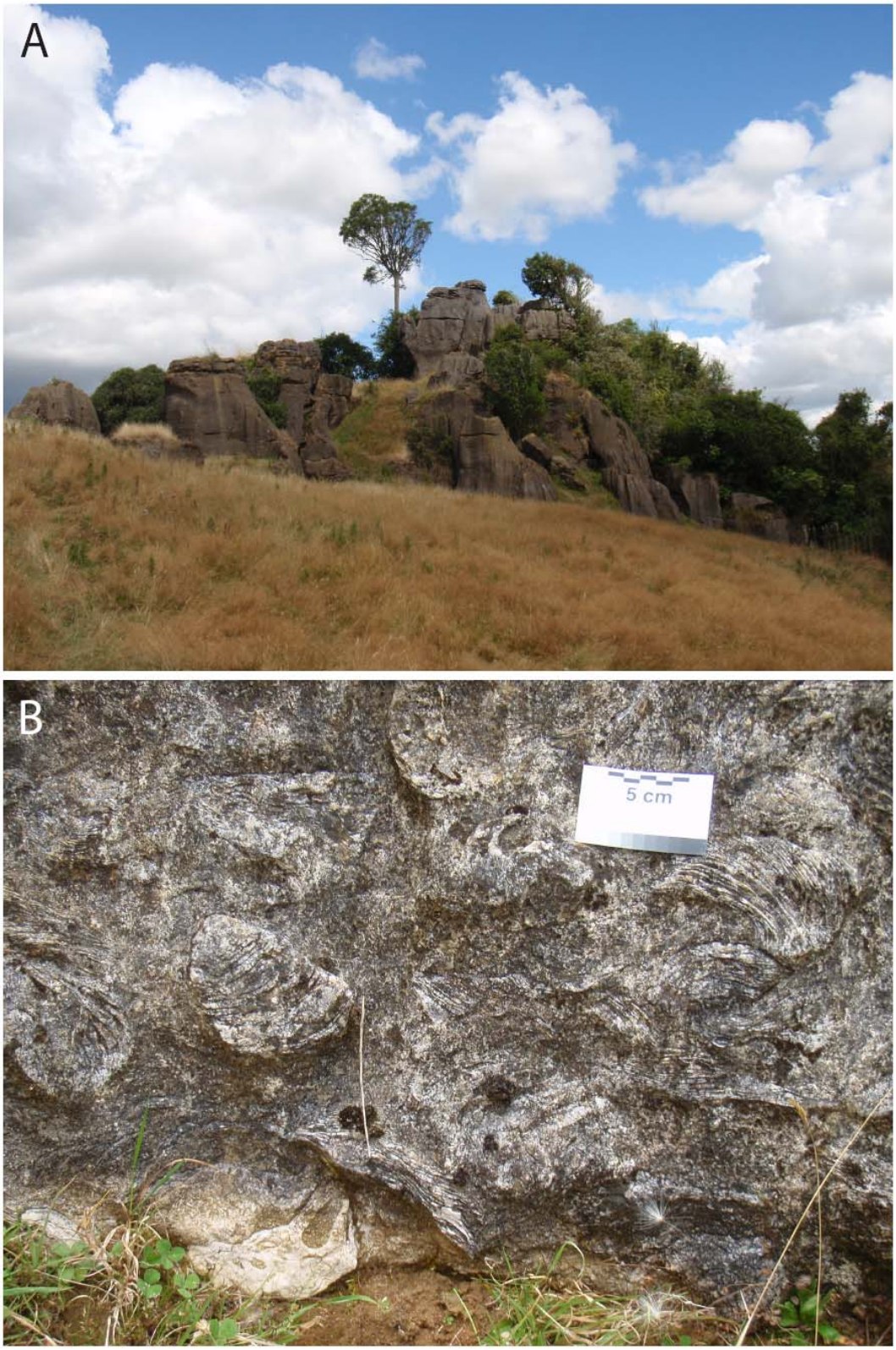

Figure 1.4 (A) Outcrop of Te Kuiti Group Orahiri Limestone on Mairoa Road, Waitomo County (more detail provided in Section 3.5.2). (B) Preferential weathering of the indurated Orahiri Limestone ensures Flemingostreini Stenzel oysters are clearly visible in some outcrops.

Figure 1.5 (A) Outcrop of the Wilkies Shellbed along the Kauarapaoa Stream in the Kauarapaoa Valley. (B) Wilkies Shellbed composed of abundant *Crassostrea ingens* at Kauarapaoa Road (see Chapter Five for localities and more detail).

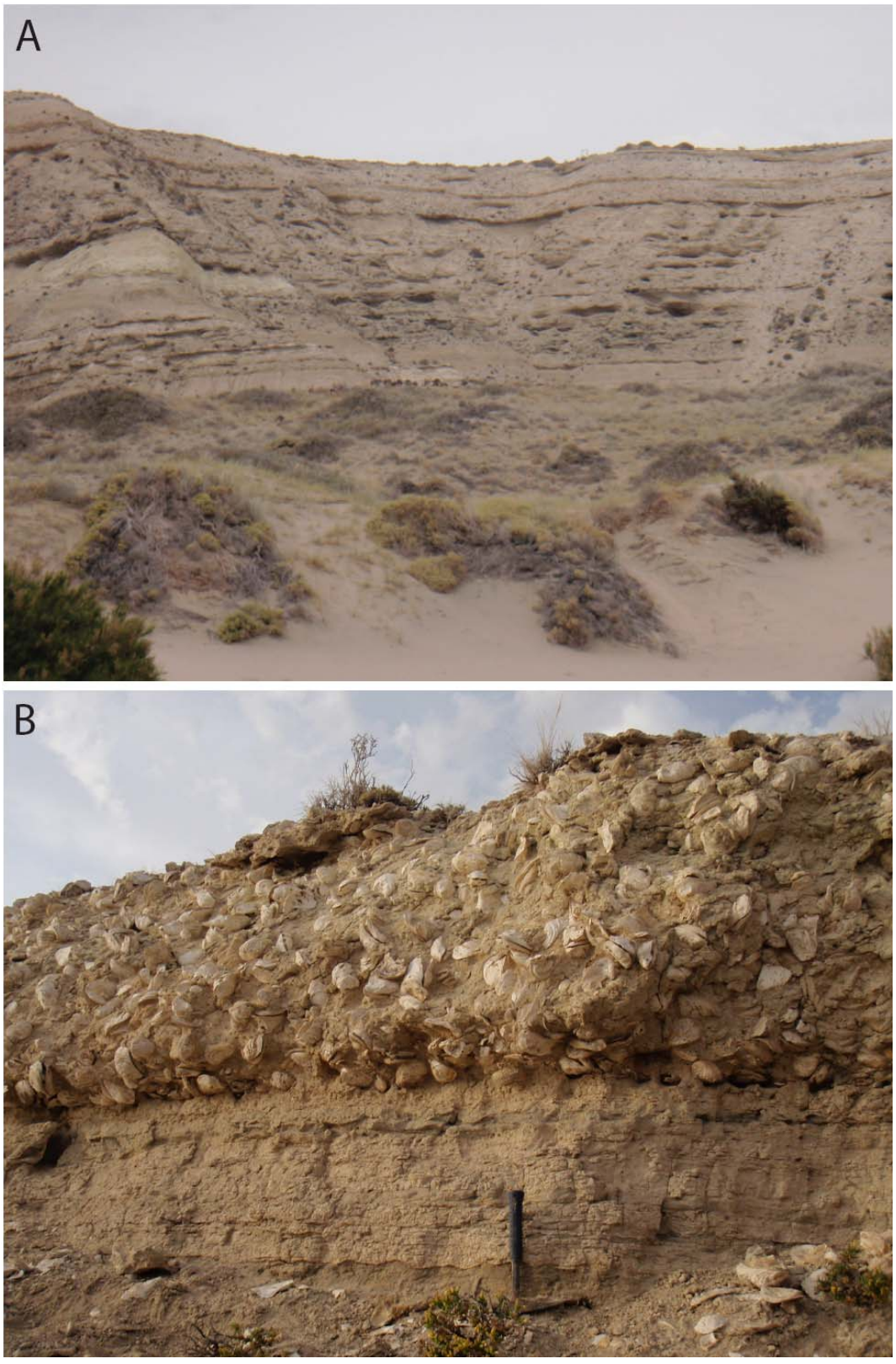

Figure 1.6 (A) A total of 90 m of the Puerto Madryn Formation is exposed at Puerto Pirámide (B) *"Ostrea" patagonica* occurrence located atop the Puerto Madryn Formation exposed at Puerto Pirámide, Península Valdés, Patagonia (See Chapter Four for more detail).

bearing Oligocene Orahiri Limestone of the Te Kuiti Group was obtained. Barrett (1962, 1967) provided additional information on the stratigraphy in the Waitomo-Te Anga area as well as suggesting that the giant oysters in the Orahiri Limestone belonged to the genus *Crassostrea*. Furthermore, he suggested that the oyster beds formed under estuarine conditions due to the fact that extant *Crassostrea* species flourish in lower salinity conditions.

Hopkins (1966, 1970) was the first to complete a study on the petrographic analysis of limestones in the Te Kuiti Group and to also offer detailed facies descriptions and stratigraphic relationships within the west Piopio area.

Nelson (1973, 1978) undertook a detailed study of the stratigraphy and sedimentology of the Te Kuiti Group in Waitomo County, delineating the distribution, thickness, lithology and contacts of units as well as the distribution and relationships between them. The study also suggested that the paleoenvironment for the giant oysters in the Orahiri Limestone was estuarine, like the extant species *Crassostrea virginica* found in Central Texas Bay today.

Nelson et al. (1983) reviewed the taxonomy and paleoenvironments of the giant oysters, using the stable oxygen and carbon isotope composition of their shells to help decipher the latter. Their findings discounted the earlier suggestions made by both Barrett (1967) and Nelson (1973) and indicated that the oysters in the Orahiri limestone (Fig. 1.4) lived in a fully marine, tide swept strait at around 25-50 m water depth.

White & Waterhouse (1993) revised the lithostratigraphy of the Te Kuiti Group to account for the considerable lithologic variation within some of the formations. The revision centred around the Whaingaroa, Aotea and Te Akatea Formations, redefining them to add consistency and ease of identification. Most recently a study of the Te Kuiti Group was completed by Tripathi (2008) which focused on basin analysis and revision of the stratigraphy and sequences.

1.1.2 Patagonia (Late Miocene)

The first mention of transgressive marine deposits in the Late Miocene of Argentina was by d'Orbigny (1842) who noted the presence of marine molluscs in

an outcrop near Paraná City. The same fauna as described by d'Orbigny four years earlier was recognised by Charles Darwin in 1846 in the costal section of Península Valdés (Fig. 1.3) (Brito 2009). Later, in 1897, Ortmann conducted a study on various giant oyster species found in Patagonia with the objective of sorting out the confusion surrounding their identification.

The occurrence of Late Miocene marine deposits from the transgression known as "Entrerriense" (further discussed in Chapter Four) found in the northwest and towards the centre of Argentina was studied by Bodenbender (1912), followed by Stappenbeck (1927) and Groeber (1929). Their work was later confirmed by micropaleontological studies carried out by Zabert & Herbst (1977), Russo & Serraiotto (1978), Zabert (1978), Bertels & Zabert (1980) and Herbst & Zabert (1987).

A general Miocene age was determined for formations situated at Paraná and Puerto Madryn by del Río (1988, 1990, 1991) by studying various molluscs contained within the "Entrerriense" formations. An age of Late Miocene was assigned by Malumián & Masiuk (1973) due to the presence of the foraminifera *Protelphidium tuberculatum* (d'Orbigny), which is recognised from the Paris Basin and has been found extensively throughout the "Entrerriense" deposits of Argentina.

Scasso et al. (2001) conducted $^{87}Sr/^{86}Sr$ analysis on pectinids and oyster shells collected from the Puerto Madryn Formation exposed at Península Valdés. The study deduced an age of 10.0 ± 0.03 Ma for the Formation. These values are close to those found by Zinsmeister et al. (1981) who gave the units an age of 9.4 Ma based on $^{40}K/^{40}Ar$ dates.

Studies carried out by Scasso & del Río (1987), del Río et al. (2001) and Casadío et al. (2005) concluded that the section exposed at Puerto Pirámides is the upper part of a depositional sequence that includes both a transgressive systems tract (TST) and a highstand systems tract (HST). Most recently, Brito (2009) has conducted a study on the oyster reef within the Puerto Madryn Formation (Fig.

1.6). The study focused on understanding the geometry of the reef and the characteristics of the communities living on the reef.

The oyster reef focused on in this study occurs on Península Valdés, northern most Patagonia, Argentina (Fig. 1.3B). Patagonia encompasses the southern portion of South America. Located in both Chile and Argentina, Patagonia is the southernmost part of the Andes Mountains to the west and south, and plateaux and low plains to the east. For the purposes of this study the locality from here on in will be referred to as Patagonia.

1.1.3 Wanganui (Pliocene)

All place names mentioned herein are contained on a locality map of the Wanganui region featured in Appendix A-1.1.

The Wilkies Shellbed is the largest and most spectacular shellbed in the Wanganui Basin succession (Fig. 1.3C). It is also thought to be the largest accumulation of fossil shells in New Zealand (Beu & Maxwell 1990). The shellbed is dominated by extinct *Crassostrea ingens* and forms large reefs up to 15 m thick in places around the Wanganui Basin (McIntyre 1997). The first formal taxonomic description was made by Zittel (1864) who described the locality from where he collected the type specimen as "Wanganui River". This description likely refers to the most prominent roadside occurrence of the shellbed situated at Parikino (Section 5.5.1).

Wilkies Shellbed was first described by Park (1887), who collected fossils and described the shellbed at the mouth of the Waitotara River. This was correlated with shellbeds seen at Parikino as part of his "Coralline Series" (Fleming 1953). Marshall & Murdoch (1920) undertook a paleontological study of the Castlecliff, Kai-Iwi, Nukumaru and Waipipi Beach sections and concluded that the shellbed found at Wilkies Bluff was faunally distinct compared to collections made at Castlecliff and Nukumaru. The fauna of the fossil molluscan bed has also been previously listed and discussed by Laws (1940) and Fleming (1953), who collected specimens from Nukumaru Beach, Wilkies Bluff, Mangapani Valley and Waipipi. Laws (1940) noted similarities between the faunal assemblages at

Wilkies Bluff and Mangapani Valley. He concluded that the shellbeds described all belonged in the New Zealand Nukumaruan Stage (Late Pliocene).

Fleming (1953) formally named the shellbed found at Wilkies Bluff as "Wilkies Shellbed" and gave it formation status. In that study he correlated the shellbed to the east where spectacular inland river valley sections occur. A total of nine new collections were made between the type locality at the Waitotara River mouth and the Parihauhau Valley. Fleming's (1953) work contributed significantly to the understanding of the stratigraphy in the Wanganui Basin. The study was particularly helpful regarding the strata of the "Waitotaran Stage", which consists of a poorly exposed outcrop on the coastal section between Waipipi and Nukumaru. Fleming's description of many new inland outcrops together with the fossil collections formed the foundation of a new, detailed basin stratigraphy and molluscan biostratigraphy (McIntyre 2002).

Christie (1973) was the first to focus on the Wilkies Shellbed as a singular unit. He re-examined Fleming's (1953) sections. The paleontology and sedimentology was investigated in an attempt to establish a depositional environment and paleoenvironmental history for the Wilkies Shellbed.

A paleomagnetic study of the Wilkies Shellbed was carried out by Wilson (1993). This study was able to demonstrate the position of the Wilkies Shellbed in relation to the Gauss/Matayama transition. McIntyre & Kamp (1998) conducted textural and sequence stratigraphic analysis, and showed that the Wilkies Shellbed, Cable Siltstone and Te Rimu Sandstone encompassed a complete cyclothem. The most recent work on the Wilkies Shellbed was by McIntyre (2002) who studied the paleontology and sedimentology to better understand the paleoenvironmetal and depositional history of the shellbed.

1.2 SUMMARY OF OBJECTIVES

The main aim of this research is to develop an understanding of the formation of fossil oyster reefs in New Zealand and Argentina and to interpret the nature of the paleoenvironments in which they formed. This will contribute to improved knowledge of paleoenvironmental, paleoceanographic and paleobiogeographical

conditions in New Zealand and Patagonia in the middle Cenozoic era. To meet this aim, the following objectives have been set:

- Develop an understanding of the geometry, internal structure, stratigraphic relations and distribution of the reefs within a sequence stratigraphic framework at sites in Waitomo, Patagonia and Wanganui.
- Determine the isotopic and elemental composition of oysters from each location.
- Describe the mineral, textural and petrographic properties of both the host materials and oysters at each study site.
- Understand the evolution of the oyster reefs from first colonizers to extinction.
- Compare the characteristics of the reefs and their fauna among the New Zealand and Patagonian examples.
- Determine the paleoenvironmental setting(s) in which these reefs formed.

1.3 OUTLINE OF STUDY

Field work for this research project was carried out in Patagonia and Waitomo and Wanganui, New Zealand. The main approaches involved basic stratigraphic section logging and an in depth description of the oyster occurrences found at each locality. This included: (a) stratigraphic features such as host materials, thickness, lateral extent, geometry, contacts, sedimentary structures and their position in sequence; (b) paleontological features including abundance, age range and mineralogy; and (c) taphonomic features such as articulation, sorting, size, fragmentation, abrasion, biological modification, orientation and packing (Kidwell 1991b).

Samples of host rock were also collected from each location to undertake analysis of their composition and texture. Oyster samples were collected to study the communities living on and within the shell and also to examine the internal structure of the oyster shells in more detail.

1.4 THESIS STRUCTURE

This thesis is divided into ten chapters followed by references and appendices.

Chapter 1 – Introduction: Introduces the geological and ecological importance of oyster reefs. It also provides background information concerning previous studies at the three field locations, and sets the objectives of the study.

Chapter 2 – Methodology: Provides a detailed account of both field and laboratory methods used for this study.

Chapter 3 – Field stratigraphy and sedimentology, Waitomo: Summarises all the information for the oyster beds collected from field areas in the Waitomo region. This includes their geological setting, stratigraphy, sedimentology, a detailed description of the oyster facies and their sequence stratigraphic interpretation.

Chapter 4 – Field stratigraphy and sedimentology, Patagonia: Collates all the information collected for the oyster beds during field work at Puerto Pirámide, Patagonia. The chapter includes their geological setting, stratigraphy, sedimentology, a detailed description of the oyster facies and a sequence stratigraphic interpretation.

Chapter 5 – Field stratigraphy and sedimentology, Wanganui: Collates information on the oyster bed from three field sites in Wanganui. This includes their geological setting, stratigraphy, sedimentology, a detailed description of the oyster facies and their sequence stratigraphic interpretation.

Chapter 6 – Oyster geochemistry: Describes the chemical and stable oxygen and carbon isotopic composition of the host rocks and oyster facies, noting similarities and differences between the study sites and also between shell species. A reconnaissance sclerochronological study reports the different elemental and stable isotopic compositions across shell growth layers. Some data from extant samples is presented for comparison.

Chapter 7 – Petrography of oysters and their host sediments: This chapter covers the following areas:

a) An introduction covering sandstone and carbonate classifications.
b) Results from detailed petrographic and cathodoluminscence (CL) microscope descriptions of host rock and oyster facies from each field location.
c) Determination of the mineral composition for each of the host rocks, and of the oysters themselves.
d) Determination of the textural characteristics of the host materials supporting the oyster reefs.

Chapter 8 – Oysters and associated communities: Describes the encrusting and boring communities living on and within the oyster shell facies at each location. Statistical analysis of each valve is carried out to determine if boring and encrusting organisms are non-randomly distributed. Similarities and differences from each study site are presented.

Chapter 9 – Discussion: Discusses key findings from each chapter.

Chapter 10 – Conclusions: Offers findings from set study objectives and concludes the thesis.

CHAPTER TWO
Methodology

2.1 INTRODUCTION

This chapter outlines all the field and laboratory methods employed during this study. This will include methods used at all three field sites and subsequent laboratory work. The laboratory work involves a variety of sedimentological analytical methods, including petrographic, geochemical, mineralogical, textural and statistical analyses.

2.2 FIELD METHODS

2.2.1 Waitomo

Reconnaissance work was carried out involving a collation of previously constructed stratigraphic columns through the Te Kuiti Group in the Waitomo area by Barrett (1967) and Nelson (1973). From this several sites, were chosen for revisiting and describing in detail, focusing on the nature and occurrence of the oysters in the oyster beds. Factors such as the orientation and density of shells and their borings were recorded, along with other features as outlined in Table 2.1. Localities of the study sections are included in Figure 3.4 in Chapter Three.

Using GPS, the grid reference at the bottom and top of each stratigraphic log was recorded for the purpose of creating a fence diagram and linking columns to each other through the recognition of common facies. Where possible, samples were collected of both oysters and host rock. Each sample was given a number relating to its collection position on the stratigraphic column. No samples were collected from the Mangapohue Natural Bridge area or Piripiri Cave as they are nature reserves and sampling is prohibited. A sample catalogue is included in Appendix A-1.2.

2.2.2 Patagonia

A sedimentological description and brief log were recorded at the Puerto Pirámide section on Península Valdés, as more detailed logs have previously been compiled by Parras & Casadío (2005) and Brito (2009) (see Chapter Three). The oyster reef was described using the attributes compiled by Kidwell (1991b) (Table 2.1).

Fossil oyster ("*Ostrea" patagonica*) and host rock samples were collected with emphasis placed on recording their position within the oyster reef. In particular, shells with a good ligamental area (beak of left valve, where growth increments are best shown) were selected for later geochemical analysis. Samples from the unit underlying the oyster reef were also collected. A sample catalogue is included in Appendix A-1.2. A modern site was also visited at San Blas where *Crassostrea gigas* was described at three different tidal locations, so allowing comparison of the ancient oyster location to a modern environment (see Chapter Six). GPS co-ordinates were taken at both locations using WGS '84 map projection.

2.2.3 Wanganui

Field work at this location chiefly involved creating a comprehensive sketch map of the largest occurrence of the Wilkies Shellbed (*Crassostrea ingens*) situated along the roadside at Parikino. As well as a sketch, a detailed stratigraphic log was made every 30 metres and included details of shell concentrations as in Kidwell (1991b) (Table 2.1). Other sites at Rangitatau East Road and Kauarapaoa Road were described in a similar manner (See Chapter Five for details). GPS was used at each location to record the grid reference of each stratigraphic log recorded.

Sample collection was difficult due to outcrop inaccessibility and the high amount of weathering that some shells had undergone. The best preserved samples were in debris piles resulting from the collapse of outcrop faces. A sample catalogue is included in Appendix A-1.2.

2.2.4 Foveaux Strait

Modern samples of *Ostrea chilensis* from Foveaux Strait were kindly provided by Keith Michael at the National Institute of Water and Atmosphere (NIWA) in Wellington. Geochemical and environmental data from these samples are used to provide a comparison of a present day environment in New Zealand with fossil samples collected from Wanganui and Waitomo (See Chapter Six).

Table 2.1 Attributes of shell concentrations for field description. Adapted from Kidwell (1991b).

	Semiquantitative scale
Stratigraphic features	
Host material	
Thickness	mm----------cm----------m----------10 m----------100 m
Lateral extent	cm ----------10,000 m
Geometry	bed----------wedge----------lens----------cluster
Physical contacts	sharp----------interbedded----------gradational
Position in sequence	e.g., base or top of fining-up sequence; within a transgressive or regressive aggradational facies tract; part of a lowstand or highstand systems tract
Association with signficant surface	e.g., local or regional unconformity; transgressive ravinement or flooding surface; downlap horizon; transport or toplap surface
Paleontological features	
Number of species	one----------few----------10----------100----------1000
Relative abundance	all individuals from one species----------one indivdual of each species
Age spectrum	juveniles only----------mixed----------adults only
Original mineralogy	aragonite-------calcite------Mg-calcite-------mixed-------silica-------other
Preserved mineralogy	original-recrystallized-replaced----------molds----------geodal fill
Taphonomic features	
Articulation	articulated----------disarticulated but closely associated---------- disarticulated and dissociated
Size sorting	very good------moderately good to poor-------very poor-------bimodal
Modal size and range	mm/phi
Shape sorting	one part only----------sorted----------unsorted
Fragmentation	all whole----------some broken----------all fragments
Abrasion	unabraded----------abraded----------highly abraded and polished
Rounding	angular----------subangular----------rounded----------well-rounded
Biological modification (bioerosion, encrustation)	none (pristine)------minor (post-moterm vs. pre-mortem)------extensive
Orientation	all in life position----------mixed----------all disturbed
Relative abundance of shells (% abundance of shells)	100%---------- --0% (visualisation estimation charts of Schäfer 1975)
Close-packing of shells	densely packed (bioclast-supported)--loosely packed (matrix-supported)--dispersed (matrix-supported)
Associated sedimentary structures	e.g., shells at base or top of size-graded beds; within concretionary bodies; along bedset boundaries, avalanche slopes; form within massive beds.

2.3 LABORATORY METHODS

2.3.1 Thin sections

Sample preparation

1. Each large sample was cut into smaller slabs using a water-cooled saw. Slabs were wet-scanned to preserve the details of the rock. This was done by lightly wetting the slab with a sponge (wetting makes features more prominent) and placing it carefully in an ACER S2W 4300V A4 flatbed scanner. The outline of the area to be thin sectioned was traced around a glass slide with a vivid marker pen and re-scanned so the feature could be

kept as a record. The slab was then trimmed down to a block measuring about 45 x 25 x 20 mm.

2. Less indurated blocks were placed on a hot plate (~ 80^{o}C) and impregnated using araldite K142 at a ratio of 5 (component): 1 (hardener). Resin was mixed slowly on the hot plate to remove any gas bubbles. One mixed, a thin layer was spread on the smooth surface of the block with a wooden spatula. Samples were left to cure overnight (this step is not required for well lithified samples).
3. The surface of the block was ground level using water and carborundum 600 powder grit on a glass plate. If necessary, impregnation was repeated. Each block was then washed clean and placed back on the hot plate until dry.
4. Friable rock samples had to be completely set in resin. Small rectangular cases were constructed out of tin foil, placed on the hot plate, and with a small amount of Araldite resin placed in the bottom of the cases. The dry friable sample was then placed in the case and then further filled with resin. This was left to cure on the hot plate overnight and then prepared as a regular block prior to mounting (See step 3).
5. A glass microscopic slide was frosted using the Struers Discoplan – TS, washed and placed on a clean hotplate. This ensures the slide surface is even prior to mounting and gives good adhesion.
6. Hillquist resin was combined at a ratio of 7 (component): 3 (hardener) on a hot plate (~ 80^{o}C). A small amount was spread evenly onto the prepared block with a spatula. Place a pre-frosted slide on to the block and work out any air bubbles using light pressure from finger tips. After air is removed the block is placed glass down on the hotplate overnight (resin set blocks must be left to cure off the hot plate).
7. Using the saw on the Discoplan TS the excess block was sawn off as close to the glass as possible. The remainder of the block was then ground down to approximately 0.03 mm thick using the lap wheel on the Discoplan. The correct slide thickness was achieved when quartz grains were light yellow under the cross polarisers.
8. A diamond tipped pen was used to carefully write the sample number on the finished slide.

2.3.2 Cathodoluminscence petrography method

Cathodoluminscence (CL) petrography was used to determine variations in mineralogy and to identify any diagenetic alteration of carbonate within the host and the oyster shells. The analysis was carried out at the University of Waikato with a Nikon Eclipse E400 POL microscope. The CL model used was a CITL CL8200 Mk5-1 run at 16-18 KV and 350-450 μA. A PC is connected to the microscope and a Nikon Digital Still camera to allow photomicrographs to be taken under CL and plain polarised light for comparison (Fig. 2.1). Images were captured using Nikon's digital interface ACT-1 software. Data from this method is included in Chapter Seven.

Figure 2.1 Cathodoluminscence stage, microscope and control unit set up at the University of Waikato.

2.3.3 Scanning electron microscope (SEM)

Samples for SEM analysis were obtained by carefully breaking small pieces the size of a thumb tack away from a larger sample. These were then mounted firmly onto carbon tape placed on aluminium stubs (Fig. 2.2A). The samples were placed into the Hitachi E-1030 Ion Sputter coater and coated with platinum, thus making them electrically conductive.

SEM was carried out at the University of Waikato using a Hitachi S-4700 Scanning Electron Microscope at an Acceleration speed of 20 kV (Fig. 2.2B). A series of magnifications were selected with images having a scale ranging from 1 mm to 30 µm. Images from this technique are included in Chapter Seven and in Appendix D-1.3.

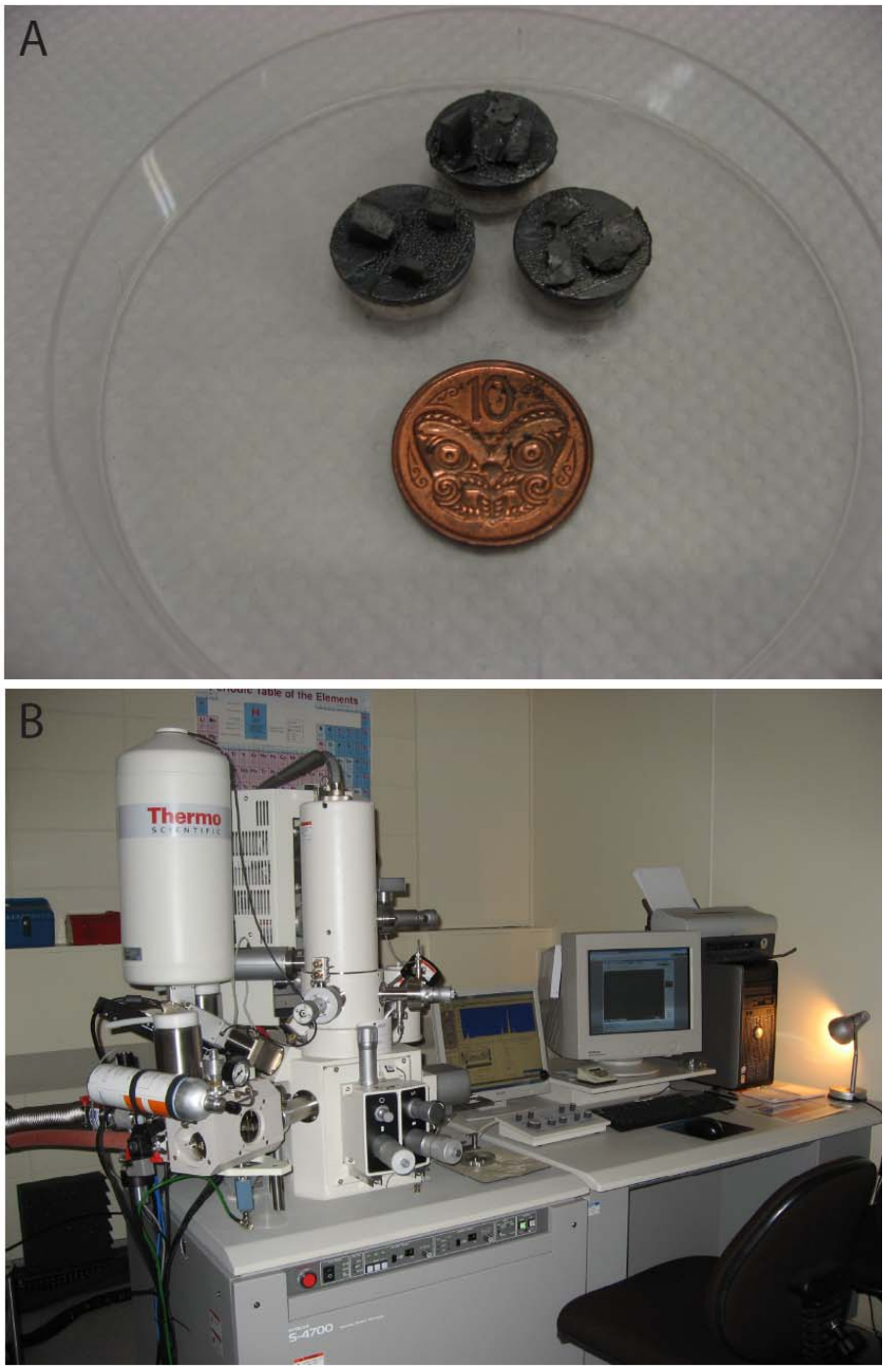

Figure 2.2 (A) Samples mounted on aluminium stubs and coated in platinum ready to be analysed under the scanning electron microscope. (B) Hitatch S-4700 Scanning electron microscope at the University of Waikato.

2.3.4 X-ray diffraction (XRD)

Samples to be analysed by XRD were crushed by breaking with a hammer. Oyster samples were removed from the host rock so that mineralogical analysis could be conducted separately. Crushed samples were then oven dried for 24 hours at 105^{o}C. Following this, each sample was run through a ring mill using a tungsten carbide head (to prevent contamination from iron head) for approximately 60 seconds, to produce a fine powder.

Analysis was carried out on a Philips (XPERT) XRD machine at the University of Waikato. X-ray powder diffraction analyses were run using two programs, the first being Absolute S set to a continuous scan mode; settings are included in Table 2.2. Secondly a General program was used during analysis; settings are also included in Table 2.2. Mineralogy was determined from the resultant graphs by the identification of peak positions. Results from this analysis are included in Chapter Seven. All data is presented in Appendix C-1.1 and also on a CD provided as a Digital Appendix.

Table 2.2 Settings for the two programs used on the Philips (XPERT) XRD machine for analysis of sample mineralogy.

X'Pert Absolute S.	
Settings	
Start Angle (^{o})	2
End Angle (^{o})	42
Step Size	0.04
Time perstep (s)	1.00

X'Pert General	
Settings	
KV	30
mA	20
2Theta	12
Omega	6

2.3.5 Stable Isotopes

2.3.5a Bulk sample preparation

1. Selected samples were broken into pieces (≤ 50 mm) using a sledge hammer. These samples were then dried in a 105^{o}C oven overnight.

2. The dried sample was then crushed into a fine powder using a ring mill with a tungsten carbide head.
3. A 15 ml vial of each sample was labelled for analysis and the remainder of the powder stored in an airtight sample bag.
4. Samples were then reacted in the Europa CAPS (Carbonate Automatic Preparation System) using the individual acid dosing or 'drip' method which allows a small amount of acid to drip onto the powdered sample, the product then being frozen out.
5. Samples are then loaded into individual reaction vessels and placed into a carousel in a 70^{o}C oven.
6. Each vessel is evacuated and a dose of 105% orthophosphoric acid is dispensed.
7. Once the reaction is complete (~ 10 minutes), the sample is run against an internal reference gas.
8. Carbon 13 and oxygen 18 isotope values are normalised and expressed per mille (‰) relative to the Vienna Peedee Belemnite, VPDB (Coplen 1988, 1994).

2.3.5b Incremental sample collection

The methodology outlined in Kirby et al. (1998) and Kirby (2000) has been followed.

1. Left valves of oyster shells were cleaned and set in resin. This prevented the shells breaking when cut. Tinfoil cases were made (as with friable rock samples) to fit shell and warm Araldite K142 resin was poured into tin foil container with sample. Samples were left to cure over night.
2. Samples were then cut radially through the hinge of the shell with a water cooled rock saw at a direction parallel to the maximum growth increments (Fig. 2.3A).
3. A 0.5 mm bit attached to a Dremel drill allowed for very small samples of powder (20 to 80 µg) to be removed from the shell. This was done at 1 to 2 mm intervals (Fig. 2.3B). Consecutive samples were collected along the ligamental area towards the beak of the shell in accordance with Kirby et al. (1998) and Kirby (2000). Individual powders were processed in the same way as described above for bulk samples (Section 2.3.5).

Data for both bulk and incremental samples is presented in Chapter Six. Data is also contained within Appendix B-1.1 and provided on a CD as Digital Appendix.

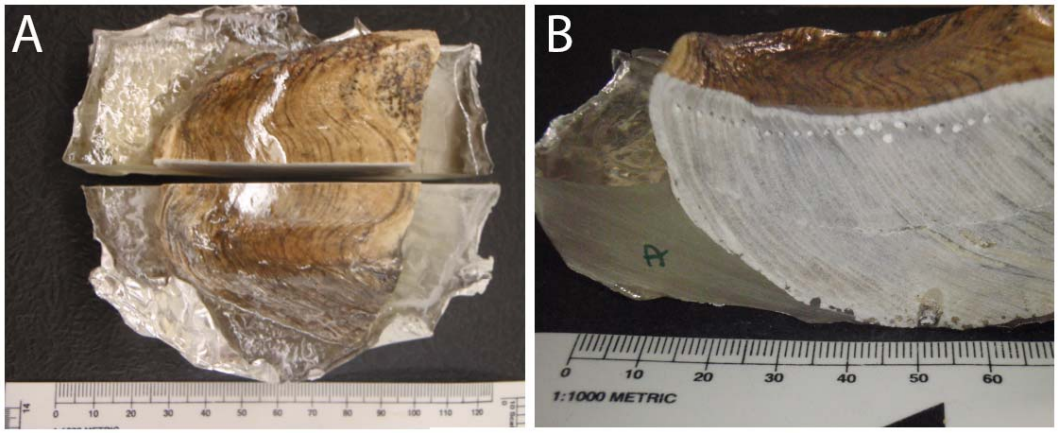

Figure 2.3 (A) Sample set in resin and cut radially through the hinge of the shell at a parallel direction to the maximum growth increments. (B) Oyster shell after being incrementally drilled using a Dremel drill with a 0.5 mm drill bit attached. Small white dots show where each sample was taken from.

2.3.6 Laser Ablation Inductively Coupled Plasma – Mass Spectrometry (LA-ICP-MS) protocol

2.3.6a Sample preparation

A left valve from each site was selected to be analysed. Two samples from Patagonia were analysed to offer a comparison with the top and bottom of the reef. Each sample was mounted in a resin block (as in Section 2.3.1). This prevented the sample from breaking when cut radially through the hinge of the shell in a direction parallel to the maximum growth increments (Fig. 2.4) (Stetcher et al. 1996). Samples were then cut into blocks and prepared for mounting on a microscopic slide as in Section 2.3.1. A thin section was prepared for each sample. This allowed information to be collected from PPL (plane polarised light) and CL (cathodoluminscence) petrography as well as via laser ablation. Thin sections were polished using silicon carbide sand paper from 200 to 1200 grit and an alumina 3 μm polishing cloth (Stetcher et al. 1996; Klünder et al. 2008) (while this is unnecessary for ablation it aided in visually identifying shell growth structures). Each sample was wiped with alcohol and air dried before analysis (Stetcher et al. 1996).

2.3.6b Sample analysis

Methods from Riceman (2008) were followed in this study and laser parameters were adjusted accordingly for each sample. Samples were analysed for Sr, Ba, Ca, Mg, Mn, Fe, Cu and Pb by LA-ICP-MS at the University of Waikato's ICP suite using a Perkin Elmer Elan 6000 SCIEX DRC II ICP-MS with a New Wave Research Nd: YAG 213-nm wave-length laser (Fig. 2.4). Instrumental parameters are recorded in Table 2.3. The mass spectrometer was calibrated with NIST612 glass external standard.

Figure 2.4 Set up of the Elan 6000 LA-ICP-MS at the University of Waikato.

Table 2.3 LA-ICP-MS parameters.

Sample	Sample Location	Spot diameter (µm)	Laser output (%)	Dwell time (sec)	Repetition rate (hz)
N14/1C	Waitomo	40	50	35	5
WLK	Wanganui	40	50	35	5
PAT2/1	Patagonia	50	50	35	5
PAT4/1	Patagonia	50	50	35	5
NIST612	External reference	60	80	60	10

A line of spots was created as a guide on each sample to make sure the analysis was carried out at even increments firstly at 750 µm apart, and secondly at 150 µm to provide greater detail. Analysis was then conducted using the spot tool option; this was able to focus the laser on each individual shell layer at a high

spatial scale. A selection of data gained from this technique is presented in Chapter Six and in full in Appendix B-1.2 and as a Digital Appendix.

2.3.7 Component mineralogy

Thin sections were analysed using a SIEMENS General Area Detector Diffraction system (GADDs) machine located at the University of Auckland. Operating conditions are featured in Table 2.4.

An image is produced by a digital camera and shows the position of the laser beam (0.5 mm width) on the sample. Using a scan time of 120 seconds, a series of detectors collect x-ray beams that are fired at the material within the point being analysed. This produces an image that consists of points with a variation in size and colour depending on the intensity of the x-ray reflection. The intensity of the reflection is influenced by crystal size, orientation and mineralogy.

From the data collected, Chi Square analysis is conducted identifying key peaks. Using EVA Software the mineralogy is determined by matching peaks with their corresponding mineral types, similar to XRD analysis (Section 2.3.4). Data gained from this technique is presented in Appendix C-1.3 and as a Digital Appendix.

Table 2.4 Operation settings for the GADDs machine.

SIEMENS General Area Detector Diffraction system	
Settings	
Generator	40 kV 30mA
$^{o}2\theta$ (detector)	40
Omega (stage)	20.00
Scan range ($^{o}2\theta$)	23-58
Collimator	0.5 mm
Count	120 sec

2.3.8 Particle size analysis

Samples were analysed using the Malvern Mastersizer 2000 laser particle size analyser (Fig. 2.5) in the Department of Earth & Ocean Sciences, University of Waikato. Methodology was adapted from Hayton (1998) to disaggregate samples in preparation for grain-size analysis. The method used is as follows:

1. Weigh a suitable amount of air-dried sample (0.25 to 2.5 g) in aggregate form into a small jar (~ 50 ml).
2. Add 10 ml of 10% hydrogen peroxide (H_2O_2) to each jar. If organic matter is present the sample will effervesce. When effervescence has ceased, place sample on a hot plate and simmer. Remove sample when majority of H_2O_2 has cooked off.
3. Cool sample and add 10 ml of 10% hydrochloric acid (HCl), which will remove any carbonate. Leave overnight to ensure reaction is complete.
4. Place the sample in an ultrasonic bath for 10 min to further disaggregate samples (note ultrasonic bath may remove any pen labels).
5. If any large particles remain it is necessary to put the sample through a 2 mm sieve before analysis.
6. Mix the sample well before placing into the Malvern laser particle size analyser to reduce bias.

Each sample was run three times and the results averaged to reduce error created when sub-sampling.

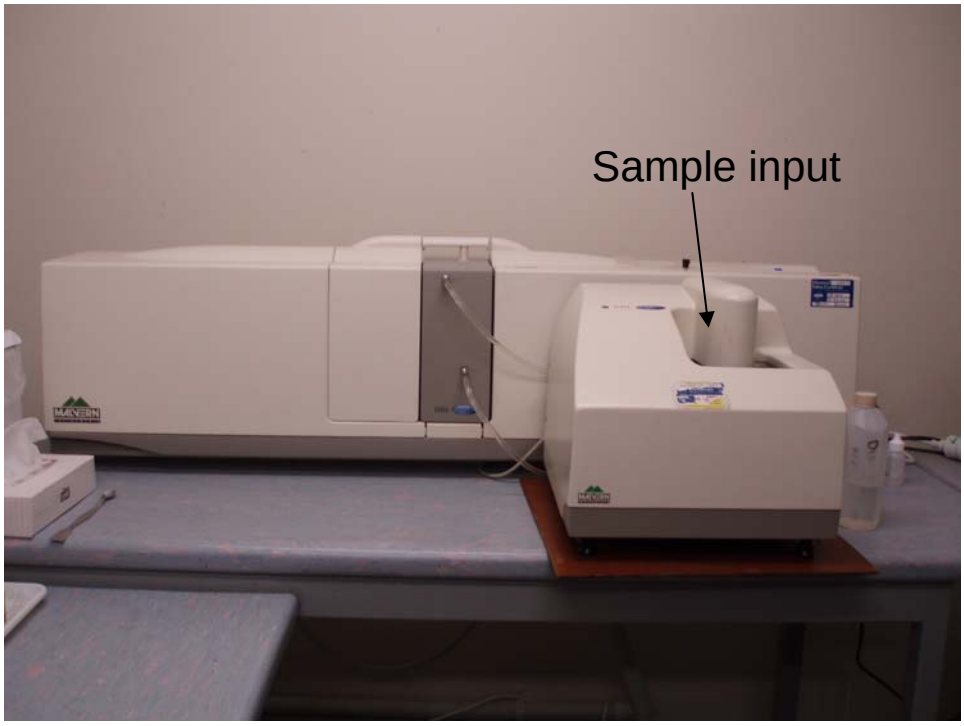

Figure 2.5 Malvern Mastersizer 2000 laser particle sizer in the Department of Earth & Ocean Sciences, University of Waikato.

2.3.9 Carbonate percentage

Carbonate percentage was carried out using the methodology of Nelson (1973) and with 1:4 acetic acid instead of hydrochloric to avoid the alteration of clay minerals in the samples (Ray et al. 1957).

1. Dry filter paper (Whatman No. 42 15 cm) at 40^{o}C for ≥ 2 hours. Weigh paper and record weight, then fold and place in a funnel over a flask.
2. Weigh about 10 g of powdered sample to four decimal places and place in a beaker.
3. Add 100 ml of 25% v/v glacial acetic to each sample, leave in room temperature for approximately 12 hours, stirring occasionally.
4. Once reaction is complete wash the insoluble residue into the filter paper funnel over flask with distilled water.
5. Once filtered, place the sample into a low heat (~ 40^{o}C) oven to allow the sample to slow-dry.
6. Weigh dried insoluble fraction on filter paper. Subtract the known weight of the filter paper.
7. $CaCO_3$% can be obtained by dividing the insoluble fraction by the original sample weight.

Data from this technique are presented in Chapter Seven.

2.3.10 Oyster trace biota analysis

Oyster shells collected from each of the three field sites were examined for the presence and/or absence of borings and encrusting organisms, and the number of valves they occurred on. The percentages of valves with encrusters and borers present at each site were then calculated using the approach of Parras & Casadío (2006).

To test the hypothesis that certain parts of the valves are colonized preferentially, sectors were defined on each valve, and the preference of each boring and encrusting organism in each sector was recorded. Sectors have been defined using the natural architectural boundaries of the oyster shell. On the left valve the exterior surface has been divided into five sectors whereas the interior is divided into six. The right valve has seven divisions on both the interior and exterior of the shell (Fig. 2.6) (Parras & Casadío 2006).

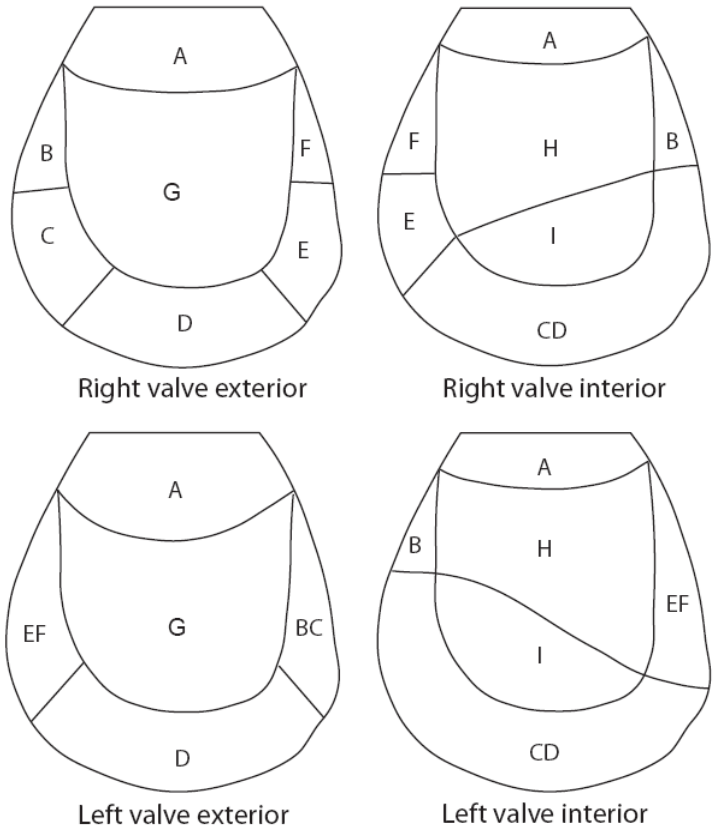

Figure 2.6 Sectors of fossil oysters. A=beak; B=posterior-dorsal; C=posterior-ventral; E=anterior-ventral; D=ventral; F=anterior-dorsal; G=central; H=central; I=muscle; BC=posterior (dorsal+ventral); CD=ventral (posterior+ventral); EF=anterior (ventral+dorsal) (Parras & Casadío 2006).

A Chi-sq independence test was used to hypothesis that borings and encrusters are non-randomly distributed between left and right valves and also between the interior and exterior surfaces of each valve, and between the different localities. Statistical analysis was performed using Microsoft Excel (Parras & Casadío 2006). Data gained from this method is presented in Chapter Eight and in Appendix D-1.5.

CHAPTER THREE

Field stratigraphy and sedimentology, Waitomo

3.1 INTRODUCTION

This chapter begins with a brief overview of the geological history of the King Country whose history goes back to at least 220 Ma, in the late Triassic. Like much of New Zealand, the development of the King Country region has been a relatively complex one. The chapter then goes on to describe the stratigraphy and sedimentology of the Orahiri Limestone, in particular providing a detailed description and field interpretation of the oyster facies at several localities in the vicinity of Waitomo.

3.2 REGIONAL GEOLGICAL SETTING

A geological time scale in support of the following account is included in Appendix A-1.3. A generalised geology map for the King Country region is provided in Figure 3.1 and a comprehensive chronostratigraphic diagram for the Te Kuiti Group in Figure 3.2.

3.2.1 Triassic-Jurassic

The oldest rocks in the Waitomo district and the wider King Country region consist of hard, bluish-grey Triassic – Jurassic sandstones and siltstones, often termed Mesozoic greywackes and argillites or simply Mesozoic basement rocks (Fig. 3.1). These rocks, or their metamorphosed equivalents, underpin most New Zealand mountain ranges. In the King Country region basement rocks make up Rangitoto and Hauhungaroa Ranges towards the east and the Herangi Ranges in the west (Nelson 1993).

The siliciclastic sediments constructing the Mesozoic basement rocks were derived from the eastern margin of the combined Australia and Antarctica continents that formed part of the supercontinent Gondwana during Triassic – Jurassic times. The total thickness of these sediments reached over 10 km and their induration largely reflects this degree of burial (Nelson 1993). Towards the west of a north-south lineament that corresponds to the Waipa Fault (Fig. 3.1), the basement rocks are both fossiliferous and include interbedded volcanic ash layers

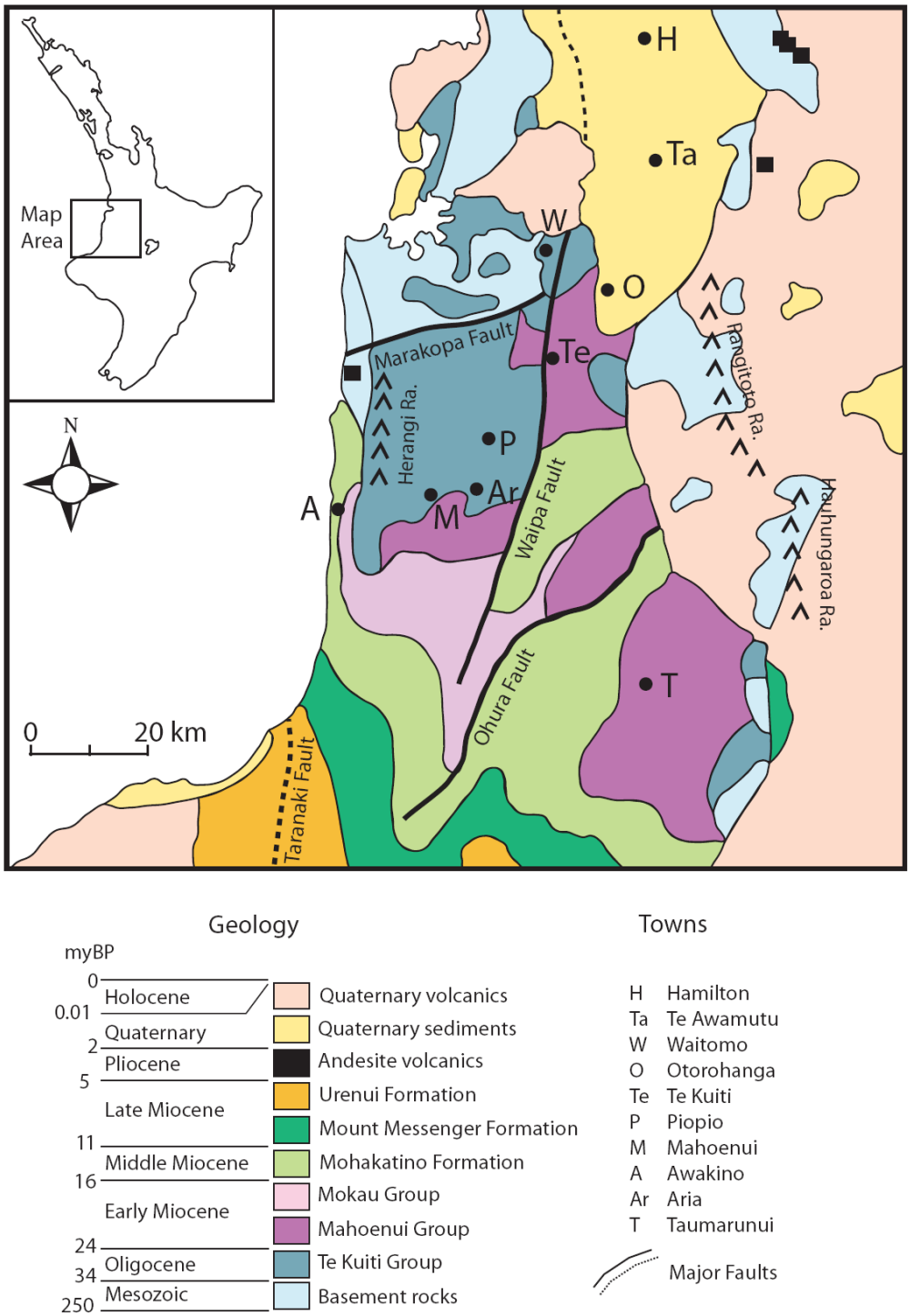

Figure 3.1 Generalised geology of the King Country region, adapted from Nelson (1993). Inset shows location of area within the North Island, New Zealand.

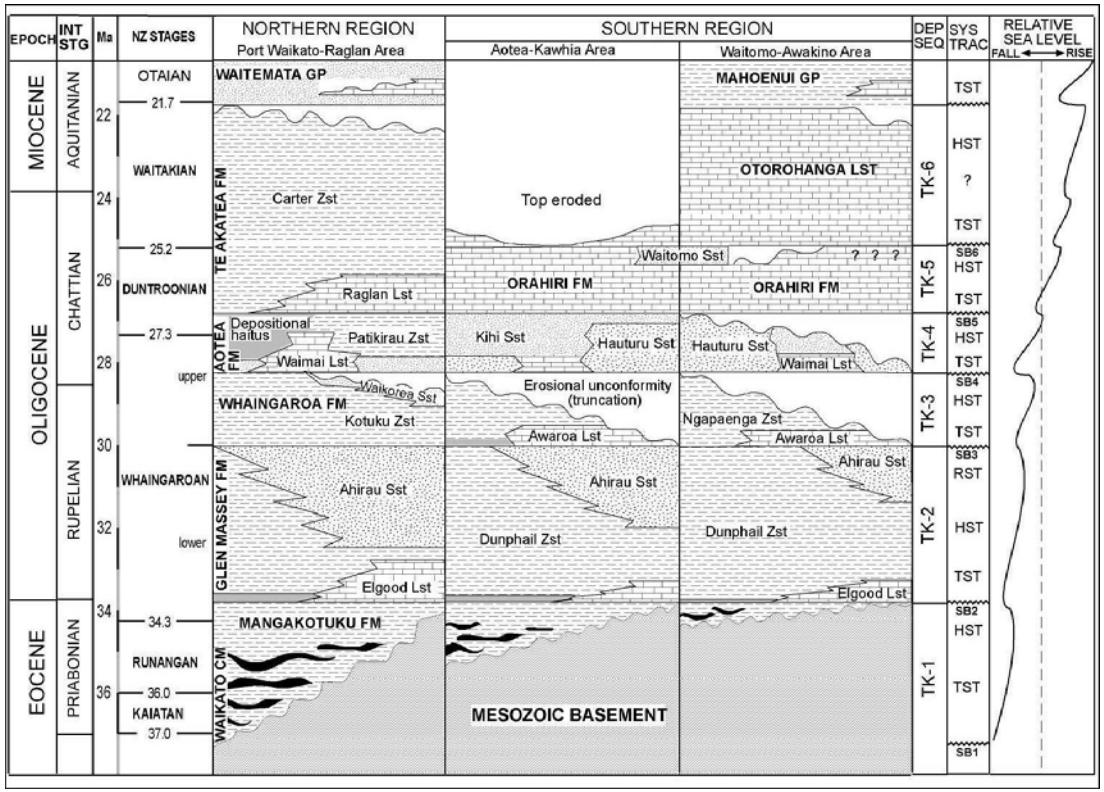

Figure 3.2 Chronostratographic panel from Tripathi (2008) for the Te Kuiti Group in the western-central North Island, showing relationships of the units between northern and southern regions. The columns on the right show Tripathi's interpretation of the depositional sequences, systems tracts and relative changes in depositional paleodepths. SB = Sequence Boundary; TST, HST and RST=transgressive, highstand and regressive systems tract, respectively.

derived from volcanism along the coastline of Gondwana. The Waipa Fault demarcates the junction of different terranes of Mesozoic basement rocks that were emplaced by sea-floor spreading in the Early Cretaceous and uplifted to add new land to the Gondwana margin. This collision event is referred to as the Rangitata Orogeny (Nelson 1993). A sliver of basaltic oceanic crust was caught up in the collision zone along the Waipa Fault and is represented by ultramafic rocks seen at the Wairere Serpentine Quarry north of Aria. The serpentinite is a mainly subsurface feature but outcrops in the South Island at Dun Mountain in Nelson and at Red Mountain in Otago. The basement rocks that lie towards the west of the Waipa Fault are structurally relatively simple and form a broad down-warped fold as part of the Kawhia Regional Syncline. Those towards the east are much more structurally complex with intensive jointing, shearing and faulting (Nelson 1993).

3.2.2 Late Cretaceous-Eocene

By 80 million years ago, part of the continent bearing the future New Zealand landmass began to break or rift away from the Australian-Antarctic continent as a result of upwelling and diverging molten material beneath the eastern margin of the Gondwana supercontinent. From 80 to 55 million years ago the New Zealand landmass drifted eastwards into the Pacific Ocean and away from Australia, leading to the formation of the Tasman Sea. The drifting ceased around 50 million years ago when Antarctica began to separate from Australia. There were no rocks laid down in the King Country region between 100 and 45 million years ago as the land was subaerially exposed. Initially, following the Rangitata Orogeny, this land was mountainous, but by the Eocene the area was reduced to a low-lying landscape (Nelson 1993).

3.2.3 Late Eocene-Oligocene

The low lying Eocene environment provided a perfect one for the development of swamps and subsequent coal deposition. Coal deposits are widespread throughout the King Country, including in the south at Bennydale, Otewa near Te Kuiti, and Okoko Road near Otorohanga (Nelson 1993), but especially in the Waikato region in the north, near Rotowaro and Huntly, where the deposits reach up to 200 m in thickness (Edbrooke 2005). By about 40 million years ago the coal deposits were transgressed by shallow seas accumulating calcareous siltstone and calcareous

sandstone and limestone, facies that continued to form from 40-25 million years ago during the Oligocene. The deposits total up to 100-200 m in thickness and are known as the Te Kuiti Group (Nelson 1993). The Oligocence was a period of relative tectonic quiescence when widespread regional subsidence took place with minor and localised faulting (Edbrooke 2005). Today, the limestone in the King Country region forms impressive relief features such as steep bluffs, isolated crags or towers, and tomos or sinkholes.

3.2.4 Early Miocene

Limestone formation ceased in the King Country region about 25 million years ago and was replaced by the deposition of 200-500 m or more thick of blue-grey mudstone and flysch beds referred to as the Mahoenui Group. These deposits formed rapidly in up to hundreds of metres water depth as a response to an increase in fault activity in the area coinciding with the development of the convergent Pacific – Australian plate boundary through New Zealand. Parts of the landscape in the region became uplifted and eroded, whereas other areas were depressed to form troughs that rapidly accumulated the sand and mud detritus. The Mahoenui mudstone areas are characterised by gently rolling, hummocky topography in the landscape (Nelson 1993).

Seas began to shallow in the region around 20 million years ago and the Mahoenui Group was overlain by porous brown sandstones of the Mokau Group which typically form blocky bluffs in the landscape. Locally the seas shallowed sufficiently enough to allow the formation of coal in coastal swamps, the resultant coal seams having been mined at Mahoenui, Ohura and Taumarunui (Fig. 3.1) (Nelson 1993).

3.2.5 Middle Miocene

Sandstone and mudstone deposition continued throughout the region from 15 to 10 million years ago, with the inclusion of a significant amount of volcanic particles and ashes sourced from andesitic volcanism situated from a now-buried source some 40 km offshore from Awakino. These volcanogenic rocks formed in relatively deep waters and are collectively referred to the Mohakatino Group (Nelson 1993).

3.2.6 Late Miocene

From around 10 million years ago the King Country region most likely emerged out of the sea, although the deposition of marine sediments continued to the south of the inland Taranaki region and to the west in offshore Taranaki. The emergence of the region was largely due to uplift along the many north-south-trending faults and other faults passing through the King Country (Fig. 3.1), including the Taranaki, Manganui, Marokopa, Waipa, Ohura and Hauhungaroa Faults. This active faulting was part of New Zealand wide activity and referred to as the Kaikoura Orgeny. The rocks in the King Country region were uplifted to different degrees causing them to be exposed at differing elevations. The resultant outcome was the entire King Country became exposed as land and the deposition of marine sediments ceased. The rocks have been exposed to the elements over the past 10 million years and weathering and other erosional processes have resulted in rugged greywacke steeplands, karst (i.e. limestone topography), gently rolling and hummocky mudstone hill country, local sandstone bluffs and broad flats of river alluvium (Nelson 1993).

3.2.7 Pliocene-Quaternary

Onshore volcanism has provided a further modification to the landscape since the region emerged. Volcanic deposits have been emplaced from lava flows, pyroclastic flows and volcanic ash fall, variably sourced from Pirongia-Karioi in the north, Taranaki in the south and Rotorua-Taupo district volcanic centres in the east (Nelson 1993).

3.2.8 Quaternary

The King Country region is blanketed with volcanic ashes sourced from Rotorua, Taupo, Tongariro and Taranaki that can be divided into three age categories. The oldest began erupting 2.3 to 0.1 million years ago and include the Kauroa-Hamilton ashes, sourced from the Rotorua-Taupo volcanic centre, that are now weathered to reddish brown clays. The middle ashes were deposited 50,000 to 10,000 years ago and include the Rotoehu Ash sourced from Lake Rotomahana which is characterised by a distinctive layer of cream sands. The pumiceous and widespread Rangitawa Ash (26 ka) erupted near Wairakei. The Holocene ashes (10,000 – 0 years ago) are brown friable ashes that form the parent material of the soil over the majority of the King Country. The Mairoa Ash is the name given to

several differing thin units that have become mixed and combined, originally sourced from Taranaki, Taupo, Rotorua and Tongariro volcanic centres (Nelson 1993).

3.3 TE KUITI GROUP STRATIGRAPHY

The majority of the mainly Oligocene aged Te Kuiti Group rocks are a transgressive sequence of basal coals overlain by marginal marine to outer shelf calcareous mudstone, calcareous sandstone and limestone. It is typical of the Te Kuiti Group strata to have more or less horizontal dips and everywhere the Group unconformably overlies an undulating surface cut into Mesozoic basement rocks (Fig 3.2) (Edbrooke 2005). The Upper Te Kuiti Subgroup includes all lithologies below the Mahoenui Group (or Waitemata Group in the north) and above the Lower Te Kuiti Subgroup (Nelson 1978). The dominant lithologies in the Upper Te Kuiti Subgroup include sandy and pure skeletal limestone with some calcareous sandstone and rare conglomerates. These are referred to the Orahiri Limestone, Waitomo Sandstone and Otorohanga Limestone formations (Fig. 3.2) (Nelson 1978). The Orahiri Limestone is host to the giant fossil oyster Flemingostreini Stenzel (Nelson et al. 1983) and is thus the main focus of the remainder of this chapter. Figure 3.3 shows the location of all the stratigraphic logs erected in this study, otherwise shown in detail on a CD as Digital Appendices.

3.3.1 Orahiri Limestone

The Orahiri Limestone is the lowest formation of the Upper Te Kuiti Subgroup and overlies any of the Mesozoic basement rocks, Aotea Formation or Whaingaroa Formation (Fig. 3.2). In most places the Orahiri Limestone is overlain by the Otorohanga Limestone, although near Te Kuiti and Waitomo the Waitomo Sandstone occurs between the two limestones. The Orahiri Limestone includes a variety of facies from massive and moderately sandy, glauconitic and pebbly lithologies through to pure flaggy limestones and thick oyster beds (Nelson 1978).

3.3.1a Name and type section of Orahiri Limestone

The type section for the Orahiri Limestone is situated at the old Otorohanga Limestone Company's Quarry (S16/963291) on Waitomo Valley Road (Nelson

1978), 2.8 km south of an earlier type section nominated by Kear & Schofield (1958) at Worth's Quarry, which is no longer exposed.

3.3.1b Boundaries of the Orahiri Limestone

The underlying contact of the Orahiri Limestone can be with any of the Mesozoic basement rocks, Whaingaroa Formation or Aotea Formation. Disconformities separate members and beds within the Orahiri Limestone (Nelson 1978). The contact with overlying Waitomo Sandstone is gradational, but where the sandstone does not occur a prominent disconformity separates the Orahiri Limestone from the overlying Otorohanga Limestone.

3.3.1c Distribution and thickness of the Orahiri Limestone

The distribution and thickness of the Orahiri Limestone is shown in Fig. 3.4.

3.3.1d Paleontology of the Orahiri Limestone

There are many macrofaunal specimens in the Orahiri Limestone including coelenterates, bryozoans, brachiopods, bivalves, gastropods, annelids, echinoderms, vertebrate remains and red algae (Nelson 1978). Giant oysters are the most common and widespread of the macrofossils. However the high degree of induration of the limestone makes the collection of whole and well preserved specimens virtually impossible. Nelson et al. (1983) suggested the characteristics of the oysters most closely resembled those belonging to the tribe Flemingostreini Stenzel.

3.3.1e Age of the Orahiri Limestone

The Orahiri Limestone lacks many age-diagnostic fossils. The overlying Waitomo Sandstone and underlying Aotea Formation have in places been assigned a Duntroonian (Late Oligocene) age, so giving the same age to the Orahiri Limestone. Stratigraphic evidence across the King Country suggests that the Orahiri remains Duntroonian in most places, although at some higher points towards the west and south it may span into the Waitakian Stage (but still Late Oligocene) (Nelson 1978).

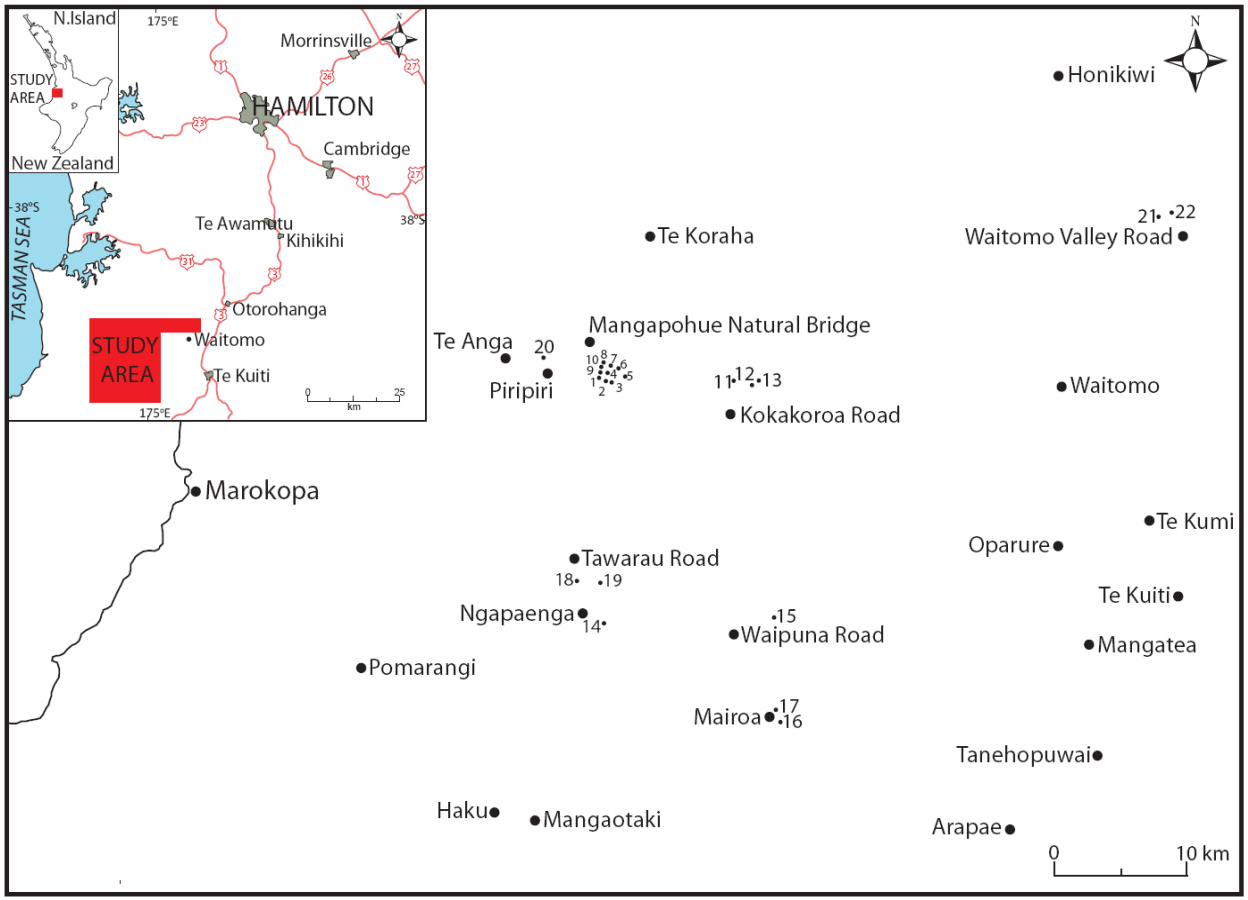

Figure 3.3 Locality map showing numbered localities of stratigraphic columns through the oyster bearing Orahiri Limestone. Inset shows field area in relation to towns in the Waikato region, main highways and also the North Island of New Zealand. Adapted from Nelson (1978). Stratigraphic columns are included in Appendix D-1.1.

3.4 SEDIMENTOLOGY OF THE ORAHIRI LIMESTONE

The Orahiri Limestone has been divided into two members by Nelson (1978). The first, Mangaotaki Limestone Member (OrA), comprises massive to massive ripply surfaced sandy limestones that occupy the lower part of the Orahiri Limestone where the formation is thickest. The overlying member, the Te Anga Limestone Member (OrB), consists of purer flaggy limestones that include oyster beds. The Te Anga Limestone Member has seven associated facies (or beds) as defined by Nelson (1978), five of which occur in the Waitomo-Te Anga area and will be described here.

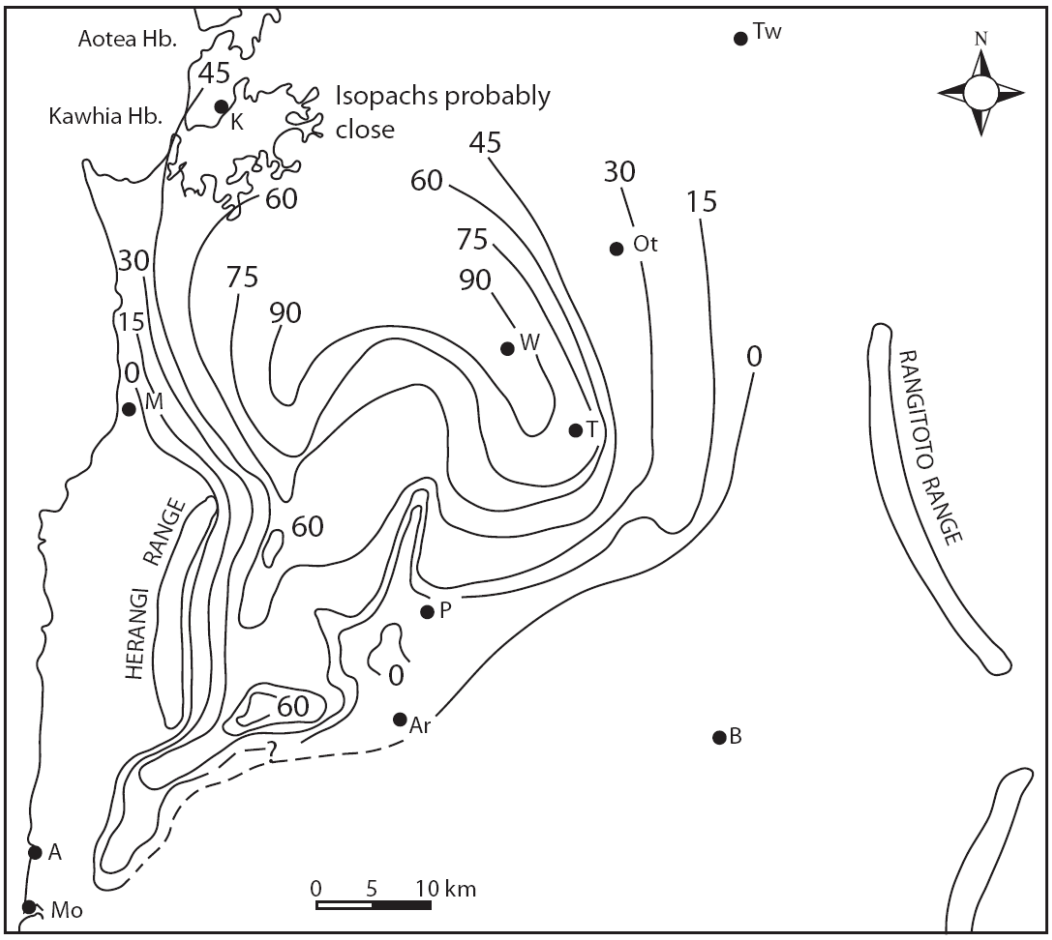

Figure 3.4 Isopach map showing thickness of the Orahiri Limestone in the King Country region. Tw=Te Awamutu; K=Kawhia; M=Marokopa; Ot=Otorohanga; W=Waitomo; T=Te Kuiti; P=Piopio; Ar=Aria; B=Benneydale; A=Awakino; M=Mokau. After Nelson (1978).

3.4.1 Flaggy Limestone Beds (OrB1)

These beds are relatively widespread and are grey to cream in colour. They typically have a low terrigenous content (< 5%), rarely reaching more than 15%. East of Te Kuiti terrigenous grit and glauconite are evident. Incipient to well developed flags are characteristic, the flags being 2.5 – 5 cm thick (Nelson 1978).

3.4.2 Oyster Beds (OrB2)

The characteristic feature of these beds is the presence of large oysters up to 250 mm and averaging around 150 mm in length. They typically have haphazard orientations within the limestone with respect to each other and to the bedding. They occur in small clusters through to extensive beds up to 8.5 m thick (Fig. 3.5). Shells of the oysters are up to 50 mm thick and can be highly bored. Valves are both articulated and disarticulated. Scattered pebbles are normally found in association with the oyster beds and at times form conspicuous bands. The matrix of the limestone is fawn to grey colour and iron stained in places. These beds lack flagginess and incipient irregular seams are common. Oyster beds can lie above or below, or be interbedded with, Flaggy Limestone Beds (OrB1).

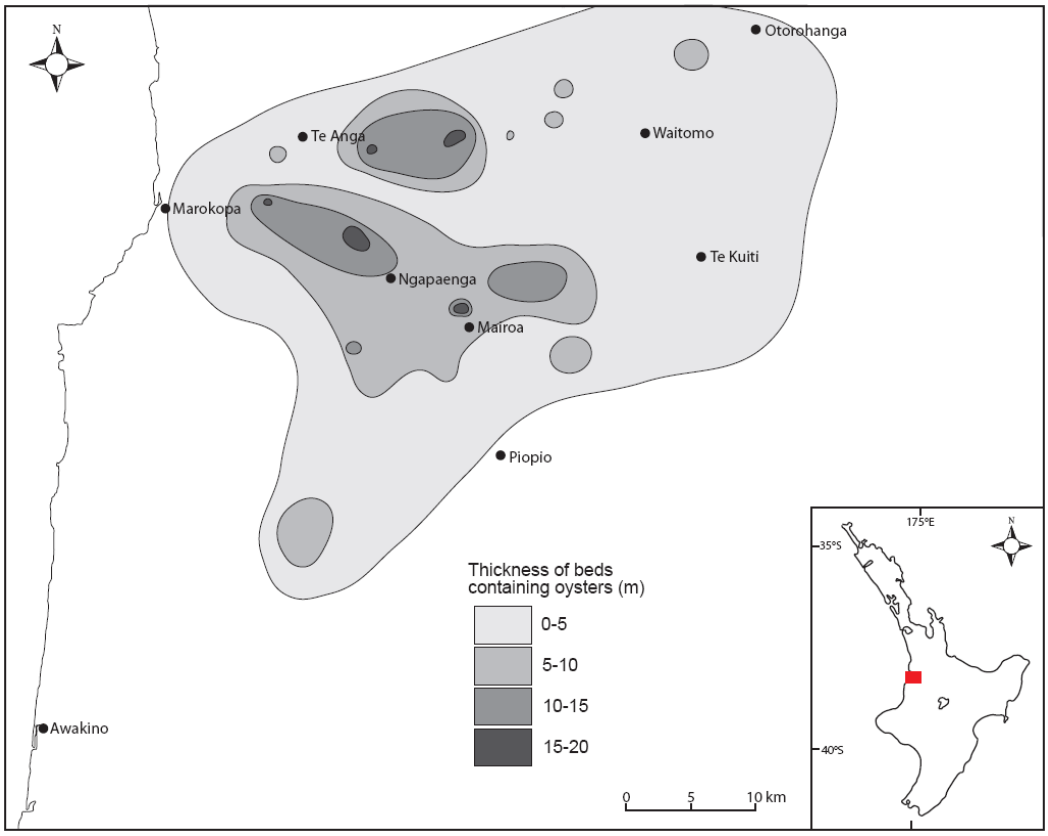

Figure 3.5 Isopach map showing distribution and combined total thickness of the oyster beds in the Orahiri Limestone. Inset shows location of map (red) in the North Island of New Zealand. Adapted from Nelson et al. (1983).

3.4.3 Semiknobbly Beds (OrB3)

These beds consist of sparry, coarse grained limestone up to 2.5 m thick. The beds support irregular seams that give outcrops a knobbly appearance. The distribution

of these beds is restricted to south of Te Anga (Fig. 3.3) where they most commonly occur at the base of the Te Anga Limestone Member (Nelson 1978).

3.4.4 Massive Sandy Limestone Beds (OrB4)

Massive sandy limestone beds with up to 30% terrigenous sand material. They occur commonly in the Ngapaenga area (Fig. 3.3) and are up to 8 m thick (Nelson 1978).

3.4.5 Fossil-hash Beds (OrB5)

Smashed up shell material is the most characteristic feature of these beds. There are also scattered oysters, calcareous red algae, sharks teeth and common pebbles, all contained with a micritic fawn to yellow-brown limestone, with iron staining adding a red colouration to some beds. Seams are incipient and irregular. OrB5, where present, forms the top of the Orahiri Limestone (Nelson 1978).

3.5 DESCRIPTION OF OYSTER FACIES (OrB2)

The accumulations of the giant oyster Flemingostreini Stenzel are found within Facies OrB2 throughout the Waitomo region. A total of 22 detailed stratigraphic logs (C1-C22) were described in the wider Waitomo region, including at Kokakoroa Road, Mairoa, Mangapohue Natural Bridge, Ngapenga, Piripiri Cave and Waitomo Valley Road (Fig. 3.3). Stratigraphic logs are featured in detail in Appendix D-1.1.

3.5.1 Kokakoroa Road

Stratigraphic columns at Kokakoroa include columns 11-13 (Appendix D-1.1).

3.5.1a Paleontological features

The giant oyster Flemingostreini Stenzel is the dominant species in the oyster beds, accompanied by rare pectinids (Fig. 3.6). Judging from the uniformly large size (c. 150 mm) of the oyster shells, juvenile specimens are seemingly absent.

3.5.1b Stratigraphic features

Oysters are contained within grey to buff, highly indurated limestone. Limestone ranges from bioclastic to increasingly terrigenous in places and weathers to an

orange colour. Poorly sorted, sub-rounded, scattered pebbles up to 50 mm in size form distinct bands in the stratigraphic logs taken at Kokakoroa Road (Fig 3.7A).

At Kokakoroa Road the thickness of oyster beds ranges from a single layer of shells up to 1.5 m thick (Fig. 3.7B). The oysters present at this location have varying geometries; bedded, scattered in clusters (possible nests) or thin lenses where oyster specimens are often only a single layer of disarticulated and fragmented shells (Fig. 3.7C). Oyster occurrences have an abruptly gradationally contact with the overlying limestone unit or tend to disperse gradationally up section (Fig. 3.7C).

3.5.1c Taphonomic features

Shells are a mixture of articulated and disarticulated specimens. The presence of articulated shells in some occurrences suggests they are a biological accumulation and thus in life position. Some smaller occurrences (both scattered and lenses) are dominantly disarticulated. The modal size of the shells is approximately 150 mm. Fragmentation and abrasion is low. Biological modification is high with most shells exhibiting large bore holes (Fig. 3.8). The relative abundance of shells varies with the type of accumulation. Dense beds can comprise up to 40% of densely packed oysters in grain support and rarely matrix supported. The oyster abundance in sparse lenses and clusters can be as low as 5% and specimens are predominantly matrix supported. In places the shells are ‘fitted’ into one another.

3.5.2 Mairoa

Combines columns 15-17 from Mairoa Road and nearby Waipuna Road to the north (Appendix D-1.1).

3.5.2a Paleontological features

The most abundant species present is the giant oyster Flemingostreini Stenzel, and all specimens appear to be adult ones.

3.5.2b Stratigraphic features

Oysters are contained within a light grey to blue-grey limestone, often massive or fluted (Fig. 3.9A), with iron stained weathering in places. Limestone varies from bioclastic to increasingly terrigenous in the majority of the oyster beds. Pebble

Figure 3.6 Fragmented pectinid in Orahiri Limestone at Kokakoroa Road (C12 R16/824251).

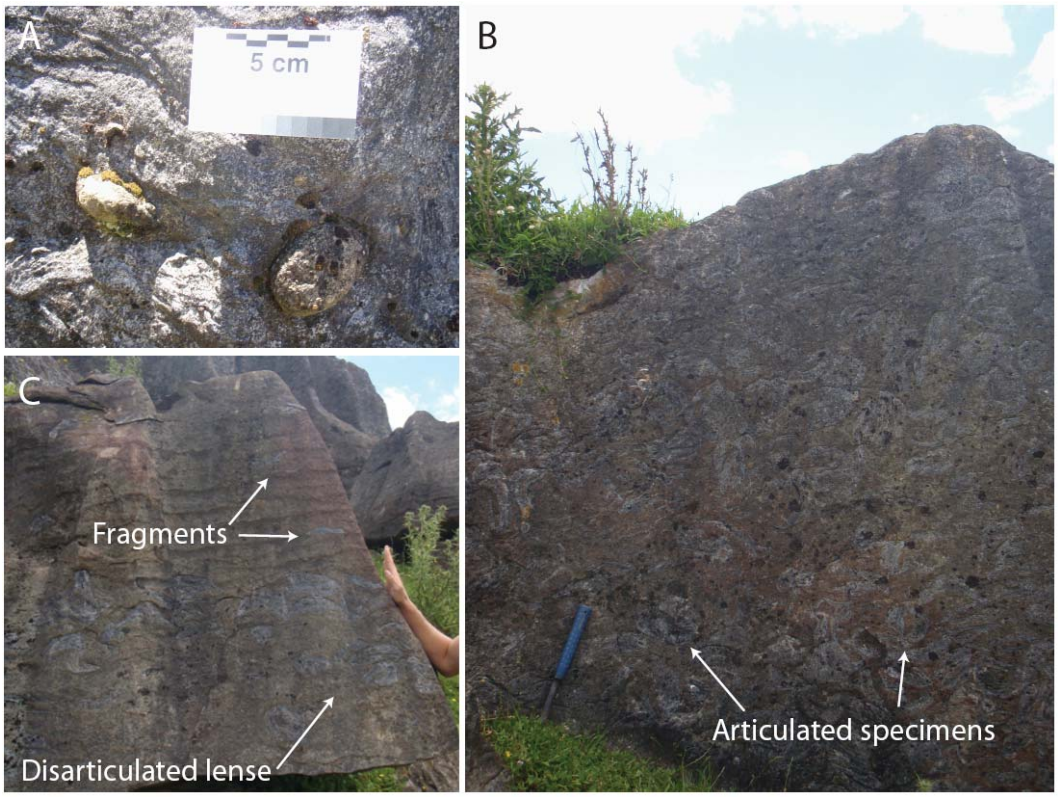

Figure 3.7 (A) Large pebbles seen in a concentrated band at Kokakoroa Road. Pebbles originated from the Mesozoic basement rocks. (B) Thick accumulation of oysters at Kokakoroa Road showing a bed type geometry. Hammer=32. 5 cm. (C) Sparse accumulation of oysters presenting in a lens geometry. Disarticulated and fragmented specimens are evident (See C11 R16/818259).

Figure 3.8 Large oyster shell with prominent borings at Kokakoroa Road (C11 R16/818259).

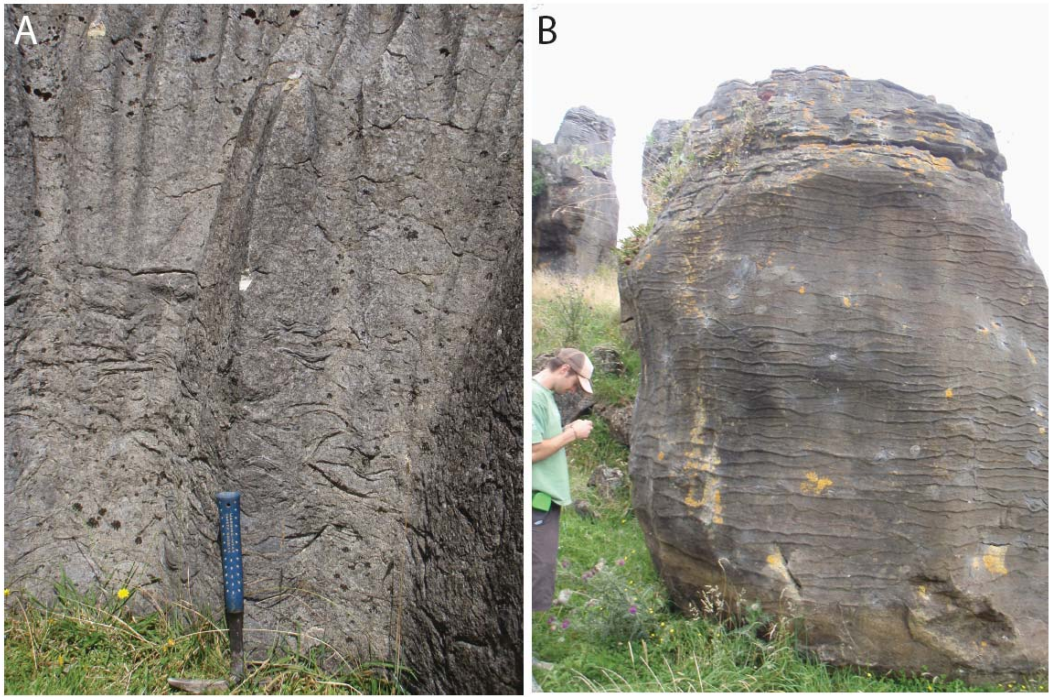

Figure 3.9 (A) Densely packed bed of oysters contained in fluted limestone (C16 R16/832118). (B) Sparse oysters 'floating' in incipiently seamed limestone at Mairoa Road (C17 R16/832228).

bands are absent at this location. The thickness of the oyster beds varies from sparse scattered individuals or lenses (Fig. 3.9B) to beds up to 2 m thick. The geometry of the oyster accumulations continues to vary, with beds being the most common (Fig. 3.9A) and scattered specimens being rare (Fig 3.9B). The majority of contacts at this locality are abruptly gradational (Fig. 3.10).

3.5.2c Taphonomic features

The majority of oyster shells are articulated with some disarticulation noted. Size sorting is good with most specimens ranging from 180-200 mm in length. Fragmentation, abrasion and rounding of shells is low. Biological modification is moderate to high with large bore holes seen in most shells (Fig 3.11). Orientation of oyster specimens is vary haphazard suggesting that some individuals have been disturbed from life position. Densely packed areas contain up to 40% abundance and are a combination of matrix and oyster supported. Sparse occurrences have as low as 10% abundance and are entirely matrix supported (Fig. 3.9B).

3.5.3 Mangapohue Natural Bridge

Combines columns 1-10 from the Mangapohue Natural Bridge area (Appendix D-1.1).

3.5.3a Paleontological features

The most abundant species seen is the giant oyster Flemingostreini Stenzel, and all specimens are adult ones.

3.5.3b Stratigraphic features

Oyster beds are typically contained within a massive to incipiently seamed, variably terrigenous grey to cream limestone, with an orange weathering stain in places. Concentrated bands of pebbles occur in columns 1, 7 and 8 (Fig. 3.12). Pebbles are sub-rounded, poorly sorted and 5–20 mm in size. The thickness of the beds in this area ranges from a single layer to dense beds up to 2.5 m thick (Fig. 3.13). The dominant geometry of the oysters involves beds, followed by thin lenses of oysters 2-3 specimens thick (Fig. 3.14A), and sometimes only a single layer of shells. Contacts in this area are abruptly gradational through to gradational (Fig. 3.14B).

3.5.3c Taphonomic features

The majority of shells are articulated, and those that are disarticulated are often closely associated or scattered and largely dissociated. Size sorting is good with most of the shells being 150-200 mm in length. Abrasion and rounding of oysters is low. Fragmentation is evident in the thin lenses containing disarticulated shells. Biological modification in the form of bioerosion is moderate to high in most shells and can include conspicuous large bore holes (Fig. 3.15). Shells are mainlyhaphazardly orientated (Fig. 3.13). Vertical shells are assumed to be in life orientation whereas horizontal specimens have been slightly disturbed. In densely packed beds the relative abundance of shells is up to 70% and as low as 10% in thin lenses. Dense beds are both matrix and oyster supported whereas sparse lenses are usually entirely matrix supported. Some oyster shells are 'fitted' into one another (Fig. 3.16).

3.5.4 Ngapaenga

This location includes column 14 from Ngapaenga and columns 18 and 19 from Tawarau Road (Appendix D-1.1).

3.5.4a Paleontological features

The main species present is the giant oyster Flemingostreini Stenzel with all specimens being adults.

3.5.4b Stratigraphic features

Oysters are contained within grey indurated limestone that is massive to incipiently seamed and commonly highly terrigenous. Pebbles are seen at all locations and form conspicuous concentrated bands of pebbles ranging from 10–20 mm in size. Oyster beds are often difficult to see because of weathering. The thickness of oyster beds ranges from bands 0.5 m thick to dense beds 1.6 m thick. The dominant geometry at this location is beds (Fig 3.17), while less common are sparse 'floating' specimens. Contacts are gradationally sharp, often with a weathering break directly above the oyster bed (Fig. 3.18).

3.5.4c Taphonomic features

Specimens at Ngapaenga are articulated and/or disarticulated and slightly dissociated. The size of the shells ranges from 150–200 mm. Slight fragmentation

Figure 3.10 Gradationally abrupt contact of oyster beds is clearly evident in this incipiently seamed limestone outcrop at Mairoa (C17 R16/832228). Hammer=32.5 cm.

Figure 3.11 Outer surface of Flemingostreini Stenzel valve showing large borings in the surface of the valve at Mairoa Road (C15 R16/840159).

Figure 3.12 Pebbles in Orahiri Limestone at Mangapohue Natural Bridge. Pebbles are sub-rounded and poorly sorted and range in size from 5-20 mm (C7 R16/772252).

Figure 3.13 Dense bed of haphazardly orientated oysters at Mangapuhoe Natural Bridge. Note oyster to the right of the scale bar is orientated vertically and others appear more horizontal. Most specimens are articulated and a little disturbed. Oysters make up approximately 80% abundance and shells are supported by both oysters and host limestone (C1 R16/767251).

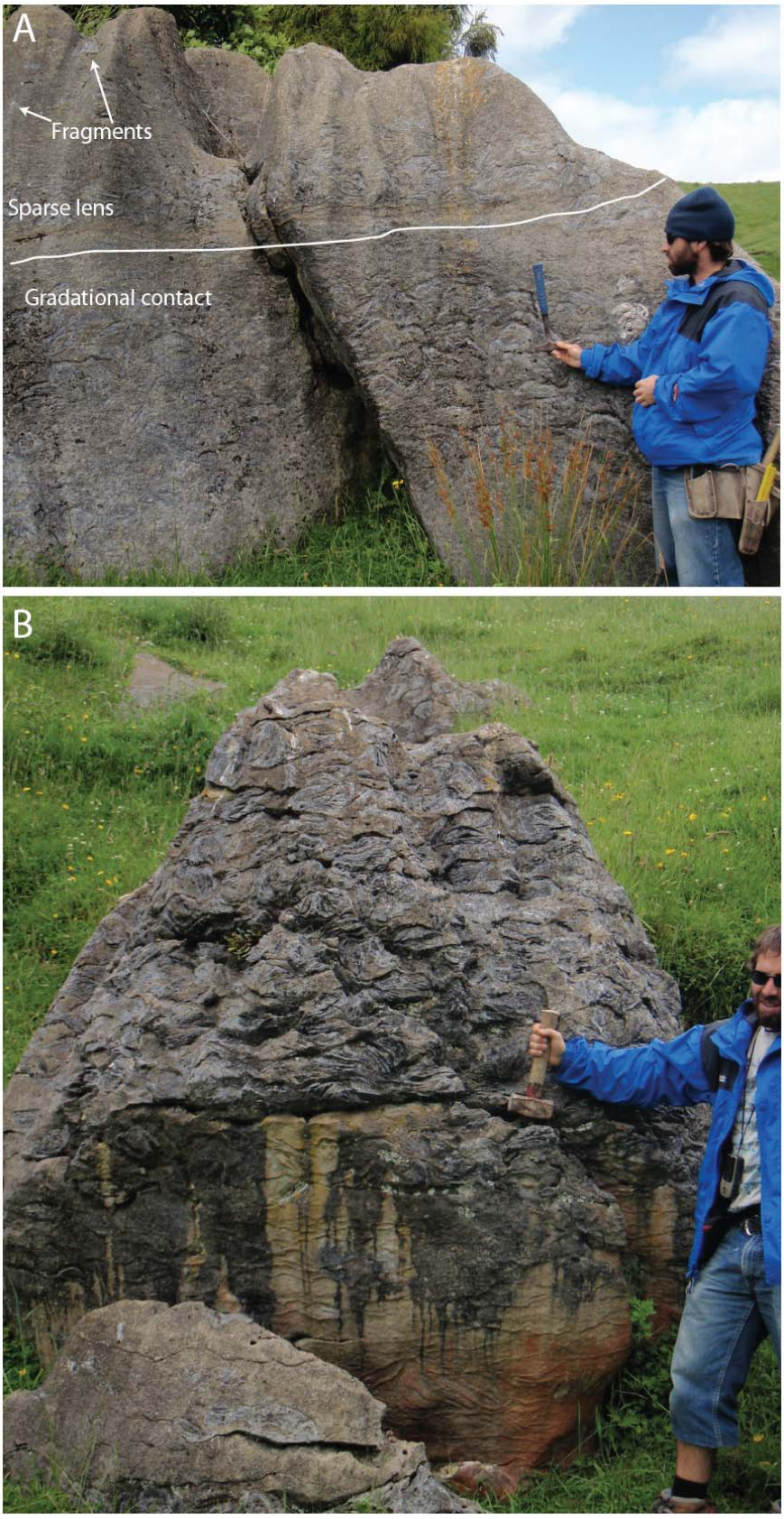

Figure 3.14 (A) Moderately packed oyster bed with an upper gradational contact into a sparser lens accumulation of oysters. A lower abundance of disarticulated and fragmented shells occurs in the upper part of the unit (C1 R16/767251). (B) Dense bed of oysters makes an abruptly gradational contact with the lower limestone unit (C2 R16/769252).

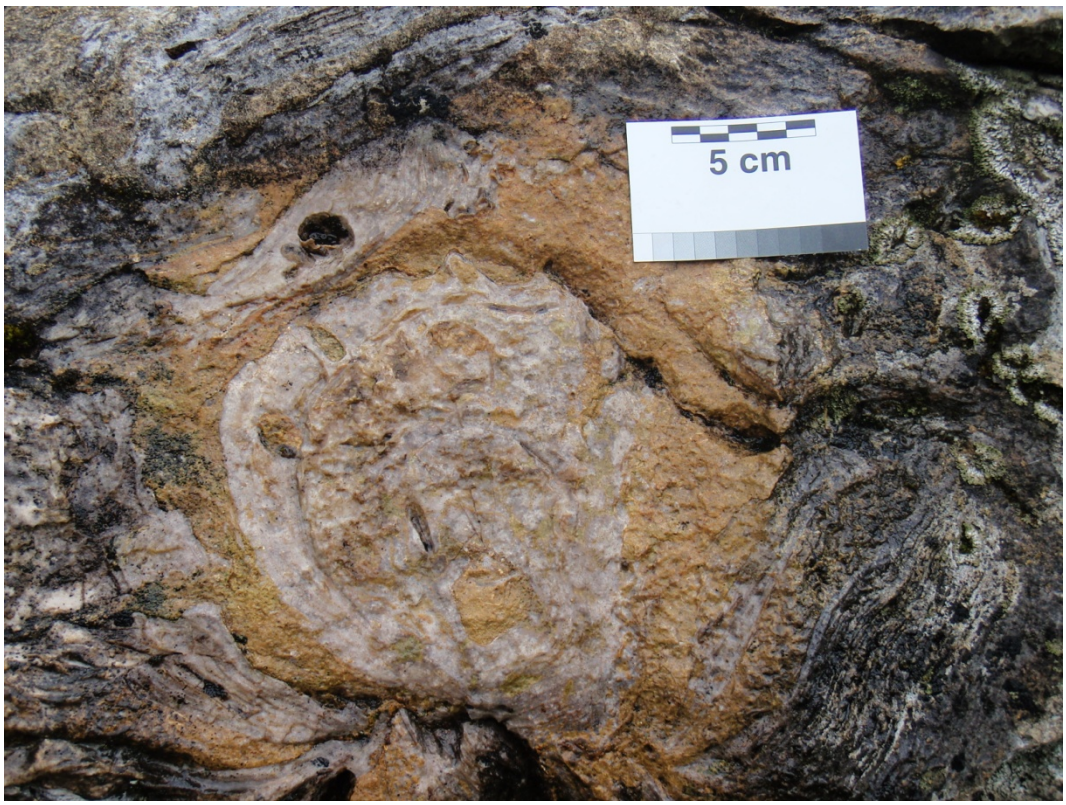

Figure 3.15 Surface of this giant oyster shell shows high biological modification. Bore holes as large as 25 mm are visible at Mangapohue Natural Bridge (C2 R16/769252).

occurs in disarticulated occurrences of shells only (Fig. 3.19). No sign of rounding or abrasion is evident. Biological modification is moderate to high in all shells. Articulated shells can be seen orientated in life position; often shells are haphazard and show signs of some disturbance. Dense beds have an abundance of up to 45% oysters, whereas sparse accumulations can be as low as 20%. Dense beds are both matrix and oyster supported, while sparse 'floating' shells are entirely matrix supported (Fig. 3.19). Moderate to sparse concentrations of shells can grade up section in places whereas dense beds show gradually abrupt contacts (Fig. 3.20).

3.5.5 Piripiri Cave

3.5.5a Paleontological features

The giant oyster Flemingostreini Stenzel is abundant at this underground locality (C20) (Appendix D-1.1). The oysters appear prominently exposed on the back wall of the Piripiri Cave, approximately 30 m from the entrance. All specimens appear to be adults as no smaller shells are noted. Many shells are covered with a secondary brown calcite precipitate.

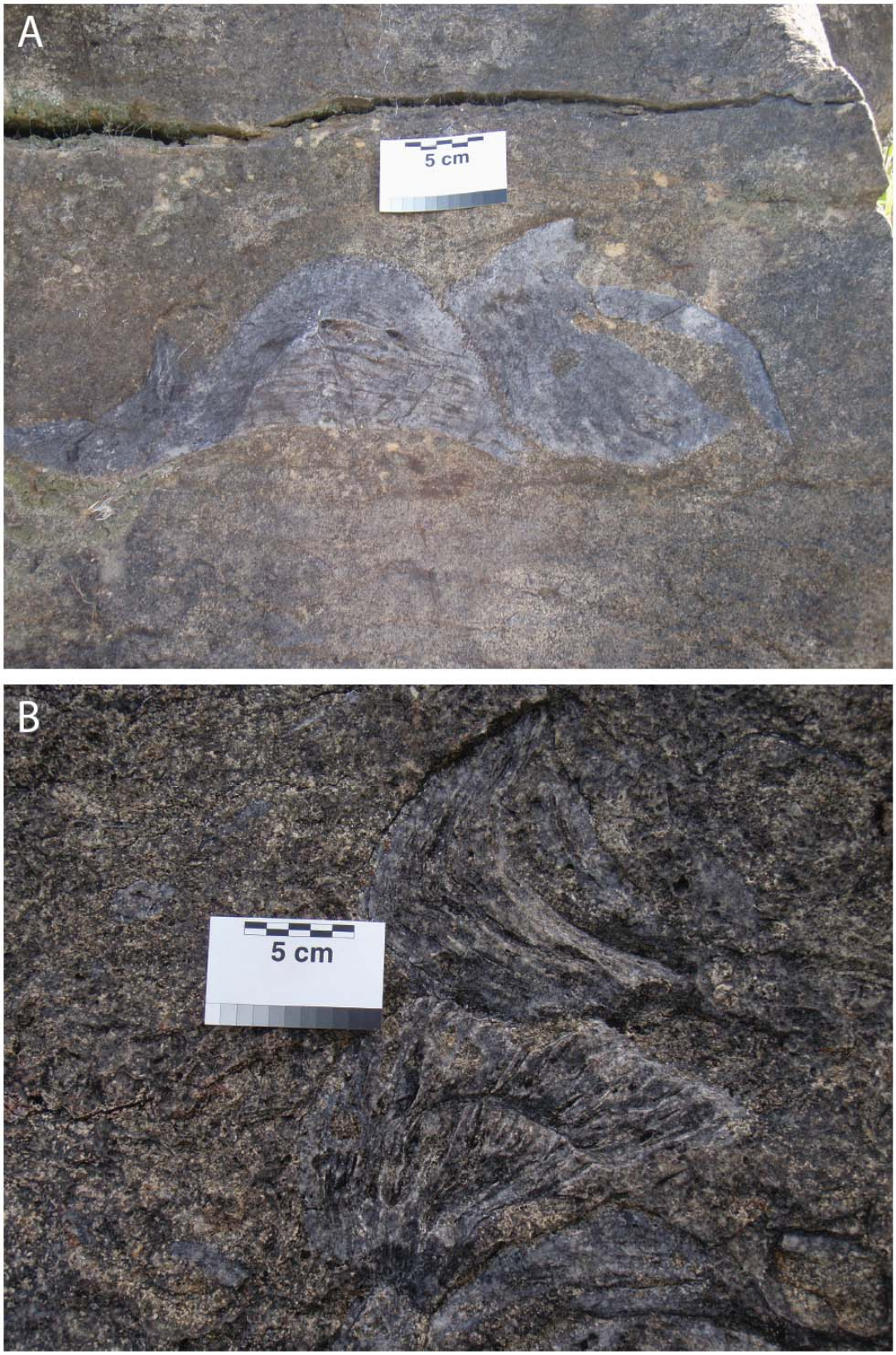

Figure 3.16 (A) Two oyster shells showing 'fitting' or suturing at Mangapohue Natural Bridge. Shells are part of a sparse concentration, horizontally orientated and the majority are matrix supported (C7 R16/771251). (B) Oyster shells supported by both host limestone and another oyster shell. Note shells are fitted (C4 R16/768251).

Figure 3.17 Dense oyster bed in outcrop at Tawarau Road. Shells are both matrix and oyster supported (C18 R16/765171).

Figure 3.18 Dense oyster bed forms a rapidly gradational sharp contact with the overlying limestone unit at Tawarua Road (C18 R16/758172).

3.5.5b Stratigraphic features

The giant oyster fossils are contained within a buff, highly indurated limestone composed of coarse fossil fragments (50-100 mm). The limestone is slightly iron stained in places. Incipient seems of limestone run around the oyster shells. The exposure of oysters in Piripiri Cave is 2.63 m thick. The occurrence is dense (Fig. 3.21A) and the lower contact of the bed is abruptly gradational while the upper limit of the bed grades into a coarse shell fragmented limestone (Fig. 3.21B). The bottom of the main oyster accumulation shows 'cones' of oysters where the development of the reef was likely initiated (Fig. 3.22).

3.5.5c Taphonomic features

The majority of the shells are articulated, but some are disarticulated. The disarticulated shells are smaller than articulated shells and show a high level of bioerosion. The oysters are well size sorted with the average size being about 150-200 mm. Bioerosion is a conspicuous feature involving a variety of small and large bore holes (Fig. 3.23). Borings are up to 50 mm in length and are infilled with host limestone or calcite precipitates. Left valves (more convex) of shells appear to be preferentially bored compared to the right valves. Most shells are in life orientation, while some shells appear to have been slightly disturbed with haphazard orientations and showing little indication of imbrication. The shells have relatively high abundances of up to about 45% and so are densely to moderately packed. Most of the shells appear to be matrix supported, but others are oyster supported. In places the oyster shells show dissolution where shells are fitted into one another.

3.5.6 Waitomo Valley Road

Columns from this area consist of C21 and C22, taken from the Old Worth's Quarry on Waitomo Valley Road (Appendix D-1.1). Worth's Quarry was previously the type section for the Orahiri Limestone (Kear & Schofield 1958).

3.5.6a Paleontological features

The main species seen at this location is again the giant oyster belonging to the tribe Flemingostreini Stenzel.

Figure 3.19 Moderately packed accumulation of oysters at Ngapaenga. Specimens are disarticulated and exhibit dissociation. They also show some fragmentation and are entirely matrix supported (C19 R16/765171).

Figure 3.20 Lower bed grades up section with the occurrence of oyster shells becoming increasingly sparse. The dense bed at the top of the section has a gradationally abrupt contact (C19 R16/765171).

3.5.6b Stratigraphic features

Oysters at this location are contained within a highly terrigenous matrix including also much shell hash and glauconite (Fig. 3.24). The matrix is also littered with many small pebbles 2-5 mm in size. The pebbles are well rounded, well sorted and comprise 5-10% of the matrix. Thickness of the oyster bed ranges from 0.5 (C21) to 2.0 (C22) m. The oysters form a bed geometry at this location and the contact with the underlying terrigenous matrix is sharp and irregular (Fig 3.25).

3.5.6c Taphonomic features

Specimens of Flemingostreini Stenzel at Waitomo Valley Road are a mixture of articulated and disarticulated shells that are about 150 mm in length. No fragmentation, abrasion or rounding of shells is evident. Biological modification in the form of bioerosion is moderate to high (Fig. 3.26). The oyster shells accumulation at this location has very haphazard orientations evident of some disturbance from the original life position of the shells. The relative abundance of shells in the moderately dense bed at C20 was about 30% abundance with a combination of both oyster and matrix support (Fig. 3.27A) whereas, the dense bed at C21 is comprised of approximately 80% oysters and the shells are almost entirely oyster supported (Fig. 3.27B).

3.6 OYSTER FACIES SUMMARY

The oyster facies accumulations can be divided into two main groups, namely dense beds or lens accumulations.

Dense accumulations have a high abundance of oysters, up to 80% and are dominated by oyster support with occasional matrix support. The average size of the shells is about 150 mm (e.g., Fig. 3.11). These accumulations have bed type geometry and consist of both articulated and disarticulated specimens. They are in life position but slightly disturbed, which is shown by the haphazard nature of the orientations. No beds have been seen to show a mound like structure that is typical of many oyster accumulations. Contacts for theses beds are often abruptly gradational below and above. In some places the denser beds appear to grade upwards into sparser accumulations. Sparse lens accumulations differ slightly from the dense beds. They have a much lower abundance of shells, as low as 5-10%, and are often entirely host matrix supported. Consequently these types of

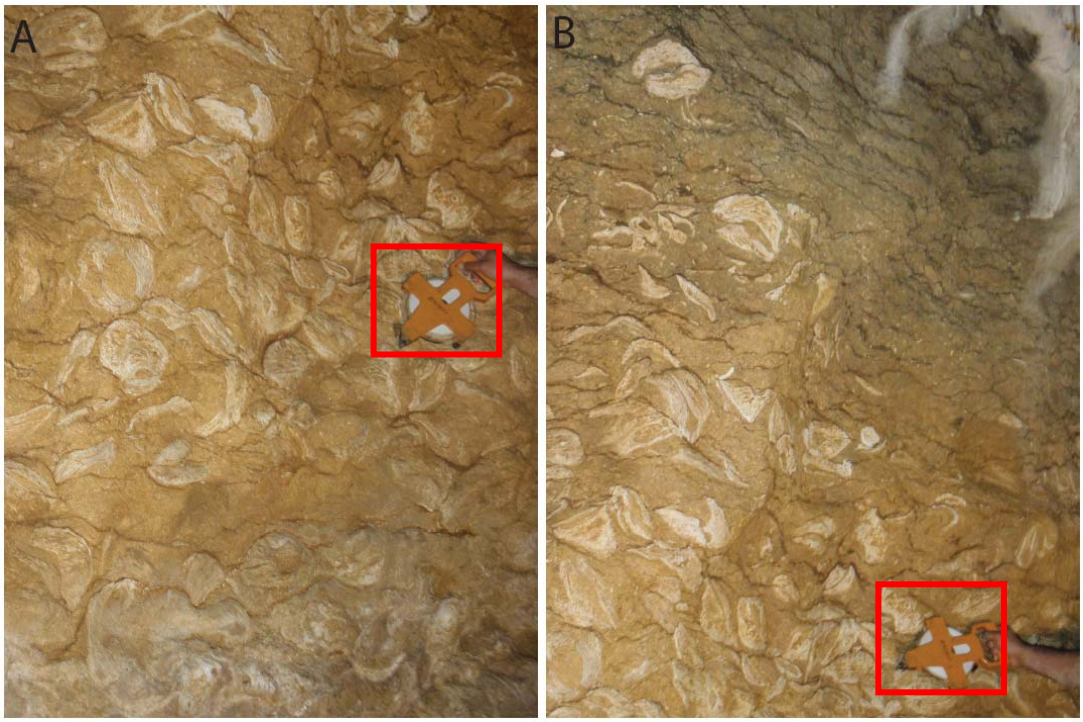

Figure 3.21 (A) Thick bed accumulation of oysters at Piripiri Cave contained within a buff-coloured, highly indurated limestone composed of coarse fossil hash and terrigenous material. (B) Oyster bed grades upwards via more disarticulated and fragmented specimens. Length of tape measure in photos=30 cm (C20 R16/739258).

Figure 3.22 Oysters at the base of the section at Piripiri Cave form 'cones', suggested to be where the beds began to develop and build up from due to the preferential settlement of larvae. Scale bar=15.3 cm.

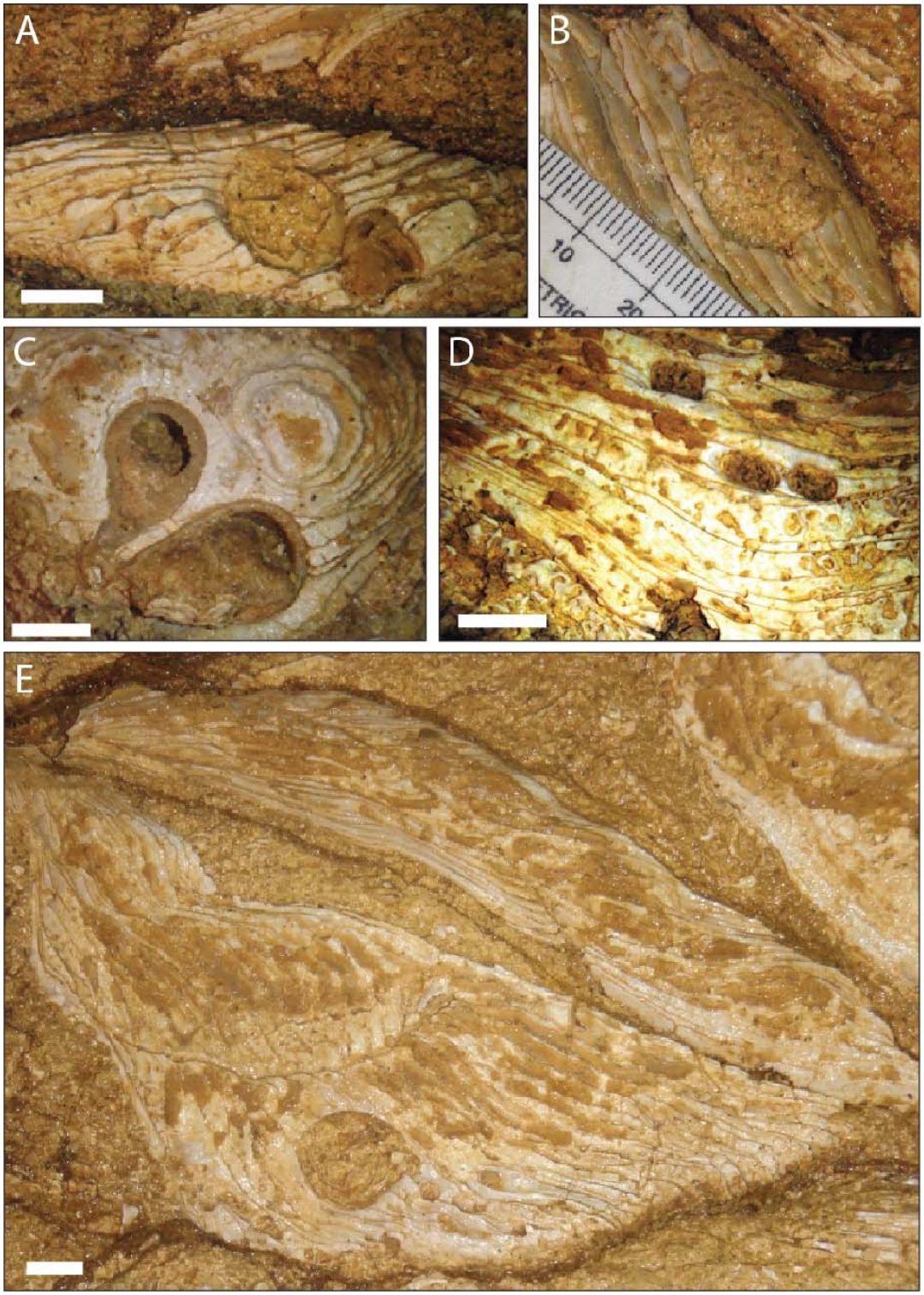

Figure 3.23 Borings in oyster shells at Piripiri Cave (A) Two large borings cut through the posterior/anterior margin of an oyster shell. (B) Large boring 30 mm in diameter, cutting through shell layers. (C) Three large bore holes variably filled with calcite precipitates. (D) Abundant small to medium sized borings in oyster shell. (E) Large bore hole (20 mm) in the thicker left valve of the oyster. Bore hole is filled with limestone host rock. Scale bars=1 cm.

Figure 3.24 Coarse terrigenous nature of host rock at Waitomo Valley Road. Small pebbles, shell hash and glauconite are common (C22 S16/988314).

accumulations are often characterised by "floating" shells which can be singular (Fig. 3.10B), in clusters of 2-3 shells (Fig. 3.17), or singular layers of shells with a high number of shells often fragmented and disarticulated (Fig 3.20). Both the dense and sparse accumulations exhibit biological modification in the form of large, conspicuous borings from 5-30 mm across which are infilled with host rock. Shells also have a host of littered microbores on the shell surfaces.

The thickness of oyster beds present in each of the stratigraphic columns varies markedly. Figure 3.28 represents the proportion of oysters seen in the total thickness of limestone logged at each location. In the smaller outcrops the occurrence of oyster beds can comprise up to 80%, whereas the larger columns such as C7 and C18 have as little as 20%.

At the local scale the lateral extent of the oyster bed occurrences could be examined. This was done in the Mangapohue Natural Bridge area where a total of ten stratigraphic columns were erected (C1 – C10) in close proximity. Figure 3.29 shows that some of the oyster beds are able to be correlated with neighbouring columns, while for others they appear to lens in and out, as do the pebble

Figure 3.25 Lower contact of oyster bed at Waitomo Valley Road is sharp and irregular. Preferential weathering has caused the oyster bed to protrude from the outcrop (C22 S16/988314).

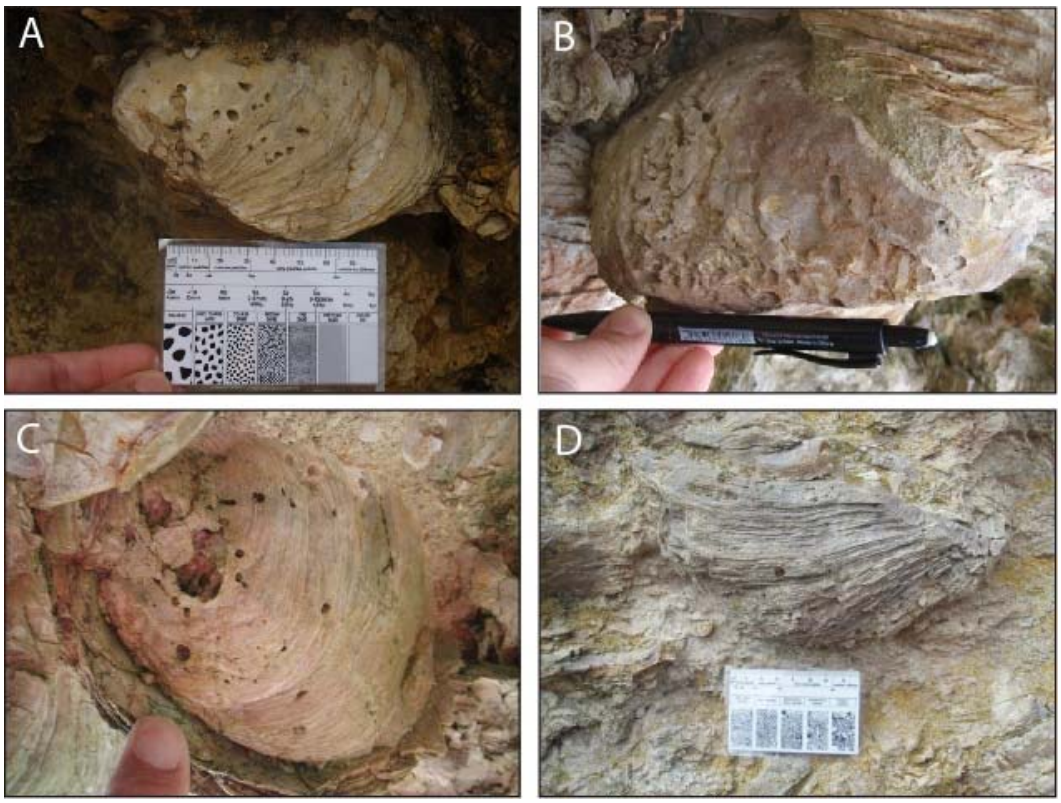

Figure 3.26 Borings in oyster shells at Waitomo Valley Road. (A) Borings litter the outer surface of this giant oyster shell. (B) Surface of this shell is highly irregular due to endolithic boring organisms. (C) A very large boring is obvious on the top of this giant oyster and is surrounded by smaller bores. (D) Bore holes in the ventral margin of this thick shell.

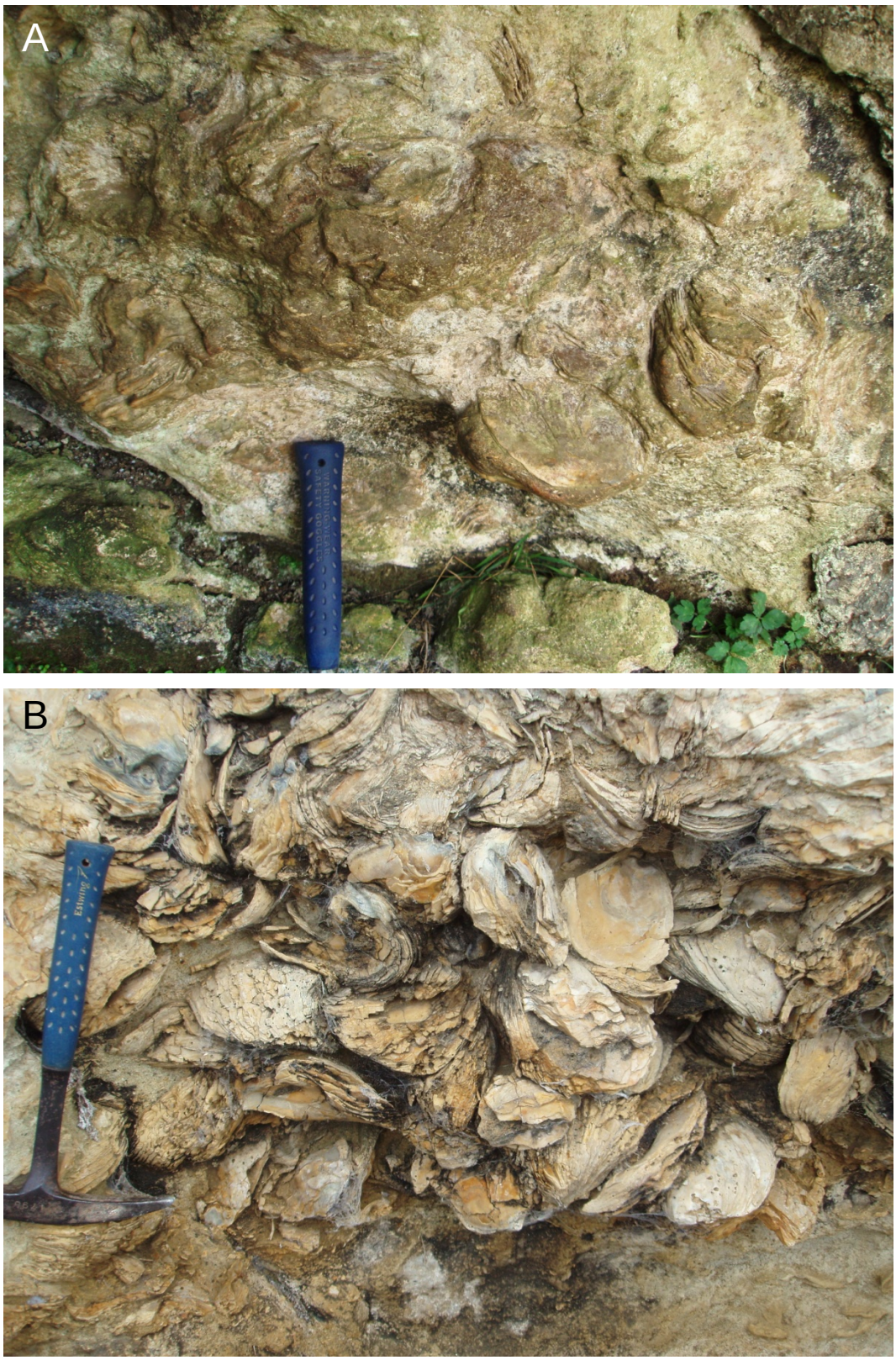

Figure 3.27 Flemingostreini Stenzel oyster bed at Waitomo Valley Road. (A) Moderately packed bed of oysters at this location are both matrix and oyster supported (C21 S16/987315). (B) Dense accumulation of oysters at this location are almost entirely oyster supported. Oysters stand out from preferentially weathered host matrix limestone. Note haphazardness of orientations of oyster specimens (C22 S16/988314).

occurrences. The majority of other stratigraphic columns show little correlation with each other and their oyster occurrences are assumed to be laterally discontinuous and the change in thickness and variation in occurrence of the oyster beds throughout most of the stratigraphic columns is clear. This is likely due to the larger spatial scale at which the other stratigraphic logs were taken.

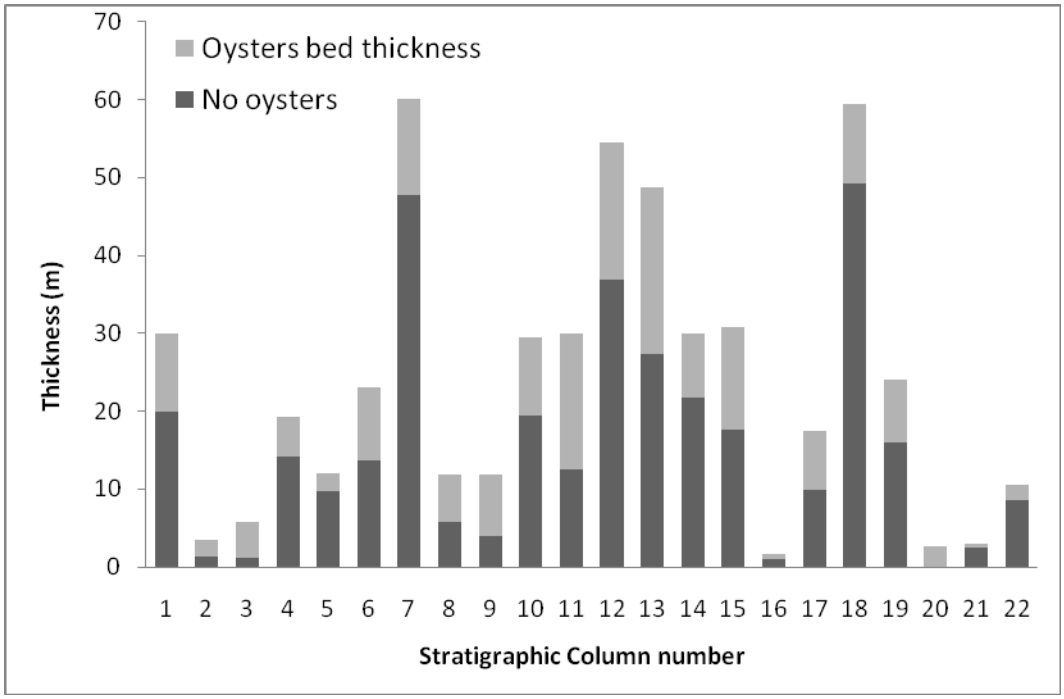

Figure 3.28 Graph showing total thickness of limestone and the proportion of oyster occurrences in each of the described stratigraphic columns.

The host rock of the oyster beds consists of limestone ranging from cream to buff and occasionally dark red due to a localised weathering stain. Pebbles occur in half of the columns (C1, C7, C8, C11, C12, C14, C18, C19, and C22), either scattered amongst the oysters or as conspicuous bands of poorly sorted pebbles. The limestone host containing the oyster beds usually lacks flags and is weakly seamed to massive. Seams may develop around the oyster shells in an irregular manner.

3.7 SEQUENCE STRATIGRAPHIC INTERPRETATION

Sequence stratigraphic development of temperate carbonates is often similar to that in siliciclastic settings (Read 1995). This is because in a temperate system the carbonate sedimentation is not dependent on light as in tropical settings. So a temperate carbonate system sees little decrease in sedimentation rates into deeper

water, and they are characterised by gently sloping ramps on prograding seaward sediment wedges (Lees 1975; Schlager 1992).

The Orahiri Limestone has been placed within a broad sequence stratigraphic framework by Tripathi (2008). The lower part of the limestone known as the Mangaotaki Limestone Member (OrA) (Nelson 1973) has been placed within a transgressive systems tract (TST) and the upper part of the limestone which is oyster bearing and known as the Te Anga Limestone Member (OrB) (Nelson 1973) in a highstand systems tract (HST) (Fig. 3.2). The HST is interpreted to form during the late part of sea level rise, during sea level standstill, or during the early part of sea level fall. It forms under conditions which allow progradation (Boggs 2001).

The repetitive and discontinuous nature of the oyster shellbed deposits suggests that late sea level rise or standstill associated with an HST was not uniform, but rather involved superimposed small scale oscillations of transgression and regressions. The HST part of the sequence is represented by a shallow, low energy shoreface which has evolved upward from the shallow shelf environment of the TST. The periods of transgression have possibly led to the formation of the two different morphological types of beds seen in the Orahiri Limestone - dense and sparse beds.

The sparser shellbeds of Flemingostreini Stenzel in the Orahiri Limestone are dominated by disarticulated and sometimes fragmented oysters. This could be interpreted as an onlap shellbed deposited in a high energy, shallow setting during transgression. An onlap shellbed often develops when winnowing and by-passing of sediment from the nearshore environment basinward leaves a shell and gravel lag (McIntyre 2002). Periods of onlap allowed for adequate energy and a shallow enough environment for rounded and poorly sorted terrigenous pebbles to be included in the transgressive lag (Fig. 3.12). As these deposits are discontinuous it is suggested that their deposition was restricted to areas of depression, and so they do not occur in all stratigraphic columns at all localities (Fig. 3.30).

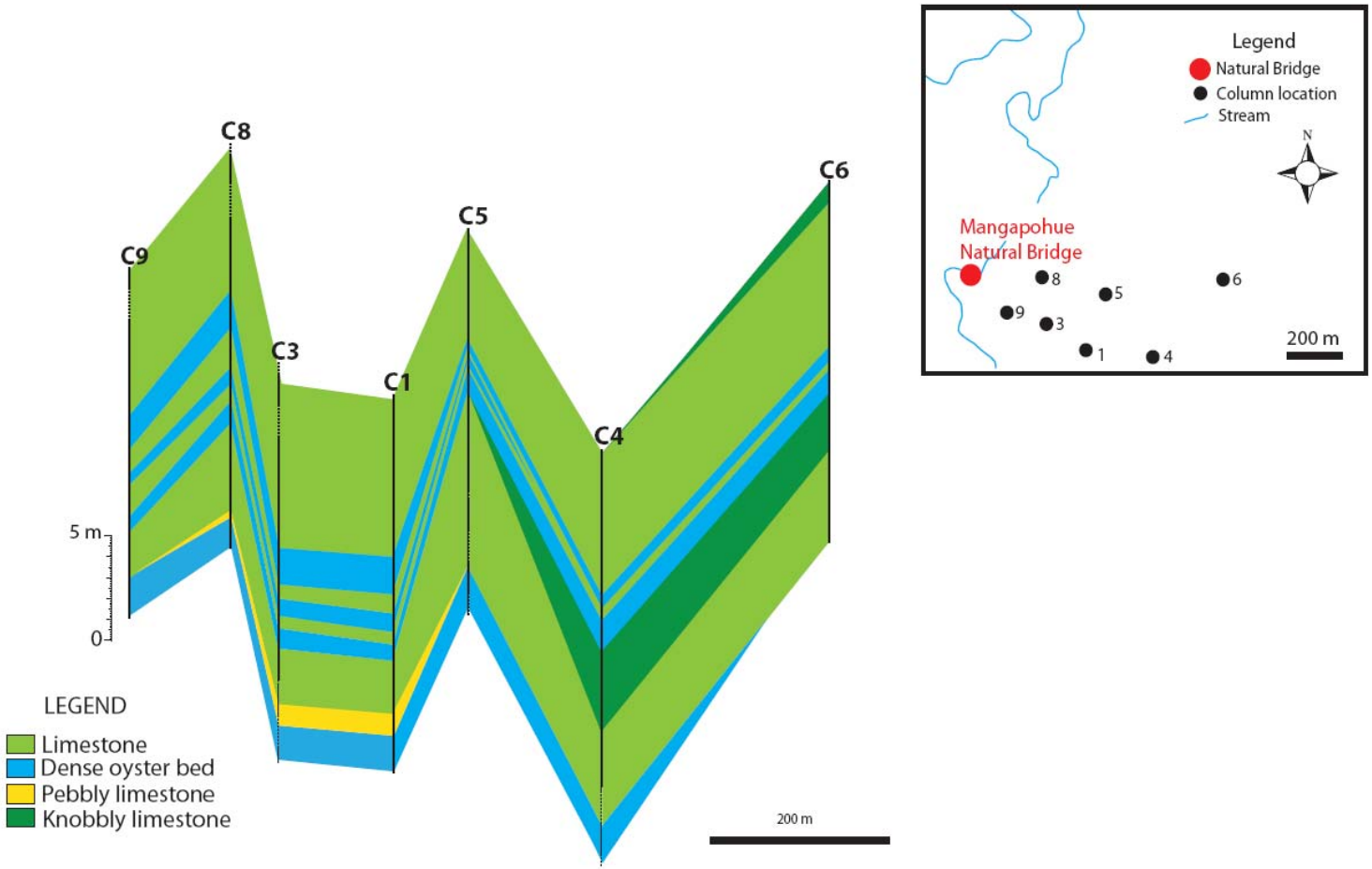

Figure 3.29 Fence diagram showing suggested distribution of dense oyster beds in selected stratigraphic columns at Mangapohue Natural Bridge. Note lithologies for this diagram are simplified in places and those occurring within a dashed line are inferred. Appendix D-1.1 for complete logs and grid references.

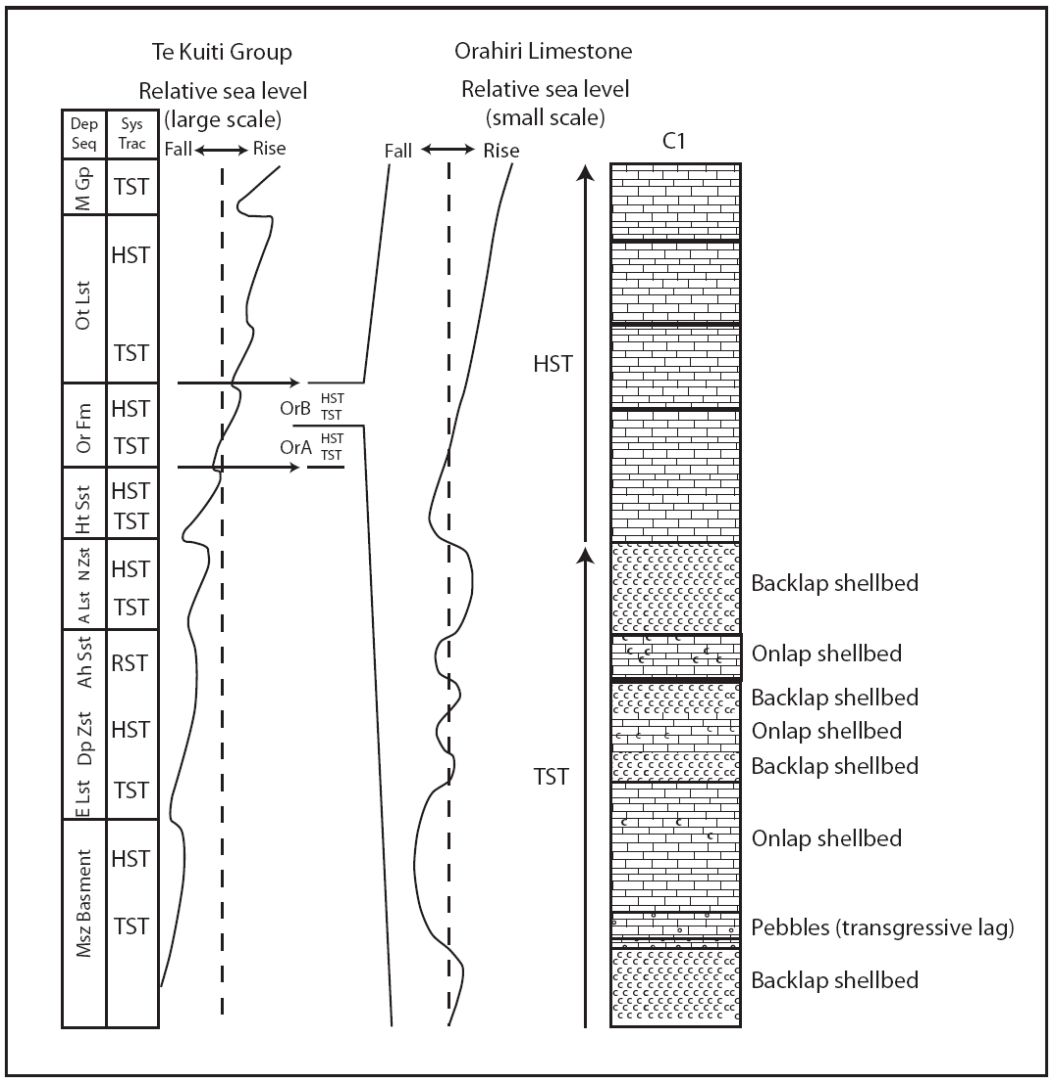

Figure 3.30 Schematic diagram showing inferred sea level curve for Orahiri Limestone from Mangapohue Natural Bridge (R16/767251). Large scale relative sea level and systems tracts for the Te Kuiti Group from Tripathi (2008) (See Fig. 3.2). Msz=Mesozoic; E=Elgood; Dp=Dunphail; Ah=Ahirau; A=Awaroa; Ng=Ngapaenga; Ht=Hauturu; Or=Orahiri; Ot=Otorohanga; M=Mahoenui.

Shellbeds overlying the fragmented shellbeds in the Orahiri Limestone typically involve coincide with dense oyster shellbeds. They are dominated by densely packed Flemingostreini Stenzel and can be interpreted as a backlap shellbed, or backstep shellbed of Kidwell (1991a). This is a deeper water shellbed and formed under conditions of reduced turbidity and low sedimentation rate. During transgression the shellbed continues to migrate shoreward, thus maintaining the depth at which the Flemingostreini Stenzel can live *in situ* within the shelly gravel sediments (Fig. 3.30).

The large and boulder-shaped size of the Flemingostreini Stezel suggests the morphotypic type of the oyster specimens were reclined and sediment supported (Seilacher et al. 1985). The free living nature of these oysters on the sea floor means that in a shallowing leading to formation of the onlap shellbed, disturbance of these underlying backlap shellbeds was likely. This possibly resulted in the haphazard nature and of the oyster shell orientations and the dominance of oyster support that is commonly seen in the field (i.e. Fig. 3.13).

HST periods of late sea level rise or stand still dominate this system as they formed the majority of the Orahiri Limestone seen in the field that is devoid of oyster shellbeds, as represented graphically in Figure 3.28.

CHAPTER FOUR

Field stratigraphy and sedimentology, Patagonia

4.1 INTRODUCTION

One of the more conspicuous features of the marine Miocene deposits of northeastern Patagonia (Argentina) is the presence of well preserved molluscan shell accumulations. Molluscan shellbeds comprise up to 55% of the total thickness of the Puerto Madryn Formation cropping out at Península Valdés (Fig 4.1) (del Río et al. 2001). Fossil oysters are one of the more common taxa in the molluscan assemblages in the Cretaceous to Neogene deposits of Patagonia (Casadío et al. 2005). This chapter describes the broad geological setting of Patagonia, including locality, stratigraphic, sedimentologic and other information about the oyster accumulations. The chapter concludes with some insights about sea level dynamics and local environmental conditions in the Miocene.

4.2 REGIONAL GEOLOGICAL SETTING

The study area locality map is provided in Figure 4.1, a generalised geology map of Argentina in Figure 4.2 and a general stratigraphic diagram in Figure 4.4. A geological time scale is also included in support of the following account in Appendix A-1.3.

Southern South America experienced a number of transgressive events throughout both the Paleogene and early Neogene (Casadío et al. 2005). Subsidence of the Atlantic margin of Patagonia is hypothesised to be the main cause. Tectonic, climatic and relative sea level changes have been responsible for at least five major sedimentary cycles and thus the widespread nature of Tertiary deposits in Argentina (Fig 4.1). The first of these cycles began with a Late Cretaceous – Paleocene (Maastrichtian – Danian, 70.6 – 61.7 Ma) marine transgression which covered a large area of South America. During the Middle Eocene the second event occurred covering all areas south of 40^{o} S (Casadío et al. 2005). The third cycle is characterised by widespread continental deposits, occurring during the Late Eocene-Oligocene, these deposits include important coal-bearing intervals. The fourth cycle includes two of the most important transgressions, in terms of the area covered and quality of the paleontological and stratigraphic record preserved.

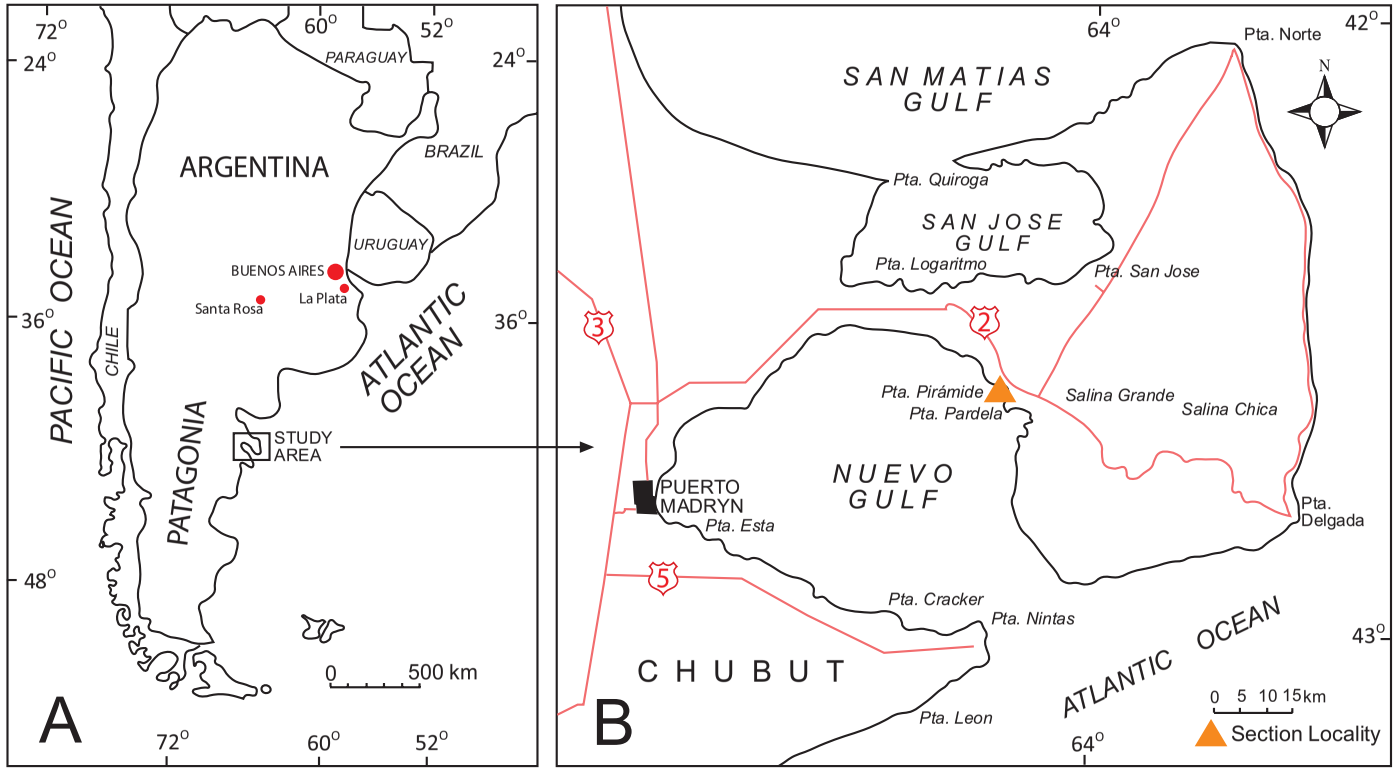

Figure 4.1 (A) Argentina and the area of study. Note Patagonia situated in the lower part of Argentina. (B) Location of the Late Miocene fossiliferous coastal section at Puerto Pirámide on Peninsula Valdés. Adapted from del Río et al. (2001).

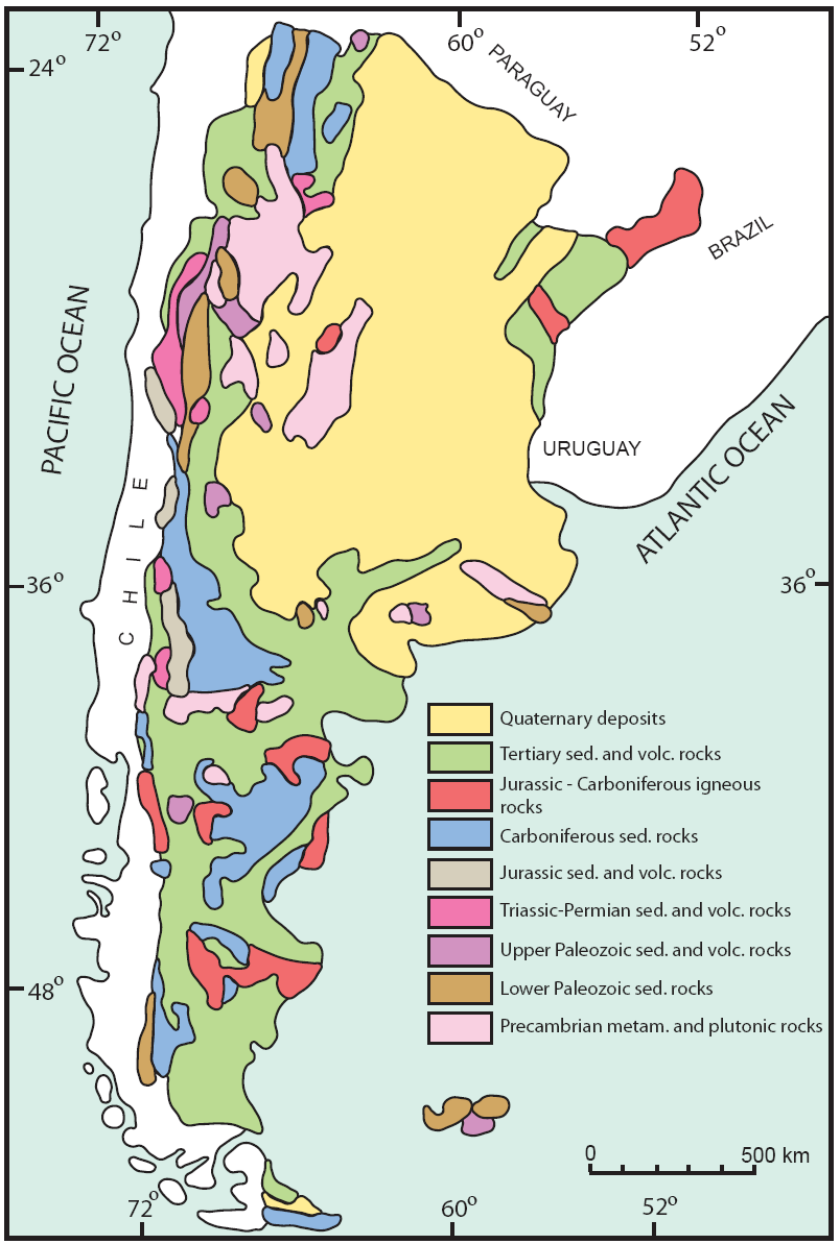

Figure 4.2 Generalised geological map of Argentina. Extent of the Tertiary sedimentary deposits is shown in green. Adapted from Pascual (2008).

The first of these transgressions occurred during the Late Oligocene - Early Miocene while the second occurred during the Late Miocene (Tortonian, 11.6 - 7.2 Ma). Finally, the fifth cycle is related to an important orogenic phase and the uplift of the Andes (Casadío et al. 2005).

The oyster fossils of interest in this chapter come from the Late Miocene Puerto Madryn Formation, exposed near Puerto Pirámide, Chubut Province, Argentina (Fig. 4.2). They occur in deposits associated with part of the fourth sedimentary cycle, during the second (Tortonian) transgression. This transgression has been given the name “Entrerriense” or “Paranense” (Fig. 4.3), and is representative of

the most widespread Cenozoic transgression in Argentina. In contrast to the first transgression during the Late Oligocene - Early Miocene, it was focused in the northern half of Argentina. The maximum thickness of the transgressive deposit is recorded in the subsurface of the Chaco-Pampeana basin (Fig. 4.3). Sections no thicker than 200 m are exposed around Península Valdés and are give the name Puerto Madryn Formation (Casadío et al. 2005).

The deposits of the Puerto Madryn Formation coincide with the end of the Neogene climatic optimum. The presence of warm water along the Atlantic coast of Argentina during the Middle Miocene is characterised by a marked diversification in calcareous nannoplankton (Malumián 1999). This warm water in the South Atlantic is related to an important change in the composition of the faunal associations that are recorded in the Puerto Madryn (Early Later Miocene) (Fig. 4.4) (del Río et al. 2001). According to del Río (2000), there was a change in the association of invertebrates in the Middle Miocene and new taxa appeared that were at the time unknown in the South Atlantic. These new taxa make up a total of 60% of the “Entrerriense” fauna.

4.3 STRATIGRAPHY

4.3.1 Puerto Madryn Formation

The Puerto Madryn Formation (Fig. 4.5) comprises coquinas, cross-bedded sandstones with mud drapes, mudstones that have heterolithic lamination, and laminated or massive, bioturbated mudstones (Scasso et al. 2001). Large scale cross-bedding with climbing ripples or with mud drapes between sets are light green to brown pyroclastic mudstones are occasionally intercalated. Some ash-fall tuffs are contained in the upper part of the unit (Scasso & Castro 1999).

4.3.2 Name and type section

The name Puerto Madryn Formation derives from the proximity of the town of Puerto Madryn (Fig. 4.1) on Península Valdés, Chubut, Argentina. The type section for the formation is situated at the cliff along the coast of Puerto Madryn, where the formation crops out clearly and reaches 270 m thick (Malumián 1999).

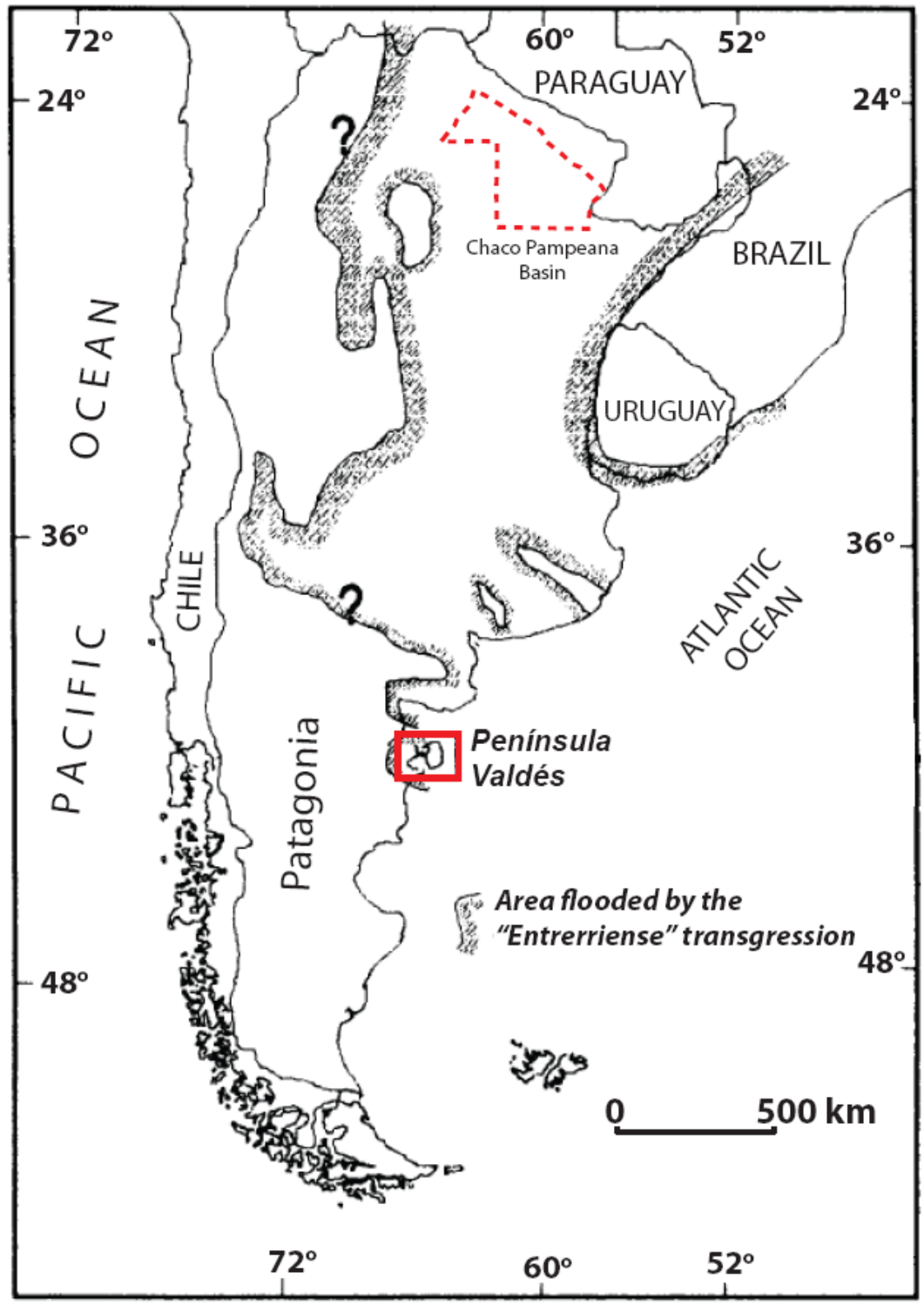

Figure 4.3 Paleogeography of Argentina during the Miocene. Area flooded by the "Entrerriense" transgression includes Península Valdés. Dashed red line pertains to the province Chaco where the thickest "Entrerriense" deposits are recorded in the Chaco-Pampeana basin. Adapted from del Río et al. (2001).

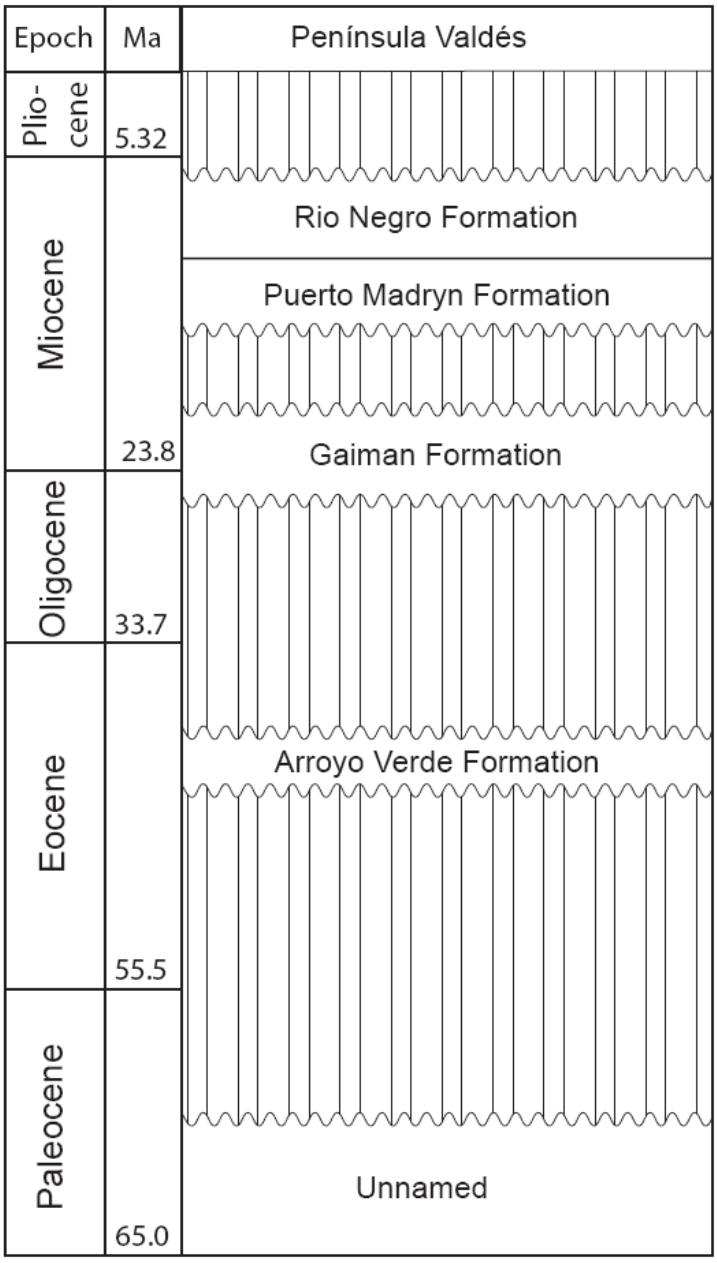

Figure 4.4 Generalised chronostratigraphic panel of geological units on Península Valdés (see Figures 4.2 & 4.3).

4.3.3 Boundaries and underlying contact

The base of the Puerto Madryn Formation is not exposed at the Puerto Pirámide locality; at other localities the formation unconformably overlies the Gaiman Formation (Casadío et al. 2005) (Upper Oligocene - Lower Miocene) (Fig. 4.4). The contact between these two units has been interpreted as a transgressive ravinement surface (Scasso & Castro 1999; del Río et al. 2001). The Puerto Madryn Formation is conformably overlain by the Rio Negro Formation, which comprises fluvial sandstone and conglomerate (Scasso & Castro 1999; Scasso et al. 2001; Casadío et al. 2005).

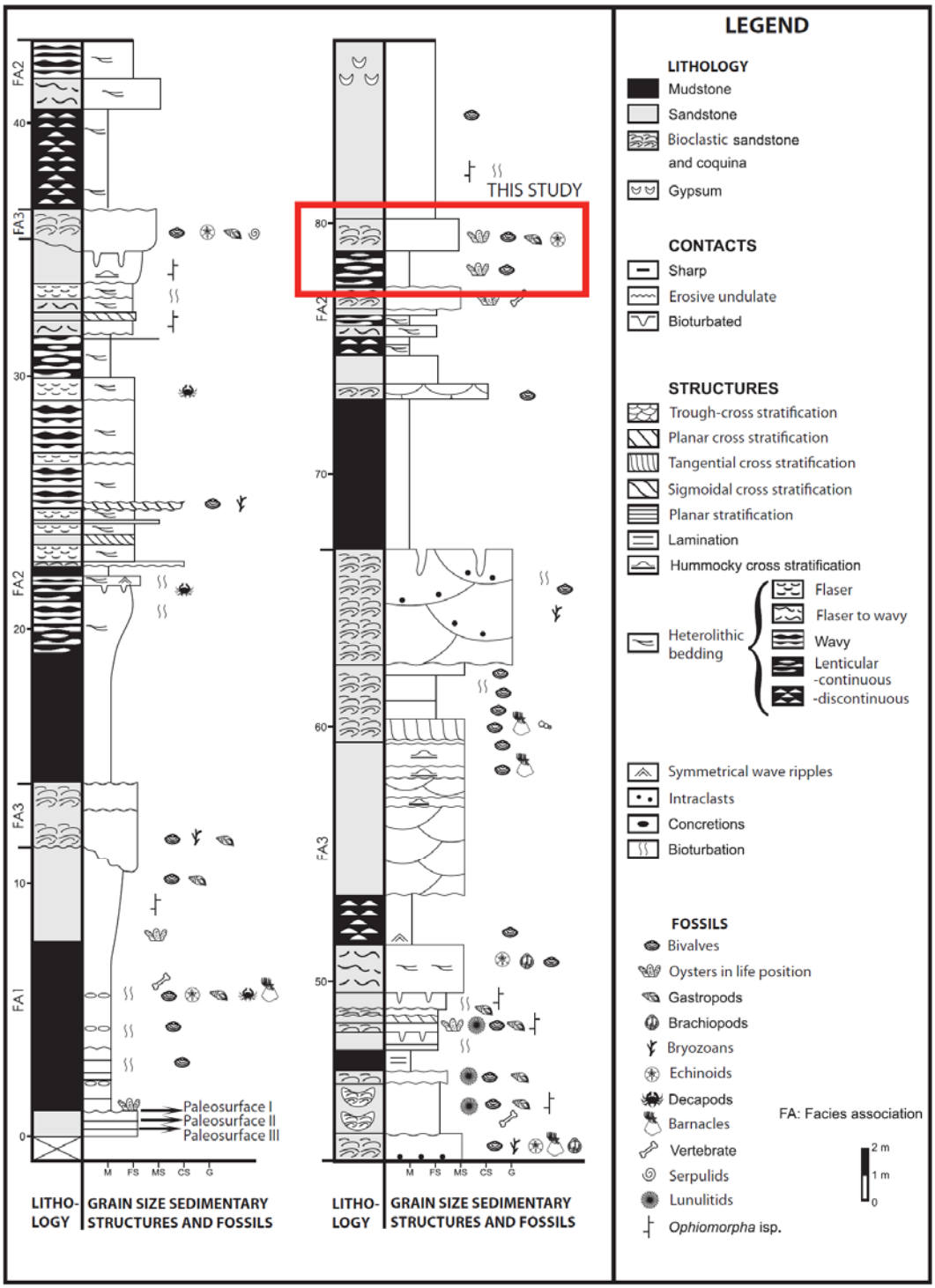

Figure 4.5 Generalised stratigraphy and sedimentology of the Late Miocene Puerto Madryn Formation on Península Valdés. Note the inclusion of facies associations FA1 – FA3. Red box shows location of oyster reef this study has focused on. After Mauna et al. (2005).

4.3.4 Distribution and thickness

The Puerto Madryn Formation comprises a 270 m thick marine succession. A total of 90 m is exposed at Puerto Pirámide (Scasso et al. 2001).

4.3.5 Paleontology

Thick fossiliferous coquinas occur throughout the sequence which has a diverse and abundant molluscan fauna that includes an assorted association of bivalves and gastropods. Also found are brachiopods, bryozoans and echinoderms (Scasso et al. 2001).

4.3.6 Age

The Puerto Madryn Formation has been given an absolute age of 10.0 ± 0.3 Ma, placing it in the Middle Tortonian Stage (Scasso et al. 2001).

4.3.7 Environment of deposition

The marine fauna in the Puerto Madryn Formation suggest generally normal marine conditions. However, the depositional environment is a shallow shelf environment with some storm influence, and it evolves upwards into a tide-dominated estuarine environment for most of the unit (Scasso et al. 2001).

4.4 SEDIMENTOLOGY OF THE PUERTO MADRYN FORMATION EXPOSED AT PUERTO PIRAMIDE

The section exposed at Puerto Pirámide (Fig. 4.5) belongs to the upper part of a depositional sequence that includes both a transgressive systems tract (TST) and a highstand systems tract (HST) (Scasso & del Río 1987; del Río et al. 2001). There are three facies associations represented at the coastal section (Fig. 4.5). The TST interval is represented by shelf sediments that were deposited below a wave base and are represented by Facies Association 1. The HST is representative of tidal channel and tidal flat deposits contained within Facies Associations 2 and 3 (Casadío et al. 2005).

4.4.1 Facies Association 1 (FA1)

Facies Association 1 represents inner-outer shelf deposits (8 - 15 m thick) and portrays a fining upwards within the sequence. This includes fine sandstone and massive, bioturbated mudstone facies. The facies contains multiple occurrences of organisms from the Cruziana ichnofacies. Invertebrates found in life position are frequent and include clusters of *"Ostrea" patagonica*. The facies grades upwards into a laminated mudstone facies. Towards the top of the facies there are thin beds

containing calcareous concretions with many bivalve borings (Casadío et al. 2005).

The fine grained nature of the deposits, trace fossil assemblages, and high level of fossil preservation suggest a low sedimentation rate in an offshore, low-energy environment below fair weather wave base. Taphonomic information suggests that sudden increases in sedimentation can be related to storm events towards the base of this lithological interval. Facies Association 1 is representative of a sedimentary retrogradation with a rising sea level (Casadío et al. 2005).

4.4.2 Facies Association 2 (FA2)

Facies Association 2, from 2 - 15 m thick, is dominantly in the middle and upper part of the stratigraphic sequence and includes facies of fine sandstone intercalated with mudstone. The majority of stratification in this facies is horizontal although flaser, wavy and lenticular bedding occurs. The facies has few invertebrate remains, but there are beds with abundant *Skolithos* and *Ophiomorpha* (Casadío et al. 2005).

Low energy conditions are suggested due to the fine grain sizes and available tide - influenced sedimentary structures. The unit has likely been deposited in a sandy to muddy sand dominated tidal flat environment. This facies association is always accompanied by Facies Association 3 (Casadío et al. 2005).

4.4.3 Facies Association 3 (FA3)

This facies association typifies large tidal channels (5 - 14 m thick). This group of lithofacies forms a clustered group in a fining upwards sequence. Beds in this association have erosive bases and a lenticular geometry. At the base of each set of beds is a shell concentration 1 – 5 m that is set in a sandy matrix. The beds are usually massive or have medium to large scale cross stratification. These deposits grade upwards into a medium grained sandstone and mudstone possessing heterolithic bedding (Casadío et al. 2005).

Infilling of tidal channels and tidal sand waves are the suggested source of deposition for these deposits due to the lenticular geometry of the beds, their erosive bases, and the upwards decreasing energy level as suggested by grain size

and sedimentary structures present. The significant lateral extent of the combined bed sets and the geometry seen in individual beds represents the lateral migration of the channels within a complex channel system. Shelly, sandy dunes and waves migrated along the deepest parts of these channels, while in other areas weaker currents were associated with small ripple migrations across sandy tidal flats. The presence of mudrock intraclasts leads to the suggestion that the channels were flanked by fine tidal flat sediments of Facies Association 2 (Casadío et al. 2005).

4.5 DESCRIPTION OF THE OYSTER REEF AT PUERTO PIRAMIDE

The "*Ostrea" patagonica* reef at Puerto Pirámide occurs within Facies Association 2 some 80 m up the exposed Puerto Madryn Section (Scasso & Castro 1999). A total of six detailed stratigraphic logs were made at various locations along the reef (Fig. 4.6). The logs provide details about the lithologic features of the reef units, and the nature of the overlying and underlying contacts and deposits, as reproduced in Appendix D-1.1.

4.5.1 Paleontological features

The oyster reef is chiefly made up of "*Ostrea" patagonica* (Fig 4.7) with some occurrences of the oyster *Ostrea alvarezii*. The genus *"Ostrea"* is inferred as it is possible the taxonomic identification of the oyster is incorrect. Rarer faunal occurrences include pectinids, brachiopods and barnacles. The age spectrum of "*Ostrea" patagonica* appears to represent predominantly adult specimens, with rare to absent juveniles.

4.5.2 Stratigraphic features

The oyster specimens are contained within a light grey, poorly to moderately indurated, slightly weathered, fine to medium homogenous sand matrix, within Facies Association 2 (Fig. 4.5). The matrix includes randomly placed inclusions of shell hash, consisting of sharp angular fragments of poorly sorted shell material. At the study site the accumulation reaches up to 1 m thick and extends laterally for over 20 m. This gives the reef a lens geometry as it thins distally in both directions (Figs. 4.6 and 4.8); such an accumulation of bivalves has been referred to as a bioherm (Dittmann 1990; Martín et al. 1997; Pruss et al. 2007; Navarro et al. 2008). The reef unit overlies heterolothic mud beds with a sharp

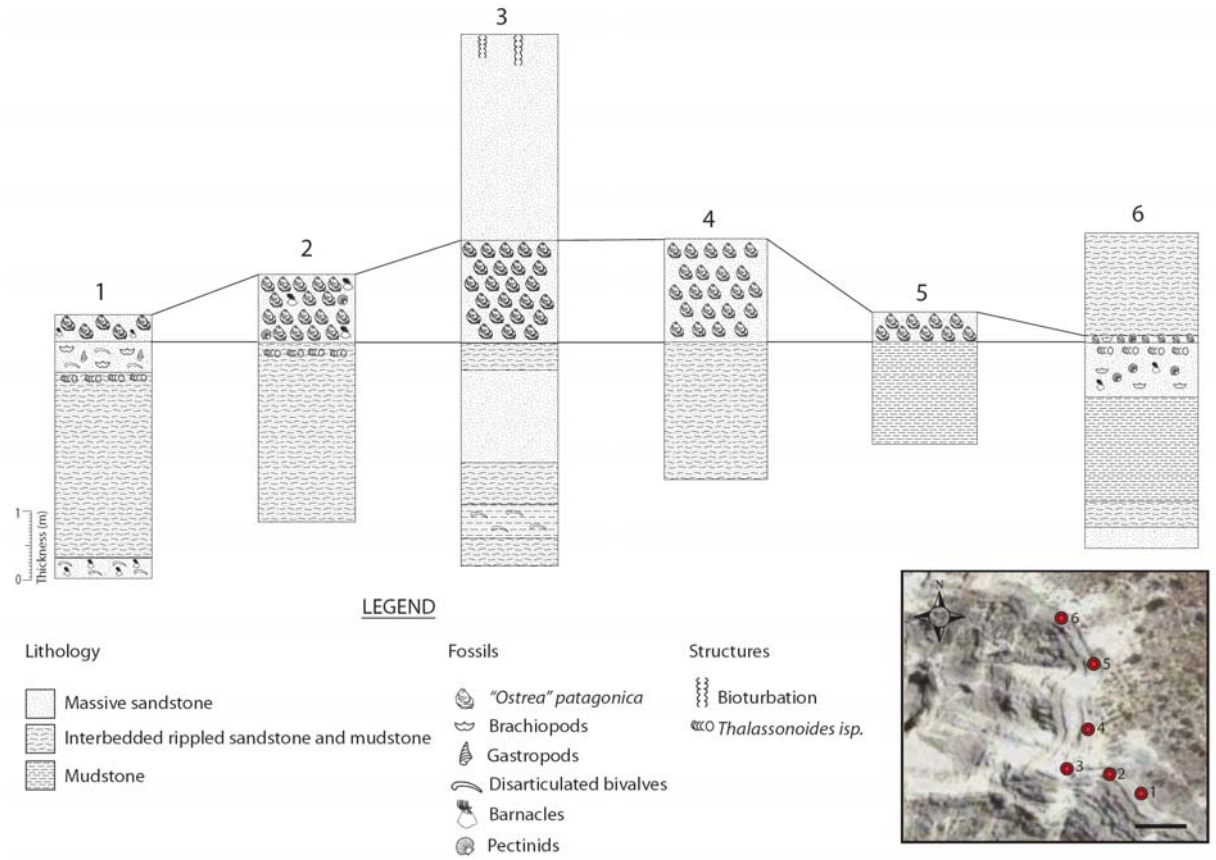

Figure 4.6 Stratigraphic columns taken from Puerto Pirámide, Peninsula Valdés, Patagonia. Adapted from Brito (2009). The *"Ostrea" patagonica* reef forms a lens geometry as the oyster accumulation thins distally. Inset: Aerial photography view showing location of columns relative to one another. Scale bar=5 m. For grid references and more detailed lithological description see Appendix D-1.1.

Figure 4.7 *"Ostrea" patagonica* (d'Obigny) specimens reach up to 20 cm in length, individual valves are up to 5 cm thick and can weigh up to >3kg.

Figure 4.8 Reef extends laterally at least 20 m atop the coastal Puerto Madryn section at Puerto Pirámide. The lens geometry (bioherm) of the accumulation is here outlined for clarity (see Fig. 4.6).

Figure 4.9 Reef composed of *"Ostrea" patagonica* forms a sharp and erosive contact with the underlying heterolithic mud bed. Scale: hammer=32.5 cm.

Figure 4.10 Development of oyster reefs in the Puerto Madryn Formation at Puerto Pirámide begins with 'cone' shaped nests at the base followed by upwards growth upon one another. Preferential settlement of oyster larvae leads to several cones developing and forming a large reef or bank of oysters. Photographs kindly provided by S. Casadío (2008).

erosive contact (Fig 4.9). V-shaped 'nests' at the base of the accumulation mark the seeding positions of earliest generation oysters (Fig. 4.10). The reef occupies a position within a suggested highstand systems tract and the upper contact forms an unconformity with overlying fluvial deposits of the Rio Negro Formation (Casadío et al. 2005).

4.5.3 Taphonomic features

All *"Ostrea" patagonica* shells in the studied reef are articulated and in life position (Fig. 4.11). Weathering over time has caused many shells to break away from the reef; singular valves can be seen as a result. Specimens are very well size sorted with the average size being about 200 mm in length. Bioerosion is moderate to high in most shells with many visible borings and traces noted on the shell surfaces (Fig. 4.12). The shells make up about 25% of the reef unit and are loosley packed, so that they are supported by the matrix and sometimes other oysters in the reef. Generational layering can be easily interpreted for the reef, making it possible to analyse the associated reef fauna over time (see Chapter Eight) (Fig. 4.11).

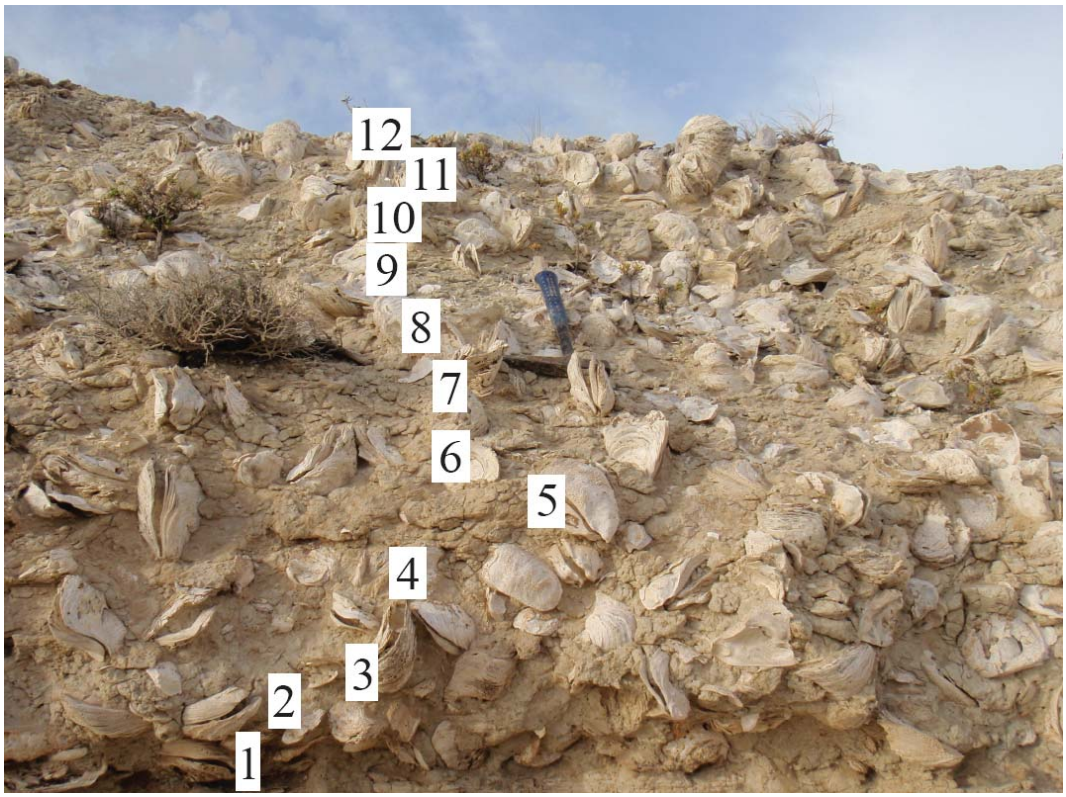

Figure 4.11 Biological accumulation of *"Ostrea" patagonica* in the Puerto Madryn Formation. All shells are articulated and in life position. Numbers 1 – 12 represent the suggested number of generations in the oyster reef.

4.6 SEQUENCE STRATIGRAPHIC INTERPRETATION

The reef of *"Ostrea" patagonica* can be interpreted within a sequence stratigraphic framework. It has been suggested by Scasso & del Río (1987) and del Rio et al. (2001) that the section exposed at Puerto Pirámide belongs to the upper part of a depositional sequence which includes a transgressive systems tract (TST) and a highstand systems tract (HST) (Fig. 4.13). The TST interval is represented by shelf sediments that were deposited below wave base and include Facies Association 1 (See section 4.4.1), whereas the HST represents tidal channel and tidal flat deposits of Facies Associations 2 and 3 (See sections 4.4.2 and 4.4.3 respectively). Shell concentrations within a sandy matrix are a common feature at

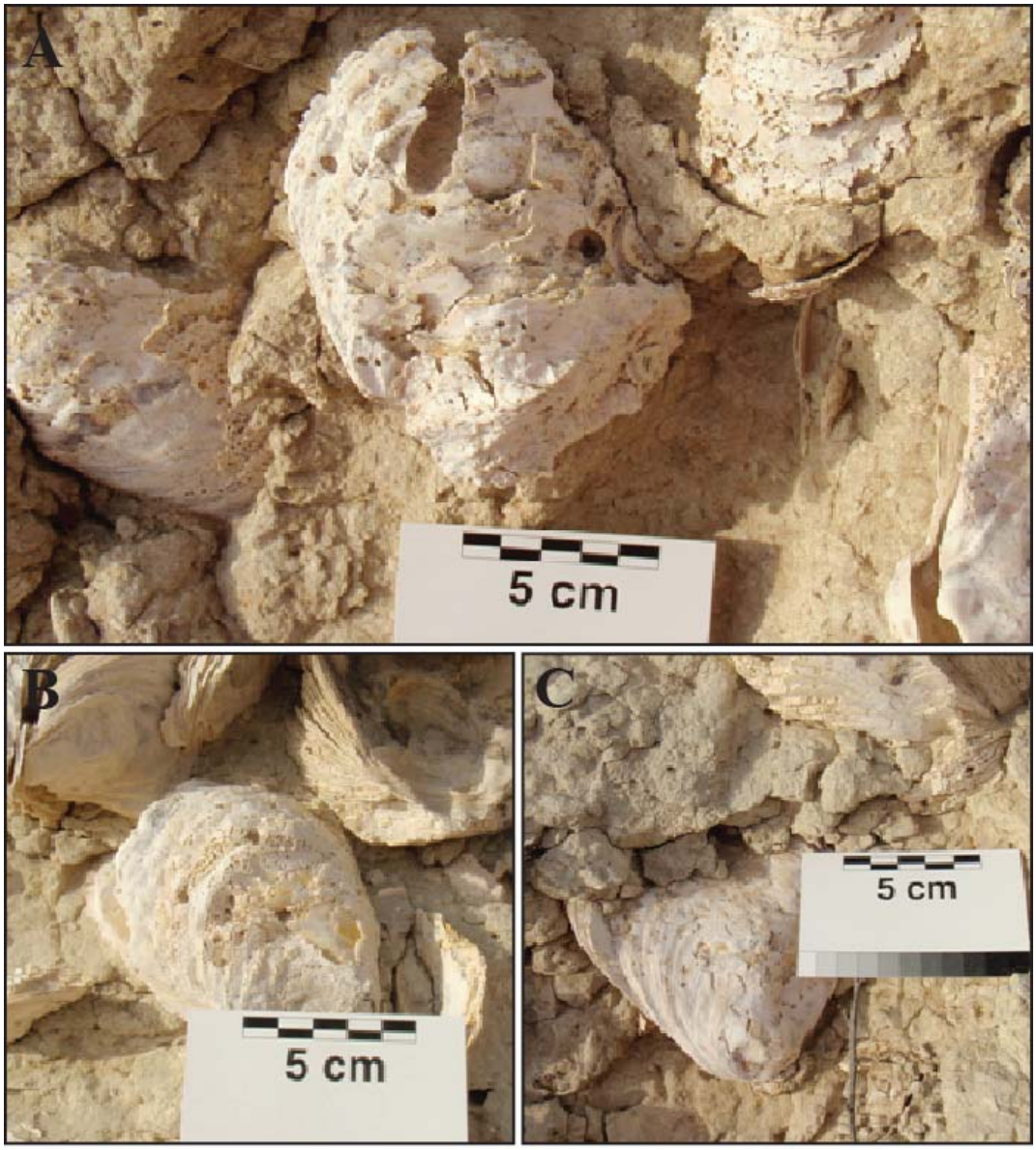

Figure 4.12 (A) Left valve exhibiting large bore holes from the bivalve *Gastrochaenolites* isp. (B) Pock marked surface of a left valve attributed to *Entobia* isp, a boring sponge. (C) A highly eroded right valve of *"Ostrea" patagonia*. Boring traces are associated with *Maendropolydora* isp.

the base of Facies Association 2 and 3. The contact between Facies Association 1 and Facies Association 3 (Fig. 4.5) is representative of a downlap surface, and thus the base of the TST.

This interpretation is consistent with the finest grained facies (Facies Association 2 and 3) occurring in the HST sequence and representing a shallow, low energy shoreface suggestive of a tidal flat environment which has evolved upward from the shallow shelf environment of the TST (Fig. 4.14). The HST is interpreted to form during the late part of sea level rise, during sea level standstill, or during the early part of sea level fall. It forms under conditions which allow progradation (Boggs 2001).

Figure 4.13 Location of the transgressive systems tract (TST) and highstand systems tract (HST) in the Puerto Madryn formation cropping out at Puerto Pirámide. Black arrow denotes the position of the *"Ostrea" patagonica* reef atop the section. Photograph kindly provided by C. Brito (2009).

The oyster reef of *"Ostrea" patagonica* occurs within Facies Association 2 which involves a group of lithofacies clustered to form fining upward sequences. Geometry of these beds often features an erosive base and lenticular geometries. The shellbed is thus interpreted as a downlap shellbed within a HST. Condensed deposits that are associated with downlap surfaces occur at the distal, basinward

portion of progradational siliciclastic sediments. Downlap shellbeds often have a diverse fauna and are preserved in life position. They pass up-section into less fossiliferous siltstone or sandy siltstone, and can be easily distinguished from underlying backlap shellbeds as they are normally matrix dominated (Naish & Kamp 1997). The base of the shellbed is bounded by a downlap surface and it is equivalent to the omission-soled type III shellbed of Kidwell (1991a) (Fig. 4.15).

The occurrence and high level of preservation of the shellbed and the dominance of matrix in the reef of *"Ostrea" patagonica* near the top of the Puerto Madryn Formation, is in accordance with the reef being a downlap shellbed within a HST (Fig. 4.15). Downlap facies typically have a high preservation as they are mantled by regressive marine deposits as occurs in the central part of the reef (Fig. 4.6).

A)

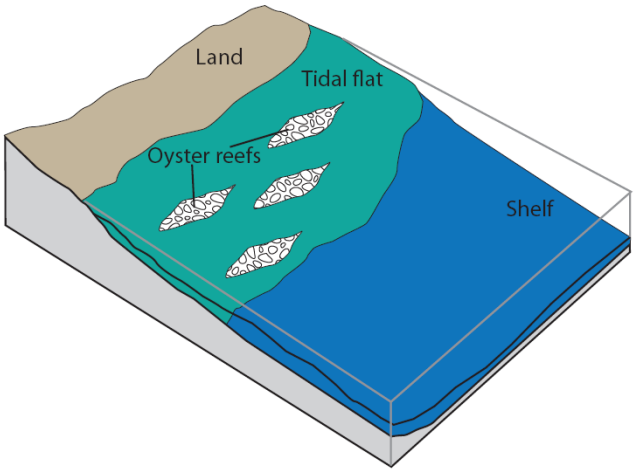

B)

Land	Tidal flat	Shelf
Subaerial	Protected/low energy	Below fairweather wave-base
Fluvial deposits	Tidal flat and tidal channel deposits	Shelf deposits
Gravels	Fine sand & mud Medium sand & heterolithic muds	Fine sand & massive mud
Rio Negro Formation	*Skolithos* Ichnofacies	*Cruziana* Ichnofacies
	FA2 & FA3	FA1
	Puerto Madryn Formation	

Figure 4.14 (A) 3-dimensional facies model of Península Valdés. (B) Diagram showing sediment distribution across a tidal flat to shelfal environment and associated ichnofacies and facies associations. Adapted from Bosence & Wilson (2003).

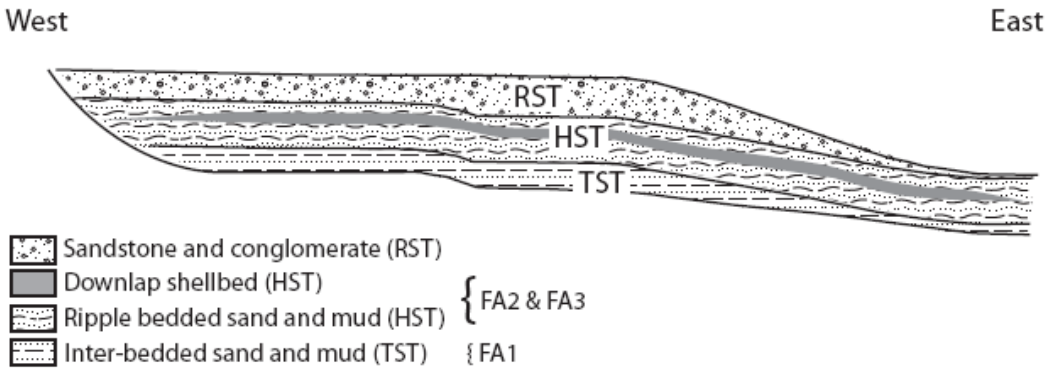

Figure 4.15 Model of sequence stratigraphic framework for the Puerto Madryn Formation, showing facies associations (FA1 - FA3) and approximate position of downlap oyster reef. Adapted from McIntyre (2002).

The high level of preservation is consistent with the dense articulated accumulation of oysters in life position in the Puerto Madryn Formation. The overlying sandstone deposit has become subsequently eroded off the top of the oyster beds towards the more distal areas of the reef.

del Río, C. J.;Martinez, S. A. & Scasso, R. A. 2001: Nature and origin of spectacular marine Miocene shell beds of northeastern Patagonia (Argentina): Paleoecological and bathymetric significance. *Palaios 16*: (1) 3-25

CHAPTER FIVE

Field stratigraphy and sedimentology, Wanganui

5.1 INTRODUCTION

In the Plio-Pleistocene Wanganui Basin (Fig. 5.1), sedimentation broadly matched subsidence until basin eversion occurred by uniform and rapid uplift during the late Quaternary. As a result the Wanganui Basin has one of the most complete and undeformed shallow marine Plio-Pleistocene records in the world (Carter & Naish 1998). The Plio-Pleistocene sediments (Fig 5.2) include coquina shellbeds usually 1-3 m in thickness (Townsend et al. 2008). The thickest and most distinctive of these shellbeds in the Wanganui Basin is named the Wilkies Shellbed (McIntyre 2002). The Wilkies Shellbed is considered to be the largest accumulation of fossil shells in New Zealand (Fleming 1953; Beu & Maxwell 1990).

This chapter presents the regional geological setting of the Wanganui Basin, including the geological history, structure and physiography. The stratigraphy of the Wilkies Shellbed is covered as well as a detailed description of the Wilkies Shellbed at each field locality (Fig. 5.3). Finally a summary of the shellbed characteristics is provided as well as some insight into the sea level dynamics and environmental conditions during the formation of this shellbed. All locations mentioned in the text are featured on a map in Appendix A-1.1. A geological time scale is located in Appendix A-1.3 in support of the following account.

5.2 REGIONAL GEOLOGICAL SETTING

5.2.1 Location and tectonic setting

The Wanganui Basin lies in the south-western part of the North Island and is a major Cenozoic sedimentary basin (McIntyre 2002). Wanganui Basin is an elliptical sedimentary basin trending NNE-SSW and occupies a back-arc position behind and parallel to the axial ranges of the North Island. The formation of the basin is a result of sublithospheric tectonic loading, highlighted by sediment loading and driven by both overlying (Australian) and underthrusting (Pacific) plates (Stern et al. 1993) (Fig. 5.1).

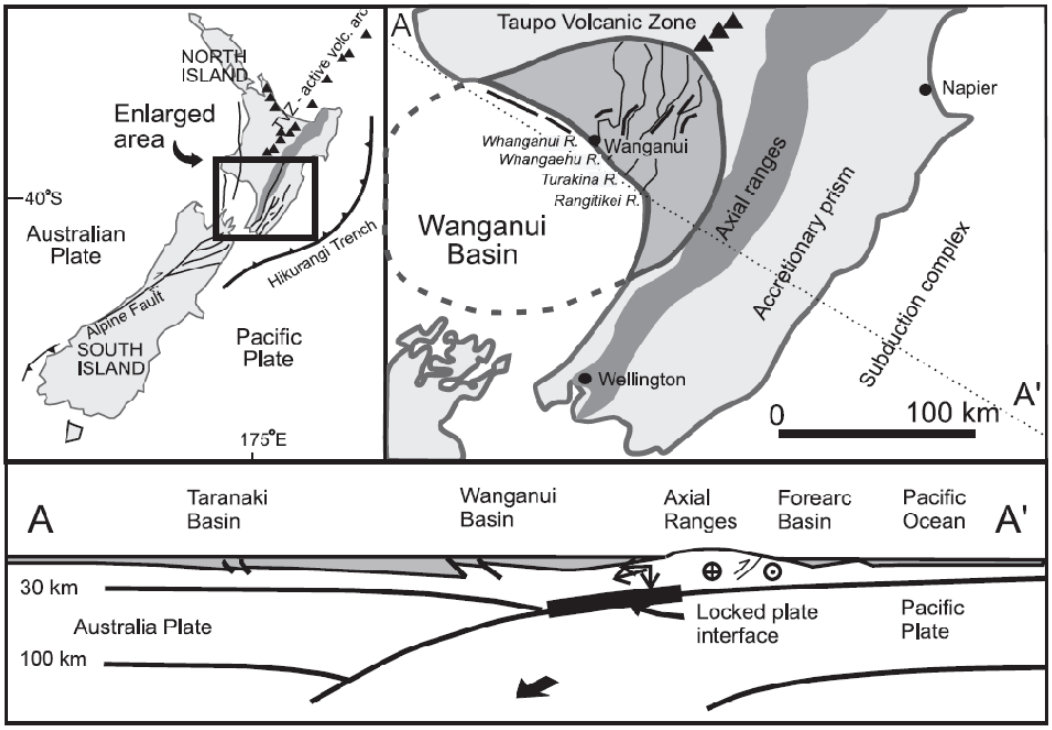

Figure 5.1 Locality map and geological setting of the Wanganui Basin. Cross section shows the regional tectonic setting across the Wanganui Basin and the main features of the Hikurangi subduction margin. After Carter & Naish (1998).

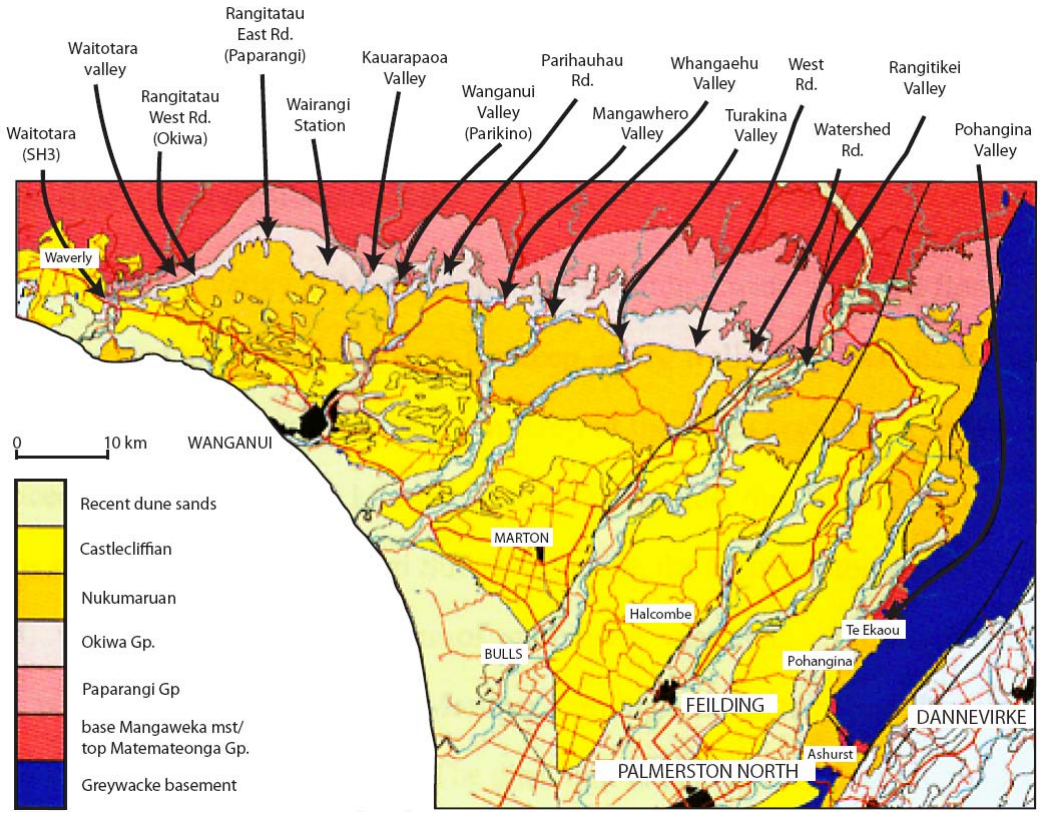

Figure 5.2 Plio-Pleistocene geology of the Wanganui Basin. Locations at the top denote key locations where strata are exposed from McIntyre (2002) .

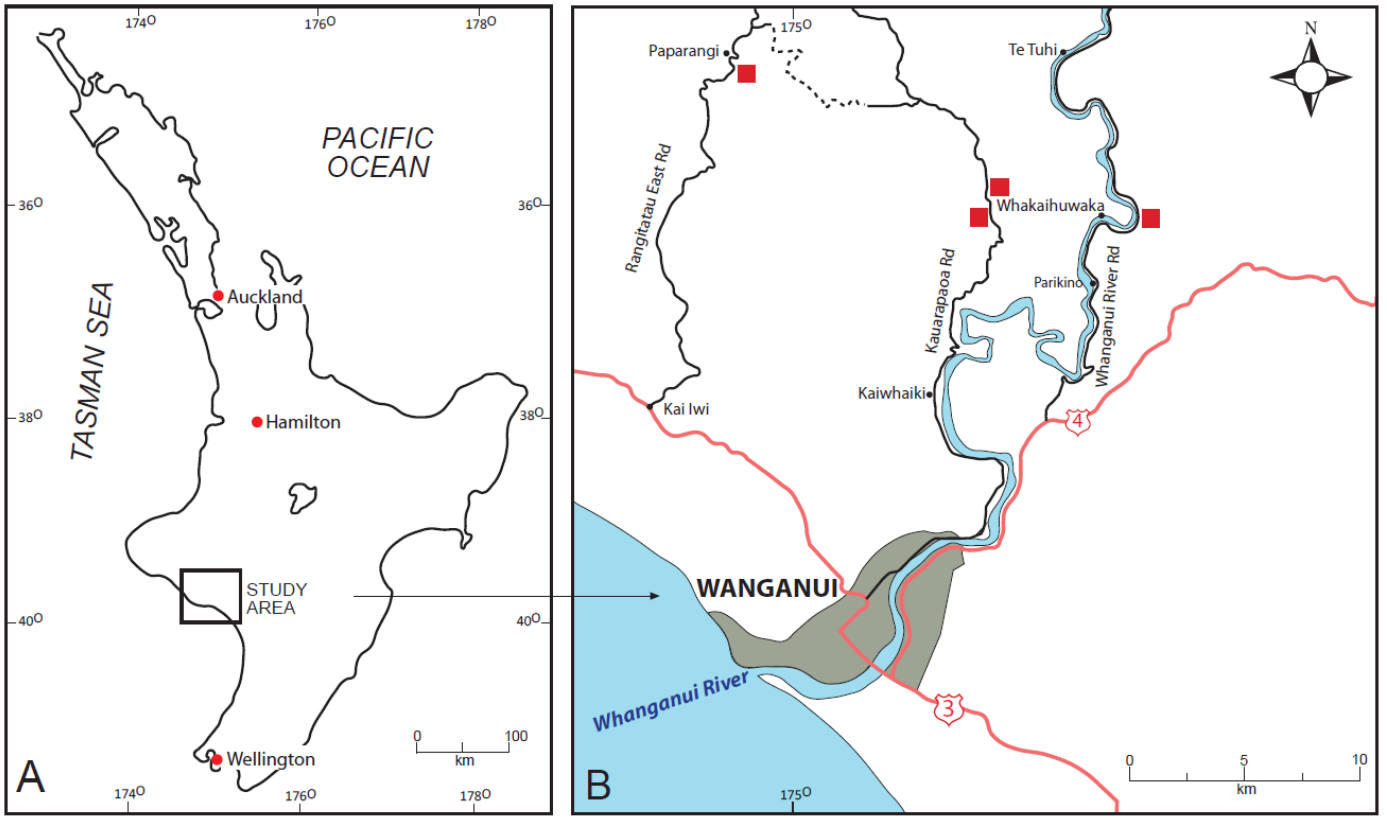

Figure 5.3 (A) North Island (New Zealand) and location of the Wanganui study area. (B) Detail of site locations with outcrops (red boxes) of Wilkies Shellbed at Paparangi, Rangitautau East Road (S22/782637); Parikino, Whanganui River Road (S22/955571); and Kauarapaua Valley – Kauarapaua Road (S22/901592).

A southwards migration of the Wanganui Basin depocentre from the vicinity of the central North Island in the Miocene to its present day position north of Cook Strait has resulted from the dextral oblique nature of the interaction of the plates. Progressive subsidence and onlap towards the south in conjunction with emergence and offlap in the north has lead to a 4 km thick deposition of gently southward-dipping (2-15^{o}) mainly shelfal sediments (Fleming 1953; Anderton 1981; Naish & Kamp 1995; McIntyre & Kamp 1998). Volcanics of the Central Volcanic Region (CVR) form the northern boundary of the basin and obscure the relationship between the sediments of the Wanganui Basin and those of the Taupo Graben towards the north. The modern eastern boundary of the basin is formed by uplifted greywackes of the Ruahine and Tararua Ranges that form part of the axial ranges in the North Island (Anderton 1981). Towards the west the Taranaki and Wanganui Basins are separated by the Patea-Tongaporutu High, bounded on the west by the Taranaki Fault. The southern edge of the basin is marked by the Marlborough Sounds (Anderton 1981) (Fig 5.4).

Towards the north of the basin the strata become progressively older, with the oldest being Oligocene in age in the Te Kuiti region. The basin fill of the Wanganui Basin consists of a near-complete sedimentary record spanning from the late Oligocene to the present, comprised of shallow to bathyal deposits. The southward migration of the basin depocentre has been accompanied by uplift in the northern parts of the basin, which has resulted in much of the basin fill becoming exposed on land (McIntyre 2002).

5.2.2 Structure

The Wanganui Basin structure is a basin in which all the beds of the Wanganui Series show gentle regional dips towards a depocentre south of Wanganui and are cut by NE-NNE-trending faults generally downthrown towards the basin (Fleming 1953; Anderton 1981). The faults in the region generally have a small throw, but a number have some expression. The sediments in the Wanganui Subdivision dip southward at angles of 2^{o} to 8^{o}. In general, the older beds in the subdivision are more inclined than the younger ones (Fleming 1953). Emergence of the northern part of the basin has been associated with progressive migration and offlap towards the sedimentary depocentre located in the south. At the margins of the basin, block faulting of the basement has led to the development of gentle

anticlines. Within the faulted zone forming the southeastern edge of the basin, structures are related to the growth of faults during deposition (Anderton 1981).

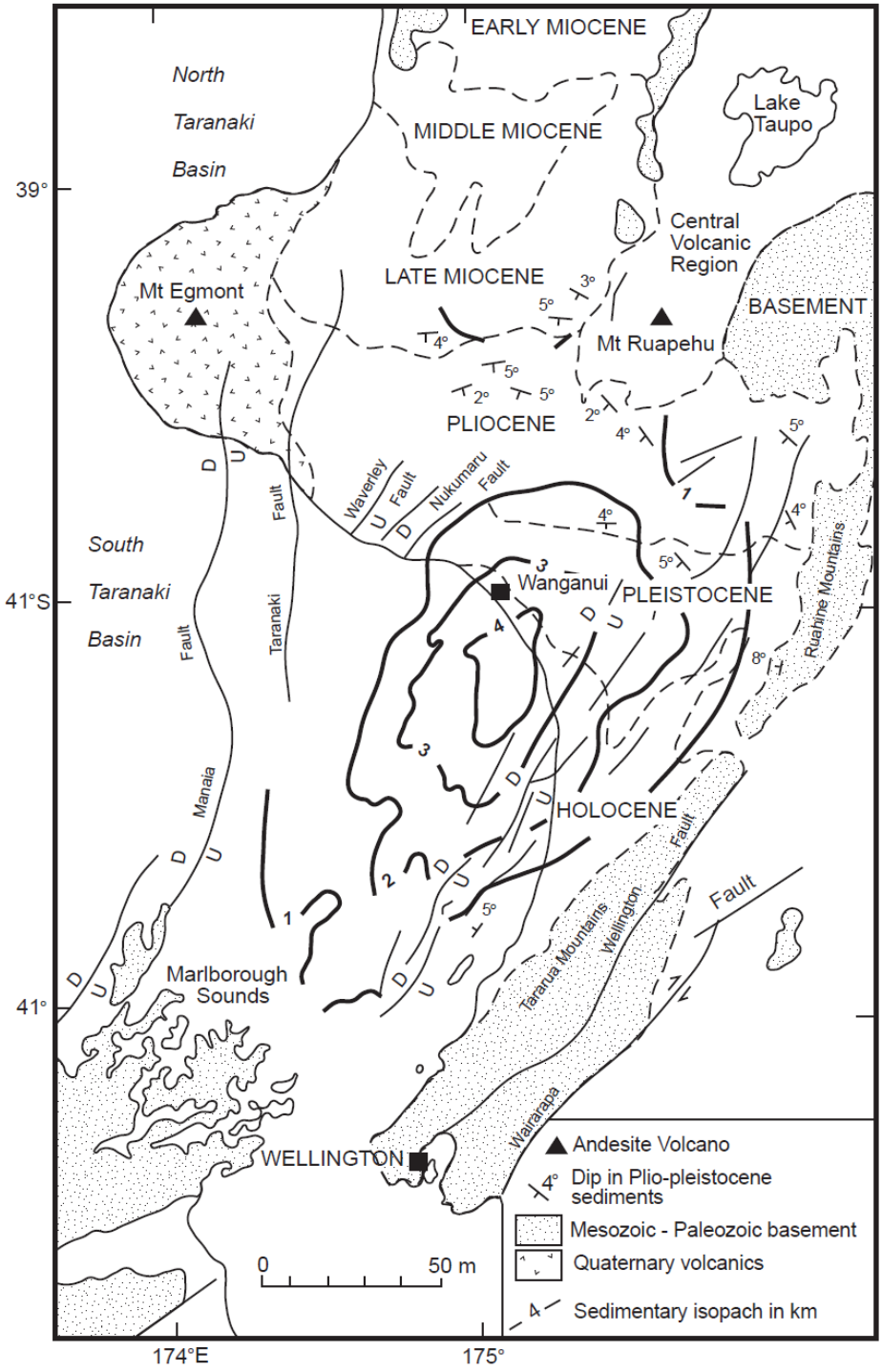

Figure 5.4 Key features of the Wanganui Basin including simplified geology, basin margins and thickness of Cenozoic beds. Adapted from Stern et al. (1993).

The regional fault pattern of the Wanganui Basin has been interpreted as a divergent dextral wrench system (Anderton 1981). The western and southeastern basin margins represent primary wrench faults, the faults trending northeast across

the central basin represent strike slip faults. This interpretation is somewhat complicated by the differing age of the boundary fault systems. Uplift along the southeastern boundary has only been recognised for Pliocene-Pleistocene sedimentation, but earlier movement is possible (Anderton 1981).

Offshore structure and stratigraphy of the Wanganui Basin has been determined from the offshore well Kupe-1 and seismic profiles. The offshore portions of the Wanganui Basin have three major fault zones: the Rangitikei, Rauoterangi and Turakina faults. Indicative of wrench structural styles are *en echelon* fault traces and abrupt changes in the throw along the individual fault planes within these zones (Anderton 1981).

5.3 STRATIGRAPHY

The Okiwa Group (Fig. 5.5) was deposited on the western margin of Wanganui Basin and is lithologically diverse, comprising mixed carbonate-siliciclastic rocks. The Owika Group includes many constituent formations (Fleming 1953; Kamp & McIntyre 1998; McIntyre & Kamp 1998; McIntyre 2002). These generally correspond to cyclothems consisting of coarse, basal bioclastic limestone (coquina shellbeds) overlain by sparsely fossiliferous siltstones and sandstones. The Okiwa Group has three formations - Parikino Formation, Whakaihuwaka Formation and Whauteihi Formation. The Whauteihi Formation is of particular interest here as it contains the Wilkies Shellbed.

5.3.1 Whauteihi Formation

5.3.1a Definition of unit

The Whauteihi Formation contains three members: Wilkies Shellbed, Cable Siltstone and Te Rimu Sandstone, in ascending stratigraphic order.

5.3.1b Name and type locality

The Whauteihi Formation is named after the Whauteihi Stream, a tributary to the Whanganui River that enters near Te Rimu. The type locality was described by McIntyre & Kamp (1998) and is situated along the Whanganui River Valley in a roadside outcrop (S22/954572).

5.3.1c Boundaries and underlying contact

The Whauteihi Fomation is bounded above by the Whakaihuwaka Formation and the underlying contact is the Moukuku Formation, part of the Paparangi Group (Fig. 5.5).

5.3.1d Distribution and thickness

The thickness of the Whauteihi Formation varies at the following locations: 22 m (Turakina); 23 m (Whangaehu); 65 m (Parihauhau); 53 m (Wanganui); 49 m (Kauarapaoa); >10 m (Wairangi); 5.5 m (Paparangi); and 3 m (Okiwa) (McIntyre 2002).

5.3.1e Age

Middle Mangapanian.

5.3.2 Wilkies Shellbed Member

5.3.2a Definition of unit

The Wilkies Shellbed is a weakly cemented, fossiliferous, massive to crudely horizontally bedded very fine sandy shellbed, comprised of abundant *in situ Crassostrea ingens* (giant oyster) shells (McIntyre 2002).

5.3.2b Name and type locality

The thick *Crassostrea*-dominated shellbed which crops out distinctively across the western part of the Wanganui Basin was named "Wilkies Shellbed" by Fleming (1953). This formalised a name for the "Shellbed near the mouth of the Waitotara River, opposite Wilkies Farm" as first described by Park (1887). The type locality for the shellbed is situated at Te Rimu in the Wanganui River valley (S22/954572) (McIntyre 2002).

5.3.2c Boundaries and underlying contact

The Wilkies Shellbed conformably overlies the Makokako Sandstone (Paparangi Group) at Parikino, with the lower boundary marked by a concretionary layer 0.5 m thick. In the Kauarapaoa Valley and in Paparangi the shellbed uncomformably overlies the sandstone with up to 2 m relief on the contact. The overlying massive blue-grey Cable Siltstone conformably overlies the shellbed.

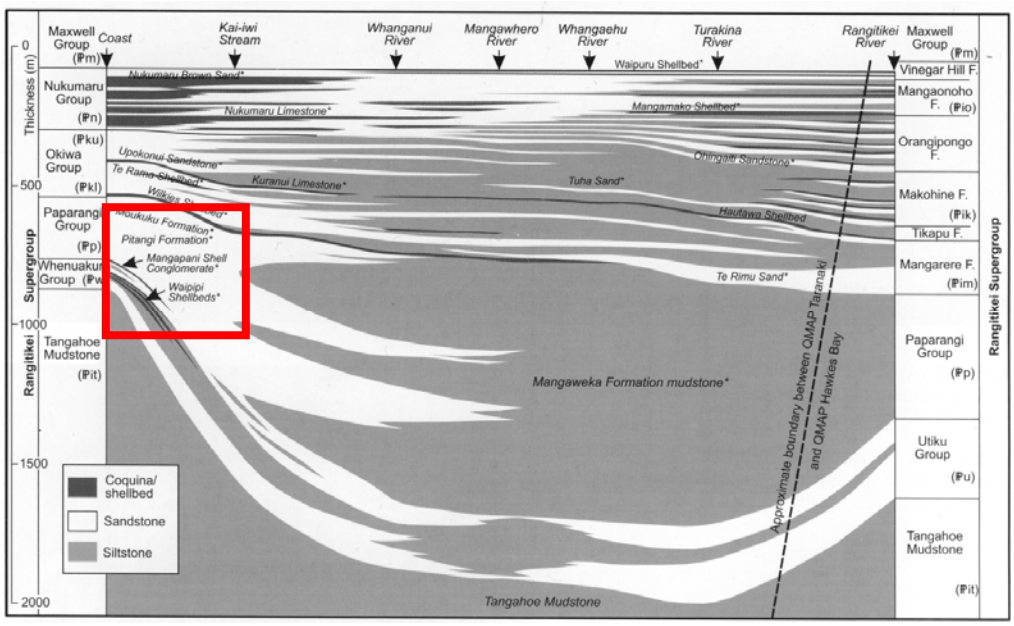

Figure 5.5 Early to middle Pliocene stratigraphy of the Rangitikei Supergroup showing lithological relationships across the Wanganui Basin. Vertical scale is representative of the relative thickness of units in the basin and the width is approximately 100 km (vertical exaggeration ~ 40X) (Townsend et al. 2008).

5.3.2d Distribution and thickness

The greatest thickness of the Wilkies Shellbed is 15 m with up to 10 m relief on the upper contact (Kamp et al. 1999). It acts as a useful marker horizon and extends over 48 km of outcrop throughout Wanganui Basin. The Wilkies Shellbed ranges in thickness at the following locations: 1m (Whangaehu); 12 m (Parihauhau); 5-15 m (Wanganui); 8 m (Kauarapaoa); 10 m (Wairangi); 3.5 m (Paparangi); and 3 m (Okiwa) (McIntyre 2002).

5.3.2e Paleontology

The shellbed is mainly composed of abundant *Crassostrea ingens* held in a sandy silt matrix. A large variety of other molluscan shells are usually also present within the shellbed (Ker 1970). The paleontology of the Wilkies Shellbed has been described in detail by McIntyre (2002) and fossils are held within the University of Waikato fossil collection and database.

5.3.2f Age

Middle Mangapanian (2.75 Ma) (McIntyre 2002).

5.3.3 Cable Siltstone Member

5.3.3a Definition of unit

The Cable Siltstone has a consistent character across the basin. It is a slightly cemented, sparsely fossiliferous, blue-grey siltstone (McIntyre 2002).

5.3.3b Name and type locality

The Cable Siltstone was first described and named by Ker (1970) in the Whanganui River Valley at Te Rimu. At this location a cableway extends across the Whanganui River. The type section for the Cable Siltstone is located at Te Rimu, Whanganui River Valley (S22/954572) (McIntyre 2002).

5.3.3c Boundaries and underlying contact

The Cable Siltstone conformably overlies the Wilkies Shellbed Member. The massive siltstone then gradationally coarsens upwards into the Te Rimu Sandstone Member (McIntyre 2002).

5.3.3d Distribution and thickness

The siltstone is distinguishable from other siltstones in the Okiwa Group by its proximity to the Wilkies Shellbed, except in the western part of the basin where the shellbed is cut out by an unconformity. The thickness of the siltstone ranges at the following locations: 14 m (Whangaehu); 51 m (Parihauhau); 28 m (Wanganui); 10 m (Kauarapaoa); and 2 m (Paparangi) (McIntyre 2002).

5.3.3e Paleontology

Rare *in situ* pectinids and other molluscs such as *Ostrea* (bivalve) and *Amalda novaezelandiae* (gastropod) are found throughout the member in most sections (Beu & Maxwell 1990; McIntyre 2002).

5.3.3f Age

Middle Mangapanian (2.75 Ma) (McIntyre 2002).

5.3.4 Te Rimu Sandstone Member

5.3.4a Definition of unit

The Te Rimu Sandstone comprises a slightly cemented, sparsely fossiliferous, micaceous, yellow-brown fine sandstone.

5.3.4b Name and type locality

The Te Rimu Sandstone was named by Fleming (1953), based on the typical occurrence of the sandstone at Te Rimu in the Whangaui River Valley. The type locality is thus at Te Rimu, Whanganui River Valley (S22/954572). This locality also includes the type Wilkies Shellbed and Cable Siltstone, where all three members have great exposures on the Whanganui River roadside (McIntyre 2002).

5.3.4c Boundaries and underlying contact

In all sections the Te Rimu Sandstone is conformable with the underlying Cable Siltstone. The upper surface is unconformably overlain by the Mangamahu Shellbed. One exception is in the Turakina Valley where the sandstone unconformably overlies the Mangaweka Mudstone (McIntyre 2002).

5.3.4d Distribution and thickness

The Te Rimu Sandstone is not observed to the west of Kauarapaoa Valley, it is covered by vegetation at Wairangi, and does not occur at both Paparangi and Okiwa sections as it is truncated by an angular unconformity at the base of the Mangamahu Shellbed. The thickness of the member varies over the following locations: 22 m (Turakina); 8 m (Whangaehu); 20 m (Wanganui); and 10 m (Kauarapaoa) (McIntyre 2002).

5.3.4e Paleontology

Where the Te Rimu Sandstone is exposed at Whakaihuwaka there is a thick layer of shells containing specimens of reworked and disarticulated *Chlamys, Divaricella, Pteromyrtea, Bassina, Gari, Ruditapes* and *Amalda*. In the Kauarapaoa Valley the sandstone presents itself as barren and massive (Beu & Maxwell 1990; McIntyre 2002).

5.3.4f Age

Middle Mangapanian (2.75 Ma) (McIntyre 2002).

5.4 SITE DESCRIPTIONS OF THE WILKIES SHELLBED

Three key locations in the Wanganui Basin (Fig 5.3) were visited where the Wilkies Shellbed is well exposed. The largest section occurs at Parikino, along

Whanganui Road, where 20 stratigraphic logs were taken as well as a detailed sketch section along the roadside. Other localities include Paparangi and the Kauarapaoa valley. The stratigraphic columns taken from each location are included on a CD as Digital Appendices.

5.4.1 Whanganui River section (Parikino)

This locality comprises the most spectacular occurrence of the Wilkies Shellbed along Whanganui River Road situated near the oxbow in the river at Parikino (Fig. 5.3B) (S22/955571). This is the most accessible and well known occurrence of the shellbed in the Wanganui Basin (McIntyre 2002). Stratigraphic columns are provided in full in Appendix D-1.1. See Enclosure 1 for a detailed sketch from this location.

5.4.1a Paleontological features

The most abundant species in the lower 3 m of the Wilkies Shellbed at this location is the extinct giant oyster *Crassostrea ingens* (Zittel) (Fig. 5.6) and *Chlamys.* The upper part of the bed is abundant with *in situ* and horizontally bedded *Crassotrea*, rare *Ostrea*, *Purpurocardia* and *Neothyris*. In sandier pockets within the shellbed a slightly difference faunal assemblage is found consisting of *Maoricolpus*, *Amalda* (Fig. 5.7), *Divaricella*, *Zenatia* and *Cyclomactra* (McIntyre 2002).

5.4.1b Stratigraphic features

The accumulation of oysters (*Crassostrea ingens*) at Parikino occurs within a light brown to grey fine grained sandy siltstone matrix. Slight to moderate weathering is sometimes evident. Thickness of the oyster beds at this location ranges from 2 to 15 m (Fig. 5.8) over a lateral distance of approximately 580 m along the riverside (Enclosure 1). Here the geometry of the oyster accumulation is crudely bedded and the beds interfinger along the road cut. Sandier pockets within the shellbed have sparse to no *Crassostrea* present (Fig. 5.8). The shellbed conformably overlies the Makokako Sandstone and a prominent concretionary horizon, 0.5 m thick, marks the lower boundary.

5.4.1c Taphonomic features

All of the *Crassostrea* shells are articulated and are approximately 120 mm in length. Abrasion, rounding and fragmentation of oysters is low. Some specimens have undergone a significant amount of weathering and crumble to a fine powder. Biological modification in the form of bioerosion is moderate in most specimens (further discussed in Chapter Eight). Shells are oriented in life position with little disturbance (Fig. 5.9). In densely - loosely packed beds the abundance of *Crassostrea* is > 45%. Dispersed beds have a lower abundance of around 10%. Densely packed shells are both matrix and oyster supported.

5.4.2 Kauarapaoa Road (Kauarapaoa Valley)

The most accessible outcrop of the Wilkies Shellbed along Kauarapaoa Road (Fig 5.3B) occurs on a farm overlooking the Kauarapaoa Stream (S22/901592). Three other small outcrops also occur along the roadside in the Kauarapaoa Valley. All stratigraphic columns from this location are featured in full in Appendix D-1.1.

5.4.2a Paleontological features

The shellbed here is divisible into two facies (Fig 5.10). The lower portion of the shellbed comprises about 0.5 m of coquina. The coquina is dominated by bivalves (*Pteromyrtea, Limatula, Ostrea, Eumarica)* and gastropods (*Maoricolpus, Amalda)* are also common. The upper part of the shellbed is predominantly comprised of the extinct giant oyster *Crassostrea ingens* and the pectinid *Chlamys* (Fig. 5.11) (McIntyre 2002).

5.4.2b Stratigraphic features

The Wilkies Shellbed is 3 m thick (Fig. 5.10) at the above farm outcrop and reaches a maximum thickness of about 8 m elsewhere in the Kauarapaoa Valley (Fig. 5.12). The geometry of the shellbed remains similar throughout the valley, with crudely bedded *Crassostrea* interfingering with matrix sandy siltstones along the outcrops at each locality. The shellbed forms an unconformable contact with the underlying Makokako Sandstone. The sharp contact between the slightly cemented Wilkies Shellbed and the underlying loose sandstone forms an overhanging ledge at all of the sites in the Kauarapaoa Valley.

Figure 5.6 Plan view of a right valve of *Crassostrea ingens* (Zittel) collected from Parikino (S22/955571). Sample number WLK11. Sample stored in the Department of Earth and Ocean Sciences, University of Waikato, Hamilton, New Zealand.

Figure 5.7 *Crassostrea ingens* contained within a fine sandy siltstone matrix. Iron stained weathering is prominent. Note the accumulation of *Amalda* (gastropods) within the Wilkies Shellbed at Parikino (S22/958573).

Figure 5.8 Thickest occurrence of the Wilkies Shellbed along Whanganui River Road, Parikino. Here the shellbed reaches 15 m thick and conformably overlies the Makokako Sandstone. Note how the *Crassostrea* are crudely bedded and horizons can be seen interfingering into the sandstone lens in the centre of the photograph (S22/955571).

Figure 5.9 *Crassostrea ingens* in life position with little disturbance. Shells along the Whanganui River, Parikino are densely packed and both matrix and oyster supported (S22/955571).

Figure 5.10 Panoramic view of the Wilkies Shellbed cropping out at the Kauarapaoa Stream (S22/901592). Two facies are differentiated within the Wilkies Shellbed, the upper Crassostrea dominated overhangs the lower coquina facies. Vertical scale bar is approximately 1 m.

5.4.2c Taphonomic features

All the oyster shells are articulated and approximately 120 mm in length. There is no apparent fragmentation, abrasion or rounding. Biological modification is moderate to high in most of the shells. All specimens are orientated in life position. Relative abundance of shells is >45% in densely packed areas of the shellbed (Fig. 5.13), and in dispersed areas the abundance is about 15%. Densely packed shells involve both matrix and oyster support whereas low to moderate accumulations are entirely matrix supported.

5.4.3 Rangitatau East Road (Paparangi)

A single site was studied at this locality that involves only a thin occurrence of the Wilkies Shellbed. Three stratigraphic columns were described (Appendix D-1.1).

5.4.3a Paleontological features

The shellbed as this location involves two facies (Fig. 5.14). In the lower part of the shellbed there is a diverse assemblage of molluscs, with common *Ostrea, Phialopecten, Patro, Purpurocardia, Crepidula* and *Neothyris*. The lower shellbed grades upwards abruptly into an increasingly *Crassostrea* and *Chlamys* dominated portion of the shellbed (McIntyre 2002).

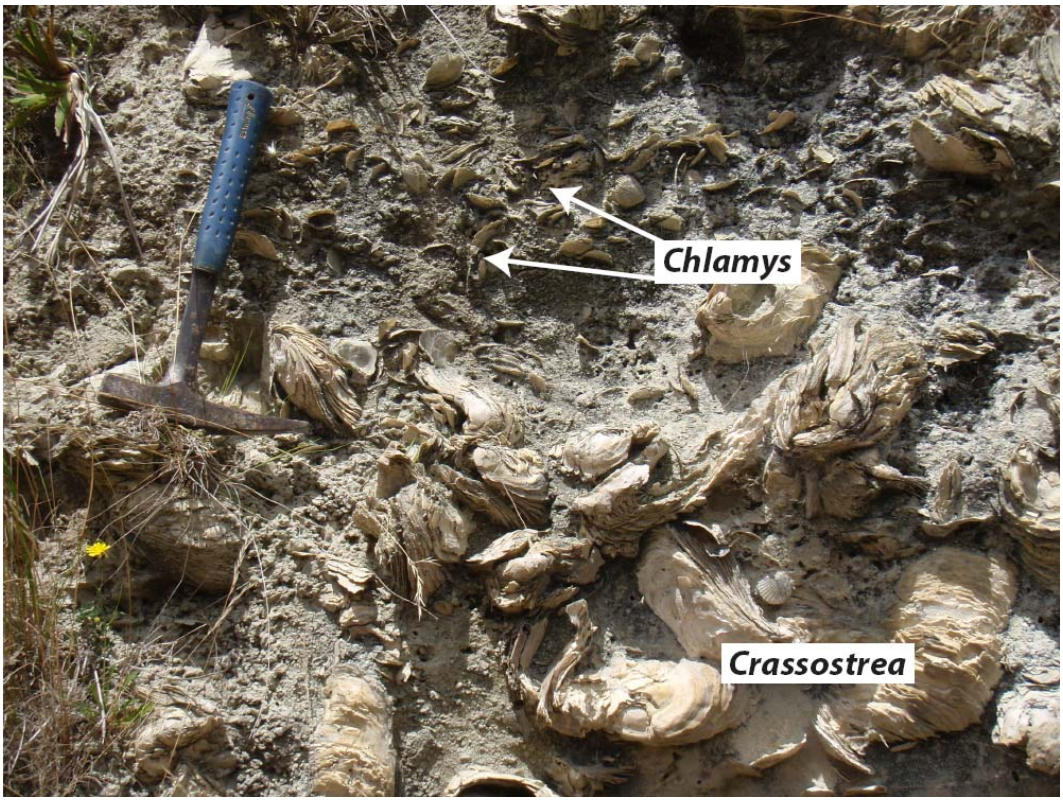

Figure 5.11 Abundant *in situ* oyster *Crassostrea* and the pectinid *Chlamys* dominate the upper part of the Wilkies Shellbed in the Kaurapaoa Valley (S22/901592).

Figure 5.12 Thickest accumulation (8 m) of Wilkies Shellbed along Kauarapaoa Road (S22/897584).

Figure 5.13 Densely packed *Crassostrea* in the upper portion of the Wilkies Shellbed in the Kauarapaoa valley (S22/901592). Dense accumulations like this involve a combination of both matrix and oyster supported specimens.

5.4.3b Stratigraphic features

The shellbed at Paparangi is contained within a massive, blue-grey siltstone matrix. This is more common in the central parts of the basin (McIntyre 2002). The shellbed is 3.5 m thick and crops out along the section for 60 m. The geometry of the shellbed at this location is again crudely bedded with the *Crassostrea* occurrences interfingering along the section. The shellbed forms an unconformable contact with the underlying Makokako Sandstone. The Wilkies Shellbed is conformably overlain by the Cable Siltstone, totalling only about 2 m thick at this location (Fig. 5.15).

Figure 5.14 An abruptly gradational contact separates the *Crassotrea* and *Chlamys* (pectinid) dominated upper Wilkies Shellbed from the lower Wilkies Shellbed at Paparangi. The lower bed has a rich assemblage of molluscs with common *Ostrea, Phialopecten, Patro, Purpurocardia, Crepidula* and *Neothyris* (S22/782637).

5.4.3c Taphonomic features

The *Crassostrea* at this location are a mixture of articulated and disarticulated specimens. Size of most specimens is approximately 120 mm. Fragmentation and abrasion is low to moderate. Shells appear very weathered at this location, making description difficult. Biological modification remains moderate to high in the majority of the shells viewed. Orientation of shells at this location is slightly more disturbed than at other localities. The relative abundance of the *Crassostrea* is higher (about 40%) in the top part of the Wilkies Shellbed at this location, dropping to as low as 10% in the lower section of the shellbed. Both portions of the shellbed exhibit dispersed shells that are matrix supported.

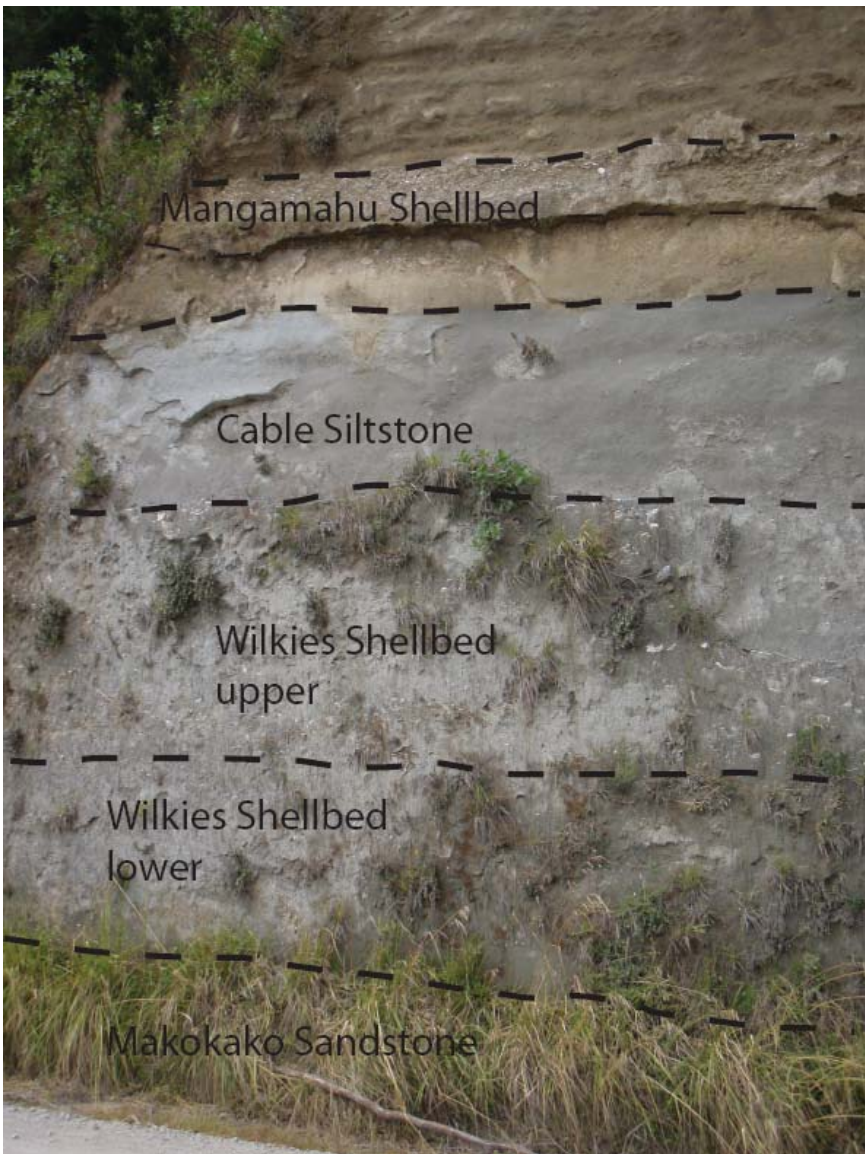

Figure 5.15 Wilkies Shellbed at Paparangi. At this locality the shellbed unconformably overlies the Makokako Sandstone and is in turn conformably overlain by the Cable Siltstone (S22782637).

5.5 WILKIES SHELLBED SUMMARY

The geometry of the shellbed is much the same at each location, involving crudely bedded shells dominated by *Crassostrea.* The Wilkies Shellbed is thus a biostrome which is defined as a layered accumulation of *in situ* organisms. A biostrome lacks a mound or "reef" type structure that is normally associated with the formation of oysters (McIntyre 2002).

The characteristics of the Wilkies Shellbed vary at each location seen. The main occurrence of the shellbed at Parikino presents itself as a 2-15 m thick densely to loosely packed accumulation of *Crassostrea ingens* that has a conformable sharp contact with the underlying Makokako Sandstone. Here the host matrix is a light

brown, fine-grained, sandy silt and all shells are in life position, densely accumulated and supported both by other oyster shells and matrix.

Moving into the Kauarapaoa Valley the shellbed ranges from 3-8 m in thickness and is relatively uniform across the valley. Here the Wilkies Shellbed involves two facies, a lower coquina and an upper *Crassostrea* dominated facies. The oysters themselves are articulated and orientated in life position, form a dense to loosely packed accumulation and are both oyster and matrix supported. The host matrix of the shellbed is light brown fine-grained sandy silt. The contact with the underlying Makokako Sandstone at this location is unconformable and the slightly cemented shellbed forms an overhang over the soft sandstone.

At the Paparangi location along Rangitatau East Road the shellbed again comprises two facies. The lower facies contains a diverse assemblage of molluscs and can be seen abruptly grading into a *Crassostrea* dominated shellbed in the upper part. The accumulation of shells here is also thinner in comparison to other localities and the abundance of shells is relatively low at 40%. The *Crassostrea* are more haphazardly orientated and more increasingly abraded and fragmented in comparison to other sites. Consequently the shells here are almost entirely matrix supported, which here is a massive, blue-grey siltstone. The underlying contact at this location with the Makokako Sandstone is unconformable.

5.6 SEQUENCE STRATIGRAPHIC INTERPRETATION

The Wilkies Shellbed has been placed within a sequence stratigraphic framework by McIntyre (2002). The base of the shellbed has been interpreted as a sequence boundary, due to unconformity occurring over parts of the basin which, however, moves into a conformable contact towards the east. The observed unconformity is likely to result from wave planation, as evidence by the reworked and fragmented shallow-water faunal coquina shellbed present at the base of the Wilkies Shellbed. The Wilkies Shellbed onlaps the unconformity in a regional sense. This unconformity can also be referred to as a transgressive surface of erosion (TSE), created by wave action as the shoreline was retreating. From this it can be depicted that the sequence boundary is also a marine flooding surface (MFS), resulting from a rapid increase in water depth (McIntyre 2002). The position of all the above surfaces is shown in Figure 5.16.

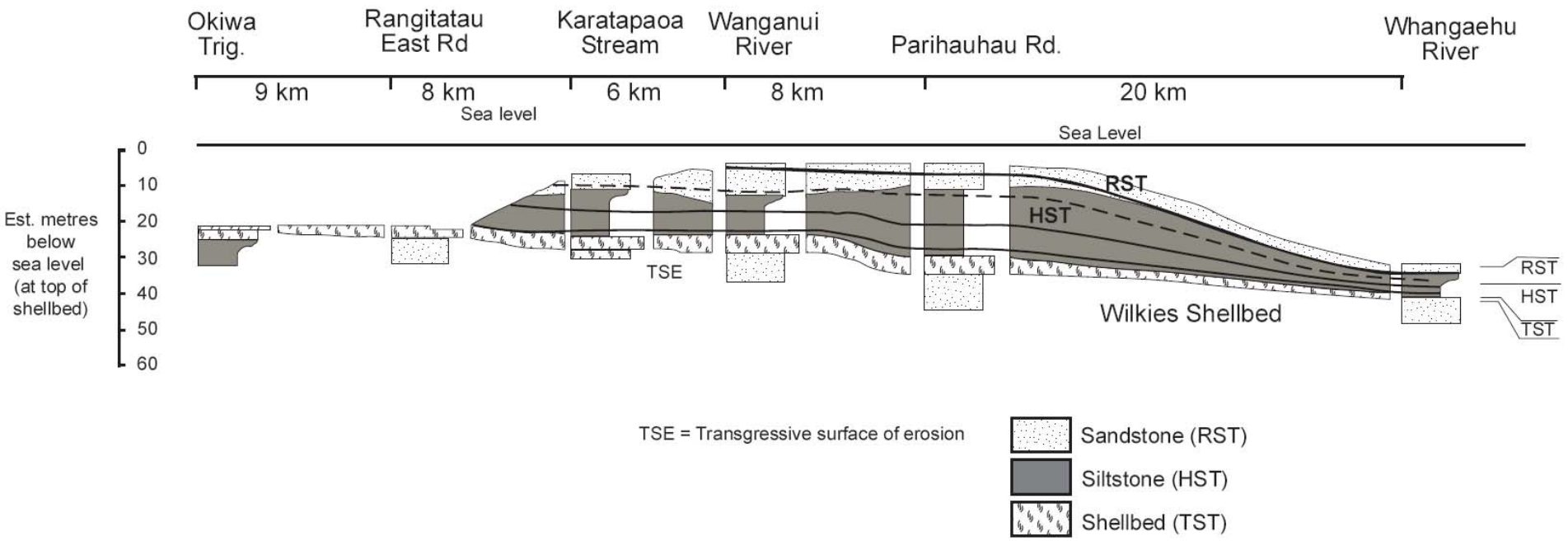

Figure 5.16 Sequence stratigraphic framework of the Whauteihi Formation, showing the main facies groups and distribution of the Wilkies Shellbed (McIntyre 2002).

The Wilkies Shellbed is part of a transgressive systems tract based on molluscan assemblages and facies evidence which suggests it accumulated in a progressively deepening marine environment. This includes more estuarine molluscan assemblages in the onlap portion moving through to more marine assemblages in the backlap part of the shellbed. The Wilkies Shellbed was dominated by a shallow, high energy shoreface which migrated upwards into lower energy mid-shelf conditions towards the upper contact of the shellbed with the Cable Siltstone. The Shellbed was thus onlapping and overlying the transgressive surface (TSE) (McIntyre 2002).

The two facies of the Wilkies Shellbed recognised at the Paparangi and Kauarapaoa Valley sections can be attributed to two different types of shellbed, both of which correspond to a different carbonate facies. Using the approach of Kidwell (1991a)(1991), Naish & Kamp (1997) have identified four different types of shellbeds within the Whauteihi Formation. The two shellbeds that have been identified within the Wilkies Shellbed correspond to onlap and backlap shellbeds. Onlap refers to the discontinuation of strata in a landward direction against a sloping surface whereas backlap refers to the termination of beds at the distal basinward edge of a retrogradational facies succession (Kidwell 1991a; Naish & Kamp 1997).

The lowermost part of the Wilkies Shellbed at Kauarapaoa Valley and Paparangi which is dominated by broken and fragmented bivalves in a sandstone matrix, corresponds to an onlap shellbed. This was deposited in a high energy, shallow setting, onlapping during transgression. An onlap shellbed (Fig. 5.17) often develops when winnowing and by-passing of sediment from the nearshore environment basinward leaves a shell lag or gravel (McIntyre 2002).

The shellbed overlying the fragmented shell facies at Kauarapaoa Valley and Paparangi is dominated by *Crassostrea* and comprises the whole shellbed seen at Parikino along the Whanganui River. This shellbed is identified as a backlap shellbed, or backstep as identified by Kidwell (1991a). This is a deeper water shellbed or biostrome and formed under conditions of reduced turbidity and low sedimentation rate. During transgression the shellbed continues to migrate

shoreward, thus maintaining the depth at which the *Crassostrea* can live *in situ*, within the fine grained sandy silt host sediments (Fig 5.17) (McIntyre 2002).

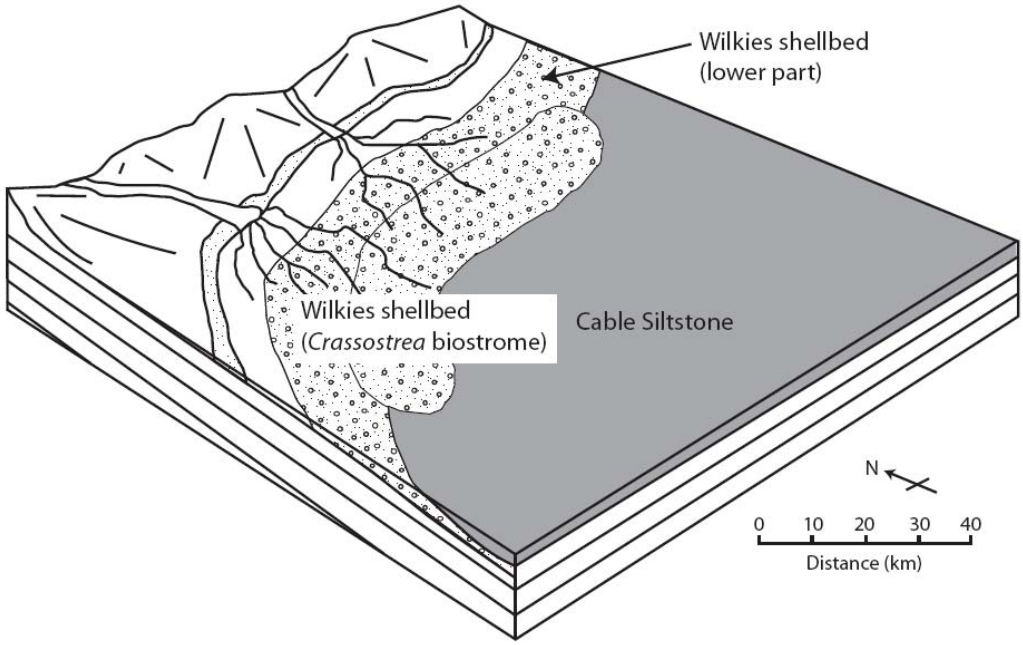

Figure 5.17 3-dimensional facies model showing the position of the Wilkies Shellbed on the shoreline of the Wanganui Basin. The diagram is representative of the shellbeds growth in the late part of a transgression. The *Crassostrea* biostrome represents the backlap shellbed and the lower part is the onlap shellbed. Adapted from McIntyre (2002).

CHAPTER SIX
Oyster geochemistry

6.1 INTRODUCTION

For more than 50 years, mollusc shells have been known archives of past environmental conditions (Emiliani et al. 1964; Clark 1968; Epstein et al. 1976; Davenport 1983). A vast amount of information about both past and present day environments is contained within the skeleton of fossil and living organisms (Rhoads & Lutz 1980). During mollusc shell growth, the layers of the shell are deposited sequentially, and the physical structure and/or chemical composition of these shells may reflect the environmental conditions at the time formed. An important goal of paleoecology is to determine the conditions under which fossil organisms lived (Kirby 2000). Molluscs are especially beneficial in this regard as they have a wide geographical range and can provide a high-resolution seasonal record of environmental conditions (Gröcke & Gillikin 2008).

This chapter seeks to interpret the broad environmental conditions for the oyster species at the study localities through the use of stable carbon and oxygen isotopes and elemental ratios of their shell carbonate. These geochemical tools can help elucidate the life spans, growth rates, season of death, temperature/salinity, and seasonality from shells that possess accretionary growth (Kirby et al. 1998). Data from extant species from Foveaux Strait and Patagonia are also included for further comparison.

6.2 MODERN SETTINGS

6.2.1 Foveaux Strait, New Zealand

The Chilean oyster *Ostrea chilensis* has been transferred to many locations around the globe for aquaculture development (Fig. 6.1). Foveaux Strait, New Zealand is home to the most extensive wild population and fishery of this oyster (Fig 6.2) (Jeffs & Hickman 2000). The oyster is a commercially important flat oyster and native to New Zealand and parts of South America. It is abundant in many intertidal and shallow subtidal environments in New Zealand (Beu & Maxwell 1990).

Figure 6.1 The flat oyster *Ostrea chilensis.* Image courtesy of Keith Micheal at National Institute of Atmosphere and Water (2008).

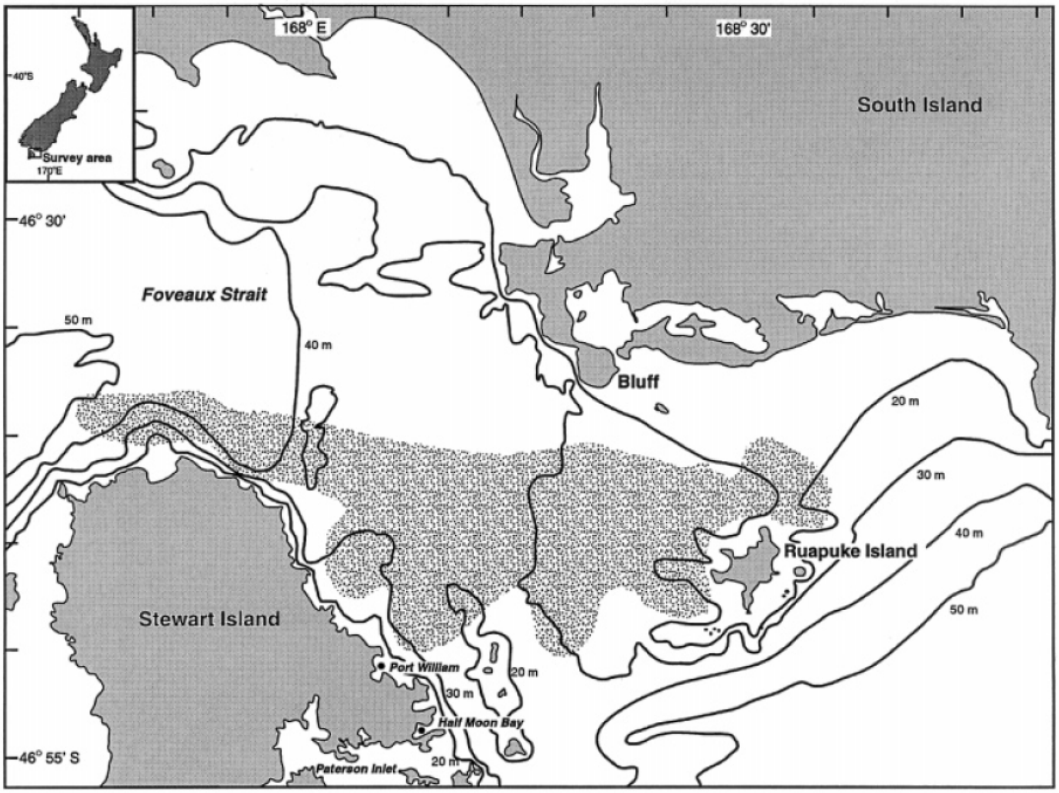

Figure 6.2 Foveaux Strait showing main features and bathymetry and extent of the commercial beds of *Ostrea* chilensis exploited between 1950 and the present. Inset: location of Foveaux Strait in New Zealand (Cranfield et al. 1999).

Foveaux Strait is about 80 km long and 23-35 km wide and follows an S-shaped course roughly northwest/southeast between New Zealand's South Island and Stewart Island (Cranfield et al. 1999, 2003). Foveaux Strait is comprised of a mixture of sand and gravel substrates. In areas where wave energy is high and strong tides dominate, the substrate is composed of gravels. Conversely, where wave energy is less and tidal currents are slower, sands overlay the gravels (K.Michael, *pers. comm.* 2009). Oysters are restricted to 18 to 45 m water depth (Fleming 1952; Cullen 1962) and high densities of oyster occur on predominately sand, gravel, and shell (mainly the shells of oysters, *Oxyperas elongata* and *Glycymeris modesta*) substrate (Fig. 6.3). The "reefs" are comprised of various shells, filled by fine sediment, with the organism living on the outside. These structures are clearly delineated by tides; they have very sharp edges between flat featureless gravels and the "reef" structure (K.Michael, *pers. comm.* 2009). Epifaunal reefs are often associated with other fauna such as bryozoans, other bivalves, echinoderms, gastropods and sponges (Cranfield et al. 1999, 2004).

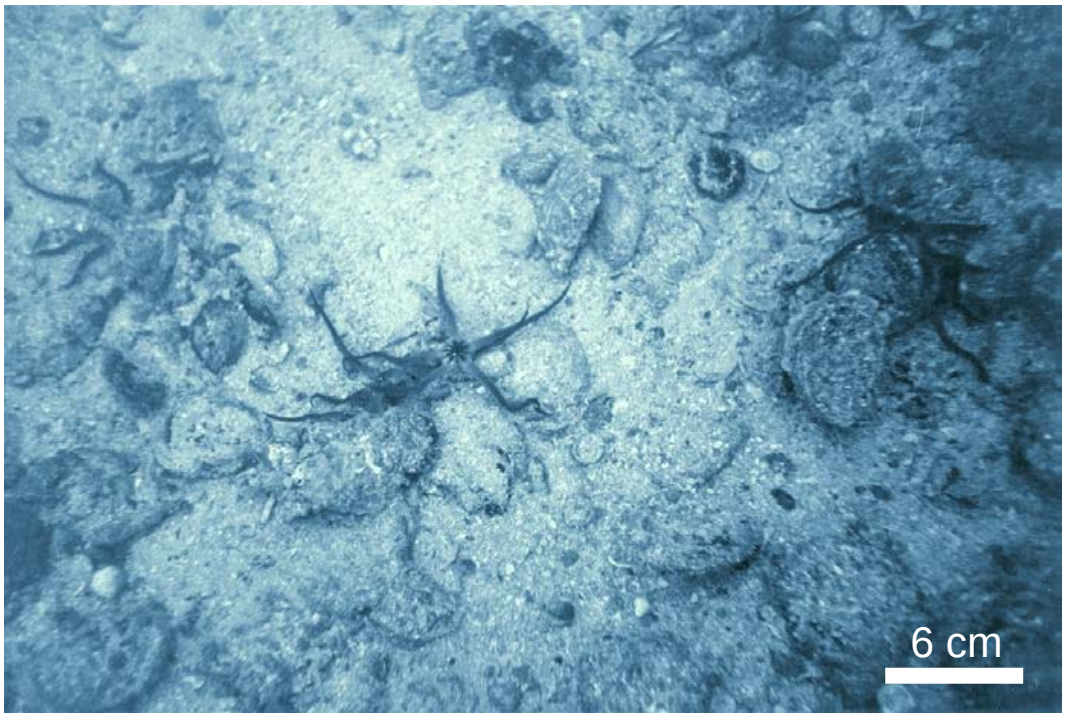

Figure 6.3 *Ostrea chilensis* on the sea floor of Foveaux Strait. Image courtesy of Keith Micheal at National Institute of Atmosphere and Water (2008).

Strong tidal streams sweep Foveaux Strait; they set to the east on the flood tide and to the west on the ebb tide (Cranfield et al. 2003). Foveaux Strait also has a high energy wave environment that is dominated by long-period swells

originating from the west to southwest. Both the strong currents and wave influence provide ideal conditions for filter feeders and as a result a diverse filter feeding community has developed on the sea floor (Cranfield et al. 1999).

6.2.2 San Blas, Patagonia

San Blas in northern Patagonia (Fig. 6.4) is home to the introduced Pacific Oyster *Crassostrea gigas* (Fig. 6.5). The Pacific Oyster *Crassotrea gigas*, a species endemic to Japan, is the most successful oyster in commercial cultivation and forms the basis of some of the largest oyster fisheries in the world (Escapa et al. 2004).

The species was introduced to Argentina in 1982 from Chile, with the purpose of beginning an aquaculture venture, but only a year later the stock was abandoned, due to small stock numbers. The remaining stock has become established in spot locations along the coast of San Blas (Fig. 6.4) (Escapa et al. 2004). The intertidal zone (area between mean high water level and mean low water level) is a mixture of sandstone and muddy bottoms. After 20 years of establishment the Pacific Oyster only covers a small area ($\leq$ 0.05%) of the intertidal zone. This is in stark contrast with other populations of this species around the world where large numbers have developed in a very short period of time. Escapa et al. (2004) suggest that the lack of hard substrate in this area, due to the large amount sediment that was once discharged from the Colorado River (Fig. 6.4A). The dominance of the muddy sediments in this area is the major limiting factor for the Pacific Oyster in San Blas.

6.3 BULK CARBON AND OXYGEN STABLE ISOTOPES

The isotopic composition of an organism is a function of both metabolism and environment (Kirby et al. 1998). For this reason oxygen and carbon stable isotopes can be used to help reconstruct the environments of molluscs (Hong et al. 1995). All isotopic results are featured in Appendix B-1.1 and as a Digital Appendix.

Diagenesis is important to recognise in fossils because it can alter the original isotopic composition of the shells. To minimise this issue in this study, all the samples analysed here were low-magnesium calcite as this mineral phase is much

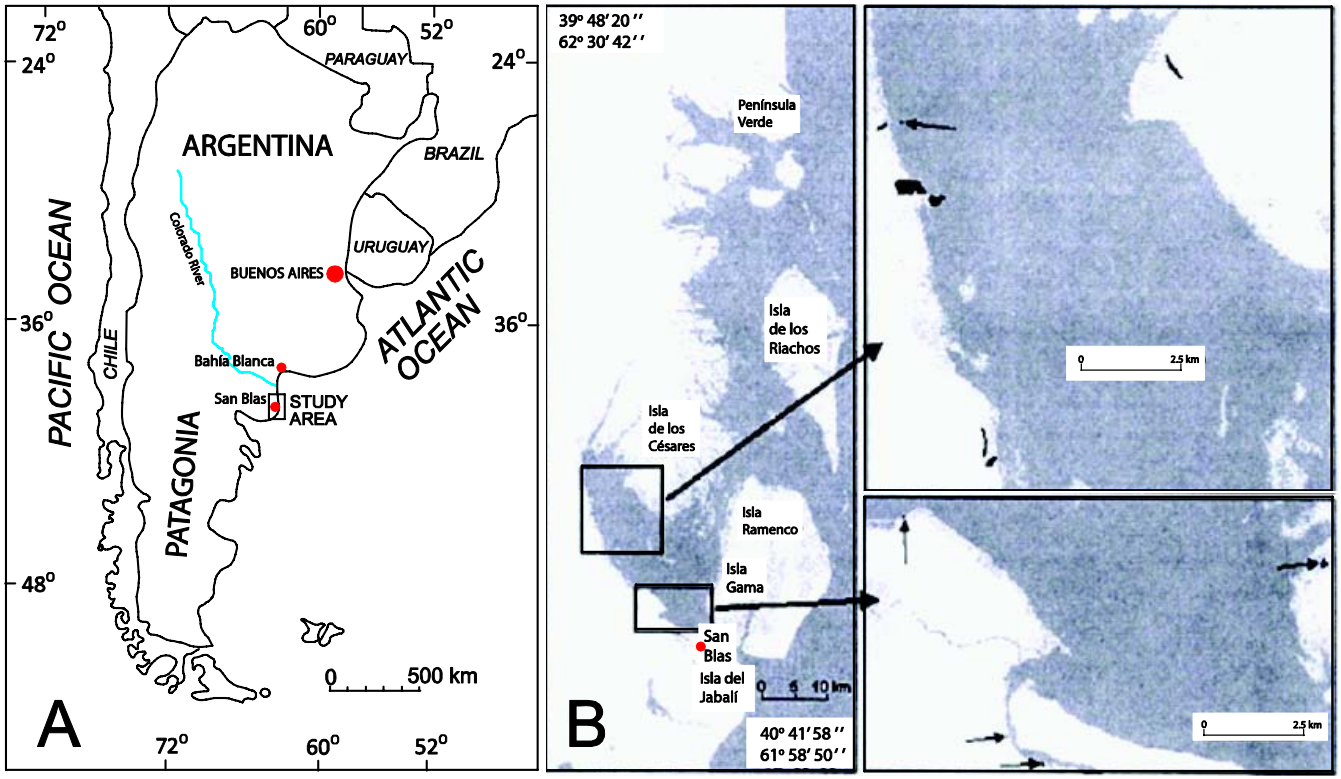

Figure 6.4 Locality maps for modern oyster *Crassostrea gigas* near San Blas, northern Patagonia. In enlargements from (B) large oyster beds are shown in black and smaller ones are indicated by arrows (Escapa et al. 2004).

less susceptible to alteration than aragonite sections of the shell. Oyster shells contain both calcite (foliated and chalky layers) and aragonite (muscle scar and ligostracum) (Stenzel 1963, 1971; Carriker & Palmer 1979), the former dominating. X-ray diffraction analysis of bulk shell samples (see Section 7.2.3) has shown no presence of aragonite, probably due to recrystallisation into a more stable form of calcium carbonate. In addition to this, cathodoluminescence was carried out on samples prior to analysis. Any samples that showed luminescence were considered altered and subsequently discarded. Samples were taken from below the ligamental area (Fig. 6.6), which is in the foliated calcite portion of the shell, using a Dremel drill (Fig. 6.7), as outlined in Section 2.3.5.

Figure 6.5 The Pacific Oysters *Crassostrea gigas* form an *in situ* mound in the intertidal zone at San Blas. The extent of the host mud is clear from the depth of the footprints in the background of this picture.

6.3.1 Results

As is presented in Figure 6.8 below the bulk isotopes from the fossil and modern oyster samples analysed show some differing patterns. Noticeably samples from Waitomo, Wanganui and also modern Foveaux Strait have higher $\delta^{18}O$ and $\delta^{13}C$

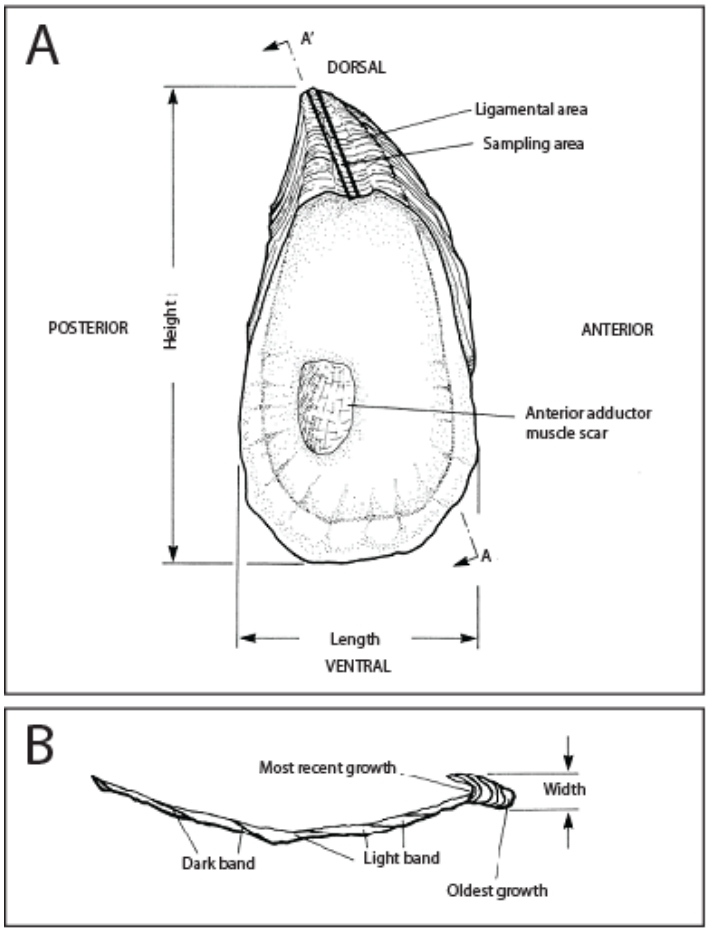

Figure 6.6 (A) Schematic of left valve of *Crassostrea virginica*, showing shell structures and ligament area where growth lines are sampled to provide a biogeochemical time series. (B) Cross section A – A' of the left valve. Adapted from Andrus & Crowe (2000).

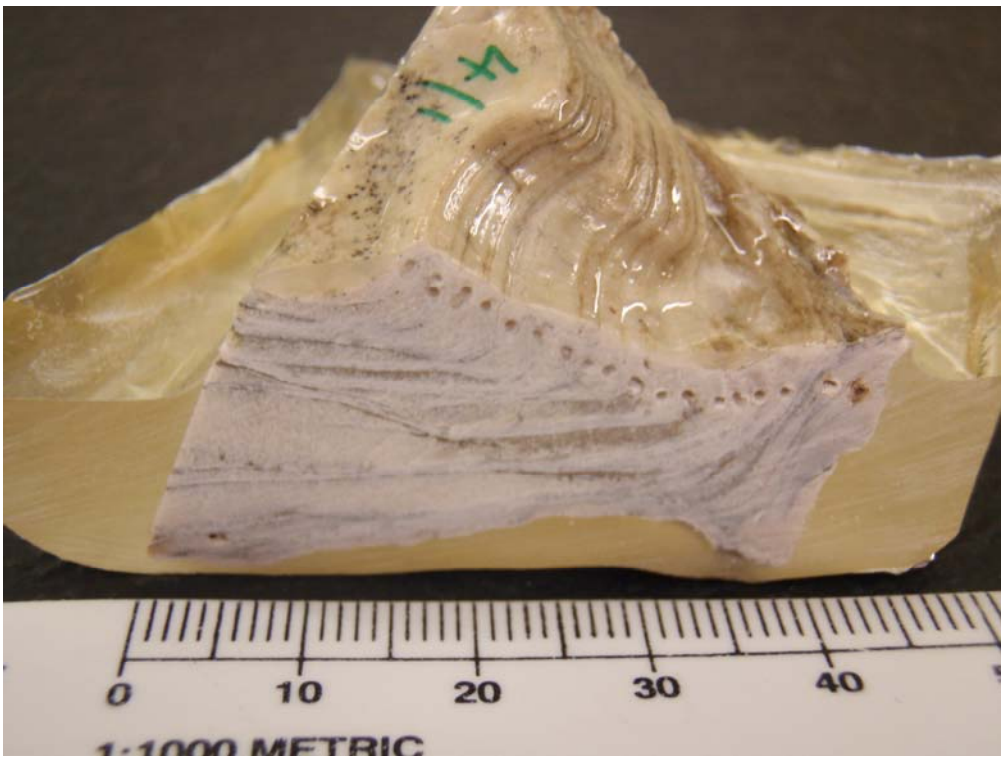

Figure 6.7 Sample PAT4/1 set in resin with drill holes for isotopic analysis taken under the ligamental area (see Fig. 6.6) using a Dremel drill.

values. Samples from Waitomo are also somewhat clustered in a tightly defined area on the graph in comparison to those from Wanganui which exert some dispersion, with samples in the outlined field and others much lower. Both modern and fossil samples from Patagonia have the most negative $\delta^{18}O$ and $\delta^{13}C$ values out of all the samples analysed. Placement of data points in relation to the marine field of Mook (1968, 1971) will be discussed in more detail in Chapter Nine.

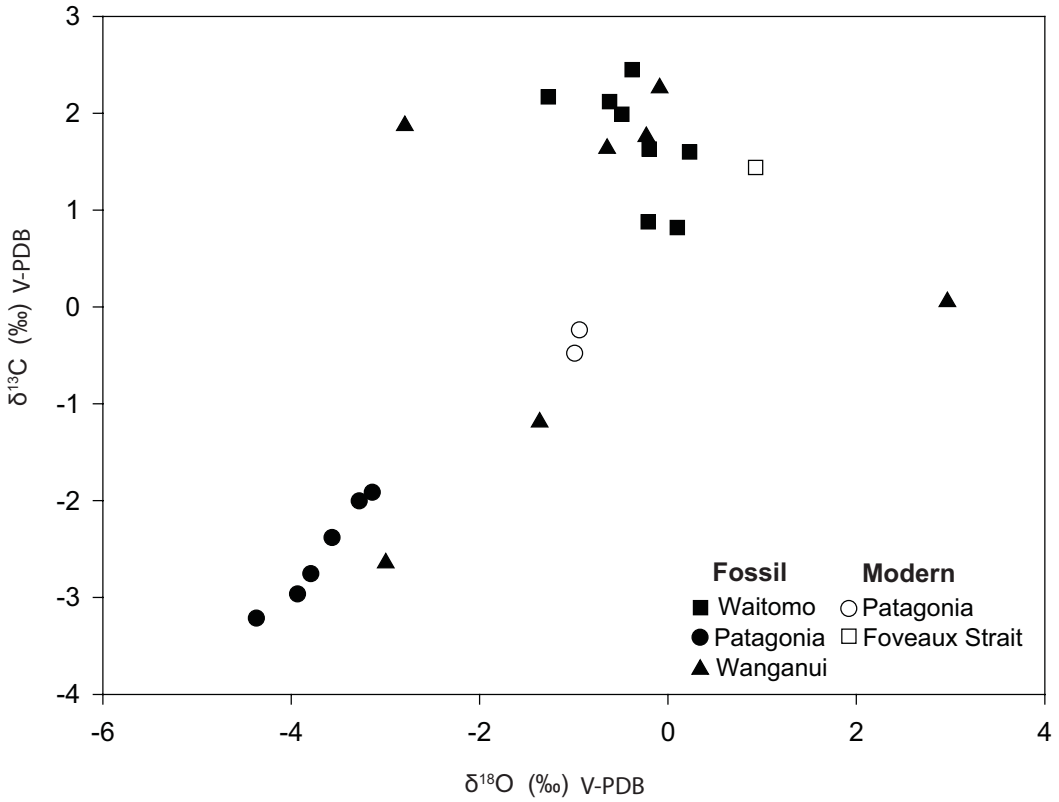

Figure 6.8 Scatter plot of $\delta^{13}C$ vs $\delta^{18}O$ values from Waitomo (Flemingostreini Stenzel), Patagonia ("*Ostrea" patagonica*) and Wanganui (*Crassostrea ingens*). Note the inclusion of modern samples from San Blas (*Crassostrea gigas)* and Foveaux Strait (*Ostrea chilensis)*.

6.4 BULK SAMPLE TRACE ELEMENT CONCENTRATIONS

Concentrations of manganese (Mn), iron (Fe), strontium (Sr) and magnesium (Mg) can provide information about the diagenetic state of calcitic fossils (Schneider et al. 2009). Concentrations of Mn and Fe usually increase during diagenesis, while fossils become depleted in Sr and Mg via the same process (Brand & Veizer 1980; Veizer 1983a, b).

Globally, many extant oyster specimens occur in environments that have reduced salinity due to the proximity of river mouths. Consequently, their shells may

display a wide range of trace element contents that originate from the heterogeneous load of river waters. However, this cannot be generally assumed to be the case and so the trace element concentrations in this study are thus compared to those in other oysters from the literature (Table 6.1) (Schneider et al. 2009). All elemental results are contained with Appendix B-1.2 and as a Digital Appendix.

In a scatter plot of Fe and Sr and Fe and Mn from each fossil oyster sample (Fig. 6.9), the relationships between elements can be examined. Results of the correlations are in Table 6.2. The Flemingostreini Stenzel sample from Waitomo shows no relationship between Fe and Mn, but Fe and Sr have a strong positive relationship which is statistically significant ($p < 0.001$). In sample PAT2/1 of *"Ostrea" patagonica* taken from the bottom of the reef at Puerto Pirámide, Fe and Mn have a statistically significant ($p < 0.01$) relationship and the relationship of Fe and Sr is insignificant. In PAT4/1 from the top of the reef, the relationships with both Fe and Mn and Fe and Sr are statistically insignificant. The sample of *Crassostrea ingens* from Wanganui Fe and Mn has a weak positive relationship ($p < 0.005$) and there is no significant relationship between Fe and Sr.

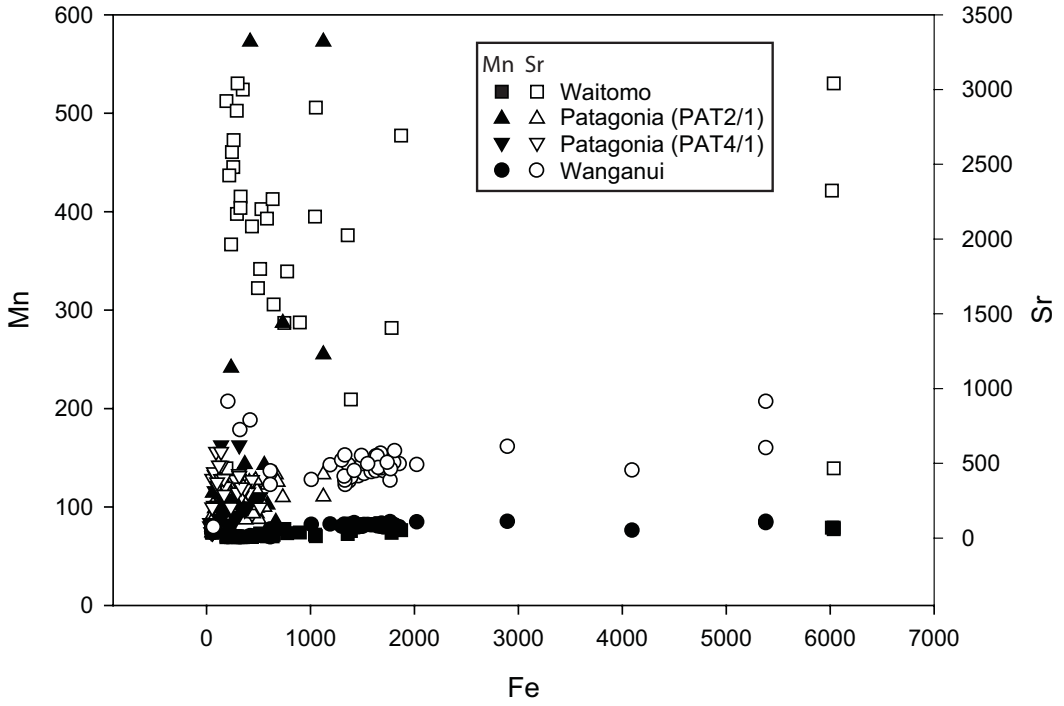

Figure 6.9 Scatter plot of Mn (black points) and Sr (white points) over Fe of fossil oyster samples from Waitomo (Flemingostreini Stenzel), Patagonia (*"Ostrea" patagonica*) and Wanganui (*Crassostrea ingens).* Note samples number PAT2/1 denotes the bottom of the reef in Puerto Pirámide and PAT4/1 is a sample from the top of the reef at Puerto Pirámide.

Table 6.1 Literature data on trace element content (Sr, Fe, Mn and Mg) of fossil and extant oysters. Adapted from Schneider et al. (2009).

Author	Taxon	Locality	Age	Sr (ppm)	Fe (ppm)	Mn (ppm)	Mg (ppm)
Pilkey and Harriss (1966)	*Crassostrea virginica*	Georgia	Extant	924-1081	159-431	18-49	1320-2540
Milliman (1974)	*Crassostrea*	-	Extant	700-1600	159-432	18-50	1100-2700
Milliman (1974)	*Ostrea*	-	Extant	700-1900	7-750	18-50	1100-2700
Carriker et al. (1980)	*Crassostrea virginica*	Delaware	Extant	1240-2580	28-37	130-178	148-252
Carriker et al. (1980)	*Crassostrea virginica*	Delaware	Extant	380-1152	20-37	141-961	183-1450
Carriker et al. (1991)	*Crassostrea virginica*	Delaware	Extant	3520-5561	28-1235	<20-673	320-739
Carriker et al. (1991)	*Crassostrea virginica*	Delaware	Extant	4103-6075	2791-4782	429-858	1747-2327
Ozhigova (1992)	*Crassostrea virginica*	Black Sea	Extant	-	200	40	1800
Ozhigova (1992)	*Crassostrea gigas*	Japan	Extant	-	300	150	1900
Ozhigova (1992)	*Ostrea edulis*	Black Sea	Extant	-	30-100	21-37	2300-2400
Ozhigova (1992)	*Ostrea edulis*	Crimea	Extant	-	50-2600	20-500	1600-5200
Ozhigova (1992)	*Pynodonte*	Russian Platform	Cretaceous	-	700-6000	30-1100	1100-2300
Anderson et al. (1994)	*Gryphaea*	Great Britian	L.Jurassic	207-473	60-15512	8-73	406-675
McArthur et al. (1994)	*Crassostrea*	Western Interior	Cretaceous	740	1300	465	865
McArthur et al. (1994)	*Ostrea*	Western Interior	Cretaceous	340-1100	315-445	365-515	615-1500
Carriker et al. (1996)	*Crassostrea virginica*	Delaware	Extant	2600-4200	600-2600	100-1600	1250-1680
Denison et al. (2003)	*Ostrea*	Texas, Oklahoma	Cretaceous	1000-1466	120-440	14-70	604-1854
Schneider et al. (2009)	*Nanogyra nana*	Portugal	U.Jurassic	667-757	254-353	20-58	1784-2252
Schneider et al. (2009)	*Praeexogyra pustulosa*	Portugal	U.Jurassic	535-979	102-4623	22-997	440-3369
Schneider et al. (2009)	*Actinostreon solitaria*	Portugal	U.Jurassic	308-639	254-353	20-58	1784-2252
This study (N14/1C)	Flemingostreini Stenzel	Waitomo, New Zealand	Oligocene	139-530	191-6034	6-70	891-3899
This study (PAT2/1)	*"Ostrea" patagonica*	Puerto Pirámide, Patagonia	L.Miocene	123-426	61-1124	64-3320	1009-2399
This study (PAT4/1)	*"Ostrea" patagonica*	Puerto Pirámide, Patagonia	L.Miocene	206-578	55-140	59-621	765-1625
This study (WLK)	*Crassostrea ingens*	Wanganui, New Zealand	Pliocene	358-914	613-5381	8-111	911-4787

Table 6.2 Correlations of Fe and Mn or Sr concentrations (see Figure 9.7).

Location	Sample	Elements	R^2	*df*	*p*
Waitomo	N14/1C	Fe vs Mn	-	-	-
		Fe vs Sr	0.487	40	<0.001
Patagonia	PAT2/1	Fe vs Mn	0.271	56	<0.01
		Fe vs Sr	0.177	56	>0.01
Patagonia	PAT4/1	Fe vs Mn	0.166	36	<0.01
		Fe vs Sr	0.020	36	>0.01
Wanganui	WLK	Fe vs Mn	0.364	49	<0.005
		Fe vs Sr	0.246	49	>0.005

6.5 SCLEROCHRONOLOGY

Recently, at the 1st International Sclerochronolgy Conference, Jones et al. (2007) defined sclerochronology as:

> "the study of physical and chemical variations in accretionary hard tissues of organisms, and the temporal context in which they formed. Sclerochronology focuses primarily upon growth patterns reflecting annual, monthly, fortnightly, tidal, daily and sub-daily increments of time entertained by a host of environmental and astronomical pacemakers. Familiar examples include daily banding in reef coral skeletons or annual growth rings in mollusc shells. Sclerochronology is analogous to dendrochronology, the study of annual rings in trees, and equally seeks to deduce organismal life history traits as well as reconstruct records of environmental and climatic change through space and time".

Oysters form a sclerochronological record within the ligamental area (Fig. 6.6), where the two valves are joined by ligament (Kirby et al. 1998). They deposit shell incrementally and therefore are able to preserve a biogeochemical time series that can be directly applied to the surrounding environment (Stetcher et al. 1996).

6.5.1 Oxygen and carbon isotopic profiles

Fossil oyster specimens with a well preserved ligamental area were selected from Waitomo, Patagonia and Wanganui. Modern oyster specimens from San Blas and Foveaux Strait were also selected to afford a comparison with modern

Table 6.3 Isotopic data for fossil Flemingostreini Stenzel (N14/1C) from Waitomo, fossil *"Ostrea" patagonica* (PAT2/1 and PAT4/1) from Patagonia, fossil *Crassostrea ingens* (WLK) from Wanganui, modern *Crassostrea gigas* (San1a and San3d) from Patagonia and modern *Ostrea chilensis* (FVX1) from Foveaux Strait in per mil relative to V-PDB.

Sample location	Sample number	Average#	Minimum	Maximum	Total range	Average seasonal range#	Average minimum#	Average maximum#	Range between minima	Range between maxima
$\delta^{18}O$ values (‰)										
Waitomo	N14/1C	-0.59 ± 0.13	-0.80	-0.40	0.40	0.3 ± 0.01	-0.72 ± 0.06	-0.47 ± 0.06	0.14	0.13
Patagonia	PAT2/1	-2.52 ± 0.71	-3.73	-0.51	3.22	0.85 ± 0.66	-2.94 ± 0.43	-1.99 ± 0.77	1.51	2.23
Patagonia	PAT4/1	-3.16 ± 0.82	-4.42	-1.48	2.94	1.37 ± 0.78	-3.48 ± 0.81	-2.37 ± 0.73	2.26	1.95
Wanganui	WLK	-1.48 ± 0.34	-2.13	-0.90	1.23	0.73 ± 0.21	-1.83 ± 0.21	-0.65 ± 0.25	0.43	2.21
San Blas	San1a	-0.39 ± 0.43	-1.99	-0.66	1.33	0.75 ± 0.45	-1.81 ± 0.18	-1.05 ± 0.40	0.35	0.93
San Blas	San3d	-1.08 ± 0.71	-2.02	0.36	2.38	-	-1.36 ± 0.94	-0.46 ± 1.16	1.32	1.64
Foveaux Strait	FVX1	0.13 ± 0.13	0.00	0.38	0.38	0.22 ± 0.08	-0.03 ± 0.03	-0.24 ± 0.12	0.21	0.06
$\delta^{13}C$ values (‰)										
Waitomo	N14/1C	0.71 ± 0.19	0.39	0.99	0.60	0.3 ± 0.26	0.593 ± 0.20	0.87 ± 0.11	0.39	0.23
Patagonia	PAT2/1	-0.90 ± 0.93	-2.03	1.68	3.71	0.95 ± 0.95	-1.32 ± 0.58	-0.32 ± 1.09	1.68	3.18
Patagonia	PAT4/1	-1.39 ± 0.58	-2.65	-0.52	2.13	0.94 ± 0.54	-2.06 ± 0.43	-1.05 ± 0.31	1.14	0.78
Wanganui	WLK	-2.13 ± 0.53	-3.38	-1.45	1.93	0.76 ± 0.58	-2.5 ± 0.46	-1.76 ± 0.25	1.29	0.55
San Blas	San1a	-0.35 ± 0.23	-0.63	0.04	0.67	0.41 ± 0.20	-0.60 ± 0.03	-0.19 ± 0.20	0.05	0.36
San Blas	San3d	-0.64 ± 0.26	-0.99	-0.14	0.85	-	-0.193 ± 1.12	-0.364 ± 0.32	1.59	0.45
Foveaux Strait	FVX1	0.02 ± 0.23	-0.22	0.38	0.60	0.33 ± 0.18	-0.11 ± 0.19	-0.24 ± 0.19	0.33	0.35

Reported as mean ± one standard deviation.

environments. All specimens were sampled as outlined in Section 2.3.5. All isotope results are contained with Appendix B-1.1 and as a Digital Appendix. Selected isotopic data are presented in Table 6.3.

6.5.1a Waitomo

Fourteen consecutive samples were taken from oyster sample N14/1C from Ngapaenga Road in Waitomo County (Fig. 3.4). The resulting isotopic values were plotted against distance across the ligamental area (Fig. 6.10). N14/1C appears to show three annual cycles. Average seasonal ranges expressed in $\delta^{18}O$ and $\delta^{13}C$ profiles are 0.3 ± 0.01‰ and 0.3 ± 0.26‰ (1.s.d), respectively (Table 6.3). Extreme values are remarkably consistent, with five of the $\delta^{18}0$ minima and maxima values differing by no more than 0.14 and 0.13‰, respectively, and four $\delta^{13}C$ minima and maxima values differing by no more than 0.39 and 0.23‰, respectively. The $\delta^{18}O$ and $\delta^{13}C$ minima and maxima tend to coincide with each other in time.

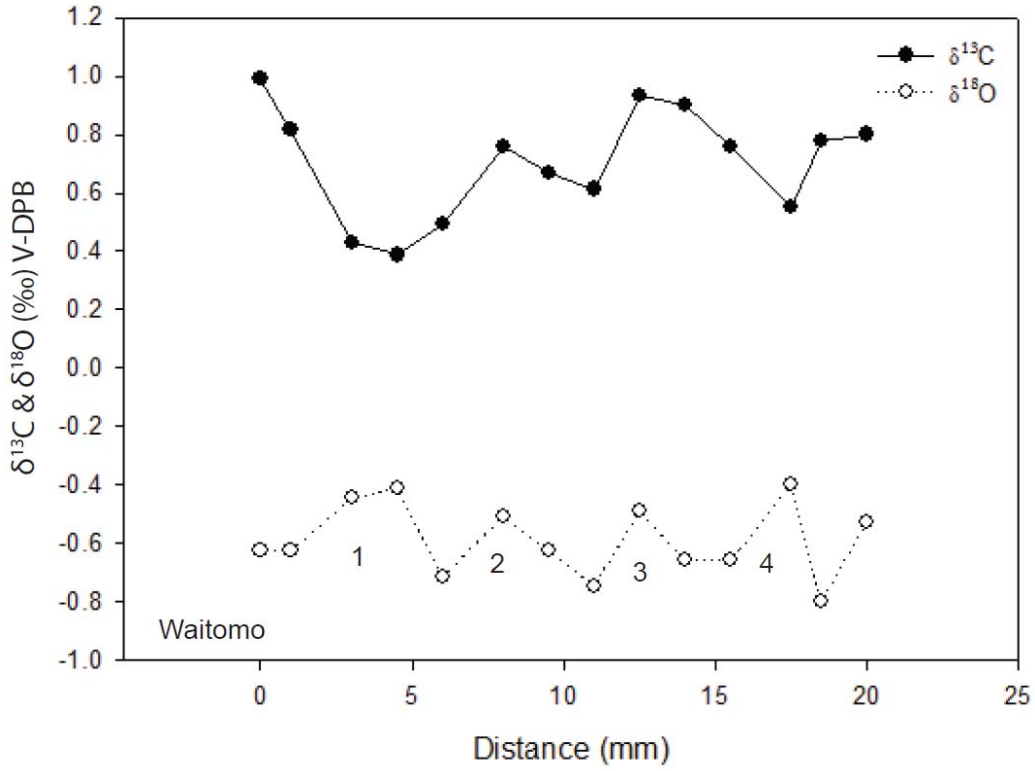

Figure 6.10 $\delta^{13}C$ and $\delta^{18}O$ profiles from the ligamental area of a Flemingostreini Stenzel specimen (N14/1C) from the Waitomo area. Numbers under oxygen profile show possible annual cycles. Growth direction of the shell is from left to right.

6.5.1b Patagonia

Samples of *"Ostrea" patagonica* were collected from both the bottom and top of the reef contained within the Puerto Madyrn Formation cropping out at Puerto Pirámide (Fig. 4.2). This was done to measure any change in the isotopic profile over time. Twenty-two consecutive samples were taken from PAT2/1, which is from the lower part of the 'reef', and sixteen consecutive samples were taken from PAT4/1 which is from the uppermost level of the reef.

The resulting isotopic values for PAT2/1 were plotted against distance across the ligamental area (Fig. 6.11). Any seasonal cycles within PAT2/1 are relatively obscure. The average seasonal value for $\delta^{18}O$ is 0.85 ± 0.66‰ and for the $\delta^{13}C$ profiles is 0.95 ± 0.95‰ (1.s.d) (Table 6.3). Extreme values show some variation, with $\delta^{18}0$ minima and maxima values ranging between 1.51 and 2.23‰, respectively, and $\delta^{13}C$ minima and maxima ranging between 1.68 and 3.18‰, respectively. Both maxima and minima values for $\delta^{18}O$ and $\delta^{13}C$ tend to coincide with each other in time.

As for PAT2/1, it is difficult to depict clear seasonal cycles from PAT4/1 (Fig. 6.12). Fluctuations in values can be seen and average seasonal ranges in the $\delta^{18}O$ and $\delta^{13}C$ profiles are 1.37± 0.78‰ and 0.94 ± 0.54‰ (1.s.d), respectively (Table 6.3). Extreme values for PAT4/1 show considerable variation, the $\delta^{18}0$ minima and maxima ranging between 2.26 and 1.95‰, respectively, and $\delta^{13}C$ minima and maxima between 1.14 and 0.78‰, respectively. Minima and maxima for $\delta^{18}O$ and $\delta^{13}C$ do not tend to coincide with each other in time as they do in PAT2/1.

6.5.1c Wanganui

Fourteen consecutive samples were taken from sample WLK from the Wilkies Shellbed at Parikino (Fig. 5.4) and isotopic values were plotted against distance across the ligamental area (Fig. 6.13). These values suggest that some seasonal cycles may exist within WLK. Average seasonal ranges expressed in $\delta^{18}O$ and $\delta^{13}C$ profiles are 0.73 ± 0.21‰ and 0.76 ± 0.58‰ (1.s.d), respectively (Table 6.3). Minima and maxima of both $\delta^{18}O$ and $\delta^{13}C$ tend to coincide with each other in time, the $\delta^{18}0$ minima and maxima ranging between 0.43 and 2.21‰ and $\delta^{13}C$ minima and maxima ranging between 1.29 and 0.55‰, respectively. This shows some considerable variation within the extreme values for this sample.

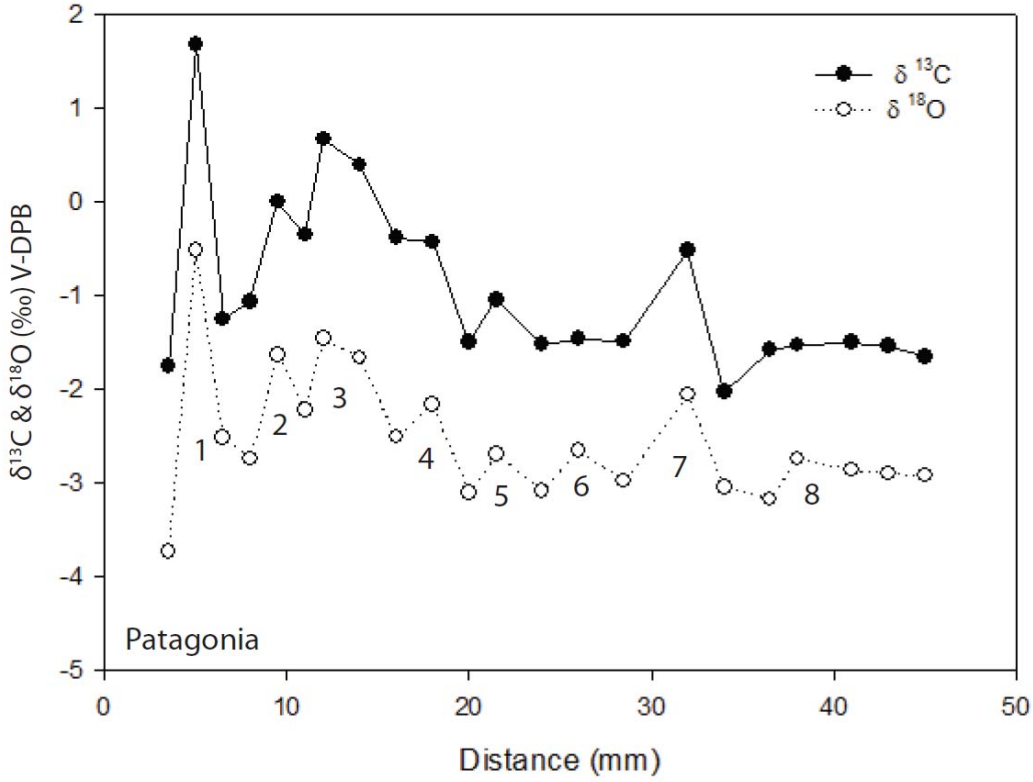

Figure 6.11 $\delta^{13}C$ and $\delta^{18}O$ profiles for *"Ostrea" patagonica* (sample PAT2/1) from the Puerto Madryn Formation in Patagonia. This sample comes from the bottom of the reef. Numbers under oxygen profile represent possible annual cycles. Growth direction of the shell is from left to right.

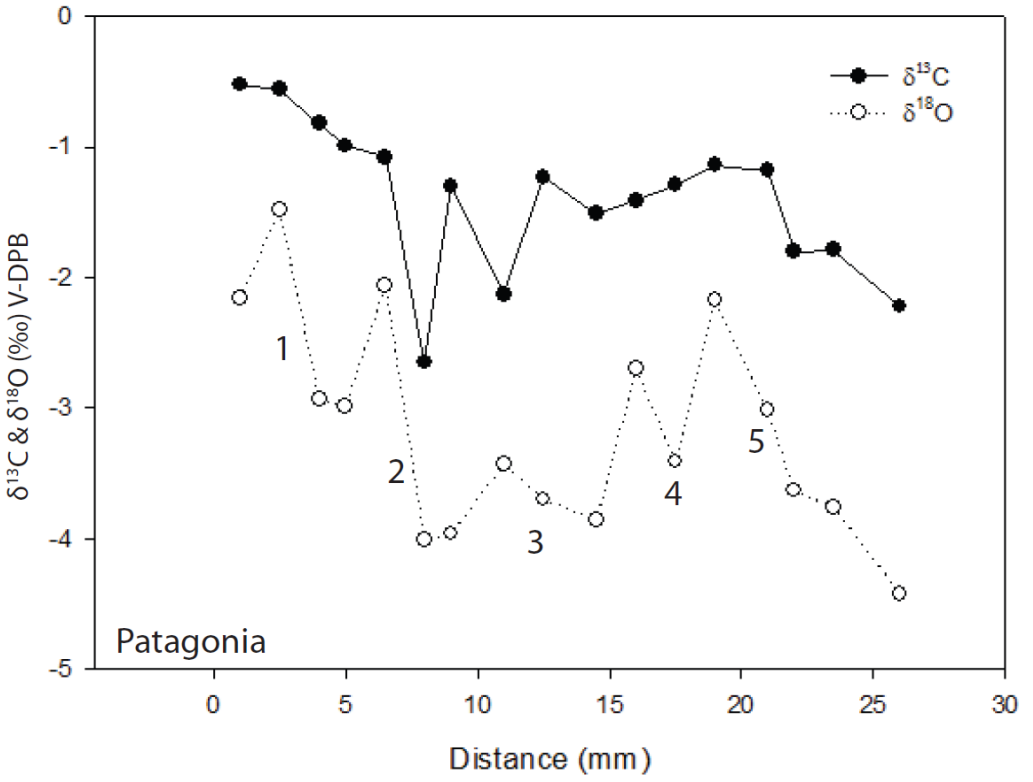

Figure 6.12 $\delta^{13}C$ and $\delta^{18}O$ profiles for "*Ostrea" patagonica* (sample PAT4/1) from the Puerto Madryn Formation in Patagonia. This sample comes from the topmost point of the reef. Numbers under oxygen profile represent possible annual cycles across the shell. Growth direction is from left to right.

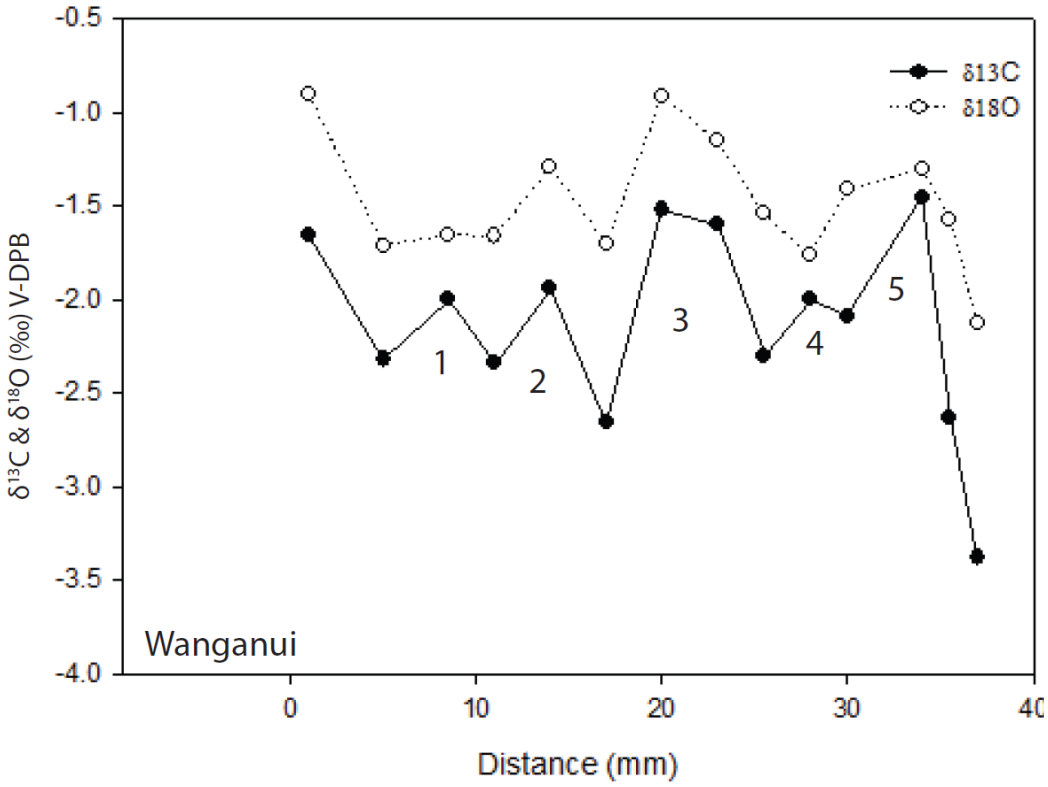

Figure 6.13 $\delta^{13}C$ and $\delta^{18}O$ profiles for *Crassostea ingens* (sample WLK) from the Wilkies Shellbed, Wanganui. Numbers shown under the oxygen profile potentially represent up to 4 annual cycles within the shell. Growth direction is from left to right.

6.5.1d Summary

Isotopic results from the Flemingostreini Stenzel samples differ from those taken from *Crassostrea ingens* in Wanganui and *"Ostrea" patagonica* from Patagonia. The most noticeable difference is that the values for Flemingostreini Stenzel are higher (Table 6.3) by 1 to 3‰ than the other oyster species, as shown in a plot of $\delta^{18}O$ vs $\delta^{13}C$ (Fig. 6.14A). Also both the total and seasonal ranges are less in both Flemingostreini Stenzel from Waitomo and in the modern *Ostrea chilensis* from Foveaux Strait (Fig. 6.14E, Table 6.4). The isotopic scatter plot shows the Flemingostreini Stenzel and *Ostrea chilensis* data forming tighter clusters than data from other samples (Fig. 6.14F). Samples PAT2/1, PAT4/1 and WLK show a strong positive correlation between $\delta^{18}O$ and $\delta^{13}C$ values (Fig. 6.14B, 6.14C; Table 6.4) which are significant at the 99% confidence level ($p < 0.001$). The modern Foveaux Strait sample has a weakly positive correlation which is significant to the 90% confidence level ($p < 0.01$) (Fig. 6.14E).

The modern Patagonian sample San 1a shows a weak, positive correlation (Fig. 6.14C), conversely the modern Patagonian sample San3d shows a weak negative

correlation (Fig. 6.14C), and both correlations are insignificant to the 99% confidence level ($p > 0.001$). The fossil sample (N14/1C) shows weak but negative correlation (Fig. 6.14A), which is insignificant to the 99% confidence level ($p > 0.001$). Reasons for these correlations will be further discussed in Chapter Nine.

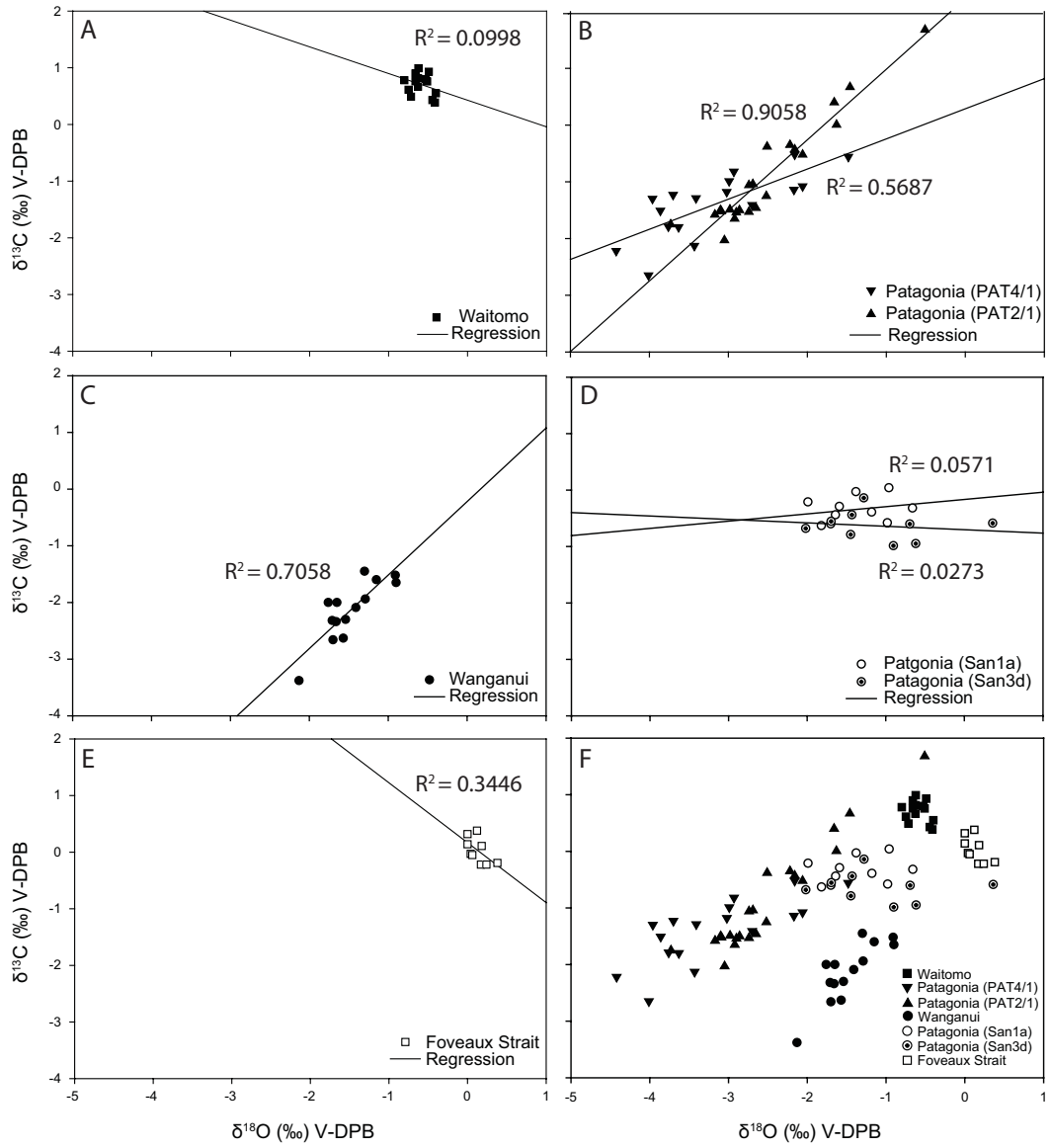

Figure 6.14 Regression and intra-shell $\delta^{13}C$ and $\delta^{18}O$ values from oysters. (A) Waitomo fossil Flemingostreini Stenzel (sample N14/1C). (B) Patagonian fossil "*Ostrea" patagonica* (samples PAT2/1 and PAT4/1). (C) Wanganui, Wilkies Shellbed *Crassotrea ingens* (sample WLK). (D) Patagonia, San Blas modern *Crassostrea gigas* (samples San1a and San3d). (E) Foveaux Strait modern *Ostrea chilensis* (sample FVX1). (F) Scatter plot for intra-shell $\delta^{13}C$ and $\delta^{18}O$ values for all oyster shells from aforementioned locations.

6.5.2 Trace element ratios

The use of Mg/Ca and Sr/Ca ratios in biogenic carbonates as geochemical proxies has increased somewhat over the last decade and complements the use of $\delta^{18}O$ and

$\delta^{13}C$ data. Factors controlling these trace element ratios and their occurrence in biogenic carbonates such as oysters are generally less well understood than those governing stable isotope ratios. The importance of elemental/Ca ratios in paleothermometry has focused research on the biological and environmental factors such as temperature, salinity and pH that may play an influencing role upon the incorporation of Mg and Sr into biogenic carbonates (Freitas et al. 2005). Studies have focused on foraminifera (Nurnberg et al. 1996; Lea et al. 1999; Elderfield & Ganssen 2000), corals (de Villiers et al. 1995) and to a lesser extent bivalves (Lorens & Bender 1980; Klein et al. 1996a, b; Stetcher et al. 1996; Putten et al. 2000). All trace element data are presented in Appendix B-1.2 and as a Digital Appendix.

Table 6.4 Correlations of $\delta^{18}O$ and $\delta^{13}C$ values (see Fig. 6.13).

Location	**Sample**	$\mathbf{R^2}$	***df***	***p***
Waitomo	N14/1C (Fossil)	0.0998	14	< 0.001
Patagonia	PAT2/1 (Fossil)	0.9058	22	> 0.001
Patagonia	PAT4/1 (Fossil)	0.5687	17	> 0.001
Wanganui	WLK (Fossil)	0.7058	14	> 0.001
Patagonia	San1a (Modern)	0.0571	10	< 0.001
Patagonia	San3d (Modern)	0.0273	9	< 0.001
Foveaux Strait	FVX1 (Modern)	0.3446	9	> 0.01

The relationship between shell Mg/Ca ratio and seawater temperature has been previously studied and attributed to a metabolic effect. This can add difficulties to use of this proxy for temperature reconstructions. It has further been suggested that Sr/Ca ratios are controlled by metabolic effects with a secondary salinity influence (Klein et al. 1996b; Putten et al. 2000).

Polished thin sections were used for analysis via laser ablation inductively coupled plasma – mass spectrometry (LA-ICP-MS). Samples were prepared as described in Section 2.3.6 and results are contained within Table 6.5.

6.5.2a Waitomo

Thirty-five consecutive samples were analysed at 750 μm spacings and results are given in Table 6.5. Elemental profiles for Sr/Ca and Mg/Ca are shown in Figure 6.15.

Table 6.5 Laser ablation data for fossil specimens from Waitomo (Flemingostreini Stenzel, sample N14/1C), Patagonia (*"Ostrea" patagonica,* samples PAT2/1 and PAT4/1) and Wanganui (*Crassostrea gigas,* sample WLK).

Sample location	Sample number	Average#	Minimum	Maximum	Total range
Mg/Ca values (ppm)					
Waitomo	N14/1C	4.84E-03 ± 1.42E-03	2.23E-03	9.74E-03	7.51E-03
Patagonia	PAT2/1	3.58E-03 ± 7.56E-03	2.52E-03	5.99E-03	3.47E-03
Patagonia	PAT4/1	2.84E-03 ± 5.40E-04	1.91E-03	4.06E-03	2.15E-03
Wanganui	WLK	62.57 ± 14.32	16.26	75.88	59.61
Sr/Ca values (ppm)					
Waitomo	N14/1C	9.86E-04 ± 2.37E-04	3.48E-04	1.32E-03	9.77E-04
Patagonia	PAT2/1	6.56E-04 ± 2.19E-04	3.07E-04	1.06E-03	7.56E-04
Patagonia	PAT4/1	9.31E-04 ± 2.22E-04	5.14E-04	1.44E-03	9.29E-04
Wanganui	WLK	9.06 ± 2.01	6.39	16.31	9.92

Reported as mean ± one standard deviation.

Sr/Ca ratios range from 3.48E-04 to 1.32E-03 (ppm) (Fig. 6.15A). Clear seasonal oscillations are not evident in this specimen but fluctuation in values do occur. The average value is 9.86E-04 ± 2.73E-04 (ppm) with the total range being 9.77E-04. The Sr/Ca ratios in N14/1C show a weak inverse correlation that is insignificant at the 95% confidence level ($R^2 = 0.072341$, $p > 0.001$).

Mg/Ca ratios range from 2.23E-03 to 9.74E-03 (ppm) for the Flemingsotreini Stenzel shell (Fig. 6.15B). Clear seasonal oscillations are not visible, but fluctuation in values is evident within the shells. The average value is 4.84E-03 ± 1.42E-03 (ppm) with the total range being 7.51E-03 (ppm). Shell Mg/Ca ratios exhibit no significant correlation with $\delta^{18}0$ values ($R^2 = 0.3878$, $p > 0.001$). Shell Mg/Ca ratios also show a weak but insignificant correlation with distance from the shell umbo ($R^2 = 0.0988$, $p > 0.001$).

6.5.2b Patagonia

Fourty eight consecutive samples were analysed from PAT2/1 at 150 μm spacings and twenty eight consecutive samples were taken from PAT4/1 at 750 μm spacing. Results are presented in Table 6.5. Sample PAT2/1 was taken from the bottom of the reef in Puerto Pirámide (Fig. 4.2) and PAT4/1 at the uppermost point. Elemental profiles for Sr/Ca and Mg/Ca in samples PAT4/1 and PAT2/1 are shown in Figures 6.16 and Figure 6.17, respectively.

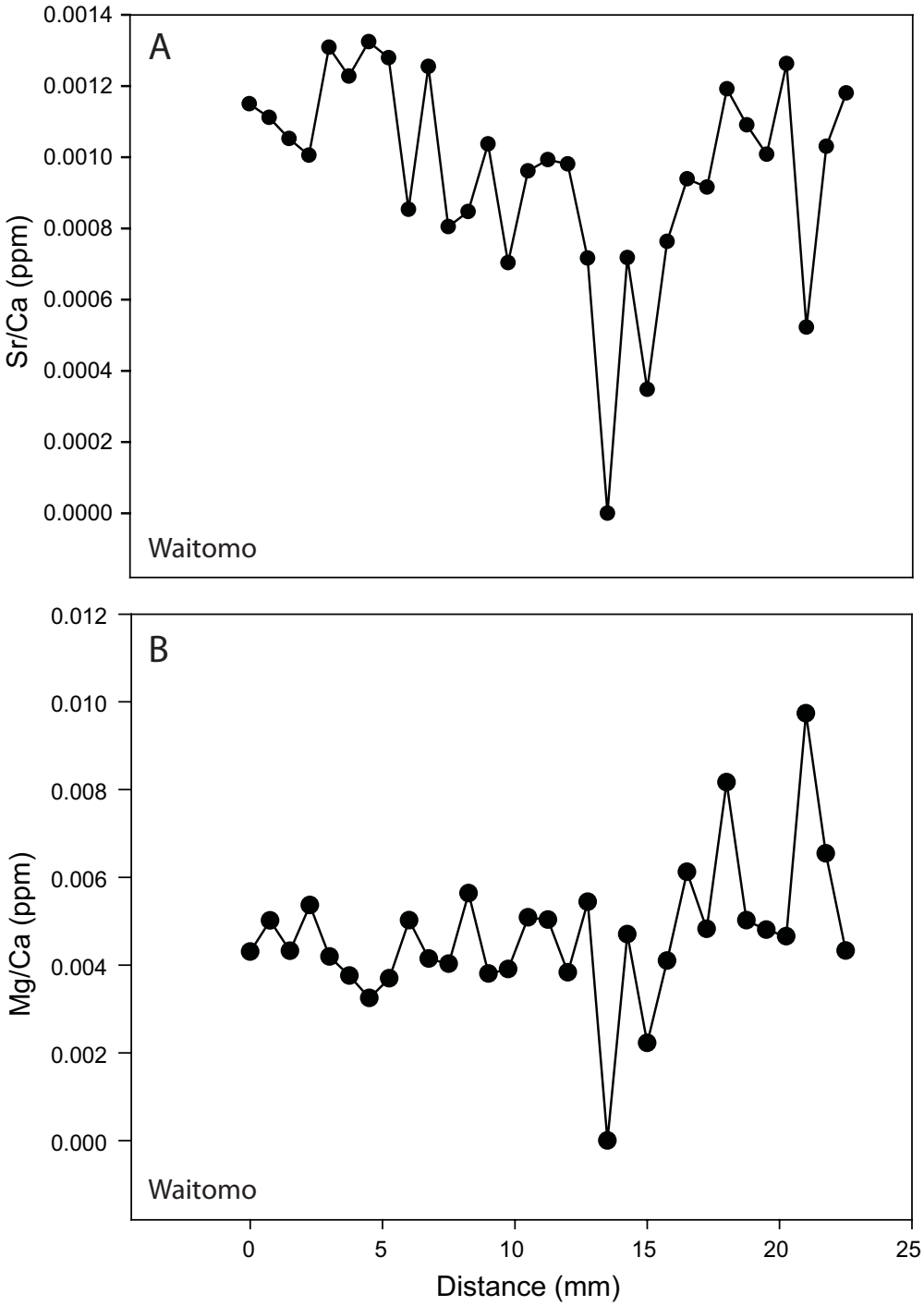

Figure 6.15 (A) Sr/Ca and (B) Mg/Ca ratios for oyster sample N14/1C from Waitomo.

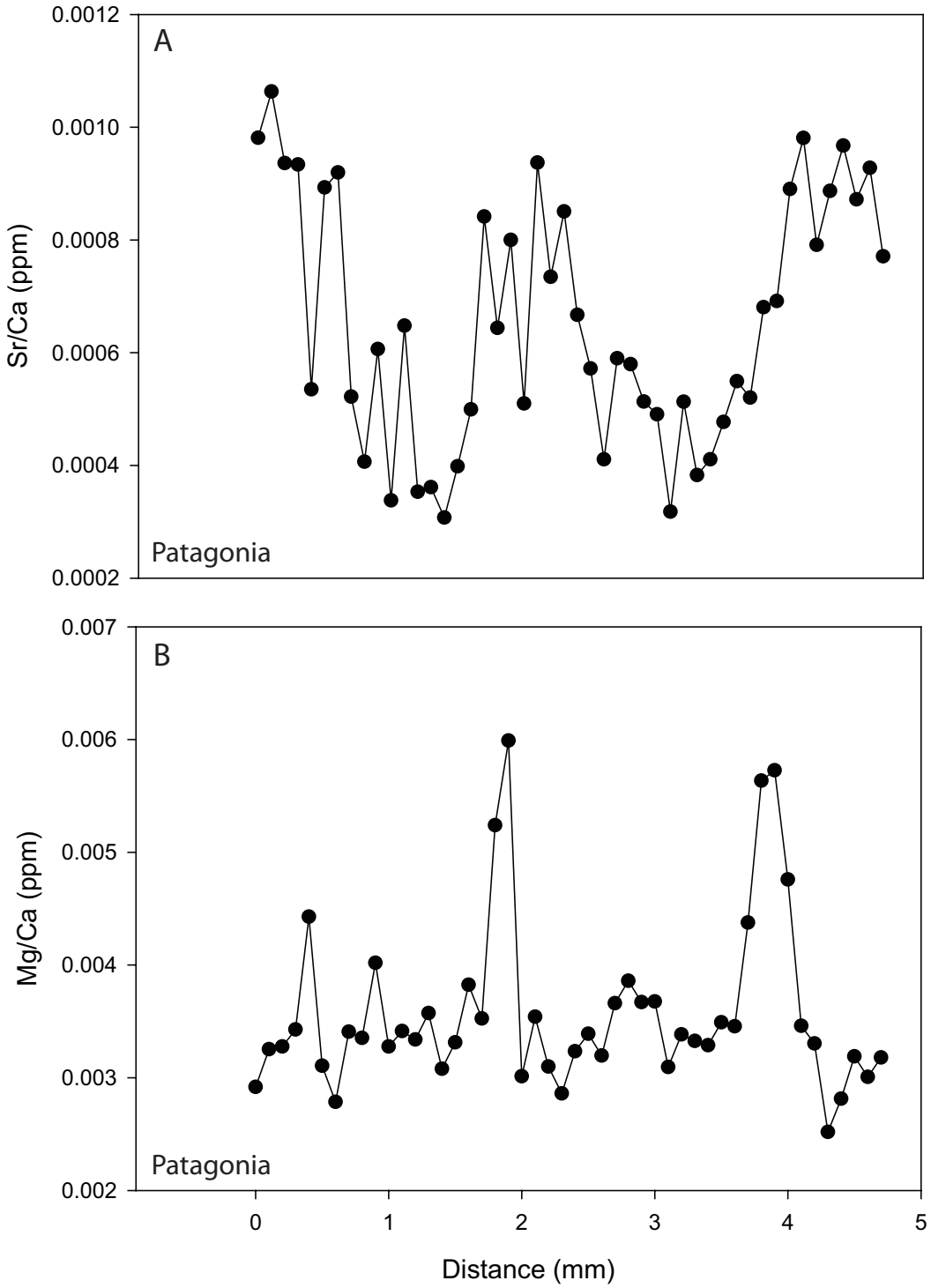

Figure 6.16 (A) Sr/Ca and (B) Mg/Ca ratios from sample PAT2/1 taken from the bottom of the oyster reef at Puerto Pirámide.

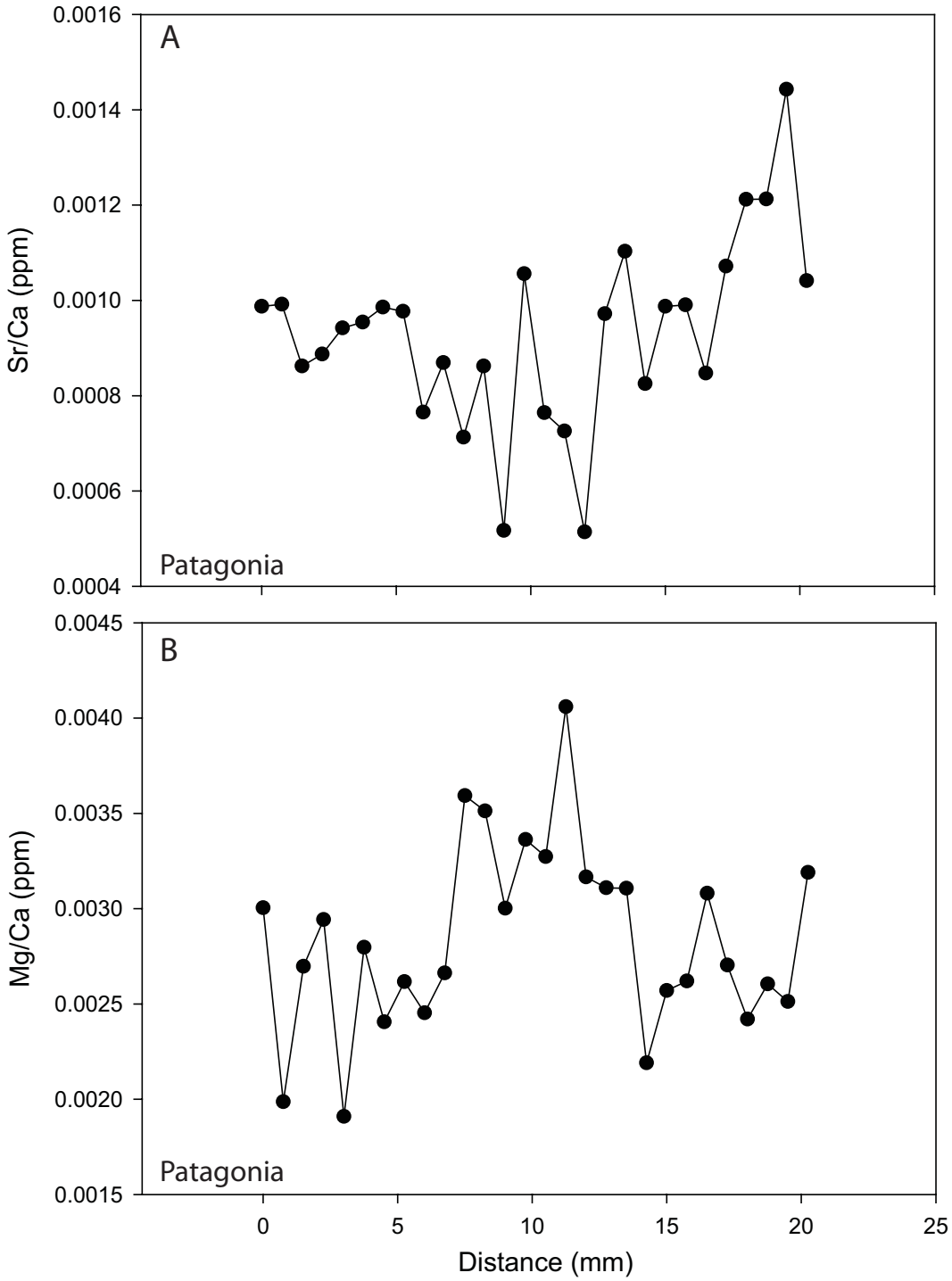

Figure 6.17 (A) Sr/Ca and (B) Mg/Ca ratios from sample PAT4/1 taken from the top of the oyster reef at Puerto Pirámide.

Sr/Ca ratios range between 3.07E-04 and 1.06E-03 (ppm) and 5.14E-04 and 1.44E-03 (ppm) for *"Ostrea" patagonica* shells PAT2/1 and PAT4/1, respectively (Fig. 6.16A, 6.17A). The average value of the shells differs slightly with PAT2/1 being slightly lower with a value of 6.56E-04 ± 2.19E-04 (ppm) and PAT4/1 being higher at 9.31E-04 ± 2.22E-04 (ppm). Samples taken at a higher resolution in PAT2/1 has allowed distinction of some clear and regular oscillations. Samples were taken over a large spatial scale for PAT4/1 so while seasonal oscillations are evident they are less regular than in PAT2/1. The total range of PAT2/1 is 7.56E-04 (pmm) and PAT4/1 is 9.29E-04 (ppm).

Mg/Ca ratios range from 2.52E-03 to 5.99E-03 (ppm) and 1.91E-03 to 4.06E-03 (ppm) for *"Ostrea" patagonica* shells PAT2/1 and PAT4/1, respectively (Fig. 6.16B, 6.17B). Clear seasonal oscillations are visible in PAT2/1 where the data were collected at a higher resolution; similar fluctuations are seen in PAT4/1 but over a larger spatial scale. The average value for the shells is remarkably similar with PAT2/1 being 3.58E-03 ± 7.56E-03 (ppm) and PAT4/1 being 2.84E-03 ± 5.40E-04 (ppm). The total range for PAT2/1 is 3.47E-03 (ppm) and for PAT4/1 is 2.15E-03 (ppm). Both samples show no significant relationship with $\delta^{18}O$ and distance across the shell umbo.

6.5.2c Wanganui

Thirty-five consecutive samples were analysed at 750 μm spacings. Elemental profiles for Sr/Ca and Mg/Ca are shown in Figure 6.18 and results are in Table 6.5. All values for Wanganui are substantially higher than those from both Waitomo and Argentina.

Sr/Mg ratios range from 6.39 to 16.31 (ppm) (Fig. 6.18A). Clear seasonal oscillations are not visible in this specimen but fluctuation in values is evident. The average value is 9.06 ± 2.01 (ppm) with the total range being 9.29 (ppm). The Sr/Ca ratios in WLK show no correlation with the distance across the umbo.

Mg/Ca ratios range from 16.26 to 75.88 (ppm) for the *Crassostrea ingens* shell (Fig. 6.18B). The average value is 62.57 ± 14.37 (ppm) with the total range being 59.61 (ppm). Shell Mg/Ca ratios exhibit no significant correlation with $\delta^{18}0$ values ($R^2 = 0.3878$, $p > 0.001$). Clear seasonal oscillations are not visible in this sample,

but fluctuation in Sr/Ca values is evident across the shell. Shell Mg/Ca ratios show a weak but insignificant correlation with distance from the shell umbo (R^2 = 0.13098, P > 0.001).

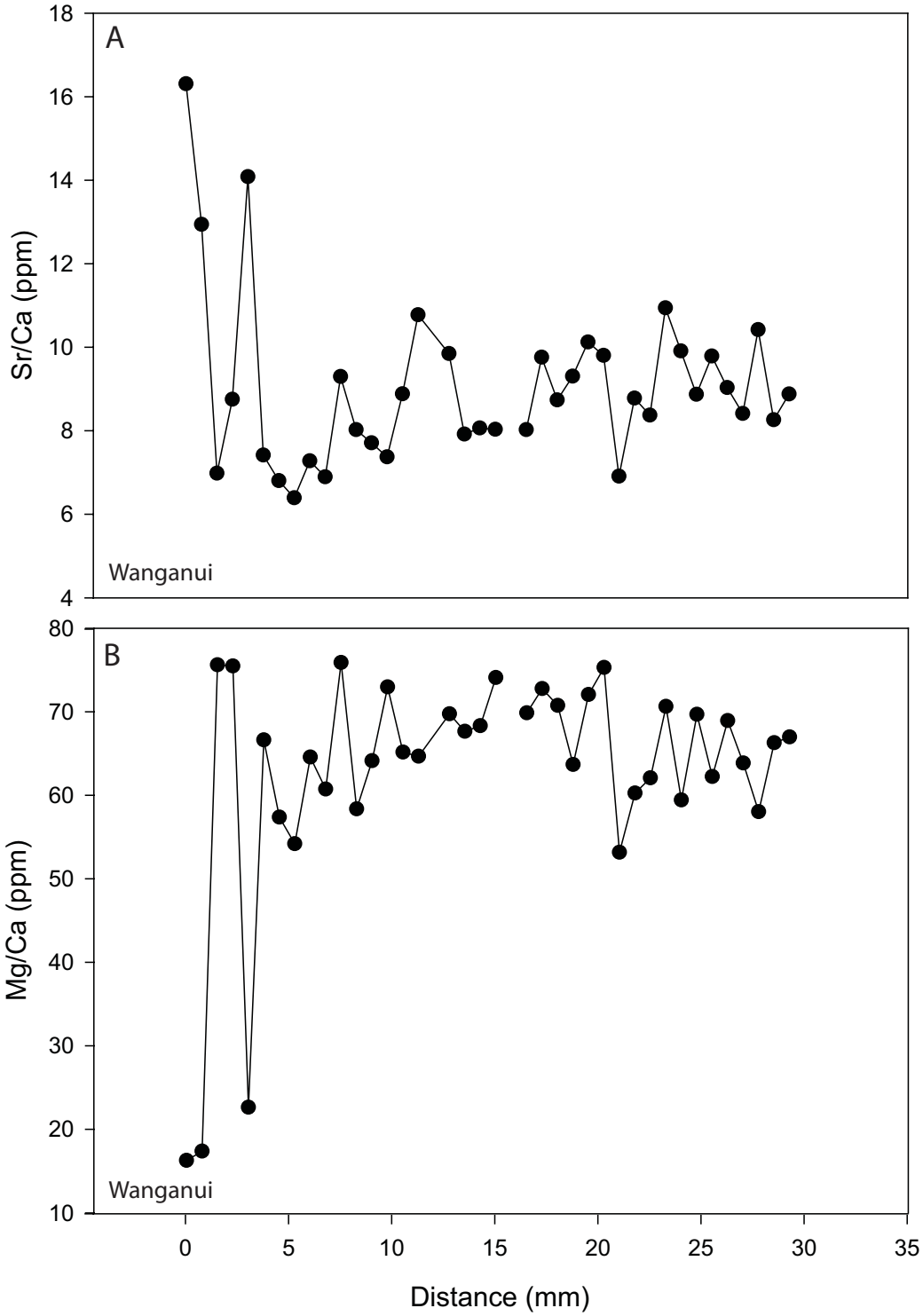

Figure 6.18 (A) Sr/Ca and (B) Mg/Ca ratios for *Crassostrea ingens* (sample WLK) from the Wilkies Shellbed at Parikino, Wanganui.

6.5.2d Summary

The elemental ratios of Mg/Ca and Sr/Ca vary across all portions of the oyster shells measured. The most noticeable difference is the extremely high values for the WLK sample from Wanganui in comparison to samples from Waitomo and Argentina. The values for Mg/Ca are 60 ppm higher and the values for Sr/Ca are 10 ppm higher. Clear seasonal cycles were not noticeable in the samples with the exception of PAT2/1. Here samples were taken at a much wider spatial scale than in the other oyster shells and the regularity of the cycles assumes seasonality is represented in this specimen. Causes for the fluctuation of elemental ratios in all the samples will be further discussed in Chapter Nine.

CHAPTER SEVEN

Petrography of oysters and their host sediments

7.1 INTRODUCTION

The objective of this chapter is to describe the mineralogical and textural composition of both the oyster shells and their host sediments from Waitomo, Patagonia and Wanganui field sites. In some cases this will also include analysis of units that bound the oyster bed formations. An introduction to carbonate terminology, limestone and other sedimentary rock classifications and the basic descriptions of techniques used are given first.

Mineralogy of the host rocks was determined using both X-ray diffraction (XRD) analysis and microscope petrography. Petrography also aided in determining the sorting, modal size and shape of grains in the host material, particularly for Waitomo samples. Texture of the siliciclastic host materials was determined for Patagonia and Wanganui samples using laser particle size analysis. Carbonate percentage tests were also carried out on all host samples.

The mineralogy of oyster shells from each field site was determined using XRD. Microscope petrography (both standard – PPL and cathodoluminescent - CL) was used to analyse features of the oyster shells, infill of borings and alteration state of the oyster shells. Scanning electron microscopy (SEM) provided some insights about the surface and internal features of selected oyster valves.

7.2 CLASSIFICATION OF HOST SEDIMENTS

7.2.1 Mixed sediment classification

Descriptive classifications of sandstones can be fundamentally based around the framework mineralogy, although the relative abundance of the matrix plays a role in some classifications. Unconsolidated siliciclastic grains >2 mm in size are termed gravel, from 0.063 – 2 mm sand, 0.004 – 0.063 mm silt and < 0.004 clay. Because many unlithified siliciclastic sediments involve mixed grain sizes their classification name can be problematic. Various classification schemes have been

devised for the naming of texturally mixed sediments and sedimentary rocks, most of which utilise textural triangles (Fig. 7.1) (Boggs 2001).

The textural classification illustrated in Figure 7.1A includes particles ranging in size from mud (clay and silt) to gravel. Note that the boundaries of each textural classification are not entirely "symmetrical". For example, the boundary between gravel and mud-sand is not 50%, but at 30% gravel in this scheme. If a sample contains only sand size grains and smaller, then the textural schemes shown in Figure 7.1B or 7.1C involving sand, silt and clay are more suitable (Boggs 2001).

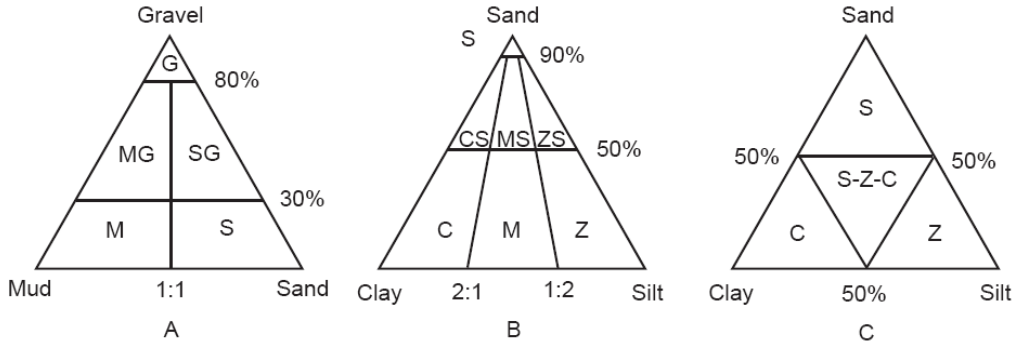

Figure 7.1 Nomenclature of mixed sediments. A, B simplified from Folk (1954). C, After Robinson (1949). G = gravel, S = sand, M = mud, Z = silt, C = clay, MG = muddy gravel, SG = sandy gravel, CS = clayey sand, MS = muddy sand, ZS = silty sand (from Boggs 2001).

7.2.1a Textural maturity

The maturity of a sandstone can be applied in two ways - compositional or textural. Compositional maturity refers to the relative abundance of stable and unstable framework grains in sandstone. A composition of mainly quartz is considered mature, whereas a sandstone with abundant unstable minerals such as feldspars or unstable rock fragments is compositionally immature. In comparison textural maturity is determined by the relative abundance of matrix and the degree of rounding and sorting of framework grains (Fig. 7.2). The level of textural maturity can range from immature, with dominant clays, and poorly sorted and poorly rounded grains, to supermature in which there are no clays and framework grains are well sorted and well rounded. Textural maturity is a measure of the degree of transport and reworking of sediment, or effectively the kinetic energy expended on forming a sediment (Boggs 2001).

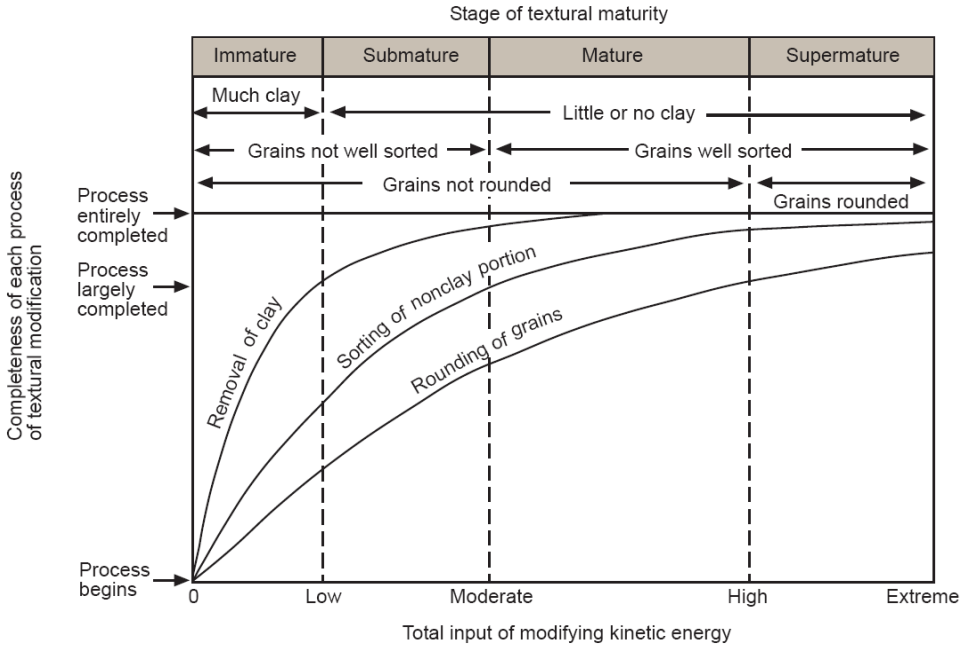

Figure 7.2 Textural maturity classification of Folk (1951). The textural maturity of sands is shown as a function of the input of kinetic energy (from Boggs 2001).

7.2.2 Carbonate classification

Limestones have been separated on the basis of the dominant size of their grains, namely as calcirudite (grains > 2 mm), calcarenite (grains 0.063 mm - 2 mm), or calcilutite (grains < 0.063 mm) (Scoffin 1987). There have been several other classification systems proposed for limestones which rely on descriptive properties as seen under the microscope. These include: (1) discrete carbonate grains or clasts; (2) fine grained carbonate matrix; (3) carbonate cement (sparry calcite) which is chemically precipitated from solution into pore spaces. Two microscope-based classifications of limestones have been universally accepted, namely the Folk (1959) and Dunham (1962) schemes. This study will use the classification system of Folk (1959).

7.2.2a Folk classification

Folk (1959, 1962) recognised three main constituents in limestones: allochems (grains), matrix (micrite), and cement (sparite). His limestone classification considers whether the carbonate particles are held together by sparite or sit within a micrite (carbonate mud) matrix (Fig. 7.3). The ratio of micrite to spar is considered representative of differing degrees of hydraulic energy during sediment deposition, the higher the energy the lower the micrite content. On this basis Folk (1962) devised a textural maturity classification for limestones which

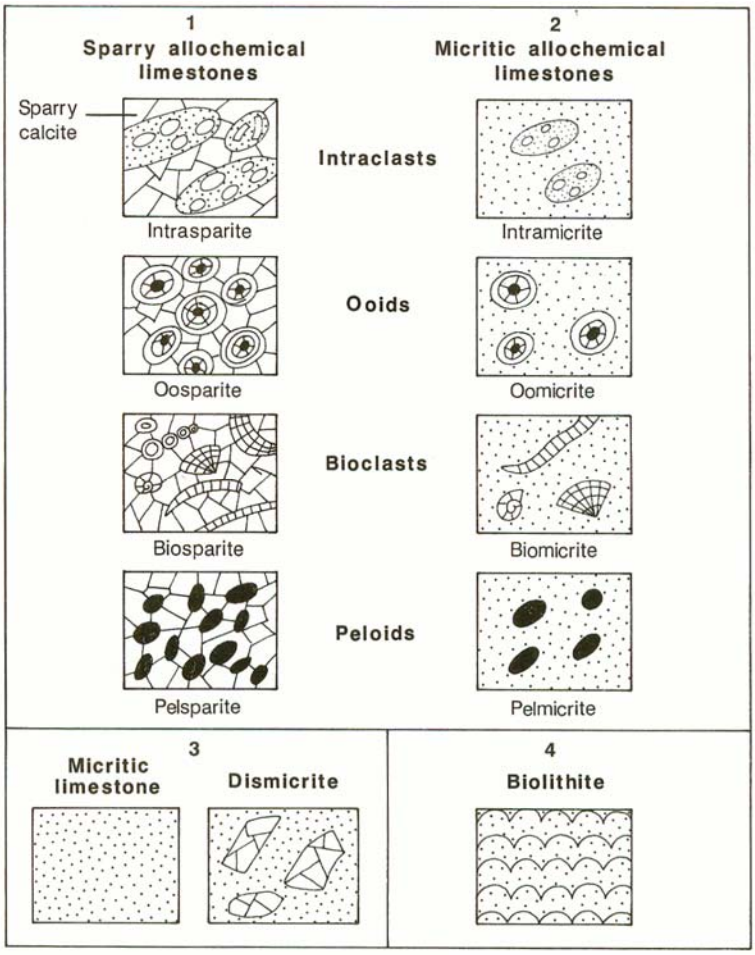

Figure 7.3 Folk's (1959) classification of basic limestone types (from Tucker & Wright 1990). Four groups are recognised and the nomenclenture is based on the types of allochems (grains) and the relative abundance of matrix versus open pore space/sparry calcite that may fill such pores. Listed in the centre of the figure are the main grain types. Box three is representative of micritic matrix lacking allochems and dismicrite ('disturbed' micrite) which has 'eyes' of sparry cement. Biolithite (box 4) is *in situ* reef carbonate.

considers the micrite:spar ratio and also the degree of sorting and rounding of the allochems (Fig. 7.4). Increasingly higher energy conditions of deposition result in a decreasing amount of micrite, increasing spar cement, and better sorting and rounding of grains.

7.2.2b Allochems

Generally, there are four main types of allochems in limestone: (1) Intraclasts (abbreviated as intra) are lithoclasts or fragments of limestone that have been derived from within the basin of deposition (Scoffin 1987). Intraclasts are rare in most New Zealand limestones. (2) Non-skeletal carbonate grains such as ooids (oo) are small round grains with a radial or concentric internal structure. They form from chemical precipitation of carbonate saturated waters. Ooids form

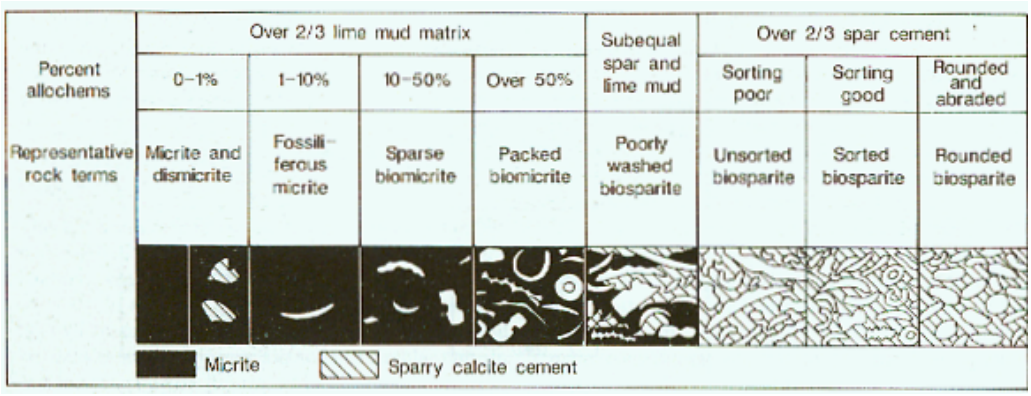

Figure 7.4 Textural maturity scheme for limestones from Folk (1962) showing 8 classes that reflect an increasing environmental energy level from left to right (from Tucker & Wright 1990).

incrementally as consecutive coatings develop around a nucleus such as a fragment of bioclast, pellet, another ooid, or a lithoclast such as a quartz grain. Ooids are characteristically 0.2-1 mm in diameter and spherical or ovoid in shape. They form mainly in carbonates at tropical latitudes and so are not found in New Zealand limestones. (3) Fossil or skeletal fragments, or bioclasts (bio), are the skeletal remains of organisms that secrete carbonate. Bioclasts are usually the only grain type in the majority of New Zealand limestones. (4) Pellets (pel) are formed as the result of ingestion of fine calcareous detritus during grazing on organic rich sediment by organisms such as gastropods and worms. $CaCO_3$ is excreted with the waste products of the organisms and the faecal pellets are often elliptical or rod-like in shape. When the faecal pellets become exposed to supersaturated carbonate waters, they may harden with interstitial precipitation of cement (Scoffin 1987). Pellets are rarely preserved in New Zealand limestones.

In the Folk scheme, the petrographic name is constructed from the various abbreviations for grain types (i.e. intra, ooid, bio, pel) followed by the matrix or cement (mic or spar), and the –ite rock suffix ending. Thus, bioclasts in a micrite matrix would be termed biomicrite and bioclasts in spar cement would be biosparite. Folk further added size terminology for bioclasts: lutite (< 0.06 mm), arenite (0.06-2.0 mm), and rudite (> 2.0 mm), giving rock names like biosparlutite, biomicarenite, and biosparrudite. Due to sand-sized grains being dominant in most limestone, Folk suggested the name arenite could be dropped, so that biomicarenite would become biomicrite, and biospararenite would be biosparite.

7.2.2c Bioclast types

At different periods throughout geological time different types of organisms have been capable of producing calcareous skeletons (Tucker & Wright 1990). The main factors controlling the change in skeletal assemblages are time and environment. Skeletal organisms can be planktic (float in the water column) or benthic (bottom dwelling). Identification of bioclasts relies on determining their shape, size and internal geometry. Common organisms in the Te Kuiti Group Limestones, such as the Orahiri Limestone, include foraminifera, bryozoans, echinoderms and bivalves (Fig. 7.5).

Most importantly in this study is one of the major molluscan groups: bivalves. Bivalves are one of the most important contributors to the bioclastic content of limestones, being present in marine environments since the Cambrian (see geological timescale in Appendix A-1.3). However, it is in the Mesozoic and Cenozoic that they become major contributors to bioclastic sediments (Adams & MacKenzie 1998). As the valves disarticulate easily after death, it is unusual to find complete shells, except in occurrences that have not been disturbed. In the majority of cases bivalves are found in small fragments in limestone, so in thin section only a small part of the usually large-growing shell is seen.

Bivalve shells can be aragonitic or wholly calcite, or a mixture of the two, and their internal structures also vary. Depending on the part of the shell that the fragment comes from and the orientation of the section, fragments may not show complete structure and mineralogy of the whole shell (Adams & MacKenzie 1998). The most important wall structures in bivalves are foliated, prismatic, and homogenous; less commonly seen are crossed lamellar, grained and single crystal microstructure. Most recent and fossil members of the Ostreidae family exhibit irregularly foliated calcite. Exceptions are seen in the family *Gryphaea* that have shells constructed of foliated and cross lamellae calcite (Majewske 1969).

The calcite lamellae that constitute the foliation seen in Ostreidae shells usually occurs in bundles and appear similar to ‘books’ of the mineral mica. Near the exterior of the shell the packets of lamellae become steeply inclined towards the outer surface. Towards the centre of the valve the bundles can be orientated in different directions - horizontal, inclined and also vertical. The bundles of

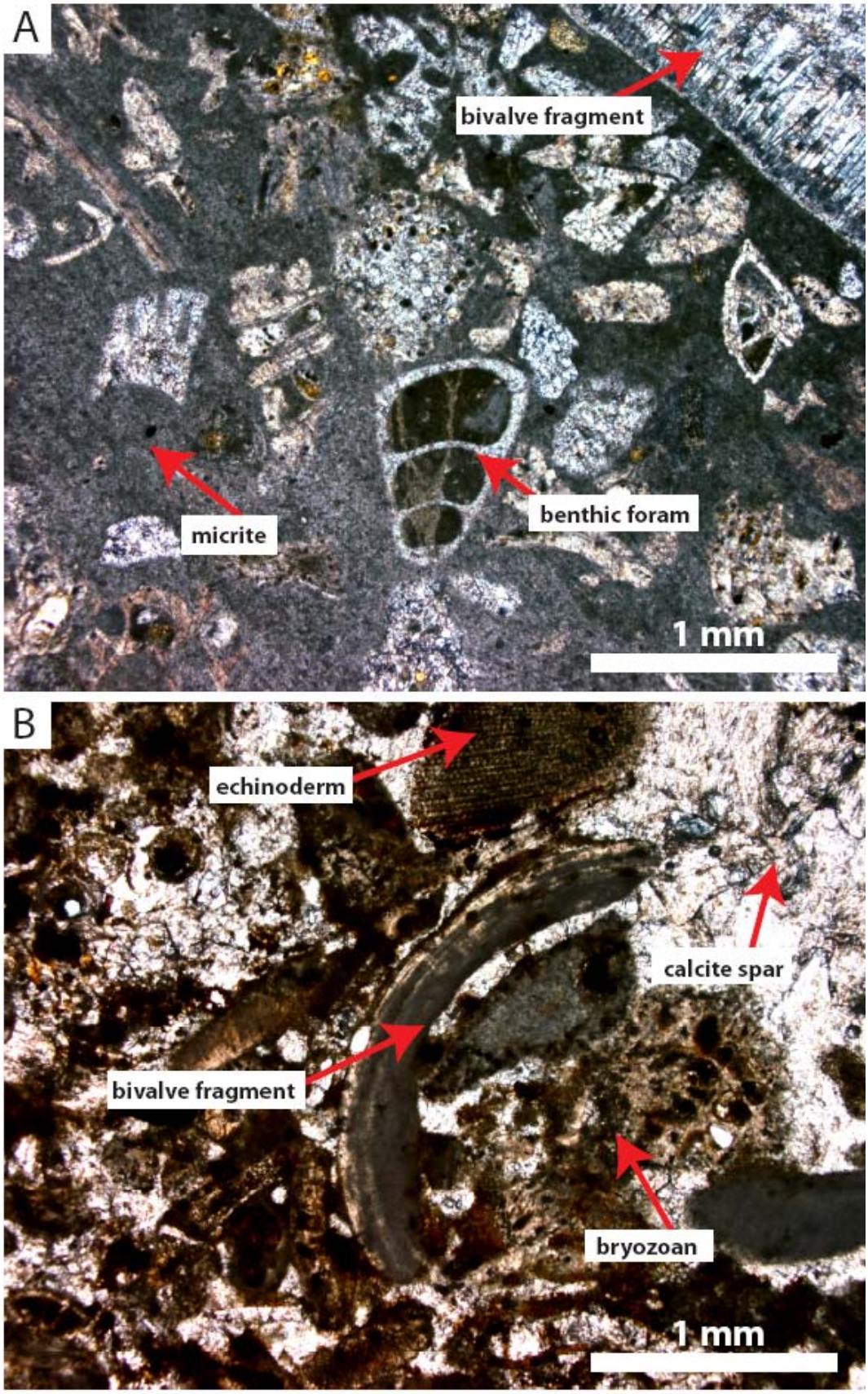

Figure 7.5 Photomicrgraphs (PPL) of samples from Mangapohue Natural Bridge, Waitomo, showing examples of the matrix and cement types and some bioclast types in the Te Kuiti Group Orahiri Limestone. (A) Bioclasts include a large bivalve fragment, benthic forams and bryozoan fragments set in micrite (field sample W04/1B). (B) Bryozoan, bivalve and echinoderm fragments in calcite spar cement (field sample W02/1A).

lamellae assume a nearly horizontal position and become more regular near the inner surface of the shell.

Thin and foliated layers are common in many oysters and commonly form a loosely fabricated lattice work of open chambers in oyster shells, or compact, horizontal foliated layers that alternate with loosely packed, 'chalky' vertical foliated layers. In some samples of fossil oysters a major portion of the valve can be represented by a vesicular lattice framework (Majewske 1969).

7.2.2d Matrix

Matrix in carbonate rocks can consist of dense, fine grained calcite crystals called microcrystalline calcite, carbonate mud, or micrite (used in this study) where carbonate crystals are <5 μm in size (Adams & MacKenzie 1998). Micrite appears dark coloured (grey to dark brown) under the microscope (e.g. Fig. 7.5A). Micrite can be directly precipitated from sea water (strictly cement) or can result from erosion of skeletal grains (Adams & MacKenzie 1998). Many matrices in limestone rocks were originally composed of carbonate crystals of aragonite or high-magnesium calcite which were unstable and later replaced by low-magnesium calcite during diagenesis. The origin of the micrite is sometimes unknown and a number of scenarios have been suggested (Tucker & Wright 1990): (1) Inorganic precipitation associated with change in partial pressure of CO_2 or high temperatures and salinities; (2) Breakdown of calcareous green algae; (3) Disintegration of skeletal organisms (other than plants) and bioerosion by organisms into carbonate substrates producing carbonate mud; (4) Direct biogenic formation of micrite with the accumulation of shells fragments of calcareous plants; and (5) By precipitation of cyanobacteria in marginal marine and freshwater algal marshes.

7.2.2e Cement

Cement is common in the Te Kuiti Group limestones (Fig 7.5B), and is mainly the result of precipitation in a burial environment (Nelson et al. 1988). These burial cements are typically clear, coarse, calcite spar cements (Tucker & Wright 1990). Sparry cement comprises crystals of calcite > 5 μm in size, often much larger (Tucker & Wright 1990), and are typically the pore filling cement responsible for the hardening of skeletal sediments into limestone. There are two common cement

patterns that can form - syntaxial and drusy. Syntaxial calcite spar often occurs as overgrowths about echinoderm fragments, and can be zoned and forms in optical continuity with its host material (Scholle & Ulmer-Scholle 2003). Drusy equant calcite is a pore filling cement that typically increases in crystal size towards the centre of a cavity. The drusy mosaic forms due to the growth competition of crystals having a preferred orientation of optic axes normal to the substrate (Tucker & Wright 1990).

7.3 ANALYTICAL METHODS

7.3.1 Petrography

Petrography is the study of rock textures and mineralogy under the electron or optical microscope (Scholle & Ulmer-Scholle 2003). Cathodoluminscence (CL) is also petrography that uses a different light source. In CL, an electron beam bombards thin sections of minerals to produce a range of luminescent colours. The most commonly observed CL emissions in biogenic carbonates are caused by substitution of Mn^{2+} into the $CaCO_3$ lattice and structural defects (Barbin 2000). CL can be useful in the determination of the spatial distribution of minerals and also the geochemical environment in which the host and fossils formed or were altered (Barbin 2000; Scholle & Ulmer-Scholle 2003).

CL is an important technique for studying carbonate fossils. It is well known that CL often reveals outlines and internal structures of fossils that are otherwise invisible in plane polarised light microscopy. CL may also reveal textures that are invisible in plane or polarised light. CL may also reveal textures more clearly which aids the identification of poorly preserved fossils (Barbin 2000). CL is also very useful for determination of non-carbonate minerals. Calcite luminesces bright yellow to orange, whereas siliceous minerals such as quartz and feldspar, which can be hard to distinguish under plane polarised light (PPL), luminesce to blue to brown (quartz) and bright green to blue (feldspar), making their distinction easier. More information on the CL method is contained in Section 2.3.2.

For this study samples of fossil oysters and the host rock containing the shells were selected from each location, except for the host rock at Wanganui because samples were extremely friable. Samples were selected on the basis of interesting features such as borings and their subsequent infillings. About 70 thin sections

were prepared using the methods outlined in Section 2.3.1. Using an optical microscope (4x objective), petrographic descriptions were recorded onto petrographic data sheets (Fig. 7.6). Light sources used for analysis included plane polarised light (PPL), cross polarised light (XPL), and cathodoluminescent light (CL).

Bioclastic and siliciclastic composition and other charateristicis (e.g. grain size, sorting, cements and shell features) were recorded. The abundance limits in the petrographic data sheets are as follows: 0% = absent, < 1% = rare, 2-5% = some, 6-15% = many, 16-25% = common, 26-50% = very common, 51-75% = abundant, and > 76% = very abundant. Three main sections make up the sheets; a section for bioclastics (carbonate component, e.g. Waitomo), a section for siliciclastics (non-carbonate, e.g. Patagonia and Wanganui) and a section for the description of shell features such as boring shapes, sizes and infill (Fig. 7.6). For the purpose of convenience in this study the siliciclastic fraction in the petrographic data sheets is inclusive of components that are not strictly siliciclastic in origin (e.g. glauconite, pyrite and gypsum), but are nonetheless non-carbonate.

7.3.2 X-ray diffraction (XRD)

The purpose of using XRD in this study is to identify the bulk mineral content of samples from the host matrix of the oyster beds, overlying and underlying lithological units and also the composition of the oysters themselves. XRD is a great tool for the confirmation of a mineral that is suspected to be present in a sample. It is also useful in shells such as oysters to determine the chemical stability of the mineral composition (i.e. low magnesium calcite or high magnesium calcite). Each sample (dried fine powder) was analysed in the XRD, and diffractograms were generated by the XRD software which recorded the mineral peaks to be interpreted. More detail on methodology for XRD is in Section 2.3.4. All results are contained within Appendix C -1.1.

An example of a diffractogram is shown in Figure 7.7. Each peak on the diffractogram is associated with a d-spacing or angstrom (symbol Å) value, position 2θ, and a corresponding mineral. Using a list of minerals that are

Petrographic data sheet - Larissa Macmillan 2009			
Sample number		K11/1A	
Sample description		Host	
Analyst		Larissa Macmillan	
BIOCLASTICS	**Total bioclast %**	77	
		%	**Abundance limit**
	Bryozoans	46	very common
	Bivalves	25	common
	Echinoderms	5	some
	Benthic foraminifera	1	rare
	Planktic foraminifera	-	absent
	Gastropods	-	absent
	Calcareous algae	-	absent
	Barnacles	-	absent
	Spicules & spines	-	absent
	Other	-	absent
	Modal size 1 (mm)	2.00	
	Modal size 2 (mm)	0.50	
	Shape/abrasion	moderately abraded	
	Sorting	poorly sorted	
SILICICLASTICS	**Siliciclastic grain %**	23	
		%	**Abundance limit**
	Quartz	2	some
	Feldspar	8	many
	Igneous rock fragments	-	absent
	Sedimentary rock fragments	-	absent
	Micas	-	absent
	Pyrite grains	3	some
	Pyrite infills	-	absent
	Glauconite pellets	4	some
	Glauconite infills	16	common
	Other	-	absent
	Modal size 1 (mm)	0.10	
	Modal size 2 (mm)	0.25	
	Shape/abrasion	subrounded	
	Sorting	poorly sorted	
SHELL FEATURES	Shell fabric - crystal shapes, weathering, ppt minerals		
	Shell increments - Thickness, colour, continuous, discontinuous		
	Borings - size, shape, boundaries, location (within layer or truncating)		
	Infill - type, bioclastics, siliciclastics, geopetal fabrics, sparite, micritic peliods		
	Recrystallisation - distribution, degree, location.		
	Modal size 1 (mm)		
	Modal size 2 (mm)		

Figure 7.6 Example of a petrographic data sheet used to record thin section information.

expected to be found in the sample, angstrom values from the main peaks were recorded and looked up in angstrom (d-spacing) mineral charts listed in JCPDS International Centre for Diffraction Data (1980). As the peak position on the graph can indicate the crystal structure, peak intensity refers to the reflection from the total scattering from each plane in the crystal structure. This is dependent on the distribution of atoms in the structure (Connolly 2003). The intensity can give a first order approximation of mineral abundance in a sample (i.e. the larger the intensity the greater the mineral content). The intensity of each mineral was also recorded.

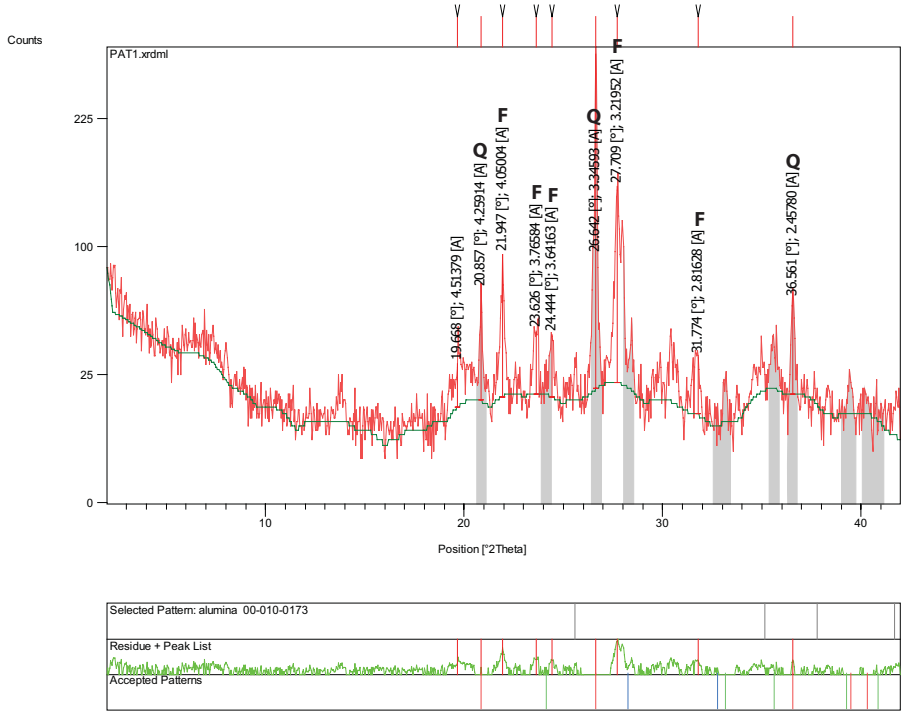

Figure 7.7 Diffractogram showing x-ray diffraction results of a sample of host material from the Puerto Madryn Formation, Patagonia. It shows peaks for the minerals quartz (Q) and feldspar (F). The lower chart shows the number of counts for each peak corresponding to the above diffractogram.

7.3.3 Scanning electron microscopy (SEM)

Scanning electron microscopy (SEM) uses an electron beam to form magnified images of specimens where special instruments can resolve detail of the sample to approximately 3 nm (Fleger et al. 1993). The SEM produces images in 3D showing the texture and morphology of a particular specimen. SEM was primarily used to analyse structure and features of the shell surface. Sample preparation for SEM is covered in Section 2.3.3. The scale of the images taken ranges from 5-500 µm. All images are included in Appendix D-1.3.

7.3.4 Laser particle size analysis

Particle size analysis is a fundamental descriptive measure for sediments and sedimentary rocks and a standard component of research involving sedimentary materials. It is an important factor in understanding the mechanisms that are in operation during transport and deposition of materials (Lindholm 1987).

To determine the size fraction below 2 mm, laser particle analysis was carried out on 16 samples of host materials from oyster accumulations at Patagonia and Wanganui and also of the overlying and underlying deposits to see if any change in grain size occurred over time. A Malvern Mastersizer 2000 instrument was used for analysis. Sample preparation included removal of both organic and carbonate content. Further methodology is included in Section 2.3.7. All generated data are included in Appendix D-1.4. Grain size classes were determined using the Wentworth size scale (Appendix C-1.2) and grain size statistics such as mean grain size and sorting were calculated using an Excel spreadsheet kindly provided by Dr Willem de Lange (*pers. comm.* 2009).

7.3.5 Carbonate percentage

Carbonate percentages were calculated to determine the amount of carbonate in the host matrix at each study location. This is particularly important at Waitomo, as by deriving the carbonate percentage the terrigenous content is in turn calculated. Further methodology for this is included in Section 2.3.8.

7.3.6 Component mineralogy (GADDs)

Component mineralogy is an x-ray technique used to evaluate suspected mineralogical changes over a fine microscopic scale. These changes were first suspected from PPL and CL petrography. Component mineralogy was performed on a sample of oyster shell showing different CL colours. Methodology for this technique is included in Section 2.3.7. Results are included in Appendix C-1.3.

7.4 RESULTS FOR WAITOMO

7.4.1 Host limestone (Orahiri Limestone OrB2)

The XRD results for host rock samples from the oyster facies (OrB2) in Waitomo are provided in Appendix C-1.1 and the petrographic data is included on a CD as Digital Appendices. XRD shows the dominant mineral in the host rocks is calcite,

specifically low magnesium calcite. In particular, the sample of host rock from Waitomo Valley Road analysed using XRD shows a composition of quartz as well as calcite, and pebbles contained within the limestone include feldspar. Under Folk's (1959, 1962) classification of limestones the oyster facies is generally a poorly sorted, packed biomicrite (Fig. 7.8, 7.9). The average bioclastic (78%) composition of the host rock is dominated by bryozoans and bivalve fragments (very common) (Fig. 7.10A). Other bioclasts include echinoderms (some), benthic forams (some) and planktic forams (some). The average siliciclastic (22%) composition is dominated by quartz and feldspar grains (common) (Fig. 7.10B). Also present in the siliciclastic fraction are pyrite grains (some), pyrite infills (rare), and glauconite pellets and infills (some).

The grain size distribution in the Orahiri Limestone host material ranges from 0.08 (very fine sand) to 3.75 mm (granule) (Fig. 7.10C). Grain size in the bioclastic fraction is mainly very coarse sand to granule sized while the siliciclastic grains are typically fine to medium sand sized. Bioclastic grains have low abrasion and are poorly sorted while siliciclastic grains are commonly subangular to subrounded and poorly sorted. Both sparite and micrite are present in samples, although micrite dominates and is often limonite stained. Carbonate percentages in the host rocks ranged from as low as 21% at Waitomo Valley Road (sample WVR-2) up to 85% at Mangapohue Natural Bridge (sample W07/1A). The average carbonate value for all the samples analysed is about 70%.

Table 7.1 Results for carbonate percentage analysis of Orahiri Limestone host from Waitomo.

Sample number	Sample location	$CaCO_3$%
W02/1B	Mangapohue Natural Bridge	82.1
W04/1B	Mangapohue Natural Bridge	82.3
W04/2	Mangapohue Natural Bridge	83.2
W04/3A	Mangapohue Natural Bridge	77.1
W07/1A	Mangapohue Natural Bridge	84.9
W10/1A.T	Mangapohue Natural Bridge	75.6
W10/2A	Mangapohue Natural Bridge	69.8
K12/1B M	Kokakoroa Road	78.3
N14/1A	Ngapaenga Road	58.2
WAP15/1B	Waipuna Road	55.7
WVR-2	Waitomo Valley Road	21.2

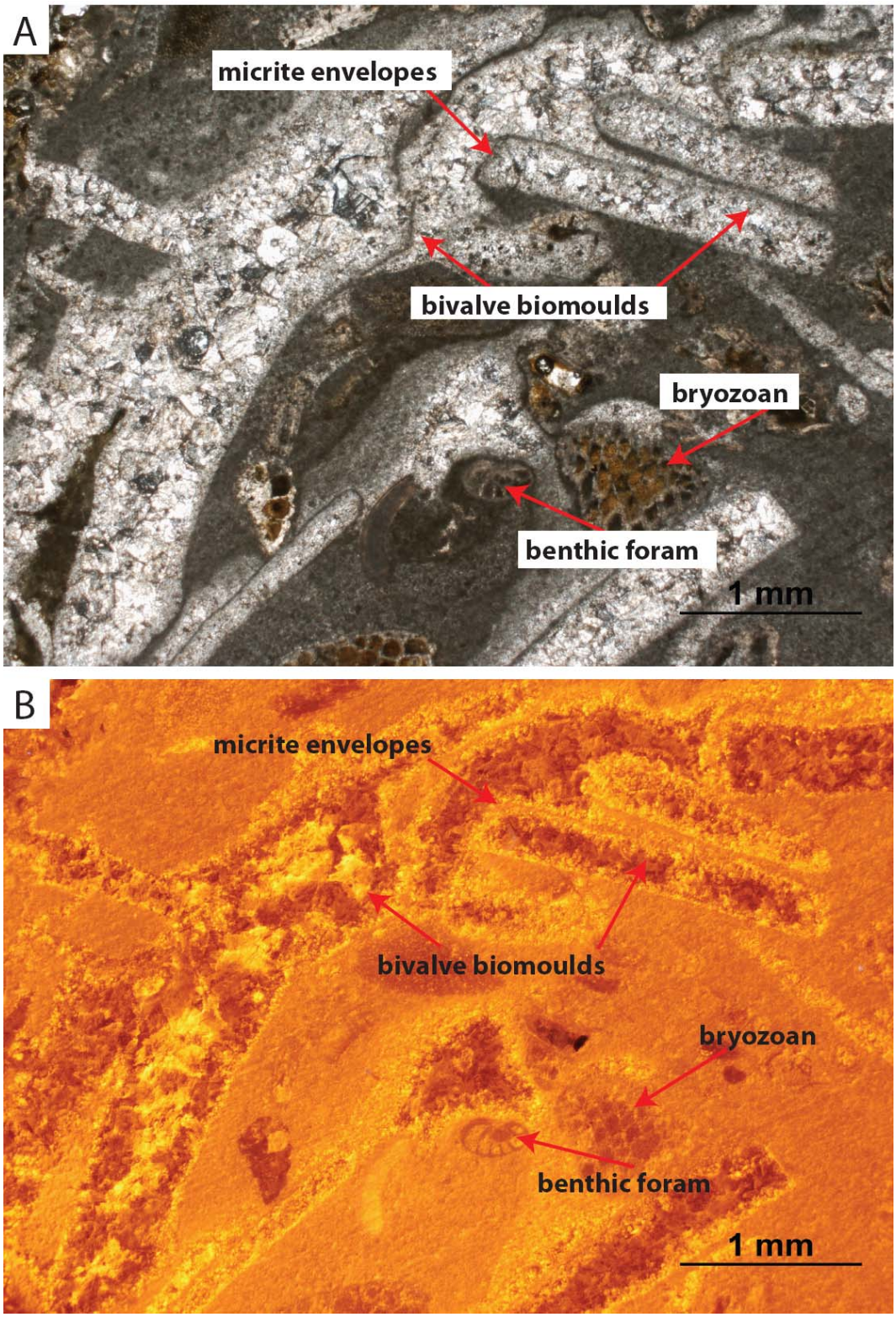

Figure 7.8 (A) Photomicrograph under PPL of the host rock from Mangapohue Natural Bridge, Waitomo (sample W04/1). The sample is dominated by biomoulds of bivalves and scattered bryozoans and micrite. (B) Photomicrograph of the same sample in (A) under CL. The calcite luminesces pale to bright orange, and indicates that the sample is predominantly calcite.

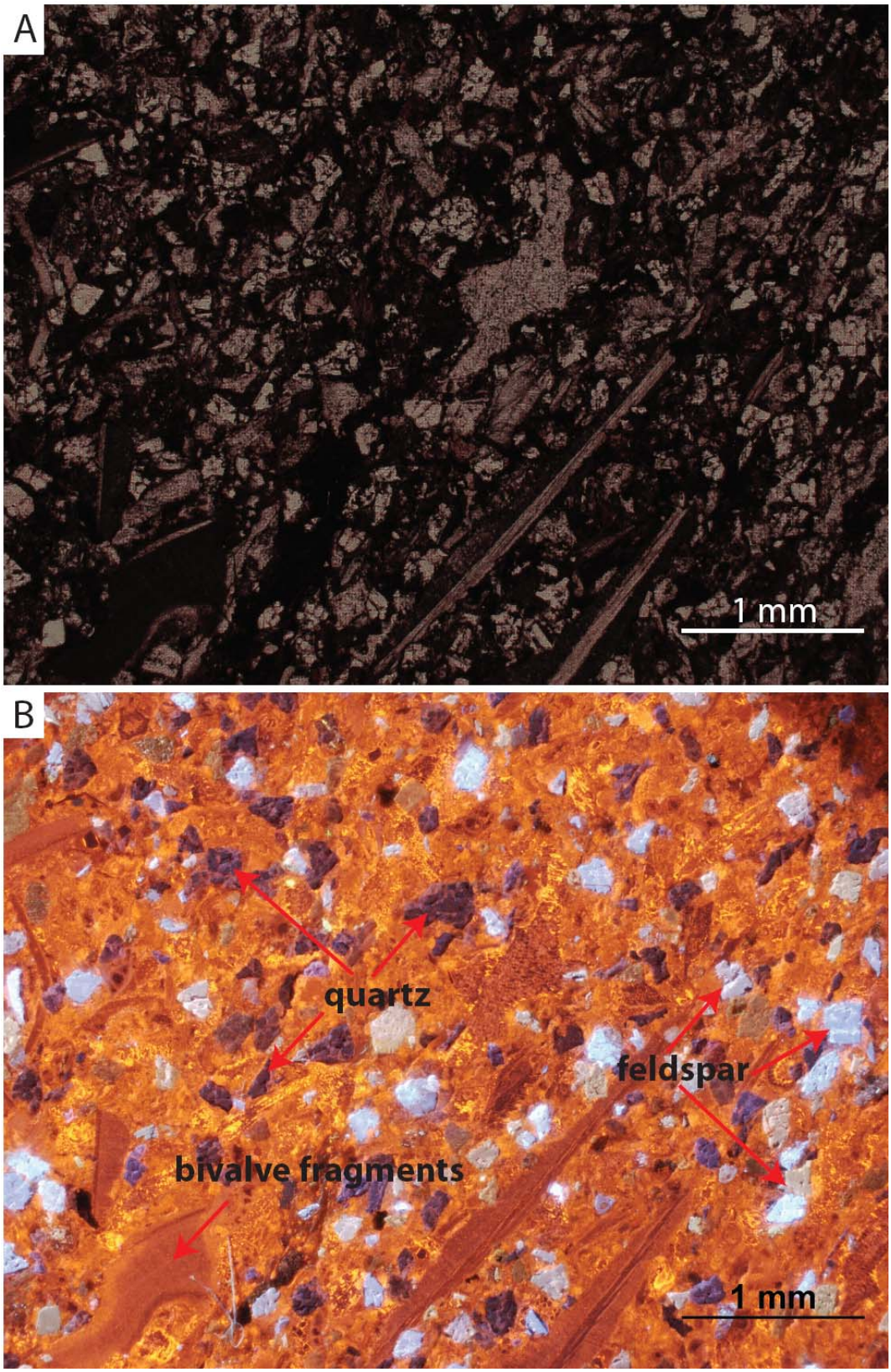

Figure 7.9 (A) Photomicrograph under PPL of host rock from Ngapaenga, Waitomo (sample N14/1C). The sample comprises a mixture of both bioclastics and siliciclastics. Siliciclastics include quartz and feldspar and bioclastics include large bivalve fragments. (B) Photomicrograph of the same sample in (A) under CL. The calcite luminesces pale to bright orange, feldspars are light blue and quartz is dark redish-brown.

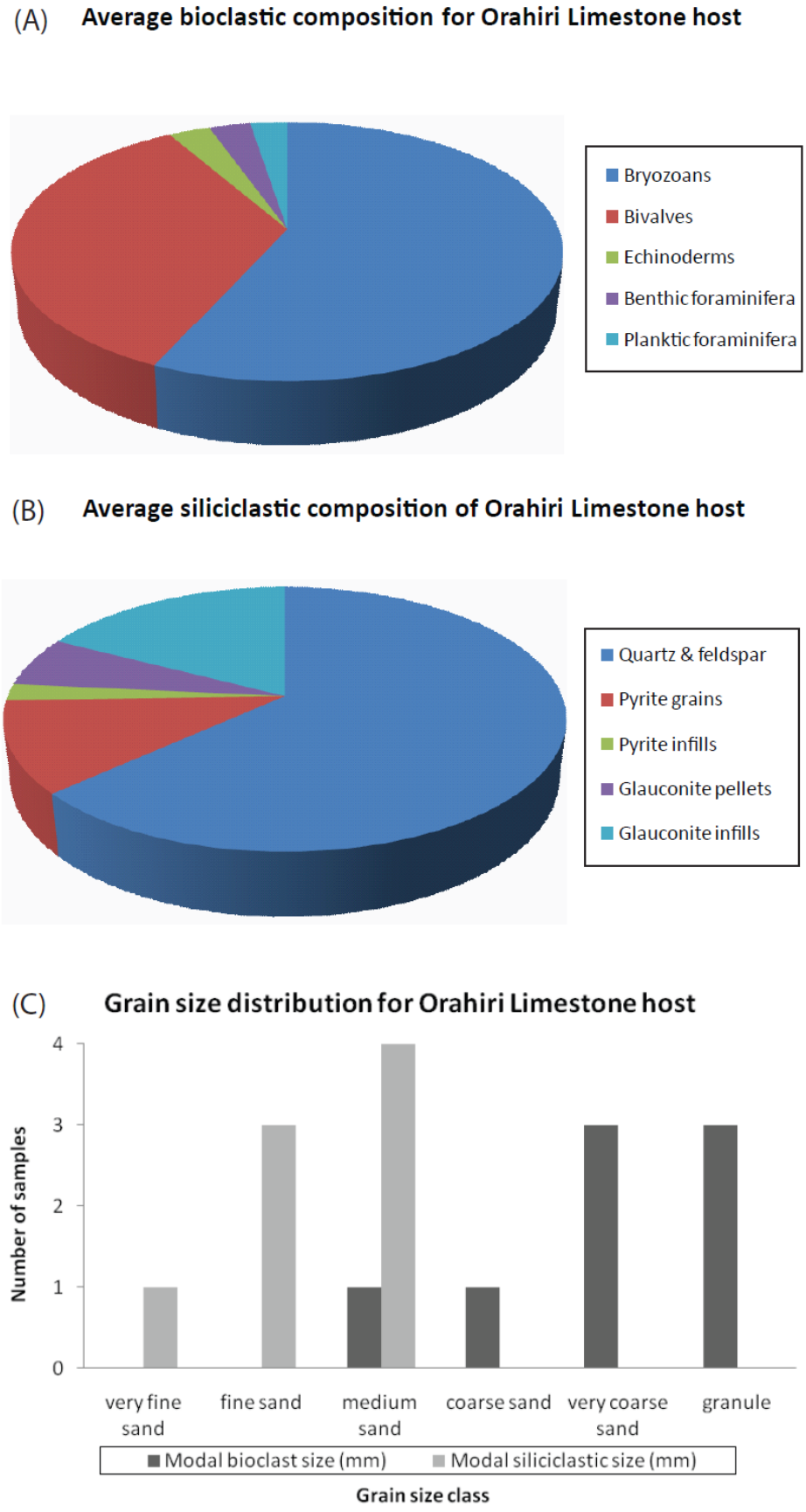

Figure 7.10 (A) Average bioclastic composition (%) of Orahiri Limestone host rock. (B) Average representative percentage of the siliciclastic component of the Orahiri Limestone host rock from petrographic descriptions. (C) Grain size distribution from petrographic descriptions including modal bioclast and siliciclastic size for Orahiri Limestone host.

7.4.2 Oyster shells (Flemingsotreini Stenzel)

XRD data for Flemingostreini Stenzel oyster shells in the Waitomo area are provided in Appendix C-1.1 and petrographic data Appendix D-1.2. XRD results show that all oyster samples are low magnesium calcite in composition. Shell layers consist of alternating thick homogenous calcite and thin foliated layers, with large blocky calcite crystals where areas have recrystallised along the margins of some shell layers. Under CL the luminescence colours are uniformly a dull orange colour in areas that do not show alteration (Fig. 7.11). Areas of recrystallisation occur in several shell samples, typically along the thin light shell layer, and show up as large blocky calcite crystals (Fig. 7.11). Crystals show a range from dull to bright orange colours under CL which indicates zoning and several stages of crystal growth. Some of the thicker layers also show a deep red to blue colour (Fig. 7.12). Results from component mineralogy (GADDs) of sample W04/3B in Figure 7.12 show that both the shell layers and recrystallised areas are composed of calcite. Shell increments range in size with dark grey coloured layers generally being about 0.4 to 3 mm thick and light brown layers being thinner, ranging from 0.05 to 0.25 mm. Layers range from sample to sample from continuous and even in thickness, to irregular and discontinuous (Fig. 7.11). Shells range from little to moderately bored, with borings being both circular and elongate in shape. The borings vary greatly in length, ranging from about 1 mm to 8 cm. Borings commonly have a sharp edge and can be infilled with biomicrite host limestone, calcite spar and sometimes by siliciclastic material (Fig. 7.13). Many have fine examples of geopetal fabrics which are characterised by coarse bioclastic sediments overlain by micrite or micritic peloids, followed by calcite spar (Fig. 7.14). The average bioclastic composition of the boring cavities is similar to that of the host limestone, with very common bryozoans and bivalves and some echinoderms and planktic and benthic foraminifera (some) (Fig. 7.15A). The siliciclastic composition of the infill is dominated by quartz and feldspar (common), pyrite grains and infills (rare), glauconite pellets (some) and glauconite infills (many) (Fig. 7.15B). Grain sizes within the borings range from about 0.1 mm (fine sand) to 2 mm (very coarse sand). The bioclastic fraction of the infill is mainly composed of coarse sand sized fragments, and is moderately abraded and poorly sorted, whereas the siliciclastic component is characterised by fine sand size grains that are subrounded but poorly sorted (Fig. 7.15C).

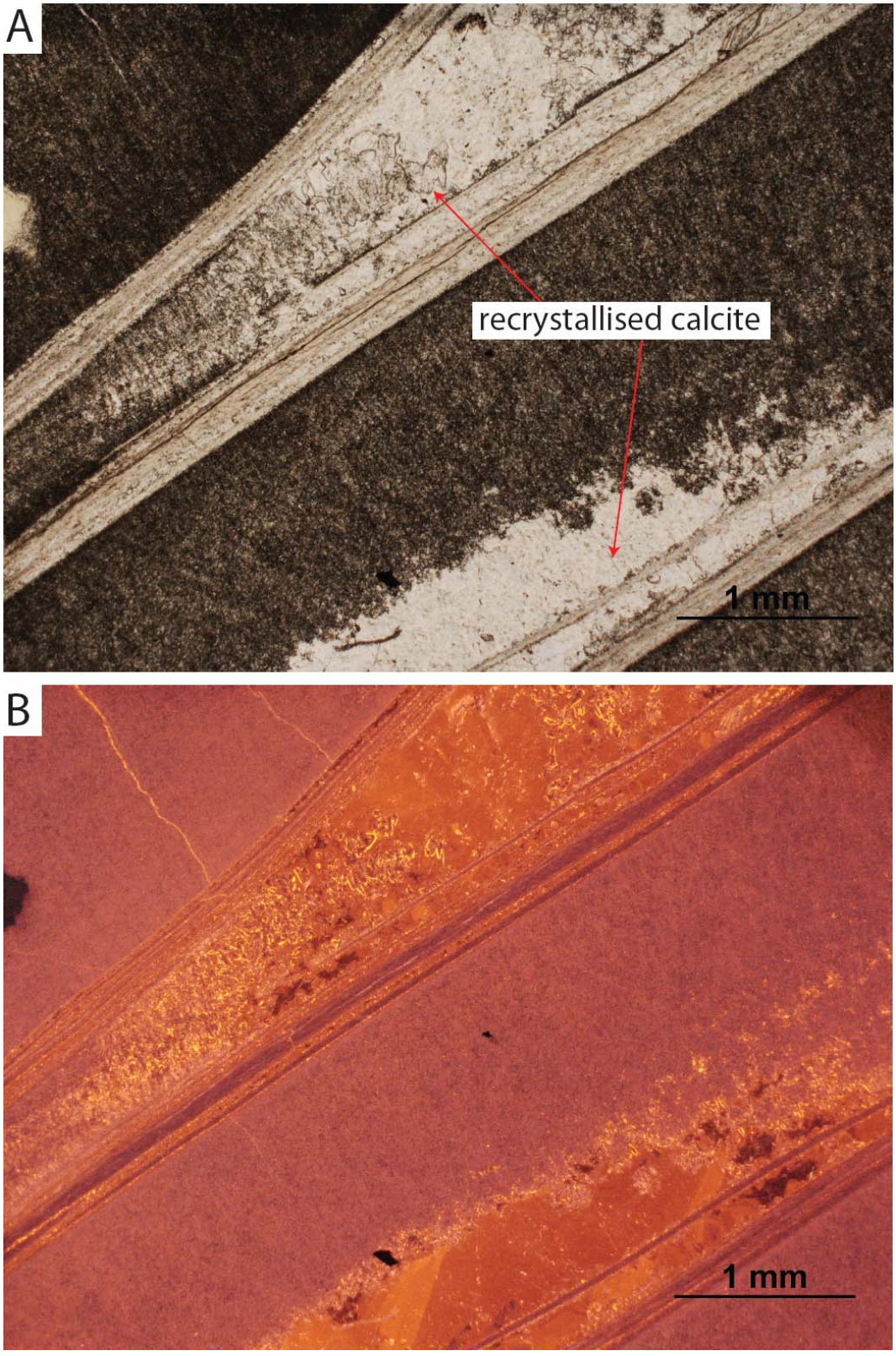

Figure 7.11 (A) Prominent layering in Flemingostreini Stenzel shell from Ngapaenga, Waitomo (sample N14/1C). Layers have a homogenous nature. Large blocky crystals of calcite have formed along the shell layers. (B) CL image of (A) showing orange colour typical of calcite.

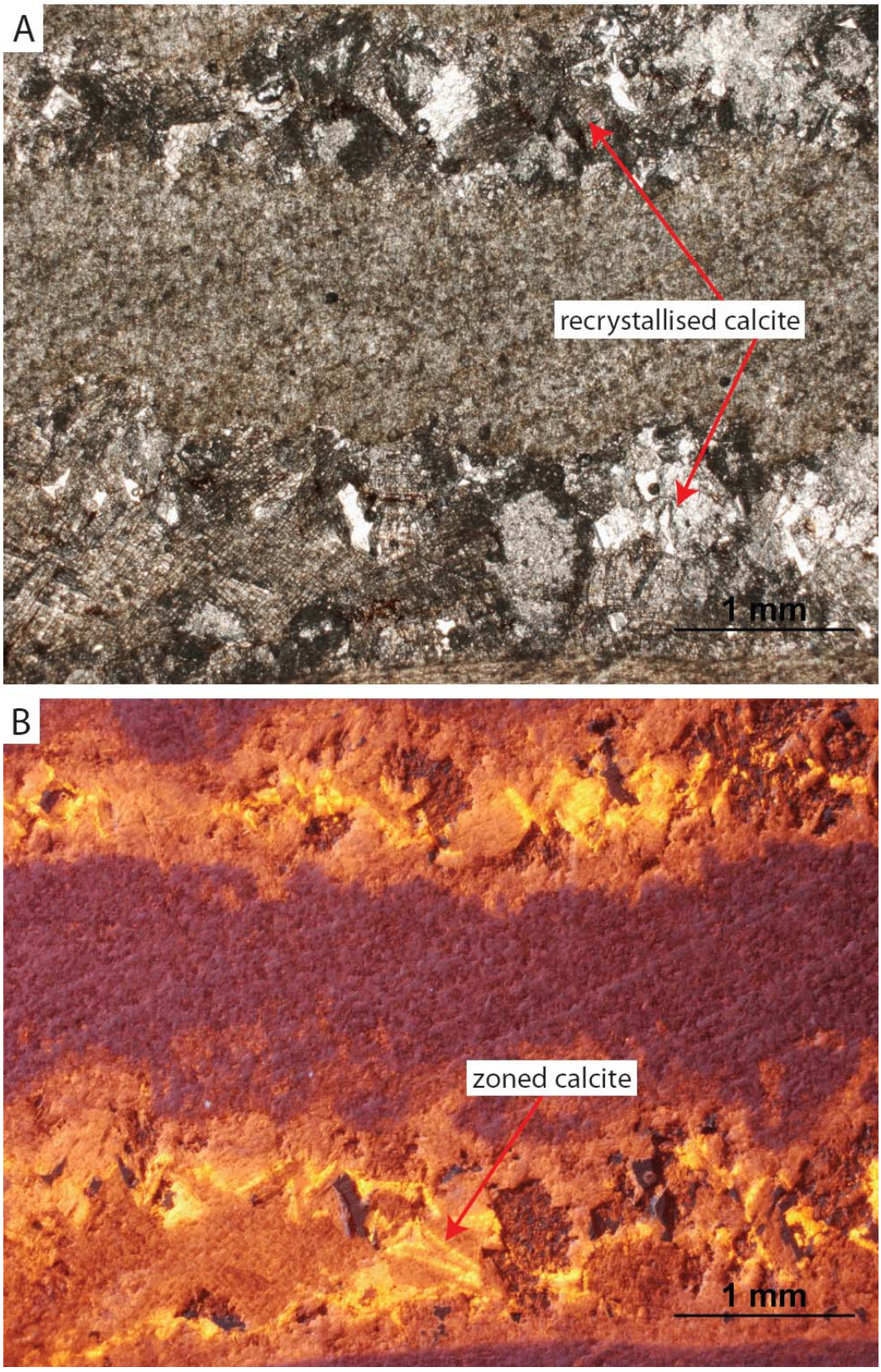

Figure 7.12 (A) Photomicrograph of oyster shell from Mangapohue Natural Bridge, Waitomo (sample W04/3B) under PPL. Large blocky calcite crystals are common in this sample. (B) Same sample under CL light. Original shell luminesces a dark red colour. Calcite crystals are orange to bright yellow with clear zoning.

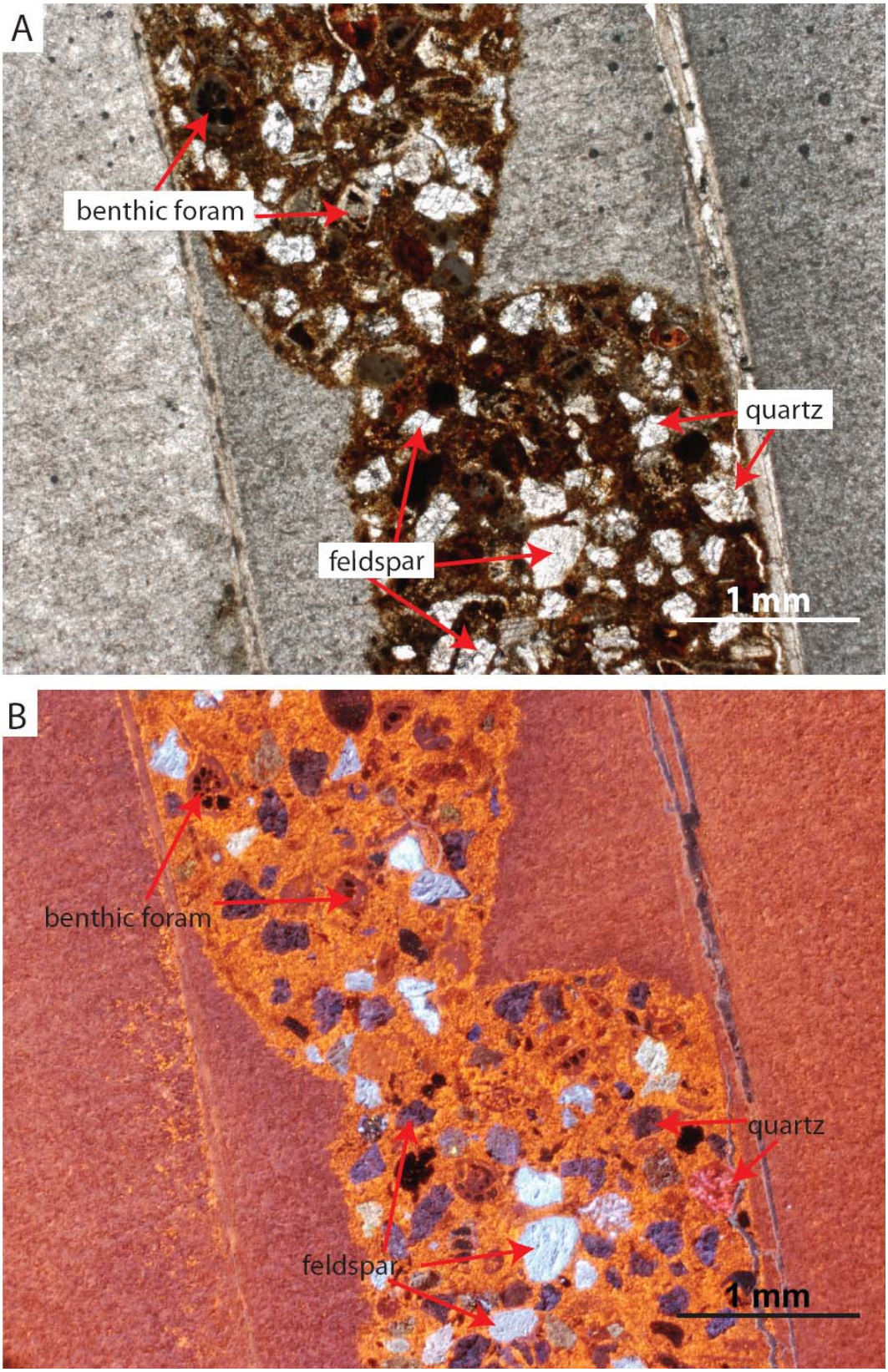

Figure 7.13 (A) Photomicrograph (PPL) of a Flemingostreini Stenzel oyster shell from Kokakoroa Road, Waitomo (sample K13/1B) with an infilled boring. Infill shows quartz, feldspar and benthic forams in a limonite stained matrix. (B) Same sample under CL light. Infill shows predominantly calcite with bright blue feldspar and dark brown quartz.

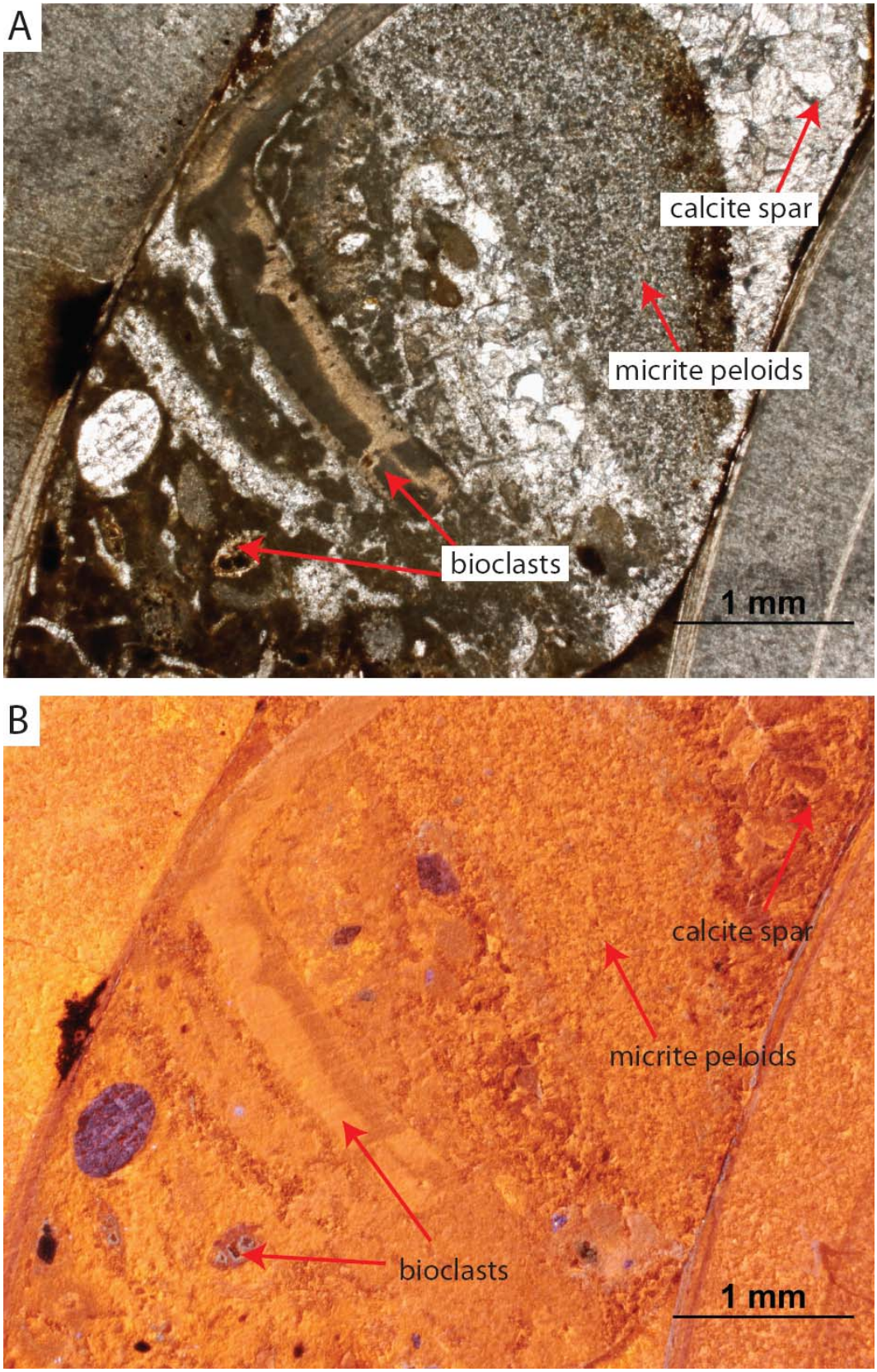

Figure 7.14 Photomicrograph (PPL) of Flemingostreini Stenzel oyster shell from Mangapohue Natural Bridge, Waitomo (sample W02/1B). Boring infill exhibits an internal geopetal fabric. Bioclasts in the lower part of the bore are overlain by micritic peloids and finally calcite spar at top right. (B) Same sample as in (A) under CL in which pale to bright orange shows dominance of calcite. Blue shows feldpar amongst bioclasts.

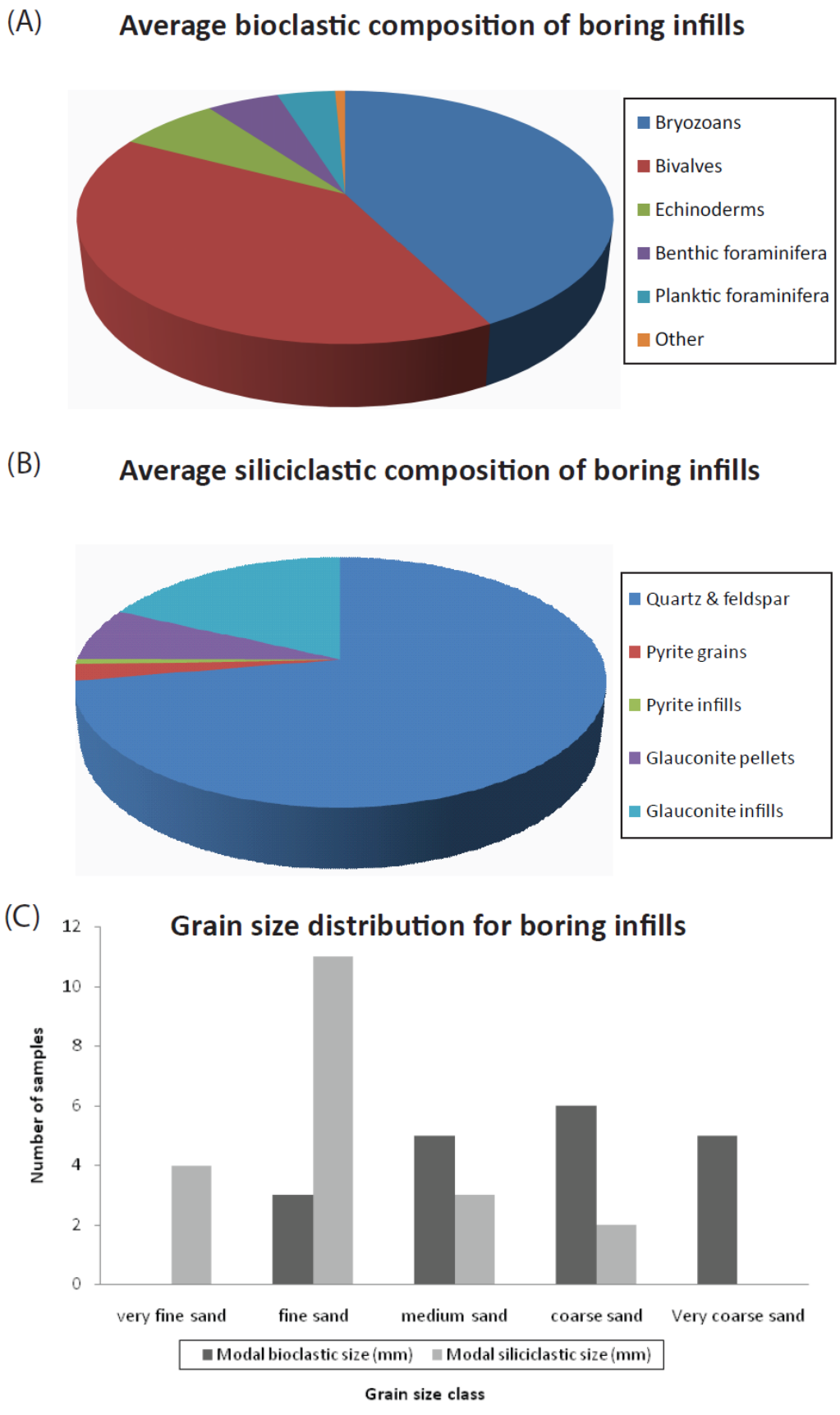

Figure 7.15 (A) Average bioclastic composition of boring infills at Waitomo localities. (B) Average composition of silicliclastic infills (C) Grain size distribution from petrographic descriptions including modal bioclast and modal siliciclastic size for boring infills from Waitomo.

7.5 RESULTS FOR PATAGONIA

7.5.1 Host sediment

XRD results for Patagonian samples are given in Appendix C-1.1 and petrography data in Appendix D-1.2. These show that the predominant mineralogy in the host sediments from Patagonia is feldspar, quartz and the evaporite mineral gypsum. XRD also shows presence of clay minerals, these are possibly contained within rock fragments, and feldspars. The underlying heterolithic muds are composed chiefly of quartz and feldspar. In thin section the host material shows an absence of bioclastic material and the top of the oyster reef in particular is dominated by well developed euhedral crystals of gypsum that appear both massive and fibrous with parallel to twinned areas within the crystal structure (Fig. 7.16A). Gypsum is absent in samples of host sediment taken from the middle and lower sections of the reef. The average siliciclastic composition (100%) of the host rock is characterised by feldspars (very common) and gypsum (common), although the latter only applies to the top of the reef (Fig. 7.16, 7.17). Opaque minerals, quartz and sedimentary rock fragments (some) are also present (Fig. 7.18). Feldspars and quartz are often highly weathered showing numerous fractures (possibly due to effects of resin impregnation) and are clear in colour (Fig. 7.16A, 7.17A). It was necessary to use CL to identify these grains (Fig. 7.16B, 7.17B).

The Patagonian host material is poorly sorted with fine sand sized grains and a bimodal distribution (Table 7.2). Siliciclastics range from angular to subrounded in grain shape. Under Folk's (1954) nomenclature for mixed sediments (Fig. 7.1) the host materials fall into the sand category (Fig. 7.18B). Considering Folk's (1951) textural maturity classification (Fig. 7.2) the host materials from the Puerto Madryn Formation in Patagonia are submature to mature, with little clay sized grains, poorly sorted and subrounded to rounded grains. Carbonate percentage analysis shows the host rock for the *"Ostrea" patagonica* reef in the Puerto Madryn Formation is very weakly calcareous with a maximum value of about 3% (Table 7.2).

Table 7.2 Results from textural and carbonate percentage analysis of host materials from the Puerto Madryn Formation, Puerto Pirámide, Patagonia

Sample no.	Sample description	Modal size (mm)	Modal size (phi)	% Sand	% Silt	% Clay	Wentworth size class	Sorting class	Size distribution	$CaCO_3$%
Pat 1	Underlying unit	0.105	3.13	74.40	16.80	0.60	Fine sand	Poorly sorted	Bimodal	3.0
Pat 5	Host middle	0.149	2.63	81.70	17.40	1.00	Fine sand	Poorly sorted	Bimodal	2.5
Pat 6	Host top	0.149	2.63	83.10	15.90	1.00	Fine sand	Poorly sorted	Bimodal	2.2
Pat 7	Host bottom	0.177	2.38	85.20	13.90	0.85	Fine sand	Poorly sorted	Bimodal	2.2

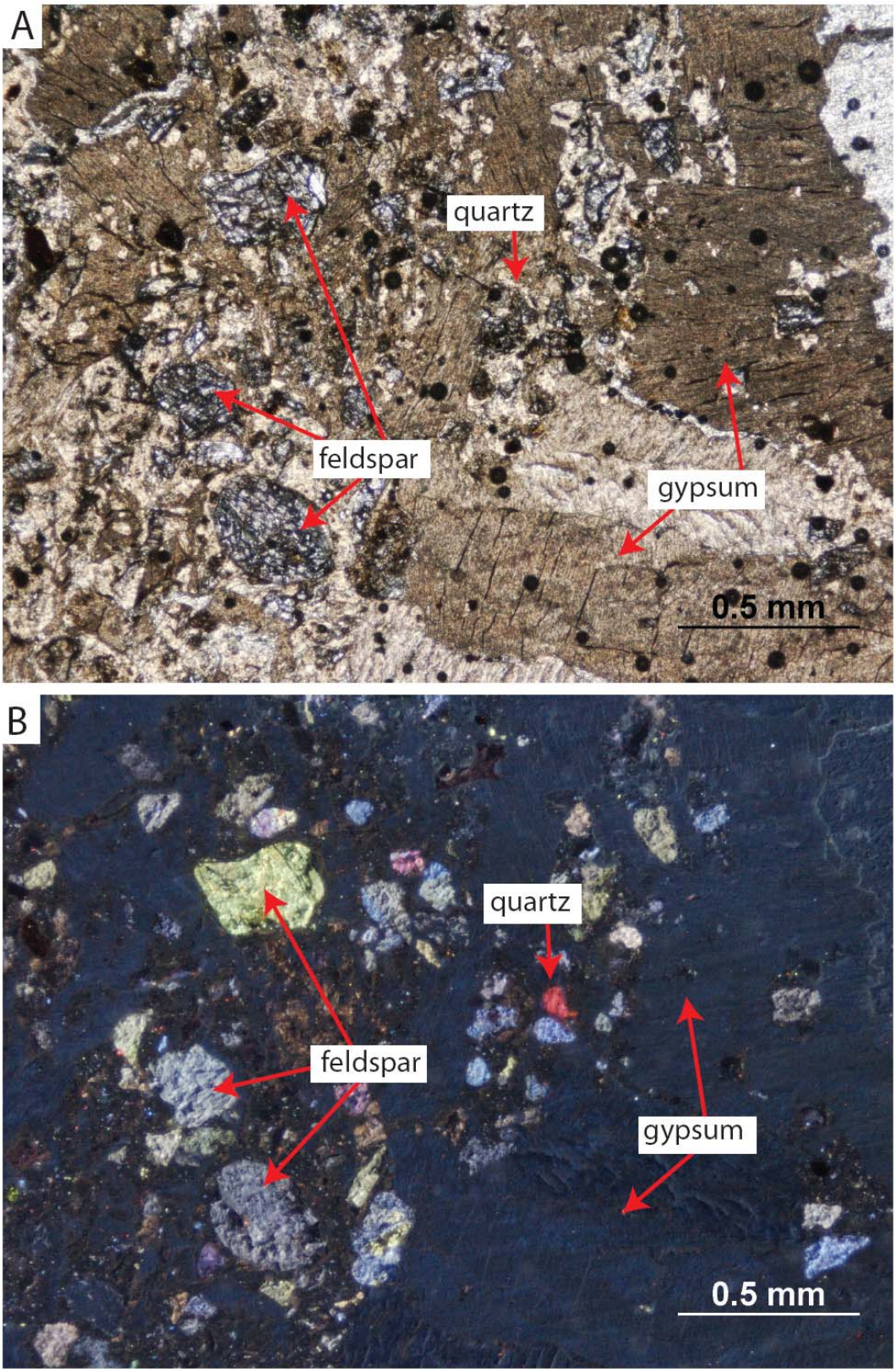

Figure 7.16 (A) Photomicrograph under PPL of the host sediment (submature-mature sand) from the top of the oyster reef in the Puerto Madryn Formation, Puerto Pirámide (sample PAT6). The sample is dominated by large platy crystals of the evaporite mineral gypsum. (B) Photomicrograph of the same sample in (A) under CL. The gypsum minerals do not luminesce and feldspars luminesce light blue.

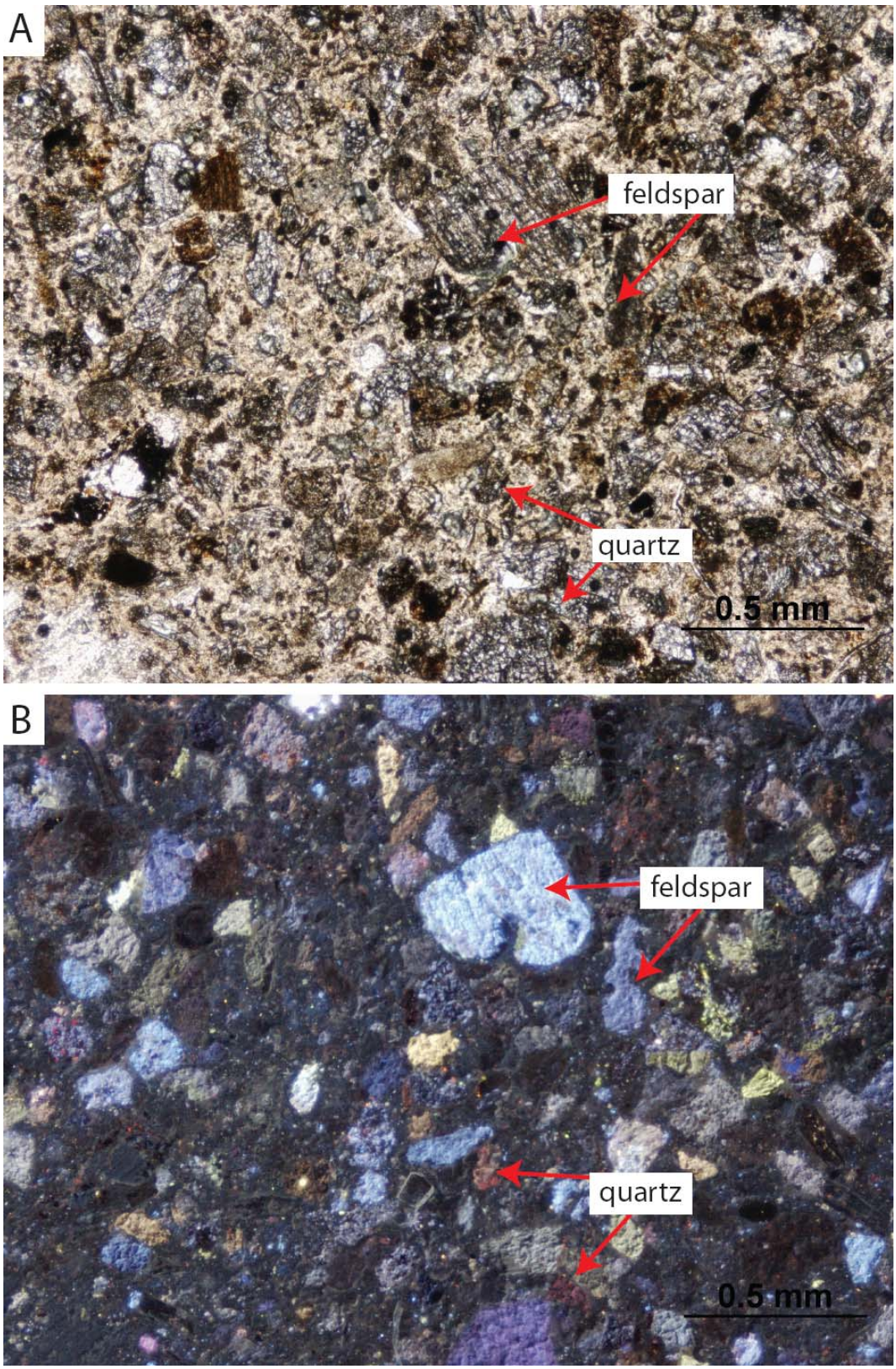

Figure 7.17 (A) Photomicrograph under PPL of the host sediment (submature-mature sand) from the middle of the oyster reef in the Puerto Madryn Formation, Puerto Pirámide (sample PAT5). The sample is dominated by subrounded and poorly sorted grains of quartz and feldspar. (B) Photomicrograph of the same sample in (A) under CL. Feldspars luminesce light blue and quartz are red brown.

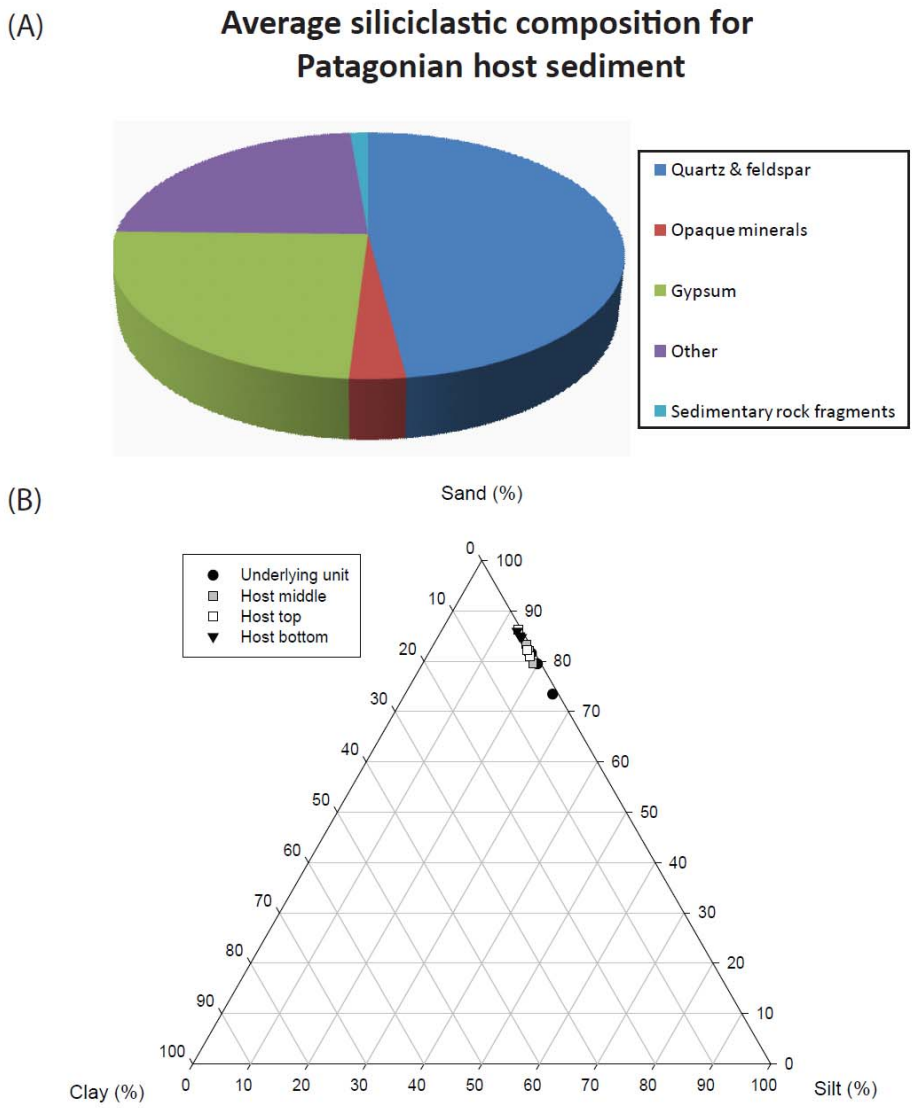

Figure 7.18 (A) Average siliciclastic composition given as a percentage from descriptions of host rock from the Puerto Madryn Formation reef. (B) Ternary plot showing sand, silt, clay composition of Patagonian host sediment. See Table 7.2.

7.5.2 Oyster shells (*"Ostrea" patagonica*)

XRD data for *"Ostrea" patagonica* oyster shells from the Puerto Madryn Formation in Patagonia are provided in Appendix C-1.1 and petrographic data in Appendix D-1.2. XRD results show that all oyster samples analysed are low magnesium calcite in composition. The shell layers consist of elongated calcite crystal laths and fine grained calcite (Fig. 7.19). The oyster shells luminescence colours range from bright to dull orange, signalling calcite (Fig. 7.19B). Weathering of samples ranges from low to moderate and some shells have dark red/brown iron oxide precipitates in the layers. This precipitate is globular to linear in occurrence and occurs mainly within the dark grey thick layer

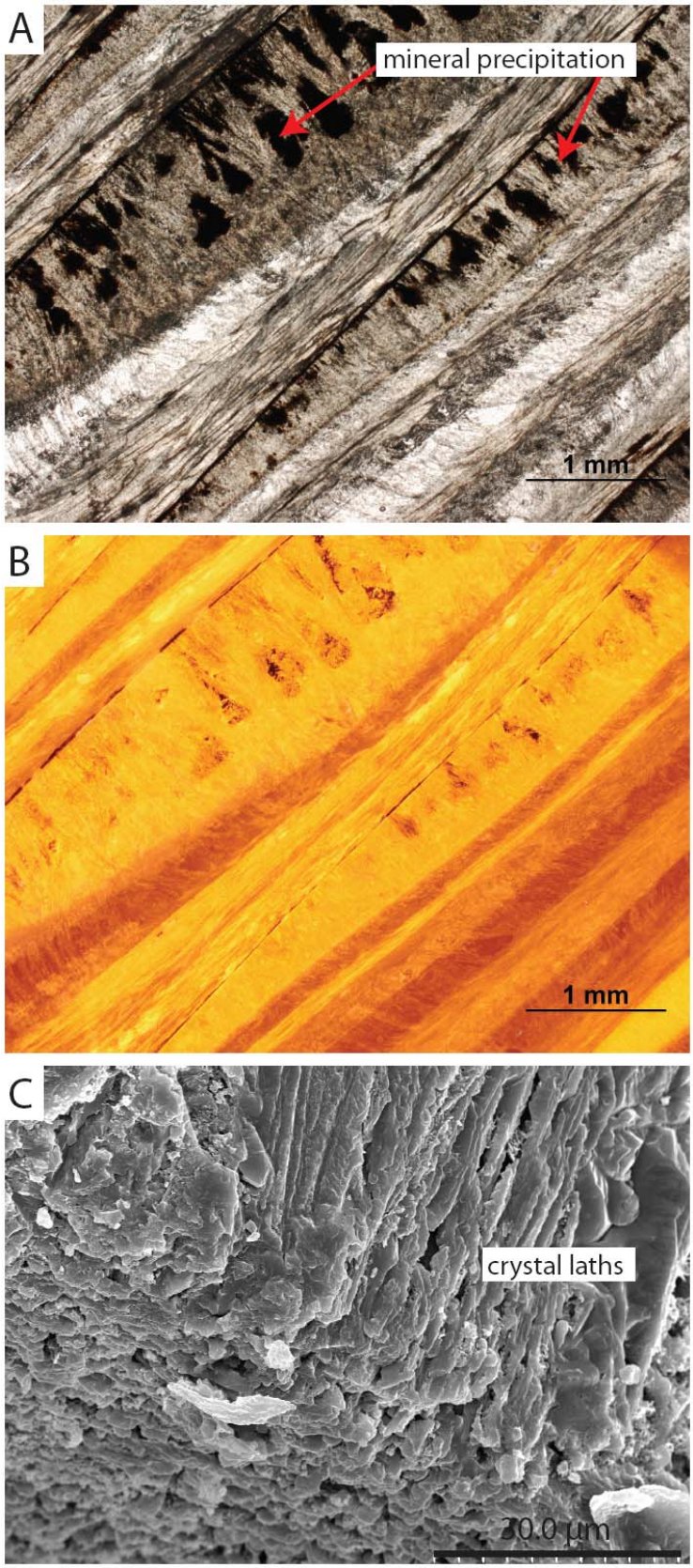

Figure 7.19 (A) Photomicrograph under PPL of *"Ostrea" patagonica* oyster shell from the Puerto Madryn Formation, Puerto Pirámide (sample PAT2/1B). Shell structure is comprised of calcite crystal laths. Dark red/brown opaque iron oxide precipitate is visible within shell layers, stemming from shell boundaries. Note the variation in thickness and colour of shell layers. (B) CL image of (A). Dull to bright orange shows calcite mineralogy of the shell. (C) SEM image showing shell structure of *"Ostrea" patagonica* comprised of calcite crystal laths. Laths are forming perpendicular to the surface of the shell (sample PAT3/3).

or in thin occurrences within the lighter layer (Fig. 7.19A). Petrography of the shells shows an alternation of light and dark shell layers, with the dark layers being much thicker (1.5-4 mm) than the lighter layers (0.2-0.5 mm). Shell layers vary from continuous with little change in thickness, to highly discontinuous and irregular with a large change in thickness. The *"Ostrea" patagonica* shells mainly have few internal borings. These are elongate in shape with sharp edges. They range from 2-4 mm in length and occur within the dark thick layer. They are commonly infilled with fine grained siliciclastic sediment such as quartz, rock fragments and opaque minerals (Fig. 7.20). CL shows the preservation state of the shells is high (i.e. no recrystallisation).

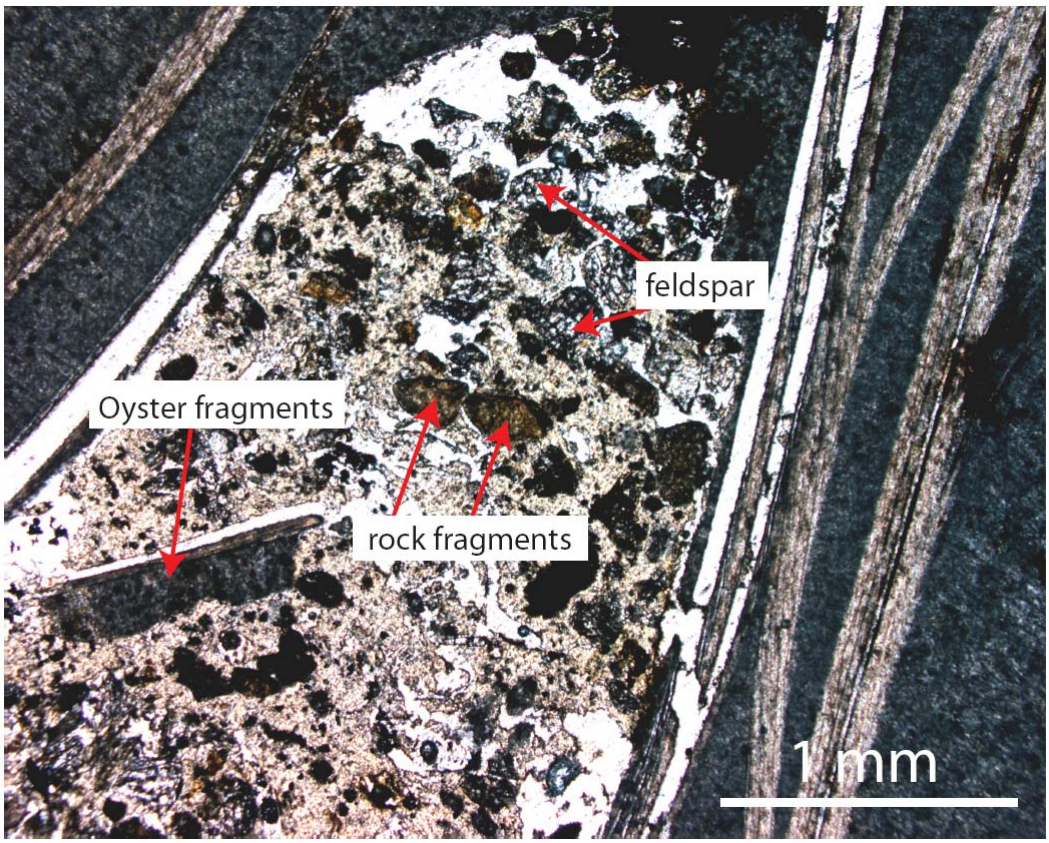

Figure 7.20 Photomicrograph taken under PPL showing boring contained within dark grey layer of oyster shell, from Patagonia (sample PAT4A). Boring is infilled with fine grained siliciclastic material and oyster fragments.

7.6 RESULTS FOR WANGANUI

7.6.1 Host sediment

XRD results for Wanganui samples are recorded in Appendix C-1.1 and petrographic data in Appendix D-1.2. XRD shows that the mineralogy of the Wilkies Shellbed host sediment is composed of quartz, calcite, feldspar,

muscovite and probably other phyllosilicates (clay minerals). The underlying sandstone unit (Makokako Sandstone) has a similar composition but is free of calcite. In thin section the host sediment of the Wilkies Shellbed is dominated by abundant fine grained siliceous material (composed of quartz, feldspars and clays) in the matrix and quartz (many) and feldspar (many) grains, often limonite stained (Fig. 7.21, 7.22). Micas (many), opaque minerals (many) and glauconite pellets (some) also occur in the host materials (Fig. 7.22). Bioclastics are commonly absent within the Wilkies Shellbed host, but where present they consist of fragmented bivalves (some to many) and abraded bryozoans (many).

Textural data (Table 7.3, Fig. 7.22B) show that the host sediment for the Wilkies Shellbed has very fine sand sized grains, which are subrounded to rounded and very poorly sorted with a bimodal size distribution. The underlying Makokako Sandstone unit ranges from medium silt to fine sand and is poorly to very poorly sorted with a bimodal distribution. The overlying Cable Siltstone has coarse silt sized grains, is poorly sorted and has a unimodal distribution (Fig. 7.22B). Using Folk's (1954) nomenclature for mixed sediments (Fig. 7.1) the host materials from Wanganui fall into the sand category and considering Folk's (1951) textural maturity classification (Fig. 7.2) the host materials are submature. Carbonate percentage data are included in Table 7.5. The host sediment at Wanganui contains 15% $CaCO_3$. The underlying Makokako Sandstone has a carbonate value ranging from about 2 to 35%. The overlying Cable Siltstone is weakly calcareous with a value near 3%. These results suggest that the carbonate percentage decreases upwards in the Whauteihi Formation (Fig. 5.5, Table 7.3).

7.6.2 Oyster shells (*Crassostrea ingens*)

XRD data for *Crassostrea ingens* oyster shells from the Wilkies Shellbed in Wanganui are provided in Appendix C-1.1 and petrographic data in Appendix D-1.2. XRD shows that all the oysters samples are low magnesium calcite in composition. Petrography of the shells shows they are composed of crystal laths of calcite (Fig. 7.23A). In some samples the calcite laths form in irregular bundles. CL imaging of the crystals shows the calcite material is relatively homogenous and dull orange in colour, suggesting calcite (Fig. 7.23B). A few samples show irregular lines of dark red/brown iron oxide staining, mostly within

Table 7.3 Results of textural and carbonate percentage analysis of host sediment from Wilkies Shellbed and the overlying and underlying units at Wanganui.

Sample no.	Sample description	Modal size (mm)	Modal size (phi)	% Sand	% Silt	% Clay	Wentworth size class	Sorting class	Size distribution	$CaCO_3$%
Wan 01	Overlying unit	0.016	5.50	21.1	66.5	4.1	Coarse silt	Poorly sorted	Unimodal	2.9
Wan 05	Underlying unit	0.177	2.38	44.8	21.8	3.4	Fine sand	Very poorly sorted	Bimodal	35.3
Wan 07	Underlying unit	0.149	2.63	78.9	18.5	2.6	Fine sand	Very poorly sorted	Bimodal	2.5
Wan 08	Underlying unit	0.125	2.63	30.6	61.4	8.0	Fine sand	Very poorly sorted	Bimodal	27.3
Wan 09	Underlying unit	0.149	2.88	71.2	25.6	3.2	Fine sand	Very poorly sorted	Bimodal	4.4
Wan 16	Underlying unit	0.149	2.63	63.3	32.3	4.4	Fine sand	Very poorly sorted	Bimodal	2.6
Wan 16A	Host sediment	0.177	2.38	77.5	20.6	1.8	Fine sand	Very poorly sorted	Bimodal	15.3
Wan 18	Underlying unit	0.149	2.63	83.6	14.7	1.7	Fine sand	Poorly sorted	Bimodal	38.8
Wan 19	Underlying unit	0.149	2.63	70.3	26.2	3.5	Fine sand	Poorly sorted	Bimodal	1.5
Wan 20	Underlying unit	0.125	2.88	70.1	26.0	3.8	Fine sand	Very poorly sorted	Bimodal	25.6
R2	Host sediment	0.210	2.13	80.1	17.8	2.1	Fine sand	Very poorly sorted	Bimodal	41.2
K2E	Host sediment	0.149	2.63	75.9	21.7	2.5	Fine sand	Very poorly sorted	Bimodal	3.2

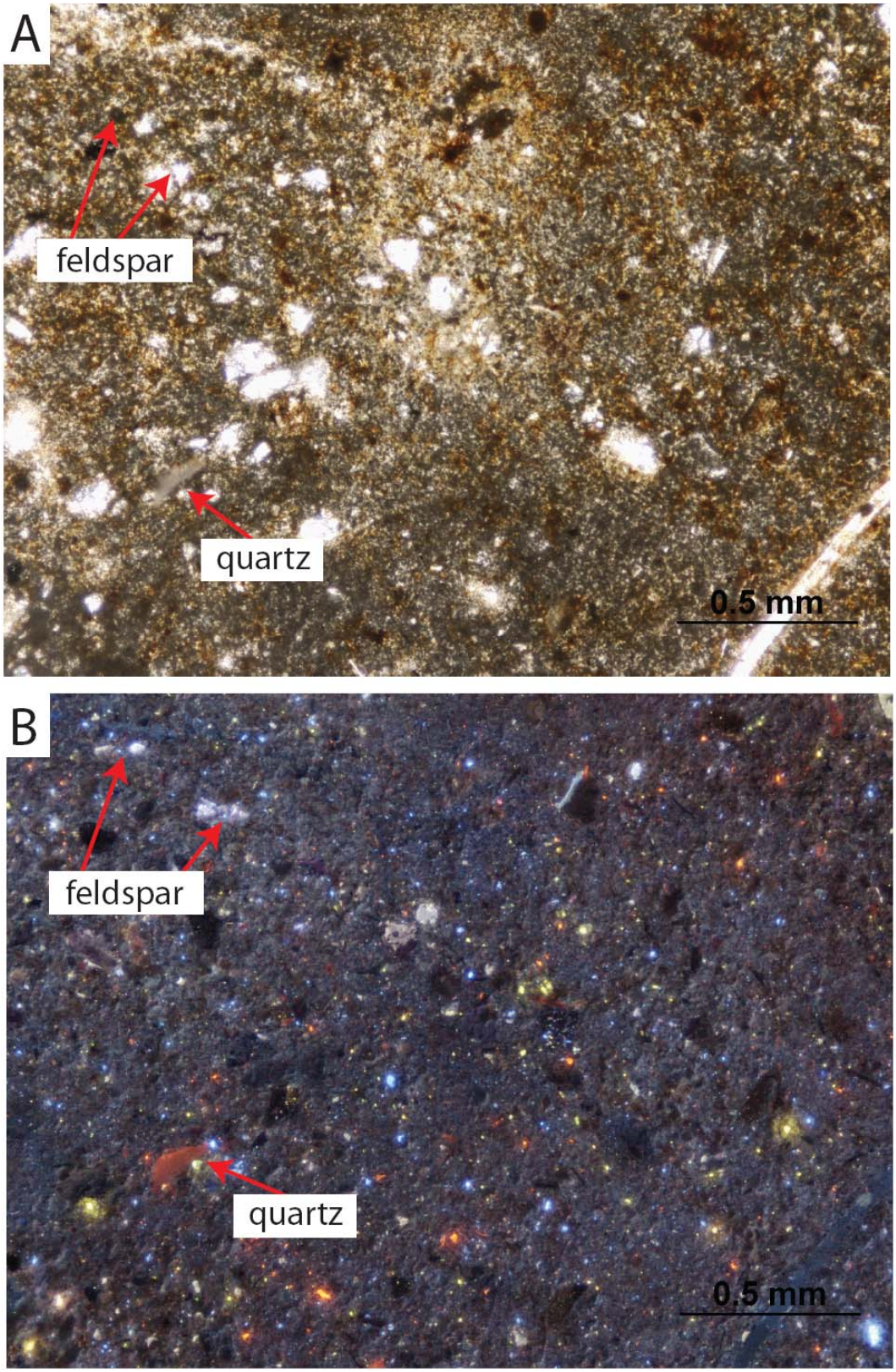

Figure 7.21 (A) Photomicrograph under PPL of host sediment (submature sand) from the Wilkies Shellbed, Parikino (Sample WLK). Sample is composed of fine grained subrounded, moderately sorted feldspar and quartz. (B) CL image of (A). Feldspar luminesces light blue and quartz red brown.

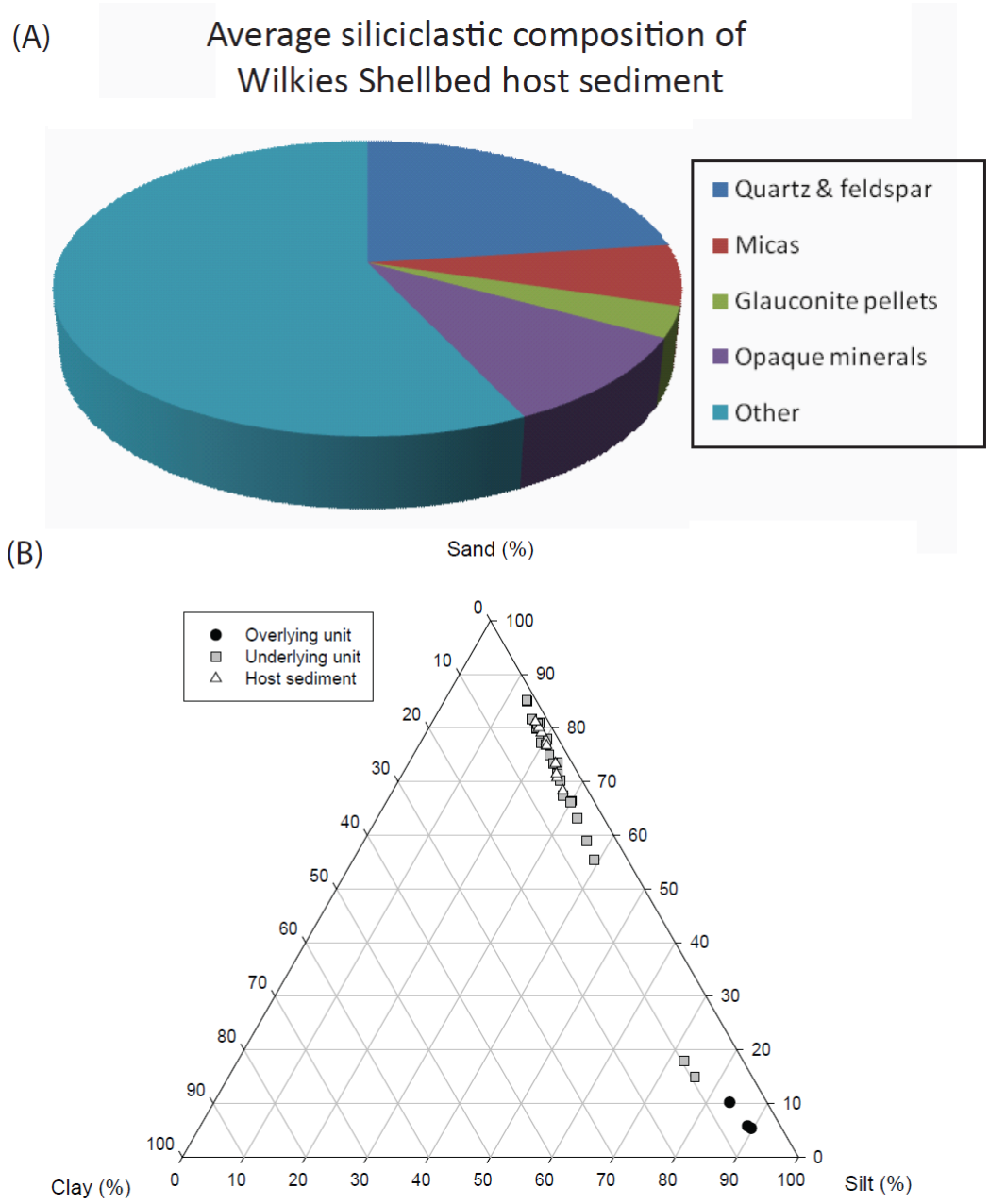

Figure 7.22 Average siliciclastic composition given as a pecentage from descriptions of host rock from the Wilkies Shellbed at Wanganui. (B) Ternary plot of sand, silt and clay fractions of Wanganui host sediments. See Table 7.3.

the thicker darker layer of the shell. Shell increments alternate in both thickness and colour. Thin layers are light brown in colour (PPL) and range from 0.1-0.3 mm thick, whereas thicker layers are dark grey in colour and range from 0.3-4 mm thick. Layers can be continuous and regular or range markedly in thickness. Many shells show fracturing and displacement of shell layers. Recrystallisation occurs in small linear patches along thin layers and in large blocks within darker thick layers (Fig. 7.24A). In both areas recrystallisation consists of fine grained calcite spar. Internal borings in *Crassostrea ingens* from the Wilkies Shellbed

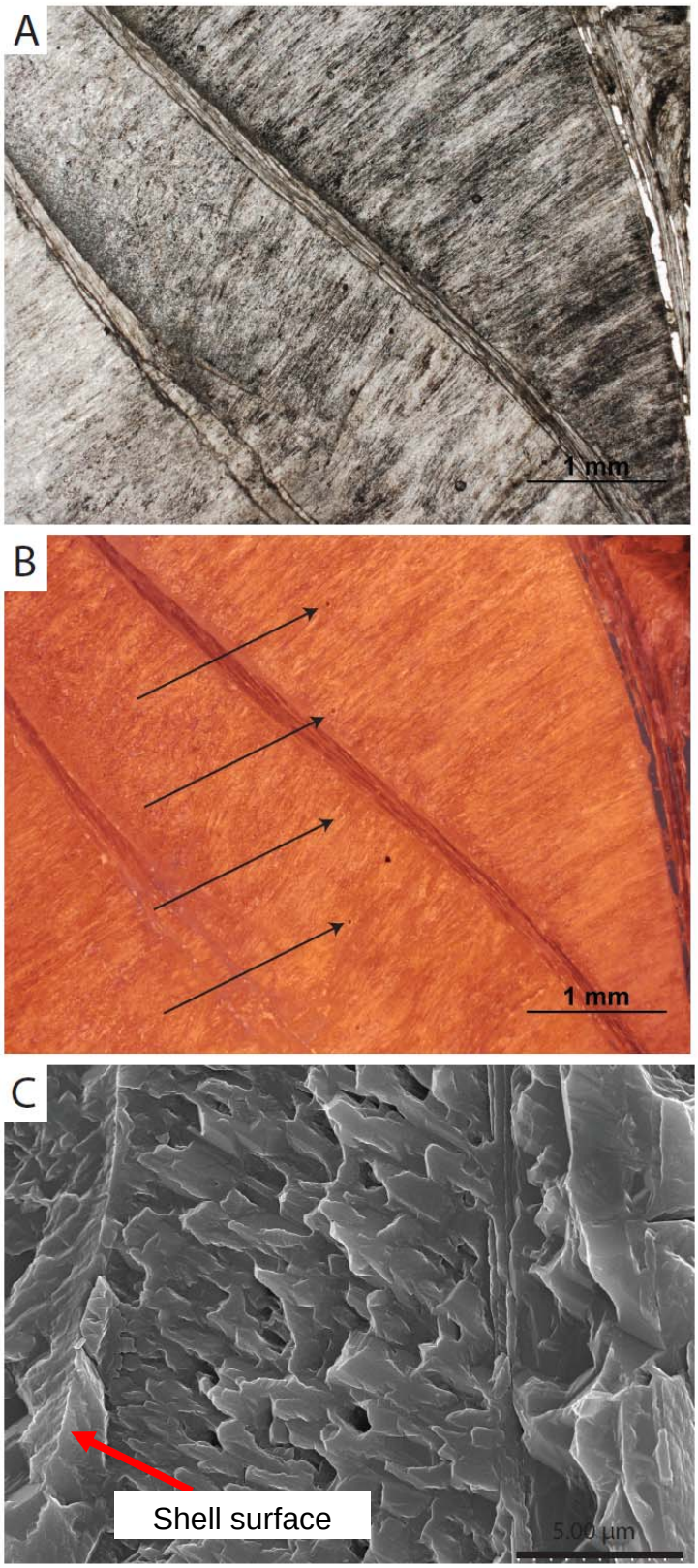

Figure 7.23 (A) Photomicrograph under PPL of *Crassostrea ingens* oyster shell from Wilkies Shellbed, Wanganui (sample WLK). Crystal lath structure can be seen in the light shell layers. (B) Same sample under CL. Bright uniform orange colour emphasises the calcitic nature of the shell. Black arrows denote small ablation pits from which elemetal analyses were made using LA-ICP-MS. (C) Shell structure from Wilkies Shellbed (WLK) under SEM. Highly porous (chalky) calcite layers. Microfractures developed parallel to the layering.

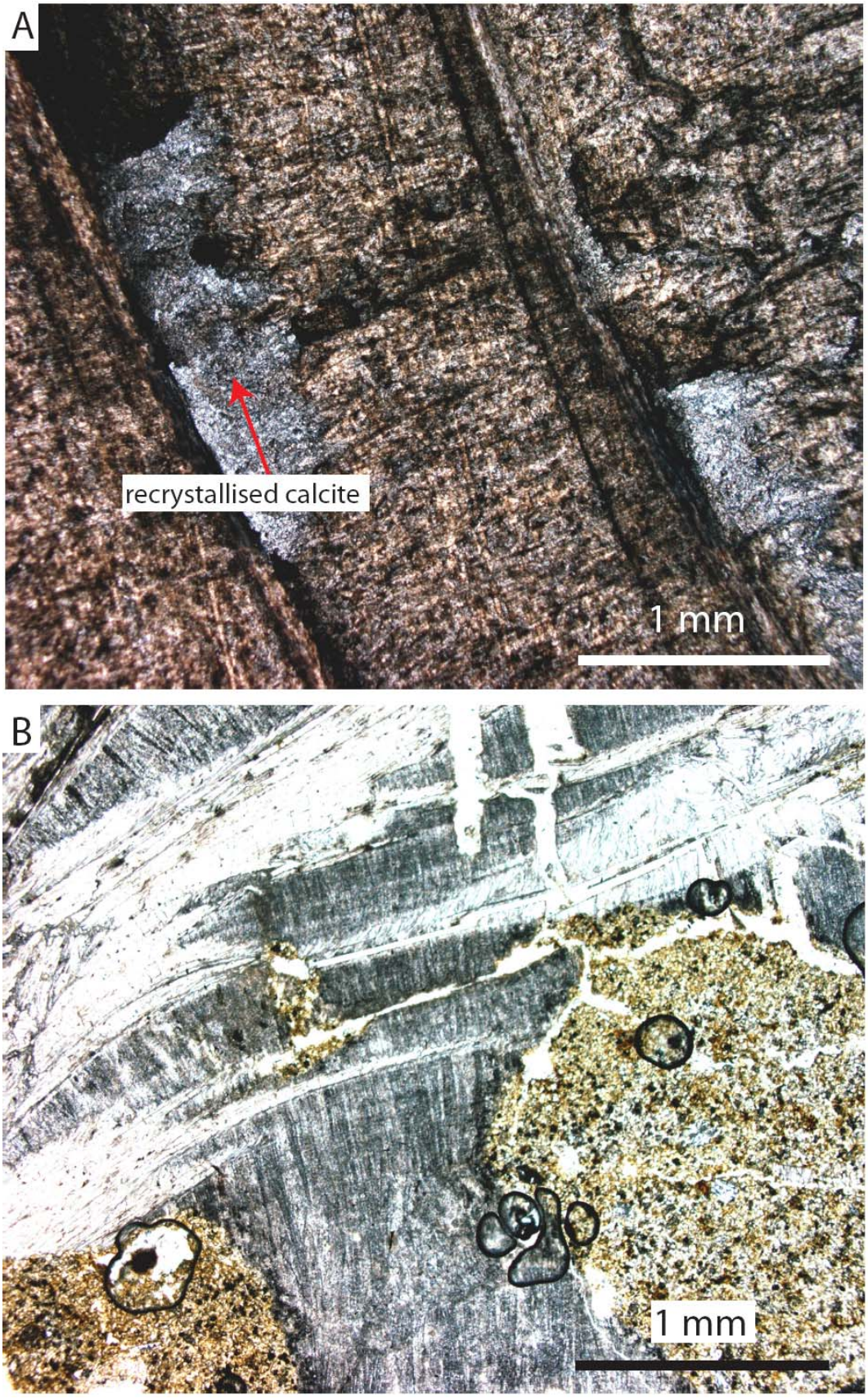

Figure 7.24 Photomicrograph of *Crassostrea ingens* oyster shells from Wanganui. (A) Areas of the oyster shell that are recrystallised with blocky patches of calcite spar (sample K4F). (B) Boring in shell infilled with fine grained siliciclastic material. Note how the edge of the boring has a sharp but irregular boundary, and the boring is contained within the darker thicker layers of the shell. Note the black circular lines are air-bubbles in the sample (sample WLK).

have sharp, but irregular edges. They are elongated in shape and range from 0.6-6 mm in length. Borings mainly occur within the thick dark layer of the shell. Infill of the borings is often absent or infilled with fine grained siliciclastic material composed of quartz, mica and opaque minerals (Fig. 7.24B). Some of this material appears weathered and limonite stained.

7.7 SUMMARY

In summary, host sediments for the oysters at each site have different petrographic and textural characteristics. Waitomo host materials are characterised by moderately abraded and poorly sorted biomicrites. Bioclasts (78%) in the limestone are chiefly bryozoans and bivalves of coarse sand size (Fig. 7.15) while siliciclastics (22%) are commonly quartz and feldspar of fine sand size (Fig. 7.15). Carbonate percentages of these samples are typically about 70%, sometimes as high as 85%.

Patagonian host sediments are submature to mature sands and Wanganui host sediments are submature sands according to the classification of Folk (1951, 1954). The texture of host sediments in Patagonia is poorly sorted fine sand. These sediments are characterised by quartz, feldspar and gypsum (top of oyster accumulation) (Fig. 7.18). Wanganui host materials are very poorly sorted fine sand. Siliciclastic sediments at this location are characterised by quartz, feldspar and mica (Fig. 7.22). Both Patagonian and Wanganui samples are very weakly calcareous with average values of about 2% and 15%, respectively.

Shell characteristics and boring features in the oyster samples are generally similar. Oyster shells from each location are composed of homogenous to crystal laths of calcite, with a marked variation in the thickness of the alternating layers (0.1-4 mm). Recrystallisation of the shells varies in each sample, and is most evident in samples from Waitomo. Borings are chiefly uniformly circular or elongate in shape and have sharp and smooth or irregular edges. The size of borings ranges from micro-scale (<0.5 mm) up to macro-scale, particularly in samples from Waitomo which can be up to 8 cm long. Infill of the borings differs according to the host material in which the oysters are contained. At Waitomo the borings are infilled with similar biomicrite to the host rock. Siliciclastic grains contained within the borings appear coarser than those in the host while the bioclastics are slightly finer. Infills in Patagonian samples are mainly composed of

feldspar within fine grained siliciclastic material and borings in Wanganui are similarly filled with very fine grained siliciclastic materials.

CHAPTER EIGHT

Oysters and associated communities

8.1 INTRODUCTION

Oysters are frequent elements of benthic populations in estuaries and shallow marine environments and play an important role in the establishment of a diverse community of fungi, algae, sponges, arthropods, bryozoans, polychaetes, brachiopods and molluscs who use the oyster shells as a substrate (Parras & Casadío 2006). Encrusting and boring organisms are significant components of marine communities, interacting in many different ways with either live or dead host substrates. They have proven to be useful tools in the understanding of the life habits and/or post-mortem histories of their hosts (Botijer 1982; Bordeaux & Brett 1990; Bien et al. 1999; Taylor & Wilson 2003; Parras & Casadío 2006).

This chapter discusses the role of oysters as physical ecosystem engineers, the processes of bioerosion and the hard substrate biota associated with the giant oysters at the study sites in Waitomo, Patagonia and Wanganui. The role of each occurrence of the oysters as a physical ecosystem engineer will also be analysed.

8.2 OYSTERS AS PHYSICAL ECOSYTEM ENGINEERS

One of the first authors to recognise the role oysters play in the establishment of a diverse community was Möbius (1877) who established the concept of biocoenosis or a social community which is defined as all the organisms living in a particular place at a particular time. While there is substantial literature on the extant *Crassostrea* oyster species, few studies are ecologically based and fail to treat the oysters as an ecosystem component. Likewise, the fauna that are associated with the commercially valuable *Crassostrea virginica* oysters (Fig. 1.1) are commonly referred to as pests (Bahr & Lanier 1981).

The interrelations between the community of organisms and the oysters can be termed facilitative or positive interactions. These are inter-species associations that benefit at least one of the taxa involved and result in no harm to either organism (Bruno et al. 2003). Physical modification and creation of habitats by

organisms such as giant oysters are positive interactions that have been termed physical ecosystem engineering by Jones et al. (1994b, 1997). Physical engineers are able to control the availability of resources such as materials, space and food, or combinations of these. Two types of ecosystem engineers are recognised: autogenic, which modify the system by means of their own physical structure (e.g. oysters and/or coral reefs), and allogenic, which modify the environment by transforming material from one physical state to another (e.g. beaver dams).

The autogenic engineering aspect of oysters attests to the dominant physical properties, rather than the biological properties, of oyster accumulations. Particularly in the Patagonian and Wanganui environments the concentrations of oysters were able to provide a hard substrate in an otherwise muddy environment devoid of such a substrate. As seen in extant shell concentrations (Zuschin et al. 1999; Gutíerrez et al. 2003), the accumulations of oysters provide a habitat for a highly diversified community of sessile boring and encrusting organisms. These organisms benefit from both the large size and great thickness of the valves that the giant oysters provide. Also of extreme benefit to these communities is the highly irregular surface of the shells, and the crevices in the 'reef' accumulations which serve as shelter for many individuals.

8.3 BIOEROSION

Bioerosion is the process by which animals, plants and microbes sculpt or penetrate surfaces of hard substrates. Bioerosion is a prominent degradation process in subtropical and tropical marine sedimentary environments (Stearley & Ekdale 1989) and results in various biogenous structures, sculptures, cavities and cavity systems. These qualify as trace fossils and are named ichnotaxa (Bromley 1994). There are two main types of substrates that are able to support bioerosion. The first is lithic substrates, which includes rock, skeletal material and manmade human substrates; the other is xylic substrates involving plant material, including wood, nuts and leaves (Bromley 1994).

8.3.1 Substrates

Lithic substrates have two contrasting surfaces that have great significance for bioerosion ecology. The difference between carbonate and non-carbonate creates two different realms. Calcium carbonate substrates are abundant in marine

environments, comprising limestone rockgrounds, carbonate hardgrounds, carbonate clasts from boulders to sand size and most skeletons of animals and calcifying algae. Bioeroders that penetrate these substrates use chemical means and are often restricted to carbonate substrates alone. However, carbonate materials are also relatively soft, which makes carbonate substrates attractive to mechanical borers. Thus diversity on these substrates can be high (Bromley 1994).

8.3.2 Macro- and microborings

Bioerosion sculptures can fall into two categories on the basis of size: macroborings down to the millimetre scale; and microborings much smaller than this. The starting point of bioerosion stems from microbes, which create microbores (e.g. fungi and algae, Fig. 8.1, 8.2). Macrobioerosion is at a larger scale, where the traces created by borers can be seen with the unaided eye or a 10x hand lens (Fig. 8.3, 8.4, and 8.5).

8.3.3 The trace makers

Organisms that have adapted to life upon hard substrates are known as epiliths (encrusters); those that dwell within a hard substrate are known as endoliths (borers). Bioerosion is a self-destructive process; the trace fossils can only be preserved when the existing habitat is covered by sediment, which suffocates the endolithic community (Bromley 1994). There are several groups into which bioerosional structures may be classified (Table 8.1). The diversity seen in the different organisms that penetrate the surface is essential in telling them apart (Ekdale et al. 1984)

8.3.4 Paleoecological significance of bioerosion

Encrusting and boring epibionts provide valuable tools in paleoecological research. The trace fossils these organisms create, such as bioerosion structures, are important as they represent the only fossil record of biological groups that lacked a skeleton (Palmer & Plewes 1993). Trace fossils (or ichnofossils) are unique as not only do they represent the morphology of the organism that made them but they are also closely linked to the environmental conditions prevailing at the time of their construction (Pemberton et al. 1990). Frey & Seilacher (1980) re-emphasised that variables such as bathymetry, temperature, sedimentation rate,

amount of sediment and cohesion of sediment all have a profound effect on the resulting trace fossil morphologies and hence aid in the determination of biological, ethological and sedimentological conditions. Encrusting and boring epibionts as paleoecological indicators can also give a good understanding of the distribution and ecology of their modern counterparts (Vogel et al. 1999).

Table 8.1. Classification of bioerosional structures and the ecological status of the producing organism (Adapted from Ekdale et al. 1984).

Bioerosion Structures	
Structure	**Producer**
Borings	Endoliths
Embedment structures	Endoliths
Raspings, scrapings	Epiliths
Superficial etching scars	Epiliths
Drill holes	Epiliths

The presence of bioerosional structures at a macro-scale is almost exclusively a marine process. The presence of well developed bioerosional structures is good evidence to suggest that active depositional conditions have been minimal or absent for a period of years. Only small amounts of sediment are required to destroy an endolithic community, although some animals are more tolerant to mud than others. Some borers like bivalves may cope beneath a few millimetres of sediment, whereas others such as sponges are a lot more sensitive to smothering, such as the ichnogenus *Entobia* which shows no environmental preferences except requiring to be sediment free (Bromley 1994).

The rate of bioerosion and also the diversity of the trace fossils decrease with increasing water depth. Bioerosional structures can provide good potential for estimating light intensity at the sea floor and also possibly as a deeper bathymetry indicator, at least to the epibathyal level (Bromley 1994). Where microborings such as algae and fungi have been identified, the photic zone is indicated. Similarly, ichnogenera such as *Radulichnus* (gastropod) produce grazing traces that also are indicative of the photic zone. These ichnogenera occur sparsely and only locally in deeper water. Species of *Gastrochaenolites* are also shallow-water

trace fossils, and where individuals are crowded and dominate the assemblage a water depth of only a few metres can be inferred (Bromley 1994).

Using bioerosional structures to infer particular aspects of an environment such as sedimentation, light intensity or bathymetry is only feasible for dominant occurrences of a particular trace fossil. Isolated individual micro- or macroborings should not be used as indicators of a general environment without caution (Bromley 1994).

8.4 COMMUNITIES ASSIOCIATED WITH OYSTER REEFS

8.4.1 Boring organisms

Fungi: Fungi are active borers on organic carbonate substrates (Mao Che et al. 1996). Endolithic fungi have a wide bathymetric range, from the intertidal to the bathyal zones, although they are more frequent in supra- to intertidal zones (Parras & Casadío 2006). Bioerosion traces attributed to fungi often consist of very small irregular drillings (Fig. 8.1).

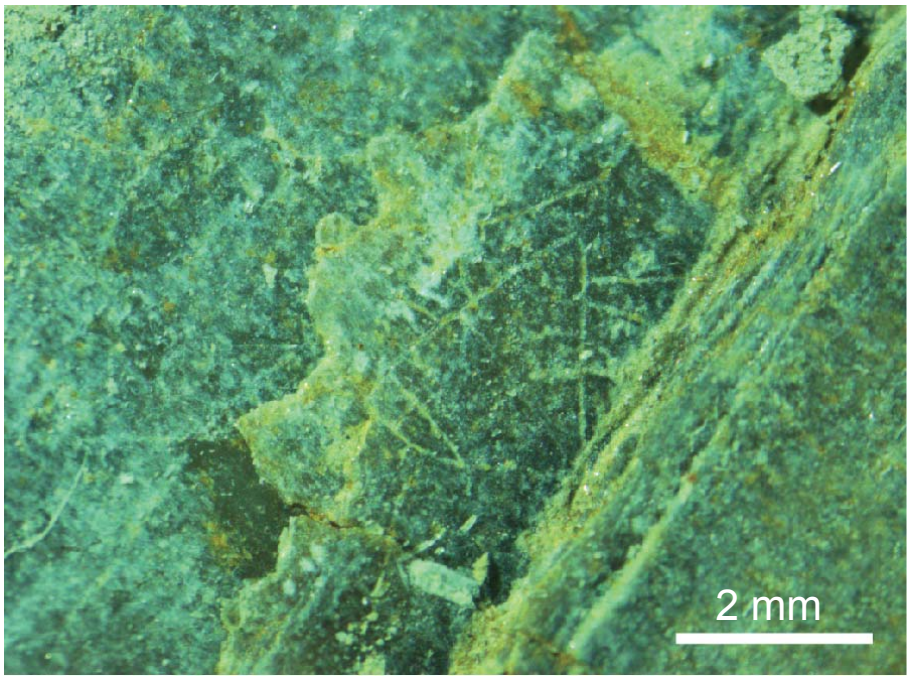

Figure 8.1 Plan view of boring traces horizontal to shell layers, on shell surface attributed to fungi (arrowed) on *Crassotrea ingens* from the Wilkies Shellbed, Parikino (sample WLK14).

Algae: Mircobores produced by algae can be good indicators of paleobathymetry as in many cases the growth and occurrence of algae are dependent on light penetration. Algal borings are restricted to the photic zone, which can be

biologically defined by the deepest growing depth of the algal genus *Ostreobium* (Akpan & Farrow 1984). The bioerosive traces that are noticed on the specimens of *"Ostrea" patagonica* from Patagonia and *Crassostrea ingens* from Wanganui are attributed to *Clionolithes?* isp (Fig. 8.2). Traces produced by *Clionolithes* are characterised by radial, irregular grooves that begin in a deep central cavity with poorly defined boundaries. Grooves shallow towards distal ends and fork into a Y shape, making the trace appear tree-like (Parras & Casadío 2006).

Polychaetes: The U-shaped pouches similar to those of *Maeandropolydora* (Fig. 8.3) are produced by polychaetes of several families (Bromley 1994). The mechanism by which polychaetes bore is not fully understood, although Blake & Evans (1973) summarised the three mechanisms in Polydora: (1) chemical, acid is secreted and dissolves the substrate; (2) mechanical, scraping of the substrate; and (3) a combination of both chemical and mechanical. Polychaete traces that are found on Flemingostreini Stenzel, *"Ostrea" patagonica* and *Crassostrea ingens* are attributed to *Maeandropolydora* isp.

Bivalves: The traces attributable to boring bivalves are commonly identified as *Gastrochaenolites* isp (Fig. 8.4), which is exclusively a mechanical borer. *Gastrochaenolites* is a generally shallow-water trace fossil and typically only a few metres of water are inferred. Details of the shape of the opening and the presence or absence of a neck to the boring can be used to differentiate ichnospecies. Traces with a narrow opening and greater elongation of the bore hole are commonly attributed to *Gastrochaenolites torpedo,* produced by the bivalve *Lithophaga* and restricted to 1-2 m water depth (Kelly& Bromley 1984; Bromley 1994). Other bivalve borers occur sparsely below this depth down to a few tens of metres (Bromley 1994).

Sponges: Sponge borings belonging to the genus *Cliona* and related taxa have been studied in detail due to their boring activity on economically important molluscs (Lauckner 1983). Most commonly their borings are assigned to *Entobia* isp. (Fig. 8.5). Borings show many apertures, and consist of a network of passages that are usually inflated to produce numerous small chambers. There is a large amount of literature on *Entobia,* but nevertheless identification of the trace can be problematic due to weathering of specimens (Parras & Casadío 2006).

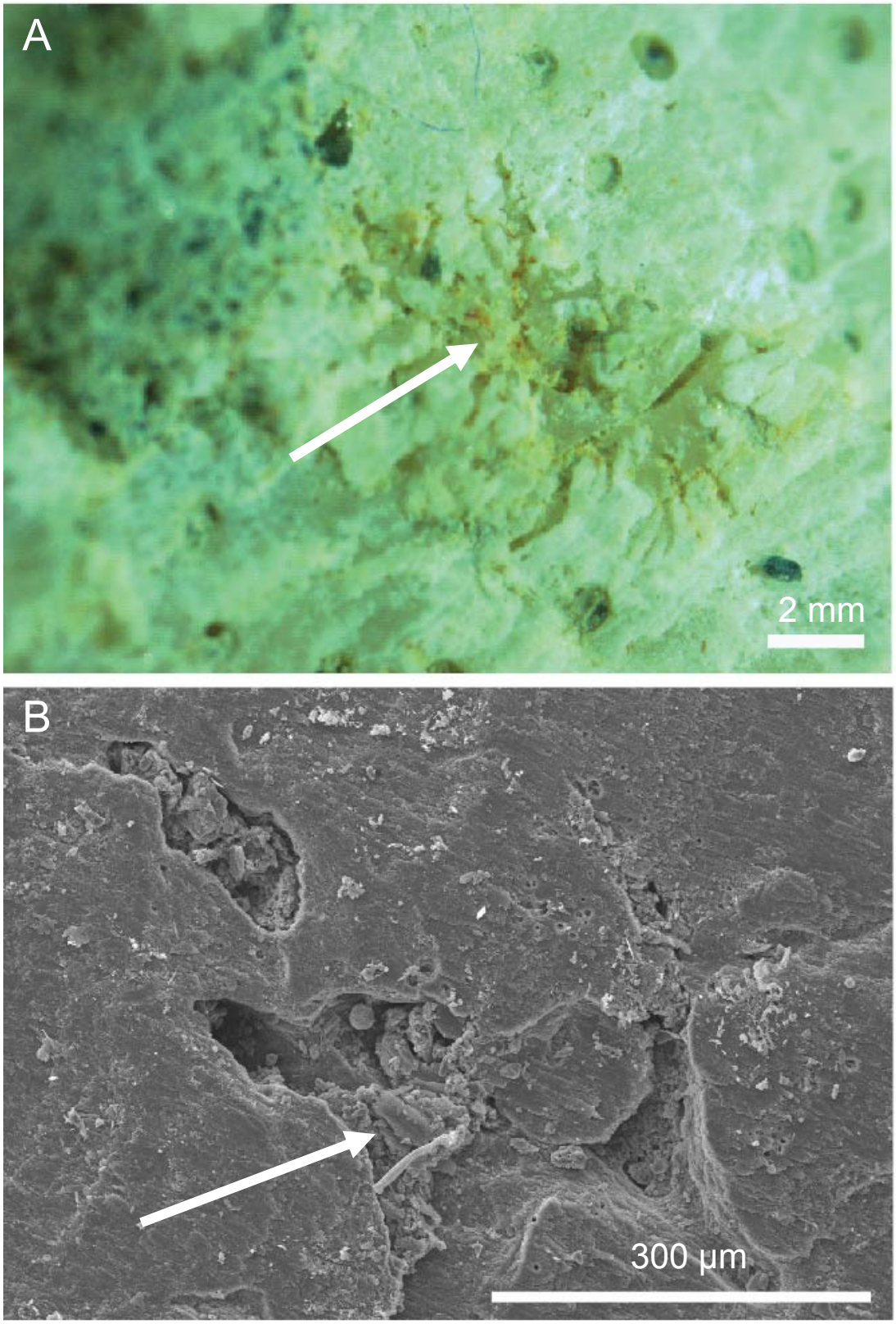

Figure 8.2 Plan view of boring traces on the shell surface of *Crassostrea ingens* from Wanganui. Borings attributed to the algae *Clionolithes?* isp (arrowed). (A) Surface of oyster sample K5C, from Wanganui. (B) SEM image of algal bore on the surface of oyster sample K5A, from Wanganui.

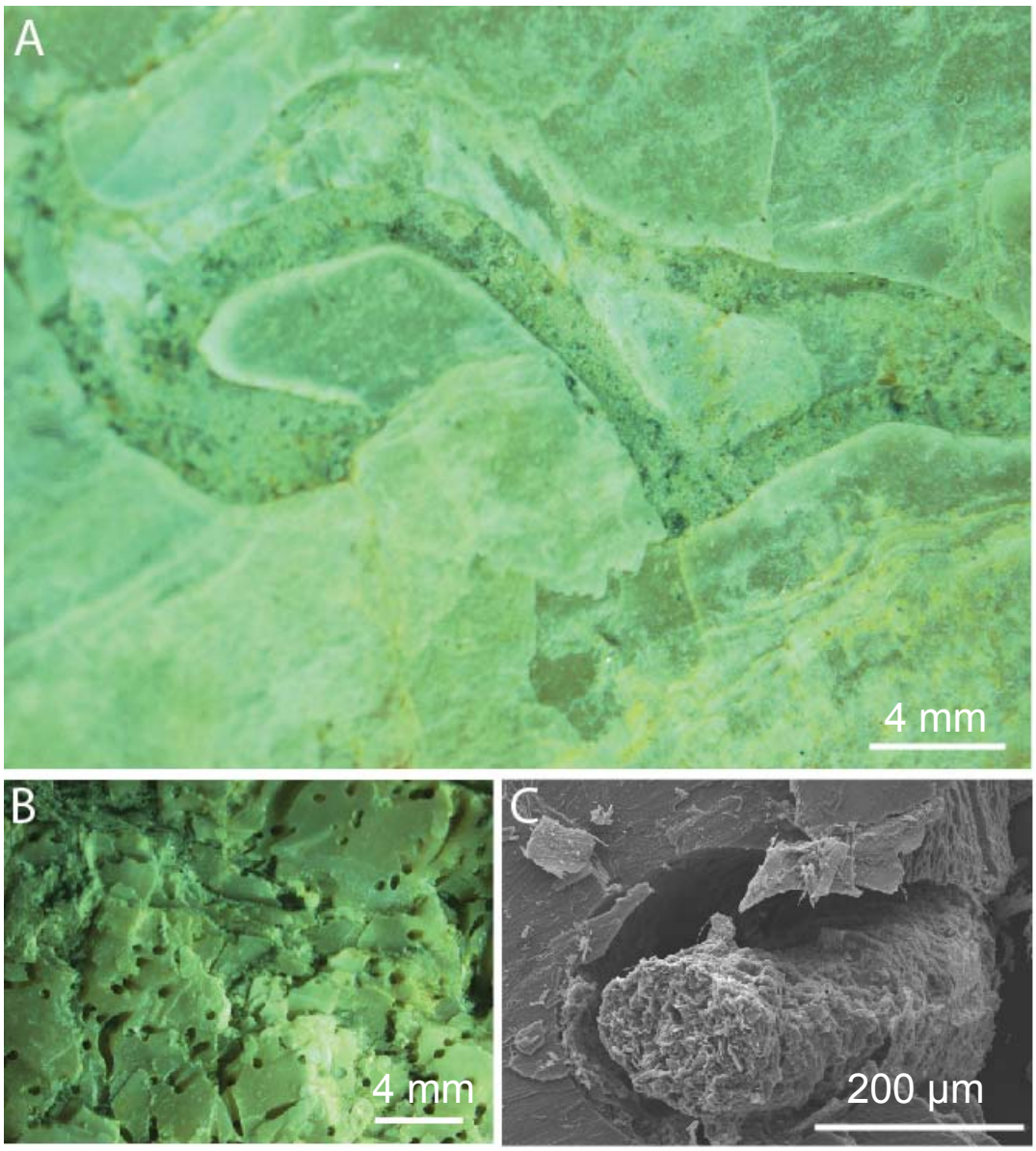

Figure 8.3 Boring traces attributed to the polychaete *Maeandropolydora* isp. on *Crassostrea ingens* from the Wilkies Shellbed, Wanganui. (A) Plan view of a U-shaped cavity similar to those of *Maeandropolydora* isp. are bored by polychaetes of several families. The borings have a wall composed of mucus and fine sand particles (sample WLK10). (B) Highly bioeroded shell supporting a network of small bore holes (sample WLK3B). Borings occur both horizontally across the shell and vertically into the shell (C) SEM image of K5A from Kauarapaoa Road showing a small, singular polychaete boring (as seen in B). Bore occurs vertically through shell layers and infill consists of sand and detritus, cemented by mucus.

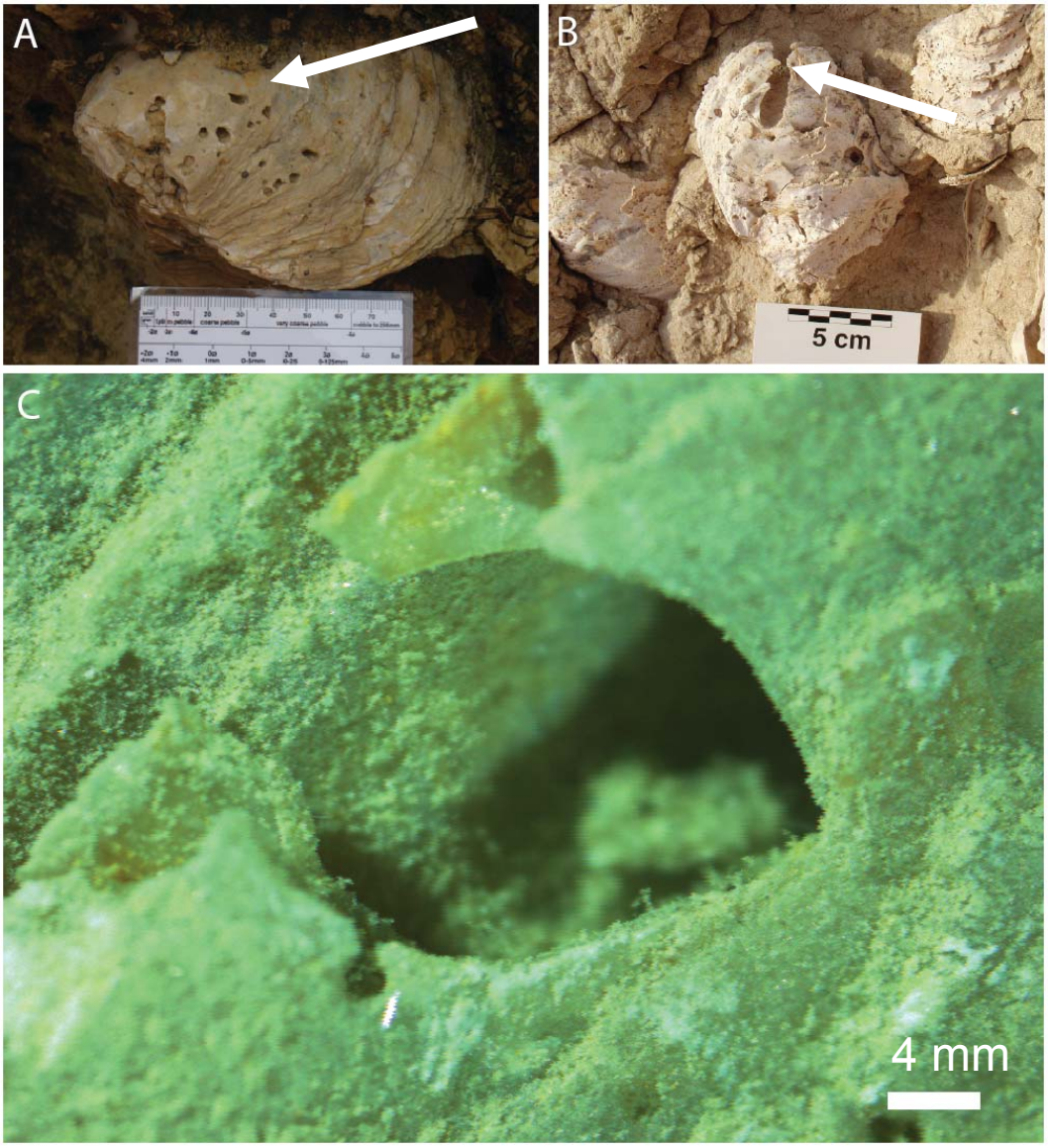

Figure 8.4 Boring traces attributed to bivalves. (A) Multiple borings on the surface of a Flemingostreini Stenzel shell from Waitomo Valley Road, Waitomo. (B) Boring attributed to *Gastrochaenolites torpedo* in the ventral portion of a left valve from *"Ostrea" patagonica* in the Puerto Madryn Formation. (C) Bore hole from a bivalve on the surface of a *Crassostrea ingens* shells from Parikino (sample WLK05A).

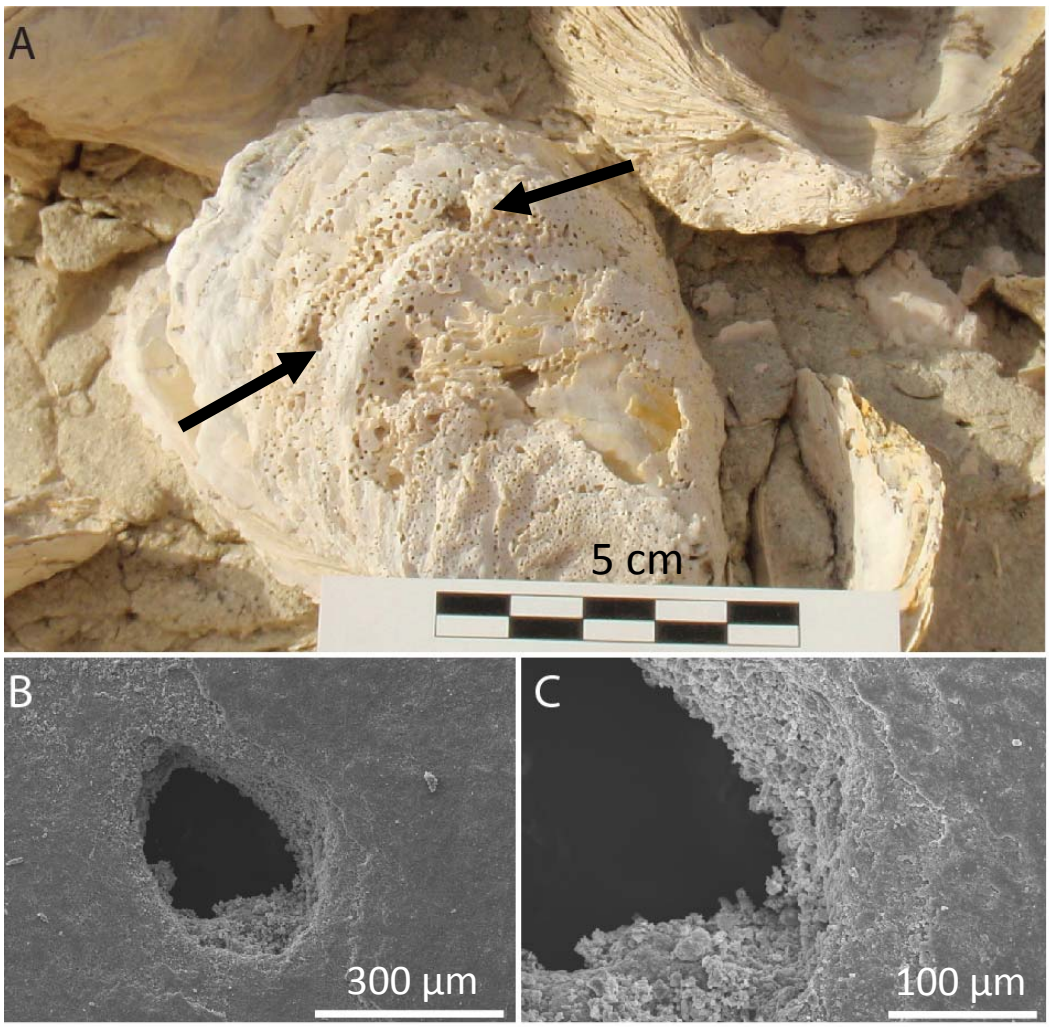

Figure 8.5 Boring traces attributed to the sponge *Entobia* isp. (A) Numerous apertures that constitute a network of passages by a boring sponge. Natural cast formation of a boring sponge consisting of many small bore holes is attributed to *Entobia* isp on the external surface of the left valve of *"Ostrea" patagonia* in the Puerto Madryn Formation at Puerto Pirámide. (B) SEM image of sample showing a bore produced by a sponge. Note how the edge of the microbore is not sharp, but appears tiered. Sample Pat4/1B. (C) Further close up of image (B) showing clear tiering and irregularity of the microbore wall.

Bryozoans: Boring bryozoans are commonly found in calcareous substrates but have also been known to excavate plant and rock materials (Warme 1975). Most of the boring bryozoans as described by Pohowsky (1978) are in the order Ctenostomata which is a group of marine taxa that live entirely immersed within calcareous substrates such as the surfaces of oyster shells. Bryozoan bores have been occasionally identified on *Crassostrea ingens* samples from Wanganui. The traces here are similar to borings produced by *Terebripora*, and are referred to as *Pinaceocladichnus.*

8.4.2 Encrusting organisms

Bryozoans: Encrusting bryozoans commonly seen are grouped into cyclostome bryozoans (Fig. 8.6). Most occurrences of encrusting bryozoans tend to have sheet like colonies which predominate over other runner-type colonies in most hard substrate bryozoan assemblages from the Ordovician to the present (Wilson & Taylor 2001). One species of bryozoan seen on valves of *Crassostrea ingens* from Wanganui etches small pits in the surface of the valves; the trace is assigned to *Leptichnus.* Often the specimens show a high degree of degradation due to shell weathering, making ichnospecific identification difficult.

Other: Vagile animals are an important component of oyster reefs. These include permanent residents which move across the surface of the shells (e.g. gastropods). The evidence for the activity of these animals is greatly reduced compared to that of boring or encrusting organisms (Taylor & Wilson 2003). Other organisms such as pectinids, barnacles and other oysters are also rarely seen on the surface of some *Crassostrea* valves from Wanganui.

8.5 DIVERSITY AND COMMUNITY SUCCESSION

This section sets out to analyse the role of the oysters as physical ecosystem engineers and the hard-substrate biota associated with fossil oysters at each study location. To do this, the placement of organisms on the oysters shell is recorded and the preferential settling of encrusters and borers assessed. The hypothesis of preference of borers and encrusters for left or right valves is tested using chi squared independence tests. Similar tests are performed in order to assess preference of borers or encrusters on other features of the shells (e.g. interior/exterior surfaces and different sectors of the valves).

The preference organism show for sections or valves of oysters can determine if traces were made while the oyster was alive, or if they are post mortem features. The identification of trace fossils on the oysters will shed light on paleoenvironmental and paleoecological conditions of the oysters and the associated communities. Methods for these analyses are outlined in Section 2.10 and the determination of the shells sectors are illustrated in Figure 2.6. All data are in Appendix D-1.5.

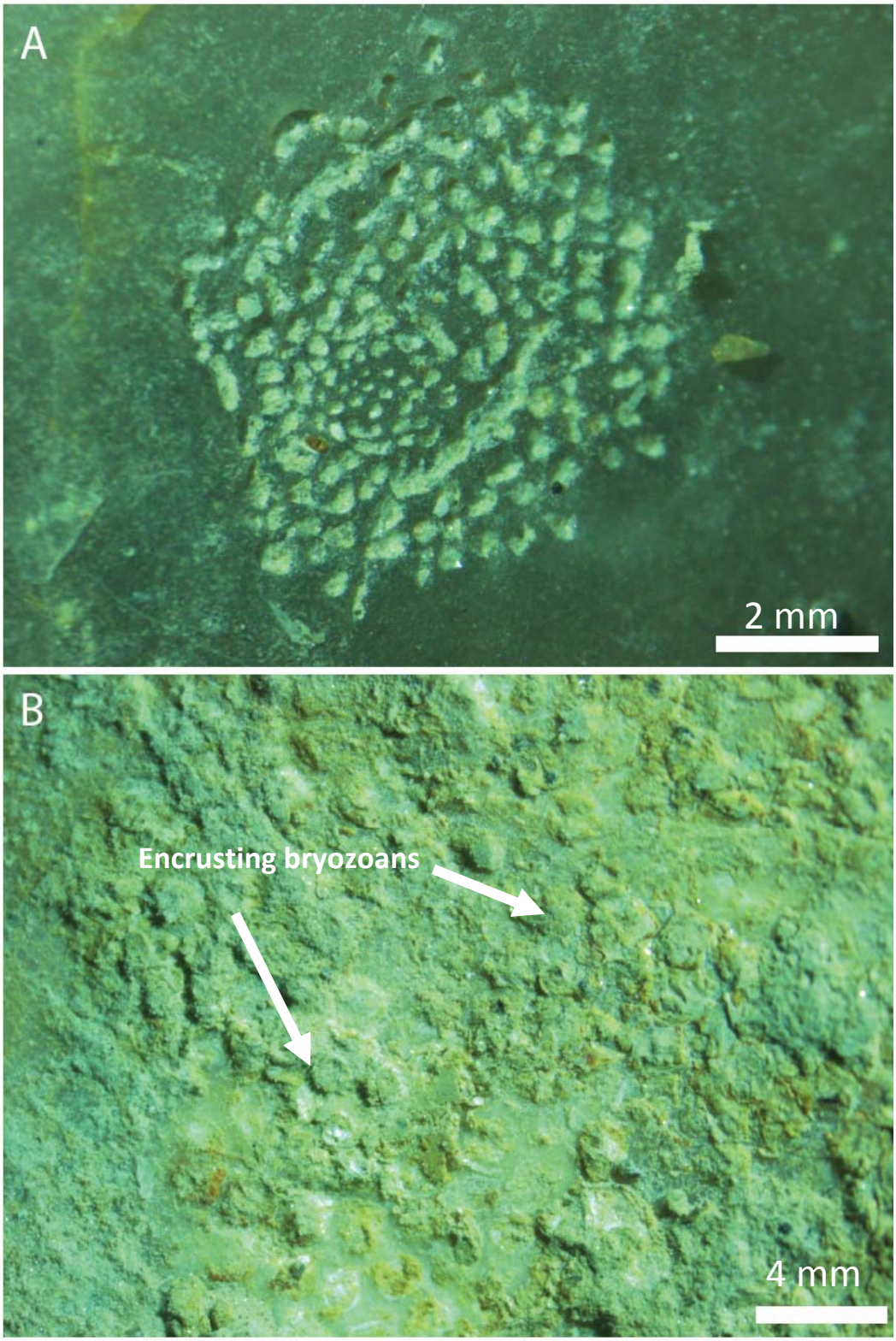

Figure 8.6 Encrusting cyclostome bryozoan traces on *Crassotrea ingens* from the Wilkies Shellbed, Wanganui. (A) Etching traces attributed to an encrusting bryozoan (sample WLK15). (B) Encrusting bryozoans (sample WLK43).

8.5.1 Waitomo (Flemingostreini Stenzel)

Extraction of fossil oyster samples at Waitomo localities is difficult due to the tenacity of the limestone host making it challenging to remove a whole and well preserved oyster sample. The orientation of the shells in the limestone rock also

meant that only on rare occasions was a shell presenting an entire outer surface of a valve for enabling the easy recording of the bioerosion traces. For this reason, only a small number of samples was able to be analysed.

8.5.1a Differences between left and right valves

Chi square tests were performed to test the hypothesis that borings or encrustations were distributed non-randomly on the right and left valves of Flemingostreini Stenzel from Waitomo. As seen in Figure 8.7, both sponges and boring bivalves show a preference for the left valves of the oysters while polychaetes only occur on the right valve.

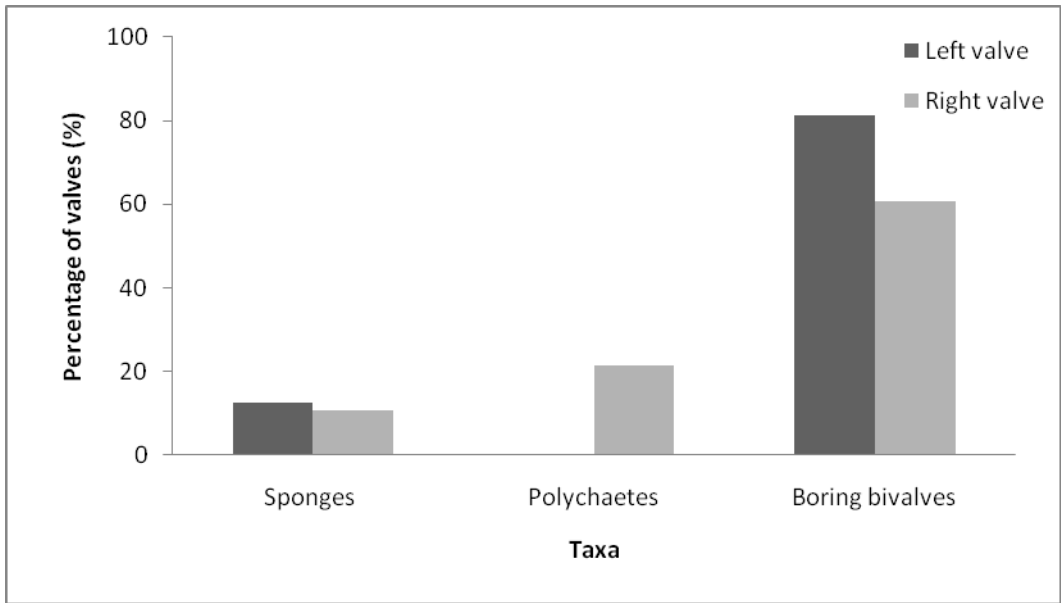

Figure 8.7 Percentages of left and right valves of Flemingostreini Stenzel from Waitomo, with associated taxa present.

The total diversity of taxa on the shell surfaces was low, ranging from zero to two. Only 18% of right valves and 6% of left valves had two taxa. A total of 61% of right valves and 80% of left valves had only one taxa. 21% of right valves had zero taxa compared with only 6% of left valves (Fig. 8.8).

8.5.1b Differences between interior and exterior surfaces

It was hypothesised that the borings and encrusters are distributed non-randomly between the surfaces of the Flemingostrieni Stenzel valves. It was found that all the taxa present on the surface of the shells have a preference for a particular

surface (Fig. 8.9). Boring bivalves and sponges both show a preference for the exterior of the shells and polychaetes prefer the interior surface of the shell.

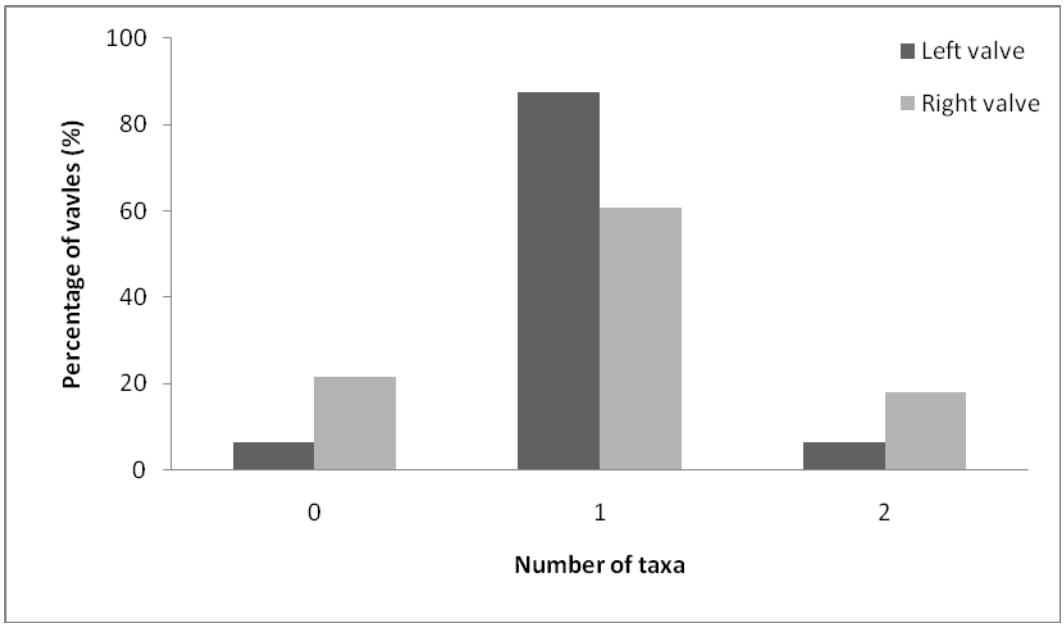

Figure 8.8 Total diversity of taxa on left (black bars) and right (grey bars) valves of Flemingostreini Stenzel from Waitomo.

The majority of the analysed oysters from Waitomo had at least one taxa on the external surface of the shell (Fig. 8.10). The external surface of the right valves carries from zero to two taxa and 21% have at least two taxa on their shell surface and 74% of the shells have only one taxa present. The external surface of left valves has one or two taxa, 93% of shells have only one taxa and 7% have a total of two taxa. On the internal surface of the left valve taxa vary from 0 to 1, with half of the examined surfaces having no taxa. On the internal surface of right valves the number of taxa recorded ranges from 0-2 with the most common being zero, represented on 56% of the valves (Fig 8.10).

8.5.1c Differences between valve sectors

Chi-square independence tests were performed to test the hypothesis that certain predefined sectors (Fig. 2.26) of the valves were preferentially colonised by boring and/or encrusting organisms. Results indicate that polychaetes and boring bivalves show preference for specific sectors of the shells.

On the exterior of the right valve boring bivalves tend to mainly occupy areas A, and G, while polychaetes show a preference for sector G and sponges show no

particular preference (Fig. 8.11). On the inner surface of the right valves organisms show no particular preference. On the external surface of the left valves boring bivalves mainly occupy areas A, D and G and sponges show no preference.

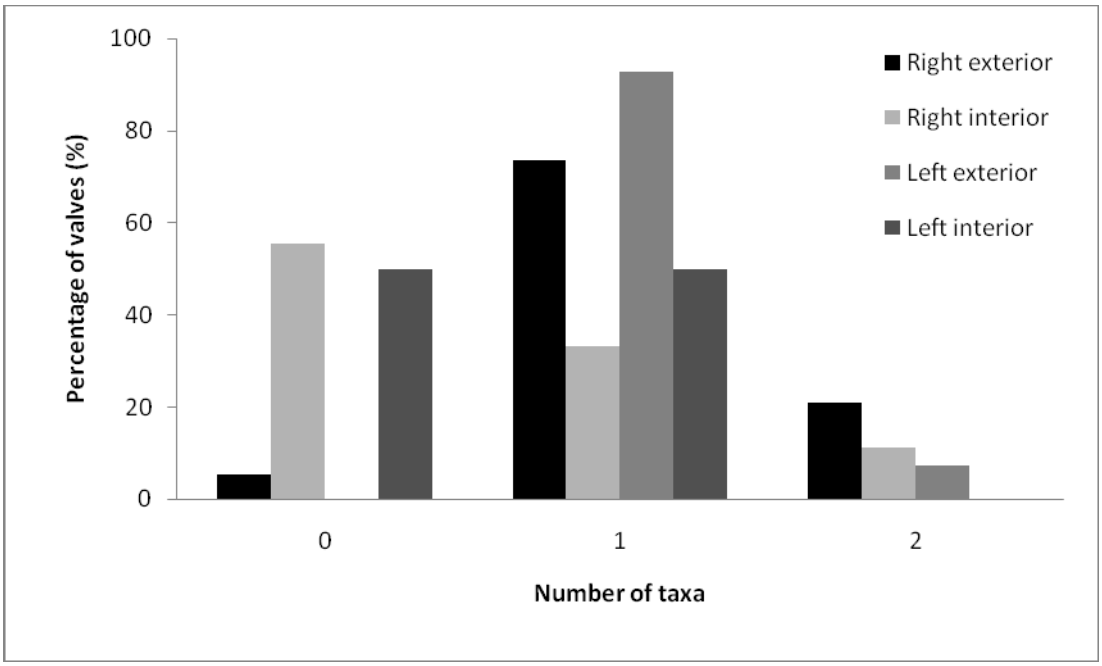

Figure 8.9 Number of taxa present on each valve surface of Flemingostreini Stenzel shells from Waitomo.

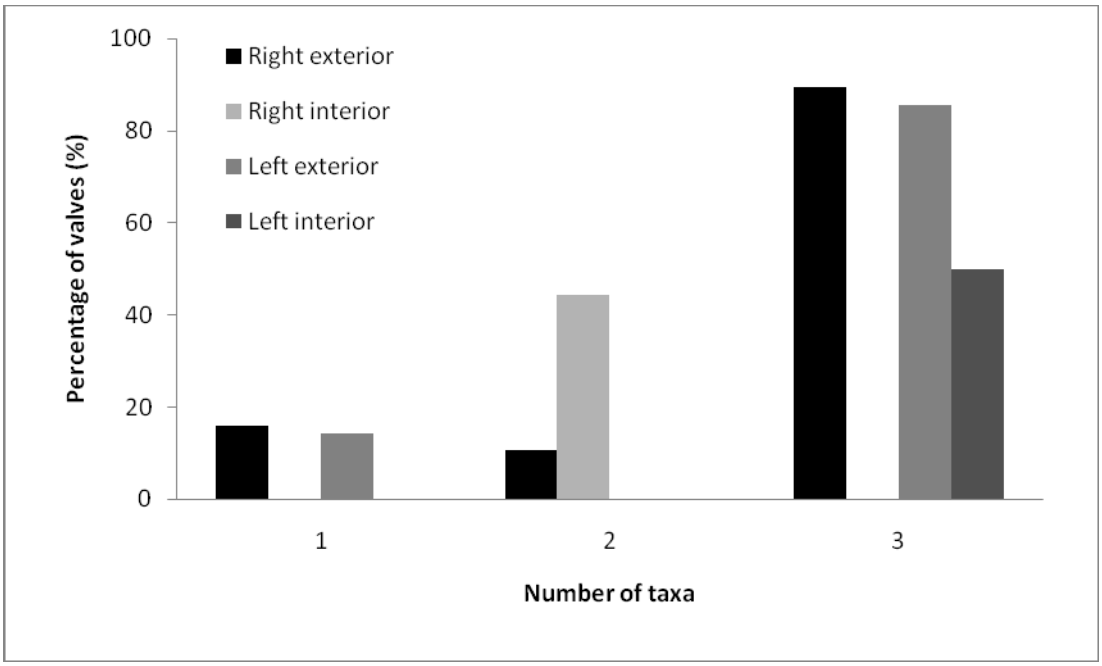

Figure 8.10 Percentage of each valve surfaces of Flemingostreini Stenzel from Waitomo containing encrusting and boring taxa.

On the inner surface there is only a slight preference of taxa to areas B and CD of the shell (Fig. 8.11). Area G on the right external valves and areas A, D and G on

the left external valve support the highest diversity of taxa (Fig. 8.11), while on the inner surface the ventral area (CD) is the most heavily colonised.

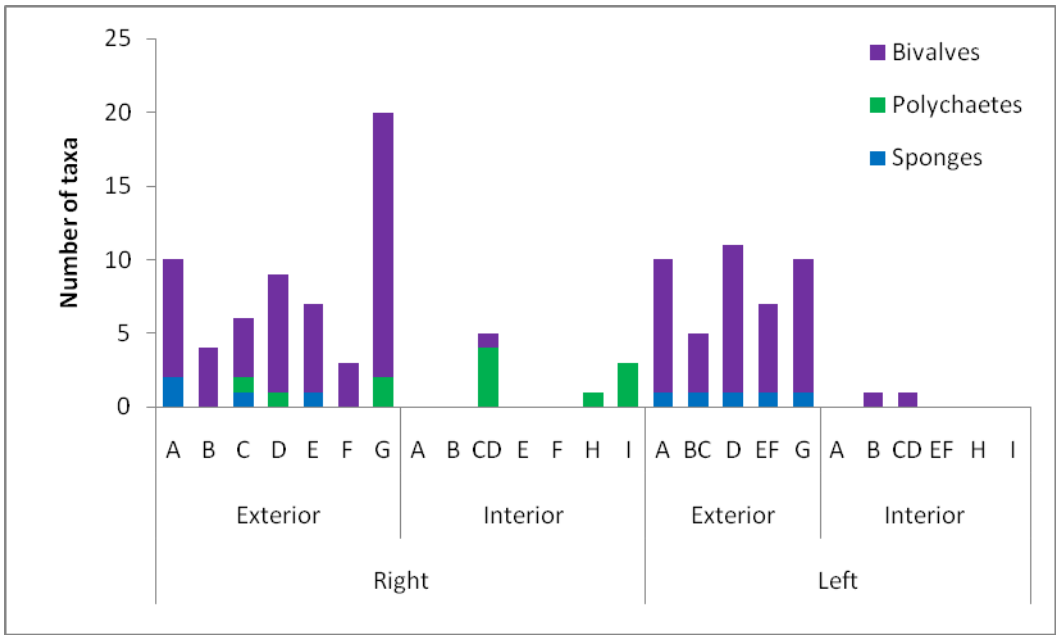

Figure 8.11 Total number of taxa per sector in species of Flemingostreini Stenzel from Waitomo.

8.5.2 Patagonia (*"Ostrea" patagonica*)

At this location fossil oyster specimens were collected from each suggested generation of shells, as in Figure 4.10. This was done by collecting a shell from each apparent layer in the reef (generations 1 – 18). Accessibility to the oyster accumulation and ease of sample collection made this possible at Puerto Pirámide. Compilation of raw data and statistical analysis were carried out by Claudia Brito (2009) and kindly made available for presentation in this study. All data is included in Appendix D-1.5.

8.5.2a Differences between left and right valves

Sponge traces attributed to *Entobia* isp. are the most common traces found on the valves of *"Ostrea" patagonica.* In samples from the Puerto Madryn Formation sponges are found on 99% of the left valves and 98% of the right valves (Fig. 8.12). Polychaetes and boring bivalves are the next most commonly occurring organisms, with polychaetes being on 69% of left valves and 79% of right valves and boring bivalves on 53% of left valves and 59% of right valves (Fig. 8.12). Algal borings occur on 1% of left valves. Grazing traces attributed to *Radulichnus* isp. (gastropod) were found on 5% of both left and right valves (Brito 2009).

The total diversity of taxa on the left and right valves of the shells ranged from 1 – 5. Only 13% of right valves and 14% of left valves had only one taxa. The most common number of taxa on 49% of right valves was two, and the most common on the left valves was three (48%). Only 1% of left valves and 5% of right valves had five taxa present (Fig. 8.13).

Chi square tests were performed to test the hypothesis that borings or encrusting organisms were distributed non-randomly between right and left valves in each generation. The results show that in generation 13 alone, fungi have a preference for the left valve ($p < 0.05$) (Brito 2009). The remainder of the generations show no preference for either left or right valves.

8.5.2b Differences between interior and exterior surfaces

Percentages of taxa present on the external and internal surface of all samples of *"Ostrea" patagonica* examined from the Puerto Madryn Formatin at Puerto Pirámide are presented in Figure 8.14. Percentage of taxa present on each of the internal and exterior surfaces for left and right valves is presented in Figure 8.15. In all the generations tested in was concluded that polychaetes, sponges, bivalves and funig prefered the external surface and not preference was shown by any taxa for the internal surface.

Generation 1 (n=10)

All valves in generation 1 show between two and three taxa on the external surface of the valves; 80% have two taxa and 20% have three taxa (Fig. 8.16A). The external surfaces of the left valves have two taxa present on at least 50% of the valves, and three taxa on the remaining 50%. The external surfaces of the right valves more commonly have two taxa present (83%). Considering the internal surfaces of the shells, 40% have no taxa (Fig. 8.16A). On the internal surface of the right valves in particular the number of taxa varies between zero and three, with the most common being two and three, with 33% of the valves in each case.
With respect to the left valves, 75% of the samples have no presence of taxa on the internal surface (Fig 8.17A).

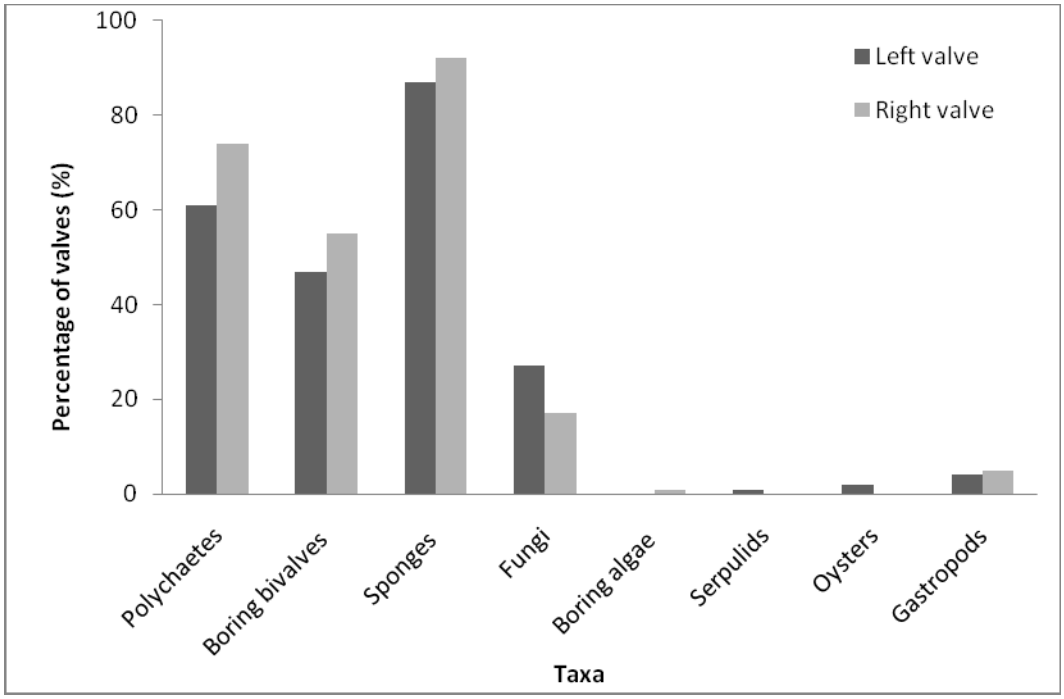

Figure 8.12 Percentage of right and left valves of *"Ostrea" patagonica* containing respective borers or encrusters in the Puerto Madryn Formation. Number of valves counted = 182.

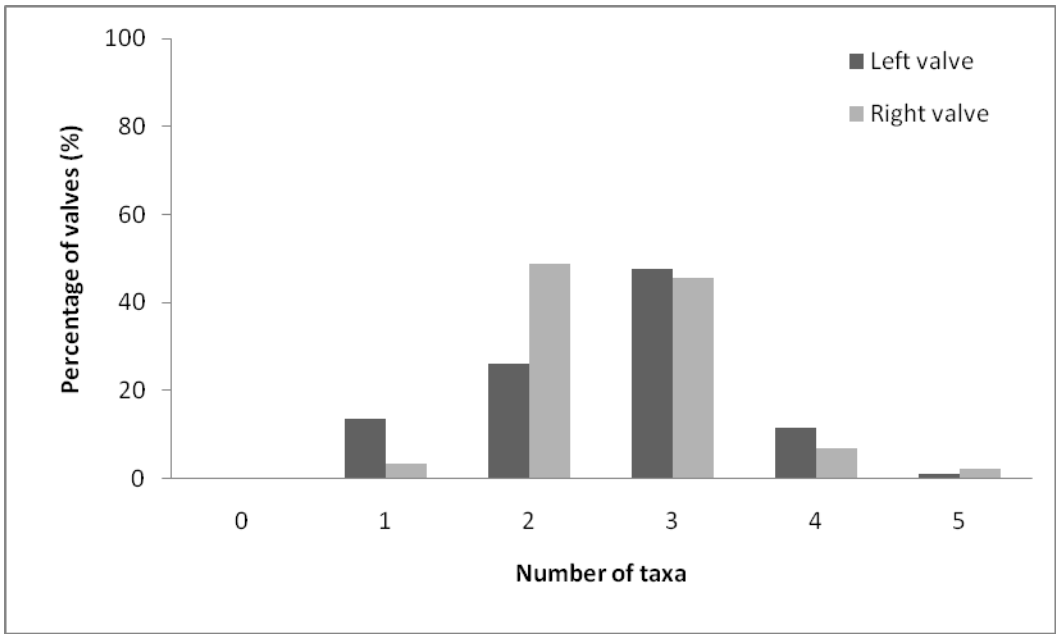

Figure 8.13 Total diversity of taxa on left (black bars) and right (grey bars) valves of *"Ostrea patagonica"* from the Puerto Madryn Formation.

Generation 2 (n=12)

All the specimens examined in this generation have at least two taxa on the external surface (Fig. 8.16B). The external surface of the left valve most commonly has two or three taxa present with three being the most common (83%). Most of the shells (67%) show no traces on their internal surface. The

number of taxa on the internal surface of the left valve varies from zero to two, with zero being the most frequent (50% of the valves) (Fig. 8.17B).

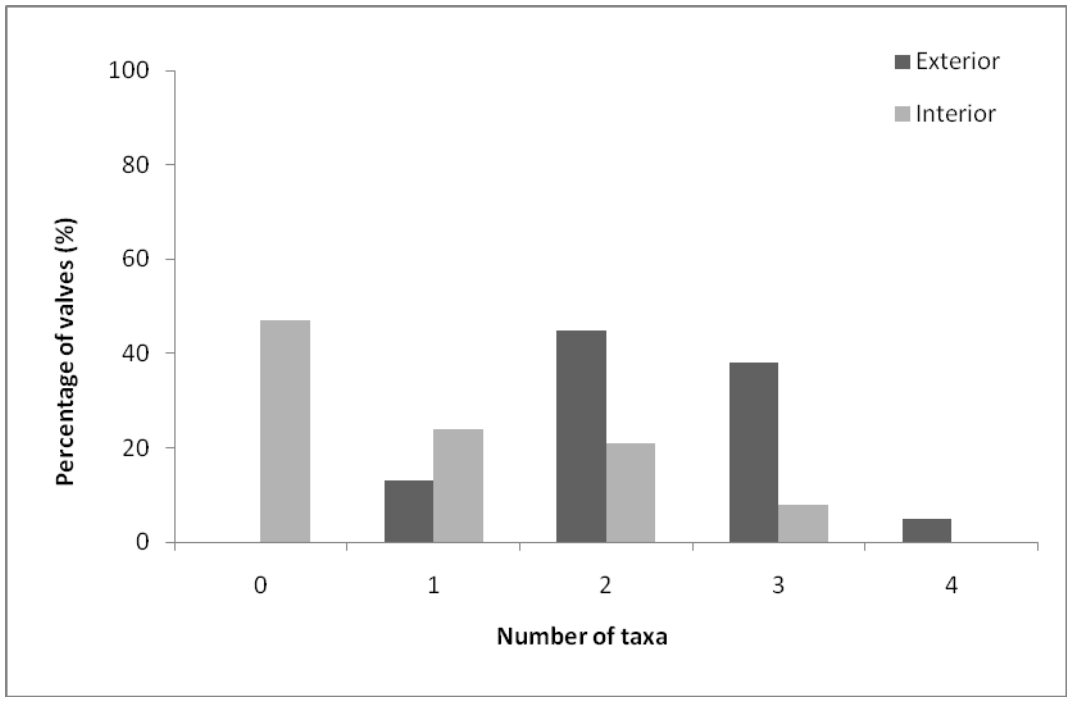

Figure 8.14 Percentage of taxa present on the external and internal surface of *"Ostrea" patagonica* from the Puerto Madryn Formatin at Puerto Pirámide.

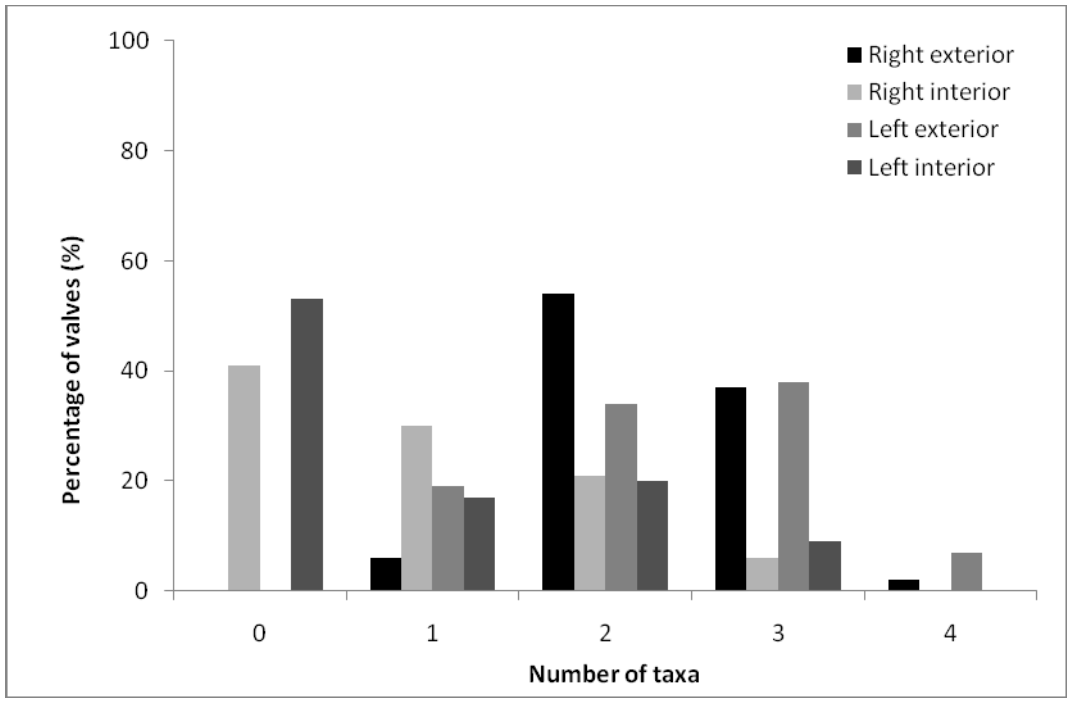

Figure 8.15 Percentage of taxa present on the left and right external and internal surface of *"Ostrea" patagonica* from the Puerto Madryn Formatin at Puerto Pirámide.

Generation 3 (n=11)

Between two and four taxa are present on shells from generation 3, with three taxa being the most common on 55% of the valves (Fig. 8.16C). On the external surface of the right valves there are between two and four taxa, with two being the most dominant on 50% of the valves. On the left valves between two and three taxa are present on the external surface, with 80% of the valves supporting three taxa. 67% of the right and 60% of the left valves show an absence of taxa on the internal surface (Fig. 8.17C).

Generation 4 (n=8)

All taxa from this generation show one to three ichnospecies with three being the most common on 50% of the valves (Fig. 8.16D). The external surface of the right valves has between two and three ichnotaxa, the most common being three on 67% of valves. On the external surface of the left valve the number of taxa varies between one and three, with two and three being the most common number representing 40% of the valves each (Fig. 8.17D). A total of 63% of the internal surfaces of the valves are absent of ichnospecies, while the remainder of the valves have three taxa (Fig. 8.16D).

Generation 5 (n=6)

83% of the valves studied in generation 5 have two taxa present on the external surface and the remainder have three present (Fig. 8.16E). The right valves have between two and three taxa present on the external surface, and all the left valves have two taxa on the external surface. When considering the internal surfaces of the valves, most had between zero and two taxa with 50% of the left and right surfaces showing no ichnospecies (Fig. 8.17E).

Generation 6 (n=9)

All shells in this generation had at least one taxa present on the external surface, the number varying from one to four with three taxa being the most common on 56% of valves (Fig. 8.16F). 75% of right valves had three taxa on their external surface, with the remainder of valves showing two taxa. 40% of the external surfaces of left valves had three taxa (Fig. 8.17F). On the internal surface of valves the greatest number of taxa varies between zero and three and a total of 44% of all the valves had no ichnospecies on the valves (Fig. 8.16F). In 50% of

the right valves two taxa were viewed on the internal surface and on the remainder of the valves there are no taxa present. 40% of the left valves have no taxa on the internal surface (Fig. 8.17F).

Generation 7 (n=9)

All shells in generation 7 have at least one taxa on the external surfaces of the shells (Fig. 8.16G). The number of taxa ranged from one to three, with one and two taxa occurring on 44% of the exterior valve surfaces. All the right valves had two taxa on the external surface of their valves. On the external surface of the left valves one taxa was most common on 67% of valves (Fig. 8.17G). On the interior surface of the valves between zero and two taxa were observed, with zero the most common on 44% of the valves (Fig. 8.16G). On the internal surface of the right valves 67% of valves had one taxa present and the remainder of samples were absent of taxa. The internal surface of the left valves most commonly supported no taxa (Fig. 8.17G).

Generation 8 (n=12)

All shells in generation 8 show at least one ichnospecies on their external surface. The number of taxa present on the external surface of valves ranges from one to four with two taxa being the most frequent on 58% of the valves (Fig. 8.16H). For right valves, 43% had two taxa on the external surface, and for left valves 80% have two taxa; the remainder of valves show three taxa (Fig. 8.17H). The internal surfaces of the shells have between zero and two taxa, with zero taxa found on 42% of the valves (Fig. 8.16H). The number of taxa on the internal surface of the right valve varies from zero to two, the predominant number being one occurring on 43% of the valves. In 60% of the left valves there were two taxa present and the remainder of shells were absent of taxa (Fig. 8.17H).

Generation 9 (n=12)

On the external surface of the shells in this generation there are one or two taxa present, with one being the most common on 56% of valves (Fig. 8.16I). In right valves 75% of shells had two taxa on the external surface, while 80% of the left valves had only one taxon on the external surface (Fig. 8.17I). The internal surface of the shells had between zero and three taxa present, with zero being the most common on 56% of valves (Fig. 8.16I). The internal surface of right valves

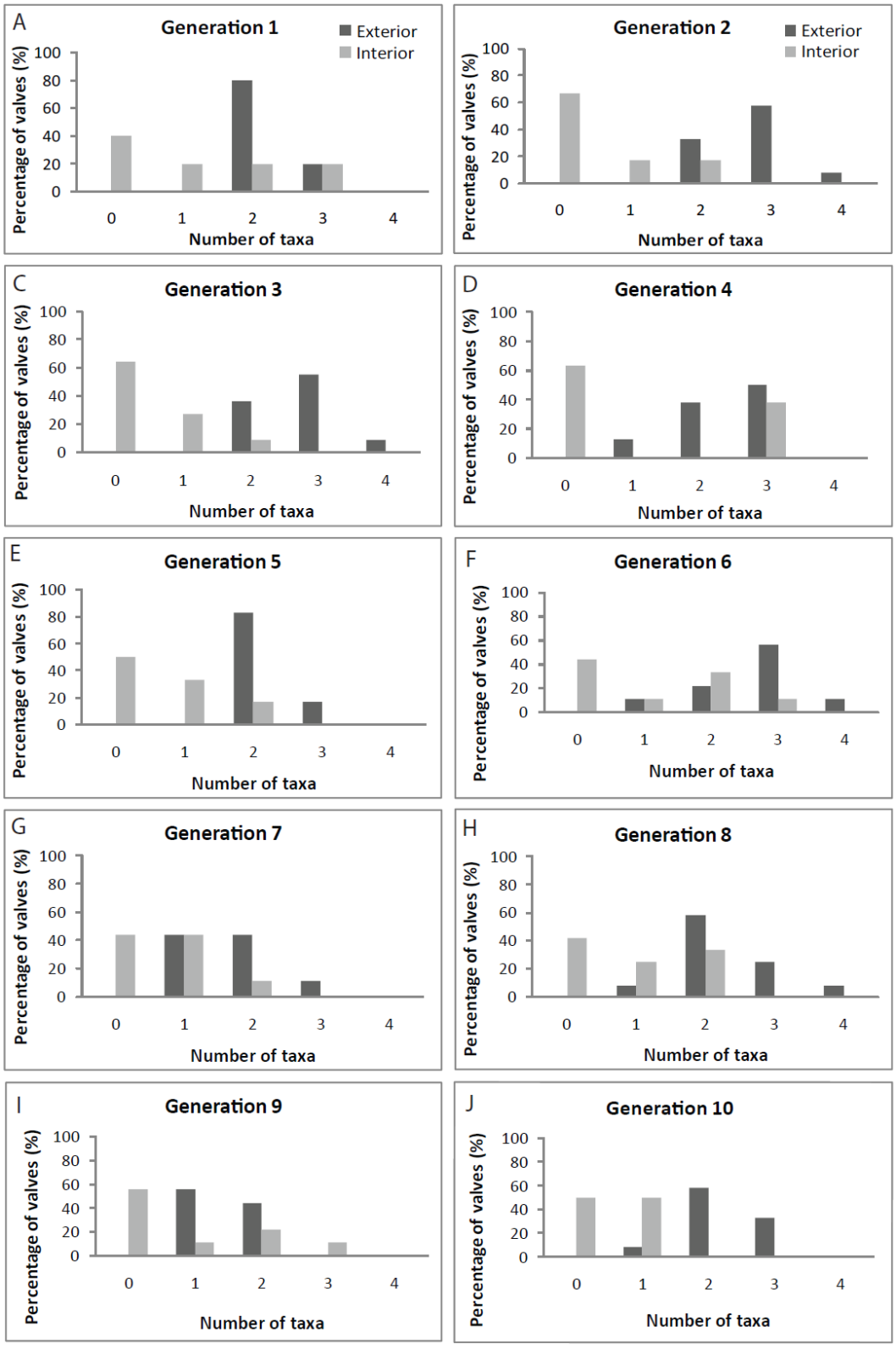

Figure 8.16 (A-J) Percentage of valves of *"Ostrea" patagonica* containing zero to four taxa of borers and encrusters on the exterior (black bars) and interior (grey bars) surfaces. Letter (A) through to (J) represent generations 1 to 10, respectively, as shown in Figure 4.10.

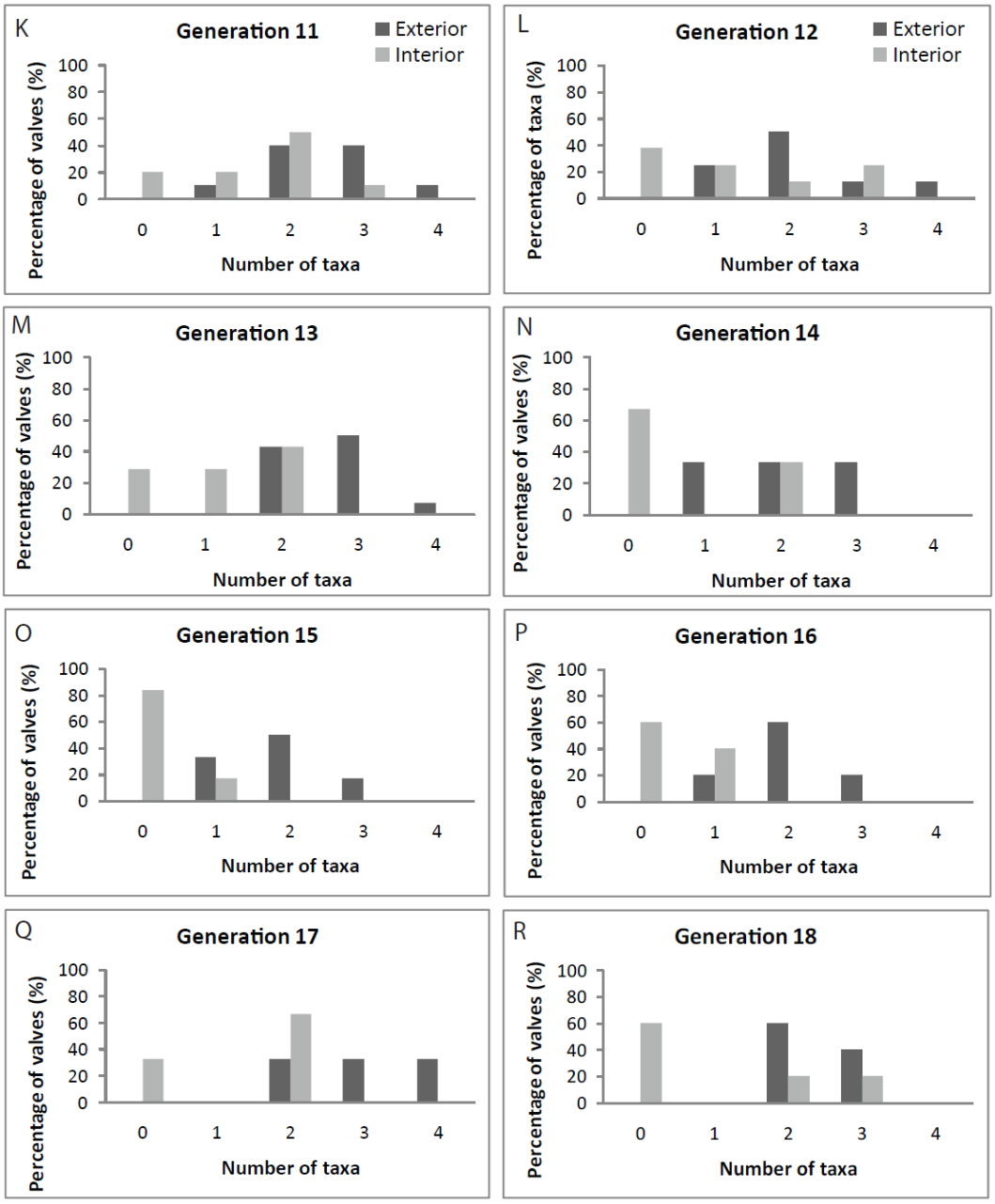

Figure 8.16 (K-R) Percentage of valves of *"Ostrea" patagonica* containing zero to four taxa of borers and encrusters on the exterior (black bars) and interior (grey bars) surfaces. Letter (K) through to (R) represent generations 11 to 18, respectively, as shown in Figure 4.10.

had an equal proportion of zero and two taxa. In the left valves there were zero, one or three taxa present on the internal surface. The majority of valves, however, had zero taxa (60%) (Fig. 8.17I).

Generation 10 (n=12)

A total of 58% of shells in generation 10 have two taxa on the external surface (Fig. 8.16J). All of the right valves examined had two taxa present on their external surface and 57% of left valves had three taxa present on their external surface (Fig. 8.17J). Half of the valves from this generation had zero taxa on the

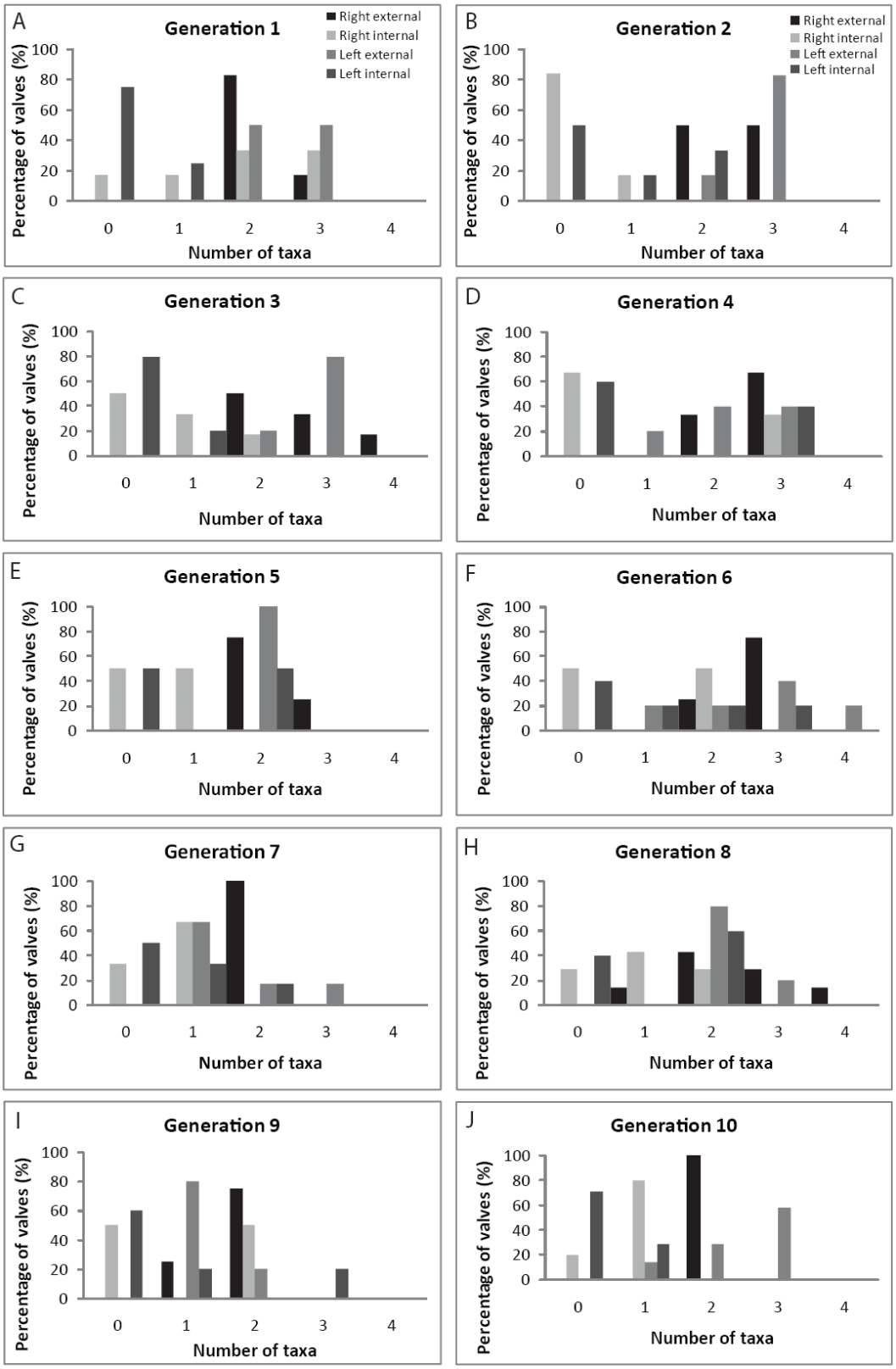

Figure 8.17 (A-J) Percentage of valves of *"Ostrea" patagonica* containing zero to four taxa of borers and encrusters on the left and right exterior (lightest grey and dark grey bars, respectively) and left and right interior (medium grey and black bars, respectively) surfaces. Letter (A) through to (J) represent oyster generations 1 to 10, respectively, as shown in Figure 4.10.

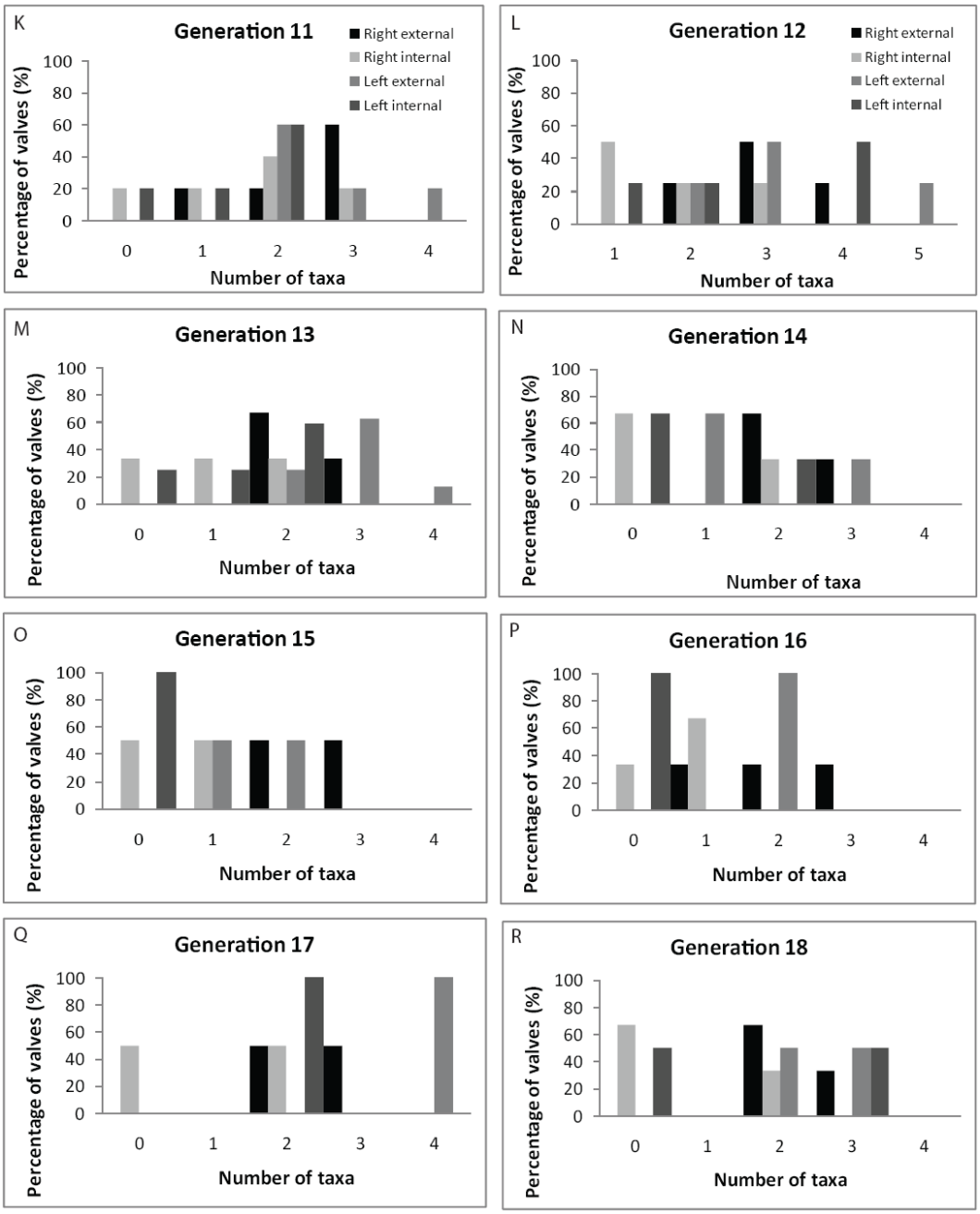

Figure 8.17 (K-R) Percentage of valves of *"Ostrea" patagonica* containing zero to four taxa of borers and encrusters on the left and right exterior (lightest grey and dark grey bars, respectively) and left and right interior (medium grey and black bars, respectively) surfaces. Letter (K) through to (R) represent oyster generations 11 to 18, respectively, as shown in Figure 4.10.

internal surface (Fig. 8.16J). On the internal surface of right valves 80% had one taxa and 71% of the left valves had no taxa present on the internal surface (Fig. 8.17J).

Generation 11 (n=10)

All the external valves of this generation had at least one taxa present on the surface of the valves. The number of taxa ranged from one to four, with two or

three taxa being the most frequent, both occurring on 40% of the valves (Fig. 8.16K). In 60% of right valves there were three taxa on the surface. The remainder of the surfaces had one or two taxa in equal proportions. The external surface of the left valves frequently had two taxa on 60% of valves (Fig. 8.17K). Taxa present on the internal surfaces of the shells varies between one and three, with two being the most frequent on 50% of the valves (Fig. 8.16K). 20% of both the left and right valves had no taxa present (Fig. 8.17K).

Generation 12 (n=8)

The number of taxa on the surface of the shells in this generation ranges from one to four, with two taxa being the most common on 50% of the valves (Fig. 8.16L). On the external surface of the right valve the taxa varied between one and three, with two being the most frequent on 50% of the valves. On the external surface of the left valves there were one, two or four taxa, with two taxa being the most common on 50% of the valves (Fig. 8.17L). The internal surface of the right valves had between zero and three taxa present with a total of 38% of the valves showing no taxa (Fig. 8.16L). The internal surface of the left valves most commonly had three taxa present (50%), whereas on the internal surface of the right valves one, two or three taxa were seen in equal proportions (Fig. 8.17L).

Generation 13 (n=14)

The number of taxa on the external surfaces of the shells in this generation ranges from two to four. The occurrence of three taxa was the most common, occurring on 50% of the valves (Fig. 8.16M). The external surface of the right valves had two or three taxa, with two taxa predominanting on 67% of the valves. The left valves have between two and four taxa on the external surface, with three taxa being the most frequent on 63% of the valves. The internal surface of the right valves had zero, one or two taxa occurring in equal proportions (33% in each case). Like the right valves, the internal surface of the left valves has zero, one or two taxa, the predominant occurrence being two taxa on 50% of the valves (Fig. 8.17M).

Generation 14 (n=6)

Valves in this generation had between one and three taxa, all in equal occurrence on the valves (Fig. 8.16N). The external surface of the right valves has two or

three taxa, with two taxa occurring on 67% of the valves. The left valves external surface had between one and three taxa present on their surface with one taxa being the most common, occurring on 67% of the valves (Fig. 8.17N). The internal surface of the valves had between zero and two taxa present; 67% of both the left and right valves had no epibionts present (Fig. 8.17N).

Generation 15 (n=6)

All the shells in this generation have at least one taxa present on the external surface of the valves. The number of taxa present varies between one and three with two being the most common occurring on 50% of the valves (Fig. 8.16O). On the external surface of the right valves there were two or three taxa present, and the external surface of the left valves had one or two taxa present in equal proportions. 83% of the valves in this generation are absent of taxa on the internal surface (Fig. 8.17O).

Generation 16 (n=5)

There are between one and three taxa present on the external surface of shells in this generation, with two being the most common occurring on 60% of the valves (Fig. 8.16P). On the external surface of the right valves only there were between one and three taxa present, and on all the external surfaces of the left valves there were two taxa present (Fig. 8.17P). A total of 60% of the valves in this generation had no evidence of taxa on the internal surface. The remainder of the shells had one taxa present (Fig. 8.16P). All of the internal surfaces of the left valves were absent of taxa, whereas only 67% of the right valves internal surfaces had zero taxa; the remainder presented one taxa (Fig. 8.17P).

Generation 17 (n=3)

All the valves in this generation had either two or four taxa on their external surfaces (Fig. 8.16Q). On the external surface of the right valves there were two or three taxa in equal proportions, and on the left external surface there were four taxa present on all valves (Fig. 8.17Q). On 67% of the internal surfaces of valves in this generation there were two taxa present on the surface; the remainder of shells were absent of epibionts (Fig. 8.16Q). On the right valves in particular 50% of the shells had no taxa present and the remaining valves show two taxa. The

internal surface of the left valves all show two taxa on the internal surface (Fig. 8.17Q).

Generation 18 (n=5)

A total of 60% of valves in this generation have two taxa present on the external surface; the remaining shells all have three taxa present (Fig. 8.16R). The external surface of right valves has two taxa on 67% of the valves; for the left valve 50% had two taxa and the rest of the valves presented with three taxa (Fig. 8.17R). The number of taxa on the internal surface of the valves ranged from zero to three. A total of 60% of the valves had no taxa on the internal surface (Fig. 8.16R).

8.5.2c Differences between valve sectors

Independence tests were carried out to hypothesis that borings or encrustations were non-randomly distributed between each predefined sector (Fig. 2.26).

Preferential settlement of sector G was noted on 33% of the left valves and 54% of the right valves. Sponges show preference for the external surface and sector G of the shells (Fig. 8.18). 78% of the right valves and 75% of the left valves have sponges present in this sector (Brito 2009).

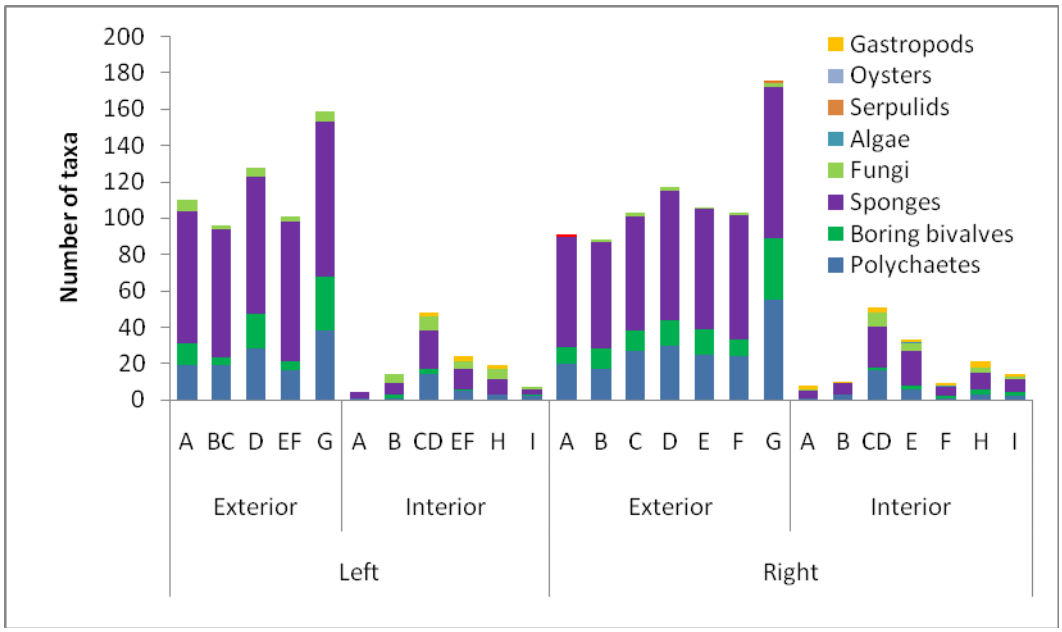

Figure 8.18 Graph showing total number of taxa occurring in each sector of *"Ostrea" patagonica* from the Puerto Madryn Formation at Puerto Pirámide.

From each generation of oysters that were tested only generations 3, 7, 10, 11 and 13 have shown preferential settlement of taxa. In generation 3, polychaetes and sponges show a preference for sector G on the external surface of the right valve. Generation 7 shows that boring bivalves also have a preference for sector G on the external surface of the right valve, whereas in generation 10 they prefer sector G on the external surface of the left valve. Polychaetes in generation 11 have a preference for sector CD of the internal surface of the right valve. In generation 13 of the *"Ostrea" patagonica* both polychaetes and sponges show preferential settlement in sector CD of the internal surface of the left valve. However, on the external surface of the right valve they occupy sector G.

Considering all the samples from the oyster reef at Puerto Pirámide it is observed that polychaetes show a preference for sector G on the left valve. Boring bivalves preferred sector H of the internal surface of the left valves. Sponges preferred sector G on the external surface of both the left and right valves. Fungi exhibited a preference for sector CD of the internal surface of the right valve and sectors B and EF of the internal surface of the left valves.

8.5.3 Wanganui (*Crassostrea ingens*)

Samples from Wanganui were chiefly collected from the prominent occurrence of the Wilkies Shellbed occurring along the Whanganui River at Parikino (see Fig. 5.3). Samples were not able to be collected in generational layers as in Patagonia due to lack of accessibility. Subsequent statistical analysis is made for a bulk collection of shells. All data is in Appendix D-1.5.

8.5.3a Differences between left and right valves

Chi square tests were performed to test the hypothesis that borings or encrustations were distributed non-randomly between right and left valves of *Crassostrea ingens* from the Wilkies Shellbed. Results show that algae, cyclostome bryozoans, pectinids, other oysters and barnacles most commonly occur on the left valves of *Crassostrea*. Both algae and pectinids have a preference for the left valve, whereas polychaetes, boring bivalves and sponges show a preference for right valves (Fig. 8.19). The preference for one or the other of the *Crassostrea* valves suggests that the traces were produced while the oyster was alive.

The number of taxa on right valves ranges from one to four with the most common number of taxa being one, occurring on 30% of the right valves. The number of taxa on left valves ranges from one to five, with 28% of left valves having one taxa; 17% of the shells have zero taxa (Fig. 8.20).

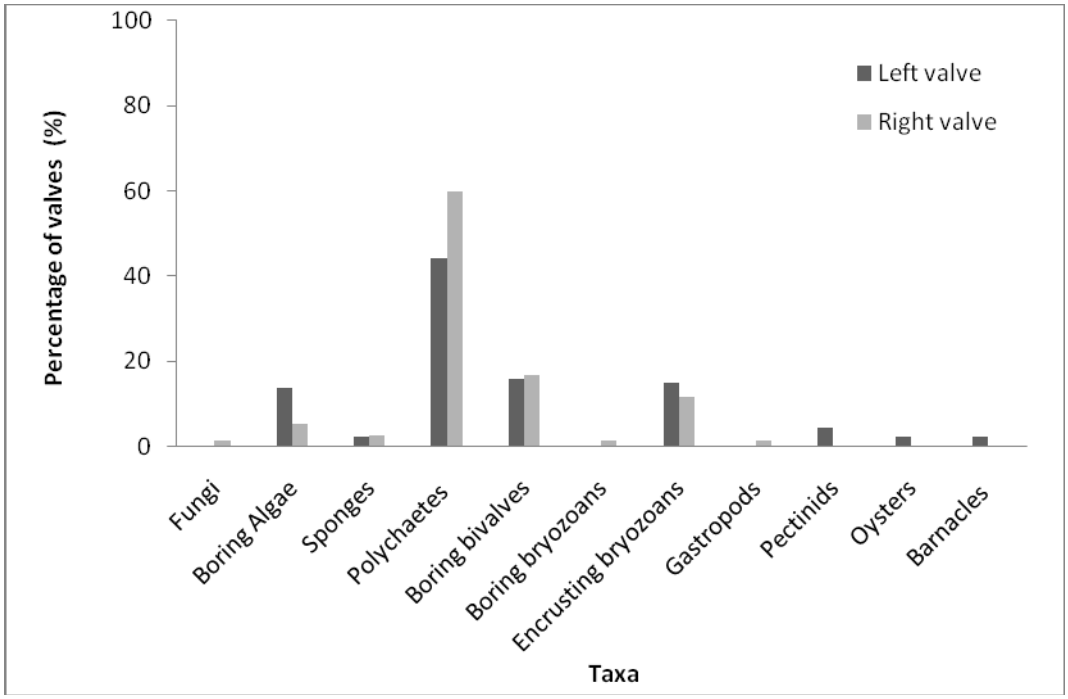

Figure 8.19 Occurrence of taxa in percentage on both left and right valves of *Crassostrea ingens* from Wanganui.

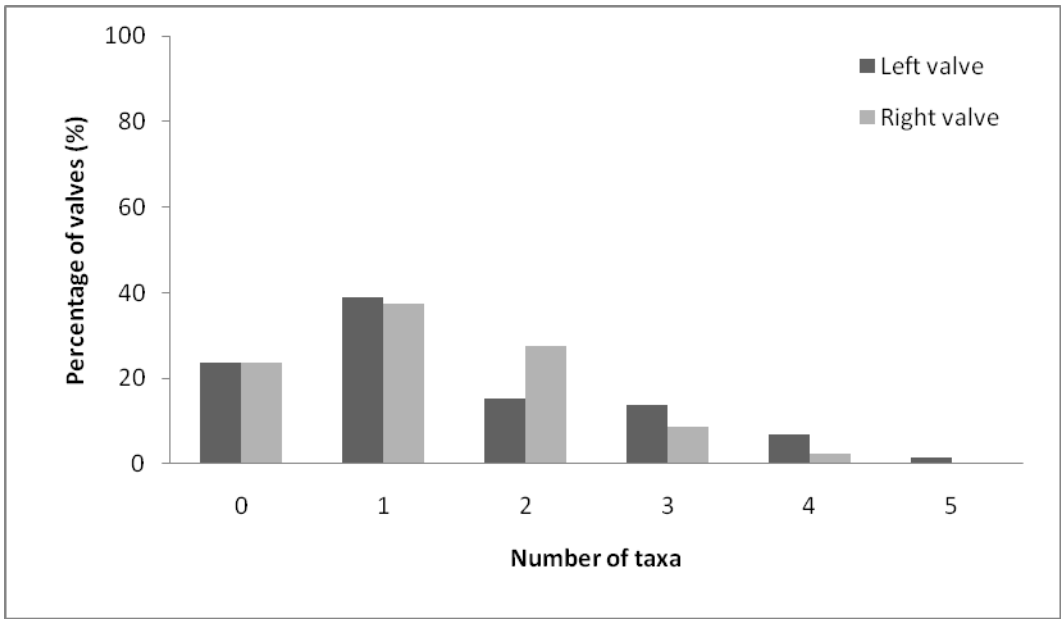

Figure 8.20 Total diversity of taxa on left (black bars) and right (grey bars) valves of *Crassostrea ingens* from Wanganui.

8.5.3b Differences between interior and exterior surfaces

When statistically testing the hypothesis that borings and encrustations were distributed non-randomly between both surfaces of the *Crassostrea ingens* valves, most taxa (e.g. polychaetes, boring bivalves, boring algae, gastropods, pectinids, other oysters and barnacles) show a preference for the external surface of the valves. None of the organisms have shown a preference for the internal surface of the valves (Fig. 8.21).

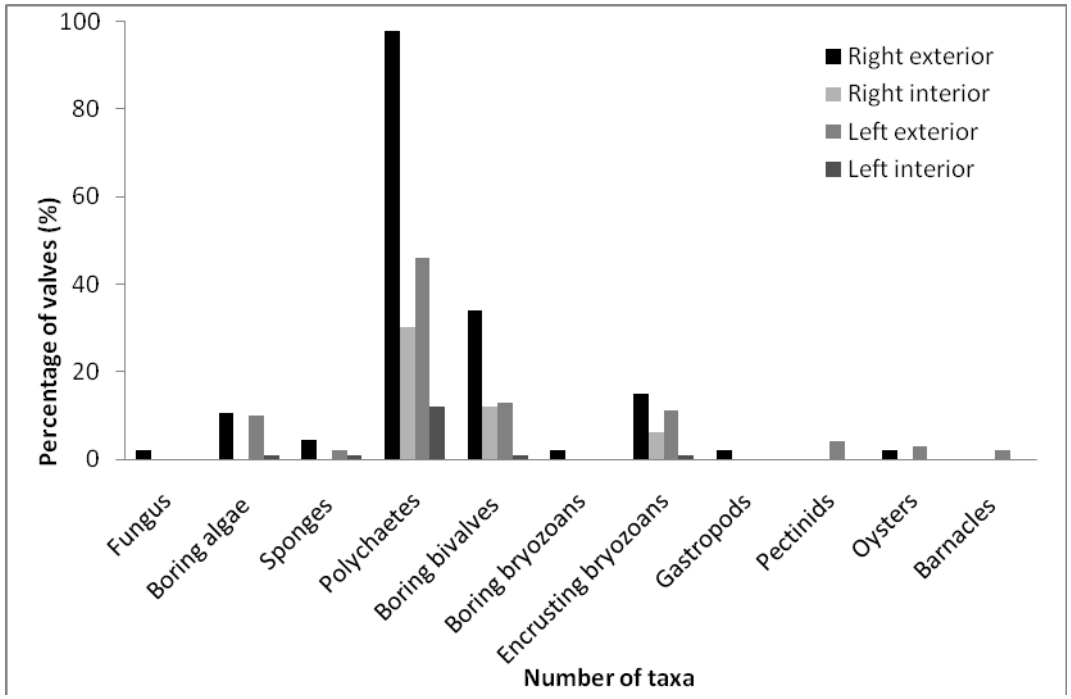

Figure 8.21 Occurrence of taxa in percentage on all surfaces of valves of *Crassostrea ingens* from Wanganui.

The large majority of all the oysters studied from the Wilkies Shellbed had at least one taxa on the external shell surface (Fig. 8.22). The total number of taxa on the shell surfaces ranges from one to five, although only 15% of the valves carry at least three taxa (Fig. 8.22). The external surface of a left valve carries between from one to five taxa and 35% have at least three taxa on their shell surface. The external surface of right valves has between one and four taxa, with two taxa being most common on 41% of valves, only 19% of shells have at least 3 taxa present. On the internal surface of right valves taxa vary from zero to two, with 58% of the valves examined having no taxa. On the internal surface of left valves the number of taxa recorded ranges from zero to four with the most common being zero, as for the right valve, at 57% (Fig. 8.22).

8.5.3c Differences between valve sectors

Chi-squared independence tests were undertaken to test the hypothesis that certain predefined sectors of oyster valves were colonised by boring and/or encrusting organisms preferentially (Fig. 2.26). Results confirm that polychaetes, boring algae, sponges, barnacles and boring bryozoans have a preference for specific sectors of the shells. On the exterior of the right valve polychaetes tend to occupy mainly areas A, D, E and G while boring bivalves, boring algae, boring bryozoans, gastropods, fungi and other oysters all prefer area G. On the inner surface of this valve only polychaetes show a preference for sector H. Other taxa on the inner surface of the right valve show no particular preference. Area G on the right and left external valve supports the highest diversity of taxa (Fig. 8.23), while on the inner surface both the central and muscle area is the most heavily colonised. On the external surface of the left valve polychaetes, boring bryozoans, boring bivalves and boring algae all show a preference for sector G, whereas on the inner surface there is only a slight preference of taxa for the central and ventral areas of the shell (Fig. 8.23).

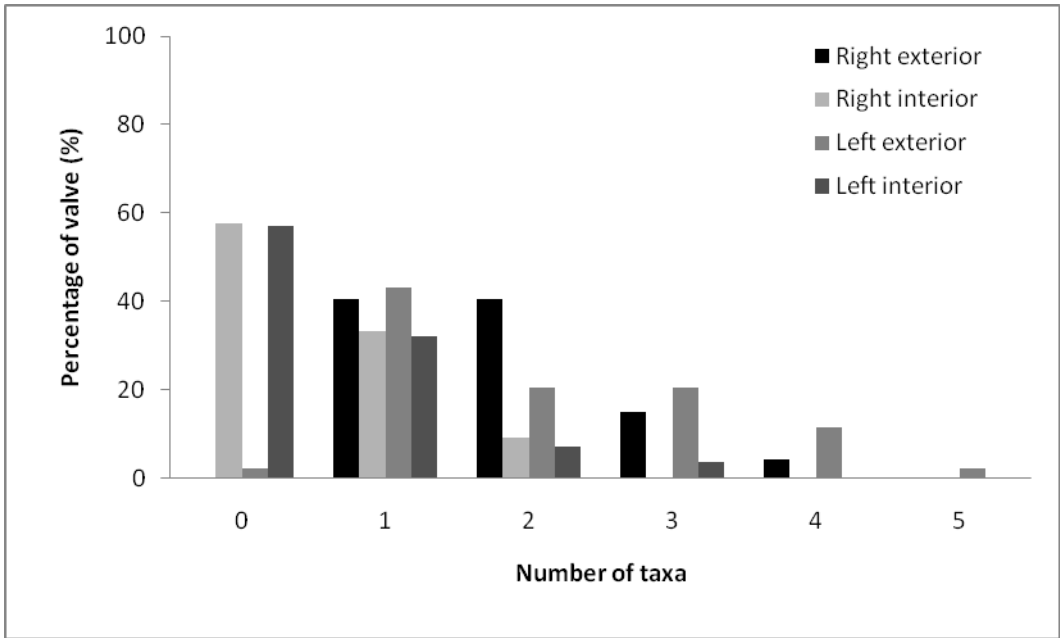

Figure 8.22 Percentage of valves of *Crassotrea ingens*, from Wanganui carrying zero to five boring and encrusting taxa on each surface of the shell.

8.6 SUMMARY

In Waitomo a preference was shown by boring bivalves and sponges for the left valve of the shells and polychaetes were only seen on the right valve of the oyster shell. In Patagonian samples preference for left or right valves was solely

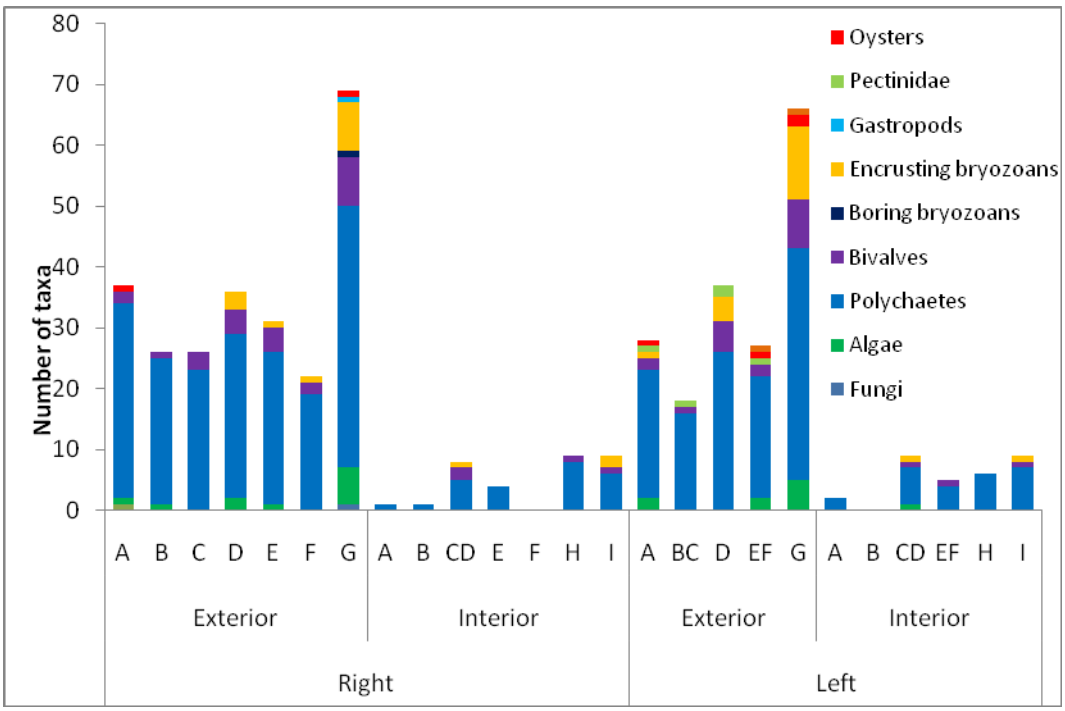

Figure 8.23 Total count of taxa occurring in each sector of the shell on different valves and surfaces of *Crassostrea ingens* from Wanganui.

exhibited by fungi on shells in generation 13, for the left valve of *"Ostrea" patagonica*. In the *Crassostrea ingens* shells analysed from Wanganui, algae and pectinids show a preference for the left valve, whereas polychaetes, boring bivalves and sponges show a preference for the right valve of the shell.

In shells examined from Waitomo it was found that all taxa present have a preference for the interior or exterior surface of the shell. Boring bivalves and sponges both show a preference for the outer surface of the shells, whereas polychaetes are found in the interior surface of the shell. In shells examined from Patagonia, a preference for the external surface of the shell is shown by polychaetes, sponges and boring bivalves. No organisms have shown a preference for the internal surface. The result for *Crassostrea ingens* from Wanganui was similar, polychaetes, boring bivalves, boring algae, gastropods, pecitinds, other oysters and barnacles all show a preference for the external surface, with no taxa having a preference for the inner surface.

On specimens of Flemingosteini Stenzel from Waitomo boring bivalves have a tendency to occupy areas A and G on the right valve and the inner surface of the right valve have no preference. On the external surface of the left valve, boring bivalves tend to occupy area A, D and G and on the internal surface of the shells

taxa show a slight preference to areas B and CD of the shell. The samples from the reef in Puerto Pirámide show that polychaetes have a preference for sector G on the left valve, and boring bivalves prefer sector H in the internal surface of the left valve. Sponges are preferential to sector G on the external surface of both left and right valves and fungi show a preference for sector CD on the internal right surface and sectors B and EF on the internal surface of the left valves. Finally, in Wanganui boring bivalves, boring algae, boring bryozoans, gastropods, fungi and other oysters all show a preference for area G. Polychaetes tend to mainly occupy area A, D, E, and G.

CHAPTER NINE
Discussion

9.1 OVERVIEW

Giant fossil oyster accumulations are a feature of Tertiary strata in both New Zealand and Argentina. Shell concentrations contain much ecological and stratigraphic information. The depositional environment of a shell concentration as seen in the field can differ from the life habit. The dynamics of shell concentrations can become complicated with feedback from other biological, physical and diagenetic systems before final burial. However, with care, details about the paleoecological and paleoenvironmental conditions of shell concentrations can be reconstructed with a combination of taphonomic, stratigraphic and geochemical techniques (Kidwell 1991b).

Field related analysis of fossils oyster concentrations in Waitomo (New Zealand), Patagonia (Argentina) and Wanganui (New Zealand) has involved construction of stratigraphic columns and sketches as well as a detailed description of the stratigraphic, paleontological and taphonomic features of shell accumulations, following Kidwell's approach (1991b). The fossil oyster taxa in this study included Flemingostreini Stenzel (Waitomo), *"Ostrea" patagoncia* (Puerto Pirámide, Patagonia) and *Crassostrea ingens* (Wanganui). To offer a modern day comparison, *Crassostrea gigas* (Patagonia) and *Ostrea chilenesis* (Foveaux Strait) were also included in some aspects of the study.

Laboratory analysis of both fossil oyster accumulations and their host sediments has involved geochemical analysis via carbon and oxygen stable isotopes and laser ablation for elemental concentrations, both for bulk and sclerochronological data. Other analyses included plane polarised light petrography (PPL), cathodoluminescent light petrography (CL), bulk mineralogy via XRD, textural analyses using a lasersizer instrument, scanning electron microscopy (SEM) and component mineralogy (GADDs).

This chapter discusses the results for both the oyster accumulations and host materials in relation to one another, and compares and contrasts the key

differences and/or similarities at each location. The synthesis will help to identify features and characteristics of the oyster accumulations as outlined in the aims of this study in Chapter One. These include: (1) Develop an understanding of the geometry, internal structure, stratigraphic relations and distribution of the oyster beds/reefs within a sequence stratigraphic framework at sites in Waitomo, Puerto Pirámide (Patagonia) and Wanganui. (2) Determine the isotopic and elemental composition of oysters from each location. (3) Describe the mineral, textural and petrographic properties of the host sediments and oysters at each study site. (4) Understand the evolution of the oyster reefs from first colonisers to extinction and compare the characteristics of the reefs and their fauna among the New Zealand and Patagonian examples. (5) Determine the paleoenvironmental setting(s) in which these reefs formed.

9.2 FIELD CHARACTERISTICS AND SEQUENCE STRATIGRAPHY

9.2.1 Terminology and geometry

Accumulations of oysters can be given many names such as bed, bar, mound, clump, pod, reef, bank, wedge, pavement, lens, bioherm, biostrome and the likes (Dittmann 1990; Kidwell 1991b; McIntyre 2002; Powell 2006; Pruss et al. 2007; Navarro et al. 2008). These terms are often based loosely around the geometry that a given oyster accumulation possesses. In this study each accumulation of oysters at the three study sites has a different geometry and so is referred to by different names. Oysters at Waitomo form tabular bed type accumulations and shells are haphazardly orientated, and so are named ‘beds’ (Fig. 3.10). In Patagonia the accumulations have a distinct lens geometry (Fig. 4.8) and the term reef or bioherm is appropriate. A bioherm is defined as a build up of largely *in situ* organisms that produce a mound or reef. Finally the *Crassostrea* that compose the Wilkies Shellbed appear crudely bedded in outcrop (Fig. 5.8) and the name biostrome is used. A biostrome is defined as a layered or sheet-like accumulation of *in situ* organisms which differs from a bioherm as occurs in Patagonia as it lacks a mound or reef structure.

9.2.2 Types of shell concentrations

Shell concentrations are able to be organised into four broad types recognised by Kidwell (1991b) based on their stratigraphy and the inferred history of accumulation (Fig. 9.1). (1) Event concentrations are single scale beds and record

one ecologically brief episode of shell concentration. (2) Multi-event or composite concentrations are complex and record accretion of multiple generations and/or event concentrations. (3) Hiatal concentrations are complex accumulations similar to multi-events except they are relatively thin due to slower rates of accumulation. And finally (4) lag concentrations, which are thin concentrations produced by erosional scour. Shells are displaced and concentrated by removal of the sedimentary matrix, or by erosion or corrosion. Each shell concentration has different stratigraphic and paleobiological implications. Note that the shell beds should not necessarily be viewed as discrete categories, as they can inter-grade somewhat. Shell concentrations 2 and 4 (as above) are recognised in this study and will be further discussed below.

The reef of *"Ostrea" patagonica* in Patagonia is a multi-event shellbed that forms an oyster-rich facies due to repeated levels of colonisation within the building bioherm (mound or reef of *in situ* organisms) (Fig. 9.2A). At Waitomo the oyster beds not only have a large lateral extent, but there are also many condensed shell beds occurring in any one stratigraphic section (i.e. they are multi-event) (Fig. 9.2C). Similarly the oyster beds in Wanganui have a large lateral extent but are characterised by the individual accretion of shells overlying a shell lag. There is a lot of uncertainty regarding the absolute completeness of a record that has had such a complex history and interpretations are most valuable when the preservation styles of shell accumulations are contrasted, such as at Waitomo and Wanganui with an alternation of *in situ* shells and shell lag(Kidwell 1991b).

One possible explanation for the occurrence of multi-event shell concentrations in Waitomo is the accretion of multiple small scale deposits, such as repeated colonisation events involving a bioherm or reef type structure, coupled with periods of shell lag. A complex history is usually inferred from such accumulations that have resulted from episodes of biohermal build up. Episodes of bioherm build up in Waitomo have resulted in thick accumulations (~2 m) alternating with periods of erosional reworking or shell lag deposits (Fig. 9.2C).

In Wanganui a composite shell bed is typified by repeated colonisation horizons within a biostrome (layered accumulation of *in situ* organisms), overlying a shell

lag. Ideal conditions of bathymetry and sedimentation have allowed the composite shellbed of *Crassostrea* to form over a long time range.

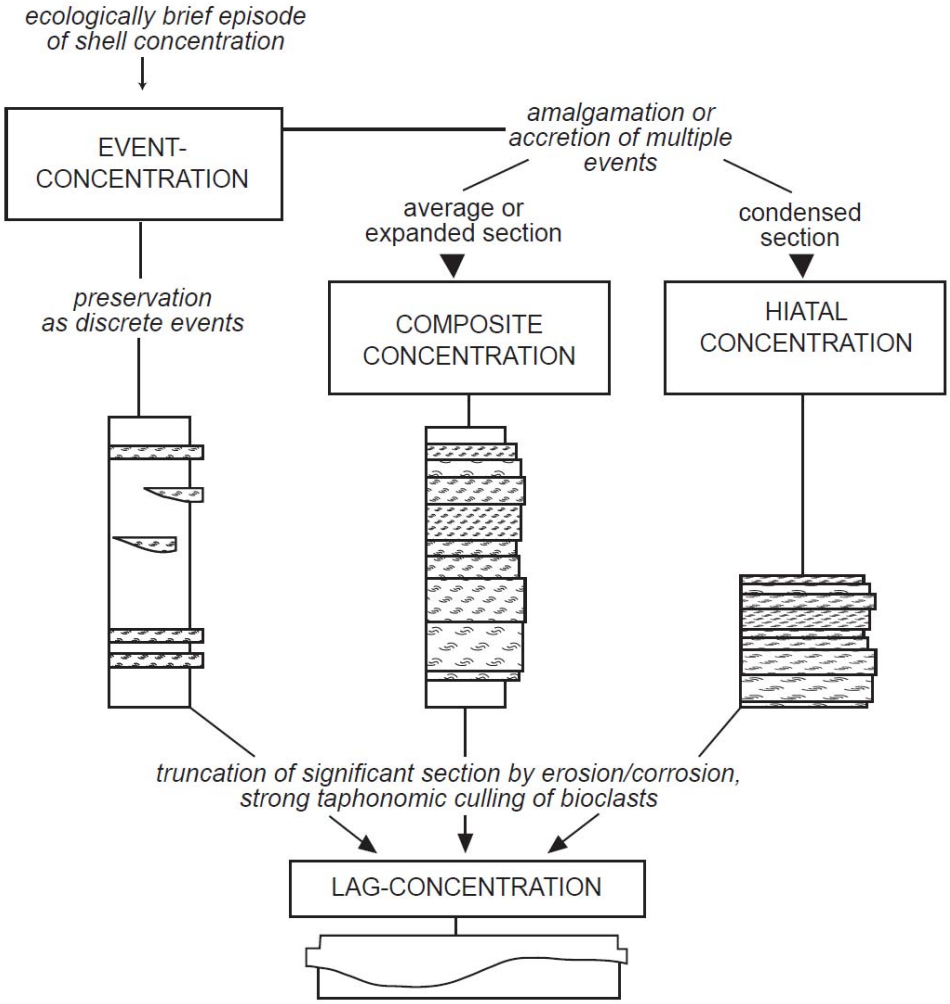

Figure 9.1 Shell concentrations can reflect a range of accumulation histories and time scales and can be grouped into four broad categories. These categories range from simple event-concentrations to accretionary multiple-event accumulations (both composite concentrations and hiatal concentrations) and finally lag-concentrations. Each category can include biogenic, sedimentological and mixed origin coquinas, which can be composed of both local and exotic shells (After Kidwell 1991b).

The very nature of accretion by which these event concentrations are placed upon one another, especially in the formation of the shell lag, means displacement of shells in underlying death assemblages is likely to occur, along with physical reworking of the shells. Portions of the record can also become eroded in between subsequent events, storm events or lags may not erode to their normal potential due to the build up of shells on the sea floor, and diagnostic shell orientations (see Section 9.2.4) may not be produced (Kidwell 1991b).

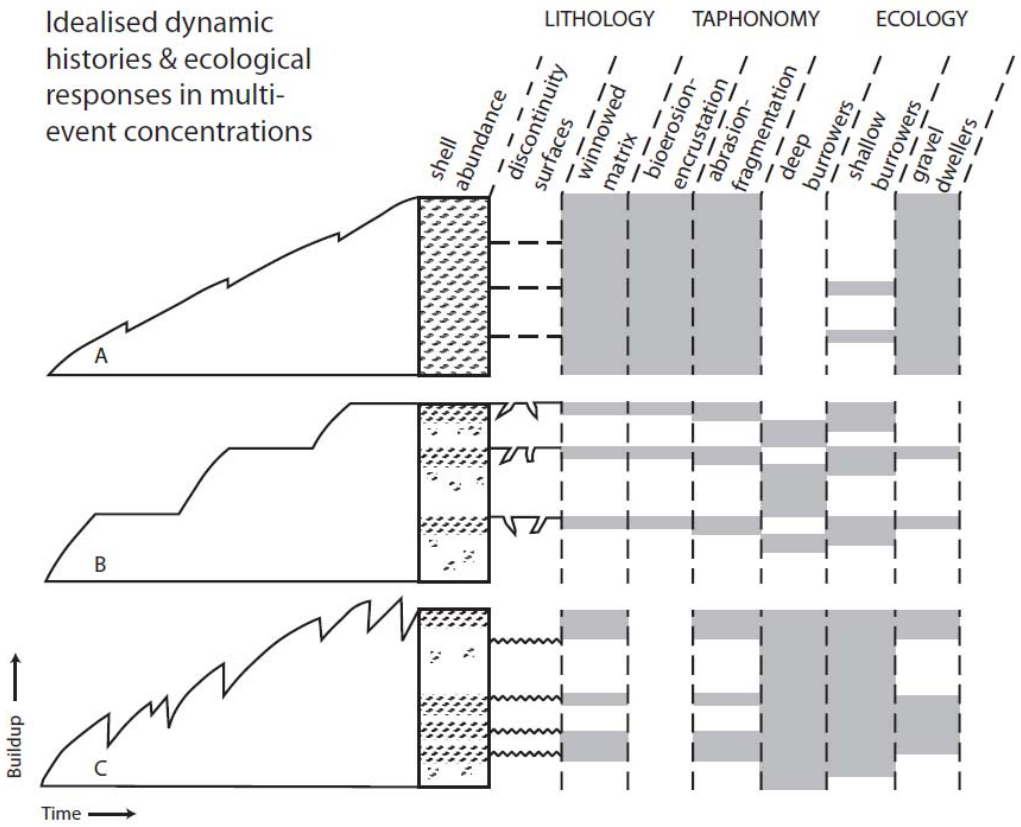

Figure 9.2 Composite concentrations can accumulate either gradually or episodically, and under an array of sedimentary conditions including idealised end-members of (A) complete sediment starvation, or repeated deposition of only temporary, thin sedimentary increments, (B) repeated deposition of thick sedimentary increments, alternating with nondeposition, and (C) repeated deposition of thick sedimentary increments, alternating with partial or complete erosional reworking. The short-term sedimentary and biological dynamics of multiple-event concentrations may be interpreted from sedimentoloigcal, taphonomic, and paleocological features (After Kidwell and Aigner 1985).

Shell lag deposits are typically thin, but this is highly dependent on the volume of shell material available and the extent to which it becomes destroyed. Transport of shells into and out of an area can also be a significant factor, so that some lags may comprise thin ‘streaks’ of shell material while others can be up to 1 m in thick. Shells in lag deposits are typically in poor condition, with abundant disarticulation and fragmentation (discussed in Section 9.2.4). Shell lags most commonly occur in subaerial and shallow marine environments, associated with initial transgression or late stage regression. Lags can have several physical forms from laterally continuous shell bodies as at Wanganui and laterally accreted lenses, as seen at Waitomo (Fig. 3.19).

9.2.3 Oyster morphology

Ostreidae is one of the most successful group of cemented bivalves. Part of their morphologic diversity is due to the fact that oysters have repeatedly evolved during the Mesozoic and Cenozoic and left their original rocky substrates and have become soft bottom dwellers (Seilacher et al. 1985) (Fig. 9.3). This is also due to the unusual shell form that oysters possess that is dictated by environmental conditions and capable of growing over or around adjacent objects, including other oysters (Powell 2006). The fossil oyster accumulations at Waitomo, Patagonia and Wanganui have different physical morphotypic varieties (Fig. 9.4) (Seilacher et al. 1985). Figure 9.4 suggests that all the oyster species in this study are recliners (heavyweights). In particular, Flemingostreini Stenzel from Waitomo and *"Ostrea" patagonica* from Patagonia are large boulder-shaped shells that were mud- and/or gravel-supported. Conversely, in Wanganui the *Crassostrea ingens* shells are recliner types but are shell supported as opposed to mud and/or gravel supported as at the other localities (Fig. 9.4, 9.5).

9.2.4 Orientation, thickness and lateral extent

Numerous studies have focused on the wave and current arrangements of detrital (or transported) bivalve shells such as oysters and mussels (Frey et al. 1987). Such orientations in fossil assemblages can have significance in paleoecological and paleoenvironmental reconstructions. Patterns in orientations of fossil accumulations seen in the field can be a response to not only life habits of the organisms but also due to hydraulic reworking and reorientation of the shells.

Oysters are dependent on current flow to supply nutrients and oxygen, to disperse gametes and larvae, and to remove silt and metabolic wastes. Presumably alignments enhance the efficiency of these functions and are advantageous to sessile organisms such as oysters. Fossil specimens preserved *in situ* can allow for representation of possible current regimes and responses of the organisms (Frey et al. 1987). The three oyster locations examined in this study show markedly different orientation features.

At Waitomo there are two different types of oyster accumulations present when studied in cross-sectional view: dense beds with haphazard orientations and dispersed lenses (shell lag) commonly horizontally (or concordant) orientated.

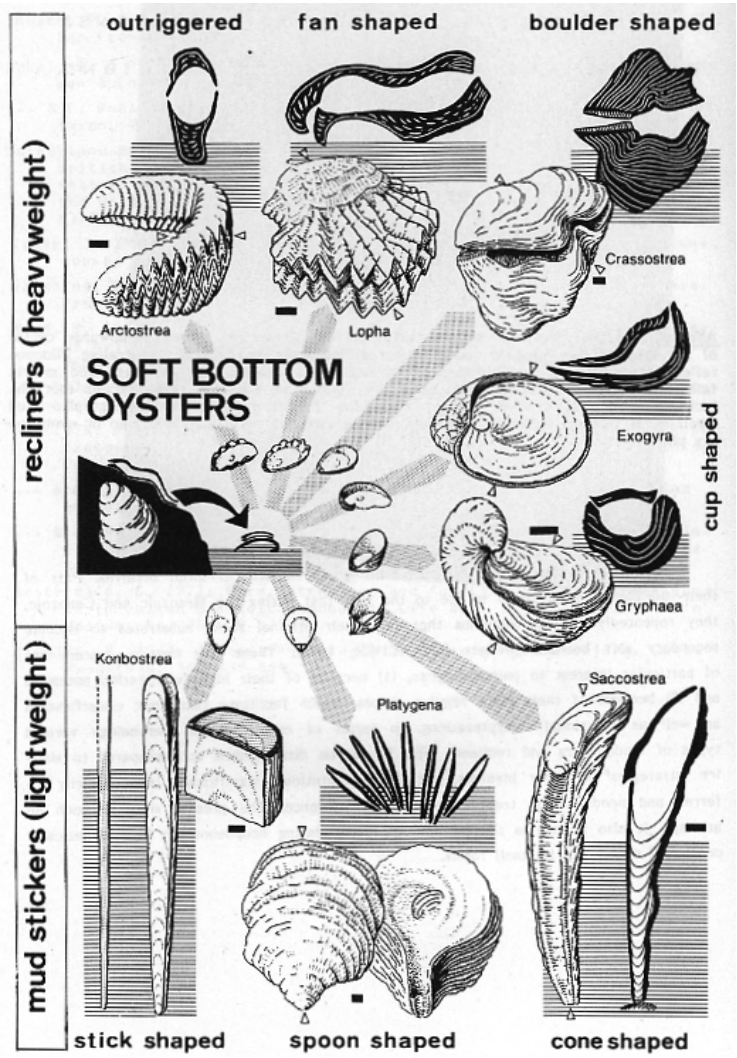

Figure 9.3 The highly irregular shell form of oysters is inherited from the original rock-encrusting habitat and has enabled oysters to adapt to substrates via a variety of strategies. Recliner type (heavyweights) fossil oysters are seen in Waitomo, Patagonia and Wanganui (from Seilacher et al. 1985).

The haphazard nature of the dense beds leads to several hypotheses as outlined by Kidwell & Bosence (1991) (Table 9.1): (1) Shells in life position. (2) Turbulent stirring of the sea floor. (3) Rapid deposition of the shells out of high-density turbulent flows such as debris flows. (4) Burial by sediment scour at subcritical velocities. The dispersed lenses show a concordant orientation which could be due to reposition of the shell fragments out of suspension. The oysters at Waitomo also exhibit a bimodal distribution in plan-view (Fig. 3.5), as do those at Puerto Pirámide, in Patagonia, as identified by Brito (2009). This suggests that they have formed a rheotaxic orientation (movement in response to current) in oscillating current conditions (Frey et al. 1987). In cross-sectional view the shell

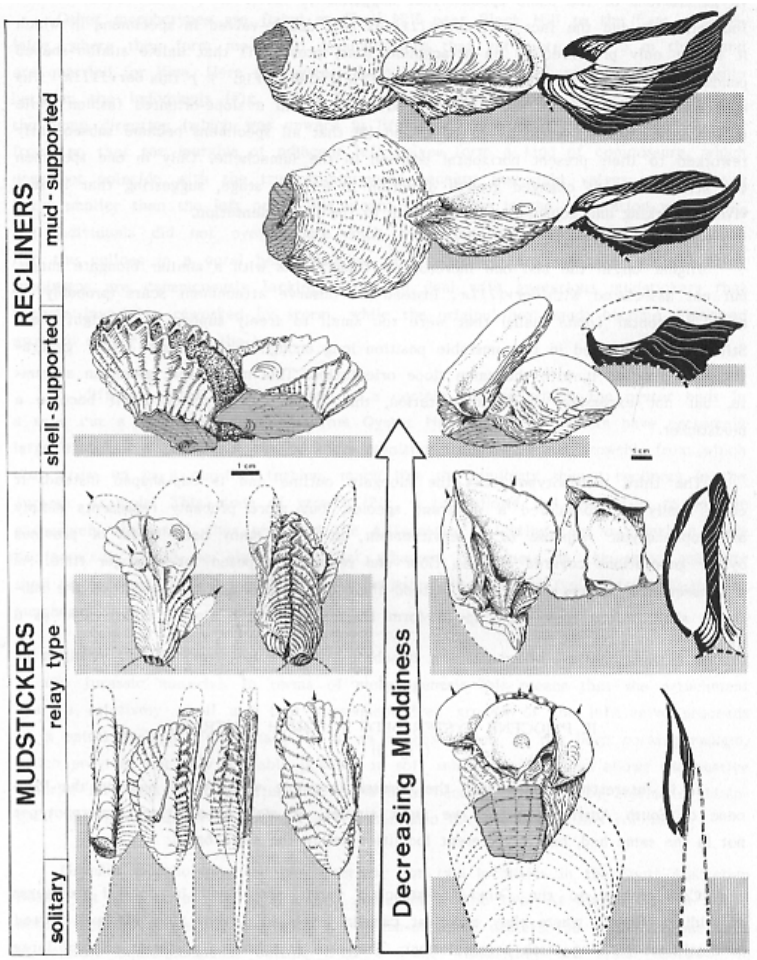

Figure 9.4 Morphotypes of oysters can be further subdivided from mudstickers and recliners to shell-supported or mud-supported. The shift from solitary mudstickers to relay type is representative of decreasing muddiness (from Seilacher et al. 1985).

Figure 9.5 *Crassostrea ingens* from Parikino, Wanganui held within a fine sand host sediment and showing a shell-supported morphotype.

accumulation in Patagonia has no strong trend, suggestive of life position. The Wilkies Shellbed in Wanganui possesses a bimodal distribution in plan-view and a concordant orientation when the cross-sectional view is analysed (Fig. 5.8), both inferring that the shells are in life position (Table 9.1) (Kidwell & Bosence 1991).

Table 9.1 Features of shell orientation of shell accumulations due to hydraulic and other processes (modified from Kidwell and Bosence 1991).

Orientation	Hydraulic processes	Other processes
PLAN VIEW		
Unimodal 	Unidirectional current acting on shells whose critical threshold velocities are lower than the surrounding sediment, the more turbulent the flow the greater the angular deviation	Rheotaxic life position
Bimodal 	Reversing currents i.e. Wave oscillations, tidal ebb and flood. Shell long axes aligned perpendicular to oscillatory current directions	Free-rolling when alive, rheotaxic life position in oscillationg currents
No strong trend 	Flow velocities below or near critical thresholds for shell movement, or sediment moves at lower velocity then shells, leading to burial without orientation, or very turbulent conditions, or interference among shells or inbetween shells and other particles	Life position
CROSS-SECTIONAL VIEW		
Concordant 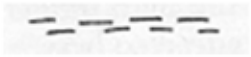	Redeposition of shells out of suspension, or rotation during compaction, or complete exhumation of vertically embedded fauna by winnowing	Life position
No strong trend 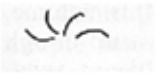	Turbulent stirring of the seafloor, or rapid deposition out of high-density turbulent flows such as debris flows, or burial by sediment scour at subcritical velocities	Life position, or bioturbation, or biogenic graded bedding

Adult oysters are sessile and fixed in position whereas spat are able to adjust their orientation slightly. Consequently, successive generations of spat are able to mimic the preferential alignment of individual oysters. Due to differences in ebb and flood tidal flows, large oyster beds can exhibit differences in alignment in one part of the bed compared to another. Individuals will tend to orientate themselves with respect to the prevailing direction of flow (Frey et al. 1987). Oysters feed on plankton and are able to test the water for presence of these nutrients and then modify their feeding behaviour accordingly (Collier et al. 1953). If an oyster was

to be located in a position that is by-passed by currents or receiving water that has already been filtered by other oysters it may not be stimulated to feed, and if these conditions continued the oyster would starve to death. Conversely, where many oysters are successfully feeding, they in turn produce waste (Stenzel 1971); unless this material is removed by currents, the oyster will become buried by their own refuse (Frey et al. 1987).

Oyster spat that settled near the centre of an accumulation may have been less likely to survive due to overcrowding and increased competition for nutrients (Frey et al. 1987). Also prolonged vertical growth of the bed by subsequent generations of spat may elevate individuals beyond their optimum bathymetric range, thus limiting the thickness of the oyster accumulation. In contrast to this, spat that have settled towards the outer limits of the accumulation are free from competition for space and nutrients and well within the bathymetric optimum. It is possible this phenomenon of spat settling on the outer limits occurred at Waitomo and Wanganui, and explains the great lateral extent of the shell accumulations.

9.2.5 Disarticulation and fragmentation

Disarticulation and fragmentation are generally attributed to physical reworking and shell transport. These phenomena are seen in outcrop at Waitomo and characterised by the occurrence of shell lag as part of multi-event shell concentrations, as discussed above. In general, the degree of disarticulation of shells should decrease with decreasing water energy (Kidwell & Bosence 1991). Rapid burial and low-energy anoxic conditions are frequently suggested to explain a high degree of preservation and articulation in shell accumulations (Seilacher et al. 1985).

Disarticulation of specimens is not always solely a function of water energy or the distance they have been transported. Life habit can also play an important role (e.g. epifaunal bivalves, as in this study, are more prone to disarticulation and transport than infaunal bivalves). Anoxic conditions are rather ineffective at preventing decay, but favour preservation as they reduce the effects of biogenic reworking and can promote an early mineralisation of connective tissues. Low temperatures are most effective at preventing the decay of shells. Therefore well articulated specimens should preferentially occur under environmental conditions

characterised by frequent and/or catastrophic burial (Brett & Seilacher 1991) or by low temperature and anoxia (Kidwell & Bosence 1991).

Fragmentation of shells occurs when waves and currents force the shells against a hard surface such as hard-packed sand, gravel or bedrock. Because water tends to have a cushioning effect, the mechanical fracture of shells is more common in a beach than a subtidal setting. Alternatively shells can be broken up by mobile gravels or by water if they become wedged in a fissure (Kidwell & Bosence 1991).

In Patagonia and Wanganui it can be inferred that the articulated and well preserved specimens of oysters are due to low temperatures and anoxic conditions or by rapid burial of the shell accumulation (Parras & Casadío 2005). In Waitomo however, the epifaunal shells have become disarticulated in a higher level of water energy and fragmented due to waves and/or currents forcing the shells against a surface, such as the shelly-gravelly host sediment.

9.2.6 Sequence stratigraphic characteristics

As discussed in Section 9.2.2, many shell accumulations can have dynamic histories with repeated cycles of shell burial, winnowing and colonisation. Such is the case for the multi-event shell accumulations seen at Waitomo and Wanganui, with colonisation coupled with shell lags. In Patagonia the shell facies is also a multi-event shellbed with repeated episodes of biohermal colonisation. Each of these shell accumulations can be characterised by their expected features and differences as a function of sequence stratigraphic position, as outlined in Table 9.2.

At Waitomo the multi-event concentrations can be interpreted as onlap and backlap shellbeds in a transgressive systems tract (TST) sequence (Fig. 3.30). The sequence stratigraphic development of temperate carbonate systems is likened to that of siliciclastic systems because the temperate carbonate system involves little decrease in carbonate sediment supply into deeper water (Read, 1995). Onlap shellbeds at Waitomo are characterised by shell lags composed of new and reworked fossils that formed in shallow water (< 50 m, see later) due to by-passing and sediment starvation. The backlap shell beds at Waitomo are typified

by a dense accumulation of shells forming from sediment starvation in deeper water (but still < 50 m) than the shell lag. Both of these shell accumulations have a good preservation potential (Table 9.2).

A similar situation applies for the Wilkies Shellbed in Wanganui, with the presence of both an onlap and backlap shellbed being identified within a TST (Table 9.2). Evidence provided by molluscan assemblages suggests the shellbed accumulated in a progressively deepening environment but probably < 40 m. The lower portion of the bed has been identified by McIntyre (2002) as a shallower water onlap shellbed, which forms a transgressive shell lag. The winnowing and by-passing of sediment has led to the carbonate accumulation in the form of a shell lag. The overlying backlap shellbed formed in conditions of reduced turbidity and sedimentation as it deepened upwards. This allowed the *Crassostrea* to live *in situ* at maintainable depths within the fine muddy sand host as the shellbed transgressed shoreward.

In Patagonia the *"Ostrea" patagonica* reef is characterised as a downlap shellbed within a highstand systems tract (HST). The shellbed formed under conditions of sediment starvation, ranging from shallow to deeper water (< 10 m) and in a shallowing upward environment as is confirmed by the conformably overlying fluvial sourced Rio Negro Formation (Fig. 4.4). Lithologies of the shellbed are distinguished by benthic and planktic fossils and also the presence of authigenic minerals (Table 9.2). The reef at Puerto Pirámide includes common authigenic gypsum in the upper part of the reef. A downlap shellbed can be distinguished from a backlap shellbed due to the dominance of matrix/host sediments (Naish & Kamp 1997) (Fig. 4.9). Downlap shellbeds often have a high diversity of mixed fauna, have excellent preservation (Kidwell 1991a, b), as occurs in the *"Ostrea" patagonica* reef, and most specimens are articulated and in life position.

9.3 ISOTOPIC AND ELEMENTAL COMPOSTION OF OYSTERS

9.3.1 Bulk stable carbon and oxygen isotopes

An important goal of paleoecology is being able to understand the environment in which fossil organisms lived. The ratio of heavy to light stable isotopes of both carbon and oxygen preserved in shell calcite may be used to address problems concerning paleoecology as in bivalve shells, such as oysters, environmental

Table 9.2 Summary of expected differences among condensed deposits as a function of position within a stratigraphic sequence (After Kidwell 1991a, b). Numbers (3 to 1) demarcate successivly older strata. Toplap, dowlap, onlap and backlap of Van Wagoner et al. (1988).

Condensed facies types	Sedimentary dynamics	Bathymetry		Lithology	Paleontology		Chronostratigraphy		Preservation potential
		Setting	History		Ecology	Taphonomy	Isochroneity	Duration	
Toplap 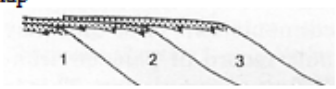 **e.g. Patagonia**	By-passing ± starvation	Shallow water	Shallowing-upward	Benthic skeletal residue, winnowed sand	Low diversity, mixed benthos	Concentration of durable elements	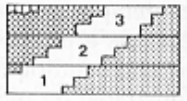	Similar over extent	Poor
Downlap 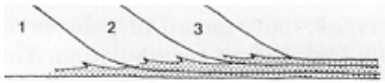 **e.g. Waitomo and Wanganui**	Starvation	Range from shallow to deep water	Shallowing-upward	Concentration of authigenic minerals & benthic + planktic fossils	High diversity, mixed benthos & plank/nekton	Variable, poor to excellent preservation	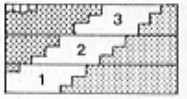	Increases basinwards	Excellent
Onlap 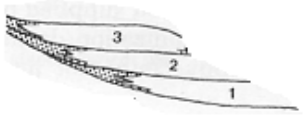 **e.g. Waitomo and Wanganui**	By-passing ± starvation	Shallow water	Deepening-upward	Benthic and skeletal lags in well sorted sand, ± authigenic minerals	High diversity, mixed benthos	Mix of new & reworked fossils	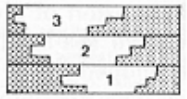	Similar over extent	Good
Backlap (backstep) 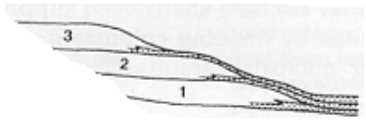	Starvation	Range from shallow to deep water	Deepening-upward	Concentration of authigenic minerals & benthic + planktic fossils	High diversity, mixed benthos & plank/nekton	Variable, poor to excellent preservation	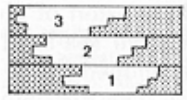	Increases basinwards	Good

conditions can be recorded geochemically within the shells at the time of calcification (Kirby 2000).

9.3.1a Paleosalinity

The basis for being able to estimate the paleosalinity of the oysters lies in the ratio of heavy to light isotopes for oxygen and carbon ($\delta^{18}O$ and $\delta^{13}C$, respectively) and the distinctive characteristics of isotopes from freshwater, brackish and marine environments (Nelson et al. 1983). Epstein & Mayeda (1953) showed that the $\delta^{18}O$ of sea and coastal waters increases with salinity and that this relationship is caused by the mixing of isotopically light freshwater with seawater.

It has also been identified that the carbon isotopic composition of carbonates varies with salinity and can be used to determine the relative influence of marine and freshwater on fauna such as oysters. A direct approach towards isotope salinity correlation was described by Mook (1968, 1971) who found a close relationship between the $\delta^{13}C$ and $\delta^{18}O$ composition of carbonate materials and salinity. He constructed a marine field of isotopic ratios which corresponds to the isotopic equilibrium precipitation of shells with normal sea water (Fig. 9.6). Samples that plot below this field are considered to have been influenced by freshwater, the amount being proportional to the distance from the marine field.

Differences in the isotopic composition of Flemingostreini Stenzel (Waitomo), *"Ostrea" patagonica* (Patagonia) and *Crassostrea ingens* (Wanganui) are most likely due to differences in paleoecology between these species. Fossil samples from Waitomo, Wanganui and the modern oyster from Foveaux Strait all mainly plot within the Mook (1968, 1971) marine field, commensurate with these samples having lived in fully marine conditions (Fig. 9.6). In particular the environment of the Foveaux Strait oyster *Ostrea chilensis* can provide a good model for the inferred environment of the Orahiri Limestone Flemingostreini oyster. As discussed in Section 6.2.1, the Foveaux Strait oyster lives in 18–45 m water depth as elongated deposits on siliciclastic gravels overlain locally with skeletal sands in a tide swept environment. The distribution of oysters in this environment is attributed to the gravelly substrate, which is suitably firm for the attachment of larvae (Fleming 1952; Cullen 1962).

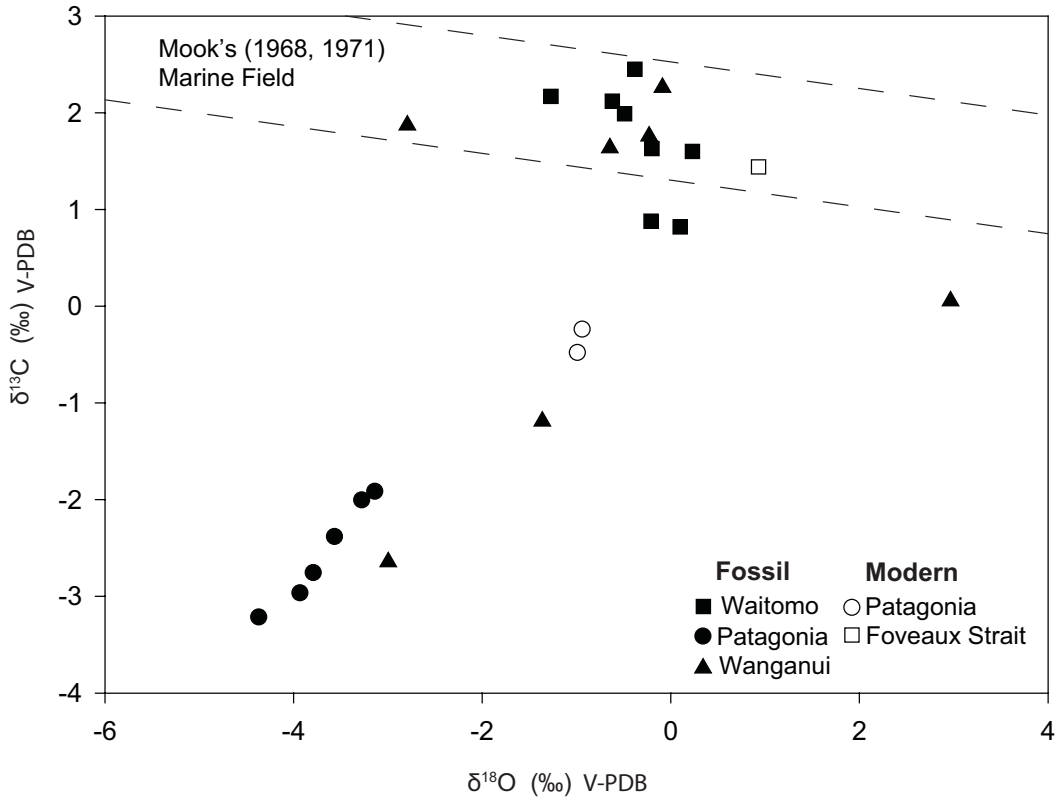

Figure 9.6 Scatter plot of $\delta^{13}C$ vs $\delta^{18}O$ values from Waitomo (Flemingostreini Stenzel), Patagonia *("Ostrea" patagonia*) and Wanganui (*Crassostrea ingens*). Note the inclusion of modern samples from Patagonia, (*Crassostrea gigas*) and Foveaux Strait (*Ostrea chilensis*). The dashed lines show the marine field of Mook (1968, 1971).

Crassostrea ingens from the Wilkies Shellbed biostrome at Wanganui show both a marine and marginal marine signal. This fits with the suggestion of McIntyre (2002) that the lower part of the Wilkies Shellbed may have some estuarine influence as supported by associated fauna, which could account for some of the lower $\delta^{13}C$ values in Figure 9.6. The upper part of the reef, however, has an abundance of moderate to high salinity marine fauna. This is supported by those Wilkies data that fall within the Mook (1968, 1971) fully marine field.

Data from San Blas (Patagonia) modern oysters (*Crassostrea gigas)* fall below the marine field, suggestive of some freshwater influence and a brackish environment. As discussed in Section 6.2.2 *Crassostrea gigas* lives in the intertidal zone, which the isotopic data presumably represent. The Patagonian fossil oysters ("*Ostrea" patagonica)* also have low $\delta^{13}C$ and $\delta^{18}O$ values, falling well below the fully marine field and supportive of a freshwater influence.

9.3.2 Stable isotope sclerochronology

Oysters form a sclerochronological record within the ligamental area (Fig. 6.6), where the two valves are joined by ligament (Kirby et al. 1998). They deposit shell incrementally which reflects the environment in which it was formed (Gröcke & Gillikin 2008). Therefore mollusc shells such as oysters are able to preserve a biogeochemical time series that can be directly applied to the surrounding environment (Stetcher et al. 1996).

9.3.2a Sclerochronological interpretation

Both $\delta^{18}O$ and $\delta^{13}C$ values for *"Ostrea" patagonica* and *Crassostrea ingens* are within the range of what would be expected for shallow marine bivalves (Table 6.2). The relative seasonal ranges of both $\delta^{18}O$ and $\delta^{13}C$ values are similar to other bivalves from shallow marine environments, such as the Quaternary age *Spisula solidissima* (Krantz et al. 1987). Conversely, values from Flemingostreini Stenzel at Waitomo are unlike those from the other oyster fossils analysed. The most noticeable difference in the data is that the $\delta^{18}O$ and $\delta^{13}C$ values are much higher in Flemingostreini Stenzel than *"Ostrea" patagonica* and *Crassostrea ingens*, which suggests that Flemingostreini Stenzel was exposed to more fully marine conditions. Generally, marine water has $\delta^{18}O$ values higher than meteoric water (Mook & Vogel 1968). The $\delta^{13}C_{DIC}$ values are higher and show less variability in marine water because the dissolved inorganic carbon (DIC) in meteoric water is mostly derived from the decomposition of organic matter from terrestrial sources and from chemical weathering, which has low $\delta^{13}C$ values (Keith et al. 1964). Values that are obtained from brackish environments will have intermediate $\delta^{18}O_{water}$ and $\delta^{13}C_{DIC}$ values between marine and meteoric waters.

In addition to the higher $\delta^{18}O$ and $\delta^{13}C$ values, both total and seasonal $\delta^{18}O$ ranges are less for Flemingostreini Stenzel than in *"Ostrea" patagonica* and *Crassostrea ingens*, and $\delta^{13}C$ ranges are either small or less in Flemingostreini Stenzel (Fig. 6.13, Table 6.2). Smaller seasonal ranges suggest less seasonality in both temperature (around 2-3^{o}C) and $\delta^{18}O_{water}$ (and also salinity) in the case of the $\delta^{18}O$ values, and less seasonality is also interpreted for $\delta^{13}C_{DIC}$ in the case of the $\delta^{13}C$ values as would be expected in a shallow marine environment. Smaller standard deviations indicate less inter-annual variability in conditions. In contrast, values from specimens from Patagonia ("*Ostrea" patagonica*) and Wanganui

(*Crassostrea ingens*) show lower isotopic values and a larger seasonal range, which is consistent with a brackish environment that received extensive freshwater input and mixing. Difference in minimum and maximum seasonal temperatures is about 0.4°C at Waitomo and from 8 to 12°C in Patagonia and 7 to 10°C in Wanganui. The low amount of seasonal variation evident in Flemingostreini Stenzel is consistent with little variation in summer and winter $\delta^{18}O_{water}$ values from year to year and thus less variation in the pattern of freshwater influx in this environment. The $\delta^{18}O$ maxima and minima values in the other fossil oysters analysed, however, show a large amount of variation (Table 6.2), which is consistent with higher levels of freshwater input common to brackish environments.

Some positive correlations are seen between values of $\delta^{18}O$ and $\delta^{13}C$ (Fig. 6.13, Table 6.3) in samples from Patagonia (both modern and fossil) and *Crassostrea ingens* from Wanganui. Kirby (2000) suggested that such relationships could be occurring for several reasons, such as (1) an influx of meteoric water decreasing both $\delta^{18}O_{water}$ and $\delta^{13}C_{DIC}$ at the same time (salinity effect), (2) as temperature increases so too does the level of primary productivity, or (3) increasing temperature leading to an increase in the metabolism of the organism and thus incorporation of respired ^{12}C into their shells. The isotopic data alone are insufficient to reject any of the above hypotheses. However, the tight cluster of isotopic values for Flemingostreini Stenzel (Fig. 6.13) suggests that an influence via meteoric water was less likely to have occurred in the Waitomo environment. Also Krantz et al. (1987) suggested that a pattern of low summer and high winter $\delta^{13}C$ values as witnessed in many shallow marine bivalves does not necessarily reflect the salinity effect, but rather the occurrence of seasonal plankton blooms. In addition to changes in $\delta^{13}C_{DIC}$ due to productivity and salinity effects, shell $\delta^{13}C$ may also reflect metabolic changes of the organism throughout the year (Kirby 2000).

9.3.3 Trace elemental composition

There is good potential to gain paleoenvironmental data from marine molluscs such as oysters as the geochemical composition of their shells reflects the ambient growth conditions (Freitas et al. 2005).

9.3.3a Bulk trace elements

As outlined in Schneider et al. (2009), concentrations of Mn, Fe and Sr can provide significant information on the diagenetic state of fossils. Concentrations of Mn and Fe are known to increase during diagenesis and fossils become depleted in Sr and Mg by the same process. However, many extant oysters are prone to environments that have reduced levels of salinity and usually are found in river mouths and are subject to fresh water input and mixing. Because of this, the shells of these oysters show a wide range of trace element contents originating from the heterogeneous loads of rivers. As this situation can hold true for oysters in this study, they have therefore been compared to other oysters in the literature (Table 6.1).

Average levels of Sr and Mn in this study are not as low as those observed by Anderson et al. (1994) in Jurassic fossils from the United Kingdom. The values range considerably below those reported by Denison et al. (2003) for Cretaceous oysters and values presented for several oysters by McArthur et al. (1994) from Western Interior, United States. Average concentrations of Fe are the highest in Flemingostreini Stenzel shells from Waitomo, but are still in accordance with values in shells analysed by Carriker et al. (1996) from Delaware and Anderson et al. (1994) from the Western Interior. The oyster sample from the top of the reef at Puerto Pirámide has the lowest concentration of Fe, but is in accordance with the majority of studies in Table 6.1. The average concentrations of Mg in sample PAT4/1 from Patagonia is comparable with the majority of studies featured in Table 6.1. PAT2/1 is comparable with values recorded by Carriker et al. (1980, 1991). Samples from Waitomo and Wanganui, however, have Mg values significantly lower than all the other studies presented here.

Compared to the broad range of concentrations in Fe, Sr, Mn and Mg in the literature (Table 6.1) the cutoffs for these elements are relatively strict (Table 9.3). A "cutoff" is an empirically derived value for which oysters falling below or above a particular value are thought to have undergone some form of diagenesis (Schneider et al. 2009). As Mn and Fe are known to increase in diagenesis all samples should fall below the maximum cutoff of 305 and 300 ppm, respectively. The Waitomo and Wanganui samples have a greater concentration in Fe, and the lower Patagonian sample has slightly higher Mn levels. Sr is said to reduce when

diagenesis occurs so all samples should be above the 605 ppm cutoff. Only the sample from Waitomo is above this level. No cutoff information for Mg is presented.

Table 9.3 Literature data on diagenetic alteration cutoffs for Sr, Fe, Mn (noted in ppm) in oysters.

Author	Sr	Fe	Mn
Jones et al. (1994c)	-	<150	<30
Jones et al. (1994a)	-	300	-
McArthur et al. (2000)	586	298	305
Holmden and Hudson (2003)	603	-	-
Wierzbowski and Joachimski (2007)	-	<250	<100

As noted in Section 6.4, some of the oyster samples do show statistically significant relationships between Fe and Mn and between Fe and Sr (Table 6.2). In none of the oysters sampled for trace elements are both of these relationships statistically significant. In the samples from Waitomo, the sample from Patagonia and the sample from Wanganui there is a statistically significant relationship between Fe and Mn, but all relationships between Fe and Sr are insignificant and the upper sample from Patagonia shows no relationship between any of Fe, Mn or Sr.

Applying the cutoffs to samples suggests that at least some diagenesis has occurred in all of the samples. However these results require further testing as such a small sample area is collected from laser ablation (see Section 2.3.6) and so may not be representative of the whole sample. The higher trace element concentrations in samples from Patagonia and Wanganui could be explained by the variable input of freshwater into the marine environment. Freshwater has a higher Fe and Mn concentration than sea water. Also all these shells are living epifaunally (above the sediment) and may be directly influenced by elements that are released from siliciclastic sediments. Compared to data from the literature all oysters sampled in this study from Waitomo, Patagonia and Wanganui retain trace element compositions that are well within the ranges known from examples of extant and fossil oysters (Table 6.1).

9.3.3b Sclerochronological interpretations

Many studies have shown the use of Sr/Ca and Mg/Ca ratios to be useful proxies for paleosalinity and paleotemperature (Stetcher et al. 1996; Freitas et al. 2005; Carroll & Romanek 2008; Gentry et al. 2008; Klünder et al. 2008; Wanamaker et al. 2008; Higuera-Ruiz & Elorza 2009). These proxies are especially useful as the oyster shells deposit material incrementally, and the shell preserves a chemical time series that is related to the environment. Molluscs live in a broad range of environments, and have diverse life habits, growth rates and specific aquatic habitats. These characteristics make the study of trace elements a potentially rich source of environmental information (Stetcher et al. 1996).

Sample PAT2/1 (bottom of reef) from Patagonia was analysed at a higher spatial scale than the other samples and the regular fluctuations in the profiles of Sr/Ca and Mg/Ca are suggestive of seasonal cycles, with a range of 7.56E-04 and an average value of 6.56E-04 (Fig. 6.16). Fluctuations across the shell show large peaks in both the Sr/Ca and Mg/Ca ratios. The highest values, the maximum being 1.06E-03 for PAT2/1, pertain to summer values. As the winter period approaches, the Sr/Ca ratio drops off rapidly, and then rises again just as rapidly during spring. The sharpness of these valleys is almost certainly a result of slow growth of the shell during the winter (Rice & Pechenik 1992). While not so well defined, similar fluctuations are seen over a larger scale in the remaining samples from Waitomo (N14/1C), Patagonia (PAT4/1) and Wanganui (WLK). All samples exhibiting the sharp peaks and valleys seen in PAT4/1 in both the Sr/Ca and Mg/Ca ratios almost certainly relate to temperature variations across seasons. The phenomenon of sharp peaks and valleys pertaining to summer and winter values has also been described for $\delta^{18}O$ profiles (Krantz et al. 1989).

The variation seen in values in the first 10 mm of the Waitomo profile is much less than in other samples (Fig. 6.15). The minimum, maximum and total range of values for Mg/Ca and Sr/Ca are comparable with samples from Patagonia, but the standard deviation on the average value is much smaller. This is suggestive of less variation in values throughout the seasons and from year to year. This is consistent with a marine environment that experiences relatively little variation in temperature and salinity. The large spike at the start of the WLK record from Wanganui (Fig. 6.18) is possibly due to a kinetic or metabolic effect at the start of

the organisms life (Freitas et al. 2005). Faster growth in the early years of the oysters life is attributed to survival and warding off of predators by thickening the shell rapidly. Across the rest of the shell more even fluctuations occur across the shell, and these are less in magnitude and show much less variation in minimum and maximum values than those in samples from Patagonia. This is indicative of an environment with less freshwater influence, and therefore less variation in temperature and salinity.

Several studies report ontogenic decreases; as the shell reaches maturity the rate of shell growth decreases (Stetcher et al. 1996; Gentry et al. 2008; Klünder et al. 2008). None of the samples analysed in this study, however, show any decrease in Sr/Ca or Mg/Ca values. A study undertaken by Stetcher et al. (1996) that different bivalve species can have opposing effects of Sr/Ca incorporation into their shells. From this it was concluded that the Sr/Ca ratio in shells is most unlikely to be controlled by ambient water temperature but rather that it is kinetically controlled and appears to increase with growth rate. Mg/Ca ratios however have been found to be a useful estimate of temperature changes during summer according to Klünder et al. (2008). Due to the large differences in spatial scale of elemental and isotopic data in this study, this information was not able to be coupled to provide an estimate of paleotemperature and paleosalinity as in some other studies.

9.4 TEXTURAL, MINERAL AND PETROGRAPHIC CHARACTERISTICS

9.4.1 Host sediment characteristics

Host sediments in Te Kuiti Group Orahiri Limestone at Waitomo are characterised by biomicritic limestones, with bryozoans and bivalves (oyster fragments) dominating the bioclastic (78%) component of the rock. The micritic nature of the host rock suggests a low environmental energy level in the Folk (1962) scheme. Micritic host rock is also suggestive of carbonate-mud being trapped amongst the oysters, but possibly some of the micrite could have formed as cement. Bioclastic grain size is commonly very coarse sand or granule sized which Nelson (1973) suggested reflects the local derivation of sediment, rather than the occurrence of strong current action. This is further supported by the poor sorting and low abrasion of the grains. The average siliciclastic (22%) fraction of the host rock is mainly composed of quartz and feldspar. The siliciclastic grain

size ranges from very fine to medium sand and is most commonly medium sand sized. These grain sizes support shallow water deposition (Nelson 1973).

The predominant mineralogy of the host sediment from the Puerto Madryn Formation at Puerto Pirámide in Patagonia involves feldspar, quartz, clay minerals and the fibrous evaporite mineral gypsum (Fig. 7.18A). The latter, however, is only prevalent in the uppermost section of the reef and is mainly diagenetic in origin (Scasso & Castro 1999). Grains in Patagonia are subrounded to rounded fine sands and generally poorly sorted (Fig. 7.18B). There is a lack of clay-sized grains, although XRD shows the presence of some clay minerals, which are probably contained within rock-fragments and as alteration products of feldspars. The poorly sorted, subrounded to rounded nature of the sediment with little clay-sized material suggests a texturally submature to mature sand sediment (Fig. 7.2). This, combined with the fine grain size, fits with the low to moderate energy tidal flat environment suggested by Casadío et al. (2005).

The host sediment from the *Crassostrea* abundant Wilkies Shellbed, Wanganui, is characterised by fine sand sized, very poorly sorted quartz, feldspar, muscovite and clay minerals plus some calcite (Fig. 7.22A). The very poorly sorted, subrounded to rounded, fine sand suggests a texturally submature-mature sediment and mainly low energy environment. This fits in with the suggestions of McIntyre (2002) that the Wilkies Shellbed maintained a low level of turbidity and sedimentation throughout the life time of the *Crassostrea* biostrome.

9.4.2 Oyster shell microstructure

As described by Majewske (1969), the shell microstructure of oysters in the family Ostreidae is commonly composed of prismatic and foliated crossed-lamellae of calcite crystals. Samples of Flemingostreini Stenzel from Waitomo have a homogeneous structure alternating with thin foliated layers (Fig. 9.7A). Closer examination of the shell under SEM shows the homogeneous calcite to be chalky and porous in nature (Fig. 9.7B). Many of the samples that have been examined show patches that appear to have been recrystallised with large blocky calcite crystals (Fig. 7.12A). These, however, are easily avoidable during analysis. Cathodoluminescene (CL) imaging of these shells shows a dominance of dull orange colours which confirms calcite. In areas that have become recrystallised,

bright orange, zoned calcite crystals are seen, with the zoning representative of several stages of growth. A purple-blue luminescence colour was rarely noted in samples (W04/3B) (Fig. 7.12B). Component mineralogy was carried out on this sample using GADDs which confirmed both CL colours were calcite. The change in colour witnessed is possibly due to an increase in Fe within the sample, as noted in the bulk trace element studies (see Section 9.3.3a), which acts as a quencher in CL intensity (Machel et al. 1991).

The *"Ostrea" patagonica* shells from Patagonia have a prismatic shell structure comprised of well formed crystal laths of calcite. All samples examined under the microscope show small well defined areas of iron and possibly manganese oxides inside cavities and also between the laminae of the shell structure (Fig. 7.19A, B). These results are comparable to a study undertaken by Scasso et al. (2001). Other areas of the shell structure remain well preserved and the apparently altered areas are easily avoided during geochemical sampling (Fig. 7.19C). Under SEM, the shell microstructure is mainly composed of prismatic calcite layers (Fig. 9.7C). CL images of *"Ostrea" patagonica* shells show an alternation between dull to light orange in different laminae of the shell, confirming the calcitic nature of the shell (Fig. 7.19B).

Wanganui *Crassotrea ingens* shells have a structure composed of foliated calcite (Fig. 7.23A) that forms bundles in some specimens. Irregular chalky layers have been identified under SEM (Fig. 9.7D), and are similar to those found by Scasso et al. (2001) in samples of *"Ostrea" patagonica.* Chalky layers in shells are known to be porous and are an adaptive strategy of oysters shells that live on soft bottoms (Carter 1990; Chinzei 1995). These layers can be susceptible to becoming infilled with diagenetic calcite. CL images of the Wanganui Basin oysters typically show a uniform dull orange colour, suggesting the oyster calcite has not undergone any significant diagenetic alteration.

The SEM study of oyster microstructures indicates that shell structure varies greatly between the oyster species and that alteration is not always clearly detected, mainly due to the complex internal structural pattern of each of the shells and the subtle nature of the recrystallisation processes that are seen in some carbonates (Mii et al. 1997; Scasso & Kiessling 2001). Furthermore, some of the

inferences drawn between the luminescence properties and alteration in carbonate shells might be challenged due to the discovery of luminescent carbonate shells from modern day environments (Rush & Chafetz 1990; Barbin et al. 1991; Barbin & Gaspard 1995). However, combined with aspects of geochemistry, CL can be a useful tool in the assessment of diagenetic alteration in fossils (Barbin 2000).

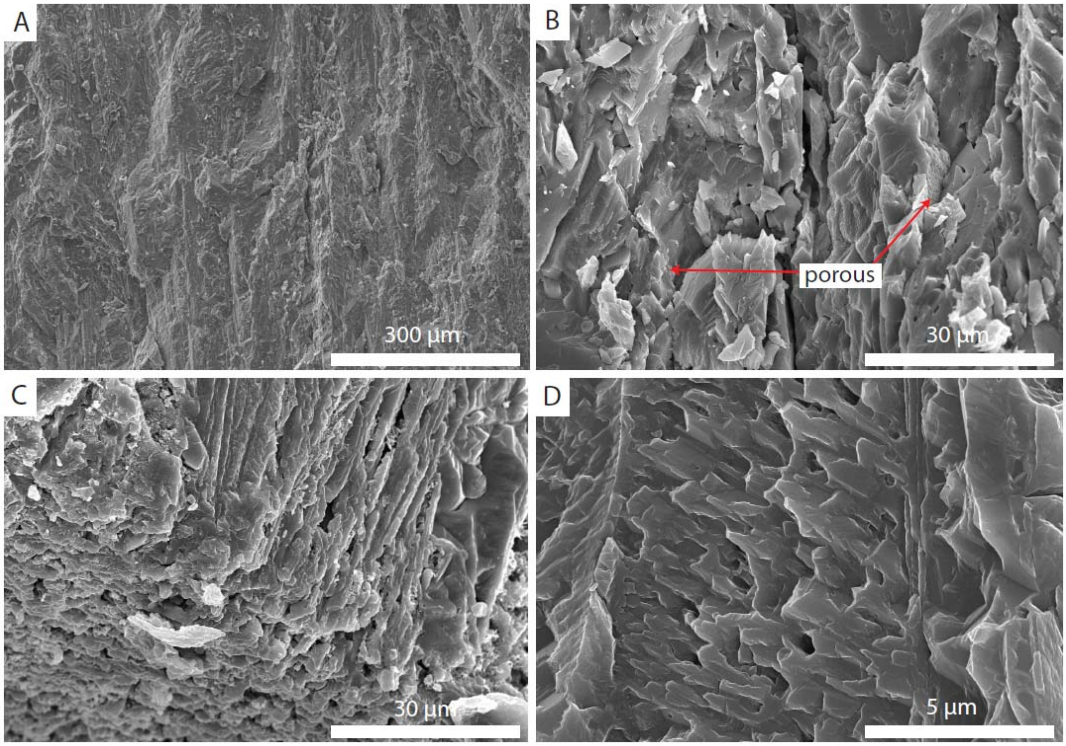

Figure 9.7 SEM images showing differences in oyster shell microstructure from each species analysed in this study. (A) Homogeneous calcite structure of Flemingostreini Stenzel from Waitomo (sample K13/1B). (B) On closer examination the shell in (A) appears chalky and porous. (C) Calcitic lath structure of *"Ostrea" patagonica* from Patagonia (sample PAT3/3). (D) Chalky structure in *Crassostrea ingens* from Parikino, Wanganui (sample WLK).

9.4.3 Borings

9.4.3a Internal geopetal fabrics

Geopetal fabrics indicate the relationship between the top and bottom of the shell at the time a particular rock was formed. In this study internal geopetals often occur in the boreholes in Flemingostreini Stenzel shells from Waitomo. They are characterised by a boring being infilled by fine bioclasts in the bottom of the borehole, overlain by micrite peloids which in turn are overlain by calcite spar cement (Fig. 7.14). It has been suggested by Flugel (2004) that not only can these internal geopetals represent the relationship between the top and bottom of a particular shell, but they also act as frozen spirit levels within the boring at the

time of deposition of the internal sediment. Most importantly, the conditions for the formation of the internal geopetals seen at Waitomo are low sedimentation rates and rapid burial of the oyster fossils.

9.5 OYSTERS AND ASSOCIATED COMMUNITIES

9.5.1 Oysters as physical ecosystem engineers

Facilitative or positive interactions are associations among species that benefit from at least one participant and cause no harm to the other (Bruno et al. 2003). These types of interactions have also been termed physical ecosystem engineering which is defined as follows:

> "Physical ecosystem engineers are organisms that directly or indirectly control the availability of resources to other organisms by causing physical state changes in biotic or abiotic materials. Physical ecosystem engineering by organisms is the physical modification, maintenance, or creation of habitats. The ecological effects of engineering on other species occur because the physical state changes directly or indirectly control resources used by these other species" (Jones, 1997, pg 1947).

Oysters are termed autogenic physical ecosystem engineers as they modify their environment by means of their own physical structure. This relationship between oysters and boring and/or encrusting communities was first enunicated by Mobiüs (1877) who stated "the territory of an oyster-bed is not inhabited by oysters alone but also by other animals". He proposed the word 'biocoenosis' for such a community.

Analysis of the oysters shells from each location in this study - Flemingostreini Stenzel (Waitomo), *"Ostrea" patagonica* (Patagonia) and *Crassostrea ingens* (Wanganui) – shows that they support diverse assemblages of fossils, mainly appearing as traces. Sessile boring and encrusting organisms such as boring fungi, algae, boring bivalves, sponges, polychaetes, bryozoans, barnacles and other organisms have depended on the hard substrate provided by the oyster shells. This suggests that the main role of these oyster species lay in their physical rather than biological properties. The presence of boring and encrusting organisms on the valves of oysters examined at each location suggests that a high diversity of communities was dependent on the substrate and/or the refuge provided by these

giant oysters. The diversity of communities supported is comparable to that observed in extant oyster reefs of *Crassostrea virginica* (Bahr & Lanier 1981), suggesting that all species of oysters examined in this study acted as autogenic physical ecosystem engineers.

A similar study conducted by Parras & Casadío (2006) found that both sedimentological and biological accumulations of *Crassostrea? hatcheri* from Late Oligocene – Early Miocene of Patagonia supported a diverse community of organisms. It was suggested that factors that have rendered it a facilitating organism included the large size of the shell (250 mm high, 210 mm long and 60 mm thick), the age of the adult specimens (25 years), high population densities, large geographic distribution and a long temporal range of over 5 My.

9.5.2 Diversity and community succession

9.5.2a Differences between left and right valves

Analyses in the form of chi square tests were performed to test the hypothesis that boring and encrusting organisms were distributed non-randomly between left and right valves in the accumulations of oysters at each study location. A summary of the results is provided in Figure 9.8. In Waitomo a preference for left valves exhibited by sponges and bivalves suggests that these traces were made while the organism was alive. On samples of *"Ostrea" patagonica* only fungi on shells in generation 13 of the reef build up show a preference for the left valves of the shell. In *Crassostrea ingens* samples analysed from the Wilkies Shellbed in Wanganui a preference for the left valve of the shells was shown by algae, cyclostome bryozoans, pectinids, other oysters and barnacles. Conversely, polychaetes, bivalves and sponges show a preference for the right valve of the *Crassostrea* shell.

A preference exhibited by boring and encrusting organisms suggests that these traces were created during the oyster's lifetime. This can possibly be explained by the shell form and morphotypic trends seen in the oysters (Fig. 9.3, 9.4). Both Flemingostreini Stenzel and *"Ostrea" patagonica* are heavyweight recliners with a boulder shape and are mud and/or gravel supported (Seilacher et al. 1985). This means it is most likely that the right valve was sitting in the sediment and the left valve (more convex) above the sediment, making a suitable and sediment free attachment environment for organisms such as sponges, boring bivalves and

fungi. Alternatively the non–random distributions that are exhibited by some of these taxa may reflect taxic behaviours of the larvae themselves to enhance its survival (Bien et al. 1999). A study conducted by Mauna et al. (2005) found that the more rugose surface of the left valves of *"Ostrea" patagonica* could possibly trigger active selection by larvae (rugophilic behaviour according to Bien et al. 1999). Larvae that settle on the rugose surface of the left valve would be better protected from grazers, thus increasing their survival rate.

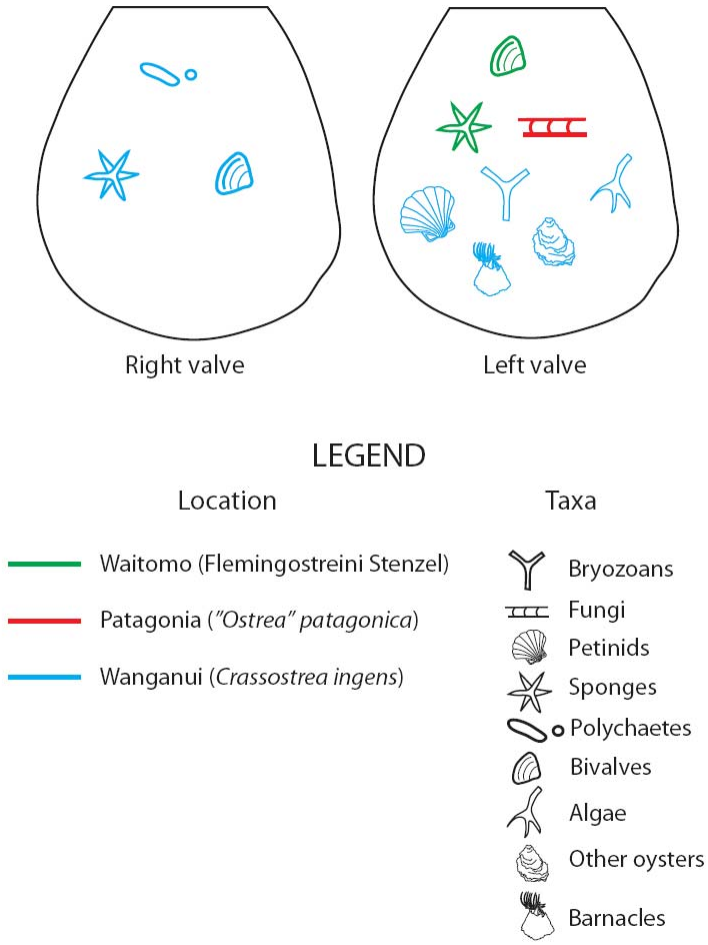

Figure 9.8 Summary of relationships exhibited by communities on left or right valves of the oyster shells found at Waitomo (green), Patagonia (red) and Wanganui (blue) study locations.

In the case of Wanganui occurrences a different morphotypic trend is seen. The *Crassostrea ingens* oysters contained within the Wilkies Shellbed are shell supported (Fig. 9.4, 9.5) (Seilacher et al. 1985). Consequently both the left and right valves of some shells can be orientated out of the sediment. So it is possible that the algae, cyclostome bryozoans, pectinids, other oysters and barnacles shown to prefer the left valve are exhibiting rugophilic behaviour (Bien et al. 1999). Organisms that prefer the right valve, such as polychaetes, bivalves and

sponges, may have done so because of their preference for the flatter surface of the less convex right valve. The suggestion that the Wanganui oysters were shell supported and not reclined in the sediment as at other localities is supported by the preference of sponges for a particularly sediment free environment (Bromley 1994).

9.5.2b Differences between internal and external surfaces

It was hypothesised that borings and encrustations are non-randomly distributed between the interior and exterior surfaces of the valves at each location. A summary of the results is contained in Figure 9.9. The majority of organisms analysed on the shell surfaces show a preference for the external surfaces of the valves. In particular the boring bivalves and sponges both show a preference for the exterior of the Flemingostreini Stenzel shells from Waitomo, while rare occurrences of polychaete worms show a preference for the interior of the shell (Fig. 8.11). This suggests that the exterior of the shell was colonised during the lifetime of the oyster and that the borings produced by polychaete worms are a post-mortem feature.

Organisms on *"Ostrea" patagonica* shells from Patagonia are found on all surfaces, including both the left and right internal surfaces of the valves. The presence of taxa on the internal valves of some oysters suggests that these are post-mortem traces. As shown in Figure 8.18, traces are mostly on the external surface of the shells. This means the majority of traces were made during the oyster's lifetime, but some after shallow burial. The presence of traces on the internal surface also suggests that these shells were not rapidly buried.

Data gained from studying each of the generations of *"Ostrea" patagonica* building the Patagonian oyster reef has show that observed differences in diversity and abundance of organisms is only very subtle and there is little clear difference in the development of the reef over time. The small change in the community on the valves of *"Ostrea" patagonica* over time (i.e. through each generation) probably signifies the stability of the established oyster-reef community at the Puerto Pirámide locality (Brito 2009).

All the taxa present on the shells from Wanganui show a preference for the external surface of the shells (Fig. 8.23). This suggests that all the traces were made during the life time of the *Crassostrea* oysters and are not post-mortem features. It has been documented by Bien et al. (1999) that sediment can become trapped within the valves of live as well as dead oysters. The presence of sediment against the internal surfaces of the oyster shells would have likely deterred the settlement of organisms here.

9.5.2c Differences between valve sectors

Chi-squared independence tests were carried out to validate the hypothesis that predefined parts of the oyster valves are colonised preferentially (Fig. 2.6). A summary of the results is provided in Figure 9.9. Oyster samples from Waitomo are mainly occupied by the boring bivalve *Gastrochaenolites* on areas A and G of the right valve exterior and polychaetes on area G. On the left external valves bivalves occupy areas A, D and G. No other taxa show any preference. In both the Patagonia and Wanganui localities, the oysters were most heavily populated on area G of both the left and right valves. On the shells of *"Ostrea" patagonica* from selected reef-growth generations some show preferential settlement of taxa. Sponges and polychaetes in generation 3 prefer sector G on the external right valve, in generation 7 boring bivalves prefer the same area, whereas in generation 10 the bivalves prefer sector G on the left valve. In the internal surface of the right valve polychaetes prefer area CD. In Wanganui, polychaetes had a preference for A, D, G and E on the right external valve while bivalves, gastropods, bryozoans, algae, fungi and other oysters all preferred sector G. On the external left valve, polychaetes, bryozoans, bivalves and algae preferred G. A slight preference towards the internal surface of the right valve was shown by polychaetes.

The preference of different organisms for particular areas of the shell is possibly related to the shell morphology, as the right valve would have been lying on the bottom and the left valve up, so that boring and encrusting organisms would have a greater chance of survival on the left valve (Mauna et al. 2005). The left valve is the most convex and, as mentioned earlier, has a more rugged surface then the right valve so that some organisms prefer this and exhibit rugophilic behaviour, perhaps most ideal in terms of protection (Bien et al. 1999). As exhibited by species from all three locations, area G is often preferentially colonised. As this

part of the shell on the left valve is the highest area of relief it is possible that the larvae are showing geophobic (anti-gravity) behaviour. This could possibly also be the case on the right external surface if the shell was to be overturned. Gravity is one of the most important factors in the orientation of larvae (Baker 1997), especially so in species that contain statocysts (balancing organs) like those of molluscan larvae (Young 1995).

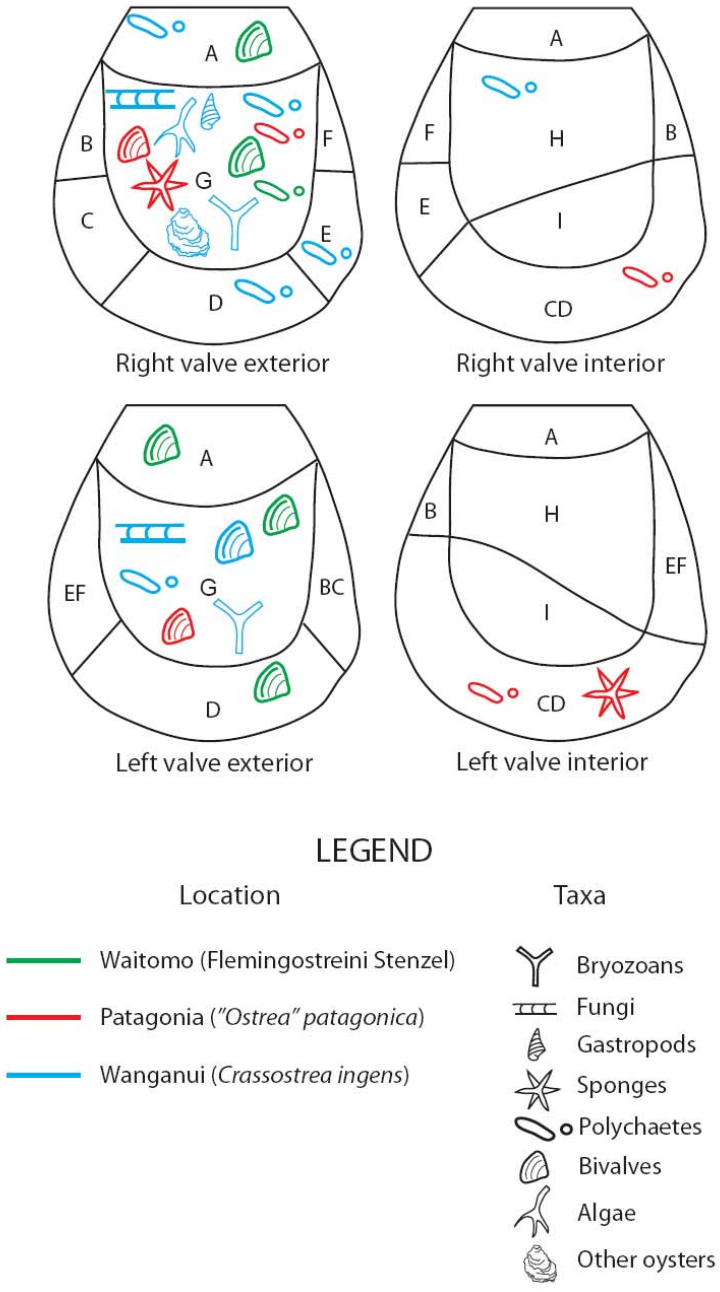

Figure 9.9 Summary of relationships exhibited by communities occupying different valve sectors of the oyster shells found at Waitomo (green), Patagonia (red) and Wanganui (blue) study locations. See Figure 2.6 for definition of shell sectors.

The non-random distribution of lithophagid (boring) larvae may be explained by rheophilic (current-seeking) behaviour. This relates to placement of these larvae in the most ideal place to filter feed and so by placing themselves in the current they have access to the greatest amount of nutrients. Rheotaxic behaviour has been documented in crustacean larvae and in the oysters themselves, but not bivalve larvae in general (Young 1995). Nevertheless, the upturned valve margins or the bulbous left valves of the oysters would have protruded from the sediment, generating a turbulent flow across the oyster shells when they were in life position. Adult lithophagid borers such as *Gastrochaenolites* would have been in an ideal position to filter food suspended in eddies around the projecting oyster shell (Bien et al. 1999).

9.5.3 Paleoecology of bioerosion

From the traces left on the oyster shells by communities of boring and encrusting organisms, important ichnofossil information can be used and applied to interpreting the paleoenvironments of the oysters and their associated communities at each location. The presence of algae (*Clinolithes* isp.) and boring fungi on *"Ostrea" patagonica* from Patagonia and *Crassostrea ingens* from Wanganui acts as a useful tool for paleobathymetric reconstructions (Bromley 1994; Vogel 1995). The presence of these organisms suggests that these oysters lived within the photic zone. Only rarely do these ichnogenera occur in deeper water (Bromley 1994). The photic limit, however, varies in accordance with latitudinal position and is influenced by turbidity, so that ideally other information is needed to make viable interpretations. Around 20-40 m depth for the photic limit is a reasonable estimate for temperate environments (Akpan & Farrow 1985), as is the case in this study. Hessland (1949) also states that endolithic algae are influenced by the energy of the water at the seabed and the highest occurrence of algae occurs in low-energy shallow marine environments.

Ichnogenera associated with gastropods, such as *Radulichnus,* produce grazing traces that can also be associated with the photic zone, as endolithic microbes such as algae and fungi constitute the main food-source for the gastropods. These traces are seen on oyster shells from Patagonia and Wanganui. Traces from gastropods can also occur sparsely and locally in deeper water (Bromley 1994). The bivalve-produced ichnospecies of *Gastrochaenolites* is generally a shallow-

water trace fossil. Where many individuals are present in an assemblage a water depth of only a few metres can be inferred. *Gastrochaenolites torpedo,* in particular, as identified by Brito (2009) on shells of *"Ostrea" patagonica,* suggests a water depth of only 1-2 m, although rare individuals may extend as deep as 10 m. Other boring bivalve species, however, can continue to a depth of a few tens of metres (Bromley 1994).

Sponges such as *Entobia* occur on all the oysters examined in this study but show no environmental preferences except for being particular to a sediment-free setting. Sponges are much less abundant and diverse in muddy environments (Stearley & Ekdale 1989; Bromley 1994). This type of environment is also preferred by polychaetes, also prevalent on every species of oyster analysed in this study. They are affected adversely by mud, and tend to be absent. Polychaetes do not exhibit observable bathymetric trends in an environment dominated by mud, but increases in their abundance do occur with increasing depth of water in a high energy environment (Stearley & Ekdale 1989).

9.6 PALEOENVIRONMENTAL SETTINGS OF OYSTER REEFS

Jones (1950) stated that there are three factors that explain the distribution of marine organisms; temperature, substrate and salinity. Temperature in particular is recognised as being the principal factor determining the extent of marine biogeographic regions. Within each of these areas the substrate largely determines the nature of the community and can be one of the greatest limiting factors in the flourishing of an oyster population (Escapa et al. 2004). Salinity becomes an important factor in brackish environments, where there is freshwater input and mixing. Another important factor is water movement which can determine the dispersal of larvae and also nutrient availability. Without adequate nutrients oysters will not be stimulated to feed and will in turn starve (Frey et al. 1987). Figure 9.10 summarises key factors that influence the distribution of marine organism such as oysters.

9.6.1 Flemingostreni Stenzel (Waitomo)

Previous studies by Barrett (1967) and Nelson (1973) likened the environment of the oysters at Waitomo to that of extant *Crassostrea virginica* living in a reduced salinity estuarine environment. Nelson et al. (1983) reviewed the taxonomy and

paleoenvironments of the giant oysters, using the stable oxygen and carbon isotope composition of their shells to help decipher the latter. Their findings discounted early suggestions and confirmed the environment of Flemingostreini Stenzel to be fully marine. Further isotopic analysis in this study has also confirmed that the oysters lived in a fully marine environment, free of fresh water input and mixing and with little variation in both temperature and salinity over seasons and from year to year.

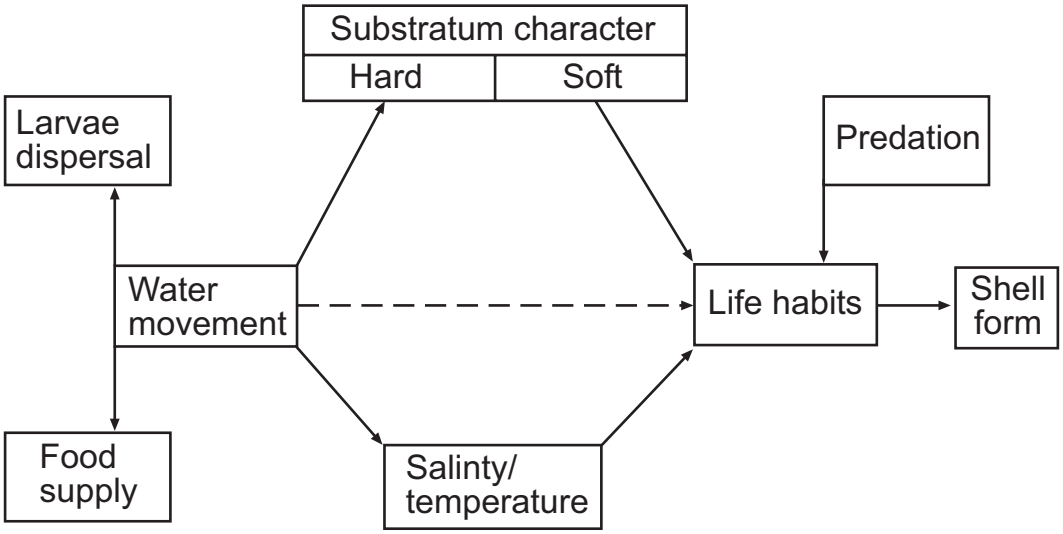

Figure 9.10 Flow diagram of key environmental factors that aid in the development of an oyster reef. All the factors ultimately dictate the shell form of the organisms. Adapted from Stanley (1970).

Following Kidwell (1991b), the presence of dense shellbeds alternating with broken and fragmented (shell lag) occurrences is suggestive of a multi-event shellbed (Fig. 9.1). Multi-event concentrations can be associated with paleohighs, occuring as current swept shells and bioherms formed by selective colonisation. This scale of shell concentrations can also be used to infer periods of high benthic production, which can also coincide with periods of low sediment dissolution (Kidwell 1991b). Disarticulation and fragmentation seen in the shell lags is representative of an increasing level of water energy, possibly associated with small scale shallowing of sea level, however the epifaunal lifestyle of the oysters makes them more prone to disarticulation and transport. Fragmentation of shells occurs when waves and currents abrade the shells against the shell-gravel substrate (Kidwell & Bosence 1991). This interpretation fits in with the sequence stratigraphic interpretation of onlap shellbeds, which are shell lags composed of new and reworked fossils that formed in shallow water due to by-passing and

sediment starvation, and backlap shell beds typified by dense accumulations of shells associated with sediment starvation in (slightly) deeper water than the shell lag (Kidwell 1991b).

The lateral extent and variation in thickness of the oyster beds is reflective of selection for survival by oyster spat. Oyster beds in the field at Waitomo average about 1.5 m in thickness and any further settlement on the top of such build ups may have caused the oysters to be out of their optimum bathymetric conditions. This would have encouraged settlement onto the outer edges of the accumulation, giving the oyster more space and food within the incoming currents (Frey et al. 1987). The discontinuous nature of the oyster beds at Waitomo is due to repeated colonisation events with a bioherm or reef type structure developing in accordance with changing environmental conditions. The thickest accumulations of these oysters in plan-view are orientated in a NW-SE direction (Fig. 3.5). In cross-section the shell lags have a concordant orientation which is due to the redeposition of shells out of suspension; the lack of trend seen in the dense beds (Table 9.1) could be due to the turbulent stirring of the sea floor affecting these relatively free-living reclined shells (Kidwell & Bosence 1991).

Taxa such as sponges have been identified on/within the surface of the shells suggesting the Waitomo oysters lived in an environment with a low sedimentation rate. Boring bivalves which are conspicuous on the shells are characteristic of a marine environment, as these organisms are more prevalent in normal salinity conditions (Bromley 1994). Polychaetes become more prominent in a higher energy environment. As these traces feature mainly on the internal surface of some of the valves it is possible the post-mortem environment of the shells was higher energy (Stearley & Ekdale 1989). The great size and impressive thickness of the Waitomo oyster shells are possibly an adaptation of the oyster to protect itself against bioerosion and predation. The large boulder-type morphology of the shell suggests the oyster was adapted to being reclined in the sediment (Fig 9.3). Sediment would have been characterised by medium sand sized shelly-gravels with local pockets of terrigenous pebbles transported during periods of low sea level, while the micritic nature of the limestone host rock is suggestive of relatively low energy conditions or of carbonate mud trapping amongst the oysters in a higher energy setting.

Foveaux Strait, New Zealand (see Section 6.2.1), provides a modern analogue for the Late Oligocene Flemingostreini Stenzel. The Foveaux Strait substrate is a mixture of sand and gravel sediments. In a fully marine environment where wave energy is high and strong tides dominate, the substrate is composed of gravels. Conversely, where wave energy is less and tidal currents are slower, sands overlie the gravels. High densities of the oyster *Ostrea chilenesis* (Fig. 9.11A) occur on predominantly sand, gravel, and shell (mainly the shells of other oysters and of *Oxyperas elongata* and *Glycymeris modesta*) (K. Michael, *pers. comm.* 2009) and are restricted to 18 to 45 m water depth (Fleming 1952; Cullen 1962). These "reefs" are comprised of various shells, filled by fine sediment, with the oysters living on the outside. These structures are clearly delineated by the tidal flow directions and have very sharp edges between the flat featureless gravels and the oyster "reef" structure (K. Michael, *pers. comm.* 2009). Mean summer sea surface temperatures are around 13-14^{o}C with sea floor values about 2^{o}C lower. The winter sea surface temperature is 11-12^{o}C with the sea floor value again about 2^{o}C lower (Head 1985), conditions probably similar to those in the Oligocene at Waitomo (Nelson et al. 1983).

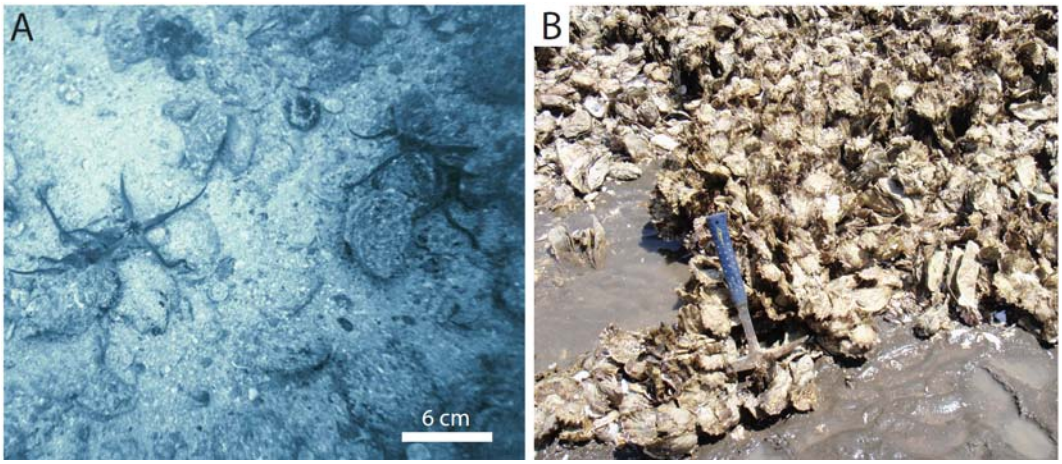

Figure 9.11 Examples of comparable modern oyster species. (A) *Ostrea chilensis* from Foveaux Strait, Southern New Zealand. The oyster occupies shelly and gravelly sediment in a fully marine, tide swept environment. Image courtesy of Keith Micheal at National Institute of Atmosphere and Water (2008). (B) *Crassostrea gigas* formining an *in situ* mound (bioherm) in the intertidal zone at San Blas, Patagonia.

9.6.2 *"Ostrea" patagonica* (Patagonia)

The Late Miocene Puerto Madryn Formation in Patagonia was deposited in a shallow marine environment evolving into an estuarine and finally continental

environment (Scasso & Castro 1999). As bulk carbon and oxygen stable isotopes suggest, the *"Ostrea" patagonica* reef evolved in a marginal marine environment with a large variation in temperature and salinity across the seasons and from year to year, which is consistent with a setting receiving extensive freshwater input and mixing. The heavy oysters were able to successfully colonise the muddy-bottomed environment using a recliner strategy, most suited to the heavyweight nature of the shell (Fig. 9.3, 9.4) (Seilacher et al. 1985). This is further confirmed by the adaptation of many oyster species to hyposaline environments (Wells 1961). Bioturbation structures in Facies Association 2 within the Puerto Madryn Formation (Fig. 4.5) consists of abundant traces from the *Skolithos* ichnofacies representative of a beach sand environment. The largely bimodal orientation of the shellbed (Table 9.1) as identified by Brito (2009) reflects a rheotaxic life position in oscillating currents due to a combination of biotic factors, such as nutrient and space availability and selective survival of spat (Frey et al. 1987). The lack of trend seen in cross-section combined with articulated specimens can be interpreted to reflect the oysters being in life position (Kidwell & Bosence 1991). The *in situ* and well preserved shellbed is characteristic of a downlap shellbed in sequence stratigraphic terms and forms within a HST (Kidwell 1991a, b). It is also characteristic of a condensed deposit shell bed which has formed from many colonisation events within the biohermal buildup. Mass mortality of the oysters resulted from unfavourable conditions such as increased sedimentation, change in nutrients or rapid burial (Kidwell 1991b).

Biota associated with the Patagonian shellbed are characterised by sponges, polychaetes, boring bivalves, algae and fungi. The presence of sponges suggests that the conditions surrounding the oyster reef consisted of low sedimentation rates, as sponges are less diverse in muddy environments. Algae and fungi traces seen on the shells suggest the oyster reef occupied the photic zone, and algae also prefer a low energy environment (Hessland 1949). Various traces created by boring bivalves have been identified by Brito (2009) as due to *Gastrochaenolites torpedo.* The presence of this trace can be used to infer only 1-2 m water depth for the oyster reef (Bromley 1994).

The environment of these oysters is comparable to that at the modern San Blas site in Patagonia (see Section 6.2.2). The extant *Crassotrea gigas* (Fig. 9.11B)

oyster occupies a low energy estuarine environment with reduced salinity, and the shells are inhabited by a similar community of boring and encrusting organisms. The accumulations are typified by lens-shaped bioherms forming on muddy bottoms (Escapa et al. 2004). The modern oyster morphotype differs from the fossil *"Ostrea" patagonica* species, those seen at San Blas being shell supported on patches of suitable substrate. Modern sea surface temperatures are 8°C in the winter and 20°C in the summer for the Península Valdés area, a similar range that is suggested for the fossil examples (S. Casadío, *pers. comm.* 2010).

9.6.3 *Crassostrea ingens* (Wanganui)

The sequence stratigraphic interpretation of McIntyre (2002) suggests that the Wilkies Shellbed is comprised of an onlap and backlap shellbed within a transgressive sequence. The lower part of the Wilkies Shellbed is an onlap shellbed, deposited in a high energy shallow marine setting with winnowing and by-passing of terrigenous material responsible for the accumulation of carbonate material in the form of a shell lag. The backlap portion of the shellbed was formed in deeper water and the migration of the shellbed shoreward would have maintained depths in which the *Crassostrea* could live *in situ* with low turbidity and sediment accumulation. The presence of a lower shell lag and an overlying biostrome is suggestive of a multi-event shellbed (Fig. 9.1). This scale of shell concentrations can also be used to infer periods of high benthic production, which coincides with periods of low sediment dissolution. Siliciclastic sediment starved, shallow-water areas are common sites for the accumulation of thick shellbed deposits. Mass mortality of the oysters resulted from an increase in water depth and sedimentation leading to the deposition of the overlying Cable Siltstone (Fig. 5.15) (Kidwell 1991b). The large thickness and lateral extent of the Wilkies Shellbed suggests the *Crassostrea* oysters had a small bathymetric optimum range. As the shellbed reached its optimum range vertically, conditions would have been more suitable on the outer reaches of the shell accumulation, so promoting the vast extent of the shellbed in the Wanganui Basin. The shell bed is characterised by articulated *Crassostrea* shells. In cross-section the shells collectively show a concordant orientation, which suggests life position (Kidwell & Bosence 1991).

In agreement with McIntyre (2002), the *Crassostrea ingens* dominated Wilkies Shellbed in Wanganui mainly formed in a fully marine environment under conditions of normal salinity. As discussed earlier, however, bulk stable isotopes indicate occasionally some reduced salinities from marine to marginal marine conditions. In the oyster sample analysed across the ligament area, there is a large variation in temperature and salinity across the seasons and from year to year, which is consistent with a marginal marine environment receiving extensive freshwater input and mixing. McIntyre (2002) suggested that the lower part of the shellbed possibly had more freshwater influence as shown by the fauna in the shellbed, whereas the upper part of the shellbed was more fully marine.

Communities associated with the Wilkies Shellbed, as identified by bioerosion structures on the surface of the *Crassostrea* valves, consist of fungi, algae, sponges, polychaetes, bryozoans, boring bivalves, gastropods, pectinids and other oysters. The presence of fungi and algae indicates the shellbed occupied the photic zone, while algae also support a preference for lower energy conditions (Hessland 1949). Gastropods also identify the photic zone as they feed on the likes of algae and fungi. Sponges have an environmental preference for sediment-free conditions. The presence of the above trace taxa suggests the *Crassostrea* reef occupied a low energy environment within the photic zone, in depths less than 40 m.

CHAPTER TEN
Conclusions

Giant oyster fossil shellbeds and/or reefs occur in Paleogene and Neogene sequences in the North Island of New Zealand and in Patagonia, southern Argentina. The aim of this study was to understand the formation of the oyster beds at each of the study locations and to interpret the paleoenvironments in which they formed. In this chapter the outcome of each study objective is noted and, in particular, a comprehensive synthesis is provided as Table 10.1 (page 251) to compare features of the shell accumulations from each study location.

The giant Flemingostreini Stenzel oysters at Waitomo, North Island (Fig. 10.1A), are characteristic of multi-event shellbeds and are inferred to represent backlap and onlap shellbeds within a transgressive systems tract. These Oligocene oyster accumulations are composed of tabular beds (0.5 to 2 m thick), and thin (up to 10-20 cm) lenses but stretched (single layer of shells). The succession of oyster beds and thin layers reflects several episodes of biohermal colonisation and transgressive shell lags, respectively. Similarly, the *Crassostrea* dominated Pliocene Wilkies Shellbed in Wanganui, North Island (Fig. 10.1C), is a multi-event shellbed comprised of an onlap and backlap portion. The lower onlap bed is interpreted as a transgressive shell lag and the overlying backlap shellbed forms a *Crassotrea* biostrome characterised by several colonisation events of oysters. The Late Miocene *"Ostrea" patagonica* reef at Puerto Pirámide, Patagonia (Fig. 10.1B), is interpreted as a downlap shellbed within a highstand systems tract. It is also a multi-event shellbed that formed an oyster-rich facies from repeated levels of colonisation on the building bioherm.

Flemingostreini Stenzel oysters (Fig. 10.1A) have high shell $\delta^{18}O$ (-2.1 to 1.4‰) and $\delta^{13}C$ (0.4 and 2.5‰) values, and minimal variation in these values across the shell ligamental area, confirming that these oysters lived in a fully marine environment not influenced by any freshwater input. Patagonian oyster (Fig. 10.1B) shell $\delta^{18}O$ (-4.4 to -3.2‰) and $\delta^{13}C$ (-2.0 to -3.2‰) values are low and show large seasonal isotopic ranges, with a large amount of variability,

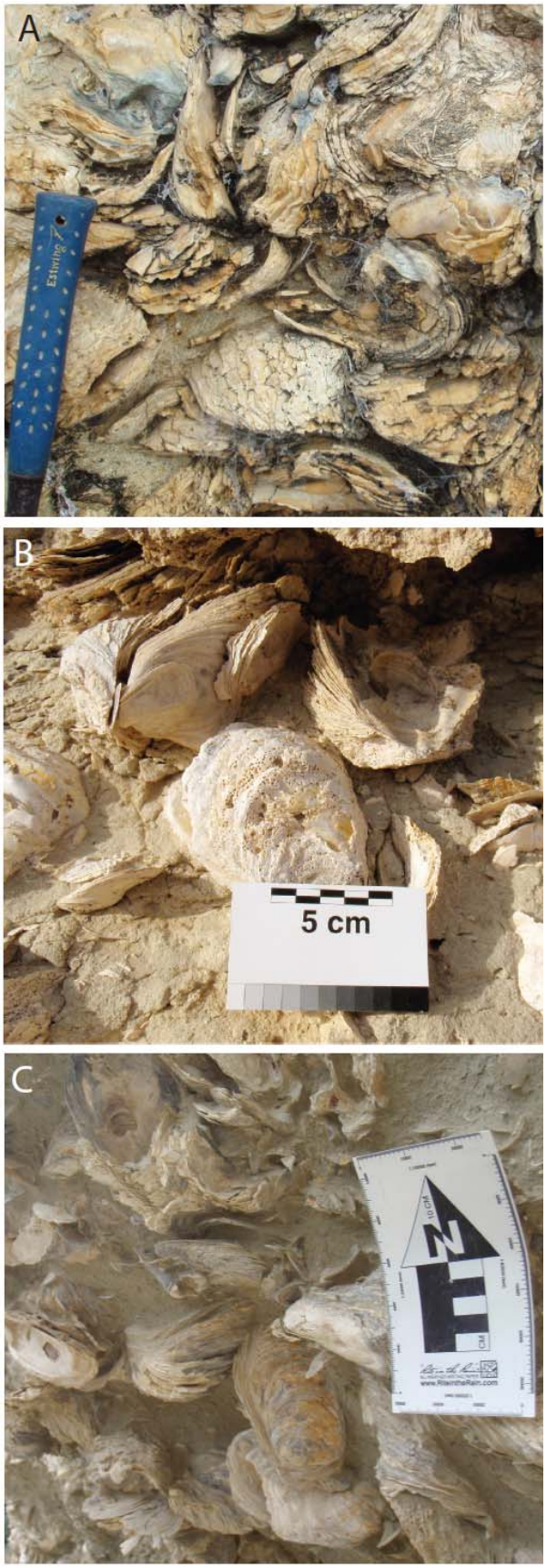

Figure 10.1 The three species of giant fossil oysters in this study. (A) Oligocene Flemingostreini Stenzel held in biomicritic Orahiri limestone from Waitomo, New Zealand. (B) *"Ostrea" patagonica* from the Late Miocene Puerto Madryn Formation, Puerto Pirámide, Patagonia. (C) Extinct giant oyster *Crassostrea ingens* from the Pliocene Wilkies Shellbed, Wanganui, New Zealand.

collectively supporting a marginal marine setting receiving extensive freshwater input and mixing. *Crassostrea ingens* at the Wanganui (Fig. 10.1C) localities has widelyspread shell $\delta^{18}O$ (-3.0 to 3.0‰) and $\delta^{13}C$ (-2.6 to 1.8‰) isotopic values which are consistent with the inferred marginal marine conditions for the lower Wilkies Shellbed (onlap) and fully marine ones for the upper portion of the Wilkies Shellbed (backlap). The oyster shells from all localities fall within element concentration (Mg, Sr, Mn & Fe) ranges of fossil and extant oysters from other studies. However, once 'cutoffs' are applied, samples from Waitomo and Wanganui show enrichment in iron and Patagonian oysters are depleted in strontium and manganese. This is consistent with samples that have undergone at least some small degree of diagenetic alternation. The trace element data coupled with CL petrographic analysis suggest that further geochemical analyses should be carried out with caution.

All oysters in this study are composed of low-Mg calcite. Flemingostreini Stenzel oysters from Waitomo (Fig. 10.1A) have a homogeneous to chalky and porous shell microstructure and the host sediments are comprised of low-Mg calcite biomicritic limestones. Borings in the oysters are infilled with fine grained host sediment, and calcite spar, commonly forming internal geopetal fabrics. Similarly, *Crassostrea ingens* from Wanganui (Fig. 10.1C) has a chalky shell microstructure and is held within a very poorly sorted fine muddy sand. The microstructure of *"Ostrea" patagonica* shells from Puerto Pirámide (Patagonia) (Fig. 10.1B) comprises calcite crystal laths and the shells are contained within a poorly sorted fine sand. The authigenic mineral gypsum is dominant at this location in the uppermost portion of the oyster reef.

All species of fossil oysters in this study show moderate to high levels of biological modification (bioerosion). Their large (up to 30 cm), thick (up to 7 cm) and heavy (up to 3 kg) shells provided suitably hard substrates for a very diverse community of encrusting and boring organisms, including the likes of *Gastrochaenolites* (bivalve), *Maeandropolydora* (polychaete), *Clionolithes* (boring algae), *Entobia* (sponge), *Leptichnus* (bryozoan) and *Radulichnus* (gastropod). These communities are comparable to those seen on extant oyster reefs. Oysters modify the environment by their own physical structure and are thus termed autogenic ecosystem engineers. Non-random distribution of

euendoliths and epiliths on oyster valves may be accounted for by different survival adaptations of larvae. Preference for the external surface of shells suggests traces were created during the life time of the oysters, while internal traces are more likely to be post-mortem features. Shell morphotypes (namely mud or shell supported recliners) and exterior architectures are inferred to have prompted active rugophilic (groove-seeking), geophobic (anti-gravity) and rheophilic (current-seeking) behaviour of larvae. These behaviours enhanced the survival rate of larvae settling on the oyster valves.

The environment of Oligocene Flemingstreini Stenzel (Fig. 10.1A) was probably similar to modern *Ostrea chilensis* from Foveaux Strait (Fig. 9.12A), southern New Zealand. Isotopic and other data suggest the reclined oysters lived in normal salinity conditions, in a shallow shelf environment in water depths of around 18-40 m and bottom temperatures of about 13^{o}C. The recliner type oysters occupied coarse, shelly and gravelly sediment, in tide swept substrates forming *in situ* biostromes of haphazardly packed oyster shells on the seafloor (Fig. 10.2).

The environment of "*Ostrea" patagonica* in the Late Miocene Puerto Madryn Formation, Península Valdés, Patagonia, is comparable with modern *Crassostrea gigas* reefs at San Blas, Patagonia (Fig. 9.12B). The *"Ostrea" patagonica* reef occupied the low energy intertidal zone in < 10 m water depth (Fig. 10.2). The oysters were not cemented firmly to the substrate, but reclined on muddy sediment and formed *in situ* bioherms of loosely packed oysters, with the living animals becoming concentrated over time to the outside of the accumulation. Summer and winter temperatures of about 20^{o}C and 8^{o}C, respectively, as recorded today from the Península Valdés region, are suggested also for the environment of *"Ostrea" patagonica.*

The Pliocene Wilkies Shellbed in the Wanganui Basin, New Zealand, evolved in two parts, the lower (onlap) with a more estuarine influence, and the upper (backlap) shellbed in a nearshore (< 40 m), marine setting under conditions of normal salinity. During transgression the backlap shellbed migrated shoreward, maintaining an ideal bathymetry in which the oysters could live *in situ* in the fine muddy sand matrix (Fig. 10.2). *Crassostrea* flourished in the low sedimentation

and turbidity levels forming a crudely-bedded biostrome as a result of successive colonisation events.

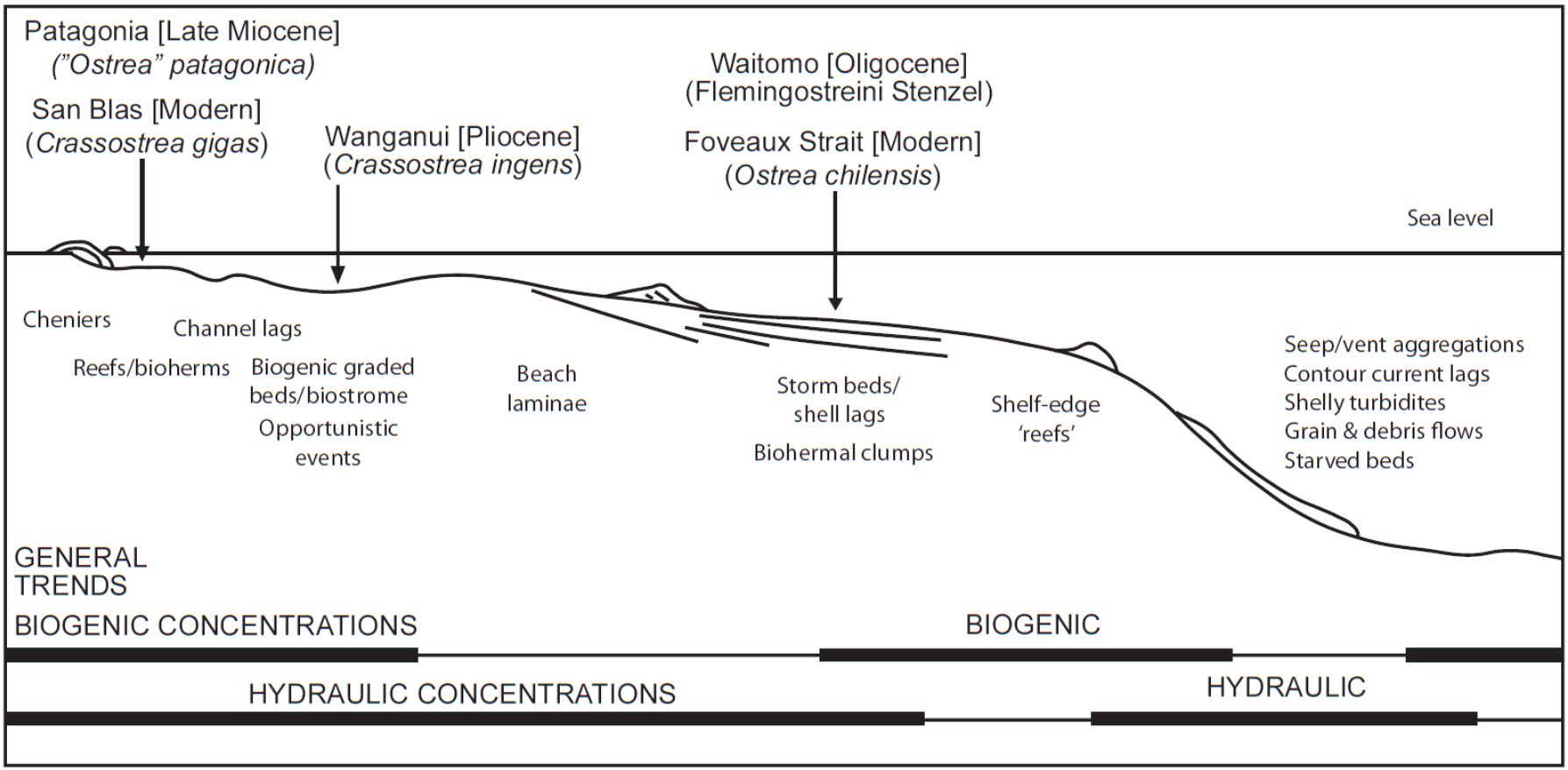

Figure 10.2 Idealised onshore-offshore trends in the distribution of event and multi-event shell concentrations. Biogenic concentrations can be found in virtually all environments, as can hydraulic concentrations of shells, but their relative proportions vary. The Patagonian oyster occurrence occupies the shallowest estuarine environment and consists of biogenic 'reefs' or biohermal build-ups. The Wanganui oyster accumulation occupies nearshore shallow marine settings with localised freshwater input and is characterised by biogenic graded beds or a biostrome that has formed in an opportunistic event. The Waitomo oysters occupy a fully marine environment and consist of biogenic accumulations and thin storm beds or shell lags. (Adapted from Kidwell 1991b).

Table 10.1 Synopsis of all associated features of giant fossil oysters from Waitomo (New Zealand), Puerto Pirámide (Patagonia) and Wanganui (New Zealand).

	Study location		
	Waitomo	**Patagonia**	**Wanganui**
STRATIGRAPHIC FEATURES			
Age	Late Oligocene	Late Miocene	Pliocene
Host formation	Orahiri Limestone	Puerto Madryn Formation	Whauteihi Formation
Shellbed name	-	-	Wilkies Shellbed
Typical thickness (max.) (m)	0.5-2 (9)	1.5	8 (15)
Lateral extent	10s km	> 20 m	10s km
Physical contacts	Abruptly gradational	Sharp/erosional	Conformable/unconformable
PALEONTOLOGICAL FEATURES			
Species/family	Flemingostreini Stenzel	*"Ostrea" patagonica*	*Crassostrea ingens*
Age spectrum	Adults	Adults	Adults
Original mineralogy	Low-Mg calcite	Low-Mg calcite	Low-Mg calcite
Preserved mineralogy	Low-Mg calcite	Low-Mg calcite	Low-Mg calcite
CONDENSED DEPOSIT FEATURES			
Sequence stratigraphic position	TST	HST	TST
Type of shellbed	Multi-event	Condensed	Multi-event
Condensed facies type	Backlap / Onlap	Downlap	Backlap / Onlap
Geometry	Tabular beds / Sparse lenses (transgressive lag)	Lens/bioherm	Sheets/biostrome / Transgressive lag
Sedimentary dynamics	Starvation / By-passing ± starvation	Starvation	Starvation / By-passing ± starvation
Bathymetric setting	Shallow to deep water / Shallow water	Shallow to deep water	Shallow to deep water / Shallow water
Bathymetric history	Deepens upward / Deepens upward	Shallows upward	Deepens upward / Deepens upward
Duration	Increases basinwards / Similar over extent	Increases basinwards	Increases basinwards / Similar over extent
Preservation potential	Good / Good	Excellent	Good / Good
OYSTER TAPHONOMY			
Articulation	Articulated and disarticulated / Disarticulated	Articulated	Articulated / Disarticulated
Size sorting	Very good / Very poor	Very good	Very good / Very poor
Modal size (mm)	150 / -	200	120 / -
Fragmentation	- / High	-	- / High
Abrasion	Low / Moderate	Low	Low / Moderate
Rounding	Low / Low	Low	Low / Low
Biological modification (bioerosion, encrustation)	Extensive, pre- and rare post-mortem / Extensive, pre- and rare post-mortem	Extensive, pre- and rare post-mortem	Extensive pre-mortem / Extensive pre-mortem
Orientation of beds			
Plan-view	Bimodal	Bimodal	Bimodal
Cross-sectional	No strong trend / Concordant	No strong trend	No strong trend / Concordant
Shell abudance (%)	30-80 / 5	25	45 / 10
Shell packing	Loose-dense / Dispersed	Loose	Dense / Dispersed
OYSTER GEOCHEMISTRY			
Shell $\delta^{18}O$ isotope values (‰)			
Average	-0.59 ± 0.13	2.84 ± 0.76	-1.48 ± 0.34
Min.	-0.80	-2.40	-2.13
Max.	-0.40	1.00	-0.90
Range	0.40	1.40	1.23
Shell $\delta^{13}C$ isotope values (‰)			
Average	-0.71 ± 0.19	-1.15 ± 0.76	2.13 ± 0.53
Min.	0.39	-2.34	-3.38
Max.	0.99	1.10	-1.45
Range	0.60	1.24	1.93
Shell trace element concentration (ppm)			
Sr	680	290	457
Fe	2331	172	1570
Mg	23	742	81
Mn	54	283	74
HOST SEDIMENT/ROCK FEATURES			
Host sediment/rock	Limestone	Sand	Muddy sand
Carbonate classification	Biomicrite	-	-
Carbonate maturity	Packed biomicrite	-	-
Mixed sediment classification	-	Sand	Sand
Wentworth size class	-	Fine sand	Fine sand
Mixed sediment maturity	-	Submature-mature	Submature-mature
Bioclasts			
Average (%)	78	0	2-25
Composition	Bryozoans, bivalves, echinoderms, benthic	-	-
Sorting	Poorly sorted	-	-
Abrasion	Moderately abraded	-	-
Siliciclastics			
Average (%)	22	100	75-98
Composition	Quartz, feldspar, pyrite grains & infills, glauconite grains & infills	Feldspar, gypsum, opaque minerals, quartz & rock fragments	Quartz, feldspar, muscovite, opaque minerals, glauconite, clay minerals
Sorting	Poorly sorted	Poorly sorted	Very poorly sorted
Shape	Subangular-subrounded	Subrounded-rounded	Subrounded
Av. Sand, silt, clay (%)	-	83, 16, 1	78, 20, 2
Av. $CaCO_3$% (%)	70	3	20

SHELL INTERNAL FEATURES				
Microstructure	Homogeneous, chalky and porous	Crystal laths	Chalky
Recrystallisation	Some	Nil	Some
Mineral alteration	Nil	Some iron-bearing	Nil
Borings	Many	Few	Few
Boundaries	Sharp	Sharp	Sharp and irregular
Min. size (mm)	1	2	0.6
Max. size (mm)	8 (cm)	4	6
Infill	Bioclasts and siliciclastics	Fine grained siliciclastic material	Fine grained siliciclastic material
Geopetal fabrics	Many	Absent	Absent
PALEOECOLOGICAL FEATURES			
Shell morphology	Recliner/mud-supported	Recliner/mud-supported	Recliner/shell-supported
Environment	Fully marine	Marginal marine	Fully marine | Marginal marine
Associated taxa	Boring bivalves, sponges, polychaetes	Polychaetes, boring bivalves, sponges, fungi, algae, serpulids, other oysters, gastropods	Fungi, algae, sponges, polychaetes, boring bivalves, boring bryozoans, encrusting bryozoans, gastropods, pectinids, other oysters, barnacles
Settlement preference of taxa			
Left or right valve	Left valve: sponges & bivalves. Right valve: polychaetes.	Left valve: fungi.	Left valve: algae, bryozoans, pectinids, barnacles & other oysters. Right valve: polychaetes, bivalves & sponges.
Internal vs external	Exterior: bivales & sponges. Internal: polychaetes.	Exterior: polychaetes, sponges, bivalves & fungi.	All taxa prefer external surface.
Valve sectors	Right external: polychaetes G. Left external: bivalves A, D & G.	Right external: polychaetes, sponges & bivalves G. Left external: bivalves G. Right internal: polychaetes CD. Left internal: polychaetes & sponges CD.	Right exterior: polychaetes A, D, E & G; bivalves, algae, bryozoans, gastropods, fungi & other oysters G. Right internal: polychaetes H. Left external: polychaetes, bivalves & algae G.

REFERENCES

Abbot, S. T. 1997: Mid-cycle condensed shellbeds from mid-Pleistocene cyclothems, New Zealand: Implications for sequence architecture. *Sedimentology 44*: 805-824.

Adams, A. E. & MacKenzie, W. S. 1998: A colour atlas of carbonate sediments and rocks under the microscope, Manson Publishing, London.

Akpan, E. B. & Farrow, G. E. 1984: Shell-boring algae on the Scottish continental sheld: identification, distribution, bathymetric zonation. *Transactions of the Royal Society of Edinburgh, Earth Sciences 75*: 1-12.

Akpan, E. B. & Farrow, G. E. 1985: Shell bioerosion in high latitude low energy environments: Firths of Clyde and Lorne. *Transactions of the Royal Society of Edinburgh, Earth Sciences 75*: 1-12.

Anderson, T. F.; Popp, B. N.; Williams, A. C.; Ho, L.-Z. & Hudson, J. D. 1994: The stable isotope records of fossils from the Peterborough Member, Oxford Clay Formation (Jurassic) UK: Paleoenvironmental implications. *Journal of the Geological Society of London 151*: 125-138.

Anderton, P. W. 1981: Structure and evolution of South Wanganui Basin, New Zealand. *New Zealand Journal of Geology and Geophysics 24*: 39-63.

Andrus, C. F. T. & Crowe D. G. 2000: Geochemical analysis of *Crassostrea virginica* as a method to determine season of capture. *Journal of Archaeological Science 27:* 33-42

Bahr, L. M. & Lanier, W. P. 1981: The ecology of intertidal oyster reefs of the South Atlantic Coast: A community profile, FWS/OBS-81/15, United States Fish and Wildlife Services, Office of Biological Services, Washington, D.C.

Baker, P. 1997: Settlement and site selection by oyster larvae, *Crassostrea virginica:* Evidence for geotaxis. *Journal of Shellfish Research 16*: 125-128

Barbin, V. 2000: Cathodoluminescence of carbonate shells: biochemical vs diagenetic process, *In:* Pagel, M.; Barbin, V.; Blanc. P. & Ohnenstetter, D. (ed.), *Cathodoluminescence in Geosciences*, Springer, Berlin.

Barbin, V.; Ramseyer, K.; Debenay, J. P.; Schein, E.; Roux, M. & Decrouez, D. 1991: Cathodoluminescence of recent biogenic carbonates: An environmental and ontogenetic fingerprint. *Geology Magazine 128*: 19-26.

Barbin, V. & Gaspard, D. 1995: Cathodoluminescence of recent articulate brachiopods shells: Implications for growth stages and diagenetic evaluation. *Geobios 18*: 39-45.

Barret, P. J. 1962: The Te Kuiti Group in the Waitomo-Te Anga Area, Unpublished thesis, University of Auckland.

Barrett, P. J. 1967: Te Kuiti Group in the Waitomo-Te Anga area. *New Zealand Journal of Geology and Geophysics 10*: 1009-26.

Bertels, A. & Zabert, L. L. 1980: Microfauna del Grupo Santa Maria (Terciario superior) en las provincias de Catamarca y Tucumán, Republica Argentina. 2º Congreso Argentino de Paleontología y Bioestratigrafía y 1º Congreso Latinoamericano de Paleontología. (Buenos Aires, 1978). *Actas 3*: 67-73.

Beu, A. G. & Maxwell, P. A. 1990: Cenozoic Mollusca of New Zealand, New Zealand Geological Survey, Lower Hutt.

Bien, W.; Wendt, J. & Alexander, R. R. 1999: Site selection and behaviour in sponge and bivalve borers in shells of the Cretaceous oysters *Exogyra cancellata* and *Pycnodonte mutabilis* from Delaware, U.S.A. *Historical biology 13*: 299-315.

Blake, J. A. & Evans, J. W. 1973: *Polydora* and related genera as borers in mollusk shells and other calcareous substrates (Polychaeta: Spionidea). *Veliger 15*: 235-246.

Bodenbender, G. 1912: Constitución geológica de la parte meridional de La Rioja y regiones limítrofes. *Boletín de la Academia Nacional de Ciencias 19*: 1-220.

Boggs, S. J. 2001: Principles of sedimentology and stratigraphy, Prentice Hall, New Jersey.

Bordeaux, Y. L. & Brett, C. E. 1990: Substrate specific associations of epibionts on Middle Devonian brachiopods: Implications for paleoecology. *Historical biology 4*: 203-220.

Bosence, D. W. J. & Wilson, R. C. L. 2003: Carbonate depositional systems, *In:* Coe. A. L. (ed.), *The Sedimentary Record of Sea-Level Change*, Cambridge University Press, Cambridge.

Botijer, D. J. 1982: Paleoecology of epizoans and borings on some Upper Cretaceous chalk oysters from the Gulf Coast. *Lethaia 15*: 75-84.

Brand, U. & Veizer, J. 1980: Chemical diagenesis of a multicomponent carbonate system: 1 trace elements. *Journal of sedimentary Petrology 50*: 1219-1236.

Brett, C. E. 1995: Sequence stratigraphy, biostratigraphy, and taphonomy in shallow marine environments. *Palaios 10*: 597-616.

Brett, C. E. & Seilacher, A. 1991: Fossil Lagerstätten: A taphonomic consequence of event sedimentation, *In:* Einsele, G.; Ricken, W. & Seilacher, A. (ed.), *Cycles and Events in Stratigraphy*, Springer-Verlag, Berlin.

Brito, C. 2009: Evolución de las comunidades de organismos incrustantes y perforantes asociadas a arrecifes de ostras gigantes del Paleógeno y Neógeno de Patagonia, Argentina, Unpublished thesis, Univesidad Nacional de La Pampa.

Bromley, R. G. 1994: The paleocology of bioerosion, *In:* Donovan, S. K. (ed.), *The Palaeobiology of Trace Fossils*, The John Hopkins University Press, Maryland, Pp. 135-155.

Bruno, J. F.; Stachowicz, J. J. & Bertness, M. D. 2003: Inclusion of facilitation into ecological theory. *Opinion 18*: 119-125.

Carriker, M. R. & Palmer, R. E. 1979: A new mineralized layer in the hinge of the oyster. *Science 206*: 691-693.

Carriker, M. R.; Palmer, R. E.; Sick, L. V. & Johnson, C. C. 1980: Interaction of mineral elements in sea water and shell of oysters [*Crasssotrea virginica* (Gmelin)] cultured in controlled and natural systems. *Journal of Experimental Marine Biology and Ecology 46*: 279-296.

Carriker, M. R.; Swan, C. P.; Prezant, R. S. & Counts, C. L. 1991: Chemical elements in the aragonitic and calcitic microstructural groups of shell of the oyster *Crassostrea virginica*: A proton probe study. *Marine Biology 109*: 287-297.

Carriker, M. R.; Swann, C. P.; Prezant, R. S. & Counts, C. L. 1996: Ontogenic trends of elements (Na to Sr) in prismatic shell of living *Crassostrea virginica* (Gmelin) grown in three ecologically dissimilar habitats for 28 weeks: A proton probe study. *Journal of Experimental Marine Biology and Ecology 201*: 87-135.

Carroll, M. & Romanek, C. S. 2008: Shell layer variation in trace element concentration for the fresh water bivalve *Elliptio complanata*. *Geo-Marine Letters 28*: 369-381.

Carter, J. G. 1990: Shell microstructal data for the bivalvia, *In:* Carter, J.G (ed.), *Skeletal Biomineralization: Patterns, Processes and Evolutionary Trends*, Van Nostrand Reinhold, New York, Pp. 297-391.

Carter, R. M. & Naish, T. R. 1998: A review of Wanganui Basin, New Zealand: Global reference section for shallow marine, Plio-Pleistocene (2.5-0 Ma) cyclostratigraphy. *Sedimentary Geology 122*: 37-52.

Casadío, S.; Feldmann, R. M.; Parras, A. & Schweitzer, C. E. 2005: Miocene fossil Decapoda (Crustacea: Brachyura) from Patagonia, Argentina, and their paleoecological setting. *Annals of Carnegie Museum 74*: 151-188.

Chinzei, K. 1995: Adaptive significance of the lightweight shell structure in soft bottom oysters. *Neues Jahrbucg Geology and Palätology, Abhandlungen 195*: 217-227.

Christie, A. B. 1973: Wilkies Shellbed, palaeontology, sedimentology, and paleoenvironmental interpretation, Unpublished thesis, Victoria University.

Clark, G. R. I. 1968: Mollusk shell: daily growth lines. *Science 161*: 800-802.

Coe, A. L. & Church, K. D. 2003: Part 2 Sequence Stratigraphy and Sea-Level Change, *In:* Coe, A. L. (ed.), *The Sedimentary Record of Sea-Level Change*, The Press Syndicate of the University of Cambridge, Cambridge.

Collier, A.; Ray, S. M.; Magnitzky, A. W. & Bell, J. O. 1953: Effect of dissolved organic substances on oysters. *United States Fish Wildlife Survey Fish Bulletin 84*: 167-185.

Connolly, J. R. 2003: Introduction to quantitative x-ray diffraction methods. *Earth and Planetary Sciences 400*: 1-14.

Coplen, T. B. 1988: Normalization of oxygen and hydrogen isotope data. *Chemical Geology 72*: 293-297.

Coplen, T. B. 1994: Reporting of stable hydrogen, carbon and oxygen isotopic abundances. *Pure Applied Chemistry 66*: 273-276.

Cranfield, J. H.; Micheal, K. P. & Doonan, I. J. 1999: Changes in the distribution of epifaunal reefs and oysters during 130 years of dredging for oysters in Foveaux Strait, southern New Zealand. *Aquatic Conservation: Marine and Freshwater Ecosystems 9*: 461-483.

Cranfield, J. H.; Manighetti, B.; Micheal, K. P. & Hill, A. 2003: Effects of oyster dredging on the distribution of bryozoan biogenic reefs and associated sediments in Foveaux Strait, southern New Zealand. *Continental Shelf Research 23*: 1337-1357.

Cranfield, H. J.; Rowden, A. A.; Smith, D. G.; Gordon, D. P. & Micheal, K. P. 2004: Macrofaunal assemblages of benthic habitat of different complexity and the proposition of a model of biogenic reef habitat generation in Foveaux Strait, New Zealand. *Journal of Sea Research 52*: 109-125.

Cullen, D. J. 1962: The influence of bottom sediments upon the distribution of oysters in Foveaux Strait, New Zealand. *New Zealand Journal of Geology and Geophysics 5*: 271-275.

d'Orbigny, A. 1842: Mollusques, *In:* C. P. Bertrand (ed.), *La Relation du Voyage dans l'Amérique Méridionale pendant les annés 1826 à 1833*, Atlas, Paris.

Davenport, C. B. 1983: Growth lines in fossil pectins as indicators of past climates. *Journal of Paleontology 12*: 514-515.

de Villiers, S.; Nelson, B. & Chivas, A. 1995: Biological controls on coral Sr/Ca and $\delta^{18}O$ reconstructions of sea surface temperatures. *Science 269*: 1247-1249.

del Río, C. J. 1988: Bioestratrigrafía y cronoestratigrafía de la Formación Puerto Madryn (Mioceno Medio). Provincia del Chubut – Argentina. *Anales del la Academia Nacional de Ciencias Exactas, Físicas y Naturales 40*: 231-254.

del Río, C. J. 1990: Composición, origen y significado paleoclimático de la malacofauna Entrerriense (Mioceno Medio) de la Argentina. *Anales de la Academia Nacional de Ciencias Exactas, Físicas y Naturales 42*: 207-226.

del Río, C. J. 1991: Revisión sistemática de los bivalvos de la Formación Paraná (provincia de Entre Ríos, Mioceno Medio) de la Argentina. *Anales de la Academia Nacional de Ciencias Exactas Físicas y Naturales, Monografía 7*: 93.

del Río, C. J. 2000: Malacofauna de las Formaciones Paraná y Puerto Madryn (Mioceno marino, Argentina): su origen, composicíon y signifcado bioestrátigrafico, *In:* Aceñolaza, F. G. & Herbst, R. (ed.), *El Neógeno de Argetina*, Serie Correlación Geológical, 14, INSUGEO.

del Río, C. J.; Martinez, S. A. & Scasso, R. A. 2001: Nature and origin of spectacular marine Miocene shell beds of northeastern Patagonia (Argentina): Paleoecological and bathymetric significance. *Palaios 16*: 3-25.

Denison, R. E.; Miller, N. R.; Scott, R. W. & Reaser, D. F. 2003: Strontium isotope stratigraphy of the Comanchean series in north Texas and southern Oklahoma. *Geological Society of America Bulletin 115*: 669-682.

Dittmann, S. 1990: Mussel beds - amensalism or amelioration for intertidal fauna. *Helogolander Meeresuntersuchungen 44*: 335-352.

Dunham, R. L. 1962: Classification of carbonate rocks according to their depositional texture, *In:* Ham, W. E. (ed.), *Classification of carbonate rocks*, American Association of Petroleum Geologists Memoir 1, Tulsa, OK, 108-121.

Edbrooke, S. W. 2005: Geology of the Waikato Area, Institute of Geological and Nuclear Sciences, Lower Hutt.

Ekdale, A. A.; Bromley, R. G. & Pemberton, S. G. 1984: Ichnology: Trace fossils in sedimentology and stratigraphy, Society of Economic Paleontologists and Mineralogists, Oklahoma.

Elderfield, H. & Ganssen, G. 2000: Past temperatures and $\delta^{18}O$ of surface ocean waters inferred from foraminifera Mg/Ca ratios. *Nature 405*: 442-445.

Emiliani, C.; Cardini, L.; Mayeda, T.; McBurney, C. B. M. & Tongiorgi, E. 1964: Paleotemperature analysis of marine molluscs (food refuse) from the site of Arene Candide Cave, Italy and the Haua Fteah Cave, Cyrenaica, *In:* Craig, H.; Miller, S. L. & Wasserburg, G. J. (ed.), *Isotopic and Cosmic Chemistry*, North Holland, Amsterdam, Pp. 133-156.

Epstein, S. & Mayeda, T. 1953: Variations of O^{18} composition of water from natural sources. *Geochemica Cosmochimca Acta 4*: 212-224.

Epstein, S.; Buchsbaum, R.; Lowenstam, H. A. & Urey, H. C. 1976: Revised carbonate-water isotopic temperature scale. *Bulletin of the Geological Society of America 64*: 1315-1326.

Escapa, M.; Isacch, J.; Daleo, P.; Alberti, J.; Iribarne, O.; Borges, M.; Dos Santos, E. P.; Gagliardini, D. A. & Lasta, M. 2004: The distribution and ecological effects of the introduced pacific oyster *Crassostrea gigas* (Thunderberg, 1973) in Northern Patagonia. *Journal of Shellfish Research 23*: 1-8.

Fleger, S. L.; Heckman, J. W. & Klomparens, K. L. 1993: Scanning and transmission electron microscopy an introduction, Oxford University press, New York.

Fleming, C. A. 1952: A Foveaux Strait oyster bed. *New Zealand Journal of Science and Technology 34B*: 73-85.

Fleming, C. A. 1953: The Geology of the Wanganui Subdivision, New Zealand Geological Survey, Bulletin 52, Government Printer, Wellington.

Flugel, E. 2004: Microfacies of carbonate rocks. Analysis, interpretation and application, Springer, Berlin.

Folk, R. L. 1951: Stages of textural maturity in sedimentary rocks: *Journal of Sedimentary Petrology 21:* 127-130.

Folk, R.L 1954: The distinction between grain size and mineral composition in sedimentary rock nomenclature. *Journal of Geology 62:* 344-359.

Folk, R. L. 1959: Practical petrographic classification of limestones. *American Association of Petroleum Geologists Bulletin 43*: 1-38.

Folk, R. L. 1962: Spectral subdivision of limestone types, *In:* Ham, W. E. (ed.), *Classification of carbonate rocks*, American Association of Petroleum Geologists Memoir 1, Tulsa, OK, Pp. 62-84.

Freitas, P.; Clarke, L. J.; Kennedy, H.; Richardson, C. & Abrantes, F. 2005: Mg/Ca, Sr/Ca, and stable isotope ($\delta^{18}O$ and $\delta^{13}C$) ratio profiles from the fan mussel Pinna nobilus: Seasonal records and temperature relationships. *Geochemistry, Geophysics, Geosystems 6*: (4) 1-16.

Frey, R. W.; Basan, P. B. & Smith, J. M. 1987: Rheotaxis and distribution of oysters and mussels, Georgia tidal creeks and salt marshes, U.S.A. *Palaeogeograpy, Palaeoclimatology, Palaeooecology 61*: 1-16.

Frey, R. W. & Seilacher, A. 1980: Uniformity in marine invertebrate ichnology. *Lethaia 13*: 183-207.

FRWI, 2005: Fish and Wildlife Research Institute, Florida. [Accessesed 28/10/2009] Last updated 2005.

Gentry, K. D.; Sosdian, S.; Grossman, E. L.; Rosenthal, Y.;Hicks, D. & Lear, C. H. 2008: Stable isotope Sr/Ca profiles from the marine gastropod *Conus ermineus*: testing a multiproxy approach for inferring paleotemperature and paleosalinity. *Palaios 23*: 195-209.

Glennie, K. W. 1956: The Oligocene Formations of Taranaki, Geological Report No. 5, Shell, B.P and Todd Oil Services Ltd, Wellington, New Zealand.

Gröcke, D. R. & Gillikin, D. P. 2008: Advance in mollusc sclerochronology and sclerochemistry: tools for understanding climate and environment. *Geo-Marine Letters 28*: 265-268.

Groeber, P. 1929: Líneas fundamentales de la geología de Neuquén, sur de Mendoze y regiones adyacentes. *Publicación de la Dirección Nacional de Geología y Minería 5.*

Gutíerrez, J. L.; Jones, C. G.; Strayer, D. L. & Iribarne, O. O. 2003: Mollusks as ecosystem engineers. *Oikos 69*: 373-386.

Hayton, S. 1998: Sequence stratigraphic, paleoenvironmental and chronological analysis of the Late Neogene Wanganui River Section, Wanganui Basin, Unpublished thesis, University of Waikato.

Head, P. S. 1985: Surficial sediments on the Snares Platform, southern New Zealand: A cold-water, carbonate-dominated shelf, Unpublished thesis, University of Waikato.

Henderson, J. & Ongley, M. 1923: The Geology of the Mokau Subdivision with an Account of the Adjoining Areas of the Te Kuiti District. *New Zealand Geological Survey Bulletin 24:* 83.

Herbst, R. & Zabert, L. L. 1987: Microfauna de la Formación Paraná (Mioceno Superior) de la cuenca Chaco-Paranense (Argentina). *FACENA 7*: 165-206.

Hessland, I. 1949: Investigations of the Lower Ordovician of the Siljan District. *Geological Institute of the University of Uppsala Bulletin 33*: 409-428.

Higuera-Ruiz, R. & Elorza, J. 2009: Biometric, microstructural, and high resolution trace element studies in *Crassostrea gigas* of Cantabria (Bay of Biscay, Spain): Anthropogenic and seasonal influences. *Estuarine, Coastal and Shelf Science 82*: 201-213.

Holdem, C. & Hudson, J. D. 2003: $^{87}Sr/^{86}Sr$ and Sr/Ca investigation of Jurassic molluscs from Scotland; implications for paleosalinites and the Sr/Ca ratio of seawater. *Geological Society of America Bulletin 115:*1249-1264.

Hong, W.; Keppens, E.; Nielsen, P. & van Riet, A. 1995: Oxygen and carbon isotope study of the Holocene oyster reefs and paleoenvironmental reconstruction on the northwest coast of Bohai Bay, China. *Marine Geology 124*: 289-302.

Hopkins, J. 1966: The Te Kuiti Group in the West Piopio Area, Unpublished thesis, University of Auckland.

Hopkins, J. C. 1970: Stratigraphy, petrography and origin of the Te Kuiti Group in the west Piopio Area. *Transactions of the Royal Society of New Zealand 8:* 1-26.

JCPDS 1980: JCPDS International Centre for Diffraction Data. Mineral powder diffraction file data book, Bayliss, P., Berry, L.G., Mrose, M.E., Smith, D.K. *ed.*, Swarthmore, Pennsylvania, USA.

Jeffs, A. G. & Hickman, R. W. 2000: Reproductive activity in a pre-epizootic wild population of the Chilean Oyster, *Ostrea chilensis*, from southern New Zealand. *Aquaculture 183*: 241-253.

Jones, N. S. 1950: Marine bottom communities. *Biological Reviews 23*: 283-313.

Jones, C. E.; Jenkyns, H. C.; Hesselbo, S. P. 1994a: Strontium isotopic in Early Jurassic seawater. *Geochim Cosmochim Acta 58:*1285-1301.

Jones, C. G.; Lawton, J. H. & Shachak, M. 1994b: Organisms as ecosystem engineers. *Oikos 69*: 373-386.

Jones, C. E.; Jenkyns, H. C.; Coe, A. L; Hesselbo, S. P. 1994c: Strontium isotopic variations in Jurassic and Cretaceous seawater. *Geochim Cosmochim Acta 58:* 3061-3074.

Jones, C. G.; Lawton, J. H. & Shachak, M. 1997: Positive and negative effects of organisms as physical ecosystem engineers. *Ecology 78*: (7) 1946-1957.

Jones, D. S.; Arnold, B.; Quitmyer, I.; Schöne, B. R. & Surge, D. 2007: 1st International Sclerochronology Conference, http://conference.ifas.ufl.edu/sclerochronology.

Kamp, P. J. J. & McIntyre, A. P. 1998: The stratigraphic architecture of Late Pliocene (2.8-2.4 Ma) asymmetrical shelf sequences, western Wanganui Basin, New Zealand. *Sedimentary Geology 122*: 53-67.

Kamp, P. J. J.; McIntyre, A.; Hayton, S.; Nelson, C. S.; Pillans, B. & Naish, T. R. 1999: Pliocene and Pleistocene Stratigraphy and Sedimentary Geology of Wanganui Basin, *Field trip guide for Geological Society of New Zealand Conference*, Palmerston North.

Kear, D. & Schofield, J. C. 1958: Te Kuiti Group. *New Zealand Journal of Geology and Geophysics 2*: 685-717.

Keith, M. L.; Anderson, G. M. & Eichler, R. 1964: Carbon and oxygen isotopic composition of mollusc shells from marine and fresh-water environments. *Geochemica Cosmochimca Acta 28*: 1757-1786.

Kelly, S. R. A. & Bromley, R. G. 1984: Ichnological nomenclature of clavate borings. *Palaeontological Association 27*: 793-807.

Ker, D. S. 1970: Stratigraphy and Engineering Geology of the Lower Wanganui Valley, Koriniti to Parikino. *New Zealand Journal of Geology and Geophysics 16*: 189-208.

Kidwell, S. M. 1991a: Condensed deposits in siliciclastic sequences expected and observed features, *In:* Einsele, G.; Ricken, W. & Seilacher, A. (ed.), *Cycles and Events in Stratigraphy*, Springer-Verlag, Berlin.

Kidwell, S. M. 1991b: The Stratigraphy of Shell Concentrations, *In:* Allison, A. P &. Briggs. D. E. G. (ed.), *Taphonomy. Releasing the Data Locked in the Fossil Record*, Plenum Press, New York, Pp. 212-279.

Kidwell, S. M. & Aigner, T. 1985: Sedimentary dynamics of complex shell beds: Implications for ecological and evolutionary patterns, *In:* Bayer, U. & Seilacher, A. (ed.) *Sedimentary and Evolutionary Cycle,* Springer-Verlag, Berlin, Pp. 382-395.

Kidwell, S. M. & Bosence, D. W. J. 1991: Taphonomy and Time-Averaging of Marine Shelly Faunas, *In:* Allison, A. P &. Briggs. D. E. G. (ed.), *Taohonomy: Releasing the Data Locked in the Fossil Record*, Plenum Press, New York, Pp. 116-188.

Kirby, M. X. 2000: Paleoecological Differences Between Tertiary and Quaternary Crassostrea Oysters, as Revealed by Stable Isotope Sclerochronolgy. *Palaios 15*: 132-141.

Kirby, M. X.; Soniat, T. M. & Spero, H. J. 1998: Stable isotope sclerochronology of Pleistocene and Recent oyster shells (*Crassostrea virginica*). *Palaios 13*: 560-569.

Klein, R.; Lohmann, K. & Thayer, C. 1996a: Bivalve skeletons record sea-surface temperatures and $\delta^{18}O$ via Mg/Ca and $^{18}O/^{16}O$ ratios. *Geology 24*: 415-418.

Klein, R.; Lohmann, K. & Thayer, C. 1996b: Sr/Ca and $^{13}C/^{12}C$ ratios in skeletal calcite of *Mytilus trossulus*: Covariation with metabolic rate, salinity and carbon isotopic composition of sea water *Geochemica Cosmochimca Acta 60*: 4207-4221.

Klünder, M. H.; D, H.; Witbaard, R. & Frei, D. 2008: Laser ablation analysis of bivalve shells - archives of environmental information. *Geological Survey of Denmark and Greenland Bulletin 15*: 89-92.

Kondo, Y.; Abbot, S. T.; Kitamura, A.; Kamp, P. J. J.; Naish, T. R.; Kamataki, T. & Saul, G. S. 1998: The relationship between shellbed type and sequence architecture: examples from Japan and New Zealand. *Sedimentary Geology 122*: 109-127.

Krantz, D. E.; Williams, D. F. & Jones, D. S. 1987: Ecological and paleoenvironmental information using stable isotope profiles from living and fossil molluscs. *Palaeogeograpy, Palaeoclimatology, Palaeooecology 58*: 249-266.

Krantz, D. E.; Jones, D. S. & Williams, D. F. 1989: Reply to "Aspects of growth and deceleration in bivalves: Clues to understanding the seasonal $\delta^{18}O$ and $\delta^{13}C$ record". *Palaeogeograpy, Palaeoclimatology, Palaeoecology 70*: 403-407.

Lauckner, G. 1983: Diseases of Mollusca: Bivalva, *In:* Kinne, O. (ed.), *Diseases of Marine Animals, Vol 2: Introduction, Bivalvia to Scaphopoda*, Biologische Anstalt Helgoland, Hamburg, Pp. 447-961.

Laws, C. R. 1940: Palaeontological study of Nukumaruan and Waitotaran rocks near Wanganui. *Transactions of the Royal Society of New Zealand: 70* 150-160.

Lea, D.; Mashiotta, T. & Spero, H. 1999: Controls on magnesium and strontium uptake in planktonic foraminifera determined by live culturing. *Geochemica Cosmochimca Acta 63*: 2369-2379.

Lees, A. 1975: Possible influence of salinity and temperature on modern shelf carbonate sedimentation. *Marine Geology 19*: 159-198.

Lindholm, R. 1987: A practical approach to sedimentology, Allen & Unwin, Inc., Winchester.

Lorens, R. & Bender, M. 1980: The impact of solution chemistry on *Mytilus edulis* calcite and aragonite. *Geochemica Cosmochimca Acta 44*: 1265-1278).

Machel, H. G.; Mason, R. A.; Mariano, A. N. & Mucci, A. 1991: Causes and emissions of luminescence from dolomite, *In:* Barker, E. C. & Kopp, O. C. (ed.), *Luminescence Microscopy: Quantitative and qualitative methods*, Society of Economic, Palaeontology and Mineralogy, Tulsa, Oklahoma.

Majewske, O. P. 1969: Recognition of invertebrate fossil fragments in rocks and thin sections, E. J. Brill, Leiden, Netherlands.

Malumián, N. 1999: La sedimentación en la Patagonia extraandina. 1. La sedimentación en la Patagonia extraadina., *In:* R. Caminos (ed.), *Anales del Instituto de Geología y Recursos Minerale 29*: 557-578.

Malumián, N. & Masiuk, V. 1973: Asociaciones foraminiferológicas fósiles de la República Argentina. 5º Congreso Geológico Argentino (Córdoba, 1973). *Actas 3*: 433-453.

Mao Che, L.; Campion-Alsumard, T.; Bourny-Esnault, N.; Payri, C.; Golubic, S. & Bézac, C. 1996: Biodegration of shells of the black pearl oyster, *Pinctada margaritifera* var. *cumingii,* by microbes and sponges of French Polynesia. *Marine Biology 126*: 509-519.

Marshall, P. & Murdoch, R. 1920: Tertiary rocks near Wanganui. *Transactions of the New Zealand Institute 52*: 115-128.

Martín, J. M.; Braga, J. C. & Riding, R. 1997: Late Miocene Halimeda alga-microbial segment reefs in the marginal Mediterranean Sorbas Basin, Spain. *Sedimentology 44*: 441-456.

Marwick, J. 1946: The Geology of the Te Kuiti Subdivision. *New Zealand Geological Survey Bulletin n.s. 41:* 89.

Mauna, C.; Casadio, S.; Parras, A. & Pascual, M. 2005: Abundance and distribution of the *Lithophaga* (Mytilidae) in extant and fossil oysters: taphonomic and paleobiological implications. *Ameghiniana 42*: 395-405.

McArthur, J. M.; Kennedy, W. J.; Chen, M.; Thirwall, M. F. & Gale, A. S. 1994: Strontium isotope stratigraphy for Late Cretaceous time: Direct numerical calibration of the Sr isotope curve based on the US Western Interior. *Palaeogeography, Palaeoclimatology, Palaeoecology 108*: 95-115.

McArthur, J. M; Crame, J. A; Thirwall, M. F. 2000: Definition of Late Cretaceous stage boundaries in Antarctica using Strontium isotope stratigraphy. *Journal of Geology 108:* 623-640.

McIntyre, A. P. 1997: Lithostratigraphy and sequence stratigraphy of Late Pliocene Strata, Whanganui River Valley, New Zealand, Unpublished thesis, The University of Waikato.

McIntyre, A. 2002: Geology of the Mangapanian (Late Pliocene) strata, Wanganui Basin: Lithostratigraphy, palaeontology and sequence stratigraphy, Unpublished thesis, The University of Waikato.

McIntyre, A. & Kamp, P. J. J. 1998: The stratigraphic architecture of Late Pliocene (2.8 - 2.4 Ma) asymmetrical shelf sequences, western Wanganui Basin, New Zealand. *Sedimentary Geology 116*: 57-80.

Mii, S. H.; Grossman, E. L. & Yancey, T. E. 1997: Stable carbon and oxygen isotope shifts in Permian seas of West Spitsbergen - global changes or diagenetic artefact? *Geology 25*: 227-230.

Milliman, J.D. 1974: Marine Carbonates. Springer, New York, Pp. 1-375.

Möbius, K. 1877: An Oyster-Bank Community is a Biocönose, or a Social Community, *In:* Kormondy, E. J. (ed.), *Readings in Ecology*, Prentice-Hall, New Jersey.

Mook, W. G. 1968: Geochemistry of the stable carbon and oxygen isotopes of natural waters in the Netherlands, Unpublished thesis, University of Greningen, Netherlands.

Mook, W. G. 1971: Palaeotemperatures and chlorinities from stable carbon and oxygen isotopes in shell carbonate. *Palaeogeograpy, Palaeoclimatology, Palaeooecology 9*: 245-263.

Mook, W. G. & Vogel, J. C. 1968: Isotopic equilibrium between shells and their environments. *Science 159*: 874-875.

Naish, T. R. & Kamp, P. J. J. 1995: Pliocene-Pleistocene marine cyclothems, Wanganui Basin, New Zealand: a lithostratigraphic framework. *New Zealand Journal of Geology and Geophysics 38*: 223-241.

Naish, T. R. & Kamp, P. J. J. 1997: Sequence stratigraphy of 6th order (41 ka) Pliocene-Pleistocene cyclothems, Wanganui Basin, New Zealand. *Bulletin of the Geological Society of America 109*: 978-999.

Navarro, V.; Reolid, M.; Molina, J. M. & Ruiz-Ortiz, P. A. 2008: Slope breccias colonized by bivalves and serpulids during the Middle Jurassic (Subbetic, SE Spain) *Facies 54*: 403-415.

Nelson, C. S. 1973: Stratigraphy and sedimentology of Te Kuiti Group Waitomo Country, South Auckland, Unpublished thesis, University of Auckland.

Nelson, C. S. 1978: Stratigraphy and paleontology of the Oligocene Te Kuiti Group, Waitomo County, South Auckland, New Zealand. *New Zealand Journal of Geology and Geophysics 21*: 553-594.

Nelson, C. S. 1993: A synopsis of the Geological History of the King Country, *Proceedings of the New Zealand Farm Forestry Association Annual Conference*, Pp. 8-12.

Nelson, C. S.; Burns, D. A. & Rodgers, K. A. 1983: The taxonomic status, and isotopic evidence for paleoenvironments, of giant oysters from the Oligocene Te Kuiti Group, South Auckland New Zealand. *New Zealand Journal of Geology and Geophysics 26*: 289-299.

Nelson, C. S.; Harris, G. J. & Young, H. R. 1988: Burial-dominated cementation in non-tropical carbonates of the Oligocene Te Kuiti Group, New Zealand. *Sedimentary Geology 60*: 233-250.

Nurnberg, D.; Bijma, J. & Hemleben, C. 1996: Assessing the reliability of magnesium in foraminiferal calcite as a proxy for water mass temperature. *Geochemica Cosmochimca Acta 60*: 803-814.

Ortmann, A. 1897: On some large oysters of Patagonia. *American Journal of Science 4*: 355-357.

Ozhigova, N. V. 1992: A comparative study of shell composition in fossil and recent bivalves molluscs. *Palaeontology Journal 26:* 40-53.

Palmer, T. & Plewes, C. 1993: Borings and bioerosion in fossils. *Geology Today* (July-August) Pp. 138-142.

Park, J. 1887: On the Geology of the Western part of the Wellington Provincial District and part of Taranaki. New Zealand Geological Survey Report, Geological Exploration 1887. Pp. 24-73.

Parras, A. & Casadío, S. 2005: Taphonomy and sequence stratigraphic significance of oyster dominated concentrations from the San Julian formation, Oligocene of Patagonia, Argentina. *Palaeogeography, Palaeoclimatology, Palaeoecology 217*: 47-66.

Parras, A. & Casadío, S. 2006: The oyster *Crassostrea? hatcheri* (Ortmann, 1897), a physical ecosystem engineer from the Upper Oligocene-Lower Miocene of Patagonia, Southern Argentina. *Palaios 21*: 168-186.

Pascual, R. 2008: Mueso de Lago Gutierrez. Bariloche, Patagonia, Argentina. http://www.bariloche.ca/mapa_geologico_argentina.jpg/view. [Accessesed 20/8/2009].

Pemberton, S. G.; Frey, R. W. & Saunders, T. D. A. 1990: Trace fossils, *In:* Briggs, D. E. G. &. Crowther, P. R (ed.), *Paleobiology a synthesis*, Blackwell Scientific Publications, London.

Pilkey, O. H. & Harriss, R. C. 1966: The effect of intertidal environment on the composition of calcareous skeletal material. *Limonology and Oceanography 11:*381-385.

Pohowsky, R. A. 1978: The boring ctenostomate Bryozoa: taxonomy and paleobiology based on cavities in calcareous substrata. *Bulletins of American Paleaontology 73*: 1-193.

Powell, E. 2006: How long does and oyster shell last on an oyster reef? *Estuarine, Coastal and Shelf Science 69*: 531-542.

.

Pruss, S. B.; Payne, J. L. & Bottjer, D. J. 2007: Placunopsis bioherms: The first metazoan buildups following the end-Permian mass extinction *Palaios 22*: 17-23.

Putten, E.; Dehairs, F.; Keppens, E. & Baeyens, W. 2000: High resolution distribution of trace elements in the calcite shell layer of modern *Mytilus edulis:* Environmental and biological controls. *Geochemica Cosmochimca Acta 64*: 997-1011.

Ray, S.; Gault, R. & Dodd, C. G. 1957: The separation of clay minerals from carbonate rocks. *The American Mineralogist 42*: 681-685.

Read, J. F. 1995: Overview of carbonate platform sequences, cycle stratigraphy and reservoirs in greenhouse and ice-house worlds, *In:* Read, J. F.; Kerans, C.; Weber, J. L.; Sarg, J. F. & Wright, F. M. (ed.), *Milankovitch sea-level changes, cycles, and reservoirs on carbonate platforms in greenhouse and ice-house worlds*, SEPM (Society for Sedimentary Geology), USA, Pp. 1-101.

Rhoads, D. C. & Lutz, R. A. 1980: Skeletal Records of Environmental Change, *In:* D. C. Rhoads & R. A. Lutz (ed.), *Skeletal Growth of Aquatic Organisms*, Plenum Press, New York, Pp. 1-19.

Rice, M. A. & Pechenik, J. A. 1992: A review of the factors affecting the growth of the Northern Quahog, *Mercenaria mercenaria* (Linnaeus, 1757). *Journal of Shellfish Research 11*: 279-287.

Riceman, M. S. 2008: The use of otolith microchemistry to investigate natal origins and movement of lacustrine wild rainbow trout (*Oncorhynchu mykiss*) and common smelt (*Retropinna retropinna*). Unpublished thesis, University of Waikato.

Robinson, G. W. 1949: Soils, their origin, constitution, and classification, Murby, London.

Rush, P. F. & Chafetz, H. S. 1990: Fabric retentive, non-luminescent brachiopods as indicators of original $\delta^{13}C$ and $\delta^{18}O$ composition: A test. *Journal of sedimentary Petrology 60*: 968-981.

Russo, A. & Serraiotto, A. 1978: Contribución al conocimiento de la estratigrafía terciaria en el Noroeste Argentino. 7º Congreso Geológico Argentino (Neuquén, 1978). *Actas 1*: 715-730.

Scasso, R. A. & del Río, C. J. 1987: Ambientes de sedimentación y proveniencia de la secuencia marina del Terciario Superior de la región de Península Valdés. *Revista de la Asociación Geológica Argentina 42*: 291-321.

Scasso, R. A. & Castro, L. N. 1999: Cenozoic phosphatic deposits in North Patagonia, Argentina. Phosphogenesis, sequence stratigraphy and paleoceanography. *Journal of South American Earth Science 12*: 471-487.

Scasso, R. A. & Kiessling, W. 2001: Diagenesis in Upper Jurassic concretions from the Antarctic Peninsula. *Journal of Sedimentary Research Part A 71*: 88-100.

Scasso, R. A.; McArthur, J. M.; del Río, C. J.; Martinez, S. & Thirlwall, M. F. 2001: $^{87}Sr/^{86}Sr$ Late Miocene age of fossil molluscs in the "Entrerriense" of the Valdés Peninsula (Chubut, Argentina). *Journal of South American Earth Sciences 14*: 319-329.

Schein, P. D.; Roux, M.; Barbin, V.; Chiesi, F.; Renard, M. & Rio, E. M. 1991: Enregistrement des paramètres écologiques par la coquille des bivalves: approche pluridisciplinaire. *Bulletin Society Geology France 162*: 687-698.

Schlager, W. 1992: Sedimentology and sequence stratigraphy of reefs and carbonate platforms. *AAPG Continuing Education Course Note 34*: 71.

Schneider, S.; Fürish, F. T. & Werner, W. 2009: Sr-isotope stratigraphy of the Upper Jurassic of central Portugal (Lusitanian Basin) based on oyster shells. *International Journal of Earth Science 98*: 1949-1970.

Scholle, P. A. & Ulmer-Scholle, D. S. 2003: A Colour Guide to the Petrography of Carbonate Rocks: Grains, textures, porosity, diagenesis, AAPG Memoir 77, The American Association of Petroleum Geologists, Oklahoma, USA.

Scoffin, T. P. 1987: An introduction to carbonate sediments and rocks, Chapman and Hall, New York.

Seilacher, A.; Matyja, B. A. & Wierzbowski, A. 1985: Oyster beds: morphologic response to changing substrate conditions, *In:* Bayer, U. & Seilacher, A. (ed.), *Sedimentary and Evolution Cycles*, Springer-Verlag, Berin, 421-435.

Stainton, P. W. 1964: The Geology of Central Taranaki (A Compilation Report), Geological Report No. 63, Shell, B.P, Todd Oil Services Ltd, Wellington, New Zealand.

Stanley, S. M. 1970: Relation of shell form to life habits in the Bivalvia. *Geological Society of America Memoir 125:* 1-296.

Stappenbeck, R. 1927: Ubre Transgressionen und Regressionen des Meeress und Gebirgsbildung in Südamerika. *Neues Jahrbuch fur Mineralogie 58*: Abt. B.

Stearley, R. F. & Ekdale, A. A. 1989: Modern Marine Bioerosion by Macroinvertibrates, Northern Gulf of California. *Palaios 4*: 453-467.

Stenzel, H. B. 1963: Aragonite and calcite as constituents of adult oyster shells. *Science 142*: 232-233.

Stenzel, H. B. 1971: Oysters, *In:* R. C. Moore (ed.), *Treatise on invertebrate paleontology*, Geological Society of America and University of Kansas, Part N, V. 3, Mollusca 6, Bivalvia, Pp. N953-N1224.

Stern, T. A.; Quinlan, G. M. & Holt, W. E. 1993: Crustal Dynamics Associated with the Formation of Wanganui Basin, New Zealand, *In:* Ballance, P. F (ed.), *South Pacific Sedimentary Basins*, Elsevier, Amsterdam.

Stetcher, H. A.; Krantz, D. E.; Lord, C. J.; Luther, G. W. & Bock, K. W. 1996: Profiles of strontium and barium in *Mercenaria mercenaria* and *Spisula solidossima* shells. *Geochemica Cosmochimica Acta 60*: 3445-3456.

Taylor, P. D. & Wilson, M. A. 2003: Palaecology and evolution of marine hard substrate communities. *Earth Science Reviews 62*: 1-103.

Townsend, D.; Vonk, A. & Kamp, P. J. J. 2008: Geology of the Taranaki Area, GNS Science, Lower Hutt.

Tripathi, A. R. P. 2008: Basin analysis of the Late Eocene-Oligocene Te Kuiti Group, Western North Island, New Zealand, Unpublished thesis, University of Waikato.

Tucker, M. E. & Wright, P. V. 1990: Carbonate Sedimentology, Blackwell Scientific Publications, Oxford.

Van Wagoner, J. C.; Posamentier, H. W.; Mithcum, R. M.; Vail, P. R.; Sarg, J. F.; Louiti, T. S. & Hardenbol, J. 1988: An overview of the fundamentals of

sequence stratigraphy and key definitions. *Society for Economic Paleontology and Mineralogy Special Publication 42*: 39-45.

Veizer, J. 1983a: Chemical diagenesis of carbonates: theory and application of trace element technique. *SEPM Short Course 10*: 3-100.

Veizer, J. 1983b: Trace elements and isotopes in sedimentary carbonates; mineralogy and chemistry. *Revisions in mineralogy 11*: 265-299.

Vogel, K. 1995: Rate of dissolution of carbonate systems of microboring organisms, Davies Reef, Australia. *Journal of sedimentary Petrology 55*: 440-447.

Vogel, K.; Gektidis, M.; Golubic, S.; Kiene, W. E. & Radtke, G. 1999: Experimental studies on microbial bioerosion and Lee Stocking Island, Bahamas and One Tree Island, Great Barrier Reef, Australia: Implications for paleoecological reconstructions. *Lethaia 33*: 190-204.

Wanamaker, A. D. J.; Kreutz, K. J.; Wilson, T.; Borns, H. W. J.; Introne, D. S. & Feindel, S. 2008: Experimentally determined Mg/Ca and Sr/Ca ratios in juvenile bivalve calcite for *Mytilus edulis:* implications for paleotemperature reconstructions. *Geo-Marine Letters 28*: 359-368.

Warme, J. E. 1975: Borings as trace fossils, and the processes of marine bioerosion, *In:* Frey, R. W (ed.), *The Study of Trace Fossils*, Springer-Verlag, Berlin, Pp. 181-227.

Wells, H. W. 1961: The fauna of oyster beds, with special reference to the salinity factor. *Ecological Monographs 31*: 240-266.

White, P. J. & Waterhouse, B. C. 1993: Lithostratigraphy of the Te Kuiti Group. *New Zealand Journal of Geology and Geophysics 36*: 255-266.

Wierzbowsi, H & Joachimski, M. 2007: Reconstruction of late Bajocian-Bathonian marine paleoenvironments using carbon and oxygen isotope ratios of calcareous fossils from Polish Jura Chain (central Poland). *Paleogeography, Paleoclimatology, Paleoecology 254*: 523-540.

Wilson, G. S. 1993: Ice induced sea level change in the Late Neogene, Unpublished thesis, Victoria University.

Wilson, M. A. & Taylor, P. D. 2001: Paleoecology of hard substrate faunas from the Cretaceous Qahlah Formation of the Oman Mountains. *Palaeontology 44*: 21-41.

Young, C. M. 1995: Behaviour and locomotion during the dispersal phase of larval life. *In:* McEdward, L. R. (ed.), *Ecology of Marine Invertebrate Larvae*, CRC Press, Boca Raton: Florida.

Zabert, L. L. 1978: Micropaleontología de la Formación Paraná (Mioceno superior) en el subsuelo de la provincia de Santa Fé, República Argentina. *FACENA 2*: 101-165.

Zabert, L. L. & Herbst, R. 1977: Revisión de la microfauna Miocena de la Formación Paraná (entre Victoria y Villa Urquiza, provincia de Entre Ríos, Argentina) con algunas consideraciones estratigráficas. *FACENA 1*: 131-174.

Zinsmeister, W. J.; Marshall, L. G.; Drake, R. E. & Curtis, G. H. 1981: First radioisotope (Potassium-Argon) age of marine Neogene Rio Negro beds in Northeastern Patagonia, Argentina. *Science 212*: 440.

Zittel, K .A 1864: Fossile Mollusken und Enchinodermen aus Neu-Seeland. Nebst beiträgen von den Harren Bergrath Franz Ritter Hauer und Professor Eduard Suess. *In:* Hochstetter, F. V; Hörnes, M.; Ritter von Hauer, F. (ed.) Paläontologie von Neu-Seeland. Beitrage zur Kenntniss der Fossilien, Flora und Fauna der Provinzen Auckland und Nelson. *Reise der Österreichischen Fregatte Novara um die Erde, Geologischer Theil 1*:16-68.

Zuschin, M.; Stachowitsch, M.; Perversler, P. & Kollmann, H. 1999: Structural features and taphonomic pathways of a high-biomass epifauna in the northern Gulf of Trieste, Adriatic Sea. *Lethaia 32*: 299-317.

Enclosure 1: Sketch of the Wilkies Shellbed, Parikino, Wanganui
NZMS 260 S22 959 574

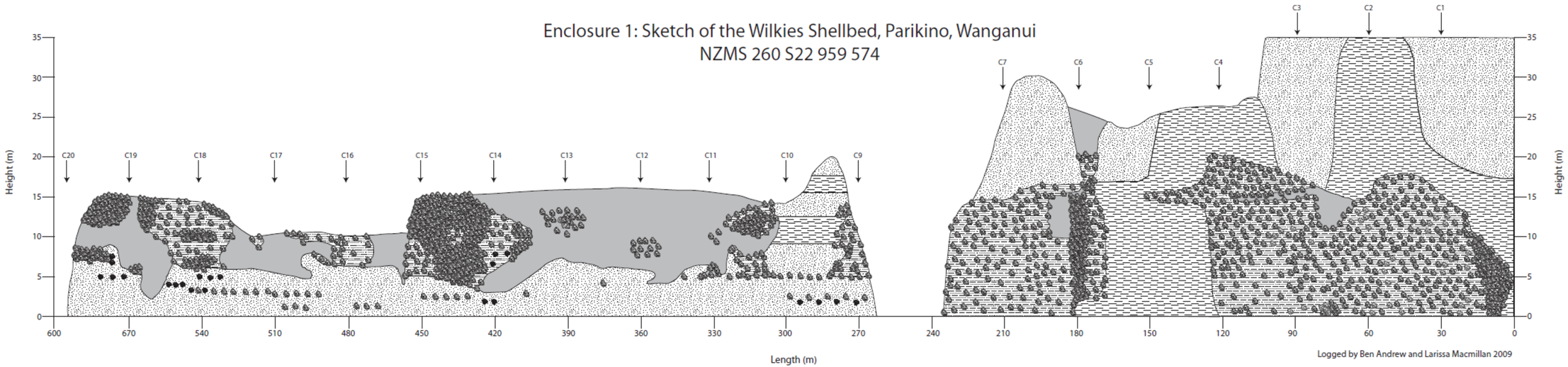

Logged by Ben Andrew and Larissa Macmillan 2009

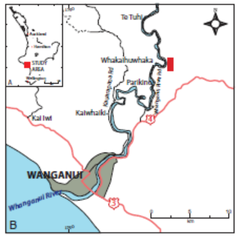

Inset (A) Location in relation to North Island, New Zealand. (B) Field area as outlined in (A). Sketch location in red.

LEGEND

- Siltstone
- Muddy sand
- Sandstone
- Unseen/vegetation
- *Crassostrea ingens*
- Pectinids
- C1 Stratigraphic column number, see Appendix D-1.1 for grid refs.

VE = 3.3

APPENDIX A
Field data

Appendix A1.1 Map of the Wanganui region including all place names featuring in Chapters One and Five.

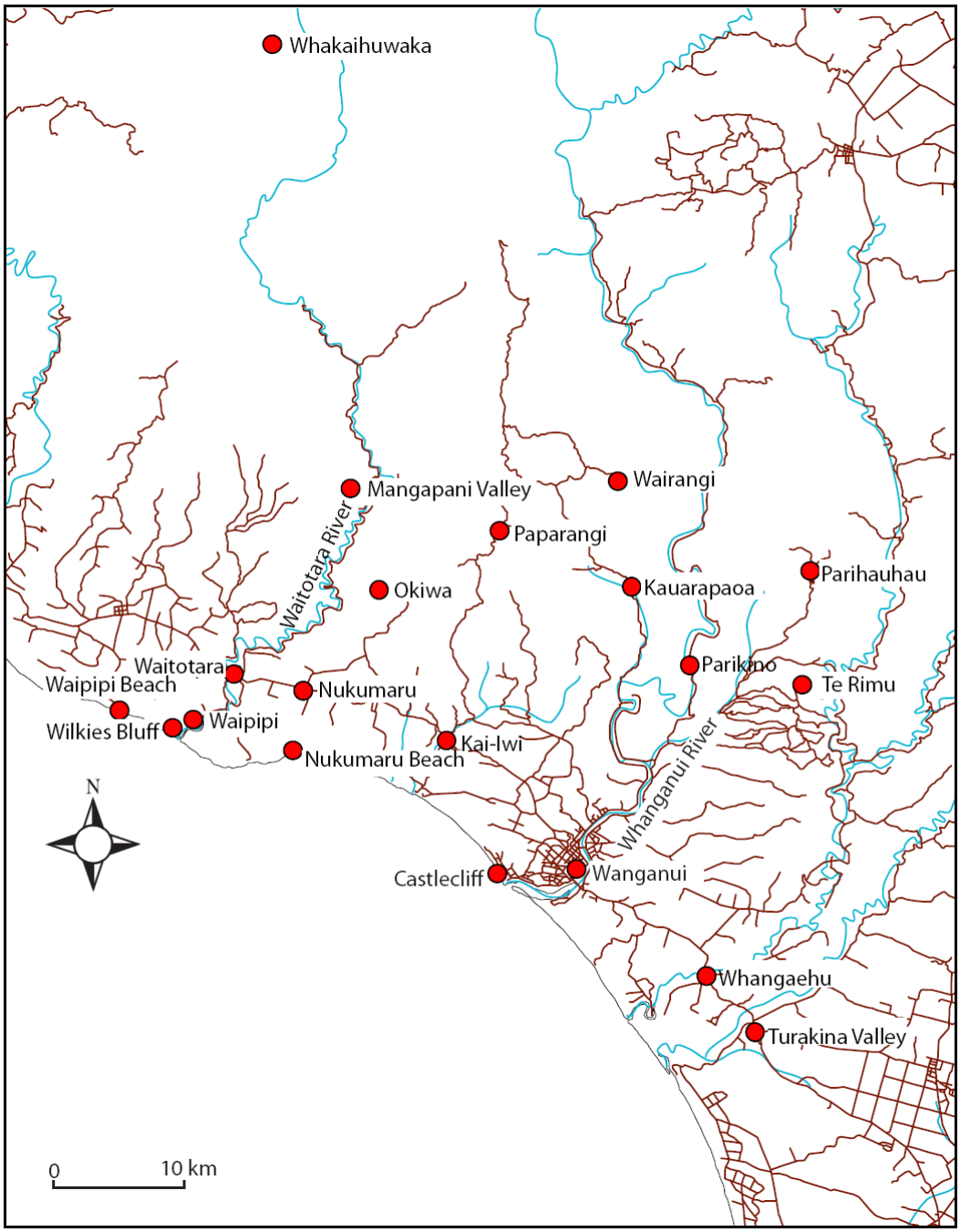

Appendix A1.2 Sample catalogue of all host sediments and fossil oyster samples referred to in this study. Includes field sample number, University of Waikato sample numbers logged in the PET database and a brief description.

Sample Number	UoW number	Description
PAT1	20100400	Muds underlying the reef
PAT2	20100401	*"Ostrea" patagonica* from bottom of the reef
PAT2_1	20100402	*"Ostrea" patagonica* from bottom of the reef
PAT2_3	20100403	*"Ostrea" patagonica* from bottom of the reef
PAT3	20100404	*"Ostrea" patagonica* from middle of the reef
PAT3_3	20100405	*"Ostrea" patagonica* from middle of the reef
PAT4	20100406	*"Ostrea" patagonica* from top of the reef
PAT4_1	20100407	*"Ostrea" patagonica* from top of the reef
PAT4_4	20100408	*"Ostrea" patagonica* from top of the reef
PAT5	20100409	Host sediment middle of the reef
PAT6	20100410	Host sediment top of the reef
PAT7	20100411	Host sediment bottom
San1a	20100412	*Crassostrea gigas* from high tide off rocks
San3a	20100413	*Crassostrea gigas* from low tide
San3d	20100414	*Crassostrea gigas* from low tide
FVX1	20100415	*Ostrea chilensis supplied by NIWA*
W02/1A	20100416	Orahiri Lst + F.Stenzel
W02/1B	20100417	Orahiri Lst + F.Stenzel
W04/1B	20100418	Orahiri Lst + F.Stenzel
W04/3A	20100419	Orahiri Lst + F.Stenzel
W04/3B	20100420	Orahiri Lst + F.Stenzel
W05/1	20100421	Orahiri Lst + F.Stenzel
W07/1A	20100422	Orahiri Lst + F.Stenzel
W07/1C	20100423	Orahiri Lst + F.Stenzel
W10/1A	20100424	Orahiri Lst + F.Stenzel
W10/2A	20100425	Orahiri Lst + F.Stenzel
K11/1A	20100426	Orahiri Lst + F.Stenzel
K12/1B	20100427	Orahiri Lst + F.Stenzel
K13/1A	20100428	Orahiri pebbles
K13/1B	20100429	Orahiri Lst + F.Stenzel
K13/1C	20100430	Orahiri Lst + F.Stenzel
N14/1A	20100431	Orahiri Lst + F.Stenzel
N14/1B	20100432	Orahiri Lst + F.Stenzel
N14/1C	20100433	Orahiri Lst + F.Stenzel
N14/1E	20100434	Orahiri Lst + F.Stenzel
W15/1B	20100435	Orahiri Lst + F.Stenzel
W15/2A	20100436	Orahiri Lst + F.Stenzel
WVR2	20100437	Glauconite rich Orahiri Limestone
PAR01	20100438	Cable Siltstone
PAR05	20100439	Makokako Sandstone
PAR07	20100440	Makokako Sandstone
PAR09	20100441	Makokako Sandstone

PAR16	20100442	Makokako Sandstone
PAR16A	20100443	Host sediment
PAR18	20100444	Makokako Sandstone
PAR20	20100445	Sst concretion from Makokao Sandstone
WANR2	20100446	Host sediment
WANK2E	20100447	Host sediment
WLK	20100448	*Crassostrea ingens*
WLK3B	20100449	*Crassostrea ingens*
WLK05A	20100450	*Crassostrea ingens*
WLK06A	20100451	*Crassostrea ingens*
WLK10	20100452	*Crassostrea ingens*
WLK11	20100453	*Crassostrea ingens*
WLK14	20100454	*Crassostrea ingens*
WLK15	20100455	*Crassostrea ingens*
WLK17	20100456	*Crassostrea ingens*
WLK24	20100457	*Crassostrea ingens*
WLK36	20100458	*Crassostrea ingens*
WLK43	20100459	*Crassostrea ingens*
K4B	20100460	*Crassostrea ingens*
K4F	20100461	*Crassostrea ingens*
K5A	20100462	*Crassostrea ingens*
K5C	20100463	*Crassostrea ingens*
Wan08	20100464	Makokako Sandstone
Par19	20100465	Makokako Sandstone
K11/2A	20100466	Orahiri Lst + F.Stenzel
W03/1	20100467	Orahiri Lst + F.Stenzel
K12/1C	20100468	Orahiri Lst + F.Stenzel
Wap17/1B	20100469	Orahiri Lst + F.Stenzel

Appendix A1.2a Sample catalogue of all other samples, namely fossil oyster samples from Wanganui used in this study. Includes field sample number, sample location and a grid reference (NZMS 260 series topographic maps).

Sample Number	Description	Location	Grid Reference
WLK1	*Crassostrea ingens*	Parikino, from fallout pile at 240 m on sketch	S22/957572
WLK2	*Crassostrea ingens*	Parikino, from fallout pile at 240 m on sketch	S22/957572
WLK3A	*Crassostrea ingens*	Parikino, from fallout pile at 240 m on sketch	S22/957572
WLK4A	*Crassostrea ingens*	Parikino, from fallout pile at 240 m on sketch	S22/957572
WLK4B	*Crassostrea ingens*	Parikino, from fallout pile at 240 m on sketch	S22/957572
WLK6A	*Crassostrea ingens*	Parikino, from fallout pile at 240 m on sketch	S22/957572
WLK6B	*Crassostrea ingens*	Parikino, from fallout pile at 240 m on sketch	S22/957572
WLK7	*Crassostrea ingens*	Parikino, from fallout pile at 240 m on sketch	S22/957572
WLK8	*Crassostrea ingens*	Parikino, from fallout pile at 240 m on sketch	S22/957572
WLK9A	*Crassostrea ingens*	Parikino, from fallout pile at 240 m on sketch	S22/957572
WLK9B	*Crassostrea ingens*	Parikino, from fallout pile at 240 m on sketch	S22/957572
WLK12	*Crassostrea ingens*	Parikino, from fallout pile at 240 m on sketch	S22/957572

WLK13A	*Crassostrea ingens*	Parikino, from fallout pile at 240 m on sketch	S22/957572
WLK13B	*Crassostrea ingens*	Parikino, from fallout pile at 240 m on sketch	S22/957572
WLK16	*Crassostrea ingens*	Parikino, from fallout pile at 240 m on sketch	S22/957572
WLK18	*Crassostrea ingens*	Parikino, from fallout pile at 240 m on sketch	S22/957572
WLK19A	*Crassostrea ingens*	Parikino, from fallout pile at 240 m on sketch	S22/957572
WLK19B	*Crassostrea ingens*	Parikino, from fallout pile at 240 m on sketch	S22/957572
WLK20A	*Crassostrea ingens*	Parikino, from fallout pile at 240 m on sketch	S22/957572
WLK20B	*Crassostrea ingens*	Parikino, from fallout pile at 240 m on sketch	S22/957572
WLK21	*Crassostrea ingens*	Parikino, from fallout pile at 240 m on sketch	S22/957572
WLK22	*Crassostrea ingens*	Parikino, from fallout pile at 240 m on sketch	S22/957572
WLK23	*Crassostrea ingens*	Parikino, from fallout pile at 240 m on sketch	S22/957572
WLK25	*Crassostrea ingens*	Parikino, from fallout pile at 240 m on sketch	S22/957572
WLK26	*Crassostrea ingens*	Parikino, from fallout pile at 240 m on sketch	S22/957572
WLK27	*Crassostrea ingens*	Parikino, from fallout pile at 240 m on sketch	S22/957572
WLK28	*Crassostrea ingens*	Parikino, from fallout pile at 240 m on sketch	S22/957572
WLK29A	*Crassostrea ingens*	Parikino, from fallout pile at 240 m on sketch	S22/957572
WLK29B	*Crassostrea ingens*	Parikino, from fallout pile at 240 m on sketch	S22/957572
WLK30	*Crassostrea ingens*	Parikino, from fallout pile at 240 m on sketch	S22/957572
WLK31A	*Crassostrea ingens*	Parikino, from fallout pile at 240 m on sketch	S22/957572
WLK31B	*Crassostrea ingens*	Parikino, from fallout pile at 240 m on sketch	S22/957572
WLK32A	*Crassostrea ingens*	Parikino, from fallout pile at 240 m on sketch	S22/957572
WLK32B	*Crassostrea ingens*	Parikino, from fallout pile at 240 m on sketch	S22/957572
WLK33A	*Crassostrea ingens*	Parikino, from fallout pile at 240 m on sketch	S22/957572
WLK33B	*Crassostrea ingens*	Parikino, from fallout pile at 240 m on sketch	S22/957572
WLK34	*Crassostrea ingens*	Parikino, from fallout pile at 240 m on sketch	S22/957572
WLK35	*Crassostrea ingens*	Parikino, from fallout pile at 240 m on sketch	S22/957572
WLK37	*Crassostrea ingens*	Parikino, from fallout pile at 240 m on sketch	S22/957572
WLK38	*Crassostrea ingens*	Parikino, from fallout pile at 240 m on sketch	S22/957572
WLK39	*Crassostrea ingens*	Parikino, from fallout pile at 240 m on sketch	S22/957572
WLK40	*Crassostrea ingens*	Parikino, from fallout pile at 240 m on sketch	S22/957572
WLK41	*Crassostrea ingens*	Parikino, from fallout pile at 240 m on sketch	S22/957572
WLK42A	*Crassostrea ingens*	Parikino, from fallout pile at 240 m on sketch	S22/957572
WLK42B	*Crassostrea ingens*	Parikino, from fallout pile at 240 m on sketch	S22/957572
WLK43	*Crassostrea ingens*	Parikino, from fallout pile at 240 m on sketch	S22/957572
WLK44A	*Crassostrea ingens*	Parikino, from fallout pile at 240 m on sketch	S22/957572
WLK44B	*Crassostrea ingens*	Parikino, from fallout pile at 240 m on sketch	S22/957572
K1A-A	*Crassostrea ingens*	Kauarapaua Rd, from column K1	R22/901592
K1A-B	*Crassostrea ingens*	Kauarapaua Rd, from column K1	R22/901592
K1B-A	*Crassostrea ingens*	Kauarapaua Rd, from column K1	R22/901592
K1B-B	*Crassostrea ingens*	Kauarapaua Rd, from column K1	R22/901592
K1C-A	*Crassostrea ingens*	Kauarapaua Rd, from column K1	R22/901592
K1C-B	*Crassostrea ingens*	Kauarapaua Rd, from column K1	R22/901592
K2A-A	*Crassostrea ingens*	Kauarapaua Rd, from column K2	R22/901592
K2A-B	*Crassostrea ingens*	Kauarapaua Rd, from column K2	R22/901592
K2B	*Crassostrea ingens*	Kauarapaua Rd, from column K2	R22/901592
K2C	*Crassostrea ingens*	Kauarapaua Rd, from column K2	R22/901592
K2D	*Crassostrea ingens*	Kauarapaua Rd, from column K2	R22/901592

K3A	*Crassostrea ingens*	Kauarapaua Rd, from column K3	R22/901592
K3B-A	*Crassostrea ingens*	Kauarapaua Rd, from column K3	R22/901592
K3B-B	*Crassostrea ingens*	Kauarapaua Rd, from column K3	R22/901592
K3C-A	*Crassostrea ingens*	Kauarapaua Rd, from column K3	R22/901592
K3C-B	*Crassostrea ingens*	Kauarapaua Rd, from column K3	R22/901592
K3D	*Crassostrea ingens*	Kauarapaua Rd, from column K3	R22/901592
K4C	*Crassostrea ingens*	Kauarapaua Rd, from column K4	R22/974586
K4D	*Crassostrea ingens*	Kauarapaua Rd, from column K4	R22/974586
K4E	*Crassostrea ingens*	Kauarapaua Rd, from column K4	R22/974586
K5B-A	*Crassostrea ingens*	Kauarapaua Rd, from column K5	R22/977584
K5B-B	*Crassostrea ingens*	Kauarapaua Rd, from column K5	R22/977584
K5D	*Crassostrea ingens*	Kauarapaua Rd, from column K5	R22/977584
K5E	*Crassostrea ingens*	Kauarapaua Rd, from column K5	R22/977584
K5F	*Crassostrea ingens*	Kauarapaua Rd, from column K5	R22/977584
K5H-A	*Crassostrea ingens*	Kauarapaua Rd, from column K5	R22/977584
K5H-B	*Crassostrea ingens*	Kauarapaua Rd, from column K5	R22/977584
K6A-A	*Crassostrea ingens*	Kauarapaua Rd, from column K6	R22/986582
K6A-B	*Crassostrea ingens*	Kauarapaua Rd, from column K6	R22/986582
K6B	*Crassostrea ingens*	Kauarapaua Rd, from column K6	R22/986582
No. 5	*Crassostrea ingens*	Bulk samples collected by Casadío, S & Nelson, C.	R16/031616
No. 6	*Crassostrea ingens*	Bulk samples collected by Casadío, S & Nelson, C. Collected from the top of a small channel.	S22/954572
No.7	*Crassostrea ingens*	Bulk samples collected by Casadío, S & Nelson, C. Taken at top of the section close to a '61' sign.	S22/954573

Appendix A1.3 Geological time scale featuring international stages and New Zealand series and stages. Time scale generated from freeware programme 'Timescale Creator'.

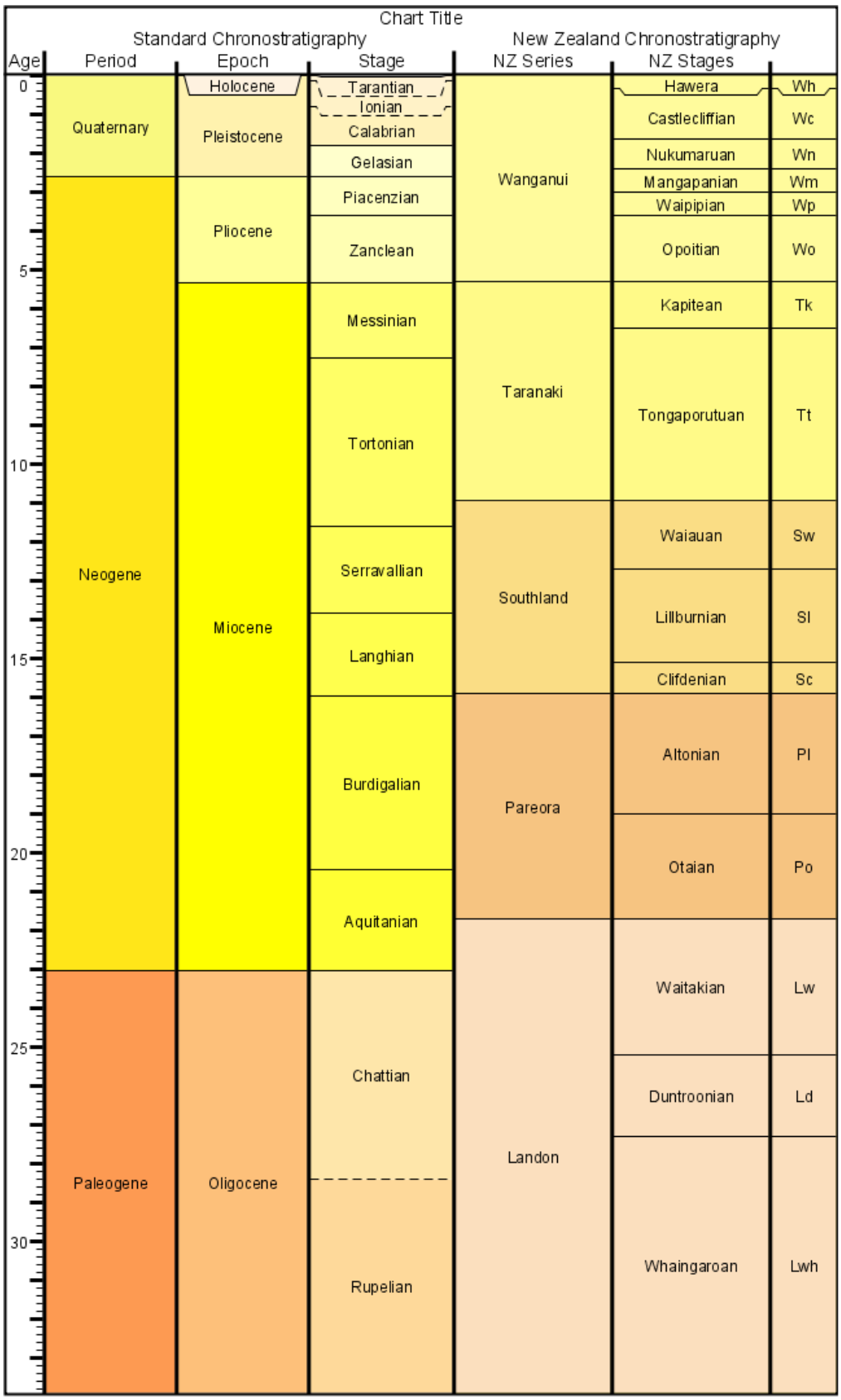
Chart Title
Standard Chronostratigraphy
New Zealand Chronostratigraphy
Age
Period
Epoch
Stage
NZ Series
NZ Stages
0
5
10
15
20
25
30
Quaternary
Neogene
Paleogene
Holocene
Pleistocene
Pliocene
Miocene
Oligocene
Tarantian
Ionian
Calabrian
Gelasian
Piacenzian
Zanclean
Messinian
Tortonian
Serravallian
Langhian
Burdigalian
Aquitanian
Chattian
Rupelian
Wanganui
Taranaki
Southland
Pareora
Landon
Hawera
Castlecliffian
Nukumaruan
Mangapanian
Waipipian
Opoitian
Kapitean
Tongaporutuan
Waiauan
Lillburnian
Clifdenian
Altonian
Otaian
Waitakian
Duntroonian
Whaingaroan
Wh
Wc
Wn
Wm
Wp
Wo
Tk
Tt
Sw
Sl
Sc
Pl
Po
Lw
Ld
Lwh

APPENDIX B

Geochemical data

Appendix B1.1 Table showing all bulk and ligamental isotope results for host sediments and fossil and extant oyster samples. Note ligamental isotopes are recorded from the outer edge of the umbo along the direction of growth. L=lower, M=middle, T=top in relation to reef position at Puerto Pirámide, Patagonia.

Sample	Location	Description	δ13C‰ V-DPB	δ18O‰ V-DPB	Distance (mm)
W04/3A	Waitomo	Orahiri Lst	1.89	-2.92	-
K13/1A	Waitomo	Orahiri Lst	-3.44	-5.15	-
WAP15/1B	Waitomo	Orahiri Lst	0.99	-2.51	-
WVR-2	Waitomo	Orahiri Lst	-3.08	-1.94	-
W02/1B	Waitomo	F. Stenzel	2.17	-1.27	-
W04/3B	Waitomo	F. Stenzel	2.45	-0.38	-
WO7/1A 0	Waitomo	F. Stenzel	1.99	-0.49	-
W10/2A O	Waitomo	F. Stenzel	1.63	-0.20	-
K12/1B O	Waitomo	F. Stenzel	2.12	-0.62	-
N14/1A O	Waitomo	F. Stenzel	0.88	-0.21	-
N14/1C O	Waitomo	F. Stenzel	0.82	0.10	-
WAP15/1BO	Waitomo	F. Stenzel	1.60	0.23	-
FVX1	Foveaux Strt, NZ	*O. chilensis*	0.93	1.44	
PAT 2	Patagonia	*O. patagonica* -L	-2.96	-3.92	-
PAT 2_3	Patagonia	*O. patagonica* -L	-2.38	-3.56	-
PAT 3	Patagonia	*O. patagonica* -M	-2.00	-3.28	-
PAT3_3	Patagonia	*O. patagonica* -M	-3.23	-4.35	-
PAT 4	Patagonia	*O. patagonica* -T	-1.91	-3.14	-
PAT4_3	Patagonia	*O. patagonica* -T	-2.76	-3.82	-
PAT 6	Patagonia	Matrix - top	-2.98	-4.02	-
PAT 7	Patagonia	Matrix - bottom	-4.01	-5.07	-
SAN1a	Patagonia	Location 1	-0.24	-0.94	-
SAN3a	Patagonia	Location 3	-0.48	-0.99	-
PAR 16	Wanganui	Underlying unit	-0.53	-0.39	-
PAR 16A	Wanganui	Reef matrix	1.50	-1.05	-
WLK06A	Wanganui	*C. ingens*	1.88	-2.78	-
WLK17	Wanganui	*C. ingens*	2.27	-0.08	-
WLK 24	Wanganui	*C. ingens*	0.08	2.96	-
WLK 36	Wanganui	*C. ingens*	1.76	-0.23	-
K5A	Wanganui	*C. ingens*	-1.17	-1.35	-
K4B	Wanganui	*C. ingens*	1.64	-0.66	-
K4F	Wanganui	*C. ingens*	-2.64	-2.99	-
N14/1C 1	Wanganui	F. Stenzel	0.99	-0.62	0.10
N14/1C 2	Waitomo	F. Stenzel	0.82	-0.63	0.30
N14/1C 3	Waitomo	F. Stenzel	0.43	-0.45	0.45

N14/1C 4	Waitomo	F. Stenzel	0.39	-0.41	0.60
N14/1C 5	Waitomo	F. Stenzel	0.49	-0.72	0.80
N14/1C 6	Waitomo	F. Stenzel	0.76	-0.51	0.95
N14/1C 7	Waitomo	F. Stenzel	0.67	-0.63	1.10
N14/1C 8	Waitomo	F. Stenzel	0.61	-0.75	1.25
N14/1C 9	Waitomo	F. Stenzel	0.93	-0.49	1.40
N14/1C 10	Waitomo	F. Stenzel	0.90	-0.66	1.55
N14/1C 11	Waitomo	F. Stenzel	0.76	-0.66	1.75
N14/1C 12	Waitomo	F. Stenzel	0.55	-0.40	1.85
N14/1C 13	Waitomo	F. Stenzel	0.78	-0.80	2.00
N14/1C 14	Waitomo	F. Stenzel	0.80	-0.53	2.10
PAT2/1 1	Patagonia	*O. patagonica* - L	-1.75	-3.73	3.50
PAT2/1 2	Patagonia	*O. patagonica* - L	1.68	-0.51	5.00
PAT2/1 3	Patagonia	*O. patagonica* - L	-1.25	-2.52	6.50
PAT2/1 4	Patagonia	*O. patagonica* - L	-1.06	-2.74	8.00
PAT2/1 5	Patagonia	*O. patagonica* - L	0.01	-1.63	9.50
PAT2/1 6	Patagonia	*O. patagonica* - L	-0.35	-2.22	11.00
PAT2/1 7	Patagonia	*O. patagonica* - L	0.67	-1.46	12.00
PAT2/1 8	Patagonia	*O. patagonica* - L	0.40	-1.66	14.00
PAT2/1 9	Patagonia	*O. patagonica* - L	-0.38	-2.51	16.00
PAT2/1 10	Patagonia	*O. patagonica* - L	-0.43	-2.16	18.00
PAT2/1 11	Patagonia	*O. patagonica* - L	-1.50	-3.10	20.00
PAT2/1 12	Patagonia	*O. patagonica* - L	-1.04	-2.69	21.50
PAT2/1 13	Patagonia	*O. patagonica* - L	-1.52	-3.09	24.00
PAT2/1 14	Patagonia	*O. patagonica* - L	-1.46	-2.65	26.00
PAT2/1 15	Patagonia	*O. patagonica* - L	-1.49	-2.98	28.50
PAT2/1 16	Patagonia	*O. patagonica* - L	-0.52	-2.06	32.00
PAT2/1 17	Patagonia	*O. patagonica* - L	-2.03	-3.05	34.00
PAT2/1 18	Patagonia	*O. patagonica* - L	-1.58	-3.17	36.50
PAT2/1 19	Patagonia	*O. patagonica* - L	-1.53	-2.74	38.00
PAT2/1 20	Patagonia	*O. patagonica* - L	-1.50	-2.86	41.00
PAT2/1 21	Patagonia	*O. patagonica* - L	-1.54	-2.90	43.00
PAT2/1 22	Patagonia	*O. patagonica* - L	-1.65	-2.92	45.00
PAT4_1Q	Patagonia	*O. patagonica* - T	-0.52	-2.16	1.00
PAT4_1P	Patagonia	*O. patagonica* - T	-0.56	-1.48	2.50
PAT4_1O	Patagonia	*O. patagonica* - T	-0.82	-2.93	4.00
PAT4_1N	Patagonia	*O. patagonica* - T	-0.99	-2.99	5.00
PAT4_1M	Patagonia	*O. patagonica* - T	-1.08	-2.06	6.50
PAT4_1L	Patagonia	*O. patagonica* - T	-2.65	-4.01	8.00
PAT4_1K	Patagonia	*O. patagonica* - T	-1.30	-3.96	9.00
PAT4_1J	Patagonia	*O. patagonica* - T	-2.13	-3.43	11.00
PAT4_1I	Patagonia	*O. patagonica* - T	-1.23	-3.70	12.50
PAT4_1H	Patagonia	*O. patagonica* - T	-1.51	-3.86	14.50
PAT4_1G	Patagonia	*O. patagonica* - T	-1.41	-2.70	16.00
PAT4_1F	Patagonia	*O. patagonica* - T	-1.29	-3.41	17.50
PAT4_1E	Patagonia	*O. patagonica* - T	-1.14	-2.17	19.00
PAT4_1D	Patagonia	*O. patagonica* - T	-1.18	-3.02	21.00

PAT4_1C	Patagonia	*O. patagonica* - T	-1.80	-3.63	22.00
PAT4_1B	Patagonia	*O. patagonica* - T	-1.79	-3.76	23.50
PAT4_1A	Patagonia	*O. patagonica* - T	-2.22	-4.42	26.00
WLK 14	Wanganui	*C. ingens*	-1.65	-0.90	0.10
WLK 13	Wanganui	*C. ingens*	-2.32	-1.71	0.50
WLK 12	Wanganui	*C. ingens*	-2.00	-1.65	0.85
WLK 11	Wanganui	*C. ingens*	-2.34	-1.66	1.10
WLK 10	Wanganui	*C. ingens*	-1.94	-1.29	1.40
WLK 9	Wanganui	*C. ingens*	-2.66	-1.70	1.70
WLK 8	Wanganui	*C. ingens*	-1.52	-0.91	2.00
WLK 7	Wanganui	*C. ingens*	-1.60	-1.15	2.30
WLK 6	Wanganui	*C. ingens*	-2.30	-1.54	2.55
WLK 5	Wanganui	*C. ingens*	-2.00	-1.76	2.80
WLK 4	Wanganui	*C. ingens*	-2.09	-1.41	3.00
WLK 3	Wanganui	*C. ingens*	-1.45	-1.30	3.40
WLK 2	Wanganui	*C. ingens*	-2.63	-1.57	3.55
WLK 1	Wanganui	*C. ingens*	-3.38	-2.13	3.70
SAN_1a 10	San Blas	*C.gigas*	0.04	-0.96	1.00
SAN_1a 9	San Blas	*C.gigas*	-0.03	-1.38	3.00
SAN_1a 8	San Blas	*C.gigas*	-0.21	-1.99	5.00
SAN_1a 7	San Blas	*C.gigas*	-0.60	-1.70	6.50
SAN_1a 6	San Blas	*C.gigas*	-0.29	-1.59	7.50
SAN_1a 5	San Blas	*C.gigas*	-0.63	-1.82	9.50
SAN_1a 4	San Blas	*C.gigas*	-0.32	-0.66	11.00
SAN_1a 3	San Blas	*C.gigas*	-0.39	-1.18	13.50
SAN_1a 2	San Blas	*C.gigas*	-0.44	-1.64	14.50
SAN_1a 1	San Blas	*C.gigas*	-0.58	-0.98	15.50
SAN_3d 2	San Blas	*C.gigas*	-0.60	-0.69	0.45
SAN_3d 1	San Blas	*C.gigas*	-0.59	0.36	0.60
SAN_3d 9	San Blas	*C.gigas*	-0.95	-0.62	0.70
SAN_3d 8	San Blas	*C.gigas*	-0.99	-0.90	0.85
SAN_3d 7	San Blas	*C.gigas*	-0.79	-1.45	1.00
SAN_3d 6	San Blas	*C.gigas*	-0.68	-2.02	1.10
SAN_3d 5	San Blas	*C.gigas*	-0.55	-1.70	1.20
SAN_3d 4	San Blas	*C.gigas*	-0.44	-1.43	1.30
SAN_3d 3	San Blas	*C.gigas*	-0.14	-1.28	1.45
FVX1_I	Foveaux Strt, NZ	*O.chilensis*	-0.03	0.04	3.00
FVX1_H	Foveaux Strt, NZ	*O.chilensis*	-0.22	0.17	4.00
FVX1_G	Foveaux Strt, NZ	*O.chilensis*	0.32	0.00	5.50
FVX1_F	Foveaux Strt, NZ	*O.chilensis*	-0.22	0.24	7.50
FVX1_E	Foveaux Strt, NZ	*O.chilensis*	-0.19	0.38	9.00
FVX1_D	Foveaux Strt, NZ	*O.chilensis*	-0.05	0.06	11.00
FVX1_C	Foveaux Strt, NZ	*O.chilensis*	0.38	0.12	14.00
FVX1_B	Foveaux Strt, NZ	*O.chilensis*	0.11	0.18	16.00
FVX1_A	Foveaux Strt, NZ	*O.chilensis*	0.14	0.00	18.00

Appendix B1.2 Table featuring all bulk and incremental trace element data collected via LA-ICP-MS. Wtm=Waitomo, Pat=Patagonia, Wng=Wanganui.

			Element					
Sample number	**Location**	**Distance (mm)**	**Na23**	**Mg24**	**Ca42**	**Fe57**	**Mn55**	**Sr88**
N14_1C_1	Wtm	0	239.3	1724.3	400447.0	244.5	10.0	460.6
N14_1C_3	Wtm	750	146.4	2008.5	400447.0	256.3	10.6	445.2
N14_1C_5	Wtm	1500	61.2	1731.1	400447.0	6016.1	70.2	421.4
N14_1C_6	Wtm	2250	415.7	2149.8	400447.0	528.6	14.5	402.6
N14_1C_7	Wtm	3000	174.7	1679.9	400447.0	348.8	7.0	524.1
N14_1C_8	Wtm	3750	363.7	1505.6	400447.0	-	17.0	491.7
N14_1C_9	Wtm	4500	955.8	1300.3	400447.0	298.3	6.3	530.3
N14_1C_10	Wtm	5250	830.9	1481.4	400447.0	191.6	15.3	512.4
N14_1C_11	Wtm	6000	237.0	2011.0	400447.0	515.6	31.6	341.8
N14_1C_12	Wtm	6750	175.3	1659.9	400447.0	290.6	10.0	502.5
N14_1C_13	Wtm	7500	69.3	1614.0	400447.0	493.7	19.5	322.3
N14_1C_14	Wtm	8250	204.2	2258.0	400447.0	774.6	32.8	339.3
N14_1C_15	Wtm	9000	326.2	1523.3	400447.0	326.7	6.9	415.4
N14_1C_18	Wtm	9750	115.1	1564.2	400447.0	1780.3	35.5	281.8
N14_1C_19	Wtm	10500	490.1	2036.8	400447.0	436.8	7.9	385.1
N14_1C_20	Wtm	11250	185.2	2015.4	400447.0	291.5	11.4	397.7
N14_1C_21	Wtm	12000	152.0	1535.6	400447.0	580.5	12.2	392.9
N14_1C_22a	Wtm	12750	60.5	2178.3	400447.0	748.2	60.8	286.9
N14_1C_23	Wtm	13500	-	-	-	-	-	-
N14_1C_24	Wtm	14250	167.8	1882.8	400447.0	896.8	37.4	287.5
N14_1C_25	Wtm	15000	7.4	891.5	400447.0	6033.9	60.3	139.2
N14_1C_26	Wtm	15750	50.3	1642.1	400447.0	645.5	22.3	305.8
N14_1C_27	Wtm	16500	114.7	2451.6	400447.0	1358.1	27.8	376.1
N14_1C_28	Wtm	17250	158.3	1931.5	400447.0	235.4	6.9	366.8
N14_1C_29	Wtm	18000	19.5	3270.7	400447.0	1872.1	53.0	477.2
N14_1C_30	Wtm	18750	214.5	2010.8	400447.0	218.4	7.5	436.8
N14_1C_31	Wtm	19500	133.9	1923.6	400447.0	326.3	10.8	403.8
N14_1C_32	Wtm	20250	419.8	1865.3	400447.0	1052.0	13.5	505.8
N14_1C_33	Wtm	21000	15.2	3899.2	400447.0	1388.8	48.2	209.3
N14_1C_34	Wtm	21750	333.7	2621.0	400447.0	635.3	12.2	412.7
N14_1C_35	Wtm	22500	269.5	1734.1	400447.0	260.3	7.8	472.7
PAT2_1	Pat	0	937.6	1168.3	400446.9	131.4	173.0	392.9
PAT2_2	Pat	100	996.2	1302.6	400446.9	666.4	108.3	425.8
PAT2_3	Pat	200	895.2	1312.3	400446.9	375.0	231.4	374.9
PAT2_4	Pat	300	776.7	1372.5	400446.9	410.3	259.6	373.9
PAT2_5	Pat	400	893.9	1773.1	400446.9	236.5	1139.1	214.2
PAT2_6	Pat	500	714.0	1243.5	400446.9	310.6	176.3	357.6
PAT2_7	Pat	600	923.7	1115.3	400446.9	452.3	164.0	368.3
PAT2_8	Pat	700	465.1	1364.8	400446.9	268.9	228.4	209.0
PAT2_9	Pat	800	343.8	1342.4	400446.9	155.6	321.0	162.8
PAT2_10	Pat	900	768.2	1609.2	400446.9	79.4	199.0	242.8
PAT2_11	Pat	1000	437.1	1312.0	400446.9	350.5	280.8	135.3

PAT2_12	Pat	1100	570.6	1366.8	400446.9	331.7	226.3	259.4
PAT2_13	Pat	1200	372.3	1337.1	400446.9	103.5	356.3	141.5
PAT2_14	Pat	1300	374.3	1430.5	400446.9	419.1	3320.2	144.7
PAT2_15	Pat	1400	311.4	1232.9	400446.9	376.4	328.4	123.1
PAT2_16	Pat	1500	471.8	1327.0	400446.9	61.3	302.9	159.5
PAT2_17	Pat	1600	714.2	1531.3	400446.9	357.9	241.7	199.9
PAT2_18	Pat	1700	1358.1	1411.6	400446.9	301.9	133.2	336.9
PAT2_19	Pat	1800	1083.3	2098.0	400446.9	367.9	494.4	257.8
PAT2_20	Pat	1900	1884.8	2398.6	400446.9	203.7	274.9	320.4
PAT2_21	Pat	2000	415.0	1206.3	400446.9	153.3	361.3	204.1
PAT2_22	Pat	2100	1545.8	1417.9	400446.9	683.6	63.8	375.3
PAT2_23	Pat	2200	793.8	1240.6	400446.9	128.9	188.2	294.1
PAT2_24	Pat	2300	967.9	1145.6	400446.9	353.2	143.7	340.5
PAT2_25	Pat	2400	761.9	1295.0	400446.9	222.5	184.0	267.1
PAT2_26	Pat	2500	616.4	1357.0	400446.9	330.0	167.2	229.0
PAT2_27	Pat	2600	393.9	1279.7	400446.9	482.4	247.7	164.5
PAT2_28	Pat	2700	528.3	1465.6	400446.9	117.0	232.1	236.3
PAT2_29	Pat	2800	966.4	1545.4	400446.9	126.8	231.9	232.1
PAT2_30	Pat	2900	643.7	1469.6	400446.9	419.1	181.9	205.5
PAT2_31	Pat	3000	401.8	1471.9	400446.9	192.1	113.9	196.4
PAT2_32	Pat	3100	291.3	1239.0	400446.9	502.0	214.4	127.2
PAT2_33	Pat	3200	571.7	1354.9	400446.9	156.1	295.3	205.4
PAT2_34	Pat	3300	456.0	1331.7	400446.9	251.8	214.9	153.3
PAT2_35	Pat	3400	509.5	1316.5	400446.9	448.0	146.6	164.4
PAT2_36	Pat	3500	533.3	1397.8	400446.9	239.5	178.5	191.0
PAT2_37	Pat	3600	642.4	1383.8	400446.9	433.6	130.8	220.0
PAT2_38	Pat	3700	837.5	1752.4	400446.9	555.2	489.8	208.3
PAT2_39	Pat	3800	736.6	2256.1	400446.9	732.9	1439.3	272.5
PAT2_40	Pat	3900	908.1	2293.4	400446.9	1123.6	1228.6	277.0
PAT2_41	Pat	4000	1497.6	1905.3	400446.9	585.7	223.5	356.5
PAT2_42	Pat	4100	1265.8	1385.6	400446.9	125.8	166.1	392.7
PAT2_43	Pat	4200	629.7	1322.9	400446.9	484.2	203.1	316.8
PAT2_44	Pat	4300	838.7	1008.6	400446.9	214.5	84.2	355.2
PAT2_45	Pat	4400	1109.7	1126.7	400446.9	471.5	158.2	387.4
PAT2_46	Pat	4500	909.3	1276.9	400446.9	238.4	143.7	349.1
PAT2_47	Pat	4600	1088.4	1204.4	400446.9	263.7	134.7	371.6
PAT2_48	Pat	4700	787.5	1272.9	400446.9	308.5	127.7	308.7
PAT4_1.1	Pat	0	882.5	1203.0	400447.0	166.3	173.1	395.4
PAT4_1.2	Pat	750	1241.3	795.5	400447.0	55.1	98.3	397.2
PAT4_1.3	Pat	1500	912.1	1079.9	400447.0	113.9	199.5	345.3
PAT4_1.4	Pat	2250	856.1	1178.2	400447.0	162.1	159.2	355.3
PAT4_1.5	Pat	3000	1229.8	764.7	400447.0	263.1	149.1	377.2
PAT4_1.6a	Pat	3750	1234.8	1120.1	400447.0	151.6	190.9	382.2
PAT4_1.7	Pat	4500	782.1	963.3	400447.0	287.2	145.0	394.8
PAT4_1.8	Pat	5250	1019.3	1047.7	400447.0	278.3	122.3	391.3
PAT4_1.9	Pat	6000	997.6	982.4	400447.0	399.5	209.3	306.4
PAT4_1.10	Pat	6750	1228.3	1066.1	400447.0	104.7	217.1	348.1
PAT4_1.11	Pat	7500	1022.2	1438.8	400447.0	337.6	288.4	285.5

PAT4_1.12	Pat	8250	1026.0	1406.6	400447.0	178.5	220.9	345.2
PAT4_1.13	Pat	9000	632.0	1202.1	400447.0	234.2	265.1	207.0
PAT4_1.14	Pat	9750	1267.3	1346.6	400447.0	79.2	314.6	422.8
PAT4_1.15	Pat	10500	968.8	1310.6	400447.0	298.4	250.5	306.1
PAT4_1.16	Pat	11250	739.3	1625.4	400447.0	169.0	242.6	290.5
PAT4_1.17a	Pat	12000	746.7	1267.9	400447.0	515.9	274.3	205.8
PAT4_1.18	Pat	12750	1171.0	1245.1	400447.0	436.6	259.5	389.2
PAT4_1.19	Pat	13500	1180.5	1244.2	400447.0	71.1	216.7	441.6
PAT4_1.20	Pat	14250	1355.5	877.3	400447.0	365.2	189.9	330.5
PAT4_1.21	Pat	15000	1557.1	1029.0	400447.0	139.8	180.9	395.5
PAT4_1.22	Pat	15750	1139.7	1049.0	400447.0	163.2	195.2	396.6
PAT4_1.23	Pat	16500	1060.0	1233.5	400447.0	333.5	295.4	339.3
PAT4_1.24	Pat	17250	1334.0	1082.5	400447.0	311.6	212.7	429.2
PAT4_1.25	Pat	18000	1886.4	969.1	400447.0	139.6	128.5	485.3
PAT4_1.26	Pat	18750	2297.6	1042.9	400447.0	117.9	128.3	485.7
PAT4_1.27	Pat	19500	2635.9	1006.1	400447.0	91.4	58.7	577.8
PAT4_1.28	Pat	20250	1078.5	1277.4	400446.9	315.0	621.0	417.0
WLK1	Wng	0	3748.5	911.3	56.0	206.0	9.1	913.8
WLK2	Wng	750	3623.5	973.5	56.0	320.7	7.6	725.0
WLK3	Wng	1500	542.2	4236.1	56.0	1007.9	91.6	391.2
WLK4	Wng	2250	569.0	4227.9	56.0	1364.2	91.3	490.3
WLK5	Wng	3000	3268.1	1268.4	56.0	418.0	15.8	788.9
WLK6	Wng	3750	570.4	3732.6	56.0	1460.6	74.7	415.6
WLK7	Wng	4500	446.7	3213.9	56.0	1370.8	80.8	381.1
WLK8	Wng	5250	365.1	3036.4	56.0	1333.3	76.5	358.2
WLK9	Wng	6000	360.7	3617.8	56.0	1390.4	91.2	407.8
WLK10	Wng	6750	401.0	3402.6	56.0	1330.4	76.0	386.3
WLK11	Wng	7500	591.0	4251.3	56.0	1715.8	86.8	520.9
WLK12	Wng	8250	2422.5	3269.9	56.0	613.0	59.9	449.6
WLK13	Wng	9000	339.0	3593.1	56.0	1514.5	90.2	431.8
WLK14	Wng	9750	1117.9	4087.7	56.0	1324.1	92.4	413.1
WLK15	Wng	10500	551.2	3650.7	56.0	1498.5	78.0	497.6
WLK16	Wng	11250	1597.8	3622.8	56.0	5380.6	102.6	603.8
WLK17	Wng	12750	686.1	3907.3	56.0	1491.3	88.3	551.7
WLK18	Wng	13500	421.9	3790.3	56.0	1584.6	88.3	443.7
WLK19	Wng	14250	536.2	3827.3	56.0	1420.5	102.6	451.8
WLK20	Wng	15000	660.3	4151.0	56.0	1627.0	91.8	450.1
WLK21	Wng	15750	-	4787.8	-	-	-	-
WLK22	Wng	16500	603.5	3914.4	56.0	1701.6	73.7	449.7
WLK23	Wng	17250	553.1	4076.4	56.0	1787.0	88.7	546.8
WLK24	Wng	18000	610.5	3963.4	56.0	1189.3	93.7	489.6
WLK25	Wng	18750	1268.9	3567.5	56.0	1300.1	78.7	521.4
WLK26	Wng	19500	600.5	4036.5	56.0	1674.8	78.1	567.2
WLK27	Wng	20250	519.2	4218.9	56.0	1629.2	92.3	549.3
WLK28	Wng	21000	340.4	2978.5	56.0	1765.8	109.2	387.1
WLK29	Wng	21750	662.2	3375.9	56.0	2023.2	107.6	492.0
WLK30	Wng	22500	391.5	3477.5	56.0	1684.3	99.1	469.0

WLK31	Wng	23250	1787.4	3957.1	56.0	2893.7	111.0	613.1
WLK32	Wng	24000	381.2	3329.5	56.0	1329.9	86.6	555.3
WLK33	Wng	24750	429.6	3903.8	56.0	1854.0	74.2	497.0
WLK34	Wng	25500	491.8	3486.2	56.0	1642.1	81.2	548.4
WLK35	Wng	26250	449.3	3862.0	56.0	1801.8	77.4	506.0
WLK36	Wng	27000	524.6	3576.9	56.0	1651.8	83.4	471.2
WLK37	Wng	27750	905.9	3250.8	56.0	1809.7	88.1	583.8
WLK38	Wng	28500	350.4	3714.1	56.0	1770.2	83.9	462.9
WLK39	Wng	29250	355.8	3751.9	56.0	1551.0	89.8	497.4

APPENDIX C

Petrographic and mineralogical data

Appendix C1.1 X-ray diffractogram results from host sediment and fossil oyster samples.

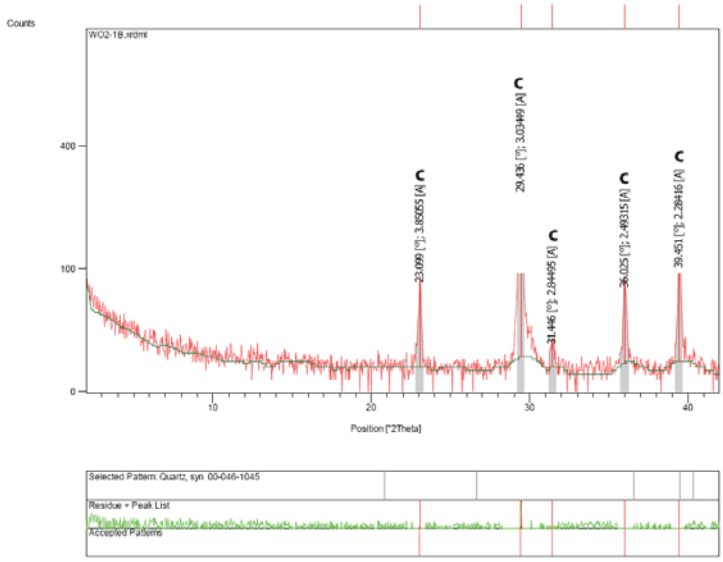

Diffractogram (top) showing XRD results of sample taken from the Orahiri Limestone at Mangapohue Natural Bridge (sample W02/1B). It shows peaks of the mineral calcite (C) which dominates this sample. The lower chart shows the number of counts for each peak corresponding to the above diffractogram.

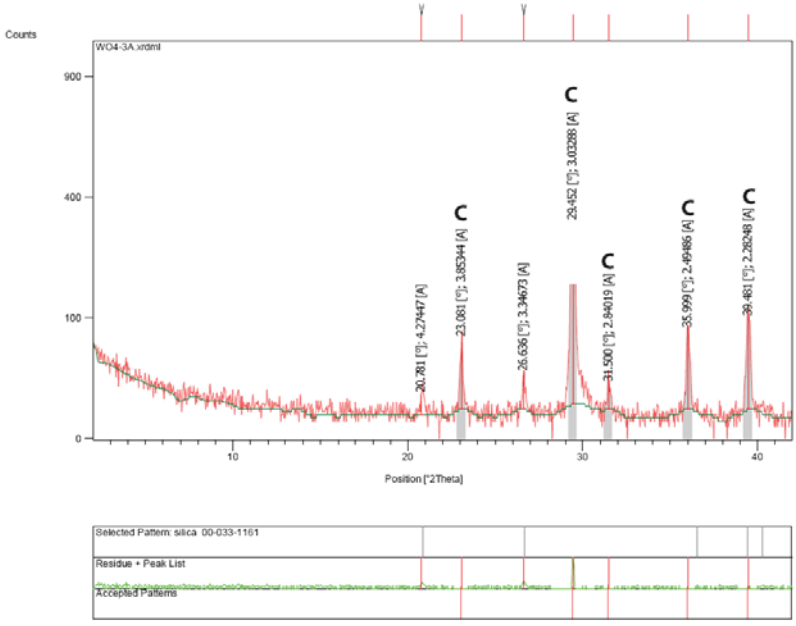

Diffractogram (top) showing XRD results of sample taken from the Orahiri Limestone at Mangapohue Natural Bridge (sample W04/3A). It shows peaks of the mineral calcite (C) which dominates this sample. The lower chart shows the number of counts for each peak corresponding to the above diffractogram.

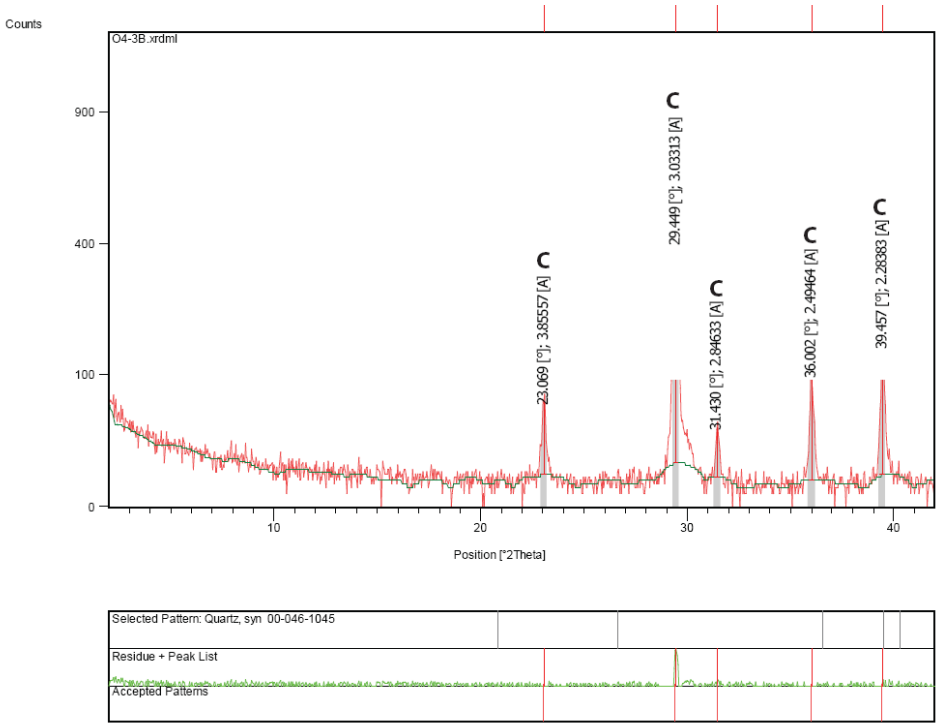

Diffractogram (top) showing XRD results of sample taken from the Orahiri Limestone at Mangapohue Natural Bridge (sample W04/3B). It shows peaks of the mineral calcite (C) which dominates this sample. The lower chart shows the number of counts for each peak corresponding to the above diffractogram.

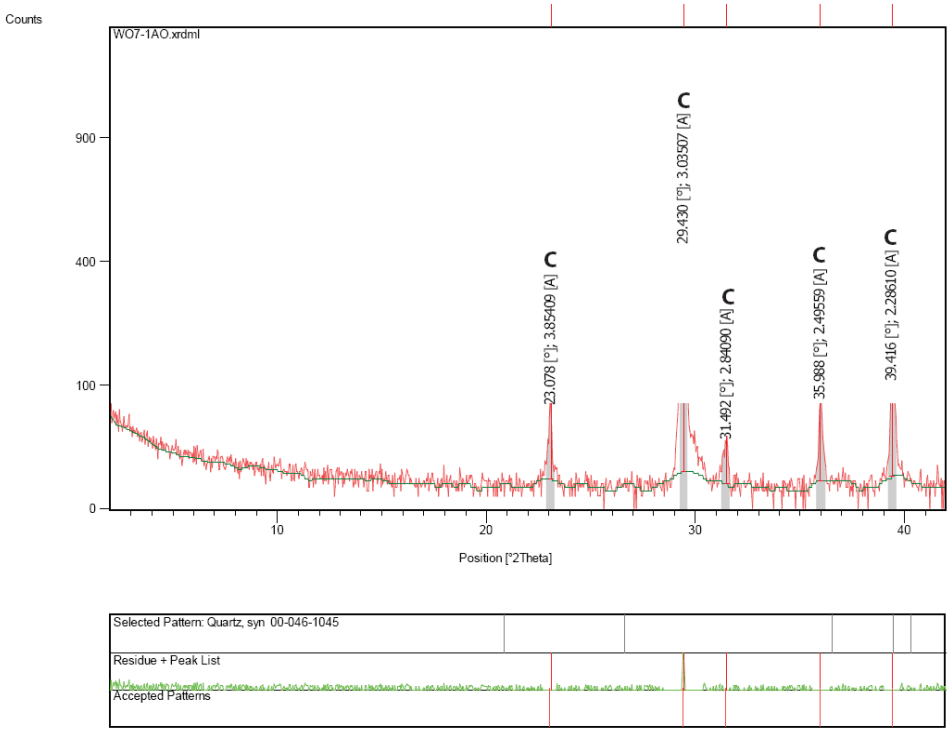

Diffractogram (top) showing XRD results of sample taken from the Orahiri Limestone at Mangapohue Natural Bridge (sample W07/1AO). It shows peaks of the mineral calcite (C) which dominates this sample. The lower chart shows the number of counts for each peak corresponding to the above diffractogram.

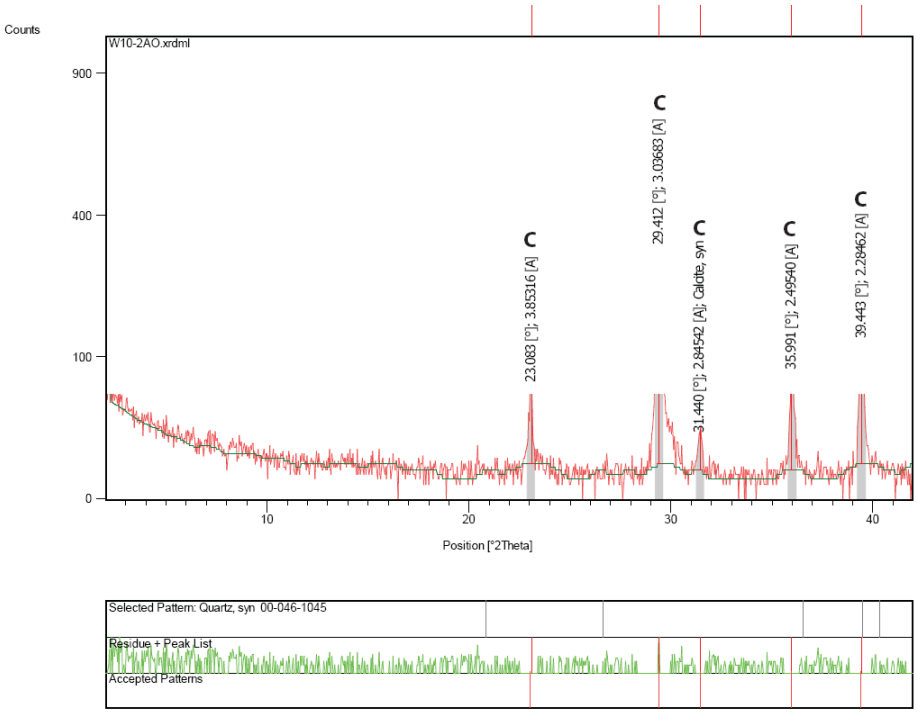

Diffractogram (top) showing XRD results of sample taken from the Orahiri Limestone at Mangapohue Natural Bridge (sample W10/2A). It shows peaks of the mineral calcite (C) which dominates this sample. The lower chart shows the number of counts for each peak corresponding to the above diffractogram.

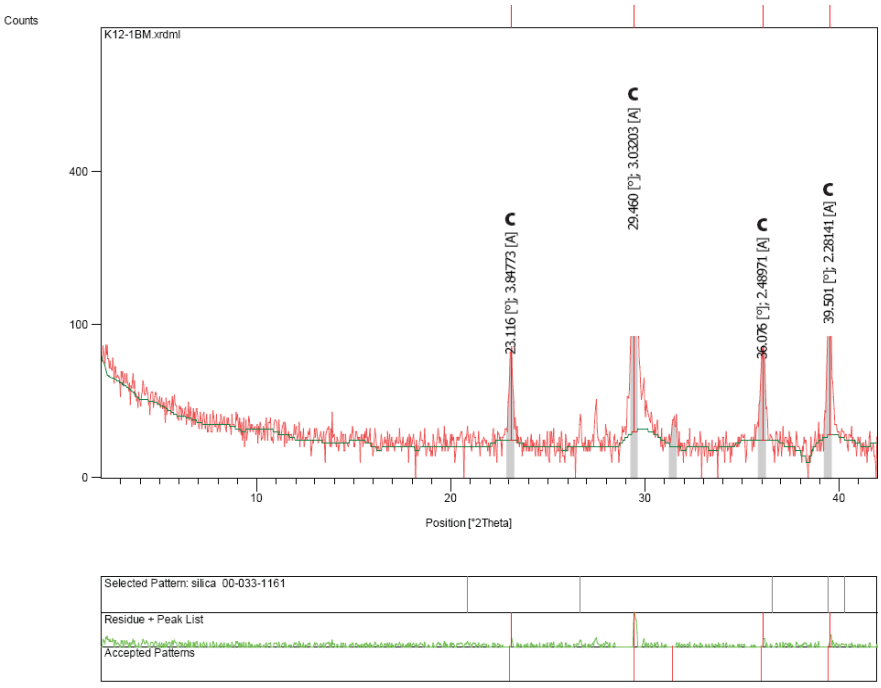

Diffractogram (top) showing XRD results of sample taken from the Orahiri Limestone at Kokakoroa Road (sample K12/1BM). It shows peaks of the mineral calcite (C) which dominates this sample. The lower chart shows the number of counts for each peak corresponding to the above diffractogram.

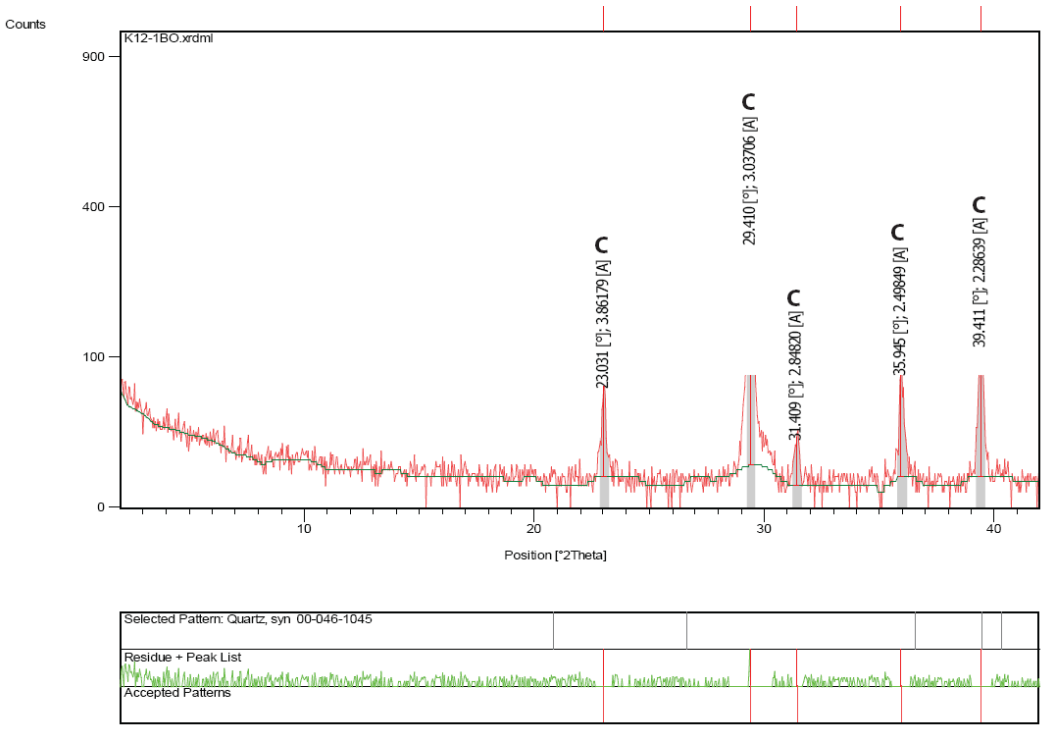

Diffractogram (top) showing XRD results of sample taken from the Orahiri Limestone at Kokakoroa Road (sample K12/1BO). It shows peaks of the mineral calcite (C) which dominates this sample. The lower chart shows the number of counts for each peak corresponding to the above diffractogram.

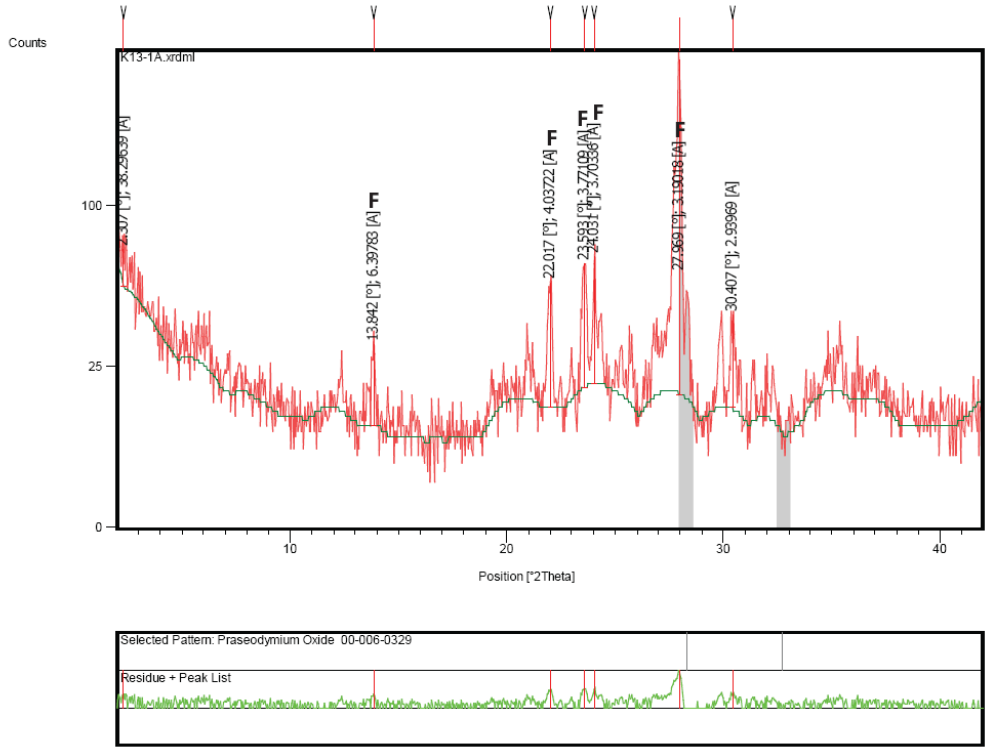

Diffractogram (top) showing XRD results of sample taken from the Orahiri Limestone at Kokakoroa Road (sample K13/1A). It shows peaks of the mineral Feldspar (F) which dominates this sample. The lower chart shows the number of counts for each peak corresponding to the above diffractogram.

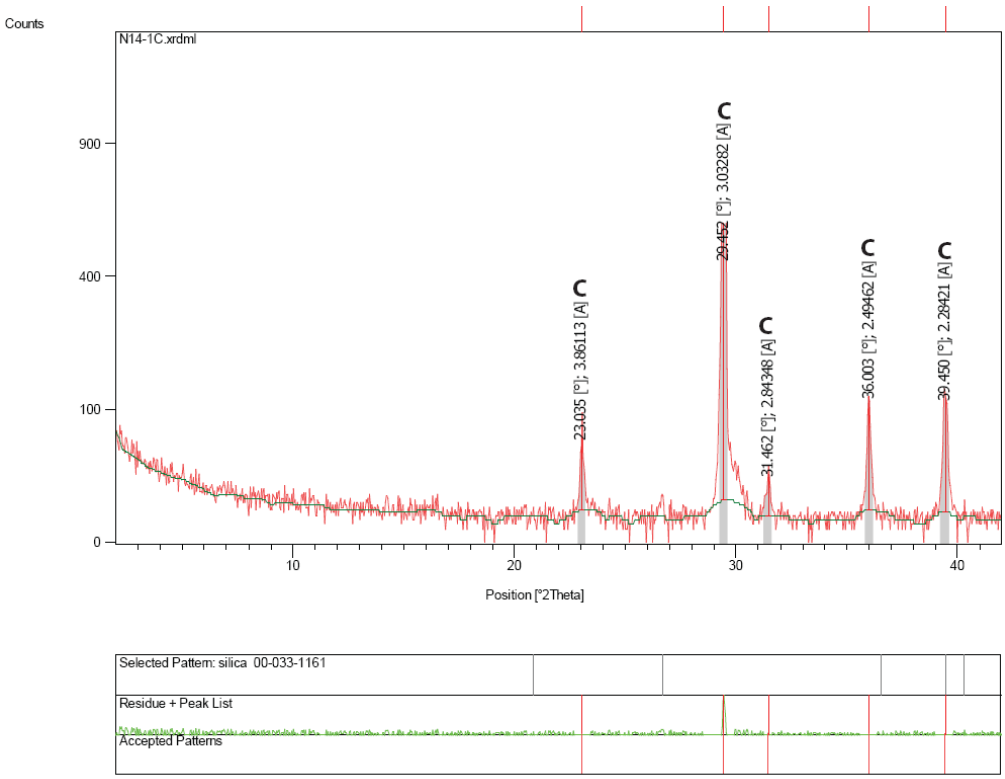

Diffractogram (top) showing XRD results of sample taken from the Orahiri Limestone at Ngapeanga (sample N14/1C). It shows peaks of the mineral calcite (C) which dominates this sample. The lower chart shows the number of counts for each peak corresponding to the above diffractogram.

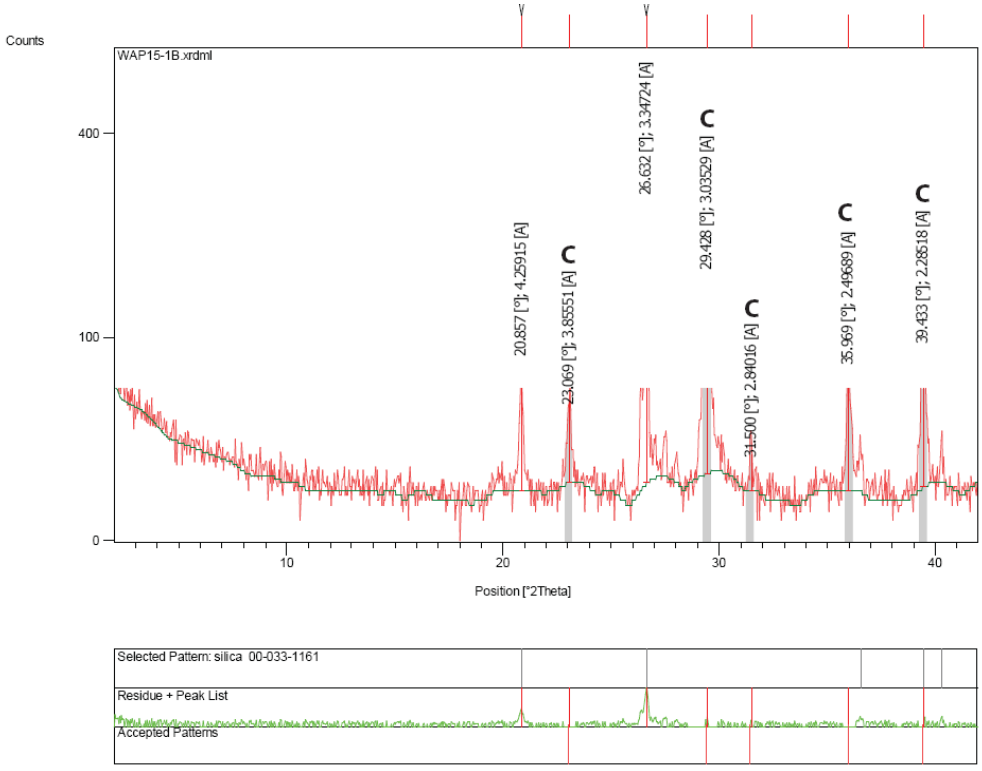

Diffractogram (top) showing XRD results of sample taken from the Orahiri Limestone at Waipuna Road (sample WAP15/1A). It shows peaks of the mineral calcite (C) which dominates this sample. The lower chart shows the number of counts for each peak corresponding to the above diffractogram.

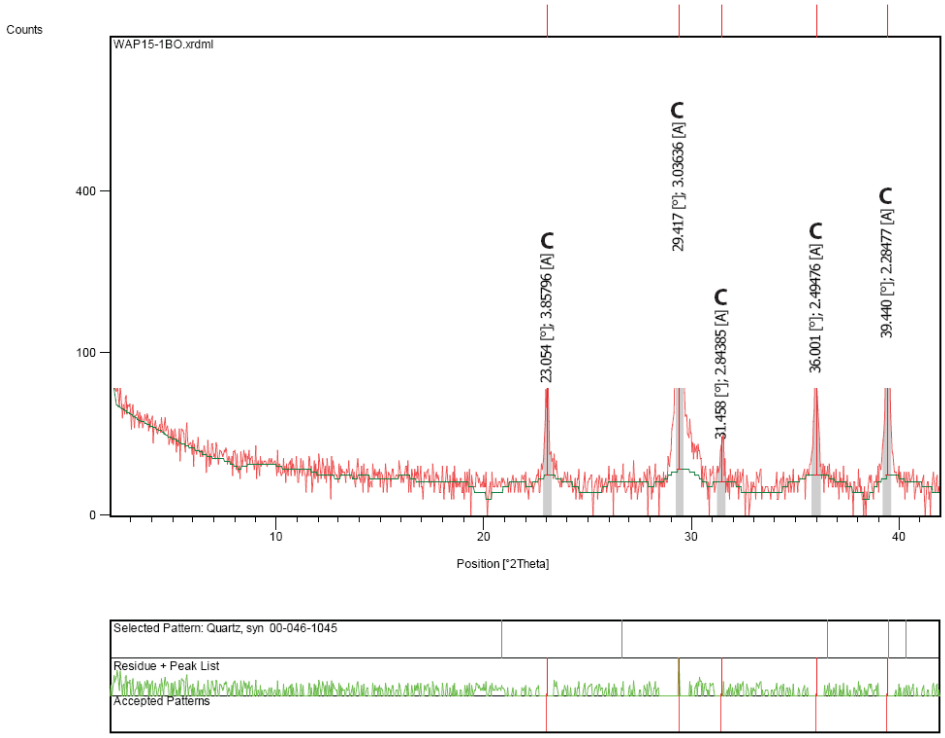

Diffractogram (top) showing XRD results of sample taken from the Orahiri Limestone at Waipuna Road (sample WAP15/1BO). It shows peaks of the mineral calcite (C) which dominates this sample. The lower chart shows the number of counts for each peak corresponding to the above diffractogram.

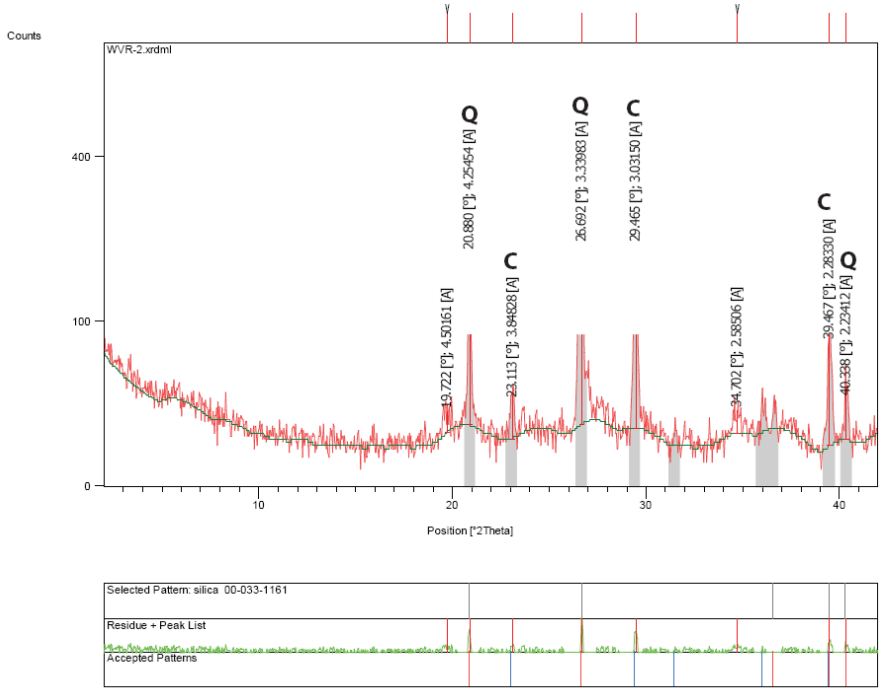

Diffractogram (top) showing XRD results of sample taken from the Orahiri Limestone at Waitomo Valley Road (sample WVR-2). It shows peaks of the mineral calcite (C) and quartz (Q). The lower chart shows the number of counts for each peak corresponding to the above diffractogram.

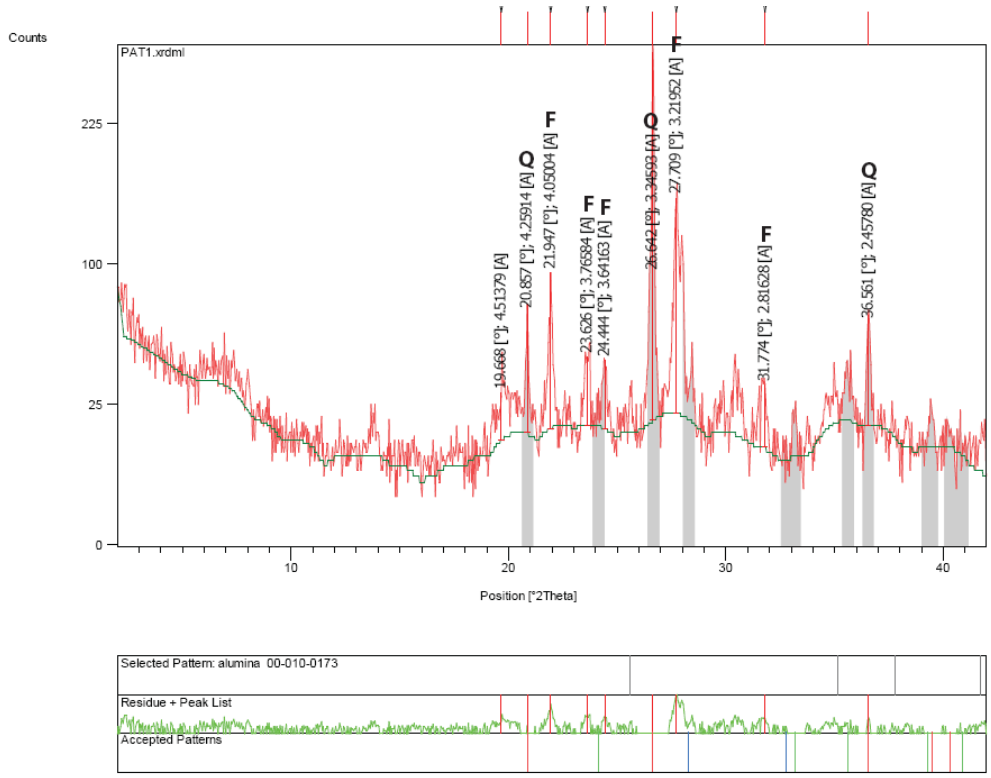

Diffractogram (top) showing XRD results of sample taken from the Puerto Madryn Formation at Puerto Pirámide (sample PAT1). It shows peaks of the mineral quartz (Q) and feldspar (F). The lower chart shows the number of counts for each peak corresponding to the above diffractogram.

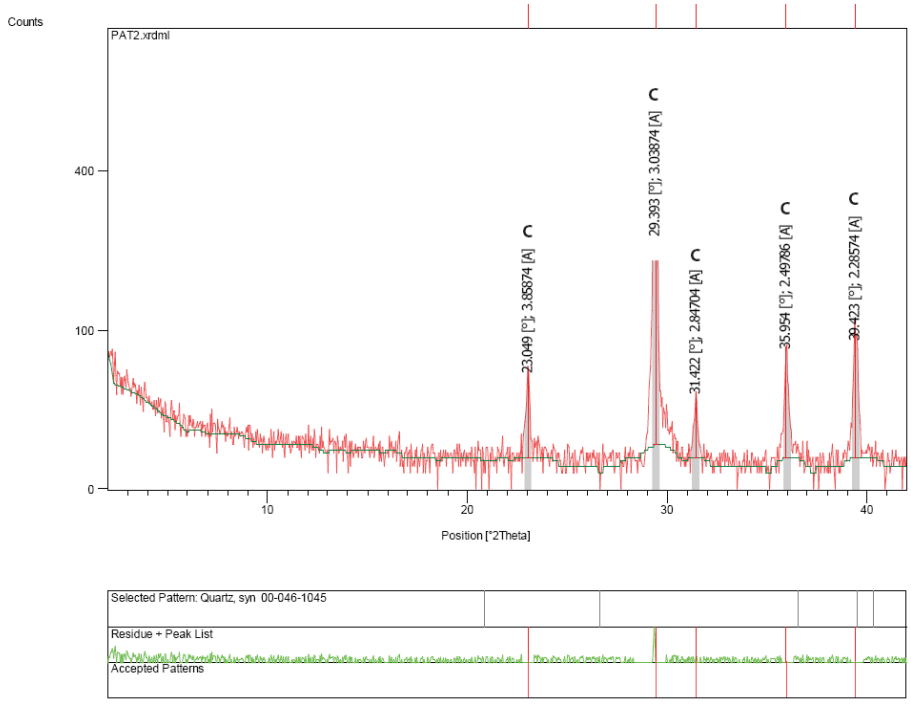

Diffractogram (top) showing XRD results of sample taken from the Puerto Madryn Formation at Puerto Pirámide (sample PAT2). It shows peaks of the mineral calcite (C) which dominates this sample The lower chart shows the number of counts for each peak corresponding to the above diffractogram.

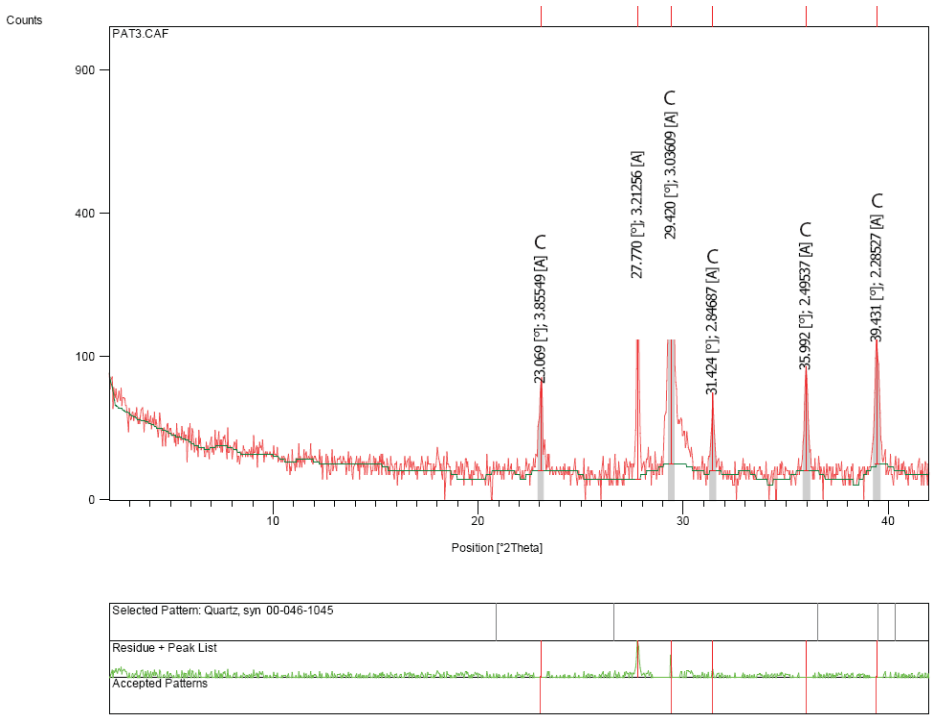

Diffractogram (top) showing XRD results of sample taken from the Puerto Madryn Formation at Puerto Pirámide (sample PAT3). It shows peaks of the mineral calcite (C) which dominates this sample The lower chart shows the number of counts for each peak corresponding to the above diffractogram.

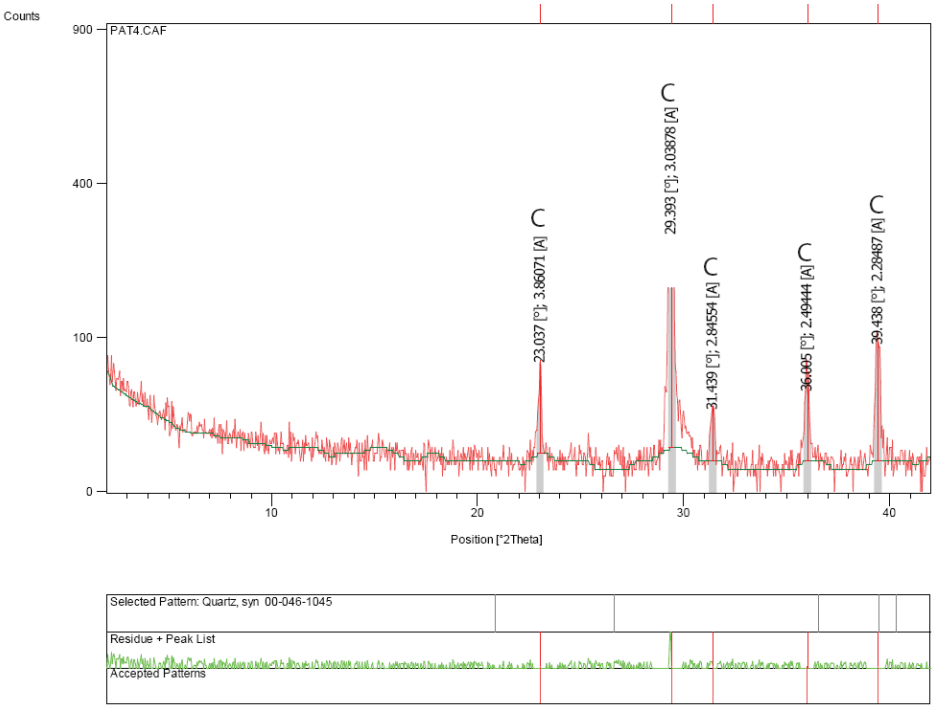

Diffractogram (top) showing XRD results of sample taken from the Puerto Madryn Formation at Puerto Pirámide (sample PAT4). It shows peaks of the mineral calcite (C) which dominates this sample The lower chart shows the number of counts for each peak corresponding to the above diffractogram.

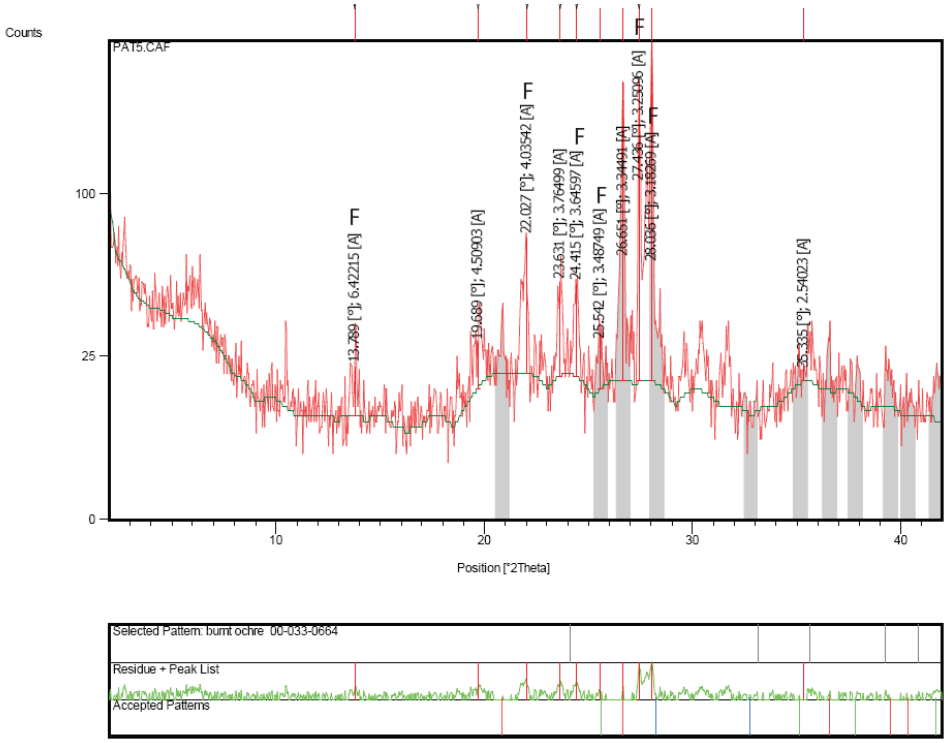

Diffractogram (top) showing XRD results of sample taken from the Puerto Madryn Formation at Puerto Pirámide (sample PAT5). It shows peaks of the mineral feldspar (F) which dominates this sample. The lower chart shows the number of counts for each peak corresponding to the above diffractogram.

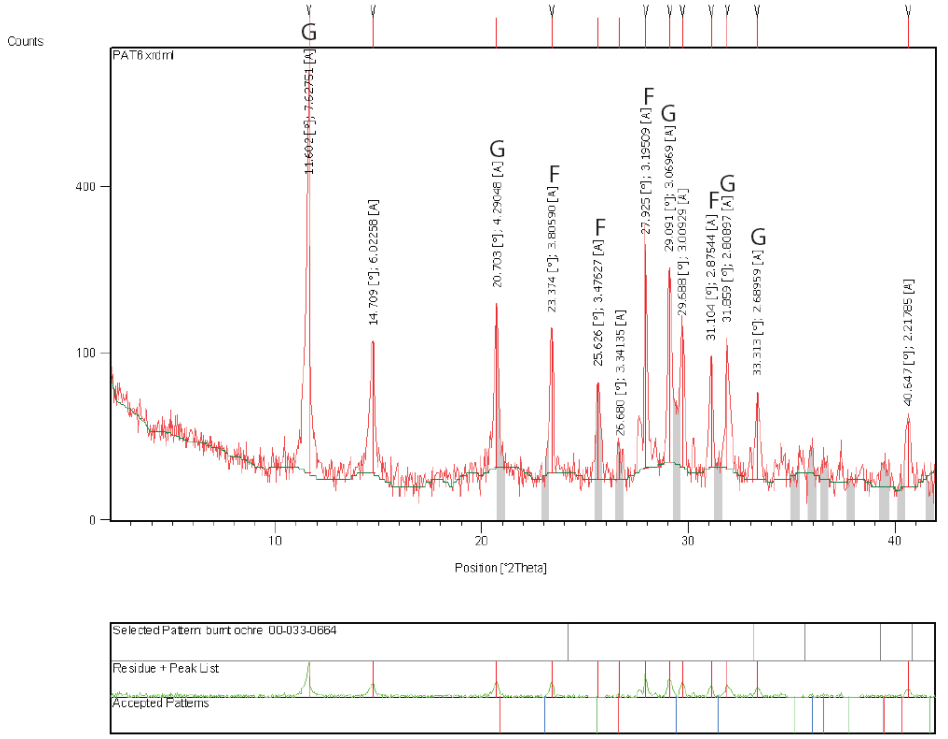

Diffractogram (top) showing XRD results of sample taken from the Puerto Madryn Formation at Puerto Pirámide (sample PAT6). It shows peaks of the mineral feldspar (F) and the evporitic mineral gypsum (G). The lower chart shows the number of counts for each peak corresponding to the above diffractogram.

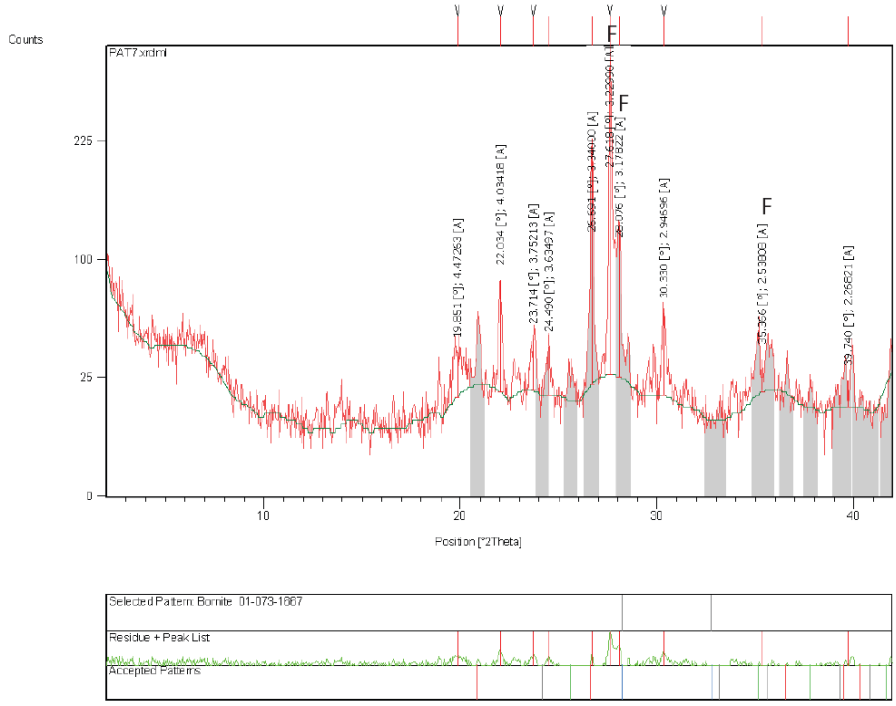

Diffractogram (top) showing XRD results of sample taken from the Puerto Madryn Formation at Puerto Pirámide (sample PAT7). It shows peaks of the mineral feldspar (F). The lower chart shows the number of counts for each peak corresponding to the above diffractogram.

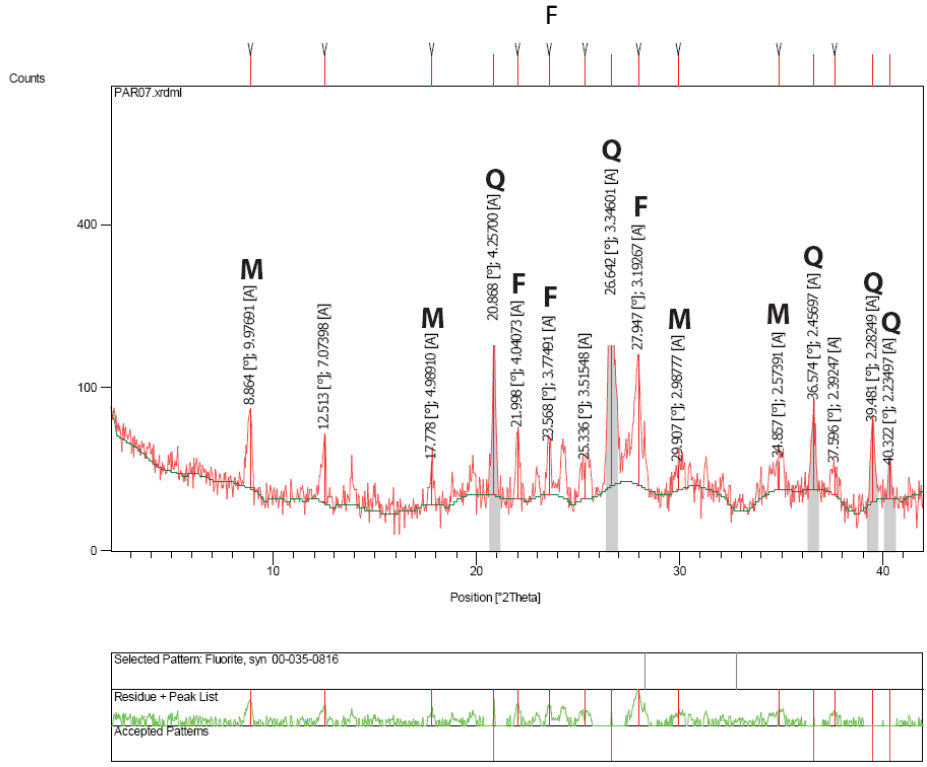

Diffractogram (top) showing XRD results of sample taken from the Wilkies Shellbed at Parikino (sample PAR07). It shows peaks of the mineral quartz (Q), feldspar (F) and muscovite (M). The lower chart shows the number of counts for each peak corresponding to the above diffractogram.

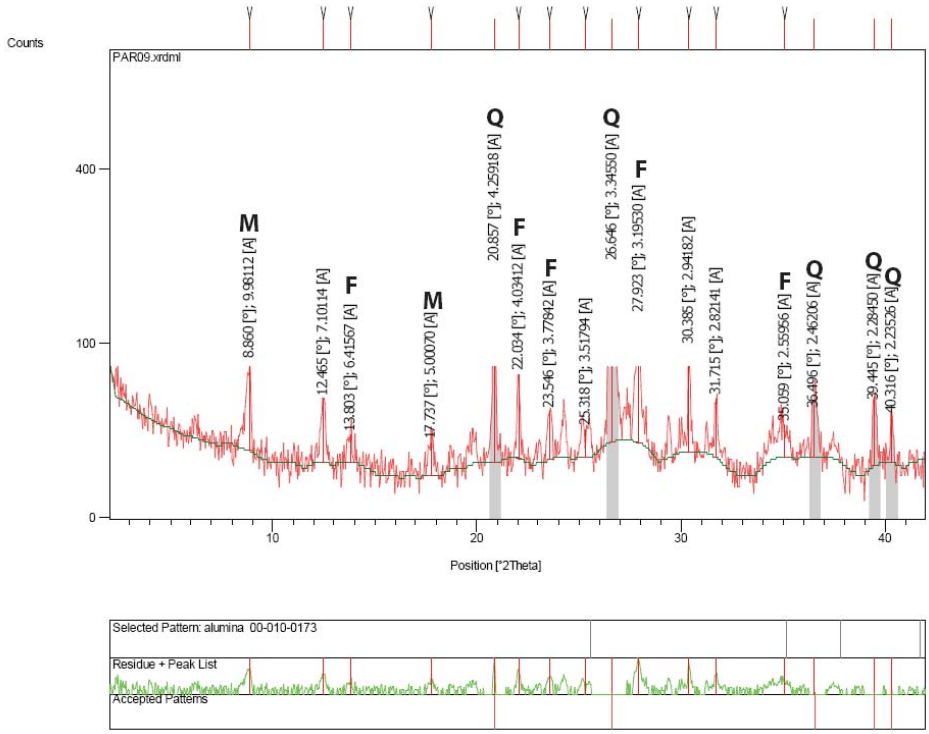

Diffractogram (top) showing XRD results of sample taken from the Wilkies Shellbed at Parikino (sample PAR09). It shows peaks of the mineral quartz (Q), feldspar (F) and muscovite (M). The lower chart shows the number of counts for each peak corresponding to the above diffractogram.

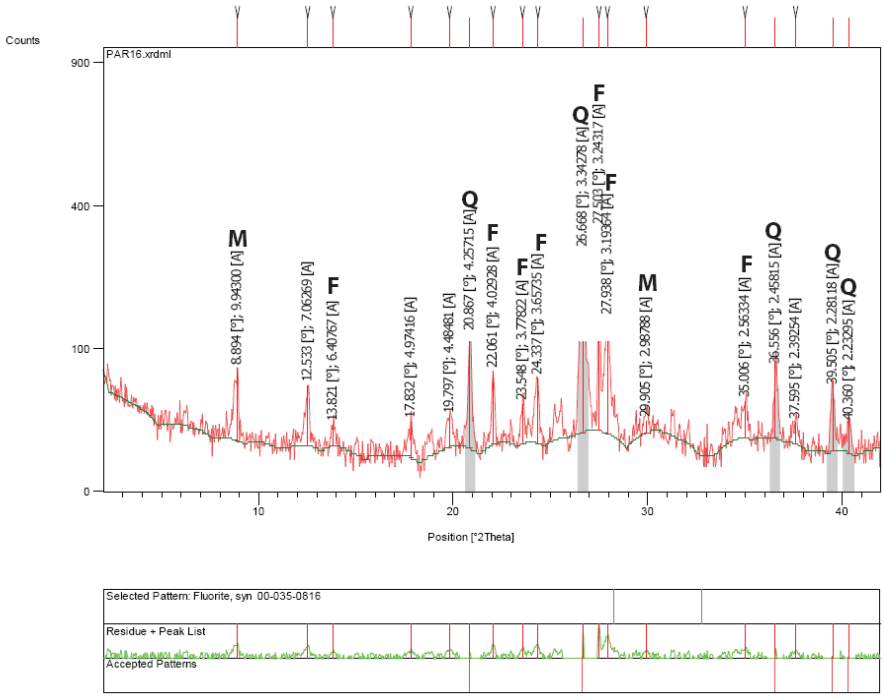

Diffractogram (top) showing XRD results of sample taken from the Wilkies Shellbed at Parikino (sample PAR16). It shows peaks of the mineral quartz (Q), feldspar (F) and muscovite (M). The lower chart shows the number of counts for each peak corresponding to the above diffractogram.

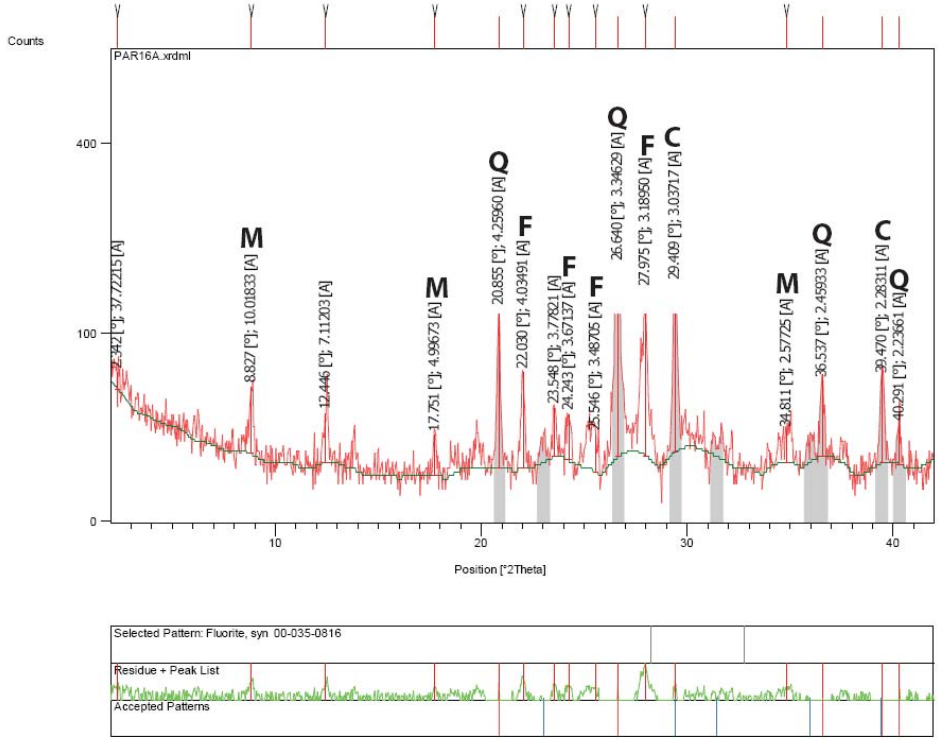

Diffractogram (top) showing XRD results of sample taken from the Wilkies Shellbed at Parikino (sample PAR16A). It shows peaks of the mineral quartz (Q), feldspar (F), calcite (C) and muscovite (M). The lower chart shows the number of counts for each peak corresponding to the above diffractogram.

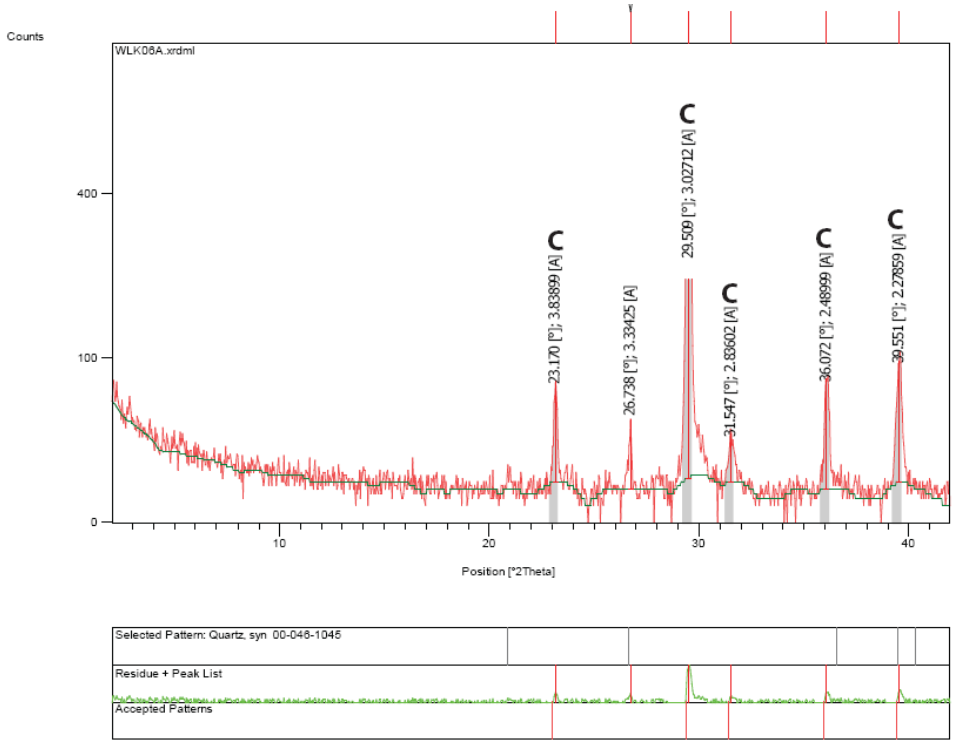

Diffractogram (top) showing XRD results of sample taken from the Wilkies Shellbed at Parikino (sample WLK06A). It shows peaks of the mineral calcite (C) which is dominant in this sample. The lower chart shows the number of counts for each peak corresponding to the above diffractogram.

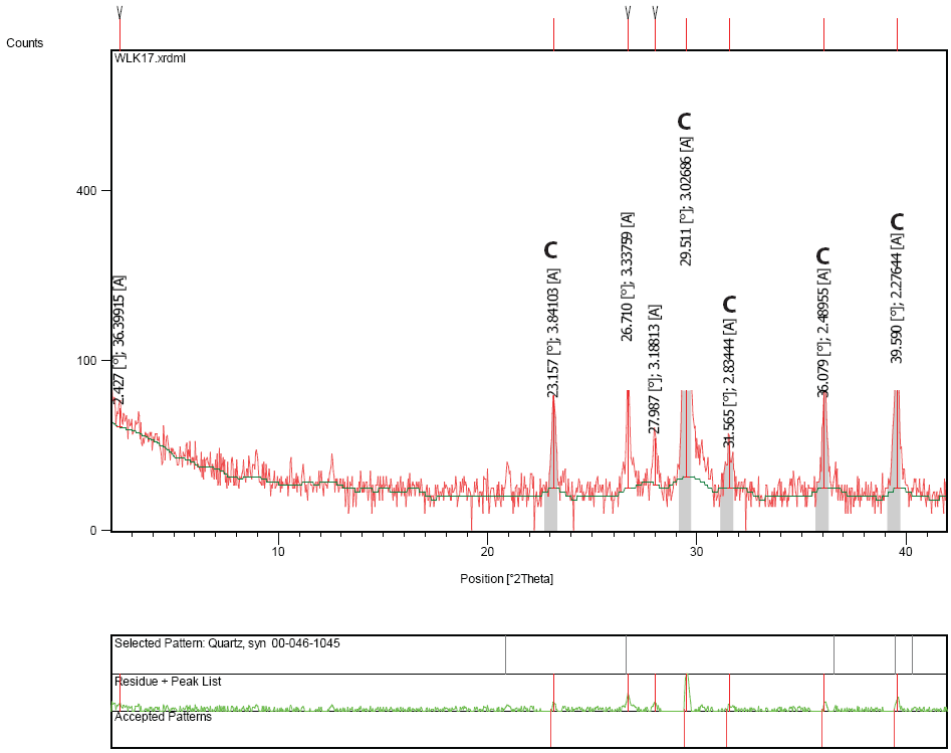

Diffractogram (top) showing XRD results of sample taken from the Wilkies Shellbed at Parikino (sample WLK17). It shows peaks of the mineral calcite (C) which is dominant in this sample. The lower chart shows the number of counts for each peak corresponding to the above diffractogram.

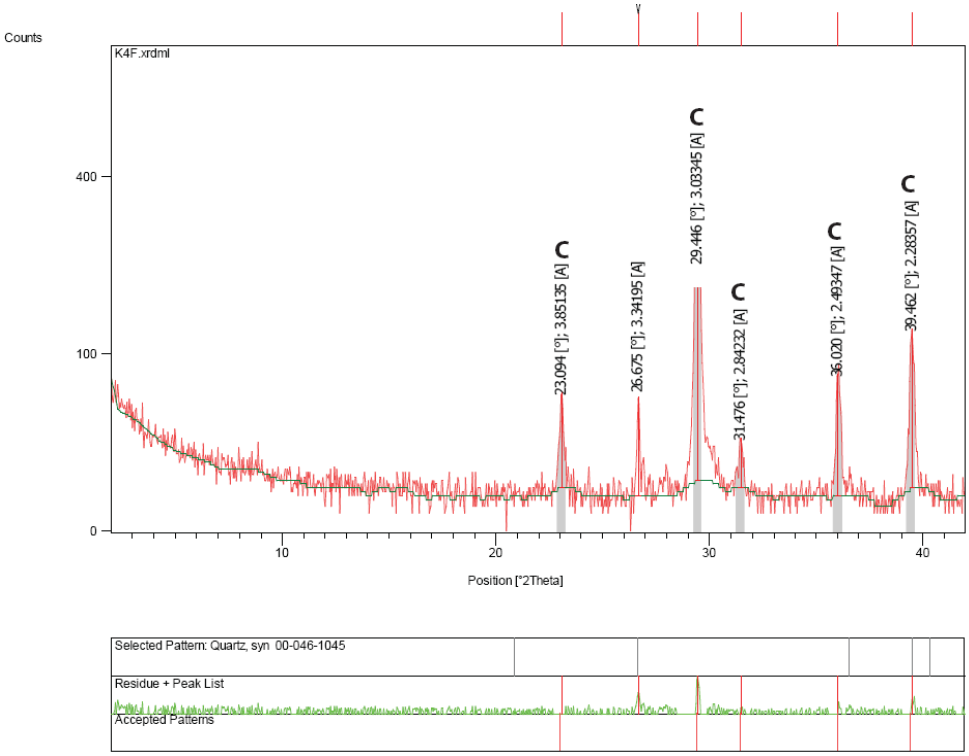

Diffractogram (top) showing XRD results of sample taken from the Wilkies Shellbed at Kauarapaoa Road (sample K4F). It shows peaks of the mineral calcite (C) which dominates this sample. The lower chart shows the number of counts for each peak corresponding to the above diffractogram.

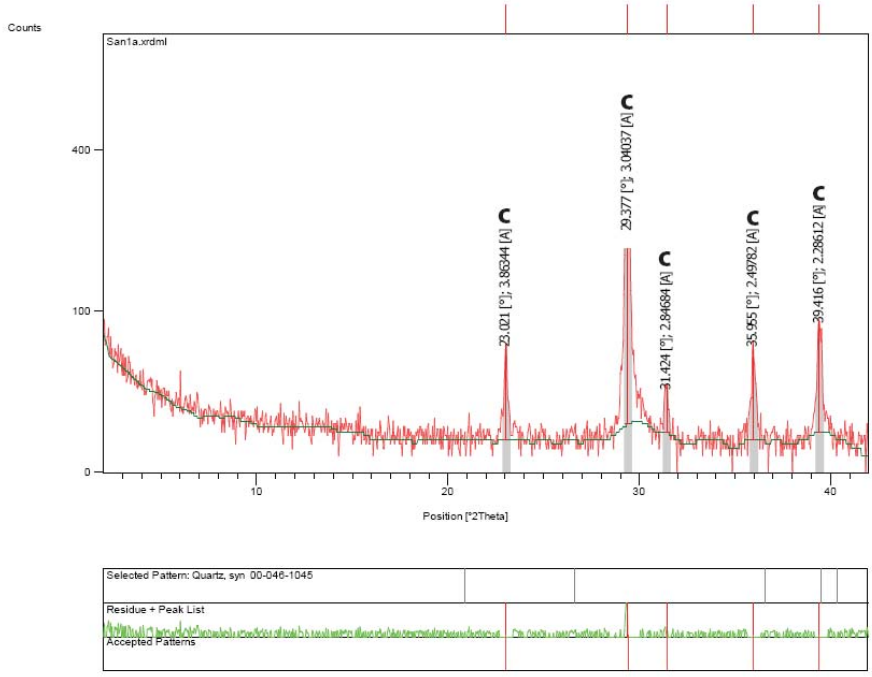

Diffractogram (top) showing XRD results of sample taken from *Crassostrea gigas* from San Blas, Patagonia (sample San1a). It shows peaks of the mineral calcite (C) which dominates this sample. The lower chart shows the number of counts for each peak corresponding to the above diffractogram.

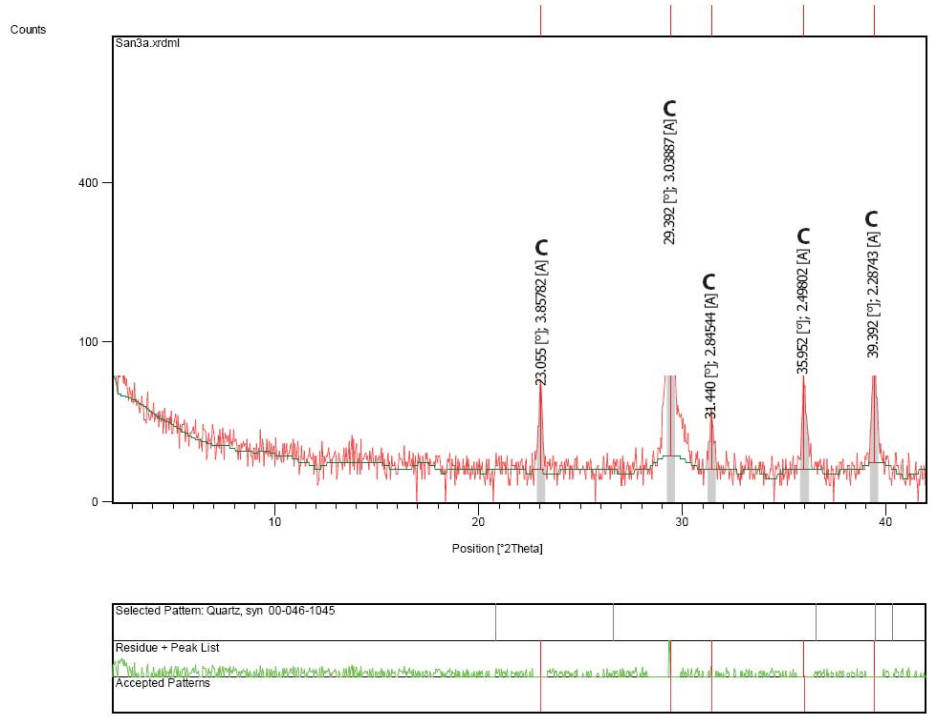

Diffractogram (top) showing XRD results of sample taken from *Crassostrea gigas* from San Blas, Patagonia (sample San3d). It shows peaks of the mineral calcite (C) which dominates this sample. The lower chart shows the number of counts for each peak corresponding to the above diffractogram.

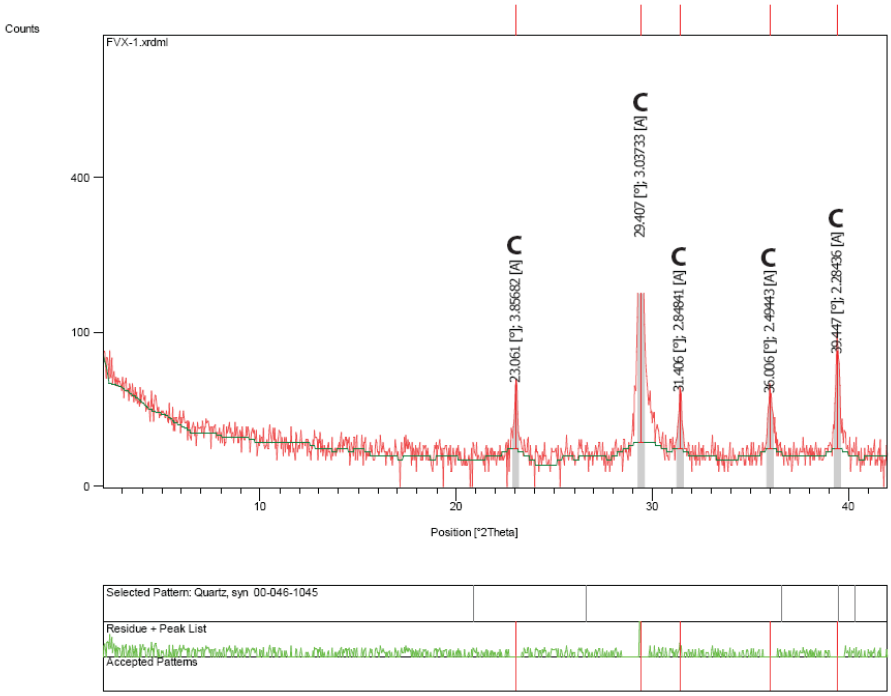

Diffractogram (top) showing XRD results of sample taken from *Ostrea chilensis* from Foveaux Strait, New Zealand (sample FVX1). It shows peaks of the mineral calcite (C) which dominates this sample. The lower chart shows the number of counts for each peak corresponding to the above diffractogram.

Appendix C1.2 Udden-Wentworth size classification for sediment grains.

	Millimetres	Millimetres	Microns	Phi (ϕ) units	Wentworth size class
GRAVEL	4096			-12	boulder
	2048			-11	
	1024			-10	
	512			-9	
	-----256-----	256	256000	-8	cobble
	128	128	128000	-7	
	64	64	64000	-6	
	32	32	32000	-5	
	16	16	16000	-4	
	8	8	8000	-3	pebble
	4	4	4000	-2	
	2	2	2000	-1	granule
SAND	1	1	1000	0	very coarse sand
	0.5	½	500	1	coarse sand
	0.25	¼	250	2	medium sand
	0.125	1/8	125	3	fine sand
	0.0625	1/16	62.5	4	very fine sand
SILT	0.0313	1/32	31.25	5	coarse silt
	0.0156	1/64	15.6	6	medium silt
	0.0078	1/128	7.8	7	fine silt
	0.0039	1/256	3.9	8	very fine silt
CLAY	0.0020		2.0	9	clay
	0.00098		0.98	10	
	0.00049		0.49	11	
	0.00024		0.24	12	
	0.00012		0.12	13	
	0.00006		0.06	14	

Appendix C1.3 Mineralogical peak graphs obtained from GADDs analysis on sample W04/3B from Mangapohue Natural Bridge, Waitomo. W04/3B1 is the area of shell laminae analysed and W04/3B2 pertains to the recrystallised portion of the shell analysed.

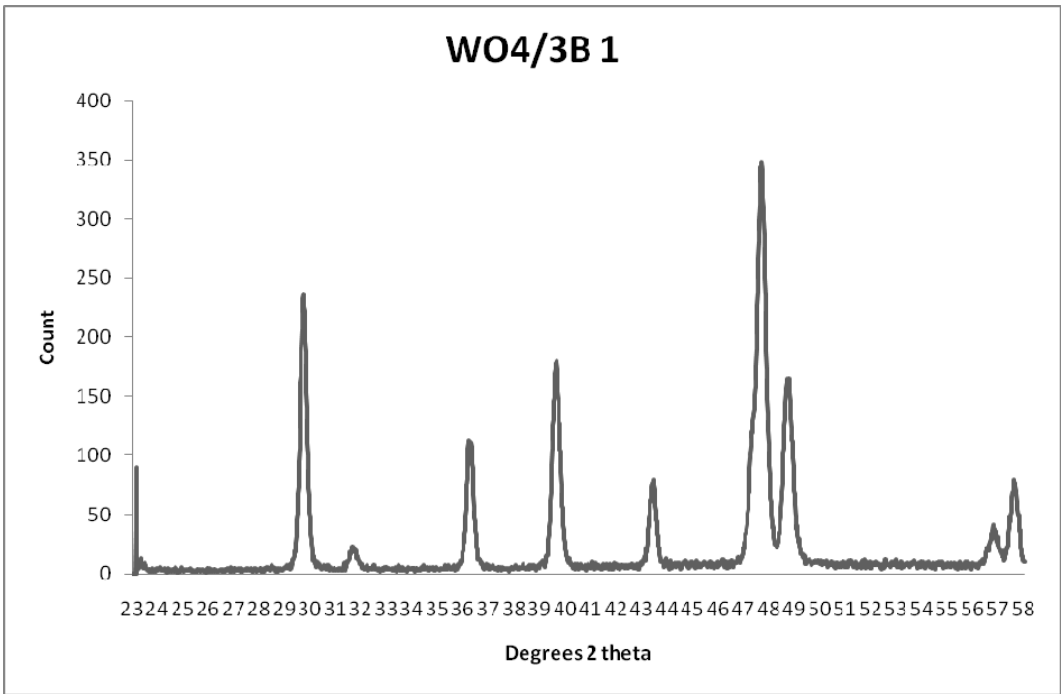

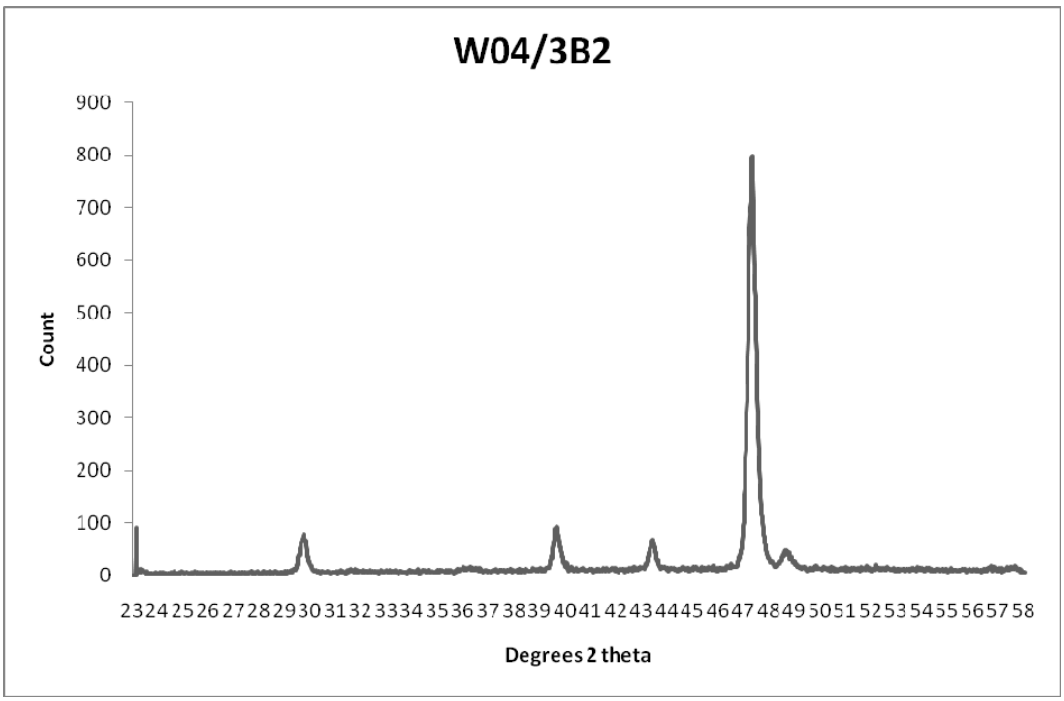

Stratigraphic Column from Mangapohue Natural Bridge 01/1

Logging and other details

Grid Reference (NZMS 260 R16):
2676779 (E)
6325208 (N)

LEGEND

Oyster Density

- Dense bed
- Moderate bed
- Sparse bed

Contacts

- Sharp
- Gradational
- Abruptly gradational

Fossils

- C Flemingostreini Stenzel

Thickness (m)

30
25
20
15
10
5
0

Limestone, flaggy, light grey, surface weathering, very indurated. Rare oyster viewd. Bioclastic matrix.

Limestone, massive, light grey, surface weathered, very indurated. Lense of fossils near the top of the unit, only sparse, majority horizontal, disarticulated, small in size (50-100 mm).

Limestone, massive, light grey, surface weathered, very indurated. Lense of fossils near the bottom of the unit, only sparse, majority horizontal.

Limestone, massive, light grey, surface weathered, very indurated.

Limestone, massive to incipiently seamed, light grey, surface weathering, very indurated. Sparse oysters at the top of the unit, thins distally and some disarticulated specimens. Regular breaks (300 mm) absent of oysters. Haphazard band majority horizontal. The thickest occurence occurs at the bottom of the unit forms a gradationally abrupt contact with underlying limestone.

Limestone, flaggy, light grey, surface weathering, very indurated. Flags 50-100mm apart.

Limestone massive, light grey, surface weathering, very indurated, gradationally abrupt contact with underlying oyster bed.

Limestone, incepiently seamed, light grey, surface weathering, very indurated, abundant oyster fossils. Fossils are abundant in the upper unit with a sharp contact and sparse scattered occurences in the lower part of the unit. Arrangement is very haphazard in the upper part of the unit, but more horizontal in the lower bands. Lower oysters are 50-150 mm in thickness and have large bore holes.

Limestone, fluted, light grey, surface weathering, very indurated, abundant fossils and bioclastic matrix. Oysters form in packed beds at the top and bottom of the unit and a sparse scattering in between, majority of specimens are horizontal, shells are articulated and 60-100mm in size.

← Medium packing.

Limestone, irregularly seamed to massive, light grey, surface weathering, very indurated, increasingly bioclastic, creamy white matrix composed of angular grains, abundant fossils. Oyster fossils horizontally scattered and form in groups of 2-3 specimens making continuous bands. Shells are 60 to 100 mm in length and 200-300 mm in thickness.

Limestone, light grey, surface weathered, very indurated with subrounded terrigenous pebbles floating in the matrix. Pebbles range in size from 8 to 35 mm. Modal size 10 mm, larger pebbles are rare. Pebbles form and abrupt contact with underlying oyster bed and grade out up the section.

Limestone, light grey, slightly weathered, liminite staining in places, very indurated, abundant fossils (20 50 cm²), highly terrigenous. Giant oyster fossils have haphazard orientations both vertical and horizontal. Shells are articulated, size ranges from 150-200mm, borings and bioerosion are obvious on shell.

Grid reference (NZMS 260 R16):
2676757 (E)
6325147 (N)

Logged by Larissa Macmillan and Glen Treweek 17/12/08

Stratigraphic Column from Mangapohue Natural Bridge 02/1

Logging and other details

LEGEND

Oyster Density

- Dense bed
- Moderate bed
- Sparse bed

Contacts

- Sharp
- Gradational
- Abruptly gradational

Fossils

- C Flemingostreini Stenzel

Grid Reference (NZMS 260 R16):
2676929 (E)
6325262 (N)

Hard to view outcrop due to scrub and topography.

Limestone, light grey, surface weathering, very indurated, abundant fossils. Fossil arrangement is mostly horizontal, articulated, individuals are up to 250 mm in length with large borings common. Occurrence forms an abruptly gradational contact with lower unit in some places, in other places it is easy to see the cone shape of nests forming.

Limestone, incipiently seamed, light brown to dark red, moderately weathered, liminite staining visible, very indurated.

Logged by Larissa Macmillan and Glen Treweek 17/12/08

Stratigraphic Column from Mangapohue Natural Bridge 03/1

Logging and other details

LEGEND

Oyster Density

- Dense bed
- Moderate bed
- Sparse bed

Contacts

- Sharp
- Gradational
- Abruptly gradational

Fossils

- C Flemingostreini Stenzel

Very weathered and very difficult to see.

Grid Reference (NZMS 260 R16):
2676929 (E)
6325262 (N)

Height (m)

30
25
20
15
10
5
0

03/1A

Limestone, abundant oyster bed. Oysters have haphazard appearance, majority are horizontal, size 120-250 mm, borings are obvious. Some disarticulated specimens noted.

Limestone, grey to light pink, slightly weathered, very indurated, accumulations of fossils are scattered in nests of 2-3 generations thick, articulated with haphazard orientations.

Limestone, grey, surface weathering very indurated, abundant fossils. Fossil oyster orientation appears haphazard with the majority horizontal, some disarticulated specimens noted, individual size 120-250 mm, thickness up to 150 mm, shells also show large borings.

Limestone, iregularly seamed, grey, surface weathering, very indurated.

Logged by Larissa Macmillan and Glen Treweek 17/12/08

Stratigraphic Column from Mangapohue Natural Bridge 04 /1

Logging and other details

LEGEND

Oyster Density

- Dense bed
- Moderate bed
- Sparse bed

Contacts

- Sharp
- Gradational
- Abruptly gradational

Fossils

- C Flemingostreini Stenzel

Grid Reference (NZMS 260 R16):
2676848 (E)
6325097 (N)

Weathering break

Grid Reference (NZMS 260 R16):
2676818 (E)
6325108 (N)

Logged by Larissa Macmillan and Glen Treweek 18/12/08

Stratigraphic Column from Mangapohue Natural Bridge 05 /1

Logging and other details

LEGEND

Oyster Density

- Dense bed
- Moderate bed
- Sparse bed

Contacts

- Sharp
- Gradational
- Abruptly gradational

Fossils

- C Flemingostreini Stenzel

Grid Reference (NZMS 260 R16):
2676978 (E)
6325316 (N)

Hard to view due to scrub and topography.

Grid Reference (NZMS 260 R16):
2676975 (E)
6325305 (N)

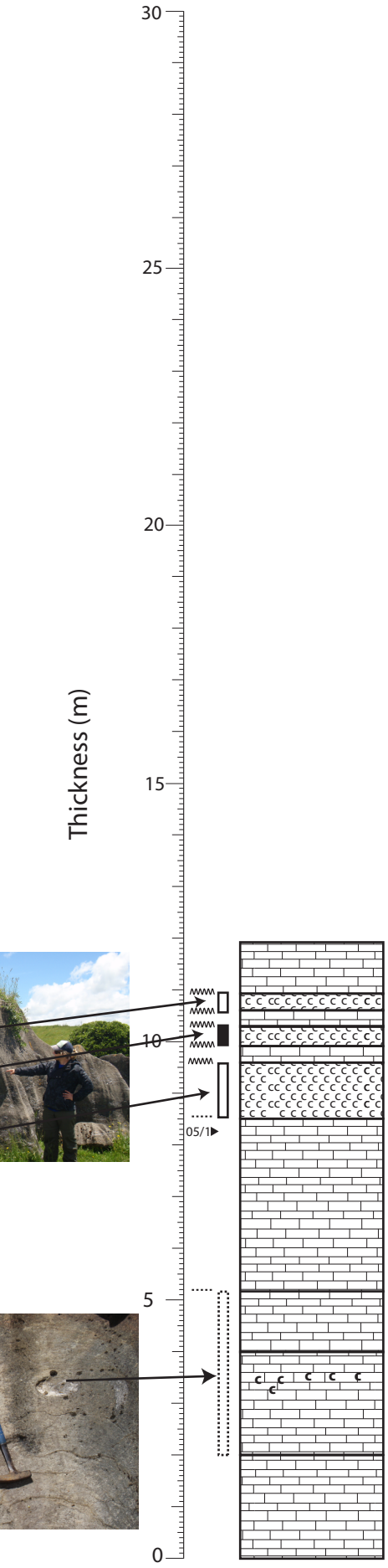

Limestone, massive, light grey, surface weathering, very indurated, moderately packed fossils, bioclastic composition. Fossils occur in bands in the lower part of the unit, majority are horizontal. Specimens mixture of articulated and disarticulated.

Limestone, light grey, surface weathering, indurated, moderately packed fossils. Oysters are haphazardly arranged but most are horizontal, articulated with few disarticulated.

Limestone, flaggy (50-100 mm), light grey, surface weathering, indurated, gradational contact into above oyster bed.

Limestone, massive, light grey, surface weathering, indurated, scattered fossils, bioclastic composition. Scattered oysters form a band, articulated and horizontally orientated.

Limestone, massive, grey, highly weathered, indurared, no fossils

Logged by Larissa Macmillan and Glen Treweek 18/12/08

Stratigraphic Column from Mangapohue Natural Bridge 06 /1

Logging and other details

LEGEND

Oyster Density

- Dense bed
- Moderate bed
- Sparse bed

Contacts

- Sharp
- Gradational
- Abruptly gradational

Fossils

- C Flemingostreini Stenzel

Grid Reference (NZMS 260 R16):
2677109 (E)
6325418 (N)

Grid Reference (NZMS 260 R16):
2677062 (E)
6325396 (N)

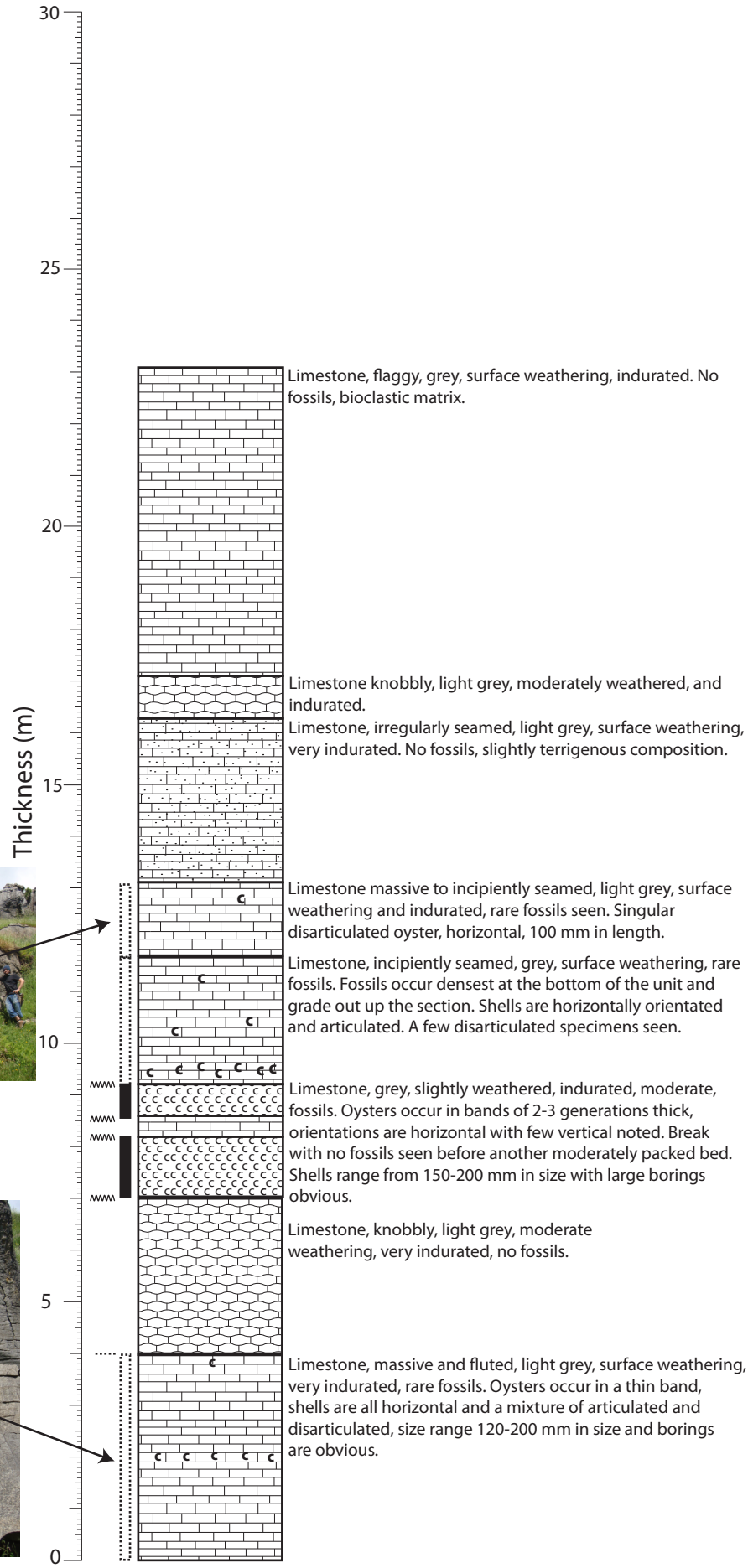

Logged by Larissa Macmillan and Glen Treweek 18/12/08

Stratigraphic Column from Mangapohue Natural Bridge 07 /1

Logging and other details

LEGEND

Oyster Density

- Dense bed
- Moderate bed
- Sparse bed

Contacts

- Sharp
- Gradational
- Abruptly gradational

Fossils

- C Flemingostreini Stenzel

Grid Reference (NZMS 260 R16):
2677241 (E)
6325253 (N)

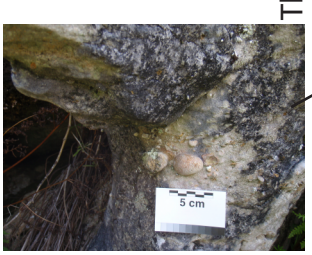

Limestone, massive to incipiently seamed, grey, surface weathering, very indurated, no fossils.

Limestone, massive, light grey, surface weathering, very indurated, rare fossils. Both articulated and disarticulated specimens, shells appear 'fitted', size 150-200 mm.

Limestone, massive, grey, surface weathering, very indurated, fossil rich. Oyster bed very dense (28 1/2 m2), hapahazardly arranged, specimens are articulated and shells appear 'fitted'. Size range 100-220 mm. Borings and bioerosion are obvious.

Limestone, massive, grey, surface weathering, indurated, moderate scattered fossils present. Fossils are concentrated in the centre of the unit and also a lense near the top. A rare disarticulated oyster can be seen at the bottom.

Limestone, massive, light grey, surface weathering, very indurated. Poorly sorted, grey-orange pebbles scattered throughout section, rounded, large size variation (5-20 mm). Greater occurence near bottom and grade out towards the top, abundant fossils. Thick occurence of oysters at the top and small lense near the base. Bottom occurence is haphazard orientations, majority horiztonal, shells articulated and 150-200 mm in size.

Limestone, massive to incipiently seamed, grey to pink, surface weathering, very indurated. Poorly sorted, grey to orange pebbles at bottom of unit, rounded, large size variation (5-30 mm). Modal size 10 mm. Only in scattered band at bottom. No grading, no fossils.

Limestone, massive, grey, surface weathering, indurated, fossil rich. Haphazard arrangement of oysters, majority are horizontal, some vertical shells seen. Specimens articulated, large size variation (100-200 mm).

Limestone, fluted and massive, light grey, surface weathering and very indurated.

Limestone, massive to incipiently seamed, light grey, surface weathering, very indurated, no fossils, composition is slightly terrigenous.

Logged by Larissa Macmillan and Glen Treweek 18/12/08

Stratigraphic Column from Mangapohue Natural Bridge 07/2

Logging and other details

Grid Reference (NZMS 260 R16):
2677198 (E)
6325149 (N)

LEGEND

Oyster Density

- Dense bed
- Moderate bed
- Sparse bed

Contacts

- Sharp
- Gradational
- Abruptly gradational

Fossils

- C Flemingostreini Stenzel

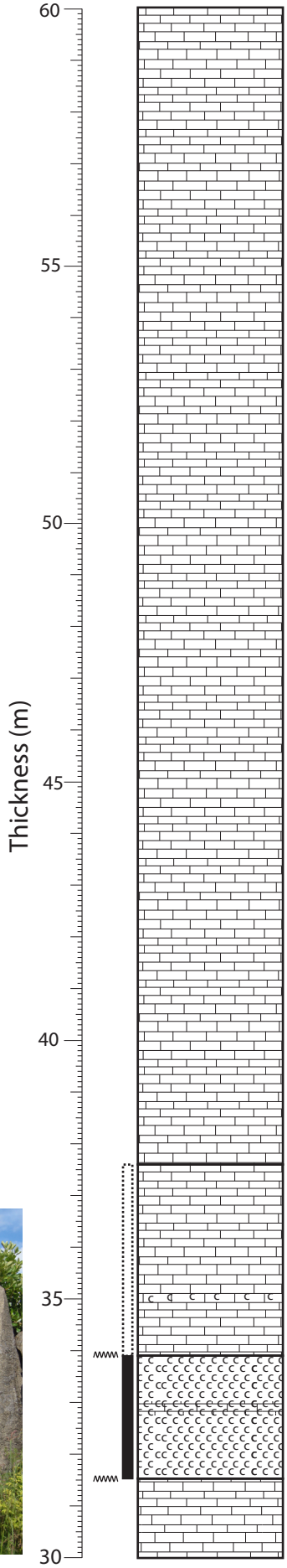

Limestone, flaggy (50 -100 mm in thickness), grey, surface weathering, very indurated, no fossils, bioclastic.

Limestone, massive, grey, surface weathering, indurated, rare fossils, bioclastic. Fossils occur in a haphazard singular band. Some specimens are disarticulated, slightly smaller in size 130-150 mm.

Limestone, massive, grey, surface weathering, indurated, abundant fossils, bioclastic sparry composition. Fossil oyster occurence is moderate, orientations are haphazard, specimens mostly articulated, gap 300 mm in thickness where no oysters appear. Size range 180-220 mm. Large borings can be seen.

Logged by Larissa Macmillan and Glen Treweek 18/12/08

Stratigraphic Column from Mangapohue Natural Bridge 08 /1

Logging and other details

LEGEND

Oyster Density

- Dense bed
- Moderate bed
- Sparse bed

Contacts

- Sharp
- Gradational
- Abruptly gradational

Fossils

- C Flemingostreini Stenzel

Thickness (m)

30
25
20
15
10
5
0

Grid Reference (NZMS 260 R16):
2676647 (E)
6325421 (N)

Grid Reference (NZMS 260 R16):
2676615 (E)
6325428 (N)

Limestone, massive, grey, surface weathering, very indurated, abundant fossils. Oyster bed is densly packed. Orientations are very haphazard, both articulated and disarticulated specimens present.

Limestone, massive to incipiently seamed, light grey, surface weathering, very indurated, moderate to dense fossils. Lower part of the unit contains dense fossils, haphazardly arranged with most shells being horizontal, some 'fitting' of shells is noted. Size varies from 150-220 mmin length. Up section the fossils form sparse lenses that branch out from each side of the out crop. Another dense bed appears followed by sparse lenses in the top of the unit. Lenses have more disarticulated specimens and borings are prevalent in all occurences.

Limestone, flaggy, grey, surface weatherd, very indurated, no fossils.

Limestone, massive, grey, surface weathering, very indurated, no fossils.

Limestone, massive, grey, surface weatherd, very indurated. Poorly sorted, grey to orange, rounded, 5 to 20 mm scattered throughout. Moderate oyster fossils, orientations are hapahazard and some shells are disarticulated.

Limestone, flaggy to knobbly in places, grey, moderately weathered, very indurated. Poorly sorted, grey to orange pebble band at the base. Pebbles are rounded and 10-20 mm in size. No fossils.

Limestone, massive, grey, surface weathering, very indurated, abundant fossils. Oysters are densly packed, have haphazard orientations and are articulated with a few disarticulated specimens noted.

Logged by Larissa Macmillan and Glen Treweek 19/12/08

Stratigraphic Column from Mangapohue Natural Bridge 09 /1

Logging and other details

LEGEND

Oyster Density

- Dense bed
- Moderate bed
- Sparse bed

Contacts

- Sharp
- Gradational
- Abruptly gradational

Fossils

- C Flemingostreini Stenzel

Grid Reference (NZMS 260 R16):
2676610 (E)
6325367 (N)

Grid Reference (NZMS 260 R16):
2676578 (E)
6325379 (N)

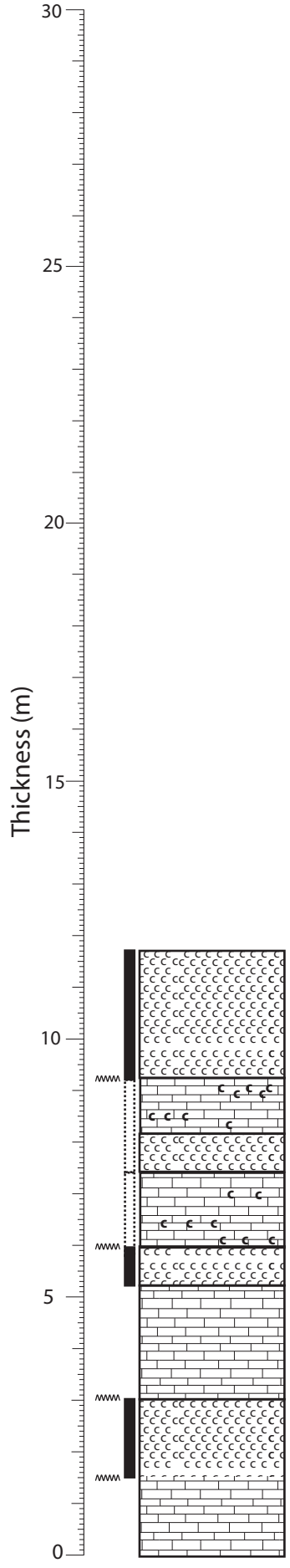

Limestone, massive, grey, surface weathering, very indurated, abundant fossils. Oyster bed is densly packed (24 1/2 m2), haphazard and has some disarticulated shells. Fitted shells and large borings (10-20 mm) are evident.

Limestone, massive, light grey, surface weathering, very indurated, sparse fossils. Oysters lens in and out of section and some appear to be arranged in nests. Shells are both articulated and disarticulated and appear to be 'fitted' in places.

Limestone, massive, light grey, surface weathering, very indurated, sparse fossils. Oysters appear to form in lenses in the section, haphazard orientations and a mixture of articulated and disarticulated shells.

Limestone, massive, light grey, surface weathering, very indurated, abundant fossils. Dense oyster bed, shells are haphazardly arranged, articulated with few disarticulated, size range 150-200 mm.

Limestone, flaggy, light grey, surface weathering, very indurated.

Limestone, massive, grey, moderate weathering, very indurated, abundant fossils. Oysters occur in a dense bed half way up the unit, samples are haphazardly arranged and articulated, size varies from 180-200 mm in length, borings in shells obvious.

Logged by Larissa Macmillan and Glen Treweek 19/12/08

Stratigraphic Column from Mangapohue Natural Bridge 10 /1

Logging and other details

Grid Reference (NZMS 260 R16):
2676767 (E)
6325529 (N)

LEGEND

Oyster Density
- Dense bed
- Moderate bed
- Sparse bed

Contacts
- Sharp
- Gradational
- Abruptly gradational

Fossils
- C Flemingostreini Stenzel

Largely unseen due to the high amount, of moss, bush and scrub.

Grid Reference (NZMS 260 R16):
2676681 (E)
6325519 (N)

Limestone, irregularly seamed, light grey, surface weathering, indurated, no fossils.

Limestone, knobbly, light grey, moderately weathered, indurated, no fossils.

Limestone, irregularly seamed, light grey, surface weathering, very indurated, no fossils.

Limestone, flaggy, light grey, surface weathering, very indurated, sparse fossils. Oysters form a band at the bottom of the unit, horizontally orientated, articulated with some disarticulation.

Limestone, massive, grey, surface weathering, very indurated, sparse fossils. Oysters form a band at the bottom of the unit, horizontally orientated, articulated with some disarticulation.

Limestone, massive, grey to orange, moderately weathered, moderately indurated, more terrigenous.

Limestone, massive, grey, surface weathering, very indurated, moderate fossils. Oysters form in single shelled beds approx. 400 mm apart. Oysters tend to form nests near the top of the unit.

Limestone, massive to incipiently seamed, grey, surface weathering, very indurated, sparse fossils. Fossils occur at the bottom of the unit.

Limestone, massive, grey, surface weathering, very indurated, abundant fossils. Fossils occur in a dense bed, shells remain haphazard in orientation and are articulated.

Limestone, massive, grey, surface weathering, very indurated, abundant fossils. Oysters form a dense bed in the middle with sparse lenses at the top at bottom. Shells are articulated and haphazard in arrangement. Majority are horizontal but some vertical specimens noted. Size ranges from 150-200 mm and borings are obvious.

Limestone, massive, grey, surface weathering, very indurated.

Logged by Larissa Macmillan and Glen Treweek 18/12/08

Stratigraphic Column from Kokakoroa Road 11 /1

Logging and other details

Grid Reference (NZMS 260 R16):
2681809 (E)
6325893 (N)

LEGEND

Oyster Density
- Dense bed
- Moderate bed
- Sparse bed

Contacts
- Sharp
- Gradational
- Abruptly gradational

Fossils
- C Flemingostreini Stenzel

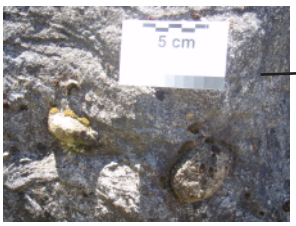

Hard to see due to weathering and algae.

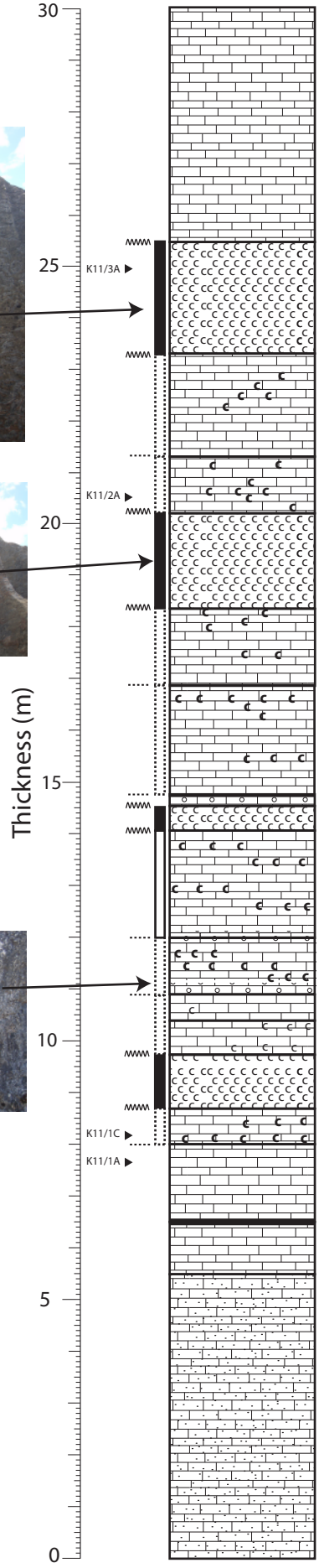

Limestone, flaggy, grey, surface weathering, indurated, no fossils, bioclastic composition. Continues for approx. 10 m.

Limestone, massive, grey, surface weathered, indurated, abundant fossils. Oysters form a dense bed, orientations are haphazard, shells are 'fitted' in places and some disarticulation can be seen. Size ranges from 150-200 mm and borings are obvious.

Limestone, incipiently seamed, grey, surface weathering, indurated, moderate fossils. Oysters only seen in bands/nest in the upper part of the unit. Shells are 'fitted' together in places and very haphazard in orientation.

Limestone, massive, grey, surface weathering, indurated, moderate fossils. Oysters form in beds in the top of the unit. Large nest seen in the centre of the unit. Shells are haphazard and a mixture of articulated and disarticulated. Size range 150-200 mm.

Limestone, fluted, grey, surface weathering, indurated, abundant fossils. Oysters form a moderately packed oyster bed. Orientations are very haphazard. Shells are articulated with some disarticualtion noted.

Limestone, incipiently seamed, grey, surface weathering, indurated, rare fossils. Oysters are scattered in bands with a possible nest at the top of the unit. Horizontally orientated, articulated and ranging from 150-200 mm in size.

Limestone, massive, grey, surface weathering, indurated, rare fossils. Oysters are scattered in lenses throughout the unit. Specimens are disarticulated and have a horizontal orientation. Some possible nests of 2-3 specimens seen.

Poorly sorted, grey-orange, rounded, 20-70 mm sized band of pebbles.

Limestone, massive, grey, surface weathering, indurated, abundant fossils. Oysters form a thick. Haphazard orientations articulation and disarticulation seen.

Limestone, massive, grey, surface weathering, very indurated, moderate fossils. Oyster bands are 2-3 generations thick, haphazardly orientated and both articulated and disarticulated shells can be seen, size ranges from 150-200 mm and borings are obvious.

Limestone, massive, grey, surface weathered, very indurated, moderate fossils. Poorly sorted, grey to orange, rounded 20-70 mm pebbles scattered throughout section. Oysters form in bands across the unit, horizontally orientated, articulated with some disarticulation. 2-3 generations thick.

Limestone, massive, grey, surface weathering, indurated, rare fossils.

Sparse lenses of oysters noted, horizontally orientated and articulated.

Dense oyster bed (22 1/2 m2), haphazard orientation, some disarticulation noted, size 150-200 mm.

Oyster bands pinching in and out of the section. Shells are haphazardly orientated and articulated.

Limestone, massive, grey, surface weathering, very indurated, no fossils.

Limestone, incipiently seamed, grey, surface weathering, indurated, no fossils, highly terrigenous.

Grid Reference (NZMS 260 R16):
2681892 (E)
6325906 (N)

Logged by Larissa Macmillan and Dirk Wallace 4/01/2009

Stratigraphic Column from Kokakoroa Road 12 /1

Logging and other details

LEGEND

Oyster Density

- Dense bed
- Moderate bed
- Sparse bed

Contacts

- Sharp
- Gradational
- Abruptly gradational

Fossils

- C Flemingostreini Stenzel

Grid Reference (NZMS 260 R16):
2682431 (E)
6325117 (N)

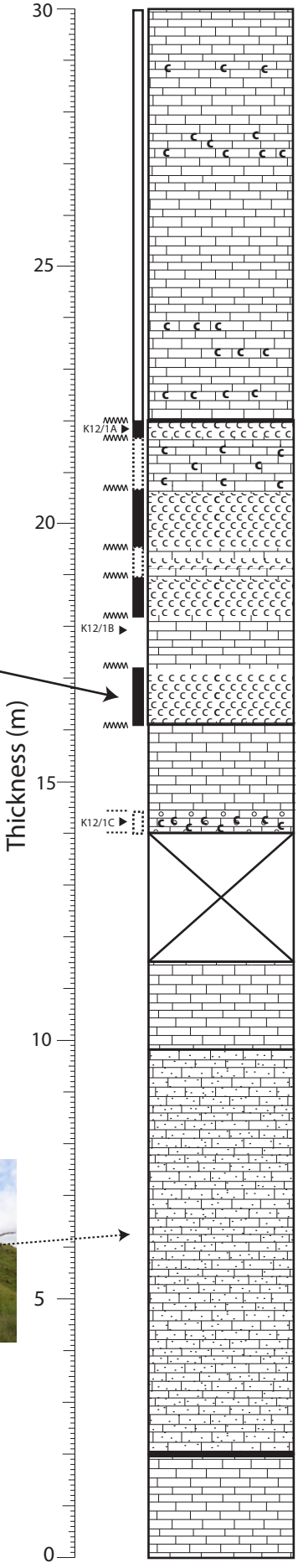

Oyster layer 2-3 shells thick, haphazard arrangement and some disarticulated shells.

Sparse scattering of oysters with some disarticulated shells.

Very dense oyster bed. Orientations are haphazard, disarticulated specimens and 'fitted' shells in places.

Abruptly contact with massive limestone. Sparse scattering of horizontal and articulated oysters.

Dense tightly packed oyster bed 5-6 generations thick. Haphazard orientations, some disarticulated shells present.

Limestone, massive, grey, surface weathered, indurated, abundant fossils. Oysters form a densly packed oyster bed, specimens are horizontal, articulated and have large borings.

Limestone, incipiently seamed, grey, surface weathering, indurated, sparse fossils. Poory sorted, grey to orange, rounded, 5 -20 mm pebbles forming a band in the base. Oysters appear in same band as pebbles. Oysters are horizontal, articulated and 150-200 mm in size.

Limestone, flaggy, grey, surface weathering, indurated, no fossils, bioclastic composition.

Limestone, massive to incipiently seamed, dark pink to dark grey, moderately weathered, indurated, no fossils, coarse grained, terrigenous matrix composition.

Limestone, massive, light pink to dark grey, moderately weathered, indurated, no fossils.

Logged by Larissa Macmillan and Dirk Wallace 5/01/2009

Stratigraphic Column from Kokakoroa Road 12/2

Logging and other details

LEGEND

Oyster Density

- Dense bed
- Moderate bed
- Sparse bed

Contacts

- Sharp
- Gradational
- Abruptly gradational

Fossils

- C Flemingostreini Stenzel

Grid Reference (NZMS 260 R16):
2682567 (E)
6324905 (N)

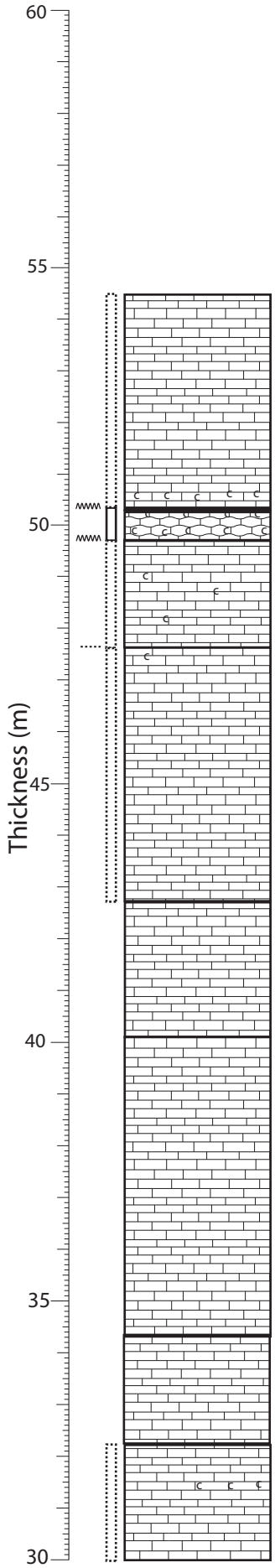

Limestone, flaggy, grey, surface weathering, indurated, rare fossils. Oysters form a sparse band at the bottom of the unit, horizontally orientated and articulated.

Limestone, knobbly, moderately weathered, indurated, moderate fossils. Oysters are horizontally orientated, some shells appear disarticulated, size range 150-200 mm.

Limestone, incipiently seamed, surface weathering, indurated, rare fossils. Fragments of oyster seen in the unit.

Limestone, flaggy, grey, surface weathering, indurated, rare fossil. Small disarticulated fragment of oyster noted in the top of the section.

Limestone, massive to incipiently seamed, grey, surface weathering, indurated, no fossils.

Limestone, massive, grey, surface weathering, indurated, no fossils.

Limestone, massive, grey, surface weathering, indurated, rare fossils. Oysters appear at random intervals up the unit, pinching in and out in singular shell layers, articulated and some disarticulation seen.

Logged by Larissa Macmillan and Dirk Wallace 05/01/09

Stratigraphic Column from Kokakoroa Road 13 /1

Logging and other details

LEGEND

Oyster Density

- Dense bed
- Moderate bed
- Sparse bed

Contacts

- Sharp
- Gradational
- Abruptly gradational

Fossils

- C Flemingostreini Stenzel

Grid Reference (NZMS 260 R16):
2682849 (E)
6325189 (N)

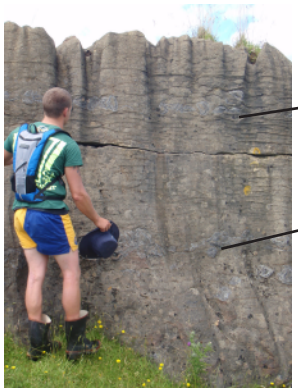

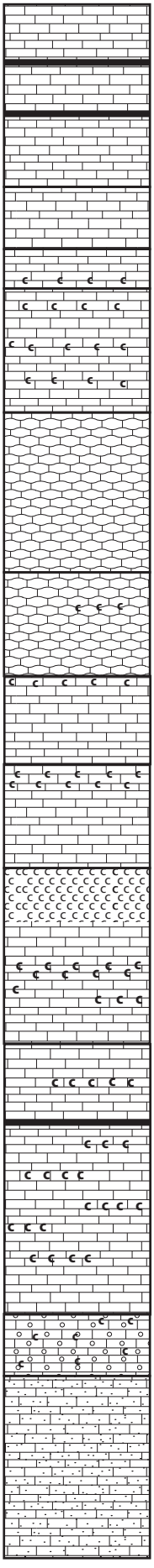

Limestone, grey, flaggy, surface weathering, indurated, rare oyster fragment seen.

Limestone, flaggy, grey, surface weathering, indurated, sparse fossils. Oysters appear in a single band, horizontal, near the bottom of the unit. Shells are a mixture of articulated and disarticulated and 150-180 mm in size.

Limestone, massive, grey, surface weathering, indurated, sparse fossils. Oysters appear in single bands, one layer thick, horizontal and articulated.

Limestone, knobbly, grey, moderatley weathered, indurated, no fossils.

Limestone, knobbly, grey, moderately weathered, indurated, rare fossils. Fossils form in a band in the top part of the unit, haphazardly orientated and articulated, 150-180 mm.

Single layer of oysters appears at the top of the unit. Randomly scattered oyster fragments can be seen as well. Layer is 2-3 generations thick and oysters have haphazard orientations.

Limestone, incipiently seamed, grey, moderately weathered, indurated, moderate fossils. Dense oyster bed developed in the top of the unit, shells are horizontal, articulated with some small disarticulated shells fragments present.

Limestone, massive, surface weathering, indurated, moderate fossils. Very dense oyster bed occurs at the top of the unit, haphazardly arranged, articulated and disarticulated specimens. Oyster bands pinch in and out of the lower part of the unit.

Limestone, flutted, grey, surface weathering, indurated, moderate fossils. Fossils lense in and out of the section in thin bands. Shells are horizontally orientated, and articulated.

Limestone, irregular, grey to pink, moderately weathered, indurated, moderate fossils. Poorly sorted, grey to orange, rounded pebbles, 10-40 mm in size. Oysters appear in scatterd lenses, articulated and disarticulated specimens, 120-200 mm in size.

Limestone, massive, grey to pink, moderately weathered, indurated, no fossils, terrigenous composition.

Logged by Larissa Macmillan and Dirk Wallace 5/01/2009

Stratigraphic Column from Kokakoroa Road 13/2

Logging and other details

LEGEND

Oyster Density

- Dense bed
- Moderate bed
- Sparse bed

Contacts

- Sharp
- Gradational
- Abruptly gradational

Fossils

- C Flemingostreini Stenzel

Grid Reference (NZMS 260 R16):
2683143 (E)
6325101 (N)

Hard to see as very weathered

Weathering break

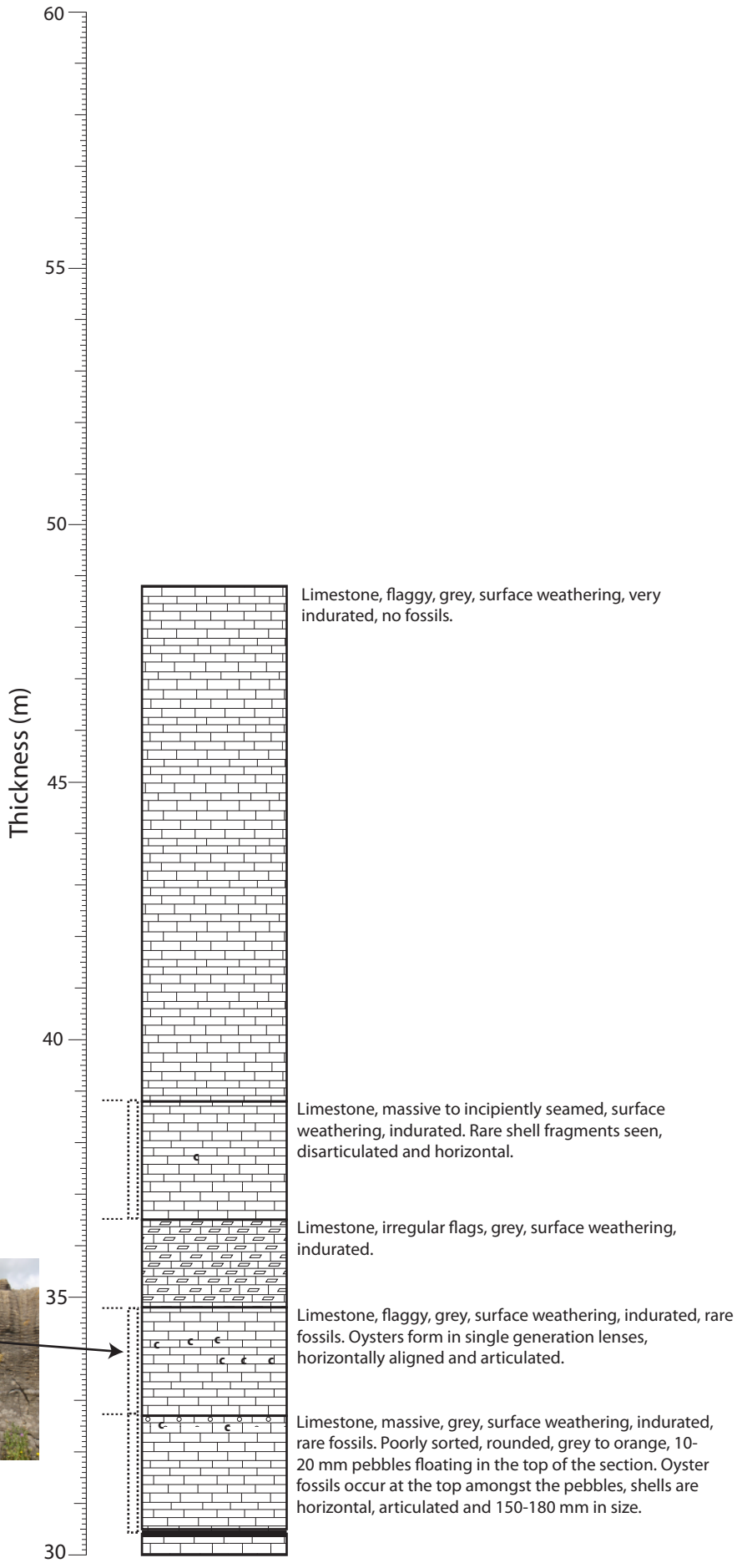

Logged by Larissa Macmillan and Dirk Wallace 05/01/09

Stratigraphic Column from Ngapaenga Road 14/1

Logging and other details

Grid Reference (NZMS 260 R16):
2676768 (E)
6315208 (N)

LEGEND

Oyster Density

- Dense bed
- Moderate bed
- Sparse bed

Contacts

- Sharp
- Gradational
- Abruptly gradational

Fossils

- C Flemingostreini Stenzel

Hard to see, tall bluff

Grid reference (NZMS 260 R16):
2676747 (E)
6315431 (N)

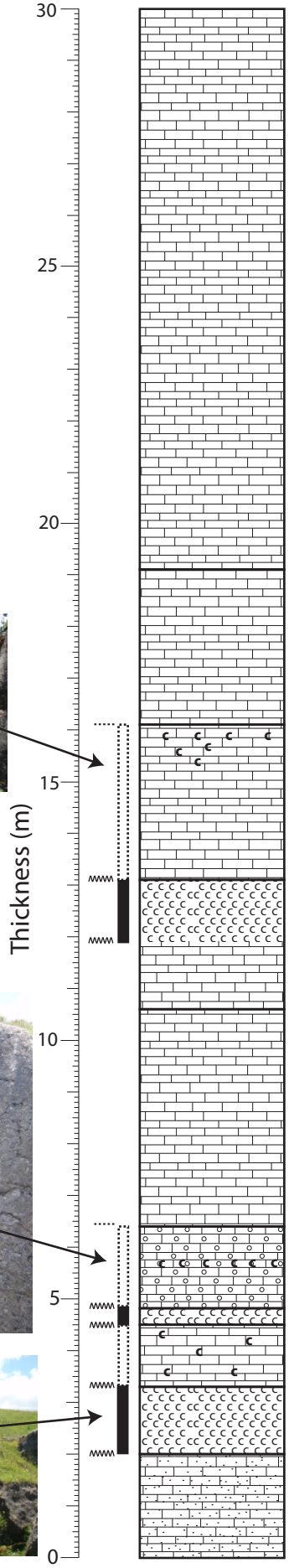

Limestone, flaggy, grey, surface weathering, indurated. Approximately 10 m.

Limestone, massive, light grey, surface weathering, indurated.

Limestone, massive, grey, surface weathering, indurated, sparse fossils. Oysters form a horizontal band 2-3 generations in thickness. Development of possible nests.

Limestone, massive, grey, surface weathering, indurated, abundant fossils. Oysters form a dense bed in the upper part of the section.

Limestone, incipiently seamed, surface weathering, indurated.

Limestone, massive, grey, surface weathering, indurated, moderate fossils. Poorly sorted, white to orange, rounded, 10-40 mm pebbles floating through section. Oyster band occurs in centre, horizontal and a mix of articulated and disarticulated.
Oysters thicken and form a band 2-3 generations thick.
Oysters become more sparse, remain horizontal and majority are articulated.

Very dense oyster bed, oysters are prominent, horizontal, articulated and 150-200 mm in lenght.

Limestone, grey, massive, surface weathering, indurated, no fossils, high terrigenous composition.

Logged by Larissa Macmillan and Dirk Wallace 6/01/09

Stratigraphic Column from Waipuna Road 15/1

Logging and other details

LEGEND

Oyster Density

- Dense bed
- Moderate bed
- Sparse bed

Contacts

- Sharp
- Gradational
- Abruptly gradational

Fossils

- C Flemingostreini Stenzel

Grid reference (NZMS 260 R16):
2684098 (E)
6315912 (N)

Thickness (m)

30
25
20
15
10
5
0

15/2C ▶ Oysters form a dense bed (24 1/2 m²), shells are haphazard, articulated, size 180-220mm. Limestone, massive, grey, surface weathering, indurated, no fossils.

15/2B ▶ Oysters form a dense bed (24 1/2 m²), shells are haphazard, articulated, size 180-220mm.

Limestone, massive, grey, surface weathering, indurated, no fossils.

15/2A ▶ Limestone, flaggy, grey, surface weathering, indurated, no fossils, sparry compostition.

15/1E ▶ Limestone, massive, grey, surface weathering, indurated, abundant fossils, sandy matrix. Oysters from a dense bed shells are haphazard, articulated, size 180-220mm.

Limestone, incipiently seamed, grey, moderately weathered, indurated, no fossils.

Limestone, massive, grey-orange, moderately weathered, indurated, abundant fossils. Dense bed formed at the top of the bluff, hard to see.

Limestone, flaggy, light grey, surface weathering, indurated, sparse fossils, sparry composition. Oysters are scattered, through unit. Only can be faintly seen due to scrub.

Limestone, massive, blue-grey, surface weathered, indurated, moderate fossils. Dense oyster bed in top of unit, very haphazard, majority of shells articulated, size range 150-200mm.

15/1A ▶
15/1B ▶
15/1C ▶
15/1D ▶ Limestone, massive to fluted, surface weathering, indurated, sparse fossils. Oysters occur randomly scattered in section, have hapahazard orientations.

Limestone, massive, blue-grey, surface weathering, indurated moderate to rare fossils. Oysters are aticulated, haphazard, some noted vertically orientated and 200 mm in length.

Logged by Larissa Macmillan and Micheal Tayler 17/02/09

Stratigraphic Column from Mairoa Road 16/1

Logging and other details

LEGEND

Oyster Density

- Dense bed
- Moderate bed
- Sparse bed

Contacts

- Sharp
- Gradational
- Abruptly gradational

Fossils

- C Flemingostreini Stenzel

Thickness (m)

30
25
20
15
10
5
0

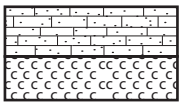

Limestone, massive, grey, surface weathering, indurated, abundant fossils, matrix has a sparry compostion. Dense bed of oysters, very haphazardly arranged, mostly horizontal, 180-220 mm in size and borings are obvious.

Grid reference (NZMS 260 R16):
2683252 (E)
6311888 (N)

Logged by Larissa Macmillan and Micheal Tayler 17/02/09

Stratigraphic Column from Mairoa Road 17/1

Logging and other details

LEGEND

Oyster Density

- Dense bed
- Moderate bed
- Sparse bed

Contacts

- Sharp
- Gradational
- Abruptly gradational

Fossils

- C Flemingostreini Stenzel

Grid reference (NZMS 260 R16):
2683218 (E)
6312283 (N)

Grid reference (NZMS 260 R16):
2683217 (E)
6312283 (N)

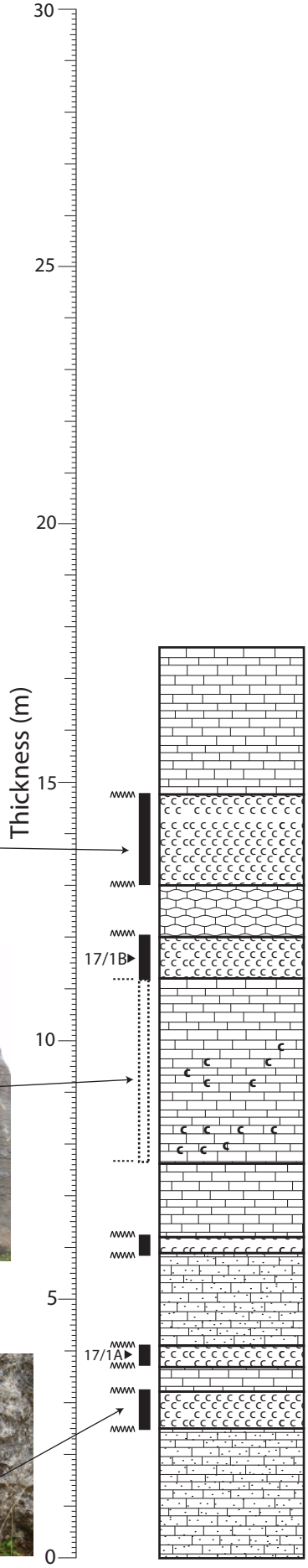

Limestone, flaggy, grey, surface weathering, indurated, no fossils, sparry compostion. Abrupt contact with lower oyster bed and pectin fossils also seen.

Dense oyster bed, very haphazard, many shells horizontal, veritcal occurences also noted. Some shells are very large, up to 250 mm, large boreholes can also be seen.

Limestone, knobbly, grey, surface weathering, indurated.

Dense oyster bed, some specimens are vertically orientated, also noted that some shells are disarticulated. Remainder of shells are horizontal and articulated.

Limestone, incipiently seamed, grey, surface weathering, indurated, sparse fossils. Oysters appear to 'float' in the unit, majority are disarticulated, horizontal and 200 mm in size.

Limestone, massive, grey, surface weathering, indurated.

Dense oyster bed, some specimens are vertically orientated, also noted that some shells are disarticulated. Remainder of shells are horizontal and articulated.

Limestone, incipiently seamed, orange to grey, moderately weathered indurated, highly terrigenous composition.

Dense oyster band, horizontally orientated, articulated, 150-200 mm.

Limestone, massive, grey, surface weathering, indurated.

Dense oyster band, horizontally orientated, articulated, 150-200 mm.

Limestone, incipiently flagged, grey, surface weathering, indurated, no fossils, highly terrigenous.

Logged by Larissa Macmillan and Micheal Tayler 17/02/09

Stratigraphic Column from Tawarau Road 18/1

Logging and other details

LEGEND

Oyster Density

- Dense bed
- Moderate bed
- Sparse bed

Contacts

- Sharp
- Gradational
- Abruptly gradational

Fossils

- C Flemingostreini Stenzel

Grid reference (NZMS 260 R16):
2685885 (E)
6317209 (N)

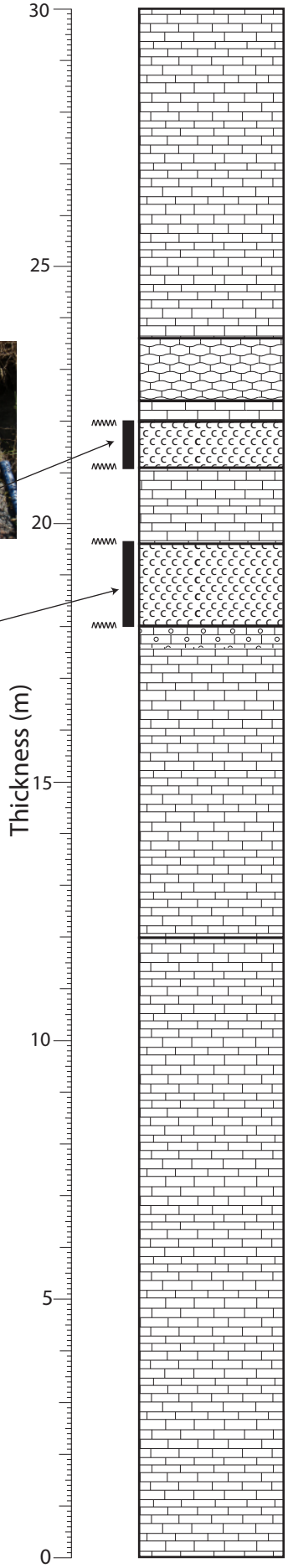

Limestone, incipiently seamed, grey to blue, surface weathering, indurated, no fossils.

Limestone, knobbly, grey, moderately weathered, indurated , no fossils.

Limestone, flaggy, grey, forms an abrupt contact with underlying oyster bed.

Dense oyster bed, very haphazard, shells are oriented both vertically and horizontally. Shell size varies from 180-200 mm and large borings can be seen.

Limestone, flaggy, grey, surface weathering, indurated, no fossils.

Dense oyster bed, very haphazard, shells are oriented both vertically and horizontally. Shell size varies from 180-200 mm and large borings can be seen.

Limestone, massive, grey, moderately weathered, indurated, sparse fossils. Poorly sorted, grey-orange, rounded, 10-20 mm pebble band at the top of the unit. Oysters occur in the upper part of the unit but very weathered and hard to see.

Limestone, massive, grey, surface weathering, indurated, no fossils.

Logged by Larissa Macmillan and Micheal Tayler 17/02/09

Stratigraphic Column from Tawarau Road 18/2

Logging and other details

Grid Reference (NZMS 260 R16):
2675723 (E)
6317051 (N)

LEGEND

Oyster Density

- Dense bed
- Moderate bed
- Sparse bed

Contacts

- Sharp
- Gradational
- Abruptly gradational

Fossils

- C Flemingostreini Stenzel

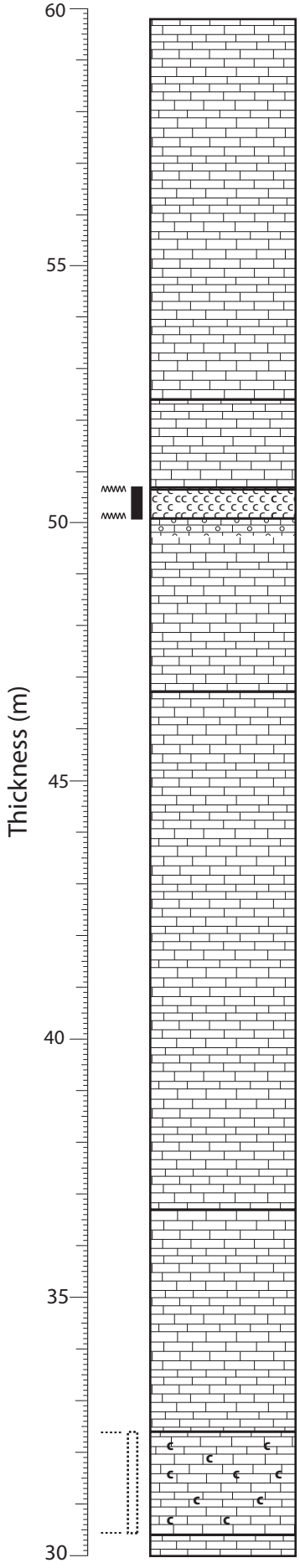

Limestone, flaggy, grey, surface weathering, indurated no fossils.

Dense oyster bed, oysters are haphazard, articulated, 180-200 mm in size.

Limestone, flaggy, grey, surface weathered, indurated, scattered fossils. Poorly sorted, grey to white, rounded, 5-10 mm pebble band at top of section. Oysters are scattered throughout section, horizontally orientated, some disarticulated specimens seen. 150-200 mm in size and large borings in places.

Limestone, flaggy, grey, surface weathered, indurated, no fossils.

Limestone, massive, grey, surface weathered, indurated, no fossils, sparry composition.

Limestone, massive, grey, surface weathering, indurated, moderate fossils. Oysters are scattered throughout the section and tend to form bands. Shells are horizontal, articulated with few disarticulated samples noted. Size ranges from 180-220 mm.

Logged by Larissa Macmillan and Micheal Tayler 17/02/09

Stratigraphic Column from Tawarau Road 19/1

Logging and other details

LEGEND

Oyster Density

- Dense bed
- Moderate bed
- Sparse bed

Contacts

- Sharp
- Gradational
- Abruptly gradational

Fossils

- C Flemingostreini Stenzel

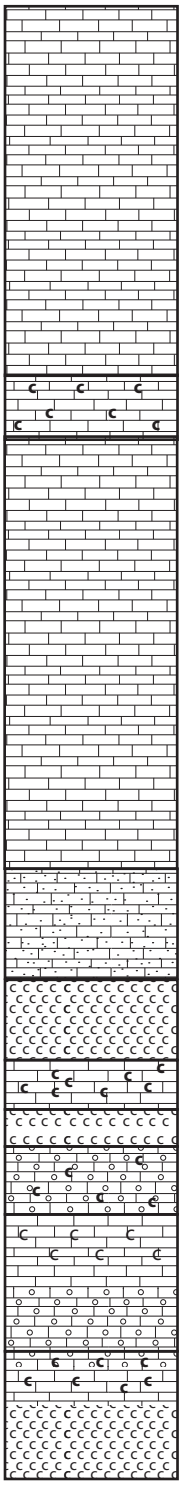

Limestone, flaggy, grey, surface weathering, indurated, no fossils.

Moderate oyster bed, very haphazard, shells are oriented both vertically and horizontally. Shell size varies from 180-200 mm and large borings can be seen.

Limestone, incipiently seamed, grey, surface weathering, indurated, no fossils.

Limestone, massive, grey, surface weathering, indurated, no fossils, highly terrigenous.

Limestone, massive, grey, moderately weathering, indurated, sparse fossils. Oysters are the densest in the top and middle of the unit, with sparse 'floating' specimens in between. Oysters are haphazard but tend towards horizontality. Majority of shells are articulated.

Limestone, massive, grey, moderately weathering, indurated, sparse fossils. Poorly sorted, grey-orange, rounded, 10 - 20 mm pebbles at the top of the unit. Oysters occur in the upper part of the unit but very weathered and hard to see.

Limestone, massive, grey, surface weathering, indurated, sparse fossils. Poorly sorted, grey-orange, rounded, pebble band at the bottom of the unit. Oysters occur in the upper part of the unit they are scattered and haphazard.

Dense oyster bed, very haphazard, shells mostly horizontally. Shell size varies from 180-200 mm and large borings can be seen.

Grid reference (NZMS 260 R16):
2676549 (E)
6317128 (N)

Logged by Larissa Macmillan and Micheal Tayler 17/02/09

Stratigraphic Column from Piripiri Cave 20/1

Logging and other details

LEGEND

Oyster Density

- Dense bed
- Moderate bed
- Sparse bed

Contacts

- Sharp
- Gradational
- Abruptly gradational

Fossils

- C Flemingostreini Stenzel

Grid reference (NZMS 260 R16):
739 (E)
258(N)

Thickness (m)

30
25
20
15
10
5
0

Buff, highly indurated limestone composed of coarse shell fragments (50-100 mm). Exposure has incipient seems and accumulation is dense in the lower part and grades up to a shell hash limestone. Shells are mostly articulated but some disarticulation is present. Disarticulated shells are smaller and fragmented with a higher level of bioerosion. Bioerosion is common and the majority of the shells have borings up to 50 mm in length. The haphazard nature of shell orientations suggest some disturbance. Shells are covered in a light brown calcite precipitate. Shells are densly packed with most shells being matrix supported.

Logged by Larissa Macmillan 19/05/09

Stratigraphic Column from Waitomo Valley 21/1

Logging and other details

LEGEND

Oyster Density

- Dense bed
- Moderate bed
- Sparse bed

Contacts

- Sharp
- Gradational
- Abruptly gradational

Fossils

- C Flemingostreini Stenzel

Grid reference (NZMS 260 R16):
2698727 (E)
6331579 (N)

Thickness (m)

30
25
20
15
10
5
0

Vegetation

Matrix is highly terrigenous with haphazard oysters with various orientations, larger shells appear to be more horizontal. Most samples are articulated, with a high amount of infilled borings. Hard to see in places due to surface weathering.

Logged by Larissa Macmillan 16/04/09

Stratigraphic Column from Waitomo Valley 22/1

Logging and other details

LEGEND

Oyster Density

- Dense bed
- Moderate bed
- Sparse bed

Contacts

- Sharp
- Gradational
- Abruptly gradational

Fossils

- C Flemingostreini Stenzel

Grid reference (NZMS 260 R16):
2698887 (E)
6331407(N)

Thickness (m)

30
25
20
15
10
5
0

Limestone, massive to large flags. Occasional scattered oyster. Section weathered and hard to see a lot of detail.

Light brown to green sandy, poorly sorted limestone. Contains scattered pebbles 2 - 5 mm in size. Pebbles are rounded and make up an abundance of 5-10% in the matrix. Highly packed oyster bed, orientations very haphazard, most shells appear articulated. Shells grade out near the top of the bed and are moderately to highly bored.

Logged by Larissa Macmillan 16/04/09

Stratigraphic Column from Puerto Pirámide - 1

Logging and other details

LEGEND

Contacts
- Sharp
- Gradational
- Abruptly gradational

Fossils
- *"Ostrea" patagonica*
- Gastropod
- Barnacle
- Bioturbation
- Brachiopods
- Bivalve-Disarticulated

Thickness (m)

Biological concentration of oysters (*"Ostrea" patagonica*) contained in a light grey fine to medium, well sorted sandy host. Oysters are articulated and in life position, they make up 55% in abundance and all specimens are adults. Fragmentation, abrasion and dissolution are neglible. Bioerosion is low to moderate and four generations of oysters are seen.

Massive fine light brown sand with an erosive upper contact. Fossiliferous material observed includes brachipods, barnacles, gastropods and disarticulated oyster shells. Oyster shells show no preferential orientation and are convex down. The geometry of the beds is tabular and fossils make up 25% abundance. Fossils are highly fragmented, have low bioerosion and average abrasion. No sign of dissolution.

Layers of dark grey mud interbedded with light grey to brown fine sandstone. The heterolithic nature of this unit diminishes up the section as the amount of mud increases. The upper contact is bioturbated with *Thalassinoides isp.* No occurrence of bioclastic material.

Massive light brown medium grained well sorted sand with intraclasts of mud and abundant fragments of oyster shells and barnacles. The upper contact is sharp and the geometry of the intraclasts is tabular. Shell fragments only approximate 25% and they are a poorly sorted, sedimentological accumulation. Orientation of fragments is horizontal and concave down. Shells are all disarticulated and have a high level of abrasion. Bioerosion of the shells is medium to high. There are equal amounts of adults and juvenile speciments present.

Grid reference (WGS 84):
42°35'47" S, 64°15'13.7" W

Logged by Claudia Brito and Larissa Macmillan 2008

Stratigraphic Column from Puerto Pirámide - 2

Logging and other details

LEGEND

Contacts
- Sharp
- Gradational
- Abruptly gradational

Fossils
- *"Ostrea" patagonica*
- Gastropod
- Barnacle
- Bioturbation
- Brachiopods
- Bivalve-Disarticulated
- Pectin

Grid reference (WGS 84):
42°35′37″ S, 64°15′14.3″W

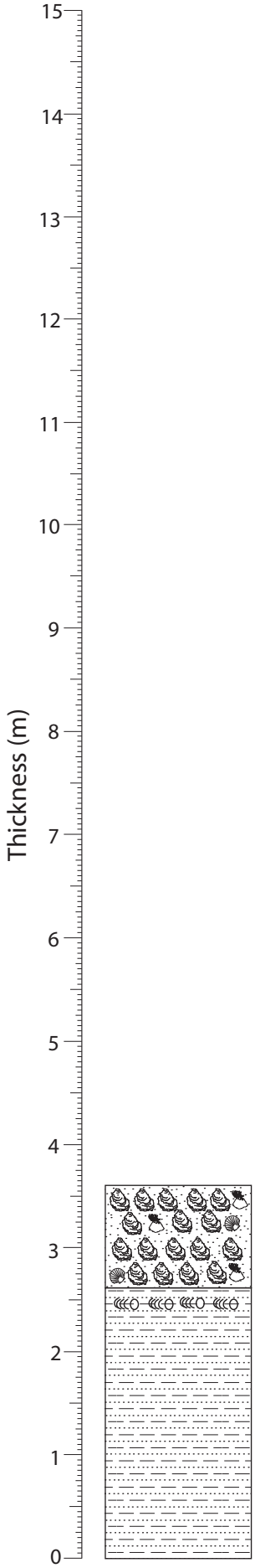

Biological concentration of oysters (*"Ostrea" patagonica*) in a fine, well sorted light grey sandstone host. The osyters are adults, articulated and found in life position, 13 generations are recognised. Scattered occurences of pectins and barnacles are also seen within the sandy matrix.

Dark grey mud interbedded with light grey fine sandstone with a discontinuous lenticular geometry. The upper contact of this unit is irregular and bioturbated with *Thalassinoides isp.*

Logged by Claudia Brito and Larissa Macmillan 2008

Stratigraphic Column from Puerto Pirámide - 3

Logging and other details

LEGEND

Contacts
- Sharp
- Gradational
- Abruptly gradational

Fossils
- *"Ostrea" patagonica*
- Gastropod
- Barnacle
- Bioturbation structures
- Brachiopods
- Bivalve-Disarticulated
- Pectin

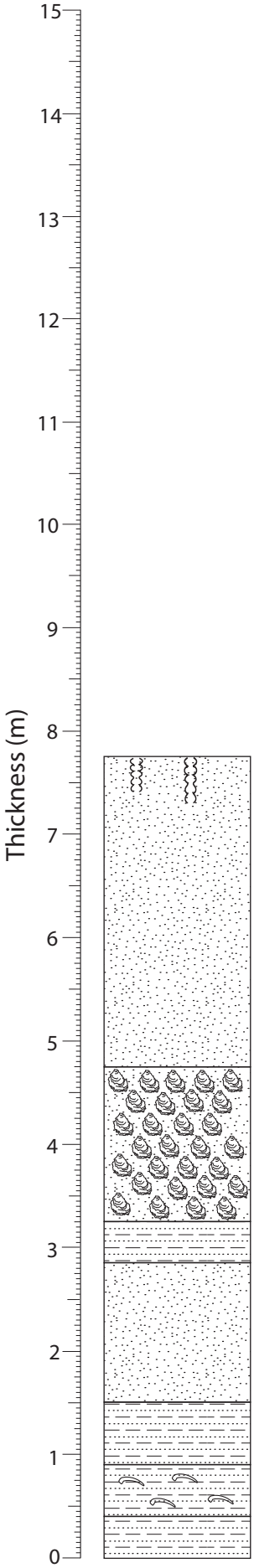

Fine light grey sandstone with laminations, bioturbation in the uppermost part of the unit is observed in the form of vertical to subvertical pipes.

Biological concentration of oysters, in a fine, light grey, well sorted, moderately indurated sandstone. Between 17 and 18 generations of oysters are noted here. Oysters are articulated and in life position.

Dark grey mudstone with lenses of sandstone, lamination is recognised as discontinuous lenticular.

Fine, well sorted, moderatley indurated flaser laminated sandstone. Upper contact is erosive.

Heterolithic continuous lenticular dark grey mudstone with intraclasts of fine to medium light grey sandstone. Upper contact is erosive.

Heterolithic beds comprised of fine to medium light grey sandstone and intercalations of dark grey mud. Sandstone is the dominant lithology. Upper contact is erosive. Disarticulated adult specimens of *"Ostrea" patagonica* are noted.

Discontinuous lenticular heterolithic dark grey mud with intercalated lenses of fine light grey sandstone beds. Upper contact is erosive.

Grid reference (WGS 84):
42°35'36.8" S, 64°15'15"W

Logged by Claudia Brito and Larissa Macmillan 2008

Stratigraphic Column from Puerto Pirámide - 4

Logging and other details

LEGEND

Contacts
- Sharp
- Gradational
- Abruptly gradational

Fossils
- *"Ostrea" patagonica*
- Gastropod
- Barnacle
- Bioturbation structures
- Brachiopods
- Bivalve-Disarticulated
- Pectin

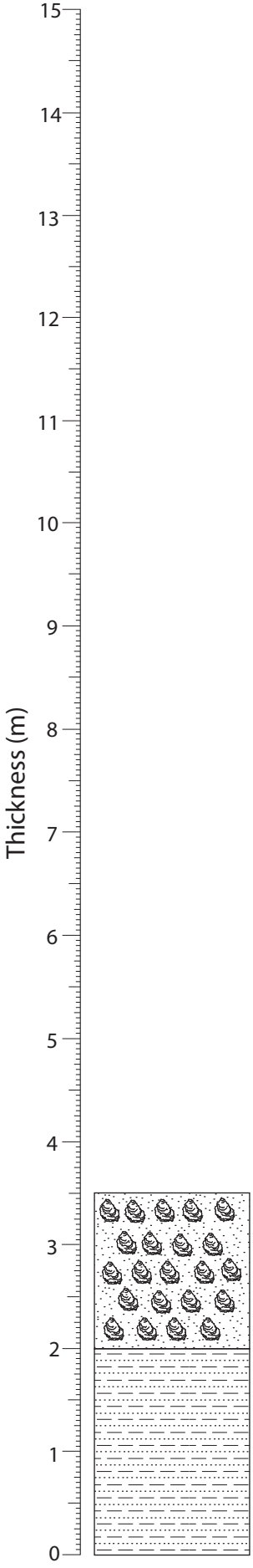

Biological concentration of oysters (*"Ostrea" patagonica*). These oysters are greater in size than previous columns. They are adult specimens, in life position and articulated. The matrix is fine to medium sand. In the medium sand portions of the matrix the oysters are more dispersed. 16 to 17 generations of oysters are recognised.

Interbedded fine moderately indurated light grey sandstone and dark grey mudstone. Upper contact is erosive.

Grid reference (WGS 84):
42°35′35.9″ S, 64°15′14.8″W

Logged by Claudia Brito and Larissa Macmillan 2008

Stratigraphic Column from Puerto Pirámide - 5

Logging and other details

LEGEND

Contacts
- Sharp
- Gradational
- Abruptly gradational

Fossils
- *"Ostrea" patagonica*
- Gastropod
- Barnacle
- Bioturbation structures
- Brachiopods
- Bivalve-Disarticulation
- Pectin

Thickness (m)

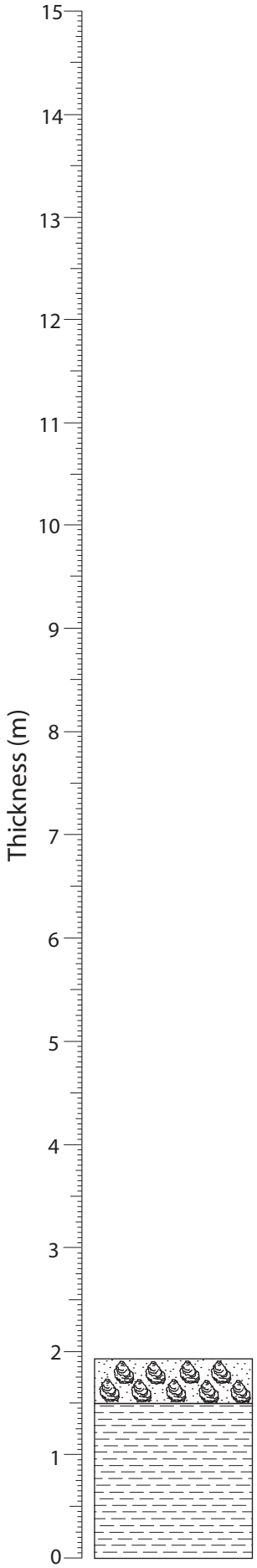

Biological accumulation of *"Ostrea" patagonica.* Four generations are recognised here, all adult and articulated. Fragmentation, abrasion and dissolution is low.

Dark grey, well indurated mudstone. Moderately weathered no presence of bioclasts.

Grid reference (WGS 84):
42°35′34.7″ S, 64°15′14.5″W

Logged by Claudia Brito and Larissa Macmillan 2008

Stratigraphic Column from Puerto Pirámide - 6

Logging and other details

LEGEND

Contacts
- Sharp
- Gradational
- Abruptly gradational

Fossils
- *"Ostrea" patagonica*
- Gastropod
- Barnacle
- Bioturbation structures
- Brachiopods
- Bivalve-Disarticulated
- Pectin

Grid reference (WGS 84):
42°35′33.4″ S, 64°18′15.8″W

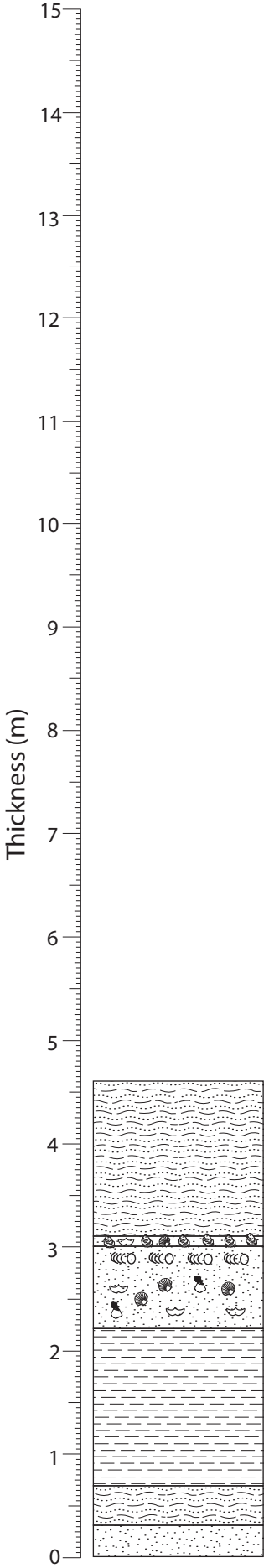

Dark grey mudstone interbedded with light grey sandstone. Stratification is lenticular and continuous.

Sinlge generation of *"Ostrea" patagonica*, held in medium grainded, moderately indurated light grey sandstone. Oysters are articulated and in life position. Articulated pectins and fragments of brachipods seen.

Medium grained, light grey, moderately indurated sandstone. Fragments of pectins and barnacles. Brachiopods also noted, articulated but not in life position. Packing of the shells is 25% and bioclasts are a sedimentological accumulation. Shells are convex up and horizontally stratified. Abrasion and bioerosion is moderate and dissolution is low. Bioturbation structures of *Thalassinoides isp* seen.

Laminated muds, light grey, moderately indurated.

Dark grey mudstone with lenses of medium grained sandstone. Stratification is lenticular and discontinuous.

Fine light grey sand.

Logged by Claudia Brito and Larissa Macmillan 2008

Stratigraphic Column from Parikino 01 - 30 m

Logging and other details

LEGEND

Oyster Density
- Dense bed
- Moderate bed
- Sparse bed

Contacts
- Sharp
- Gradational
- Abruptly gradational

Fossils
- *Crassostrea ingens*
- Gastropod
- Pectinidae
- Fossils (general)

Grid reference (NZMS 260 R16):
2695529 (E)
6157173 (N)

Thickness (m)

30
25
20
15
10
5
0

WAN01

Sandstone, bedded, brown-orange, moderately weathered, poorly indurated, well sorted, rounded, sand.

Siltstone, massive, blue-grey, moderately weathered, poorly indurated, well sorted, rounded, fine silt. No fossils.

Siltstone, massive, blue-grey, moderately weathered, poorly indurated, well sorted, massive, fine silt. Moderate *Crassostrea* fossils. Fossils are scattered in section, very weathered hard to tell if articulated or disarticulated, some borings seen.

Logged by Larissa Macmillan and Micheal Tayler 17/01/09

Stratigraphic Column from Parikino 02 - 60 m

Logging and other details

LEGEND

Oyster Density
- Dense bed
- Moderate bed
- Sparse bed

Contacts
- Sharp
- Gradational
- Abruptly gradational

Fossils
- *Crassostrea ingens*
- Gastropod
- Pectinidae
- Fossils (general)

Grid reference (NZMS 260 R16):
2695582 (E)
6157176 (N)

Thickness (m)

30
25
20
15
10
5
0

Siltstone, blue-grey, moderately weathered, poorly indurated, well sorted, massive, fine silt. No fossils.

Sandy siltstone, blue-grey, moderately weathered, poorly indurated, moderately sorted, massive, fine silt. Moderate *Crassostrea* fossils, presence of pectins and gastropods. *Crassostrea* are scattered in section, very weathered hard to tell if articulated or disarticulated, some borings seen (see photo). Siltstone slightly calcareous.

Logged by Larissa Macmillan and Micheal Tayler 17/01/09

Stratigraphic Column from Parikino 03 - 90 m

Logging and other details

LEGEND

Oyster Density
- Dense bed
- Moderate bed
- Sparse bed

Contacts
- Sharp
- Gradational
- Abruptly gradational

Fossils
- *Crassostrea ingens*
- Gastropod
- Pectinidae
- Fossils (general)

Grid reference (NZMS 260 R16):
2695613 (E)
6157178 (N)

Thickness (m)

30
25
20
15
10
5
0

Siltstone, massive, blue-grey, moderately weathered, poorly indurated, well sorted, fine silt. No fossils.

Silty sandstone, massive, grey to brown, moderately weathered, poorly indurated, possible presence of oysters, hard to see due to height.

Denser bed of *Crassostrea*. Specimens appear articulated, hard to see due to weathering. Beds are crudely horizontal and interfinger.

Denser lense of *Crassostrea*.

Denser lense of *Crassostrea*.

Silty sandstone, massive, grey to brown, moderatley weathered, poorly indurated, sparse oysters with fossil hash. Oysters hard to see as section weathered.

Logged by Larissa Macmillan and Micheal Tayler 17/01/09

Stratigraphic Column from Parikino 04 - 120 m

Logging and other details

LEGEND

Oyster Density
- Dense bed
- Moderate bed
- Sparse bed

Contacts
- Sharp
- Gradational
- Abruptly gradational

Fossils
- *Crassostrea ingens*
- Gastropod
- Pectinidae
- Fossils (general)

Thickness (m)

30
25
20
15
10
5
0

Siltstone, massive, blue-grey, moderately weathered, poorly indurated, well sorted, fine silt. No fossils.

Sandstone, massive, brown to orange in colour, moderately, weathered, poorly indurated, well sorted, sand, moderate fossils. *Crassostrea* have no preferential orientation, are articulated and around 120 mm in size.

Dense lense of oysters, articulated, haphazard.

Sandstone, massive, light brown to orange, moderate weathering, poorly indurated, well sorted, sand, rare fossils. Oysters can be seen scattered in the base, crudely bedded. Rare occurence and very weathered.

Grid reference (NZMS 260 R16):
2695545 (E)
6157327 (N)

Logged by Larissa Macmillan and Micheal Tayler 17/01/09

Stratigraphic Column from Parikino 05 - 150 m

Logging and other details

LEGEND

Oyster Density
- Dense bed
- Moderate bed
- Sparse bed

Contacts
- Sharp
- Gradational
- Abruptly gradational

Fossils
- *Crassostrea ingens*
- Gastropod
- Pectinidae
- Fossils (general)

Thickness (m)

30
25
20
15
10
5
0

Siltstone, massive, blue-grey, moderately weathered, poorly indurated, well sorted, fine silt. No fossils.

Sandstone, massive, brown to orange in colour, moderately, weathered, poorly indurated, well sorted, rounded sand, moderate fossils. *Crassostrea* are found in the top most of unit, forming the distal end of a lens. Smaller hashy shell bed can be seen underlying the oysters. *Crassostrea* bed are articulated, haphazard and around 120 mm in size. Rilling and erosional structures suggest a slump or other disturbance.

Oysters can be seen scattered in the base. Rare occurence, articulated, haphazard and highly weathered.

Grid reference (NZMS 260 R16):
2695669 (E)
6157193 (N)

Logged by Larissa Macmillan and Micheal Tayler 17/01/09

Stratigraphic Column from Parikino 06 - 180 m

Logging and other details

LEGEND

Oyster Density
- Dense bed
- Moderate bed
- Sparse bed

Contacts
- Sharp
- Gradational
- Abruptly gradational

Fossils
- *Crassostrea ingens*
- Gastropod
- Pectinidae
- Fossils (general)

Thickness (m)

30
25
20
15
10
5
0

Sandstone, massive, brown to orange, moderatley weathered, poory indurated, well sorted.

Sandstone, massive, brown to orange in colour, moderately, weathered, moderatley indurated, well sorted, rounded sand, abundant fossils. *Crassostrea* are dense and crudely bedded. Shells are articulated and haphazard. Size range 120-150 mm. Pectins form in small bands in the bottom of the unit, and grade out up section.

Sandstone, massive, brown to orange, moderatley weathered, poory indurated, well sorted, rounded.

Grid reference (NZMS 260 R16):
2695694 (E)
6157212 (N)

Logged by Larissa Macmillan and Micheal Tayler 17/01/09

Stratigraphic Column from Parikino 07 - 210 m

Logging and other details

LEGEND

Oyster Density
- Dense bed
- Moderate bed
- Sparse bed

Contacts
- Sharp
- Gradational
- Abruptly gradational

Fossils
- *Crassostrea ingens*
- Gastropod
- Pectinidae
- Fossils (general)

Grid reference (NZMS 260 R16):
2695720 (E)
6157227 (N)

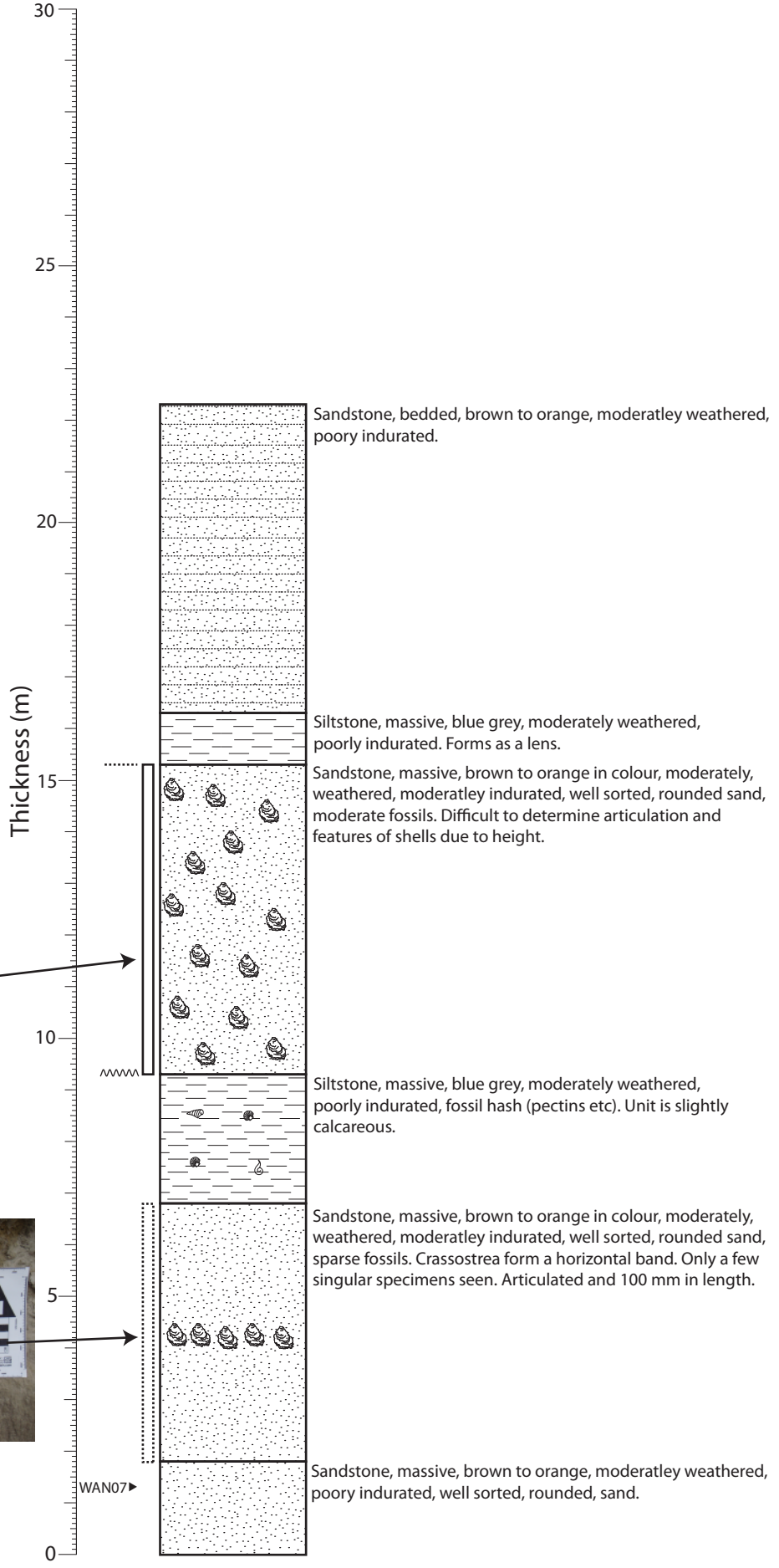

Sandstone, bedded, brown to orange, moderatley weathered, poory indurated.

Siltstone, massive, blue grey, moderately weathered, poorly indurated. Forms as a lens.

Sandstone, massive, brown to orange in colour, moderately, weathered, moderatley indurated, well sorted, rounded sand, moderate fossils. Difficult to determine articulation and features of shells due to height.

Siltstone, massive, blue grey, moderately weathered, poorly indurated, fossil hash (pectins etc). Unit is slightly calcareous.

Sandstone, massive, brown to orange in colour, moderately, weathered, moderatley indurated, well sorted, rounded sand, sparse fossils. Crassostrea form a horizontal band. Only a few singular specimens seen. Articulated and 100 mm in length.

Sandstone, massive, brown to orange, moderatley weathered, poory indurated, well sorted, rounded, sand.

Logged by Larissa Macmillan and Micheal Tayler 17/01/09

Stratigraphic Column from Parikino 09 - 270 m

Logging and other details

LEGEND

Oyster Density
- Dense bed
- Moderate bed
- Sparse bed

Contacts
- Sharp
- Gradational
- Abruptly gradational

Fossils
- *Crassostrea ingens*
- Gastropod
- Pectinidae
- Fossils (general)

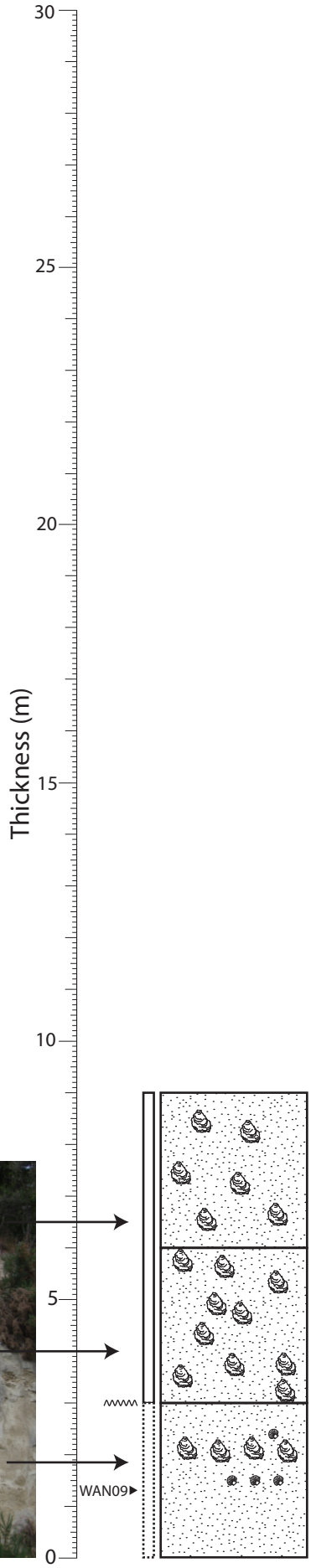

Sandstone, massive, brown to orange in colour, moderately, weathered, moderatley indurated, well sorted, rounded, fine sand, moderate fossils. Shells are scattered throughout section, articulated and 120 mm in size.

Sandstone, massive, brown to orange in colour, moderately, weathered, moderatley indurated, well sorted, rounded, fine sand, moderate fossils. Shells are articulated and 120 mm in size. They are scattered throughout section, show crude bedding and tend to form clumps in the centre.

Sandstone, massive, brown to orange, moderatley weathered, poory indurated, well sorted, rounded, sand, sparse fossils. Fossils include *Crassostrea* horizontally aligned and beds of small pectins. *Crassostrea* are articulated and 120-150mm in size.

Grid reference (NZMS 260 R16):
2695774 (E)
6157252 (N)

240-270m ph80-ph89

Logged by Larissa Macmillan and Micheal Tayler 17/01/09

Stratigraphic Column from Parikino 10 - 300 m

Logging and other details

LEGEND

Oyster Density
- Dense bed
- Moderate bed
- Sparse bed

Contacts
- Sharp
- Gradational
- Abruptly gradational

Fossils
- *Crassostrea ingens*
- Gastropod
- Pectinidae
- Fossils (general)

Thickness (m)

30
25
20
15
10
5
0

Sandstone, massive, grey to brown in colour, moderately, weathered (limonite stain), moderately indurated, well sorted, rounded, medium sand. Rare oysters seen in upper most of unit.

Siltstone, massive, blue to grey, slightly weathered, poorly indurated, fossil pectinid bed present. Siltstone appears in a lens.

Sandstone, massive, grey to brown in colour, moderately, weathered (limonite stain), fossiliferous, micaceous moderatley indurated, well sorted, rounded, medium sand. Slightly calcareous.

Grid reference (NZMS 260 R16):
2695795 (E)
6157275 (N)

Logged by Larissa Macmillan and Micheal Tayler 17/01/09

Stratigraphic Column from Parikino 11 - 311 m

Logging and other details

LEGEND

Oyster Density
- Dense bed
- Moderate bed
- Sparse bed

Contacts
- Sharp
- Gradational
- Abruptly gradational

Fossils
- *Crassostrea ingens*
- Gastropod
- Pectinidae
- Fossils (general)

Thickness (m)

30
25
20
15
10
5
0

Sandstone, massive, grey to brown in colour, moderately, weathered (limonite stain), moderatley indurated, well sorted, rounded, medium sand. Moderate to abundant *Crassostrea* fossils. Oysters form a dense lens in the centre of the unit, these shells are haphazard, articulated and 120 mm in size. Other areas shells thin out and possible become slighty disarticulated.

Vegetation.

Sandstone, massive, grey to brown in colour, moderately, weathered (limonite stain), moderatley indurated, well sorted, rounded, medium sand.

Moderate bed of *Crassostrea*. Shells are haphazard, articulated and 120 -150 mm. Reef can be seen developing from cones.

Sandstone, massive, grey to brown in colour, moderately, weathered (limonite stain), moderatley indurated, well sorted, rounded, medium sand. Pectins occur in thin bands, sparsly scattered and 50 mm thick. Single disarticulated fossil sighted. Slightly calcareous.

Grid reference (NZMS 260 R16):
2695800 (E)
6157278 (N)

Logged by Larissa Macmillan and Micheal Tayler 17/01/09

Stratigraphic Column from Parikino 12 - 330 m

Logging and other details

LEGEND

Oyster Density
- Dense bed
- Moderate bed
- Sparse bed

Contacts
- Sharp
- Gradational
- Abruptly gradational

Fossils
- *Crassostrea ingens*
- Gastropod
- Pectinidae
- Fossils (general)
- Bivalve (Disarticulated)

Thickness (m)

30
25
20
15
10
5
0

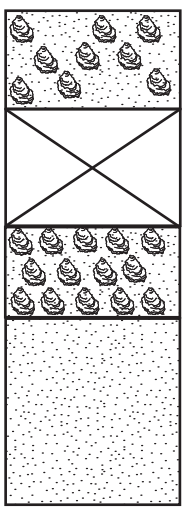

Moderate bed of *Crassostrea*. Shells are haphazard, articulated and 120 -150 mm.

Vegetation.

Abundant bed of *Crassostrea*. Shells are haphazard, articulated and 120 -150 mm.

Sandstone, massive, grey to brown in colour, moderately, weathered (liminite stain), moderatley-poorly indurated, well sorted, rounded, fine sand.

Grid reference (NZMS 260 R16):
2695822 (E)
6157290 (N)

Logged by Larissa Macmillan and Micheal Tayler 17/01/09

Stratigraphic Column from Parikino 13 - 360 m

Logging and other details

LEGEND

Oyster Density
- Dense bed
- Moderate bed
- Sparse bed

Contacts
- Sharp
- Gradational
- Abruptly gradational

Fossils
- *Crassostrea ingens*
- Gastropod
- Pectinidae
- Fossils (general)

Grid reference (NZMS 260 R16):
2695822 (E)
6157290 (N)

Thickness (m)

30
25
20
15
10
5
0

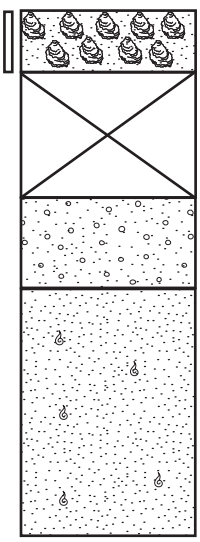

Moderate bed of *Crassostrea*. Shells are haphazard, articulated and 120 -150 mm.

Vegetation.

Sandstone, blocky, grey to brown in colour, moderately, weathered (liminite stain), moderatley-poorly indurated, well sorted, rounded, fine sand. Round fist sized rock inclusions, probably re-working. Bed filled with plant roots.

Sandstone, massive, grey to brown in colour, moderately, weathered (liminite stain), moderatley-poorly indurated, well sorted, rounded, fine sand. Contains some fossil hash.

Logged by Larissa Macmillan and Micheal Tayler 17/01/09

Stratigraphic Column from Parikino 14 - 390 m

Logging and other details

LEGEND

Oyster Density
- Dense bed
- Moderate bed
- Sparse bed

Contacts
- Sharp
- Gradational
- Abruptly gradational

Fossils
- *Crassostrea ingens*
- Gastropod
- Pectinidae
- Fossils (general)

Grid reference (NZMS 260 R16):
2695863 (E)
6157334 (N)

Thickness (m)

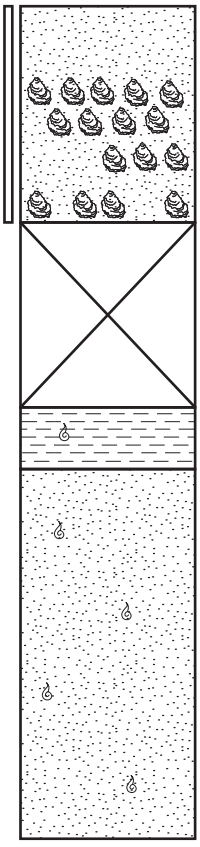

Oyster reef. Oysters appear to be more sparse in the lower part of the unit. Denser clumps form in the central part of the reef. Oyster shells grade out in the lower part of the section and in distal areas. From a distance the shells remain haphazard and articulated.

Vegetation.

Muddy sandstone, light grey, possibly reworked. A lot of roots and fossil has present.

Sandstone, massive, grey to brown, moderatley weathered (iron staining), poorly-moderately indurated, well sorted, rounded, sand. Common occurence of shell material throughout the unit. Peices up to 6cm. Some of the shell peices form small beds.

Logged by Larissa Macmillan and Micheal Tayler 18/01/09

Stratigraphic Column from Parikino 15 - 420 m

Logging and other details

LEGEND

Oyster Density
- Dense bed
- Moderate bed
- Sparse bed

Contacts
- Sharp
- Gradational
- Abruptly gradational

Fossils
- *Crassostrea ingens*
- Gastropod
- Pectinidae
- Fossils (general)

Grid reference (NZMS 260 R16):
2695899 (E)
6157341 (N)

Thickness (m)

30
25
20
15
10
5
0

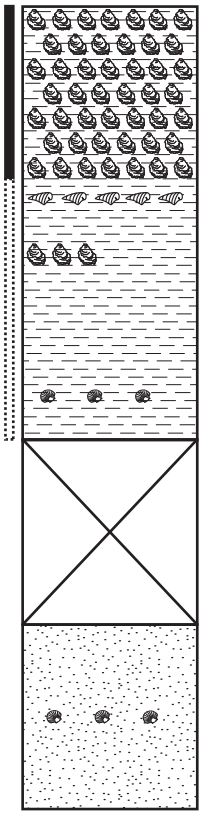

Oyster bed, densely packed through top half of the bed, oysters become sparse near the bottom of the bed. Oysters are haphazardly orientated and articulated. Below dense bed there is a bed of gastropods followed by sparser oysters, and a thin bed of pectins. Shell material is weathered to powder in places. Matrix consists of massive sandy siltstone, light grey moderately weathered, poorly-moderately indurated, well sorted, fine silty sand.

Vegetation.

Sandstone, massive, grey to light brown, moderately weathered (iron stain) poorly to moderatley indurated, well sorted, fine sandstone. Scattered bed of pectins.

Logged by Larissa Macmillan and Micheal Tayler 18/01/09

Stratigraphic Column from Parikino 16 - 450 m

Logging and other details

LEGEND

Oyster Density
- Dense bed
- Moderate bed
- Sparse bed

Contacts
- Sharp
- Gradational
- Abruptly gradational

Fossils
- *Crassostrea ingens*
- Gastropod
- Pectinidae
- Fossils (general)

Grid reference (NZMS 260 R16):
2695912 (E)
6157374 (N)

Thickness (m)

30
25
20
15
10
5
0

WAN16A ▶

WAN16 ▶

Very dense oyster bed. Shells are haphazard, articulated and are part of a thicker reed which extends laterally to column 15 (30 m).

Matrix between shells consists of a light grey sandy siltstone. Many gastropod shells amongst reef.

Sandstone, massive, buff to orange colour, moderately weathered, poorly to moderatley indurated. Moderatley packed oyster bed, thicker towards the right of the column, shells are articulated, and form in nests, no abrupt boundary to denser above bed.

Sandstone, massive, buff to orange colour, moderately weathered (iron stain), poorly-moderately indurated. Thin beds of shell material run through the section, sparse oysters present. Formation of nests?

Logged by Larissa Macmillan and Micheal Tayler 18/01/09

Stratigraphic Column from Parikino 17 - 480 m

Logging and other details

LEGEND

Oyster Density
- Dense bed
- Moderate bed
- Sparse bed

Contacts
- Sharp
- Gradational
- Abruptly gradational

Fossils
- *Crassostrea ingens*
- Gastropod
- Pectinidae
- Fossils (general)

Thickness (m)

30
25
20
15
10
5
0

Sandstone, massive, brown to grey, moderately weathered, poorly to moderatley indurated. Sparse number of oysters. Seen at 7 m and 10 m. Hard to see, possibly more.

Sandstone, massive, brown to grey, moderately weathered (iron stain), poorly-moderately indurated. Well indurated concretion found at 1.5 m. Slightly larger than fist size, shell fragments throughout section. Small patch of oysters found next to hard concretion.

Grid reference (NZMS 260 R16):
2695930 (E)
6157390 (N)

Logged by Larissa Macmillan and Micheal Tayler 18/01/09

Stratigraphic Column from Parikino 18 - 510 m

Logging and other details

LEGEND

Oyster Density
- Dense bed
- Moderate bed
- Sparse bed

Contacts
- Sharp
- Gradational
- Abruptly gradational

Fossils
- *Crassostrea ingens*
- Gastropod
- Pectinidae
- Fossils (general)

Grid reference (NZMS 260 R16):
2695946 (E)
6157414 (N)

Thickness (m)

30
25
20
15
10
5
0

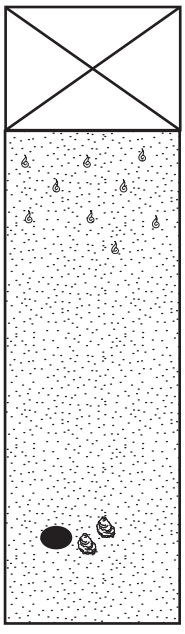

Sandstone, massive, brown to grey, moderately weathered (iron stain), poorly-moderately indurated. Shell fragments can be seen throughout bed with density increasing in the upper part of the bed. Indurated concretion seem at 1.5 m approx from the bottom of the section. Concretions have oysters in and around.

Logged by Larissa Macmillan and Micheal Tayler 18/01/09

Stratigraphic Column from Parikino 19 - 540 m

Logging and other details

LEGEND

Oyster Density
- Dense bed
- Moderate bed
- Sparse bed

Contacts
- Sharp
- Gradational
- Abruptly gradational

Fossils
- *Crassostrea ingens*
- Gastropod
- Pectinidae
- Fossils (general)

Grid reference (NZMS 260 R16):
2695989 (E)
6157441 (N)

Logged by Larissa Macmillan and Micheal Tayler 18/01/09

Stratigraphic Column from Parikino 20 - 584 m

Logging and other details

LEGEND

Oyster Density
- Dense bed
- Moderate bed
- Sparse bed

Contacts
- Sharp
- Gradational
- Abruptly gradational

Fossils
- *Crassostrea ingens*
- Gastropod
- Pectinidae
- Fossils (general)

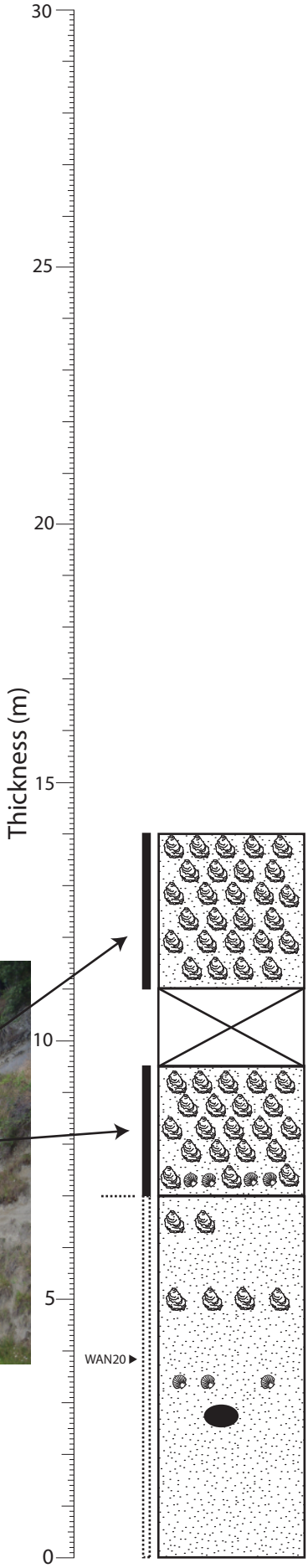

Oysters dense oyster bed, hard to view here due to outcrop height.

Dense oyster bed, haphazard and articulated. Nests can be seen in the upper parts of the sandstone unit. Also in the centre of the dense unit. Bands of pectins occur at the bottom of the oyster occurence.

Sandstone, massive, buff to grey, moderately weathered (iron stain), poorly-moderately indurated, medium to fine well sorted sand. Small fine beds of pectins and fossil hash can be seen in the lower parts of the unit. Also nests of oysters can be seen in the top of the section. Hard concretions as in 17 and 18 can be seen in the lower part of the unit.

Grid reference (NZMS 260 R16):
2695978 (E)
6157466 (N)

Logged by Larissa Macmillan and Micheal Tayler 18/01/09

Stratigraphic Column from Rangitatau East Road R1

Logging and other details

LEGEND

Oyster Density
- Dense bed
- Moderate bed
- Sparse bed

Contacts
- Sharp
- Gradational
- Abruptly gradational

Fossils
- *Crassostrea ingens*
- Gastropod
- Pectinidae
- Fossils (general)

Thickness (m)

30
25
20
15
10
5
0

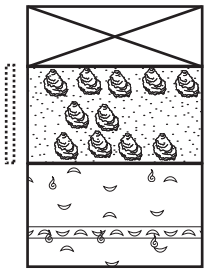

Poor exposure of oysters. Sparsely packed, haphazardly orientated within a moderately indurated fine sandstone or very fine sandsonte matrix.

Shell hash bed. Section covered in moss making identification difficult. Possible presence of *Ostrea* Shells are contained in a moderate to well indurated siltstone or very fine sandstone.

Grid reference (NZMS 260 R16):
2678262 (E)
6163717 (N)

Logged by Larissa Macmillan and Micheal Tayler 20/01/09

Stratigraphic Column from Rangitatau East Road R2

Logging and other details

LEGEND

Oyster Density
- Dense bed
- Moderate bed
- Sparse bed

Contacts
- Sharp
- Gradational
- Abruptly gradational

Fossils
- *Crassostrea ingens*
- Gastropod
- Pectinidae
- Fossils (general)

Grid reference (NZMS 260 R16):
2678292 (E)
6163741 (N)

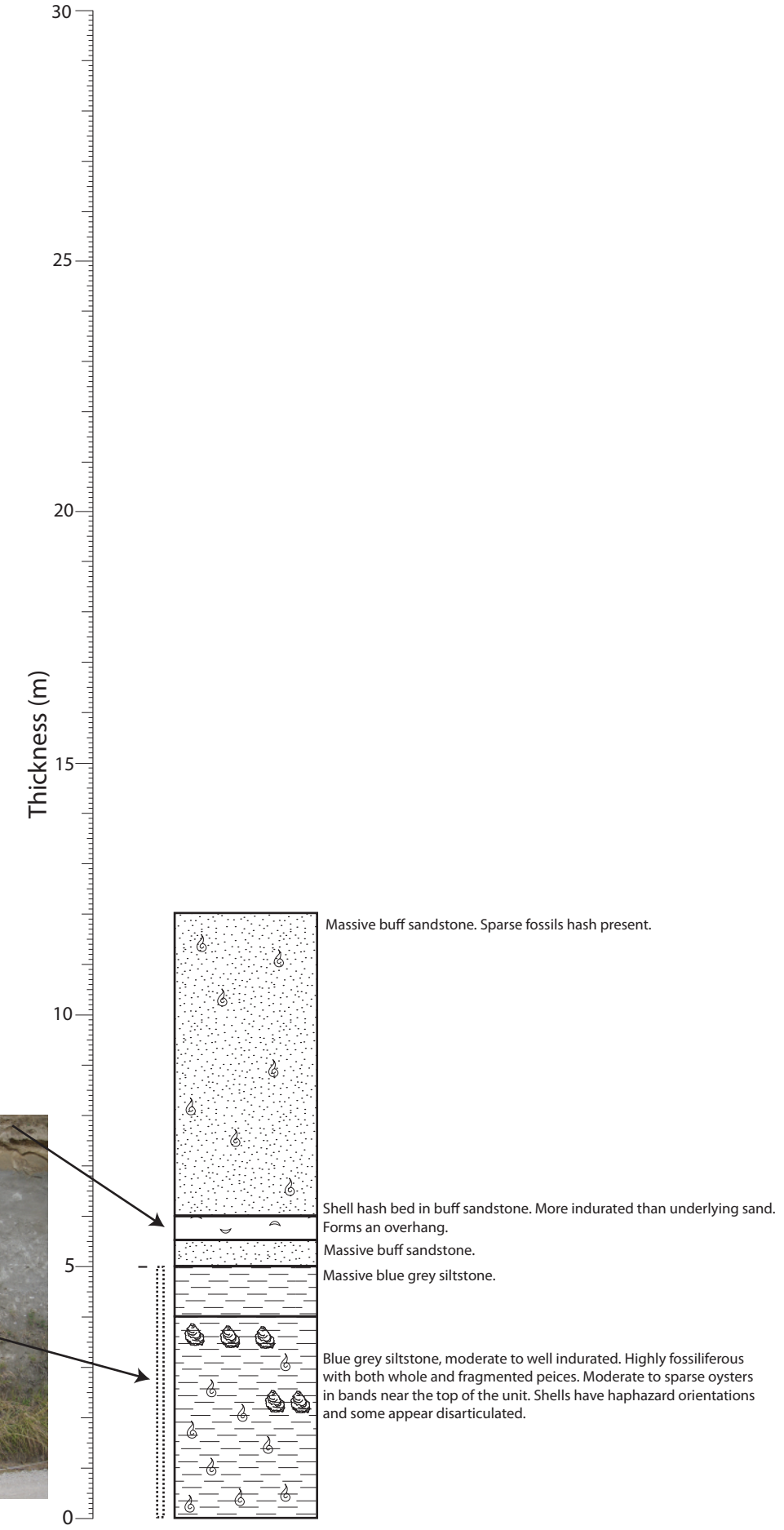

Logged by Larissa Macmillan and Micheal Tayler 20/01/09

Stratigraphic Column from Rangitatau East Road R3

Logging and other details

LEGEND

Oyster Density
- Dense bed
- Moderate bed
- Sparse bed

Contacts
- Sharp
- Gradational
- Abruptly gradational

Fossils
- *Crassostrea ingens*
- Gastropod
- Pectinidae
- Fossils (general)

Thickness (m)

30
25
20
15
10
5
0

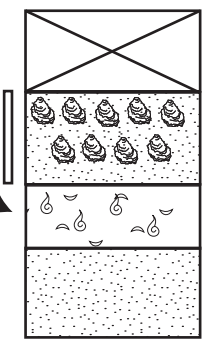

Buff sandstone. Dense to moderate shellbed. Oysters are denser towards the left of the bed and begin to pinch out towards the centre of the outcrop.

Densely packed shell hash bed in buff sandstone. Presence of bivalves, bryozoans and *Ostrea?* Moderately indurated and slightly weathered.

Massive buff sandstone, medium grained, poorly indurated.

Grid reference (NZMS 260 R16):
2678315 (E)
6163741 (N)

Logged by Larissa Macmillan and Micheal Tayler 20/01/09

Stratigraphic Column from Rangitatau East Road R4

Logging and other details

LEGEND

Oyster Density
- Dense bed
- Moderate bed
- Sparse bed

Contacts
- Sharp
- Gradational
- Abruptly gradational

Fossils
- *Crassostrea ingens*
- Gastropod
- Pectinidae
- Fossils (general)

Thickness (m)

30
25
20
15
10
5
0

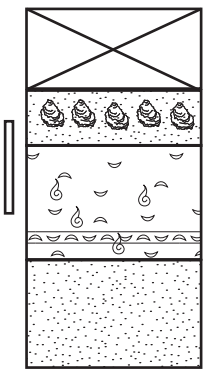

Moderate packed oyster bed. Oysters orientations are haphazard. Weathered and poor outcrop quality makes it hard to see.

Densely packed shell hash bed in buff fine sandstone mtrix. Presence of bivalves, bryozoans and *Ostrea?* Moderately indurated and slightly weathered with iron stain present.

Massive buff sandstone, medium grained, poorly indurated, fine sandstone. Weathers to a light grey.

Grid reference (NZMS 260 R16):
2678326 (E)
6163760 (N)

Logged by Larissa Macmillan and Micheal Tayler 20/01/09

Stratigraphic Column from Kaurapaoa Road K1 1.7 m

Logging and other details

LEGEND

Oyster Density
- Dense bed
- Moderate bed
- Sparse bed

Contacts
- Sharp
- Gradational
- Abruptly gradational

Fossils
- *Crassostrea ingens*
- Gastropod
- Pectinidae
- Fossils (general)

Grid reference (NZMS 260 R16):
2690152 (E)
6159215 (N)

Thickness (m)

30
25
20
15
10
5
0

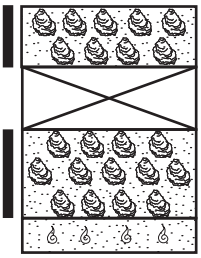

Densley packed oyster bed. Oyster orientation appears haphazard. Cannot see details due to height.

Densley packed oyster bed. Oyster orientation is random, shells are articulated and pectins are in the matrix. Matrix is fine sandstone.

Sandstone, massive, brown, moderately, poorly indurated, fine sandstone. Weathers to light brown. Some shell fragments.

Logged by Larissa Macmillan and Micheal Tayler 19/01/09

Stratigraphic Column from Kaurapaoa Road K2 7.3 m

Logging and other details

LEGEND

Oyster Density
- Dense bed
- Moderate bed
- Sparse bed

Contacts
- Sharp
- Gradational
- Abruptly gradational

Fossils
- *Crassostrea ingens*
- Gastropod
- Pectinidae
- Fossils (general)

Thickness (m)

30
25
20
15
10
5
0

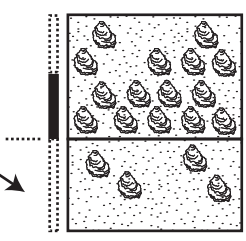

Oyster bed, very densely packed, alot of pectins throughout the unit. Shells remain haphazard and many are articulated. Shells are highly bioeroded and are denser in the lower part of the unit. Become sparse in places at the top.

Sandstone, massive, buff to grey, slightly weathered, poorly to moderately indurated, medium grained. Large amount of fossil hash, pectins visible. Some large oyster can be seen as a 'nest' in the lower part of the section.

Grid reference (NZMS 260 R16):
2690156 (E)
6159210 (N)

Logged by Larissa Macmillan and Micheal Tayler 19/01/09

Stratigraphic Column from Kaurapaoa Road K3 12.4 m

Logging and other details

LEGEND

Oyster Density
- Dense bed
- Moderate bed
- Sparse bed

Contacts
- Sharp
- Gradational
- Abruptly gradational

Fossils
- *Crassostrea ingens*
- Gastropod
- Pectinidae
- Fossils (general)

Grid reference (NZMS 260 R16):
2690156 (E)
6159210 (N)

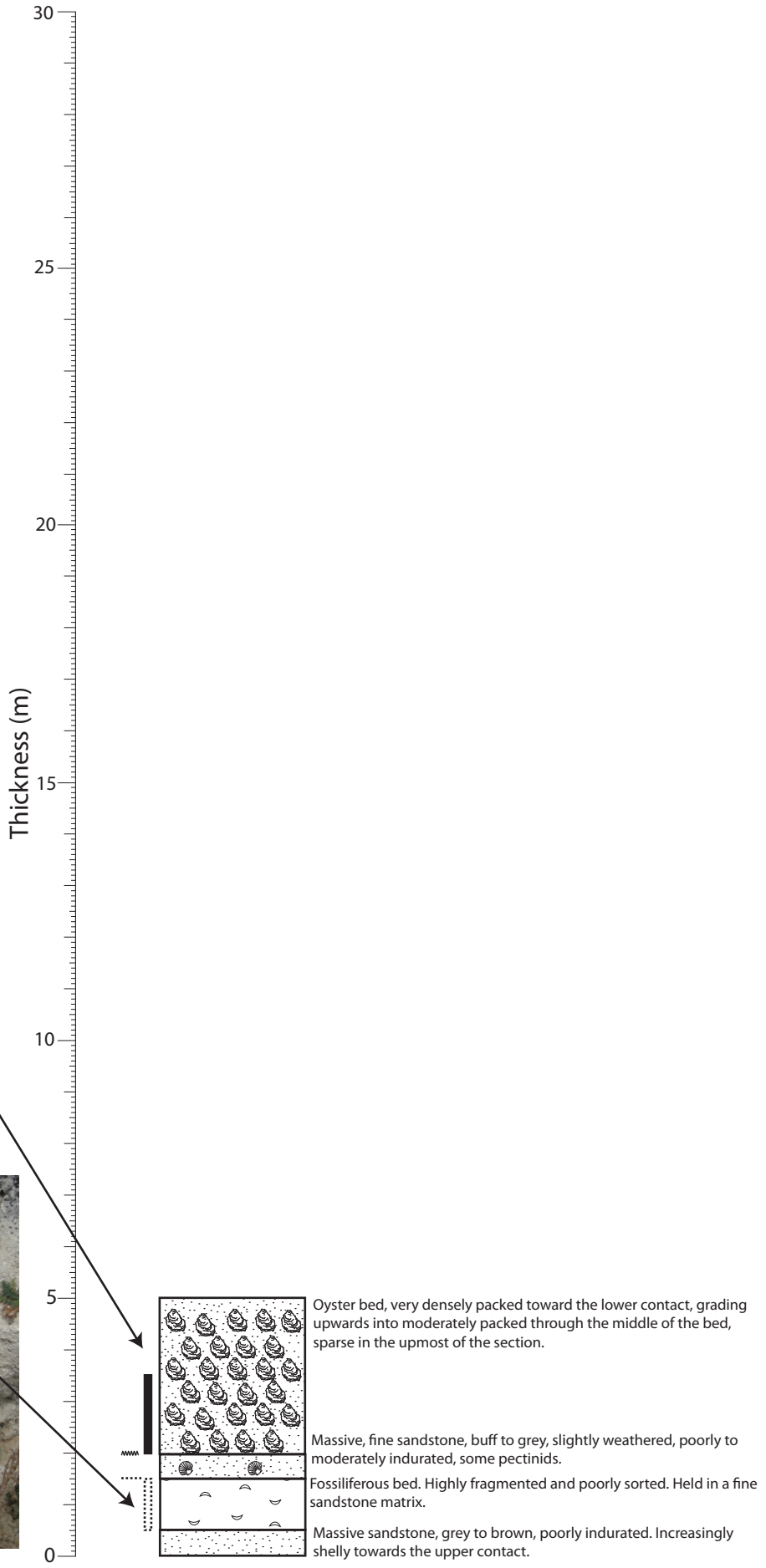

Logged by Larissa Macmillan and Micheal Tayler 19/01/09

Stratigraphic Column from Kaurapaoa Road K4

Logging and other details

LEGEND

Oyster Density
- Dense bed
- Moderate bed
- Sparse bed

Contacts
- Sharp
- Gradational
- Abruptly gradational

Fossils
- *Crassostrea ingens*
- Gastropod
- Pectinidae
- Fossils (general)

Thickness (m)

30
25
20
15
10
5
0

Oyster bed, moderately packed. Shells are haphazard and many are articulated. Shells are highly bioeroded.

Sandstone, massive, buff to grey, weathered, conspicuous iron stain poorly to moderately indurated, medium grained. Some fossil hash, hard concretions present.

Grid reference (NZMS 260 R16):
26989745 (E)
6158656 (N)

Logged by Larissa Macmillan and Micheal Tayler 19/01/09

Stratigraphic Column from Kaurapaoa Road K5

Logging and other details

LEGEND

Oyster Density
- Dense bed
- Moderate bed
- Sparse bed

Contacts
- Sharp
- Gradational
- Abruptly gradational

Fossils
- *Crassostrea ingens*
- Gastropod
- Pectinidae
- Fossils (general)

Grid reference (NZMS 260 R16):
2689775 (E)
6158413 (N)

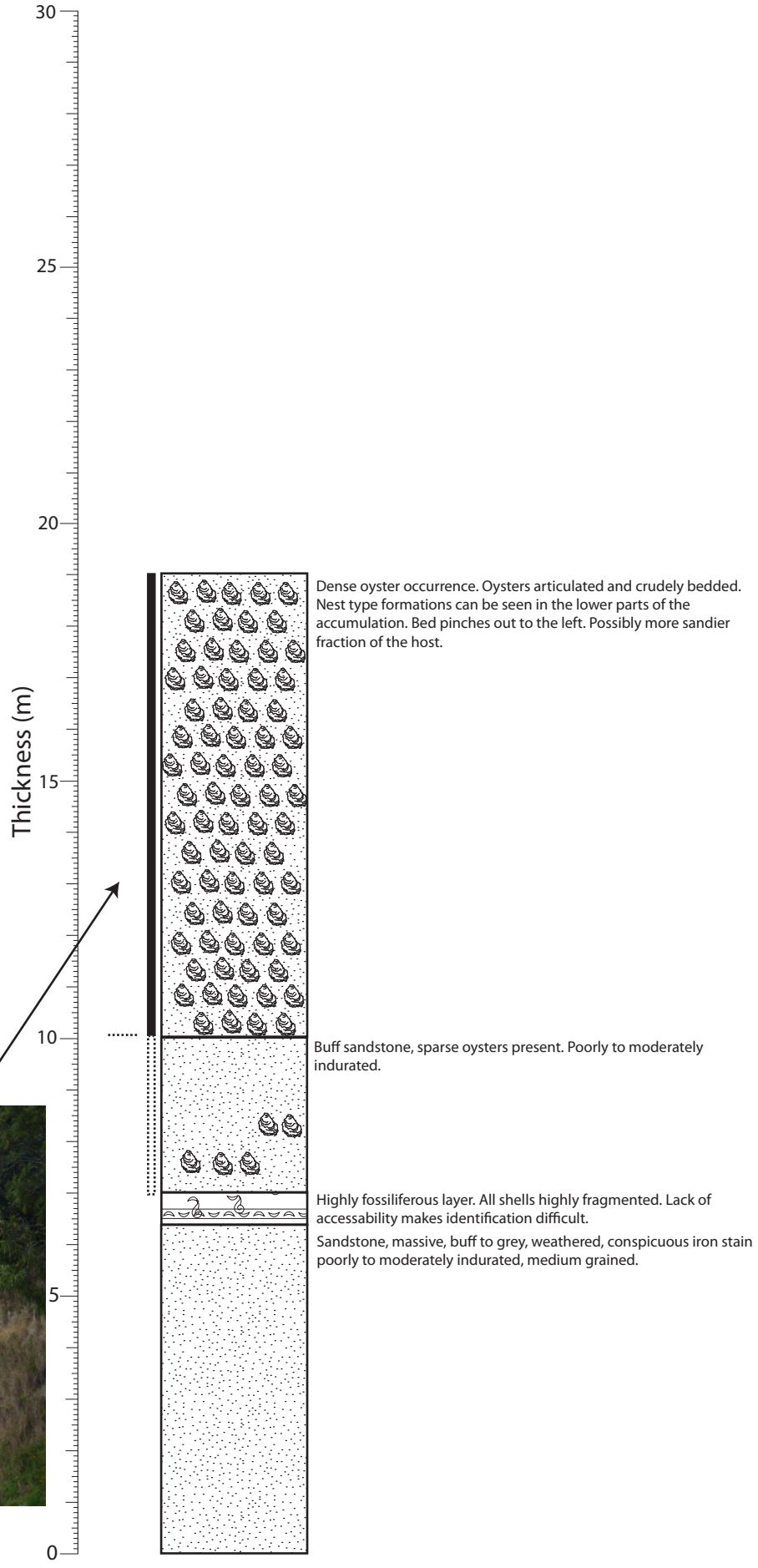

Logged by Larissa Macmillan and Micheal Tayler 19/01/09

Stratigraphic Column from Kaurapaoa Road K6

Logging and other details

LEGEND

Oyster Density
- Dense bed
- Moderate bed
- Sparse bed

Contacts
- Sharp
- Gradational
- Abruptly gradational

Fossils
- *Crassostrea ingens*
- Gastropod
- Pectinidae
- Fossils (general)

Thickness (m)

30
25
20
15
10
5
0

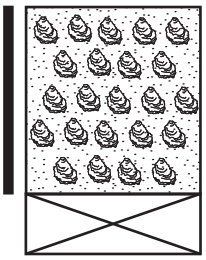

Dense oyster occurrence in a blue-grey sandy silt matrix. Oysters articulated and crudely bedded. Nest type formations can be seen in the lower parts of the accumulation.

Grid reference (NZMS 260 R16):
2689868 (E)
6158413 (N)

Logged by Larissa Macmillan and Micheal Tayler 19/01/09

Petrographic data sheet - Larissa Macmillan			
Sample number		WAP15/1B	
Sample description		Host	
Analyst		Larissa Macmillan	
BIOCLASTICS	**Total bioclast %**	55	
		%	**Abundance limit**
	Bryozoans	-	absent
	Bivalves	51	abundant
	Echinoderms	3	some
	Benthic foraminifera	-	absent
	Planktic foraminifera	1	some
	Gastropods	-	absent
	Calcareous algae	-	absent
	Barnacles	-	absent
	Spicules & spines	-	absent
	Other	-	absent
	Modal size 1 (mm)	3.75	
	Modal size 2 (mm)	0.75	
	Shape/abrasion	moderatley abraded	
	Sorting	poorly sorted biomicrite	
SILICICLASTICS	**Siliciclastic grain %**	45	
		%	**Abundance limit**
	Quartz	6	many
	Feldspar	32	very common
	Igneous rock fragments	-	absent
	Sedimentary rock fragments	-	absent
	Micas	-	absent
	Pyrite grains	5	some
	Pyrite infills	2	some
	Glauconite pellets	-	absent
	Glauconite infills	-	absent
	Other	-	absent
	Modal size 1 (mm)	0.30	
	Modal size 2 (mm)	0.18	
	Shape/abrasion	subangular	
	Sorting	moderately sorted	
SHELL FEATURES	Shell fabric - crystal shapes, weathering, ppt minerals		
	Shell increments - Thickness, colour, continuous, discontinuous		
	Borings - size, shape, boundaries, location (within layer or truncating)		
	Infill - type, bioclastics, siliciclastics, geopetal fabrics, sparite, micritic peliods		
	Recrystallisation - distribution, degree, location.		
	Modal size 1 (mm)		
	Modal size 2 (mm)		

Petrographic data sheet - Larissa Macmillan 2009			
Sample number		W04/1B	
Sample description		Host	
Analyst		Larissa Macmillan	
BIOCLASTICS	**Total bioclast %**	95	
		%	**Abundance limit**
	Bryozoans	60	abundant
	Bivalves	23	common
	Echinoderms	-	absent
	Benthic foraminifera	8	many
	Planktic foraminifera	4	some
	Gastropods	-	absent
	Calcareous algae	-	absent
	Barnacles	-	absent
	Spicules & spines	-	absent
	Other	-	absent
	Modal size 1 (mm)	0.25	
	Modal size 2 (mm)	0.75	
	Shape/abrasion	moderately abraded	
	Sorting	poorly sorted biomicrite	
SILICICLASTICS	**Siliciclastic grain %**		
		%	**Abundance limit**
	Quartz	1.00	rare
	Feldspar	4.00	some
	Igneous rock fragments	-	absent
	Sedimentary rock fragments	-	absent
	Micas	-	absent
	Pyrite grains	-	absent
	Pyrite infills	-	absent
	Glauconite pellets	-	absent
	Glauconite infills	-	absent
	Other	-	absent
	Modal size 1 (mm)	0.08	
	Modal size 2 (mm)	0.30	
	Shape/abrasion	subangular	
	Sorting	poorly sorted	
SHELL FEATURES	Shell fabric - crystal shapes, weathering, ppt minerals		
	Shell increments - Thickness, colour, continuous, discontinuous		
	Borings - size, shape, boundaries, location (within layer or truncating)		
	Infill - type, bioclastics, siliciclastics, geopetal fabrics, sparite, micritic peliods		
	Recrystallisation - distribution, degree, location.		
	Modal size 1 (mm)		
	Modal size 2 (mm)		

Petrographic data sheet - Larissa Macmillan 2009			
Sample number		K11/1A	
Sample description		Host	
Analyst		Larissa Macmillan	
BIOCLASTICS	**Total bioclast %**	77	
		%	**Abundance limit**
	Bryozoans	46	very common
	Bivalves	25	common
	Echinoderms	5	some
	Benthic foraminifera	1	rare
	Planktic foraminifera	-	absent
	Gastropods	-	absent
	Calcareous algae	-	absent
	Barnacles	-	absent
	Spicules & spines	-	absent
	Other	-	absent
	Modal size 1 (mm)	2.00	
	Modal size 2 (mm)	0.50	
	Shape/abrasion	moderately abraded	
	Sorting	poorly sorted	
SILICICLASTICS	**Siliciclastic grain %**	23	
		%	**Abundance limit**
	Quartz	2	some
	Feldspar	8	many
	Igneous rock fragments	-	absent
	Sedimentary rock fragments	-	absent
	Micas	-	absent
	Pyrite grains	3	some
	Pyrite infills	-	absent
	Glauconite pellets	4	some
	Glauconite infills	16	common
	Other	-	absent
	Modal size 1 (mm)	0.10	
	Modal size 2 (mm)	0.25	
	Shape/abrasion	subrounded	
	Sorting	poorly sorted	
SHELL FEATURES	Shell fabric - crystal shapes, weathering, ppt minerals		
	Shell increments - Thickness, colour, continuous, discontinuous		
	Borings - size, shape, boundaries, location (within layer or truncating)		
	Infill - type, bioclastics, siliciclastics, geopetal fabrics, sparite, micritic peliods		
	Recrystallisation - distribution, degree, location.		
	Modal size 1 (mm)		
	Modal size 2 (mm)		

Petrographic data sheet - Larissa Macmillan 2009			
Sample number		WAI15/2A	
Sample description		Host	
Analyst		Larissa Macmillan	
BIOCLASTICS	**Total bioclast %**	85	
		%	**Abundance limit**
	Bryozoans	71	abundant
	Bivalves	10	many
	Echinoderms	1	rare
	Benthic foraminifera	-	absent
	Planktic foraminifera	3	some
	Gastropods	-	absent
	Calcareous algae	-	absent
	Barnacles	-	absent
	Spicules & spines	-	absent
	Other	-	absent
	Modal size 1 (mm)	0.88	
	Modal size 2 (mm)	2.75	
	Shape/abrasion	moderately abraded	
	Sorting	poorly sorted biomicrite	
SILICICLASTICS	**Siliciclastic grain %**	15	
		%	**Abundance limit**
	Quartz	1	rare
	Feldspar	8	many
	Igneous rock fragments	-	absent
	Sedimentary rock fragments	-	absent
	Micas	-	absent
	Pyrite grains	3	some
	Pyrite infills	-	absent
	Glauconite pellets	2	some
	Glauconite infills	1	rare
	Other	-	absent
	Modal size 1 (mm)	0.18	
	Modal size 2 (mm)	0.30	
	Shape/abrasion	subangular	
	Sorting	moderately sorted	
SHELL FEATURES	Shell fabric - crystal shapes, weathering, ppt minerals		
	Shell increments - Thickness, colour, continuous, discontinuous		
	Borings - size, shape, boundaries, location (within layer or truncating)		
	Infill - type, bioclastics, siliciclastics, geopetal fabrics, sparite, micritic peliods		
	Recrystallisation - distribution, degree, location.		
	Modal size 1 (mm)		
	Modal size 2 (mm)		

Petrographic data sheet - Larissa Macmillan 2009			
Sample number		WAI17/1B	
Sample description		Shell	
Analyst		Larissa Macmillan	
BIOCLASTICS	**Total bioclast %**	0	
		%	**Abundance limit**
	Bryozoans		
	Bivalves		
	Echinoderms		
	Benthic foraminifera		
	Planktic foraminifera		
	Gastropods		
	Calcareous algae		
	Barnacles		
	Spicules & spines		
	Other		
	Modal size 1 (mm)		
	Modal size 2 (mm)		
	Shape/abrasion		
	Sorting		
SILICICLASTICS	**Siliciclastic grain %**	0	
		%	**Abundance limit**
	Quartz		
	Feldspar		
	Igneous rock fragments		
	Sedimentary rock fragments		
	Micas		
	Pyrite grains		
	Pyrite infills		
	Glauconite pellets		
	Glauconite infills		
	Other		
	Modal size 1 (mm)		
	Modal size 2 (mm)		
	Shape/abrasion		
	Sorting		
SHELL FEATURES	Shell fabric - crystal shapes, weathering, ppt minerals	homogenous calcite	
	Shell increments - Thickness, colour, continuous, discontinuous	Shell layers are harder to determine. Grey layers (1.75 mm) and light brown layers (0.05-0.25 mm).	
	Borings - size, shape, boundaries, location (within layer or truncating)	-	
	Infill - type, bioclastics, siliciclastics, geopetal fabrics, sparite, micritic peliods	-	
	Recrystallisation - distribution, degree, location.	occurs within dark grey layers as blocky spar and along the margin of thinner layers	
	Modal size 1 (mm)		
	Modal size 2 (mm)		

Petrographic data sheet - Larissa Macmillan			
Sample number		WAP15_1B_A	
Sample description		Shell	
Analyst		Larissa Macmillan	
BIOCLASTICS	**Total bioclast %**	0	
		%	**Abundance limit**
	Bryozoans		
	Bivalves		
	Echinoderms		
	Benthic foraminifera		
	Planktic foraminifera		
	Gastropods		
	Calcareous algae		
	Barnacles		
	Spicules & spines		
	Other		
	Modal size 1 (mm)		
	Modal size 2 (mm)		
	Shape/abrasion		
	Sorting		
SILICICLASTICS	**Siliciclastic grain %**	0	
		%	**Abundance limit**
	Quartz		
	Feldspar		
	Igneous rock fragments		
	Sedimentary rock fragments		
	Micas		
	Pyrite grains		
	Pyrite infills		
	Glauconite pellets		
	Glauconite infills		
	Other		
	Modal size 1 (mm)		
	Modal size 2 (mm)		
	Shape/abrasion		
	Sorting		
SHELL FEATURES	Shell fabric - crystal shapes, weathering, ppt minerals	crystal laths of calcite	
	Shell increments - Thickness, colour, continuous, discontinuous	increments vary in thickness. Dark grey (1.125-2.5 mm) and light brown thinner layers (0.25-0.75 mm). Shell layers are irregular and fluctuate in size	
	Borings - size, shape, boundaries, location (within layer or truncating)	-	
	Infill - type, bioclastics, siliciclastics, geopetal fabrics, sparite, micritic peliods	-	
	Recrystallisation - distribution, degree, location.	Recrysatlisation occurs along both layers. In light layers it occurs as blocks of fine grained spar. In the grey layers it occurs as more irregular patches of coarser spar.	
	Modal size 1 (mm)		
	Modal size 2 (mm)		

Petrographic data sheet - Larissa Macmillan 2009			
Sample number		N14/1C	
Sample description		Shell	
Analyst		Larissa Macmillan	
BIOCLASTICS	**Total bioclast %**	0	
		%	**Abundance limit**
	Bryozoans		
	Bivalves		
	Echinoderms		
	Benthic foraminifera		
	Planktic foraminifera		
	Gastropods		
	Calcareous algae		
	Barnacles		
	Spicules & spines		
	Other		
	Modal size 1 (mm)		
	Modal size 2 (mm)		
	Shape/abrasion		
	Sorting		
SILICICLASTICS	**Siliciclastic grain %**	0	
		%	**Abundance limit**
	Quartz		
	Feldspar		
	Igneous rock fragments		
	Sedimentary rock fragments		
	Micas		
	Pyrite grains		
	Pyrite infills		
	Glauconite pellets		
	Glauconite infills		
	Other		
	Modal size 1 (mm)		
	Modal size 2 (mm)		
	Shape/abrasion		
	Sorting		
SHELL FEATURES	Shell fabric - crystal shapes, weathering, ppt minerals	Homogenous calcite to developed crystal laths in places	
	Shell increments - Thickness, colour, continuous, discontinuous	Dark grey layers (2 mm) and light brown layers (0.225 mm). Layers pinch in and out and vary greatly in size. Shell very fractured, many layers broken and discontinuous.	
	Borings - size, shape, boundaries, location (within layer or truncating)	-	
	Infill - type, bioclastics, siliciclastics, geopetal fabrics, sparite, micritic peliods	Layers are filled with terrigenous dominated material (subrounded feldspar and quartz)	
	Recrystallisation - distribution, degree, location.	-	
	Modal size 1 (mm)		
	Modal size 2 (mm)		

Petrographic data sheet - Larissa Macmillan			
Sample number		N14/1B	
Sample description		Shell and infill	
Analyst		Larissa Macmillan	
BIOCLASTICS	**Total bioclast %**	58	
		%	**Abundance limit**
	Bryozoans	5	some
	Bivalves	50	very common
	Echinoderms	-	absent
	Benthic foraminifera	2	some
	Planktic foraminifera	1	rare
	Gastropods	-	absent
	Calcareous algae	-	absent
	Barnacles	-	absent
	Spicules & spines	-	absent
	Other	-	absent
	Modal size 1 (mm)	0.25	
	Modal size 2 (mm)	1.50	
	Shape/abrasion	moderately abraded	
	Sorting	poorly sorted	
SILICICLASTICS	**Siliciclastic grain %**		
		%	**Abundance limit**
	Quartz	8	many
	Feldspar	30	very common
	Igneous rock fragments	-	absent
	Sedimentary rock fragments	-	absent
	Micas	-	absent
	Pyrite grains	1	rare
	Pyrite infills	-	absent
	Glauconite pellets	2	some
	Glauconite infills	1	rare
	Other	-	absent
	Modal size 1 (mm)	0.30	
	Modal size 2 (mm)	0.18	
	Shape/abrasion	subangular	
	Sorting	poorly sorted	
SHELL FEATURES	Shell fabric - crystal shapes, weathering, ppt minerals	homogenous to crystal laths of calcite	
	Shell increments - Thickness, colour, continuous, discontinuous	dark grey layers (0.5-2.5 mm) and light brown layers (0.05-0.15 mm).	
	Borings - size, shape, boundaries, location (within layer or truncating)	many elongate borings with both sharp and irregular boundaries, occur withing grey layer	
	Infill - type, bioclastics, siliciclastics, geopetal fabrics, sparite, micritic peliods	see above	
	Recrystallisation - distribution, degree, location.	-	
	Modal size 1 (mm)	-	
	Modal size 2 (mm)	-	

Petrographic data sheet - Larissa Macmillan			
Sample number		N14/1A	
Sample description		Shell	
Analyst		Larissa Macmillan	
BIOCLASTICS	**Total bioclast %**	0	
		%	**Abundance limit**
	Bryozoans		
	Bivalves		
	Echinoderms		
	Benthic foraminifera		
	Planktic foraminifera		
	Gastropods		
	Calcareous algae		
	Barnacles		
	Spicules & spines		
	Other		
	Modal size 1 (mm)		
	Modal size 2 (mm)		
	Shape/abrasion		
	Sorting		
SILICICLASTICS	**Siliciclastic grain %**	0	
		%	**Abundance limit**
	Quartz		
	Feldspar		
	Igneous rock fragments		
	Sedimentary rock fragments		
	Micas		
	Pyrite grains		
	Pyrite infills		
	Glauconite pellets		
	Glauconite infills		
	Other		
	Modal size 1 (mm)		
	Modal size 2 (mm)		
	Shape/abrasion		
	Sorting		
SHELL FEATURES	Shell fabric - crystal shapes, weathering, ppt minerals	Homogenous calcite to crystal laths.	
	Shell increments - Thickness, colour, continuous, discontinuous	Variation in shell layers dark grey (1.875 mm) and light brown layers (0.25 mm). Great amount of variation in thickness, many layers are broken and discontinuous	
	Borings - size, shape, boundaries, location (within layer or truncating)	-	
	Infill - type, bioclastics, siliciclastics, geopetal fabrics, sparite, micritic peliods	Some layers filled with terrigenous dominated material (feldspar, quartz and rare glaunconite).	
	Recrystallisation - distribution, degree, location.	-	
	Modal size 1 (mm)		
	Modal size 2 (mm)		

Petrographic data sheet - Larissa Macmillan 2009			
Sample number		K12/1B	
Sample description		Oyster shell	
Analyst		Larissa Macmillan	
BIOCLASTICS	**Total bioclast %**	0	
		%	**Abundance limit**
	Bryozoans		
	Bivalves		
	Echinoderms		
	Benthic foraminifera		
	Planktic foraminifera		
	Gastropods		
	Calcareous algae		
	Barnacles		
	Spicules & spines		
	Other		
	Modal size 1 (mm)		
	Modal size 2 (mm)		
	Shape/abrasion		
	Sorting		
SILICICLASTICS	**Siliciclastic grain %**	0	
		%	**Abundance limit**
	Quartz		
	Feldspar		
	Igneous rock fragments		
	Sedimentary rock fragments		
	Micas		
	Pyrite grains		
	Pyrite infills		
	Glauconite pellets		
	Glauconite infills		
	Other		
	Modal size 1 (mm)		
	Modal size 2 (mm)		
	Shape/abrasion		
	Sorting		
SHELL FEATURES	Shell fabric - crystal shapes, weathering, ppt minerals	Homgenous calcite material	
	Shell increments - Thickness, colour, continuous, discontinuous	Thick grey layers (0.625-1.125 mm) and finer light brown layers (0.1-0.125 mm).	
	Borings - size, shape, boundaries, location (within layer or truncating)	-	
	Infill - type, bioclastics, siliciclastics, geopetal fabrics, sparite, micritic peliods	One small area of the shell infilled with limonitised micritic limestone with rare planktic forams.	
	Recrystallisation - distribution, degree, location.	Highly recrystalised shell. Large block calcite spar crystals occur within the dark grey layers. Some portions are highly limonitised. Calcite forms as continous portions or patches of spar.	
	Modal size 1 (mm)		
	Modal size 2 (mm)		

Petrographic data sheet - Larissa Macmillan			
Sample number		W10/2A C	
Sample description		Oyster shell	
Analyst		Larissa Macmillan	
BIOCLASTICS	**Total bioclast %**	0	
		%	**Abundance limit**
	Bryozoans		
	Bivalves		
	Echinoderms		
	Benthic foraminifera		
	Planktic foraminifera		
	Gastropods		
	Calcareous algae		
	Barnacles		
	Spicules & spines		
	Other		
	Modal size 1 (mm)		
	Modal size 2 (mm)		
	Shape/abrasion		
	Sorting		
SILICICLASTICS	**Siliciclastic grain %**	0	
		%	**Abundance limit**
	Quartz		
	Feldspar		
	Igneous rock fragments		
	Sedimentary rock fragments		
	Micas		
	Pyrite grains		
	Pyrite infills		
	Glauconite pellets		
	Glauconite infills		
	Other		
	Modal size 1 (mm)		
	Modal size 2 (mm)		
	Shape/abrasion		
	Sorting		
SHELL FEATURES	Shell fabric - crystal shapes, weathering, ppt minerals	Homogenous calcite material	
	Shell increments - Thickness, colour, continuous, discontinuous	Shell increments vary. Dark grey layers (2.25 mm) and light brown layers (0.25 mm).	
	Borings - size, shape, boundaries, location (within layer or truncating)	-	
	Infill - type, bioclastics, siliciclastics, geopetal fabrics, sparite, micritic peliods	Only a small amount of terrigenous material in localised area (quartz, feldspars and glauconite pallets) within layers	
	Recrystallisation - distribution, degree, location.	Large blocky calcite crystals along shell margins	
	Modal size 1 (mm)		
	Modal size 2 (mm)		

Petrographic data sheet - Larissa Macmillan			
Sample number		W10/2A A	
Sample description		Oyster shell	
Analyst		Larissa Macmillan	
BIOCLASTICS	**Total bioclast %**	0	
		%	**Abundance limit**
	Bryozoans		
	Bivalves		
	Echinoderms		
	Benthic foraminifera		
	Planktic foraminifera		
	Gastropods		
	Calcareous algae		
	Barnacles		
	Spicules & spines		
	Other		
	Modal size 1 (mm)		
	Modal size 2 (mm)		
	Shape/abrasion		
	Sorting		
SILICICLASTICS	**Siliciclastic grain %**	0	
		%	**Abundance limit**
	Quartz		
	Feldspar		
	Igneous rock fragments		
	Sedimentary rock fragments		
	Micas		
	Pyrite grains		
	Pyrite infills		
	Glauconite pellets		
	Glauconite infills		
	Other		
	Modal size 1 (mm)		
	Modal size 2 (mm)		
	Shape/abrasion		
	Sorting		
SHELL FEATURES	Shell fabric - crystal shapes, weathering, ppt minerals	Homogenous calcite	
	Shell increments - Thickness, colour, continuous, discontinuous	Variation in layers. Dark grey (2.125-3.75 mm) and light brown layers (0.2 mm). Layers are continuous throughout	
	Borings - size, shape, boundaries, location (within layer or truncating)	-	
	Infill - type, bioclastics, siliciclastics, geopetal fabrics, sparite, micritic peliods	Areas within the shell contain a large amount of terrigenous material, subangular quartz and glauconite pellets.	
	Recrystallisation - distribution, degree, location.	Highly recrystallised. Occurs along light brown shell margins and also in the centre of the shell as large blocky calcite crystals.	
	Modal size 1 (mm)		
	Modal size 2 (mm)		

Petrographic data sheet - Larissa Macmillan 2009			
Sample number		W05/1B	
Sample description		Oyster shell	
Analyst		Larissa Macmillan	
BIOCLASTICS	**Total bioclast %**	0	
		%	**Abundance limit**
	Bryozoans		
	Bivalves		
	Echinoderms		
	Benthic foraminifera		
	Planktic foraminifera		
	Gastropods		
	Calcareous algae		
	Barnacles		
	Spicules & spines		
	Other		
	Modal size 1 (mm)		
	Modal size 2 (mm)		
	Shape/abrasion		
	Sorting		
SILICICLASTICS	**Siliciclastic grain %**	0	
		%	**Abundance limit**
	Quartz		
	Feldspar		
	Igneous rock fragments		
	Sedimentary rock fragments		
	Micas		
	Pyrite grains		
	Pyrite infills		
	Glauconite pellets		
	Glauconite infills		
	Other		
	Modal size 1 (mm)		
	Modal size 2 (mm)		
	Shape/abrasion		
	Sorting		
SHELL FEATURES	Shell fabric - crystal shapes, weathering, ppt minerals	Homogenous calcite to developed crystal laths.	
	Shell increments - Thickness, colour, continuous, discontinuous	Shell increments vary in thickness. Light brown (0.375-7.5 mm) and dark grey layers (1.25-2.25 mm). Fractured in	
	Borings - size, shape, boundaries, location (within layer or truncating)	-	
	Infill - type, bioclastics, siliciclastics, geopetal fabrics, sparite, micritic peliods	-	
	Recrystallisation - distribution, degree, location.	Recrystalised along the margins of the light brown layer in the shell with large blocky calcite crystals. Fractures are infilled with fine spar.	
	Modal size 1 (mm)	-	
	Modal size 2 (mm)	-	

Petrographic data sheet - Larissa Macmillan 2009			
Sample number		W05/1A	
Sample description		Oyster shell	
Analyst		Larissa Macmillan	
BIOCLASTICS	**Total bioclast %**	0	
		%	**Abundance limit**
	Bryozoans		
	Bivalves		
	Echinoderms		
	Benthic foraminifera		
	Planktic foraminifera		
	Gastropods		
	Calcareous algae		
	Barnacles		
	Spicules & spines		
	Other		
	Modal size 1 (mm)		
	Modal size 2 (mm)		
	Shape/abrasion		
	Sorting		
SILICICLASTICS	**Siliciclastic grain %**	0	
		%	**Abundance limit**
	Quartz		
	Feldspar		
	Igneous rock fragments		
	Sedimentary rock fragments		
	Micas		
	Pyrite grains		
	Pyrite infills		
	Glauconite pellets		
	Glauconite infills		
	Other		
	Modal size 1 (mm)		
	Modal size 2 (mm)		
	Shape/abrasion		
	Sorting		
SHELL FEATURES	Shell fabric - crystal shapes, weathering, ppt minerals	Homogenous calcite to developed crystal laths.	
	Shell increments - Thickness, colour, continuous, discontinuous	Increments very in thickness, dark grey (1.5-3 mm) and light brown layers (0.125-0.45 mm). Fractured in places and infilled with calcite.	
	Borings - size, shape, boundaries, location (within layer or truncating)	-	
	Infill - type, bioclastics, siliciclastics, geopetal fabrics, sparite, micritic peliods	-	
	Recrystallisation - distribution, degree, location.	Shell recrystallised with large blocky calcite crystals.	
	Modal size 1 (mm)		
	Modal size 2 (mm)		

Petrographic data sheet - Larissa Macmillan			
Sample number		W04/3B	
Sample description		Oyster shell	
Analyst		Larissa Macmillan	
BIOCLASTICS	**Total bioclast %**	0	
		%	**Abundance limit**
	Bryozoans		
	Bivalves		
	Echinoderms		
	Benthic foraminifera		
	Planktic foraminifera		
	Gastropods		
	Calcareous algae		
	Barnacles		
	Spicules & spines		
	Other		
	Modal size 1 (mm)		
	Modal size 2 (mm)		
	Shape/abrasion		
	Sorting		
SILICICLASTICS	**Siliciclastic grain %**	0	
		%	**Abundance limit**
	Quartz		
	Feldspar		
	Igneous rock fragments		
	Sedimentary rock fragments		
	Micas		
	Pyrite grains		
	Pyrite infills		
	Glauconite pellets		
	Glauconite infills		
	Other		
	Modal size 1 (mm)		
	Modal size 2 (mm)		
	Shape/abrasion		
	Sorting		
SHELL FEATURES	Shell fabric - crystal shapes, weathering, ppt minerals	homogenous calcite to crystal laths of calcite	
	Shell increments - Thickness, colour, continuous, discontinuous	increments vary with thicker grey layers (1.25-2.5 mm) and light brown layers (0.25-1 mm). Increment thickness is continuous	
	Borings - size, shape, boundaries, location (within layer or truncating)	-	
	Infill - type, bioclastics, siliciclastics, geopetal fabrics, sparite, micritic peliods	One layer within the shell has been infilled with host material containin some bivalve fragments, planktic forams and bryozoans held in limonite stained micrite.	
	Recrystallisation - distribution, degree, location.	High level of recrstalisation. Large block calcite crystals form in many of the grey layers.	
	Modal size 1 (mm)	-	
	Modal size 2 (mm)	-	

Petrographic data sheet - Larissa Macmillan 2009			
Sample number		WAP15/1B B	
Sample description		Shell and host/infill	
Analyst		Larissa Macmillan	
BIOCLASTICS	**Total bioclast %**	55	
		%	**Abundance limit**
	Bryozoans	2	some
	Bivalves	40	very common
	Echinoderms	2	some
	Benthic foraminifera	2	some
	Planktic foraminifera	4	some
	Gastropods	-	absent
	Calcareous algae	-	absent
	Barnacles	-	absent
	Spicules & spines	-	absent
	Other	5	some
	Modal size 1 (mm)	0.23	
	Modal size 2 (mm)	0.63	
	Shape/abrasion	moderately abraded	
	Sorting	poorly sorted	
SILICICLASTICS	**Siliciclastic grain %**	45	
		%	**Abundance limit**
	Quartz	5	some
	Feldspar	38	very common
	Igneous rock fragments	-	absent
	Sedimentary rock fragments	-	absent
	Micas	-	absent
	Pyrite grains	2	some
	Pyrite infills	-	absent
	Glauconite pellets	-	absent
	Glauconite infills	-	absent
	Other	-	absent
	Modal size 1 (mm)	0.28	
	Modal size 2 (mm)	0.13	
	Shape/abrasion	subrounded	
	Sorting	poor to moderate	
SHELL FEATURES	Shell fabric - crystal shapes, weathering, ppt minerals	crystal laths of calcite to homogenous	
	Shell increments - Thickness, colour, continuous, discontinuous	layers range in thickness. Dark grey (0.5-1 mm) and light brown (0.15-0.25 mm).	
	Borings - size, shape, boundaries, location (within layer or truncating)	Irregular boundaries occuring withing the dark grey layers. Elongated in shape.	
	Infill - type, bioclastics, siliciclastics, geopetal fabrics, sparite, micritic peliods	Dominated by micrite. See above.	
	Recrystallisation - distribution, degree, location.	calcite spar occurs within fractures in the shell.	
	Modal size 1 (mm)		
	Modal size 2 (mm)		

Petrographic data sheet - Larissa Macmillan 2009			
Sample number		N14/1E	
Sample description		Shell and infill	
Analyst		Larissa Macmillan	
BIOCLASTICS	**Total bioclast %**	53	
		%	**Abundance limit**
	Bryozoans	10	many
	Bivalves	35	very common
	Echinoderms	-	absent
	Benthic foraminifera	6	many
	Planktic foraminifera	2	some
	Gastropods	-	absent
	Calcareous algae	-	absent
	Barnacles	-	absent
	Spicules & spines	-	absent
	Other	-	absent
	Modal size 1 (mm)	0.38	
	Modal size 2 (mm)	1.75	
	Shape/abrasion	moderately abraded	
	Sorting	poorly sorted	
SILICICLASTICS	**Siliciclastic grain %**	47	
		%	**Abundance limit**
	Quartz	10	many
	Feldspar	30	very common
	Igneous rock fragments	-	absent
	Sedimentary rock fragments	-	absent
	Micas	-	absent
	Pyrite grains	-	absent
	Pyrite infills	-	absent
	Glauconite pellets	4	some
	Glauconite infills	3	some
	Other	-	absent
	Modal size 1 (mm)	1.00	
	Modal size 2 (mm)	0.23	
	Shape/abrasion	subangular	
	Sorting	poorly sorted	
SHELL FEATURES	Shell fabric - crystal shapes, weathering, ppt minerals	homogenous calcite	
	Shell increments - Thickness, colour, continuous, discontinuous	Variation in layers, dark grey thick layers (3.75 mm) and light brown layers (0.1 mm).	
	Borings - size, shape, boundaries, location (within layer or truncating)	-	
	Infill - type, bioclastics, siliciclastics, geopetal fabrics, sparite, micritic peliods	-	
	Recrystallisation - distribution, degree, location.	-	
	Modal size 1 (mm)	-	
	Modal size 2 (mm)	-	

Petrographic data sheet - Larissa Macmillan 2009			
Sample number		K13/1C_A	
Sample description		Shell and infill	
Analyst		Larissa Macmillan	
BIOCLASTICS	**Total bioclast %**	59	
		%	**Abundance limit**
	Bryozoans	20	common
	Bivalves	15	many
	Echinoderms	4	some
	Benthic foraminifera	5	some
	Planktic foraminifera	15	many
	Gastropods	-	absent
	Calcareous algae	-	absent
	Barnacles	-	absent
	Spicules & spines	-	absent
	Other	-	absent
	Modal size 1 (mm)	0.30	
	Modal size 2 (mm)	0.88	
	Shape/abrasion	moderately abraded	
	Sorting	poorly sorted	
SILICICLASTICS	**Siliciclastic grain %**	41	
		%	**Abundance limit**
	Quartz	8	many
	Feldspar	13	many
	Igneous rock fragments	-	absent
	Sedimentary rock fragments	-	absent
	Micas	-	absent
	Pyrite grains	-	absent
	Pyrite infills	-	absent
	Glauconite pellets	-	absent
	Glauconite infills	20	common
	Other	-	absent
	Modal size 1 (mm)	0.13	
	Modal size 2 (mm)	0.63	
	Shape/abrasion	subrounded	
	Sorting	poorly sorted	
SHELL FEATURES	Shell fabric - crystal shapes, weathering, ppt minerals	homogenous calcite material	
	Shell increments - Thickness, colour, continuous, discontinuous	variation in thickness dark grey layers (2-3.75 mm) and light brown (0.1 mm).	
	Borings - size, shape, boundaries, location (within layer or truncating)	many small elongate borings occuring within the dark grey layer	
	Infill - type, bioclastics, siliciclastics, geopetal fabrics, sparite, micritic peliods	Calcite spar, siliciclastic and bioclastic. See above	
	Recrystallisation - distribution, degree, location.	occurs in some of the thick grey layers, large blocky spar crystals	
	Modal size 1 (mm)	0.25	
	Modal size 2 (mm)	1.25	

Petrographic data sheet - Larissa Macmillan 2009			
Sample number		K13/1B	
Sample description		Shell and infilled bore	
Analyst		Larissa Macmillan	
BIOCLASTICS	**Total bioclast %**	96	
		%	**Abundance limit**
	Bryozoans	12	many
	Bivalves	80	very abundant
	Echinoderms	2	some
	Benthic foraminifera	2	some
	Planktic foraminifera	-	absent
	Gastropods	-	absent
	Calcareous algae	-	absent
	Barnacles	-	absent
	Spicules & spines	-	absent
	Other	-	absent
	Modal size 1 (mm)	1.75	
	Modal size 2 (mm)	0.38	
	Shape/abrasion	moderately abraded	
	Sorting	poorly sorted	
SILICICLASTICS	**Siliciclastic grain %**	4	
		%	**Abundance limit**
	Quartz	-	absent
	Feldspar	2	some
	Igneous rock fragments	-	absent
	Sedimentary rock fragments	-	absent
	Micas	-	absent
	Pyrite grains	-	absent
	Pyrite infills	2	some
	Glauconite pellets	-	absent
	Glauconite infills	-	absent
	Other	-	absent
	Modal size 1 (mm)	0.25	
	Modal size 2 (mm)	0.15	
	Shape/abrasion	subrounded	
	Sorting	poorly sorted	
SHELL FEATURES	Shell fabric - crystal shapes, weathering, ppt minerals	homogenous calcite material	
	Shell increments - Thickness, colour, continuous, discontinuous	alternating continuous layers. Dark grey (2 mm) and light brown (0.125 mm).Fractured in places and infilled with calcite.	
	Borings - size, shape, boundaries, location (within layer or truncating)	Large circular and elongate. Irregular boundaries. Large circular bore truncates all layers, small elongate bores within grey layer.	
	Infill - type, bioclastics, siliciclastics, geopetal fabrics, sparite, micritic peliods	Variety. Majority biomicrite, also spar. Geopetal fabrics and micrite peliods	
	Recrystallisation - distribution, degree, location.	Within some grey layers. Also along margins of light brown laters. Consists of blocky spar crystals.	
	Modal size 1 (cm)	8	
	Modal size 2 (mm)	11.25	

Petrographic data sheet - Larissa Macmillan 2009			
Sample number		W10/1A A	
Sample description		Shell and small borings	
Analyst		Larissa Macmillan	
BIOCLASTICS	**Total bioclast %**	83	
		%	**Abundance limit**
	Bryozoans	50	very common
	Bivalves	20	common
	Echinoderms	8	many
	Benthic foraminifera	5	some
	Planktic foraminifera	3	some
	Gastropods	-	absent
	Calcareous algae	-	absent
	Barnacles	-	absent
	Spicules & spines	-	absent
	Other	-	absent
	Modal size 1 (mm)	0.75	
	Modal size 2 (mm)	1.25	
	Shape/abrasion	Highly abraded	
	Sorting	poorly sorted	
SILICICLASTICS	**Siliciclastic grain %**	17	
		%	**Abundance limit**
	Quartz	3.00	
	Feldspar	7.00	
	Igneous rock fragments	-	
	Sedimentary rock fragments	-	
	Micas	-	
	Pyrite grains	-	
	Pyrite infills	-	
	Glauconite pellets	5.00	
	Glauconite infills	2.00	
	Other	-	
	Modal size 1 (mm)	0.18	
	Modal size 2 (mm)	1.93	
	Shape/abrasion	subangular	
	Sorting	poorly sorted	
SHELL FEATURES	Shell fabric - crystal shapes, weathering, ppt minerals	homogenous calcite	
	Shell increments - Thickness, colour, continuous, discontinuous	Alternating dark grey (2.25 mm) and light brown (0.05 mm)	
	Borings - size, shape, boundaries, location (within layer or truncating)	circiular and elongate, sharp edges, withing grey layer.	
	Infill - type, bioclastics, siliciclastics, geopetal fabrics, sparite, micritic peliods	Spar and micritic limestone matrix, see above.	
	Recrystallisation - distribution, degree, location.		
	Modal size 1 (mm)	1.05	
	Modal size 2 (mm)	2.5	

Petrographic data sheet - Larissa Macmillan 2009			
Sample number		W10/1AT	
Sample description		Shell with large boring	
Analyst		Larissa Macmillan	
BIOCLASTICS	**Total bioclast %**	75	
		%	**Abundance limit**
	Bryozoans	40	very common
	Bivalves	23	common
	Echinoderms	8	many
	Benthic foraminifera	5	some
	Planktic foraminifera	-	absent
	Gastropods	-	absent
	Calcareous algae	-	absent
	Barnacles	-	absent
	Spicules & spines	-	absent
	Other	-	absent
	Modal size 1 (mm)	1.75	
	Modal size 2 (mm)	1.25	
	Shape/abrasion	moderately abraded	
	Sorting	poorly sorted	
SILICICLASTICS	**Siliciclastic grain %**	25	
		%	**Abundance limit**
	Quartz	2	some
	Feldspar	3	some
	Igneous rock fragments	-	absent
	Sedimentary rock fragments	-	absent
	Micas	-	absent
	Pyrite grains	-	absent
	Pyrite infills	-	absent
	Glauconite pellets	-	absent
	Glauconite infills	20	common
	Other	-	absent
	Modal size 1 (mm)	0.08	
	Modal size 2 (mm)	0.18	
	Shape/abrasion	subrounded	
	Sorting	poorly sorted	
SHELL FEATURES	Shell fabric - crystal shapes, weathering, ppt minerals	homogenous calcite material. Majority of shell is an infilled boring	
	Shell increments - Thickness, colour, continuous, discontinuous	almost equal thickness. Dark grey layers (0.175 mm) and light brown layers (0.3 mm). Discontinuous layers	
	Borings - size, shape, boundaries, location (within layer or truncating)	Large circular boring, small irregular elongate borings. Circular boring has a sharp boundaties, smaller bores more irregular.	
	Infill - type, bioclastics, siliciclastics, geopetal fabrics, sparite, micritic peliods	Variety of infill, mainly biomicrite, with spar cement in patches. Geopetal farbics present. See above for infill composition	
	Recrystallisation - distribution, degree, location.		
	Modal size 1 (mm)		
	Modal size 2 (mm)		

Petrographic data sheet - Larissa Macmillan 2009			
Sample number		W10/2A	
Sample description		Host	
Analyst		Larissa Macmillan	
BIOCLASTICS	**Total bioclast %**	92	
		%	**Abundance limit**
	Bryozoans	80	very abundant
	Bivalves	6	many
	Echinoderms	6	many
	Benthic foraminifera	5	some
	Planktic foraminifera	-	absent
	Gastropods	-	absent
	Calcareous algae	-	absent
	Barnacles	-	absent
	Spicules & spines	-	absent
	Other	-	absent
	Modal size 1 (mm)	1.25	
	Modal size 2 (mm)	0.75	
	Shape/abrasion	moderately abraded	
	Sorting	poorly sorted	
SILICICLASTICS	**Siliciclastic grain %**	8	
		%	**Abundance limit**
	Quartz	1	rare
	Feldspar	4	some
	Igneous rock fragments	-	absent
	Sedimentary rock fragments	-	absent
	Micas	-	absent
	Pyrite grains	-	absent
	Pyrite infills	-	absent
	Glauconite pellets	3	some
	Glauconite infills	1	rare
	Other	-	absent
	Modal size 1 (mm)	0.75	
	Modal size 2 (mm)	0.13	
	Shape/abrasion	subrounded-subangular	
	Sorting	poorly sorted	
SHELL FEATURES	Shell fabric - crystal shapes, weathering, ppt minerals		
	Shell increments - Thickness, colour, continuous, discontinuous		
	Borings - size, shape, boundaries, location (within layer or truncating)		
	Infill - type, bioclastics, siliciclastics, geopetal fabrics, sparite, micritic peliods		
	Recrystallisation - distribution, degree, location.		
	Modal size 1 (mm)		
	Modal size 2 (mm)		

Petrographic data sheet - Larissa Macmillan 2009			
Sample number		W07/1C	
Sample description		Shell layers and host	
Analyst		Larissa Macmillan	
BIOCLASTICS	**Total bioclast %**	15	
		%	**Abundance limit**
	Bryozoans	6	many
	Bivalves	7	many
	Echinoderms	-	absent
	Benthic foraminifera	-	absent
	Planktic foraminifera	-	absent
	Gastropods	-	absent
	Calcareous algae	-	absent
	Barnacles	-	absent
	Spicules & spines	-	absent
	Other	-	absent
	Modal size 1 (mm)	0.23	
	Modal size 2 (mm)	0.63	
	Shape/abrasion	moderatley abraded	
	Sorting	poorly sorted	
SILICICLASTICS	**Siliciclastic grain %**	85	
		%	**Abundance limit**
	Quartz	5	some
	Feldspar	65	abundant
	Igneous rock fragments	-	absent
	Sedimentary rock fragments	-	absent
	Micas	-	absent
	Pyrite grains	4	some
	Pyrite infills	-	absent
	Glauconite pellets	4	some
	Glauconite infills	3	some
	Other	-	absent
	Modal size 1 (mm)	0.25	
	Modal size 2 (mm)	0.10	
	Shape/abrasion	subangular	
	Sorting	poorly sorted	
SHELL FEATURES	Shell fabric - crystal shapes, weathering, ppt minerals	homogenous calcite	
	Shell increments - Thickness, colour, continuous, discontinuous	layers alternate, dark grey (0.2-1.75 mm) and light brown (0.075-0.275 mm)	
	Borings - size, shape, boundaries, location (within layer or truncating)	none apparent. Parts of shell infilled but possibly fractures. See above for composition. Mainly micritic with	
	Infill - type, bioclastics, siliciclastics, geopetal fabrics, sparite, micritic peliods		
	Recrystallisation - distribution, degree, location.		
	Modal size 1 (mm)		
	Modal size 2 (mm)		

Petrographic data sheet - Larissa Macmillan 2009			
Sample number		W02/1B B	
Sample description		Shell and large boring	
Analyst		Larissa Macmillan	
BIOCLASTICS	**Total bioclast %**	91	
		%	**Abundance limit**
	Bryozoans	40	very common
	Bivalves	3	some
	Echinoderms	16	common
	Benthic foraminifera	1	rare
	Planktic foraminifera	5	some
	Gastropods	-	absent
	Calcareous algae	-	absent
	Barnacles	-	absent
	Spicules & spines	-	absent
	Other	-	absent
	Modal size 1 (mm)	0.75	
	Modal size 2 (mm)	1.00	
	Shape/abrasion	moderately abraded	
	Sorting	poorly sorted	
SILICICLASTICS	**Siliciclastic grain %**	9	
		%	**Abundance limit**
	Quartz	1.00	rare
	Feldspar	4.00	some
	Igneous rock fragments	-	absent
	Sedimentary rock fragments	-	absent
	Micas	-	absent
	Pyrite grains	-	absent
	Pyrite infills	-	absent
	Glauconite pellets	2.00	some
	Glauconite infills	2.00	some
	Other	-	absent
	Modal size 1 (mm)	0.38	
	Modal size 2 (mm)	0.13	
	Shape/abrasion	subrounded	
	Sorting	poorly sorted	
SHELL FEATURES	Shell fabric - crystal shapes, weathering, ppt minerals	homogenous calcite	
	Shell increments - Thickness, colour, continuous, discontinuous	majority of shell is boring	
	Borings - size, shape, boundaries, location (within layer or truncating)	large with a sharp boring, takes up entire lenght of thin section	
	Infill - type, bioclastics, siliciclastics, geopetal fabrics, sparite, micritic peliods	dominated by micrite peliods and localised spar cement. Siliciclastics occur in rough clusters. See above for composition.	
	Recrystallisation - distribution, degree, location.	-	
	Modal size 1 (mm)		
	Modal size 2 (mm)		

Petrographic data sheet - Larissa Macmillan 2009			
Sample number		W02/1B	
Sample description		Shell and large bore	
Analyst		Larissa Macmillan	
BIOCLASTICS	**Total bioclast %**	93	
		%	**Abundance limit**
	Bryozoans	34	very common
	Bivalves	50	very common
	Echinoderms	4	some
	Benthic foraminifera	5	some
	Planktic foraminifera	-	absent
	Gastropods	-	absent
	Calcareous algae	-	absent
	Barnacles	-	absent
	Spicules & spines	-	absent
	Other	-	absent
	Modal size 1 (mm)	0.38	
	Modal size 2 (mm)	0.13	
	Shape/abrasion	moderatley abraded	
	Sorting	poorly sorted	
SILICICLASTICS	**Siliciclastic grain %**	7	
		%	**Abundance limit**
	Quartz	2.00	some
	Feldspar	3.00	some
	Igneous rock fragments	-	absent
	Sedimentary rock fragments	-	absent
	Micas	-	absent
	Pyrite grains	-	absent
	Pyrite infills	-	absent
	Glauconite pellets	2.00	some
	Glauconite infills	-	absent
	Other	-	absent
	Modal size 1 (mm)	0.15	
	Modal size 2 (mm)	0.20	
	Shape/abrasion	subrounded	
	Sorting	poorly sorted	
SHELL FEATURES	Shell fabric - crystal shapes, weathering, ppt minerals	homogenous calcite with some limonitisation	
	Shell increments - Thickness, colour, continuous, discontinuous	dark grey thick (1.5 mm) and light brown (0.625 mm)	
	Borings - size, shape, boundaries, location (within layer or truncating)	Large boring sharp edges and circular in shape. Truncates many layers in the shell.	
	Infill - type, bioclastics, siliciclastics, geopetal fabrics, sparite, micritic peliods	Fine micrite and calcite spar and geopetal fabrics. See above for composition	
	Recrystallisation - distribution, degree, location.	-	
	Modal size 1 (mm)	7.5	
	Modal size 2 (mm)	-	

Petrographic data sheet - Larissa Macmillan			
Sample number			
Sample description			
Analyst		Larissa Macmillan	
BIOCLASTICS	**Total bioclast %**	0	
		%	**Abundance limit**
	Bryozoans		
	Bivalves		
	Echinoderms		
	Benthic foraminifera		
	Planktic foraminifera		
	Gastropods		
	Calcareous algae		
	Barnacles		
	Spicules & spines		
	Other		
	Modal size 1 (mm)		
	Modal size 2 (mm)		
	Shape/abrasion		
	Sorting		
SILICICLASTICS	**Siliciclastic grain %**	0	
		%	**Abundance limit**
	Quartz		
	Feldspar		
	Igneous rock fragments		
	Sedimentary rock fragments		
	Micas		
	Pyrite grains		
	Pyrite infills		
	Glauconite pellets		
	Glauconite infills		
	Other		
	Modal size 1 (mm)		
	Modal size 2 (mm)		
	Shape/abrasion		
	Sorting		
SHELL AND BORING FEATURES	Shell fabric - crystal shapes, weathering, ppt minerals	Fine grained calcite crystals. Slight weathering of shell, dark orange/brown ppt mineral at layer margins	
	Shell increments - Thickness, colour, continuous, discontinuous	Dark layers thick (3.75 mm), light thin layers (0.25 mm). Bands are continuous with no size flucutuation.	
	Recrystallisation - distribution, degree, location.	Absent	
	Borings - size, shape, boundaries, location (within layer or truncating)	Absent	
	Infill - type, bioclastics, siliciclastics, geopetal fabrics, sparite, micritic peliods	Absent	
	Modal size 1 (mm)		
	Modal size 2 (mm)		

Petrographic data sheet - Larissa Macmillan			
Sample number		PAT2C	
Sample description		Oyster shell	
Analyst		Larissa Macmillan	
BIOCLASTICS	**Total bioclast %**		
		%	**Abundance limit**
	Bryozoans		
	Bivalves		
	Echinoderms		
	Benthic foraminifera		
	Planktic foraminifera		
	Gastropods		
	Calcareous algae		
	Barnacles		
	Spicules & spines		
	Other		
	Modal size 1 (mm)		
	Modal size 2 (mm)		
	Shape/abrasion		
	Sorting		
SILICICLASTICS	**Siliciclastic grain %**		
		%	**Abundance limit**
	Quartz		
	Feldspar		
	Igneous rock fragments		
	Sedimentary rock fragments		
	Micas		
	Pyrite grains		
	Pyrite infills		
	Glauconite pellets		
	Glauconite infills		
	Other		
	Modal size 1 (mm)		
	Modal size 2 (mm)		
	Shape/abrasion		
	Sorting		
SHELL AND BORING FEATURES	Shell fabric - crystal shapes, weathering, ppt minerals	Fine grained, homogenous calcite. Highly weathered with large globular dark red/brown iron stain foring around layer margins	
	Shell increments - Thickness, colour, continuous, discontinuous	Light brown thin layer (0.25 mm), thick dark grey layers (3.75 mm). Layers thin and pinch in towards what appears to be the edge of the shell.	
	Recrystallisation - distribution, degree, location.	Absent	
	Borings - size, shape, boundaries, location (within layer or truncating)	Borings oval and enlogate shapped with sharp edges.	
	Infill - type, bioclastics, siliciclastics, geopetal fabrics, sparite, micritic peliods	Absent	
	Modal size 1 (mm)	1.5	
	Modal size 2 (mm)	2.25	

Petrographic data sheet - Larissa Macmillan 2009			
Sample number		PAT2D	
Sample description		Oyster shell	
Analyst		Larissa Macmillan	
BIOCLASTICS	**Total bioclast %**		
		%	**Abundance limit**
	Bryozoans		
	Bivalves		
	Echinoderms		
	Benthic foraminifera		
	Planktic foraminifera		
	Gastropods		
	Calcareous algae		
	Barnacles		
	Spicules & spines		
	Other		
	Modal size 1 (mm)		
	Modal size 2 (mm)		
	Shape/abrasion		
	Sorting		
SILICICLASTICS	**Siliciclastic grain %**		
		%	**Abundance limit**
	Quartz		
	Feldspar		
	Igneous rock fragments		
	Sedimentary rock fragments		
	Micas		
	Pyrite grains		
	Pyrite infills		
	Glauconite pellets		
	Glauconite infills		
	Other		
	Modal size 1 (mm)		
	Modal size 2 (mm)		
	Shape/abrasion		
	Sorting		
SHELL AND BORING FEATURES	Shell fabric - crystal shapes, weathering, ppt minerals	Fine grained homogenous calcite. Moderate weathering. Dark red/brown ppt on thin layers.	
	Shell increments - Thickness, colour, continuous, discontinuous	Light thin layers (0.25 mm), thick dark layers (4.25 mm). Layers appear continuous with no size fluctuation.	
	Recrystallisation - distribution, degree, location.	Absent	
	Borings - size, shape, boundaries, location (within layer or truncating)	Absent	
	Infill - type, bioclastics, siliciclastics, geopetal fabrics, sparite, micritic peliods	Absent	
	Modal size 1 (mm)		
	Modal size 2 (mm)		

Petrographic data sheet - Larissa Macmillan 2009			
Sample number		PAT2E	
Sample description		Oyster shell	
Analyst		Larissa Macmillan	
BIOCLASTICS	**Total bioclast %**	0	
		%	**Abundance limit**
	Bryozoans		
	Bivalves		
	Echinoderms		
	Benthic foraminifera		
	Planktic foraminifera		
	Gastropods		
	Calcareous algae		
	Barnacles		
	Spicules & spines		
	Other		
	Modal size 1 (mm)		
	Modal size 2 (mm)		
	Shape/abrasion		
	Sorting		
SILICICLASTICS	**Siliciclastic grain %**	0	
		%	**Abundance limit**
	Quartz		
	Feldspar		
	Igneous rock fragments		
	Sedimentary rock fragments		
	Micas		
	Pyrite grains		
	Pyrite infills		
	Glauconite pellets		
	Glauconite infills		
	Other		
	Modal size 1 (mm)		
	Modal size 2 (mm)		
	Shape/abrasion		
	Sorting		
SHELL AND BORING FEATURES	Shell fabric - crystal shapes, weathering, ppt minerals	Fine grained, homogenous calcite crystals, moderately weathered occuring along fine layers in shell. Dark	
	Shell increments - Thickness, colour, continuous, discontinuous	Increment thickness varies markedly thin light brown layers (0.25 mm), thick dark grey layers (1.5-4.25 mm)	
	Recrystallisation - distribution, degree, location.	Absent	
	Borings - size, shape, boundaries, location (within layer or truncating)	Absent	
	Infill - type, bioclastics, siliciclastics, geopetal fabrics, sparite, micritic peliods	Absent	
	Modal size 1 (mm)		
	Modal size 2 (mm)		

Petrographic data sheet - Larissa Macmillan 2009			
Sample number		PAT3A	
Sample description		Oyster shell	
Analyst		Larissa Macmillan	
BIOCLASTICS	**Total bioclast %**	0	
		%	**Abundance limit**
	Bryozoans		
	Bivalves		
	Echinoderms		
	Benthic foraminifera		
	Planktic foraminifera		
	Gastropods		
	Calcareous algae		
	Barnacles		
	Spicules & spines		
	Other		
	Modal size 1 (mm)		
	Modal size 2 (mm)		
	Shape/abrasion		
	Sorting		
SILICICLASTICS	**Siliciclastic grain %**	0	
		%	**Abundance limit**
	Quartz		
	Feldspar		
	Igneous rock fragments		
	Sedimentary rock fragments		
	Micas		
	Pyrite grains		
	Pyrite infills		
	Glauconite pellets		
	Glauconite infills		
	Other		
	Modal size 1 (mm)		
	Modal size 2 (mm)		
	Shape/abrasion		
	Sorting		
SHELL AND BORING FEATURES	Shell fabric - crystal shapes, weathering, ppt minerals	Crystal laths of calcite. Highly weatherd with abundant amounts of mineral ppt. Irregular patternts seen in shells where the ppt occurs mainly along the thin layers	
	Shell increments - Thickness, colour, continuous, discontinuous	Alternation of thin and thick layers. Thick light layers (1.5 mm) and thin darker layers (0.25 mm). Layers are relatively continuous.	
	Recrystallisation - distribution, degree, location.	absent	
	Borings - size, shape, boundaries, location (within layer or truncating)	absent	
	Infill - type, bioclastics, siliciclastics, geopetal fabrics, sparite, micritic peliods	absent	
	Modal size 1 (mm)		

Petrographic data sheet - Larissa Macmillan 2009			
Sample number		PAT4A	
Sample description		Oyster shell	
Analyst		Larissa Macmillan	
BIOCLASTICS	**Total bioclast %**		
		%	**Abundance limit**
	Bryozoans		
	Bivalves		
	Echinoderms		
	Benthic foraminifera		
	Planktic foraminifera		
	Gastropods		
	Calcareous algae		
	Barnacles		
	Spicules & spines		
	Other		
	Modal size 1 (mm)		
	Modal size 2 (mm)		
	Shape/abrasion		
	Sorting		
SILICICLASTICS	**Siliciclastic grain %**		
		%	**Abundance limit**
	Quartz		
	Feldspar		
	Igneous rock fragments		
	Sedimentary rock fragments		
	Micas		
	Pyrite grains		
	Pyrite infills		
	Glauconite pellets		
	Glauconite infills		
	Other		
	Modal size 1 (mm)		
	Modal size 2 (mm)		
	Shape/abrasion		
	Sorting		
SHELL AND BORING FEATURES	Shell fabric - crystal shapes, weathering, ppt minerals	Homogenous, fine grained, calcite crystals, mod weathering, dark red/brown globular ppt in shell layers	
	Shell increments - Thickness, colour, continuous, discontinuous	Increment thickness varies markedly thin light brown layers (0.25 mm), thick dark grey layers (1.5-4.25 mm). Increments are discontinous and show variation. Pinching in and out and branching.	
	Recrystallisation - distribution, degree, location.	absent	
	Borings - size, shape, boundaries, location (within layer or truncating)	Borings have smooth edges lenth-ways and irregular ends. Contained within the thicker, darker shell layer.	
	Infill - type, bioclastics, siliciclastics, geopetal fabrics, sparite, micritic peliods	Siliciclastic and biocalsts. Fine grained sediment in the background (gypsum?). Highly fracutured quartz, opaque minerals and rock fragments. Bioclasts inlcude bivalve fragments.	
	Modal size 1 (mm)	3.75	
	Modal size 2 (mm)	3.5	

Petrographic data sheet - Larissa Macmillan 2009			
Sample number		PAT4B	
Sample description		Oyster shell	
Analyst		Larissa Macmillan	
BIOCLASTICS	**Total bioclast %**		
		%	**Abundance limit**
	Bryozoans		
	Bivalves		
	Echinoderms		
	Benthic foraminifera		
	Planktic foraminifera		
	Gastropods		
	Calcareous algae		
	Barnacles		
	Spicules & spines		
	Other		
	Modal size 1 (mm)		
	Modal size 2 (mm)		
	Shape/abrasion		
	Sorting		
SILICICLASTICS	**Siliciclastic grain %**		
		%	**Abundance limit**
	Quartz		
	Feldspar		
	Igneous rock fragments		
	Sedimentary rock fragments		
	Micas		
	Pyrite grains		
	Pyrite infills		
	Glauconite pellets		
	Glauconite infills		
	Other		
	Modal size 1 (mm)		
	Modal size 2 (mm)		
	Shape/abrasion		
	Sorting		
SHELL AND BORING FEATURES	Shell fabric - crystal shapes, weathering, ppt minerals	Homogenous, fine grained calcite crystals. Slightly weathered, dark mineral ppt forming in globules and linear	
	Shell increments - Thickness, colour, continuous, discontinuous	Thick dark grey layers (3 mm) and thin light brown layers (0.2 mm). Layers show irregularity and discontinuity.	
	Recrystallisation - distribution, degree, location.	Absent	
	Borings - size, shape, boundaries, location (within layer or truncating)	Elongated shape, sharp edges and contained within dark grey layer.	
	Infill - type, bioclastics, siliciclastics, geopetal fabrics, sparite, micritic peliods	Infilled with fine grained material (gypsum?) and opaque minerals. Material has dark red brown stain.	
	Modal size 1 (mm)	2	
	Modal size 2 (mm)		

Petrographic data sheet - Larissa Macmillan 2009			
Sample number		PAT4C	
Sample description		Oyster shell	
Analyst		Larissa Macmillan	
BIOCLASTICS	**Total bioclast %**		
		%	**Abundance limit**
	Bryozoans		
	Bivalves		
	Echinoderms		
	Benthic foraminifera		
	Planktic foraminifera		
	Gastropods		
	Calcareous algae		
	Barnacles		
	Spicules & spines		
	Other		
	Modal size 1 (mm)		
	Modal size 2 (mm)		
	Shape/abrasion		
	Sorting		
SILICICLASTICS	**Siliciclastic grain %**		
		%	**Abundance limit**
	Quartz		
	Feldspar		
	Igneous rock fragments		
	Sedimentary rock fragments		
	Micas		
	Pyrite grains		
	Pyrite infills		
	Glauconite pellets		
	Glauconite infills		
	Other		
	Modal size 1 (mm)		
	Modal size 2 (mm)		
	Shape/abrasion		
	Sorting		
SHELL AND BORING FEATURES	Shell fabric - crystal shapes, weathering, ppt minerals	Fine grained, homogenous calcite crystals. Moderate weathering with dark red/brown ppt minerals forming along shell boundaries.	
	Shell increments - Thickness, colour, continuous, discontinuous	Variation in increment thickness. Dark grey layer (2-3 mm) and light brown layers (0.125-1 mm). Irregularity in size, pinch in and out.	
	Recrystallisation - distribution, degree, location.	absent	
	Borings - size, shape, boundaries, location (within layer or truncating)	absent	
	Infill - type, bioclastics, siliciclastics, geopetal fabrics, sparite, micritic peliods	absent	
	Modal size 1 (mm)		
	Modal size 2 (mm)		

Petrographic data sheet - Larissa Macmillan			
Sample number		PAT4D	
Sample description		Oyster shell	
Analyst		Larissa Macmillan	
BIOCLASTICS	**Total bioclast %**		
		%	**Abundance limit**
	Bryozoans		
	Bivalves		
	Echinoderms		
	Benthic foraminifera		
	Planktic foraminifera		
	Gastropods		
	Calcareous algae		
	Barnacles		
	Spicules & spines		
	Other		
	Modal size 1 (mm)		
	Modal size 2 (mm)		
	Shape/abrasion		
	Sorting		
SILICICLASTICS	**Siliciclastic grain %**		
		%	**Abundance limit**
	Quartz		
	Feldspar		
	Igneous rock fragments		
	Sedimentary rock fragments		
	Micas		
	Pyrite grains		
	Pyrite infills		
	Glauconite pellets		
	Glauconite infills		
	Other		
	Modal size 1 (mm)		
	Modal size 2 (mm)		
	Shape/abrasion		
	Sorting		
SHELL AND BORING FEATURES	Shell fabric - crystal shapes, weathering, ppt minerals	Homogenous fine grained calcite, mod-low weathering. Low occurence of dark red/brown ppt.	
	Shell increments - Thickness, colour, continuous, discontinuous	Dark grey layer (0.75-3 mm). Light brown layer (0.5 mm). Variation in thickness is great. All layers are continous with no pinching.	
	Recrystallisation - distribution, degree, location.	Absent	
	Borings - size, shape, boundaries, location (within layer or truncating)	Absent	
	Infill - type, bioclastics, siliciclastics, geopetal fabrics, sparite, micritic peliods	Absent	
	Modal size 1 (mm)		
	Modal size 2 (mm)		

Petrographic data sheet - Larissa Macmillan 2009			
Sample number		PAT1	
Sample description		Heterolithic muds	
Analyst		Larissa Macmillan	
BIOCLASTICS	**Total bioclast %**	0	
		%	**Abundance limit**
	Bryozoans		
	Bivalves		
	Echinoderms		
	Benthic foraminifera		
	Planktic foraminifera		
	Gastropods		
	Calcareous algae		
	Barnacles		
	Spicules & spines		
	Other		
	Modal size 1 (mm)		
	Modal size 2 (mm)		
	Shape/abrasion		
	Sorting		
SILICICLASTICS	**Siliciclastic grain %**	100	
		%	**Abundance limit**
	Quartz	15	many
	Feldspar	15	many
	Igneous rock fragments	-	absent
	Sedimentary rock fragments	-	absent
	Micas	-	absent
	Pyrite grains	-	absent
	Pyrite infills	-	absent
	Glauconite pellets	-	absent
	Opaques	10	many
	Other	70	abundant
	Modal size 1 (mm)	0.10	
	Modal size 2 (mm)	0.05	
	Shape/abrasion	subrounded	
	Sorting	poorly sorted	
SHELL AND BORING FEATURES	Shell fabric - crystal shapes, weathering, ppt minerals		
	Shell increments - Thickness, colour, continuous, discontinuous		
	Recrystallisation - distribution, degree, location.		
	Borings - size, shape, boundaries, location (within layer or truncating)		
	Infill - type, bioclastics, siliciclastics, geopetal fabrics, sparite, micritic peliods		
	Modal size 1 (mm)		
	Modal size 2 (mm)		

Petrographic data sheet - Larissa Macmillan 2009			
Sample number		PAT5	
Sample description		Host - middle	
Analyst		Larissa Macmillan	
BIOCLASTICS	**Total bioclast %**	0	
		%	**Abundance limit**
	Bryozoans		
	Bivalves		
	Echinoderms		
	Benthic foraminifera		
	Planktic foraminifera		
	Gastropods		
	Calcareous algae		
	Barnacles		
	Spicules & spines		
	Other		
	Modal size 1 (mm)		
	Modal size 2 (mm)		
	Shape/abrasion		
	Sorting		
SILICICLASTICS	**Siliciclastic grain %**	100	
		%	**Abundance limit**
	Quartz	5	many
	Feldspar	56	some
	Igneous rock fragments	-	absent
	Sedimentary rock fragments	-	absent
	Micas	-	absent
	Pyrite grains	-	absent
	Pyrite infills	-	absent
	Glauconite pellets	-	absent
	Opaque minerals	2	absent
	Other	40	very abundant
	Modal size 1 (mm)	0.25	
	Modal size 2 (mm)	0.08	
	Shape/abrasion	subrounded-rounded	
	Sorting	poorly sorted	
SHELL AND BORING FEATURES	Shell fabric - crystal shapes, weathering, ppt minerals		
	Shell increments - Thickness, colour, continuous, discontinuous		
	Recrystallisation - distribution, degree, location.		
	Borings - size, shape, boundaries, location (within layer or truncating)		
	Infill - type, bioclastics, siliciclastics, geopetal fabrics, sparite, micritic peliods		
	Modal size 1 (mm)		
	Modal size 2 (mm)		

Petrographic data sheet - Larissa Macmillan			
Sample number		PAT6	
Sample description		Matrix - top	
Analyst		Larissa Macmillan	
BIOCLASTICS	**Total bioclast %**	0	
		%	**Abundance limit**
	Bryozoans		
	Bivalves		
	Echinoderms		
	Benthic foraminifera		
	Planktic foraminifera		
	Gastropods		
	Calcareous algae		
	Barnacles		
	Spicules & spines		
	Other		
	Modal size 1 (mm)		
	Modal size 2 (mm)		
	Shape/abrasion		
	Sorting		
SILICICLASTICS	**Siliciclastic grain %**	100	
		%	**Abundance limit**
	Quartz	2	some
	Feldspar	16	common
	Igneous rock fragments	-	absent
	Sedimentary rock fragments	4	some
	Micas	-	absent
	Pyrite grains	-	absent
	Pyrite infills	-	absent
	Glauconite pellets	-	absent
	Opaques	5	many
	Other (Gypsum)	73	abundant
	Modal size 1 (mm)	1.50	
	Modal size 2 (mm)	0.25	
	Shape/abrasion	rounded	
	Sorting	poorly sorted	
SHELL AND BORING FEATURES	Shell fabric - crystal shapes, weathering, ppt minerals		
	Shell increments - Thickness, colour, continuous, discontinuous		
	Recrystallisation - distribution, degree, location.		
	Borings - size, shape, boundaries, location (within layer or truncating)		
	Infill - type, bioclastics, siliciclastics, geopetal fabrics, sparite, micritic peliods		
	Modal size 1 (mm)		
	Modal size 2 (mm)		

Petrographic data sheet - Larissa Macmillan			
Sample number		PAT7	
Sample description		Matrix - bottom	
Analyst		Larissa Macmillan	
BIOCLASTICS	**Total bioclast %**	0	
		%	**Abundance limit**
	Bryozoans		
	Bivalves		
	Echinoderms		
	Benthic foraminifera		
	Planktic foraminifera		
	Gastropods		
	Calcareous algae		
	Barnacles		
	Spicules & spines		
	Other		
	Modal size 1 (mm)		
	Modal size 2 (mm)		
	Shape/abrasion		
	Sorting		
SILICICLASTICS	**Siliciclastic grain %**	100	
		%	**Abundance limit**
	Quartz	2	some
	Feldspar	66	abundant
	Igneous rock fragments	-	absent
	Sedimentary rock fragments	-	absent
	Micas	-	absent
	Pyrite grains	-	absent
	Pyrite infills	-	absent
	Glauconite pellets	-	absent
	Opaque minerals	2.00	some
	Other	30	abundant
	Modal size 1 (mm)	0.25	
	Modal size 2 (mm)	0.38	
	Shape/abrasion	Subrounded	
	Sorting	Poorly sorted	
SHELL AND BORING FEATURES	Shell fabric - crystal shapes, weathering, ppt minerals		
	Shell increments - Thickness, colour, continuous, discontinuous		
	Recrystallisation - distribution, degree, location.		
	Borings - size, shape, boundaries, location (within layer or truncating)		
	Infill - type, bioclastics, siliciclastics, geopetal fabrics, sparite, micritic peliods		
	Modal size 1 (mm)		
	Modal size 2 (mm)		

Petrographic data sheet - Larissa Macmillan 2009			
Sample number		PAR01	
Sample description		Makokako Sandstone	
Analyst		Larissa Macmillan	
BIOCLASTICS	**Total bioclast %**	0	
		%	**Abundance limit**
	Bryozoans		
	Bivalves		
	Echinoderms		
	Benthic foraminifera		
	Planktic foraminifera		
	Gastropods		
	Calcareous algae		
	Barnacles		
	Spicules & spines		
	Other		
	Modal size 1 (mm)		
	Modal size 2 (mm)		
	Shape/abrasion		
	Sorting		
SILICICLASTICS	**Siliciclastic grain %**	100	
		%	**Abundance limit**
	Quartz	73	abundant
	Feldspar	-	absent
	Igneous rock fragments	-	absent
	Sedimentary rock fragments	-	absent
	Micas	2	some
	Pyrite grains	-	absent
	Pyrite infills	-	absent
	Glauconite pellets	-	absent
	Glauconite infills	-	absent
	Other (clay)	25	common
	Modal size 1 (mm)	0.0475	
	Modal size 2 (mm)	0.0190	
	Shape/abrasion	Subrounded	
	Sorting	Poorly sorted	
SHELL AND BORING FEATURES	Shell fabric - crystal shapes, weathering, ppt minerals		
	Shell increments - Thickness, colour, continuous, discontinuous		
	Recrystallisation - distribution, degree, location.		
	Borings - size, shape, boundaries, location (within layer or truncating)		
	Infill - type, bioclastics, siliciclastics, geopetal fabrics, sparite, micritic peliods		
	Modal size 1 (mm)		
	Modal size 2 (mm)		

Petrographic data sheet - Larissa Macmillan			
Sample number		PAR05A	
Sample description		Sandstone concretion	
Analyst		Larissa Macmillan	
BIOCLASTICS	**Total bioclast %**	50	
		%	**Abundance limit**
	Bryozoans	-	absent
	Bivalves	48	very common
	Echinoderms	-	absent
	Benthic foraminifera	-	absent
	Planktic foraminifera	-	absent
	Gastropods	1	rare
	Calcareous algae	-	absent
	Barnacles	-	absent
	Spicules & spines	-	absent
	Other	1	rare
	Modal size 1 (mm)	0.5	
	Modal size 2 (mm)	5	
	Shape/abrasion	moderately abraded	
	Sorting	poorly sorted	
SILICICLASTICS	**Siliciclastic grain %**	50	
		%	**Abundance limit**
	Quartz	18	very common
	Feldspar	13	many
	Igneous rock fragments	-	absent
	Sedimentary rock fragments	-	absent
	Micas	2	some
	Pyrite grains	5	some
	Pyrite infills	-	absent
	Glauconite pellets	-	absent
	Glauconite infills	-	absent
	Other	12	some
	Modal size 1 (mm)	0.25	
	Modal size 2 (mm)	0.125	
	Shape/abrasion	subrounded	
	Sorting	moderatley sorted	
SHELL AND BORING FEATURES	Shell fabric - crystal shapes, weathering, ppt minerals		
	Shell increments - Thickness, colour, continuous, discontinuous		
	Recrystallisation - distribution, degree, location.		
	Borings - size, shape, boundaries, location (within layer or truncating)		
	Infill - type, bioclastics, siliciclastics, geopetal fabrics, sparite, micritic peliods		
	Modal size 1 (mm)		
	Modal size 2 (mm)		

Petrographic data sheet - Larissa Macmillan 2009			
Sample number		PAR05B	
Sample description		Sandstone concretion	
Analyst		Larissa Macmillan	
BIOCLASTICS	**Total bioclast %**	20	
		%	**Abundance limit**
	Bryozoans	-	absent
	Bivalves	19	common
	Echinoderms	-	absent
	Benthic foraminifera	-	absent
	Planktic foraminifera	-	absent
	Gastropods	1	rare
	Calcareous algae	-	absent
	Barnacles	-	absent
	Spicules & spines	-	absent
	Other	-	absent
	Modal size 1 (mm)	1.00	
	Modal size 2 (mm)	2.50	
	Shape/abrasion	Moderately abraded	
	Sorting	poorly sorted	
SILICICLASTICS	**Siliciclastic grain %**	80	
		%	**Abundance limit**
	Quartz	45	very common
	Feldspar	13	many
	Igneous rock fragments	-	absent
	Sedimentary rock fragments	-	absent
	Micas	8	many
	Pyrite grains	-	absent
	Pyrite infills	-	absent
	Glauconite pellets	2	some
	Glauconite infills	-	absent
	Other (clays)	12	some
	Modal size 1 (mm)	0.25	
	Modal size 2 (mm)	0.13	
	Shape/abrasion	subrounded	
	Sorting	moderately sorted	
SHELL AND BORING FEATURES	Shell fabric - crystal shapes, weathering, ppt minerals		
	Shell increments - Thickness, colour, continuous, discontinuous		
	Recrystallisation - distribution, degree, location.		
	Borings - size, shape, boundaries, location (within layer or truncating)		
	Infill - type, bioclastics, siliciclastics, geopetal fabrics, sparite, micritic peliods		
	Modal size 1 (mm)		
	Modal size 2 (mm)		

Petrographic data sheet - Larissa Macmillan 2009			
Sample number		PAR05C	
Sample description		Sandstone concretion	
Analyst		Larissa Macmillan	
BIOCLASTICS	**Total bioclast %**	20	
		%	**Abundance limit**
	Bryozoans	-	absent
	Bivalves	20	common
	Echinoderms	-	absent
	Benthic foraminifera	-	absent
	Planktic foraminifera	-	absent
	Gastropods	-	absent
	Calcareous algae	-	absent
	Barnacles	-	absent
	Spicules & spines	-	absent
	Other	-	absent
	Modal size 1 (mm)	1.50	
	Modal size 2 (mm)	2.50	
	Shape/abrasion	Moderately abraded	
	Sorting	poorly sorted	
SILICICLASTICS	**Siliciclastic grain %**	80	
		%	**Abundance limit**
	Quartz	40	very common
	Feldspar	13	many
	Igneous rock fragments	-	absent
	Sedimentary rock fragments	-	absent
	Micas	8	many
	Pyrite grains	-	absent
	Pyrite infills	-	absent
	Glauconite pellets	2	some
	Glauconite infills	-	absent
	Other (clays)	17	common
	Modal size 1 (mm)	0.25	
	Modal size 2 (mm)	0.13	
	Shape/abrasion	subrounded	
	Sorting	moderately sorted	
SHELL AND BORING FEATURES	Shell fabric - crystal shapes, weathering, ppt minerals		
	Shell increments - Thickness, colour, continuous, discontinuous		
	Recrystallisation - distribution, degree, location.		
	Borings - size, shape, boundaries, location (within layer or truncating)		
	Infill - type, bioclastics, siliciclastics, geopetal fabrics, sparite, micritic peliods		
	Modal size 1 (mm)		
	Modal size 2 (mm)		

Petrographic data sheet - Larissa Macmillan 2009			
Sample number		WAN07	
Sample description		M.SST	
Analyst		Larissa Macmillan	
BIOCLASTICS	**Total bioclast %**	2	
		%	**Abundance limit**
	Bryozoans	-	absent
	Bivalves	2	some
	Echinoderms	-	absent
	Benthic foraminifera	-	absent
	Planktic foraminifera	-	absent
	Gastropods	-	absent
	Calcareous algae	-	absent
	Barnacles	-	absent
	Spicules & spines	-	absent
	Other	-	absent
	Modal size 1 (mm)	0.30	
	Modal size 2 (mm)	0.13	
	Shape/abrasion	highly abraded	
	Sorting	poorly sorted	
SILICICLASTICS	**Siliciclastic grain %**	98	
		%	**Abundance limit**
	Quartz	30	very common
	Feldspar	15	many
	Igneous rock fragments	-	absent
	Sedimentary rock fragments	-	absent
	Micas	8	many
	Pyrite grains	-	absent
	Pyrite infills	-	absent
	Glauconite pellets	2	some
	Glauconite infills	4	some
	Other	45	abundant
	Modal size 1 (mm)	0.20	
	Modal size 2 (mm)	0.08	
	Shape/abrasion	subrounded	
	Sorting	poorly sorted	
SHELL AND BORING FEATURES	Shell fabric - crystal shapes, weathering, ppt minerals		
	Shell increments - Thickness, colour, continuous, discontinuous		
	Recrystallisation - distribution, degree, location.		
	Borings - size, shape, boundaries, location (within layer or truncating)		
	Infill - type, bioclastics, siliciclastics, geopetal fabrics, sparite, micritic peliods		
	Modal size 1 (mm)		
	Modal size 2 (mm)		

Petrographic data sheet - Larissa Macmillan			
Sample number		WAN09	
Sample description		M.SST	
Analyst		Larissa Macmillan	
BIOCLASTICS	**Total bioclast %**	2	
		%	**Abundance limit**
	Bryozoans	-	absent
	Bivalves	2	some
	Echinoderms	-	absent
	Benthic foraminifera	-	absent
	Planktic foraminifera	-	absent
	Gastropods	-	absent
	Calcareous algae	-	absent
	Barnacles	-	absent
	Spicules & spines	-	absent
	Other	-	absent
	Modal size 1 (mm)	0.10	
	Modal size 2 (mm)	0.25	
	Shape/abrasion	highly abraded	
	Sorting	poorly sorted	
SILICICLASTICS	**Siliciclastic grain %**	98	
		%	**Abundance limit**
	Quartz	28	very common
	Feldspar	15	many
	Igneous rock fragments	-	absent
	Sedimentary rock fragments	-	absent
	Micas	7	many
	Pyrite grains	-	absent
	Pyrite infills	-	absent
	Glauconite pellets	-	absent
	Glauconite infills	-	absent
	Other	48	abundant
	Modal size 1 (mm)	0.225	
	Modal size 2 (mm)	0.075	
	Shape/abrasion	subrounded	
	Sorting	poorly sorted	
SHELL AND BORING FEATURES	Shell fabric - crystal shapes, weathering, ppt minerals		
	Shell increments - Thickness, colour, continuous, discontinuous		
	Recrystallisation - distribution, degree, location.		
	Borings - size, shape, boundaries, location (within layer or truncating)		
	Infill - type, bioclastics, siliciclastics, geopetal fabrics, sparite, micritic peliods		
	Modal size 1 (mm)		
	Modal size 2 (mm)		

Petrographic data sheet - Larissa Macmillan 2009			
Sample number		WAN18	
Sample description		M.SST	
Analyst		Larissa Macmillan	
BIOCLASTICS	**Total bioclast %**	20	
		%	**Abundance limit**
	Bryozoans	-	-
	Bivalves	20	common
	Echinoderms	-	-
	Benthic foraminifera	-	-
	Planktic foraminifera	-	-
	Gastropods	-	-
	Calcareous algae	-	-
	Barnacles	-	-
	Spicules & spines	-	-
	Other	-	-
	Modal size 1 (mm)	one large frag	
	Modal size 2 (mm)		
	Shape/abrasion	low	
	Sorting	poorly sorted	
SILICICLASTICS	**Siliciclastic grain %**	80	
		%	**Abundance limit**
	Quartz	20	common
	Feldspar	10	many
	Igneous rock fragments	-	absent
	Sedimentary rock fragments	-	absent
	Micas	15	common
	Pyrite grains	-	absent
	Pyrite infills	-	absent
	Glauconite pellets	-	absent
	Glauconite infills	15	common
	Other	30	very common
	Modal size 1 (mm)	0.35	
	Modal size 2 (mm)	0.20	
	Shape/abrasion	sub angular	
	Sorting	poorly sorted	
SHELL AND BORING FEATURES	Shell fabric - crystal shapes, weathering, ppt minerals		
	Shell increments - Thickness, colour, continuous, discontinuous		
	Recrystallisation - distribution, degree, location.		
	Borings - size, shape, boundaries, location (within layer or truncating)		
	Infill - type, bioclastics, siliciclastics, geopetal fabrics, sparite, micritic peliods		
	Modal size 1 (mm)		
	Modal size 2 (mm)		

Petrographic data sheet - Larissa Macmillan 2009			
Sample number		WAN16	
Sample description		M.SST	
Analyst		Larissa Macmillan	
BIOCLASTICS	**Total bioclast %**	0	
		%	**Abundance limit**
	Bryozoans		
	Bivalves		
	Echinoderms		
	Benthic foraminifera		
	Planktic foraminifera		
	Gastropods		
	Calcareous algae		
	Barnacles		
	Spicules & spines		
	Other		
	Modal size 1 (mm)		
	Modal size 2 (mm)		
	Shape/abrasion		
	Sorting		
SILICICLASTICS	**Siliciclastic grain %**	100	
		%	**Abundance limit**
	Quartz	25	common
	Feldspar	15	many
	Igneous rock fragments	-	absent
	Sedimentary rock fragments	-	absent
	Micas	10	many
	Pyrite grains	-	absent
	Pyrite infills	-	absent
	Glauconite pellets	8	many
	Glauconite infills	-	absent
	Other	52	abundant
	Modal size 1 (mm)	0.25	
	Modal size 2 (mm)	0.10	
	Shape/abrasion	subrounded	
	Sorting	poorly sorted	
SHELL AND BORING FEATURES	Shell fabric - crystal shapes, weathering, ppt minerals		
	Shell increments - Thickness, colour, continuous, discontinuous		
	Recrystallisation - distribution, degree, location.		
	Borings - size, shape, boundaries, location (within layer or truncating)		
	Infill - type, bioclastics, siliciclastics, geopetal fabrics, sparite, micritic peliods		
	Modal size 1 (mm)		
	Modal size 2 (mm)		

Petrographic data sheet - Larissa Macmillan 2009			
Sample number		WAN19	
Sample description		M.SST	
Analyst		Larissa Macmillan	
BIOCLASTICS	**Total bioclast %**	0	
		%	**Abundance limit**
	Bryozoans		
	Bivalves		
	Echinoderms		
	Benthic foraminifera		
	Planktic foraminifera		
	Gastropods		
	Calcareous algae		
	Barnacles		
	Spicules & spines		
	Other		
	Modal size 1 (mm)		
	Modal size 2 (mm)		
	Shape/abrasion		
	Sorting		
SILICICLASTICS	**Siliciclastic grain %**	100	
		%	**Abundance limit**
	Quartz	20	common
	Feldspar	15	many
	Igneous rock fragments	-	absent
	Sedimentary rock fragments	-	absent
	Micas	10	many
	Pyrite grains	-	absent
	Pyrite infills	-	absent
	Glauconite pellets	-	absent
	Opaque minerals	15	common
	Other	30	very common
	Modal size 1 (mm)	0.15	
	Modal size 2 (mm)	0.30	
	Shape/abrasion	subangular	
	Sorting	poorly sorted	
SHELL AND BORING FEATURES	Shell fabric - crystal shapes, weathering, ppt minerals		
	Shell increments - Thickness, colour, continuous, discontinuous		
	Recrystallisation - distribution, degree, location.		
	Borings - size, shape, boundaries, location (within layer or truncating)		
	Infill - type, bioclastics, siliciclastics, geopetal fabrics, sparite, micritic peliods		
	Modal size 1 (mm)		
	Modal size 2 (mm)		

Petrographic data sheet - Larissa Macmillan 2009			
Sample number		WAN20	
Sample description		M.SST	
Analyst		Larissa Macmillan	
BIOCLASTICS	**Total bioclast %**	0	
		%	**Abundance limit**
	Bryozoans		
	Bivalves		
	Echinoderms		
	Benthic foraminifera		
	Planktic foraminifera		
	Gastropods		
	Calcareous algae		
	Barnacles		
	Spicules & spines		
	Other		
	Modal size 1 (mm)		
	Modal size 2 (mm)		
	Shape/abrasion		
	Sorting		
SILICICLASTICS	**Siliciclastic grain %**	100	
		%	**Abundance limit**
	Quartz	30	very common
	Feldspar	17	common
	Igneous rock fragments	-	absent
	Sedimentary rock fragments	-	absent
	Micas	8	many
	Pyrite grains	-	absent
	Pyrite infills	-	absent
	Glauconite pellets	-	absent
	Opaque minerlas	15	many
	Other	30	very common
	Modal size 1 (mm)	0.25	
	Modal size 2 (mm)	0.10	
	Shape/abrasion	sub angular	
	Sorting	poorly sorted	
SHELL AND BORING FEATURES	Shell fabric - crystal shapes, weathering, ppt minerals		
	Shell increments - Thickness, colour, continuous, discontinuous		
	Recrystallisation - distribution, degree, location.		
	Borings - size, shape, boundaries, location (within layer or truncating)		
	Infill - type, bioclastics, siliciclastics, geopetal fabrics, sparite, micritic peliods		
	Modal size 1 (mm)		
	Modal size 2 (mm)		

Petrographic data sheet - Larissa Macmillan 2009			
Sample number		K2E	
Sample description		Kaurapaoa Valley Road Matrix	
Analyst		Larissa Macmillan	
BIOCLASTICS	**Total bioclast %**	3	
		%	**Abundance limit**
	Bryozoans	-	absent
	Bivalves	3	some
	Echinoderms	-	absent
	Benthic foraminifera	-	absent
	Planktic foraminifera	-	absent
	Gastropods	-	absent
	Calcareous algae	-	absent
	Barnacles	-	absent
	Spicules & spines	-	absent
	Other	-	absent
	Modal size 1 (mm)	1.50	
	Modal size 2 (mm)	1.00	
	Shape/abrasion	Highly abraded	
	Sorting	poorly sorted	
SILICICLASTICS	**Siliciclastic grain %**	97	
		%	**Abundance limit**
	Quartz	15	very common
	Feldspar	10	many
	Igneous rock fragments	-	absent
	Sedimentary rock fragments	-	absent
	Micas	10	many
	Pyrite grains	-	absent
	Pyrite infills	-	absent
	Glauconite pellets	5	some
	Opaques	15	common
	Other	45	very common
	Modal size 1 (mm)	0.15	
	Modal size 2 (mm)	0.30	
	Shape/abrasion	subrounded	
	Sorting	poorly sorted	
SHELL AND BORING FEATURES	Shell fabric - crystal shapes, weathering, ppt minerals		
	Shell increments - Thickness, colour, continuous, discontinuous		
	Recrystallisation - distribution, degree, location.		
	Borings - size, shape, boundaries, location (within layer or truncating)		
	Infill - type, bioclastics, siliciclastics, geopetal fabrics, sparite, micritic peliods		
	Modal size 1 (mm)		
	Modal size 2 (mm)		

Petrographic data sheet - Larissa Macmillan 2009			
Sample number		R2	
Sample description		Rangitatau East Matrix	
Analyst		Larissa Macmillan	
BIOCLASTICS	**Total bioclast %**	15	
		%	**Abundance limit**
	Bryozoans	6	many
	Bivalves	9	many
	Echinoderms	-	absent
	Benthic foraminifera	-	absent
	Planktic foraminifera	-	absent
	Gastropods	-	absent
	Calcareous algae	-	absent
	Barnacles	-	absent
	Spicules & spines	-	absent
	Other	-	absent
	Modal size 1 (mm)	0.38	
	Modal size 2 (mm)	0.63	
	Shape/abrasion	Highly abraded	
	Sorting	Poorly sorted	
SILICICLASTICS	**Siliciclastic grain %**	85	
		%	**Abundance limit**
	Quartz	12	many
	Feldspar	10	many
	Igneous rock fragments	-	absent
	Sedimentary rock fragments	-	absent
	Micas	7	many
	Pyrite grains	-	absent
	Pyrite infills	-	absent
	Glauconite pellets	5	some
	Opaques	15	many
	Other	51	abundant
	Modal size 1 (mm)	0.13	
	Modal size 2 (mm)	0.30	
	Shape/abrasion	subrounded	
	Sorting	poorly sorted	
SHELL AND BORING FEATURES	Shell fabric - crystal shapes, weathering, ppt minerals		
	Shell increments - Thickness, colour, continuous, discontinuous		
	Recrystallisation - distribution, degree, location.		
	Borings - size, shape, boundaries, location (within layer or truncating)		
	Infill - type, bioclastics, siliciclastics, geopetal fabrics, sparite, micritic peliods		
	Modal size 1 (mm)		
	Modal size 2 (mm)		

Petrographic data sheet - Larissa Macmillan 2009			
Sample number		WLK	
Sample description		Oyster shell + small section of host	
Analyst		Larissa Macmillan	
BIOCLASTICS	**Total bioclast %**	0	
		%	**Abundance limit**
	Bryozoans		
	Bivalves		
	Echinoderms		
	Benthic foraminifera		
	Planktic foraminifera		
	Gastropods		
	Calcareous algae		
	Barnacles		
	Spicules & spines		
	Other		
	Modal size 1 (mm)		
	Modal size 2 (mm)		
	Shape/abrasion		
	Sorting		
SILICICLASTICS	**Siliciclastic grain %**	100	
		%	**Abundance limit**
	Quartz	10	many
	Feldspar	12	many
	Igneous rock fragments	-	absent
	Sedimentary rock fragments	-	absent
	Micas	3	some
	Pyrite grains	-	absent
	Pyrite infills	-	absent
	Glauconite pellets	-	absent
	Glauconite infills	-	absent
	Other	75	abundant
	Modal size 1 (mm)	0.10	
	Modal size 2 (mm)	0.05	
	Shape/abrasion	subrounded	
	Sorting	poorly sorted	
SHELL AND BORING FEATURES	Shell fabric - crystal shapes, weathering, ppt minerals	Crystals laths of calcite	
	Shell increments - Thickness, colour, continuous, discontinuous	Thin brown layer (0.2 mm) and thicker grey layer (3 mm). Layer are irregular and discontinuous.	
	Recrystallisation - distribution, degree, location.	absent	
	Borings - size, shape, boundaries, location (within layer or truncating)	borings elongate in shape and lack a sharp boundary	
	Infill - type, bioclastics, siliciclastics, geopetal fabrics, sparite, micritic peliods	fine grained siliciclastic material, quartz, mica, opaque minerals.	
	Modal size 1 (mm)	0.625	
	Modal size 2 (mm)	1.25	

Petrographic data sheet - Larissa Macmillan 2009			
Sample number		WLK06	
Sample description		Oyster shell	
Analyst		Larissa Macmillan	
BIOCLASTICS	**Total bioclast %**	0	
		%	**Abundance limit**
	Bryozoans		
	Bivalves		
	Echinoderms		
	Benthic foraminifera		
	Planktic foraminifera		
	Gastropods		
	Calcareous algae		
	Barnacles		
	Spicules & spines		
	Other		
	Modal size 1 (mm)		
	Modal size 2 (mm)		
	Shape/abrasion		
	Sorting		
SILICICLASTICS	**Siliciclastic grain %**	0	
		%	**Abundance limit**
	Quartz		
	Feldspar		
	Igneous rock fragments		
	Sedimentary rock fragments		
	Micas		
	Pyrite grains		
	Pyrite infills		
	Glauconite pellets		
	Glauconite infills		
	Other		
	Modal size 1 (mm)		
	Modal size 2 (mm)		
	Shape/abrasion		
	Sorting		
SHELL AND BORING FEATURES	Shell fabric - crystal shapes, weathering, ppt minerals	Homogenous, fine grained calcite crystals, no weathering of mineral ppt	
	Shell increments - Thickness, colour, continuous, discontinuous	Light layers (0.38-2.375 mm) thinner layers (0.19-0.38 mm). Some layers fractured, layers are irregular and vary in size.	
	Recrystallisation - distribution, degree, location.	absent	
	Borings - size, shape, boundaries, location (within layer or truncating)	absent	
	Infill - type, bioclastics, siliciclastics, geopetal fabrics, sparite, micritic peliods	absent	
	Modal size 1 (mm)	-	
	Modal size 2 (mm)	-	

Petrographic data sheet - Larissa Macmillan			
Sample number		WLK06A2	
Sample description		Oyster shell	
Analyst		Larissa Macmillan	
BIOCLASTICS	**Total bioclast %**	0	
		%	**Abundance limit**
	Bryozoans		
	Bivalves		
	Echinoderms		
	Benthic foraminifera		
	Planktic foraminifera		
	Gastropods		
	Calcareous algae		
	Barnacles		
	Spicules & spines		
	Other		
	Modal size 1 (mm)		
	Modal size 2 (mm)		
	Shape/abrasion		
	Sorting		
SILICICLASTICS	**Siliciclastic grain %**	0	
		%	**Abundance limit**
	Quartz		
	Feldspar		
	Igneous rock fragments		
	Sedimentary rock fragments		
	Micas		
	Pyrite grains		
	Pyrite infills		
	Glauconite pellets		
	Glauconite infills		
	Other		
	Modal size 1 (mm)		
	Modal size 2 (mm)		
	Shape/abrasion		
	Sorting		
SHELL AND BORING FEATURES	Shell fabric - crystal shapes, weathering, ppt minerals	Homogenous, fine grained calcite crystals.	
	Shell increments - Thickness, colour, continuous, discontinuous	Light layers are thicker (1.75 mm), dark layer (0.25-3.75 mm). Layers show fracturing and vary in thickness.	
	Recrystallisation - distribution, degree, location.	Occurs in the thicker lighter layer. Areas are liner in shape and composed of fine grained calcite spar.	
	Borings - size, shape, boundaries, location (within layer or truncating)	Borings are oval to globular in shape with sharp edges. Some show weathering/iron stain around edges. Occur within the thicker layer.	
	Infill - type, bioclastics, siliciclastics, geopetal fabrics, sparite, micritic peliods	Majority of infill no present, few quartz crystals, limonite stained.	
	Modal size 1 (mm)	2.875	
	Modal size 2 (mm)	6.25	

Petrographic data sheet - Larissa Macmillan 2009			
Sample number		WLK17A	
Sample description		Oyster shell	
Analyst		Larissa Macmillan	
BIOCLASTICS	**Total bioclast %**	0	
		%	**Abundance limit**
	Bryozoans		
	Bivalves		
	Echinoderms		
	Benthic foraminifera		
	Planktic foraminifera		
	Gastropods		
	Calcareous algae		
	Barnacles		
	Spicules & spines		
	Other		
	Modal size 1 (mm)		
	Modal size 2 (mm)		
	Shape/abrasion		
	Sorting		
SILICICLASTICS	**Siliciclastic grain %**	0	
		%	**Abundance limit**
	Quartz		
	Feldspar		
	Igneous rock fragments		
	Sedimentary rock fragments		
	Micas		
	Pyrite grains		
	Pyrite infills		
	Glauconite pellets		
	Glauconite infills		
	Other		
	Modal size 1 (mm)		
	Modal size 2 (mm)		
	Shape/abrasion		
	Sorting		
SHELL AND BORING FEATURES	Shell fabric - crystal shapes, weathering, ppt minerals	Homogenous calcite.	
	Shell increments - Thickness, colour, continuous, discontinuous	Vary greatly darker thick layers (1 mm) and lighter layers (0.05-0.125 mm). Thickness of layers is irregular. Layers	
	Recrystallisation - distribution, degree, location.	Mostly occurs along dark thicker layers. Occurs in linear patterns and large blocks of calcite spar.	
	Borings - size, shape, boundaries, location (within layer or truncating)	Irregular borings which are generally elongate in shape. Dull, blurred edges. Contained within the larger darker layer.	
	Infill - type, bioclastics, siliciclastics, geopetal fabrics, sparite, micritic peliods	Infill absent	
	Modal size 1 (mm)	1.5	
	Modal size 2 (mm)	2.25	

Petrographic data sheet - Larissa Macmillan 2009			
Sample number		WLK17B	
Sample description		Oyster shell	
Analyst		Larissa Macmillan	
BIOCLASTICS	**Total bioclast %**	0	
		%	**Abundance limit**
	Bryozoans		
	Bivalves		
	Echinoderms		
	Benthic foraminifera		
	Planktic foraminifera		
	Gastropods		
	Calcareous algae		
	Barnacles		
	Spicules & spines		
	Other		
	Modal size 1 (mm)		
	Modal size 2 (mm)		
	Shape/abrasion		
	Sorting		
SILICICLASTICS	**Siliciclastic grain %**	0	
		%	**Abundance limit**
	Quartz		
	Feldspar		
	Igneous rock fragments		
	Sedimentary rock fragments		
	Micas		
	Pyrite grains		
	Pyrite infills		
	Glauconite pellets		
	Glauconite infills		
	Other		
	Modal size 1 (mm)		
	Modal size 2 (mm)		
	Shape/abrasion		
	Sorting		
SHELL AND BORING FEATURES	Shell fabric - crystal shapes, weathering, ppt minerals	Crystal laths of calcite to homogenous calcite material. No ppt.	
	Shell increments - Thickness, colour, continuous, discontinuous	Vary greatly darker thick layers (0.5-1.75 mm) and lighter layers (0.05-0.125 mm).	
	Recrystallisation - distribution, degree, location.	Mostly occurs along dark thicker layers. Occurs as tabular sections of fine calcite spar.	
	Borings - size, shape, boundaries, location (within layer or truncating)	Irregular borings which are generally elongate in shape. Irregular boundaries. Contained within the larger darker layer. Often limonite stained. Contained withing the	
	Infill - type, bioclastics, siliciclastics, geopetal fabrics, sparite, micritic peliods	Mixture of siliciclastic material. Quartz, clay and mica. Poorly sorted.	
	Modal size 1 (mm)	3.75	
	Modal size 2 (mm)	5	

Petrographic data sheet - Larissa Macmillan 2009			
Sample number		WLK17A-2	
Sample description		Oyster shell	
Analyst		Larissa Macmillan	
BIOCLASTICS	**Total bioclast %**	0	
		%	**Abundance limit**
	Bryozoans		
	Bivalves		
	Echinoderms		
	Benthic foraminifera		
	Planktic foraminifera		
	Gastropods		
	Calcareous algae		
	Barnacles		
	Spicules & spines		
	Other		
	Modal size 1 (mm)		
	Modal size 2 (mm)		
	Shape/abrasion		
	Sorting		
SILICICLASTICS	**Siliciclastic grain %**	0	
		%	**Abundance limit**
	Quartz		
	Feldspar		
	Igneous rock fragments		
	Sedimentary rock fragments		
	Micas		
	Pyrite grains		
	Pyrite infills		
	Glauconite pellets		
	Glauconite infills		
	Other		
	Modal size 1 (mm)		
	Modal size 2 (mm)		
	Shape/abrasion		
	Sorting		
SHELL AND BORING FEATURES	Shell fabric - crystal shapes, weathering, ppt minerals	Crystal laths to homogenous calcite.	
	Shell increments - Thickness, colour, continuous, discontinuous	Shell increments vary, lighter layers (0.125 mm), darker thicker layers (0.5-1.75 mm). Very irregular, many layers fractured and displaced.	
	Recrystallisation - distribution, degree, location.	absent	
	Borings - size, shape, boundaries, location (within layer or truncating)	Borings have irregular boundaries, are elongate in shape and occur within the larger dark layer of shell material.	
	Infill - type, bioclastics, siliciclastics, geopetal fabrics, sparite, micritic peliods	Siliciclastica material includeds, quartz, mica and clays. In larger bores fragmented bivalves are common.	
	Modal size 1 (mm)	1.75	
	Modal size 2 (mm)	8.75	

Petrographic data sheet - Larissa Macmillan 2009			
Sample number		K4F	
Sample description		Oyster shell	
Analyst		Larissa Macmillan	
BIOCLASTICS	**Total bioclast %**	0	
		%	**Abundance limit**
	Bryozoans		
	Bivalves		
	Echinoderms		
	Benthic foraminifera		
	Planktic foraminifera		
	Gastropods		
	Calcareous algae		
	Barnacles		
	Spicules & spines		
	Other		
	Modal size 1 (mm)		
	Modal size 2 (mm)		
	Shape/abrasion		
	Sorting		
SILICICLASTICS	**Siliciclastic grain %**	0	
		%	**Abundance limit**
	Quartz		
	Feldspar		
	Igneous rock fragments		
	Sedimentary rock fragments		
	Micas		
	Pyrite grains		
	Pyrite infills		
	Glauconite pellets		
	Glauconite infills		
	Other		
	Modal size 1 (mm)		
	Modal size 2 (mm)		
	Shape/abrasion		
	Sorting		
SHELL AND BORING FEATURES	Shell fabric - crystal shapes, weathering, ppt minerals	Fine grained calcite, irregualr to linear lath crystals.	
	Shell increments - Thickness, colour, continuous, discontinuous	Alternating dark (0.25 mm) and light layers (1.25 mm). Fractures forming in irregular patterns.	
	Recrystallisation - distribution, degree, location.	Fine grained calcite spar occuring in small linear patches along thinner darker layers.	
	Borings - size, shape, boundaries, location (within layer or truncating)	absent	
	Infill - type, bioclastics, siliciclastics, geopetal fabrics, sparite, micritic peliods	absent	
	Modal size 1 (mm)	-	
	Modal size 2 (mm)	-	

Petrographic data sheet - Larissa Macmillan 2009			
Sample number		K4FA	
Sample description		Oyster shell	
Analyst		Larissa Macmillan	
BIOCLASTICS	**Total bioclast %**	0	
		%	**Abundance limit**
	Bryozoans		
	Bivalves		
	Echinoderms		
	Benthic foraminifera		
	Planktic foraminifera		
	Gastropods		
	Calcareous algae		
	Barnacles		
	Spicules & spines		
	Other		
	Modal size 1 (mm)		
	Modal size 2 (mm)		
	Shape/abrasion		
	Sorting		
SILICICLASTICS	**Siliciclastic grain %**	0	
		%	**Abundance limit**
	Quartz		
	Feldspar		
	Igneous rock fragments		
	Sedimentary rock fragments		
	Micas		
	Pyrite grains		
	Pyrite infills		
	Glauconite pellets		
	Glauconite infills		
	Other		
	Modal size 1 (mm)		
	Modal size 2 (mm)		
	Shape/abrasion		
	Sorting		
SHELL AND BORING FEATURES	Shell fabric - crystal shapes, weathering, ppt minerals	Shell structure formed from crystal laths of calcite. Long and irregular patterns in shells. Poss. From weathering.	
	Shell increments - Thickness, colour, continuous, discontinuous	darker layer (0.125-0.25 mm) light layer (1-2.5 mm). Layers are highly fracutred and irregular.	
	Recrystallisation - distribution, degree, location.	Occurs in patches of calcite spar crystals	
	Borings - size, shape, boundaries, location (within layer or truncating)	Within lighter layer. Are elongeted and oval in shape, have sharp edges and are contained within the lighter, thicker layer of shell material.	
	Infill - type, bioclastics, siliciclastics, geopetal fabrics, sparite, micritic peliods	Fine grained siliciclastic material, quartz, opaque minerals.	
	Modal size 1 (mm)		
	Modal size 2 (mm)		